



NEA/CSNI/R(97)9

**JOINT WANO/OECD - NEA WORKSHOP
PRESTRESS LOSS IN NPP CONTAINMENTS**

*Civaux NPP
(Poitiers, France)
25-26 August 1997*

**Organised by EDF/IPSN
with the participation of RILEM/FIP/IASMiRT**



**COMMITTEE ON THE SAFETY OF NUCLEAR INSTALLATIONS
OECD NUCLEAR ENERGY AGENCY**

Le Seine Saint-Germain – 12, boulevard des Îles
F-92130 Issy-les-Moulineaux (France)
Tel. (33) 1 45 24 82 00 Fax (33) 1 45 24 11 10

**JOINT WANO/OECD-NEA WORKSHOP PRESTRESS LOSS
IN NPP CONTAINMENTS**

Civaux NPP (Poitiers, France), 25-26 August 1997

Organised by EDF/IPSN with the participation of RILEM/FIP/IASMiRT

ORGANISATION FOR ECONOMIC CO-OPERATION AND DEVELOPMENT

Paris

60512

**Document incomplet sur OLIS
Incomplete document on OLIS**

ORGANISATION FOR ECONOMIC CO-OPERATION AND DEVELOPMENT

Pursuant to Article 1 of the Convention signed in Paris on 14th December 1960, and which came into force on 30th September 1961, the Organisation for Economic Co-operation and Development (OECD) shall promote policies designed:

- to achieve the highest sustainable economic growth and employment and a rising standard of living in Member countries, while maintaining financial stability, and thus to contribute to the development of the world economy;
- to contribute to sound economic expansion in Member as well as non-member countries in the process of economic development; and
- to contribute to the expansion of world trade on a multilateral, non-discriminatory basis in accordance with international obligations.

The original Member countries of the OECD are Austria, Belgium, Canada, Denmark, France, Germany, Greece, Iceland, Ireland, Italy, Luxembourg, the Netherlands, Norway, Portugal, Spain, Sweden, Switzerland, Turkey, the United Kingdom and the United States. The following countries became Members subsequently through accession at the dates indicated hereafter: Japan (28th April 1964), Finland (28th January 1969), Australia (7th June 1971), New Zealand (29th May 1973), Mexico (18th May 1994) the Czech Republic (21st December 1995), Hungary (7th May 1996), Poland (22nd November 1996) and the Republic of Korea (12th December 1996). The Commission of the European Communities takes part in the work of the OECD (Article 13 of the OECD Convention).

NUCLEAR ENERGY AGENCY

The OECD Nuclear Energy Agency (NEA) was established on 1st February 1958 under the name of the OEEC European Nuclear Energy Agency. It received its present designation on 20th April 1972, when Japan became its first non-European full Member. NEA membership today consists of all OECD Member countries, except New Zealand and Poland. The Commission of the European Communities takes part in the work of the Agency.

The primary objective of the NEA is to promote co-operation among the governments of its participating countries in furthering the development of nuclear power as a safe, environmentally acceptable and economic energy source.

This is achieved by:

- *encouraging harmonization of national regulatory policies and practices, with particular reference to the safety of nuclear installations, protection of man against ionising radiation and preservation of the environment, radioactive waste management, and nuclear third party liability and insurance;*
- *assessing the contribution of nuclear power to the overall energy supply by keeping under review the technical and economic aspects of nuclear power growth and forecasting demand and supply for the different phases of the nuclear fuel cycle;*
- *developing exchanges of scientific and technical information particularly through participation in common services;*
- *setting up international research and development programmes and joint undertakings.*

In these and related tasks, the NEA works in close collaboration with the International Atomic Energy Agency in Vienna, with which it has concluded a Co-operation Agreement, as well as with other international organisations in the nuclear field.

© OECD 1997

Permission to reproduce a portion of this work for non-commercial purposes or classroom use should be obtained through Centre français d'exploitation du droit de copie (CCF), 20, rue des Grands-Augustins, 75006 Paris, France, for every country except the United States. In the United States permission should be obtained through the Copyright Clearance Center, Inc. (CCC). All other applications for permission to reproduce or translate all or part of this book should be made to OECD Publications, 2, rue André-Pascal, 75775 PARIS CEDEX 16, France.

COMMITTEE ON THE SAFETY OF NUCLEAR INSTALLATIONS

The NEA Committee on the Safety of Nuclear Installations (CSNI) is an international committee made up of scientists and engineers. It was set up in 1973 to develop and co-ordinate the activities of the Nuclear Energy Agency concerning the technical aspects of the design, construction and operation of nuclear installations insofar as they affect the safety of such installations. The Committee's purpose is to foster international co-operation in nuclear safety amongst the OECD Member countries.

CSNI constitutes a forum for the exchange of technical information and for collaboration between organisations which can contribute, from their respective backgrounds in research, development, engineering or regulation, to these activities and to the definition of its programme of work. It also reviews the state of knowledge on selected topics of nuclear safety technology and safety assessment, including operating experience. It initiates and conducts programmes identified by these reviews and assessments in order to overcome discrepancies, develop improvements and reach international consensus in different projects and International Standard Problems, and assists in the feedback of the results to participating organisations. Full use is also made of traditional methods of co-operation, such as information exchanges, establishment of working groups and organisation of conferences and specialist meeting.

The greater part of CSNI's current programme of work is concerned with safety technology of water reactors. The principal areas covered are operating experience and the human factor, reactor coolant system behaviour, various aspects of reactor component integrity, the phenomenology of radioactive releases in reactor accidents and their confinement, containment performance, risk assessment and severe accidents. The Committee also studies the safety of the fuel cycle, conducts periodic surveys of reactor safety research programmes and operates an international mechanism for exchanging reports on nuclear power plant incidents.

In implementing its programme, CSNI establishes co-operative mechanisms with NEA's Committee on Nuclear Regulatory Activities (CNRA), responsible for the activities of the Agency concerning the regulation, licensing and inspection of nuclear installations with regard to safety. It also co-operates with NEA's Committee on Radiation Protection and Public Health and NEA's Radioactive Waste Management Committee on matters of common interest.

FOREWORD

This workshop was organised by EDF and IPSN. It was sponsored by WANO Paris Centre and by Principal Working Group 3 (PWG-3) of the NEA CSNI, with the participation of RILEM (Réunion Internationale des Laboratoires d'Essais et de recherches sur les Matériaux et les constructions), FIP-CEB (Fédération Internationale de la Précontrainte et Comité Euro-international du Béton) and IASMiRT (International Association for Structural Mechanics in Reactor Technology).

PWG-3 deals with the integrity of structures and components, and has three sub-groups, dealing with the integrity of metal structures and components, ageing of concrete structures, and the seismic behaviour of structures.

A status report on the ageing of concrete NPP structures was prepared during 1995 by a task group to initiate activities in this field under PWG3. The topic of tendon prestress loss was identified as one of the highest priority issues, and accordingly it was decided to organise this workshop. The other first priority topic was NDE, and a workshop to address this was also organised in 1997.

This document is published under the responsibility of the Secretary-General of the OECD.

ACKNOWLEDGEMENTS

The organising Committee would like to thank the sponsors of the Workshop :

- FIP-CEB (Fédération internationale de la précontrainte et Comité euro-international du béton),
- IASMiRT (International Association for Structural Mechanics In Reactor Technology),
- OECD - AEN/NEA (OECD Nuclear Energy Agency),
- RILEM (Réunion internationale des laboratoires d'essais et de recherches sur les matériaux et les constructions),
- WANO (World Association of Nuclear Operators),

and the two organisers :

- EDF - SEPTEN (Electricité de France - Service Etudes et Projets Thermiques Et Nucléaires),
- IPSN (Institut de Protection et de Sécurité Nucléaire).

Finally, the organisers gratefully thank the authors for their excellent contributions. They hope that all the knowledge contained in this volume will help the civil-engineering community for a better mastery of prestress concrete, a key technique associated with a wonderful material for the next century !

The Organising Committee :

President : Pierre LABBÉ (EDF / SEPTEN)

Secretary : Laurent GRANGER (EDF / SEPTEN)

Members : Bernard BARBÉ (IPSN / DES)

Pierre JARTOUX (Freyssinet International)

Alex MILLER (OECD / NEA)

Jack PICAUT (Coyne et Bellier)

Pierre ROUSSELLE (EDF / EPN)

Claude SENI (AECL)

TABLE OF CONTENTS

	Page
Opening Remarks by OECD & EDF	11
Alex Miller, OECD Nuclear Energy Agency, Secretary CSNI PWG-3 Pierre Labbé, EDF SEPTEN	
Creep and Shrinkage of Concrete: Physical Origins, Practical Measurements	15
Paul Acker, Laboratoire Central des Ponts et Chaussées, Paris, France	
Past, Present and Future Techniques for Predicting Creep and Shrinkage of Concrete	33
Prof. Zdenek P. Bazant, Technological Institute, Evanston, Ill. USA	
Assessment of Creep Methodologies for Predicting Prestressing Forces Losses in Nuclear Power Plant Containments	49
Laurent Granger, Zdenek Bittnar and Tibor Javor, Members of RILEM TC-MLN	
Prestress Behaviour in Belgian NPP Containments	65
L. de Marneffe, Tractebel, Belgium	
Presentation of Gentilly 2 NPP Containment (abstract only)	87
Nelson Garceau, Hydro-Québec	
Containment Structure Monitoring and Prestress Losses	89
Experience from Daya Bay Nuclear Power Plant XuYao Zhang, Guangdong Nuclear Power Joint Venture Corporation, People's Republic of China	
Prestress losses in NPP containments - the EDF experience	95
E. Martinet, P. Guinet, H. Rousselle, L. Granger, EDF, France	
Prestress Force Monitoring on the THTR Prestressed Concrete Reactor Vessel During 19 Years	115
E. Stangenberg, M. Borgerhoff, K. Schimmelpfennig	
NPP Containment Design: Evolution and Indian Experience	127
A. S. Warudkar, Nuclear Power Corporation, India	

	Page
In-Service Inspections and R&D of PCCVs in Japan	151
Watanabe Yukio, Kawai Ikuro, JAERI	
Kowada Akira, Akita Shodo, Kansai Electric	
Itou Yoshitetsu, Sono Youichi, Kyushu Electric Power Co.	
Koyanagi Mitsuo, Yamamoto Mikio, Obayashi Corporation	
Comparison of Grouted and Ungouted Tendons in NPP Containments	187
Munir Ahmad, Chashma Nuclear Power Project, Pakistan Atomic Energy Commission	
Prestress Losses in Containment of VVER 1000 Units	205
V. Maliavine, Atomenergoproekt, Russian Federation	
Prestressing in Nuclear Power Plants	221
Anchor Lift-off Measuring System for 37 T 15 Tendons	
M. Victor Vives, S. Luis Ubalde, Ascó, Spain	
Monitoring of Stressed-Strained State and Forces in Reinforcing Cables of Prestressed Containment Shells of Nuclear Power Plants	233
J. Klimov, State Research Institute of Building Construction, Kiev, Ukraine	
Long-Term In-Service Monitoring of Pre-stressing in Magnox Pre-stressed Concrete Pressure Vessels	259
D.W. Twidale, Magnox Electric plc	
The Measurement of Unbonded Tendon Loads in PCPV and Primary Containment Buildings	283
J. Irving, M.S. Hinley, D. McCluskey	
The Long Term In-service Performance of Corrosion Protection to Prestressing Tendons in AGR Prestressed Concrete Pressure Vessels	315
L.M. Smith, Scottish Nuclear Limited, M.F. Taylor, NNC Limited	
Prestress Force Losses in Containments of U.S. Nuclear Power Plants	337
H. Ashar, J. Costello, H. Graves, USNRC, Washington	
Discussion	357
Round Table	361
Synthesis	363
Workshop Programme	369
List of Participants	371

Opening remarks by OECD

Alex Miller, OECD Nuclear Energy Agency, Secretary CSNI PWG-3

I welcome the participants to this joint OECD-NEA, WANO Specialists Meeting on prestress losses in NPP containments. I take this opportunity to thank EDF and IPSN for hosting and organising this meeting. RILEM, FIP and IASMiRT also support this meeting. For those of you who may not be familiar with the activities of the OECD Nuclear Energy Agency, I would like to say how this meeting fits into the activities of the Agency.

The NEA is one of 15 bodies that make up the Paris based Organisation for Economic Co-operation and Development (OECD). Since the majority of the OECD's activities are oriented towards economics, the role of the Agency is less well known, and may sometimes be confused with the IAEA in Vienna, which is part of the United Nations system. There are 29 member countries of OECD, essentially the industrialised democracies. In 1996 the Czech Republic, Hungary, Poland and South Korea joined OECD. NEA has 27 Member countries, and 80 staff.

I work for the Nuclear Safety Division, which provides the secretariat for the Committee on the Safety of Nuclear Installation, a committee of senior scientist and technologists, and also for the Committee on Nuclear Regulatory Activities. CSNI works through five Principal Working groups (PWG's), dealing with Operating Experience and Human Factors (PWG-1), Coolant System Behaviour (PWG-2), Integrity of Structures and Components (PWG-3), Accidental Radioactivity Releases (PWG-4), and Risk Assessment (PWG-5). I am the secretary of PWG-3, concerned with structural integrity.

Since 1996 PWG-3 has had 3 sub-groups, dealing with the integrity of metal structures and components, the ageing of concrete structures, and the seismic behaviour of structures. Typical activities are the organisation of Workshops and Specialists Meetings, the preparation of State Of the Art Reports, and organisation of round robin or benchmark exercises. As an example, in order to start the activities of the new groups on concrete structures and seismic behaviour of structures, a status report was prepared on each topic in 1995 and 1996 respectively, suggesting future PWG-3 activities in these areas. For the concrete structures group, this report was prepared by Dan Naus of ORNL, with the assistance of a small number of people nominated by member countries.

The concrete group is organising two workshops in 1997. This is the first one. The second workshop is on NDE, being organised by the NII in Warrington in the UK, November 12. Future topics to be considered are a workshop on Finite Element analysis (maybe jointly with the seismic group), and the desirability of an operating experience database. The group carries out its work taking into account the activities of other international organisations such the IAEA, CEC and RILEM.

The metal components group deals with NDE, fracture mechanics and material ageing. The seismic group has carried out a benchmark on a NUPEC test on a shaking table test of a shear wall model, and is preparing a status report on the seismic re-evaluation of old plant. Future topics include ground motion, and further benchmarks. PWG-3 itself has the role of synthesising the work of the sub-groups, especially in the context of ageing, and of addressing topics not covered by the sub-groups, for example the ageing of organic materials.

The papers from this meeting have been distributed to you. There will be a summary prepared of the discussions, and in particular, of the concluding

synthesis. This will be further discussed at the next meeting of the PWG3 subgroup, and the final proceedings will be issued by OECD-NEA as a CSNI report. In closing, I thank our hosts again, and I look forward to hearing the papers and discussions.

Introduction by EDF

Pierre Labbé, EDF, Service Etudes et Projets Thermiques et Nucléaires

On the behalf of Electricité de France, I welcome all the participants to this workshop, here in Civaux Nuclear Power Plant. From an original idea of a Working Group of OECD, this meeting is organised by EDF and IPSN with the help of Coyne et Bellier and Freyssinet; yet I would emphasise the very efficient help of the World Association of Nuclear Operators network, without which it would not have been possible to obtain a so large international panel. I would also thank international scientific associations who sponsor this workshop, namely RILEM, FIP, and also IASMiRT although this is not a post-SMiRT conference.

However, in my mind, first people I have to thank are all the participants at this meeting who answered positively the invitation and accepted to discuss this item, which is very important for life duration or extension of NPP: Prestress losses in containments. During these two days, a delegate of a Utility of each attending country will give a lecture on its approach and its experience of the problem; we shall have opportunities of comparisons, exchanges, discussions about safety criteria, prestressing technology, monitoring and data treatment, non destructive methods and in situ walkdown, ageing management programs and results already obtained. As you know the particularity of this meeting is that are also invited Regulators of the country of a Utility presenting a contribution.

Post-tensioning is not a nuclear orientated technology; most of industrial applications are in the field of bridge construction, and most significant progress appeared in this field. Yet, despite a common technology, significant differences are observed between bridges and containments; the main one is obviously the thickness of the walls; another one is the relatively low level of prestresses in containments with a tendons capacity much higher than in bridges; we can also mention the elapsed time from pouring of concrete to tensioning. So it will certainly be very informative for all of us to follow the discussion with experts of bridge construction, which is scheduled today at the end of the afternoon. In particular we shall have information about experience of Freyssinet International which has operated tensioning of French nuclear containments.

In order also to present to you a large and useful information, we have invited two professors to give a lecture on the more recent evolution in the knowledge of creep and shrinkage of concrete:

- Professor Acker will present methods and results available from Laboratory experiments.

- Professor Bazant will present past, present, and tendency for future modelling of the phenomena.

The two State of the Art papers will open our first session; so I introduce now Professor Acker as our first speaker and I wish you a fruitful meeting in Civaux.

CREEP AND SHRINKAGE OF CONCRETE: PHYSICAL ORIGINS, PRACTICAL MEASUREMENTS

P. ACKER

Laboratoire Central des Ponts et Chaussées, Paris, FRANCE

ABSTRACT

Subcommittee 4 of RILEM TC 107-CSP has established recommendations for shrinkage and creep tests. These recommendations are based on physical and mechanical analysis of these tests, to ensure that they provide reproducible and objective results. But the complete specification of these tests must also make it possible to respond to diversified needs: in particular, industrial users (contractors, suppliers of materials, etc.) are increasingly led to request such tests, and the type of experimental data they expect can be quite different from what is expected by people who draft regulations or develop numerical models. Our paper therefore presents, in a first part, thinking about these needs, which are found to be highly varied and rapidly evolving. In a second part, we review the importance of the scale effect that makes it tricky to attempt any extrapolation of the available experimental results in two directions (to the long term and to large thicknesses). In the absence of a satisfactory explanation of this scale effect, a practical method is proposed that can be used to get round this difficulty experimentally and to deal with certain engineering problems.

Key words: Creep, Shrinkage, Concrete, Test, Recommendation, Cracking, Drying, Modelling.

1. INTRODUCTION

Concrete is by far (and for a long time still to come) the material most widely used in the world: the range of performance (physical and mechanical) it can provide continues to grow. At the same time, it is beginning to be possible to determine precisely the parameters of composition and production that best meet a "*specification*" of the material, i.e. a set of functional properties fixed or chosen by the designer. The industry will undoubtedly make more and more use of this mastery.

In this context, moreover, numerical simulation tools are destined to play a larger and larger role: no longer merely, as in the last step of design work, calculating quantities of steel, checking limit-state stresses, etc., but rather comparing different constructive solutions to one another, optimizing in a larger and larger "*solutions space*", and therefore using quantitative tools as early as possible in the design stage.

But it is clear today that there is still a substantial gap between the power and performance of the calculation programs, on the one hand, and the poverty, on the other, or low pertinence, of the laws and mathematical models put into these programs to describe the behaviour of the materials. What is most lacking in the engineer's toolbox today are constitutive laws that are pertinent, in the context of the structure, to the material being used. Here, the expression "*pertinence of the laws*" has a precise meaning: it means that the laws must reflect those aspects of the behaviour of the material that are specific to the type of structure. We shall give here a few examples:

- the choice of concrete and its formulation: mechanical strength is no longer the only criterion of choice of the material; today, various mechanical, and also physical and aesthetic, properties may be required, and this is true in an ever wider range; in some cases, a characteristic regarded as secondary can become basic to the mechanical behaviour of the structure (heat of hydration in concrete dams, for example) or to safety (permeability to gas of nuclear reactor containments, etc.); in the case of short- and intermediate-span bridges, the great variety of creep values observed in high-performance concretes has made this characteristic decisive in the choice of concretes for this type of structure; it will then be possible to settle for a mean creep coefficient, possibly completed by a function of the age of loading.
- innovation in constructive arrangements: this requires a clear understanding of local behaviour, in order to be able to situate the innovation objectively with respect to common practice; some regulation constructive details are imposed by the limitations of beam theory (concentrated forces, end and connecting zones, various singularities, etc.): in this case, a finite element calculation, in linear elasticity, will generally be sufficient; in other cases, they are related to physical phenomena (drying shrinkage, thermal expansions, etc.): it is clear that the justification must then take the physical phenomenon in question into account explicitly and describe its phenomenology (changes in time, gradients, etc.).
- the design of new structures: the introduction of new types of concrete or new techniques of construction should lead to the emergence of new structural designs; in this operation, the structural calculations can be finely interpreted and analyzed only if the physical meaning of each term of the constitutive law is explicit.
- checking the risk of early-age cracking: the stresses produced by the heat of cement hydration can be considered as resulting from competition between two separate kinetic processes: the hydration of cement and the diffusion of this heat towards the exterior, which depends to a great extent on the size of the elements and occurs in accordance with an invariate relationship of the form T/L^2 . On the other hand, hydration is a *thermoactivated* process and the kinetics of hydration does not remain uniform through the cross-section. This thermoactivation complies quite closely, at least in the range which concerns us, with the *ARRHENIUS* equation. This coupling has been accurately analyzed and current engineering models are able to predict, with sufficient accuracy for engineering purposes, the temperatures in large structures [TORRENTI, 95].
- checking the level of safety of a structure: in the current state of our knowledge, the failure process of a concrete structure can not be predicted directly by a simple and unique numerical calculation since it has been possible, in simple laboratory tests, to identify several mechanisms of failure, of which the characteristics depend, in a way still not adequately understood, on the type of loading and the size of the zone loaded; the only dependable approach, for the moment, involves in-depth analysis of pathological cases, supported by numerical simulations with various models of increasing complexity; the typical case is that of a structure having a complex geometry, for which a first, linear elastic, calculation serves to localize zones at risk and determine the type of risk, i.e. the system of loadings, which can then be reproduced in the boundary conditions of a partial, but more precise, simulation of the zone, etc.; an attempt will then be made to bracket the effects of creep; in the case of prestressed concrete, an upper bound or a lower bound of the losses of prestress will be used, according to the type of check.

- the diagnosis of damage and the choice of repair methods: even for the maintenance of structures, it is not sure that the best approach requires sophisticated models; according to our experience, the most important step, here too, is to identify the cause or mechanism that underlies the damage (this mechanism is always unique, as the practice of medical diagnosis shows, even if the damage only appears because it is amplified or triggered by a few concomitant factors): as long as this cause is not understood, it may, just, be possible to rehabilitate or strengthen the structure, but not to predict the response of the structure to this repair or its evolution; examples of inadequate repairs abound; here again, the physical approach will therefore be basic; especially since, in structures in service, the stress condition may have been extensively redistributed by the effects of shrinkage and creep.

2. THE CASE OF NUCLEAR REACTOR CONTAINMENTS

The question of the long-term behaviour of the containments of nuclear power plant is a safety problem the importance of which is obvious to everyone. But predicting this behaviour is delicate, because the material exhibits a paradoxical behaviour (PICKETT effect, see figure 1):

1. at constant humidity (drying, i.e. any exchange of water with the ambient medium, is stopped and one waits for hygrometric equilibrium before loading) and under a constant compression, in effect, the less evaporable water it contains the less it creeps; the strain obtained by this test is called *basic creep*;
2. at decreasing humidity (it then loses water during loading), it creeps more (a lot more) than if it had remained at the initial humidity; the strain obtained by this test is called *drying creep*.

In other words, the hygrometric conditions acts in opposite directions on the creep rates according to whether the water contents in the specimens are uniform or not.

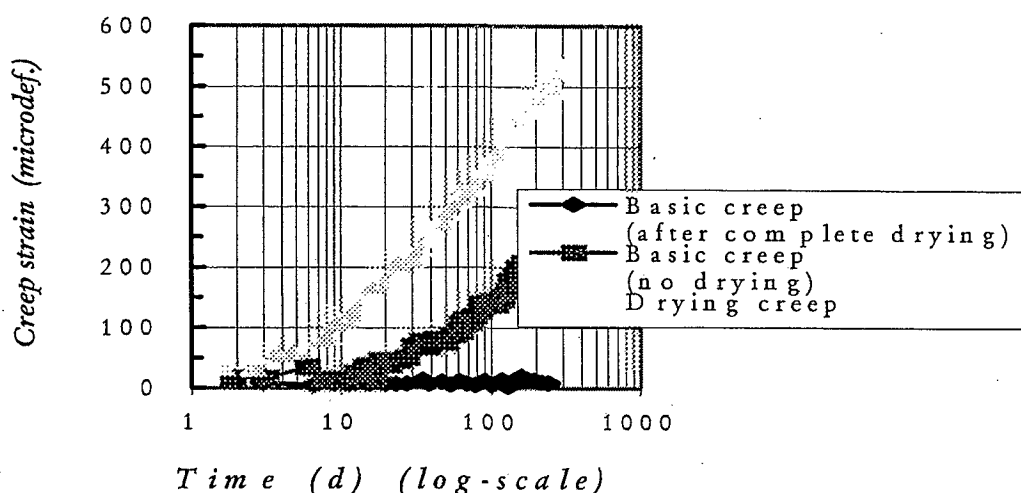


Fig.1. PICKETT's paradox: a previously dried concrete (\circ) exhibits practically no creep; in the case of a concrete in which any exchange of moisture during loading is prevented (basic creep), the more evaporable water it contains, the more it creeps (\square); on the other hand a concrete that dries during loading (drying creep) creeps even more (\triangle), although it changes gradually from the hydric state of (\square) to the hydric state of (\circ).

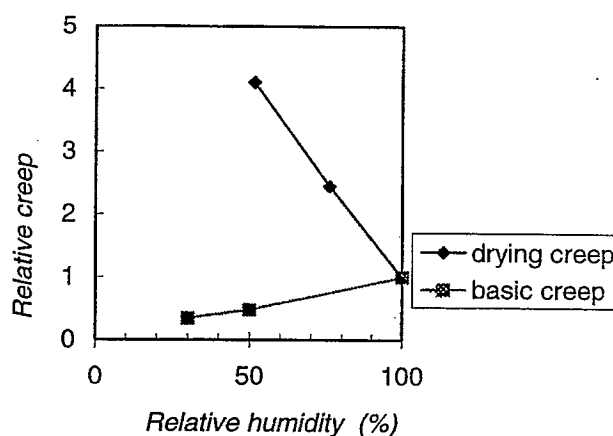


Fig. 2 : Long term creep under various hygral conditions.

For the moment, two theories coexist: one explains this by a structural effect involving the skin cracking of the shrinkage specimens (the "shrinkage" strains measured on a non-loaded control specimen are always subtracted from the experimental creep results: if this non-loaded specimen cracks under the effect of the self-stresses, the loaded specimen will crack less in proportion as it is loaded more, and its apparent strain will be so much larger) [WITTMANN 1980]; the other theory proposes that the creep rate depends not only on the water potential w , but also on the rate of variation of this potential, $\partial w / \partial t$ [BAZANT, 1982].

The first explanation is more attractive, on the physical and mechanical point of view, but it fails (at least with the description of the mechanical behaviour of the cracked zone available today) to explain more than 50 % of the difference in strain [THELANDERSSON, 1988]. The question therefore remains.

Now extrapolation to the long term of the experimental results (the longest creep tests do not exceed two or three years) is very different according to which theory is applied: in the former, the final strains will depend in particular on the degree of reversibility of the strains of the cracked zone (poorly known, but surely decreasing with the scale of the cracks, which leads to final strains that decrease as the thickness of concrete increases); in the second, the creep rates should tend to become uniform, independently of the size of the parts [GRANGER, 1993].

Whichever theory is applied, a precise analysis of these mechanisms here requires taking the humidity (or the evaporable water content) into account as a variable, and not as a parameter.

3. THREE PHYSICAL ORIGINS OF SHRINKAGE: CHEMICAL, THERMAL AND HYGRAL PROCESS

As a porous solid, the concrete is deformed as soon as it is subjected to mechanical, thermal, or hygral actions:

1. mechanical actions: external forces (concentrated or distributed) applied to the surface or in the volume (self weight) or displacements imposed by the boundary conditions (settlement of bearings, etc.); these actions will not be considered here;
2. thermal actions:
 - due to temperature variations applied at the surface . of natural origin (climate)

- . of industrial origin (thermal treatment used, for example, to accelerate the hardening of the material),
 - due to the heat produced in the mass of the concrete by the hydration of the cement (this effect is significant only in parts of some thickness, when the rate at which heat is given off is large with respect to the rate of diffusion towards the exterior);
3. hygral actions, because concrete is a *porous* material (with pores, between 10^{-6} and 10^{-9} m in size, in which the *capillary* tensions increase considerably as the largest pores are emptied, putting the solid skeleton in compression), it is therefore also subjected to strains that can result:
- from variations of the *external* humidity:
 - . of natural origin (hygral –and thermal– variations),
 - . of industrial origin (form removal, steam curing or dry heat treatment),
 - from inputs of water:
 - . of natural origin (rain),
 - . of industrial origin (curing by water spray or by soaked burlap),
 - from variations of the *internal* humidity (selfdesiccation due to the hydration of the cement).

Mechanical effects of thermal or hygral origin are often large and may, in some structures, largely predominate over strictly mechanical actions (dams or foundation blocks for thermal effects, nuclear reactor containments, concrete pavements for hygral effects, etc.), especially at early age.

Hygral actions, like thermal actions, result either from variations of ambient conditions –which generate *flows* (respectively of heat or water) and in consequence *gradients* (respectively of temperature or hygral potential)–, or from an internal source (such as the heat produced by the hydration of the cement) or from an internal sink (such as the self-desiccation that results from the continuation of hydration after setting) - which also engenders a loss of equilibrium with the ambient medium, and therefore flows and gradients. The strains that result are therefore never uniform, engendering structural effects and stresses. For a temperature field that is not plane (*i.e.*, in a cross section, a nonlinear function of the spatial co-ordinates), the mechanical effects can be broken down into two components:

- a **plane strain**, which itself includes:
 - a mean elongation or (more often in the case of concrete) shortening, obtained by calculating the mean value, over the section, of the imposed strain;
 - when the imposed field is not symmetrical, a rotation, obtained simply by writing the equality of its moments with those of the true field;
- a **field of eigenstresses**, obtained by difference between the true field and the equivalent linear field, defined and calculated as above.

The same breakdown into three terms (apparent shrinkage, bending strain, and system of eigenstresses) applies, of course, to hygral actions.

Climate-related thermal actions are basically cyclic, and their long-term mechanical effects are therefore related primarily to the difference between the initial temperature and the *mean* temperature of the place where the structure is located. Hygral actions are also cyclic, but drying is 1,000 to 10,000 times slower than cooling, and in consequence the effect of these actions on long-term behaviour is insensitive to short cycles and will be related primarily to the mean humidities of the driest periods of the year.

3.1 Relevant characteristics and properties of the material

Finally, apart from strictly mechanical effects (which are not described here), the engineer, to understand, analyze, and quantify all these effects, needs information about the following four elements:

1. for the mechanical effects of temperature variations: the values of the thermal transfer and exchange coefficients, of the coefficient of thermal expansion (CTE), and of the E-modulus of the concrete with, in some cases, its law of evolution in time;
2. to describe the thermal effects of the hydration of the cement: the foregoing parameters, but also, and especially, the law that describes the evolution of heat in the course of hydration (which must replicate the phenomenon of *thermo-activation*);
3. for hygral effects, one must, by contrast, make do with *macroscopic* data, because the processes of drying and drying shrinkage are today less well known and, especially, less well modelled than the thermal effects: it is still not known, for example, how to determine experimentally the coefficient of *hygral* contraction (the analogue, for the strains and stresses due to drying, of the CTE), because it is impossible to dry a concrete specimen, however small, without cracking it; these *macroscopic* data are the following:

- for hygral effects related to hydration: the law of evolution of the shrinkage recorded in the absence of any hygral exchange with the ambient medium. On relatively small specimens, the temperature rise due to the hydration of the cement remains very small and can be corrected; this gives the *autogenous shrinkage*, which is uniform (at least starting from a certain scale, of the order of five times that of the coarsest aggregate: this is the scale on which concrete, a granular material, can be regarded as homogeneous); autogenous shrinkage is therefore independent of the size of the specimen; it is an *intrinsic* characteristic of the material;
- for hygral effects related to climate: the law of evolution of shrinkage under ambient conditions representative of natural drying (however, these conditions are still more or less *conventional*, most often constant involving temperature and humidity); moreover, this law must be parameterized by a quantity which *characterizes the dimension that controls the kinetics of drying* of the specimen; this gives the *drying shrinkage*, which depends on the size of the part and is therefore not an *intrinsic* characteristic of the material.

3.2 Common values, factors of influence, determination of these characteristics

E-modulus

The E-modulus of the concrete acts in all structures that are subjected to boundary conditions of displacements that are more or less prevented. This function is further amplified when these conditions apply from a very young age (pavements, dams, concrete slabs of composite structures, massive parts poured in successive layers). The E-modulus, in effect, evolves substantially with the hardening of the material and, like the mechanical strengths, it increases continually from zero to a value near its service value (fig. 3).

The scale of this change is an indication of important internal modifications and cannot simply be explained by the amount of additional solid material, even if all the added material were connected and contributed to the stiffness of the material.

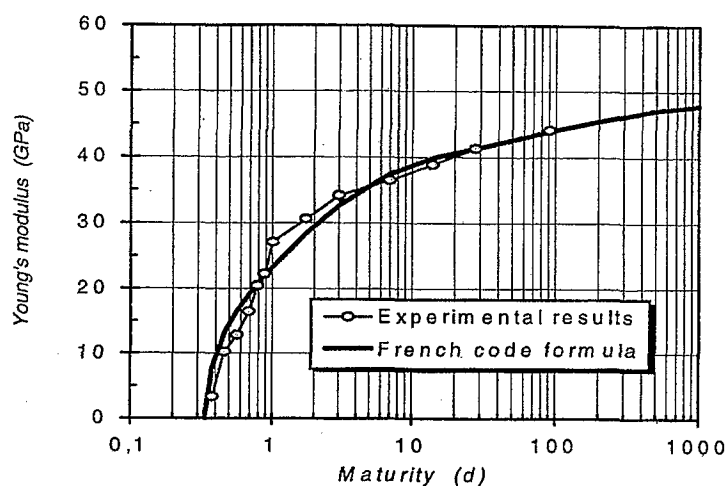


Fig. 3 : *Change in Young's modulus with the age of concrete.*

Furthermore, the kinetics of this hardening is highly activated by heat. Like many chemical reactions, the kinetics of hydration is rather well described by the *ARRHENIUS* equation. The modulus can therefore be regarded, like the compressive strength, as a monotonically increasing continuous function of the *maturity* of the concrete, this maturity being defined as the (theoretical) age at which, if the material had been kept at a constant *reference* temperature T_0 , the modulus would have reached the same value as it actually reached under the true conditions of a temperature $T(t)$ that may in fact vary. In the context of the *ARRHENIUS* equation, the maturity is written as follows:

$$\mu = \int_0^t \exp\left(\frac{k}{T_0} - \frac{k}{T(\tau)}\right) d\tau$$

where k is a constant of the material and T the absolute temperature. For an ordinary Portland cement, k is of the order of 5,000 K, which means that the rate of hardening of the concrete doubles every 12 or 13 degrees [BRESSION, 1982]; [ACKER, 1988].

The most effective way to act on the E-modulus is to choose the aggregates according to their specific modulus, first because the aggregates influence the modulus of the composite more than does the cement matrix, but also because there is generally less freedom to alter the parameters that vary the modulus of the cement paste, because of their effect on the mechanical strength, fixed elsewhere.

Calorific and thermal characteristics of the concrete

The coefficient of thermal expansion (CTE) plays an important role in parts that are subjected to conditions of blocked displacement and are also either thick (like dams) or exposed to large temperature variations (like pavements). Like the E-modulus, and for the same reasons of volumetric ratios, the CTE of concrete depends more on that of the aggregates than on that of the cement paste. Its value can range from 6 or $7 \cdot 10^{-6}$ for a concrete with calcareous aggregates to 12 or $13 \cdot 10^{-6}$ for a concrete with all siliceous aggregates. This is why, in concrete pavements, preference is often given to calcareous aggregates, but not to those that have too high an E-modulus (the stresses are proportional to the product of the two characteristics).

On the other hand, unlike the E-modulus, the CTE is practically constant from the first hours following setting. The *ARRHENIUS* equation can in fact be used, in the experiment, to separate autogenous shrinkage and thermal strain, to show that these two strains are additive and that the CTE is, at the end of a few hours, constant. For this, it suffices to record the strains of two identical specimens, kept under two different thermal conditions (for example isothermal and

quasi-adiabatic); calculating the maturity and plotting the curve that expresses the difference, at equal maturity, between the two measured strains and the difference of the two temperatures at this same maturity [LAPLANTE, 94].

Fig.4 shows a plot of strain difference against temperature difference for two identical samples of the same maturity preserved under different conditions of insulation. This line, of which the slope represents a coefficient of thermal expansion (CTE), has a steep gradient before setting because of the CTE of water ($50 \cdot 10^{-6} \text{ K}^{-1}$) which is significantly higher than that of aggregates (6 to $12 \cdot 10^{-6}$) and that of cement paste (12 to $14 \cdot 10^{-6}$). After setting it can be seen that the CTE of the concrete remains constant, which is what one would expect for a non-saturated porous material: more accurately, the expansion of unbound water displaces the liquid-vapour interface towards the larger pores. This displacement can be seen, on the pore size spectrum, as an extension of the surface area corresponding to saturated pores: in increase of 100 degrees results in a 0.5 % increase in this surface area, which corresponds to only a slight increase in the radius of the menisci, therefore to a very small hygral disequilibrium. There is thus one less coupling (in fact, there is a coupling, but when identified and thoroughly analyzed it is reduced to an ordinary effect which must be corrected for).

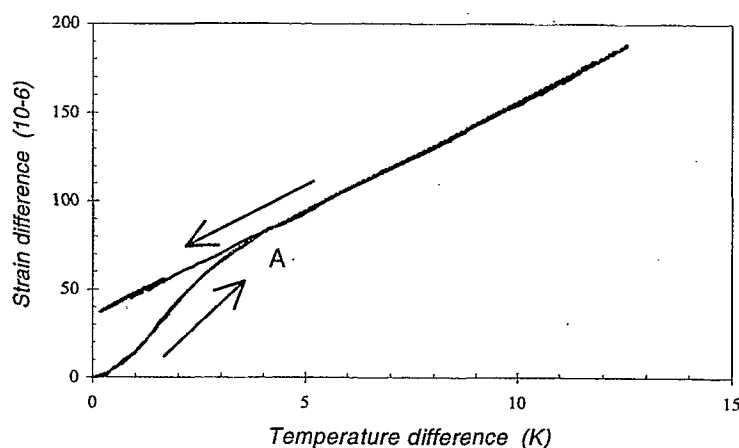


Fig.4: Strain difference, at the same level of maturity, between two samples subjected to different thermal histories (respectively quasi-adiabatic and quasi-isothermal) according to the difference between their temperatures at the same maturity. The gradient of this line represents a coefficient of thermal expansion and the point A corresponds to a maturity of 12 hours, which is the end of setting [LAPLANTE, 94].

The (higher) value observed up to about 16 h (explained by the contribution of the liquid phase, since water has a much higher CTE) has no mechanical consequence, because of the very low value of the E-modulus in this (short) period.

The exchange and heat transfer coefficients can be regarded, in most cases, as constant in the course of hardening, as can the specific heat of the material [BASTIAN, 1995].

Hydration heat of the cement

The hydration heat of the cement is an important factor in massive parts (dams, foundation blocks) but also, when they are subjected to boundary conditions of blocked displacement (pavements, concrete slabs of composite structures), in structures of more modest thickness (as little as 20 cm, when one side is thermally insulated). In these two types of structures, the effects of thermal shrinkage are superposed on those of autogenous shrinkage (concretes that have a high hydration heat are also often those that have a high autogenous shrinkage, such as, in many cases, high-strength concretes). The hydration heat depends on the chemical composition of the cement - it increases with the C_3A content - and on the fineness of grinding. It can be measured, in particular

by a standardized test (the LANGAVANT bottle test), which consists of recording, under semi-adiabatic conditions, the temperature rise of a standardized mortar as it sets. Depending on the cement, the total quantity of heat given off is between 150 and 450 Joules per gram of cement. This heat is not produced instantaneously, but in several hours, with one, sometimes two, peaks and a long period of decrease, characteristic of the evolution of the material, that becomes slower and slower, but can remain significant in the very long term (hardening due to the existence of a layer of hydrates, increasingly thick and compact, that coats the grains of anhydrous cement).

For the moment, it is not known how to predict which happens in a concrete from only the hydration heat characteristics of the cement. It is found simply that the total heat given off in the concrete often increases faster, relatively, than the proportion of cement. It is known, on the other hand, how to characterize the concrete, using a test that consists of recording the temperature rise in a specimen placed under *quasi-adiabatic* conditions. The curve so obtained constitutes, in the context of the ARRHENIUS equation, an expression of the law of behaviour of the material. It in fact makes it possible, via a transformation that uses the ARRHENIUS equation, to predict the heat given off (and therefore the temperature, the strain, and the thermomechanical characteristics) under any conditions. This makes it possible to calculate, by including this law in the data of a finite-element calculation program, the temperature field that results in a structure. This calculation is coupled with the diffusion (in the vicinity of the surface, for example, which is cooled by the external temperature, the evolution of heat is slowed, and so lasts longer; the slower growth of the modulus and strength in these zones is also reproduced by the model). This type of calculation is today operational, extensively validated by a large number of applications that have served to confirm, by *in situ* measurements, the predicted values, and is used systematically for exceptional structures or structures having zones *at risk of thermal cracking*.

The experience acquired at sites clearly shows that, as long as the thickness of concrete remains less than 30 cm (or 20 when only one side is cooled), thermal effects are zero or very small. Conversely, as soon as there is a zone of concrete more than 50 cm from the nearest cooled surface, the temperature of the concrete there will rise by 30 to 50 degrees (even 55 with high-performance cement in large proportions), and cracking in the course of cooling is then practically inevitable. Recent observations on sites where high-performance concretes are used - they often exhibit higher hydration heats, but also a faster kinetics of evolution than conventional concretes - show, however, that it is possible, with HP concretes, to have non-negligible thermal effects at thicknesses of less than 30 cm.

Thermal shrinkage can therefore reach, according to the proportion and type of cement, 400 to 500×10^{-6} at the core of the parts as soon as the thickness exceeds a certain value. The kinetics of this shrinkage is simple: it starts with the end of setting (the maximum temperature is reached between 20 and 40 h), and the duration of the cooling (an exponential decay) is proportional to the square of the thickness (the mean temperature is divided by two, for a slab 20 centimetres thick ventilated on both sides, every hour).

Thermal cracking can be of two types:

- either skin cracking (as in continuously-poured foundation blocks, joists, or segments on piers), due in this case to the local gradient; this skin cracking is however rarely very open because the distance between consecutive main cracks is of the order of the depth of the zone in tension, which can not exceed a quarter of the thickness;
- or, in the case of concreting joints (thick shell poured in successive layers) or of end-fixing (dam, shell fixed on a foundation block or on a strip footing, pavement on rigid layer or soil), localized cracking, which can then be much more widely spaced (on "CRC" - continuously-reinforced concrete - pavements, distances between cracks greater than 50 m have been observed) and therefore much more open. The spacing between cracks can thus be quite variable (the range of distances observed on structures is from a few centimetres to a few tens

of metres) and the large *span* of crack openings observed is therefore in fact linked to the capital function of the mechanical boundary conditions of the structure, much more than to the thermal and mechanical parameters of the material.

3.3 Autogenous shrinkage

The hydration of cement continues long after setting, as shown by the evolution, sometimes not negligible, of the mechanical characteristics of the concrete in the long term. But it consumes a relatively small share (except in HP concretes) of the mixing water of the concrete: 15 to 20 litres per 100 kg of cement, or less than half of the initial water in an ordinary concrete. This is the main reason for the very high porosity of ordinary concretes: 8 to 16 % of the total volume, which is 20 to 50 % of the volume of the binding paste.

Furthermore, and in spite of this excess water, the continuation of the hydration leads, from the start of setting, to drying within the material (called *self-desiccation* to distinguish it from "*drying*", which means drying with loss of water to the exterior), simply because the reduction of volume by water consumption is only partially offset by the increase of volume of solid matter. The volumetric balance shows a deficit of the order of 10 % of the volume of hydrates formed. This reduction of the relative volume occupied by the liquid phase in the pore space therefore leads, like drying, to a strain of the mineral matrix. Noting that pressurizing a fluid that filled the pores would cause an apparent swelling, it can be seen that, conversely, the tensions in the liquid phase (which follow, precisely, the laws of surface tension, up to pore sizes of a few nanometres [CRASSOUS, 1993]) cause a contraction of the matrix, called shrinkage. The effect of the capillary tension on the mineral matrix clearly prevails over the other mechanical effects, and is therefore in fact the origin of hygral shrinkage [HUA, 1994].

However, autogenous shrinkage remains less than 10^{-4} in concretes of which the W/C ratio is greater than 0.45, but it increases quickly when this ratio falls below 0.40, and can reach 3×10^{-4} (fig. 5). This is simply an effect of pore size: the tensions in the liquid phase (which engender a compression of the mineral matrix) vary inversely with the pore size at the interface with the gaseous phase. The time law of evolution of this strain is directly related to the kinetics of hydration of the cement, which also controls the evolution of the mechanical strength values of the concrete, and the parameters that influence this kinetics are therefore the same ones that act on the

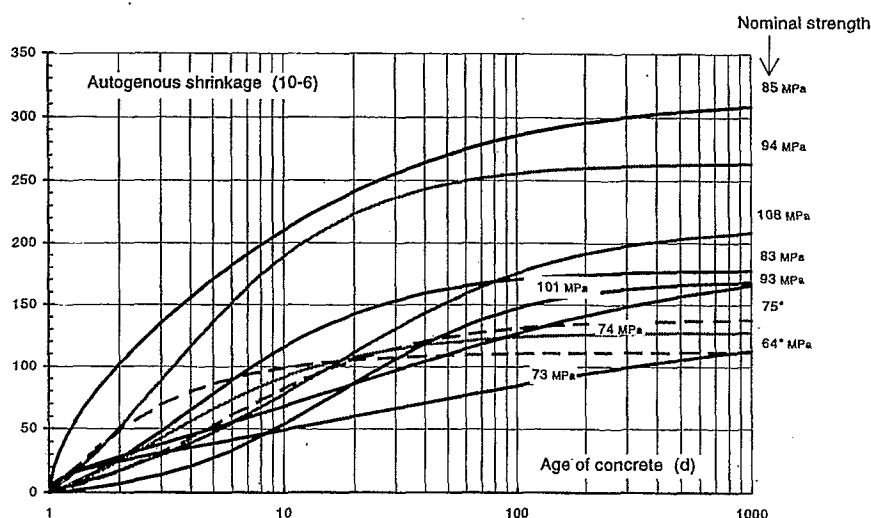


Fig.5: Autogenous shrinkage over time for various concretes [LE ROY, 96].

rate of growth of the strength values: type and fineness of cement first of all, then the W/C ratio. The curve of evolution of the autogenous shrinkage therefore rather closely matches the evolution of the mechanical strengths: very fast in the first few days, reaching 60 to 90 % at 28 days. The total intensity of the autogenous shrinkage remains moderate, but may, when added to the other shrinkages, be non-negligible: 100 to 300 $\times 10^{-6}$. The rate of its evolution at early age is such that this shrinkage was long overlooked by practitioners, because the conventional shrinkage tests - at least those used to determine the laws cited in design rules (originally, basically for the purpose of estimating losses of prestress) - started at 48 h or at 3 days.

Because hydration is generally accompanied by a reduction of the hygrometric unbalance with the ambient medium (except for high-performance concretes with very low W/C ratios), this does not activate any diffusion process, and therefore gradient, and autogenous shrinkage is basically an intrinsic phenomenon, which can nearly always be regarded as uniform in the volume of a part, at least within a zone corresponding to a single concreting operation (in the case of concreting joints, it is the phase shift of the kinetics that engenders mechanical effects). That means that in a precast part, or one poured in only one phase or continuously, and not blocked by its bearings or its formwork, this shrinkage has no mechanical effect.

On the other hand, when the shrinkage is prevented, or even merely restrained, from the start of setting (continuous rigid support, fixed bearings, concreting joint, etc.), it often constitutes a non-negligible component (often overlooked) of the early cracking. It must be recalled that, under conditions of total restraint (as in the *cracking frame* test, for example, used to evaluate pavement concrete recipes in terms of cracking risks), the specimen always ends by breaking, even in the absence of any drying and temperature rise, which means that, in spite of the relaxation of the stresses (even though this phenomenon is particularly rapid at early age), the stresses due to autogenous shrinkage alone quickly reach values equal to the tensile strength of the material.

3.4 Drying shrinkage

The drying process does not start until form removal (except on the side without formwork, which because of this is very sensitive to early drying, and so requires an appropriate treatment: *curing*). Two cracking modes can occur. The first mode, which occurs only in the very first hours (a period all the shorter in that self-desiccation is large) corresponds to the domain of water contents for which the liquid phase is still contiguous, and is reflected by cracks that are rather shallow and irregular, limited to the upper surface of the concrete. The second mode results from long-term drying; this process is extremely slow - 10 years for a specimen 16 cm in diameter or for a shell 12 cm thick - and its duration increases with the square of this thickness. Beyond a thickness of 50 cm, the duration of drying is counted in centuries! In massive parts, the duration of drying often exceeds the specified life and, for the engineer, the "final" amplitude is then much less important than the rate of evolution. The cracks that result appear much later, they are straighter and are oriented by the geometry of the structure (the boundary conditions), and their opening evolves very slowly.

By contrast with self-desiccation shrinkage, the kinetics of this shrinkage does not reflect that of the mechanism that causes it, within the material, but reflects the spread within the structure of the phenomenon that engenders it: the degree of drying varies across the thickness of the part (this applies during most of the transient phase) between its maximum value (at the surface) and its minimum value (at the core), and the apparent shrinkage is therefore related to the *mean value* of this degree in the volume: the calculation of this mean involves only the final value and the *shape* of the spatial distribution in the cross section...

In fact, the slowness of the process also indicates the importance of the gradients that develop in the first phase of the process, which produce *eigenstresses* known to lead to shallow cracking of the structures, but also of the specimens used to measure this shrinkage. The strains measured on these

specimens are substantially affected and reduced by this cracking (which depends significantly on size and geometry), and drying shrinkage is therefore only an apparent mechanism. It must accordingly be borne in mind that these values include skin cracking (which does not always exist in the actual structures, because of compressions of mechanical origin, such as prestressing, in particular).

For a slab of which one side is protected from drying, the drying gradient must be taken into account: depending on the mechanical boundary conditions, the slab will have a spherical strain of its midplane or, if this curvature is prevented, a stress gradient with the maximum tensions in the skin.

The apparent drying shrinkages, so measured, vary between 2 and 6×10^{-4} , and depend on many parameters, which are, in order of decreasing influence:

- the thickness of the part (the drying of a slab having one tight surface is comparable, in its kinetics, to that of a slab of twice the thickness, but not in its mechanical effects: if nothing opposes the bending of the slab, this bending reduces the cracking and, to a lesser extent, the apparent shrinkage),
- the porosity, or the free water content of the concrete ($e - \alpha c$, where αc is the volume of water consumed by the hydration of the cement),
- the volume of paste $e + c$
- the fineness of the binder (of its finest component, which is either the cement, or, if there is any, an ultrafine addition, the global effect of which, unlike that on autogenous shrinkage, is to substantially reduce this shrinkage, because of the drastic reduction of the initial water content to which the use of these additions leads).

4. THE ORIGIN OF CREEP

The first observation is the importance of the viscous component in the behaviour of concrete. The strain which is produced in the course of a creep test, for example, (after subtracting shrinkage) at the end of loading may be 3 or 4 times greater than the initial (elastic) strain, which is utterly exceptional for a mineral. The role of water content is very important here and is paradoxical: if tests are conducted in which there is no exchange of water with the ambient environment (*basic creep*) the lower the evaporable water content of the sample the lower the creep, to the extent that it can become negligible. However, if the tests are conducted in a dry atmosphere, the greater the drying the greater the creep - up to five times more than the basic creep of the concrete with the highest water content (Fig. 2). Water therefore plays a central role in this area [ACKER, 1988].

The water content of concrete plays an essential role in creep: concrete which has dried to the state where evaporable water has been totally eliminated is not subject to creep. Two mechanisms are apparent from kinetic analysis of basic creep for a pure paste which is completely protected from desiccation (Fig. 6), and both are compatible with the mobility of water. In the case of the first (with a characteristic time of the order of 10 days), the front moves towards the largest diameter pores (characteristic distance of the order of 0.1 to 1 mm) which changes the hygral equilibrium in the gas filled space and generates strain which is the short term component of creep. The activation energy of this first mechanism could be that of permeation in the saturated capillary pores [ULM, 1997].

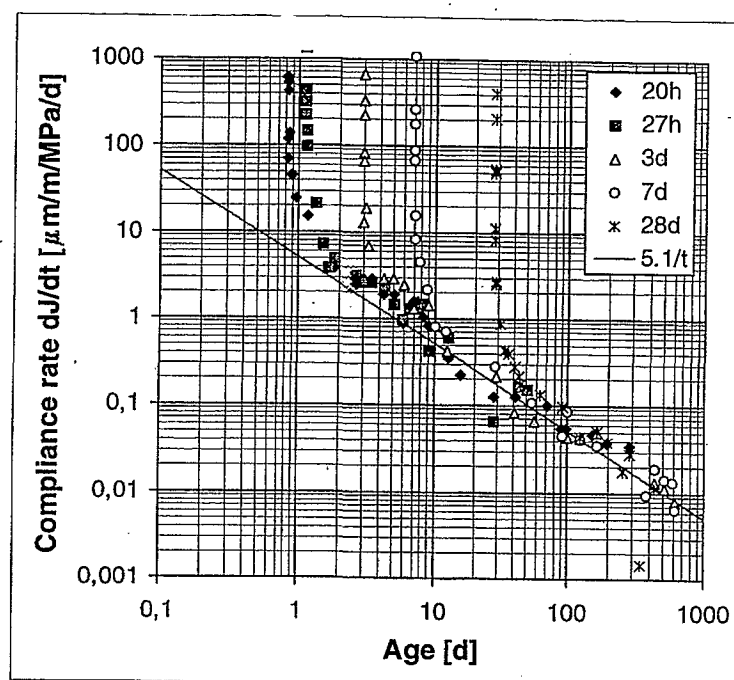


Fig.6: Rate of viscous flow in the course of a number of loaded creep tests at different ages: after a phase of rapid decrease it can be observed that the rates are solely dependent on the age of the material [ULM, 1997].

The second mechanism corresponds to non-reversible viscoplastic behaviour and would seem to be more related to viscous flow in the hydrates (slippage between layers which is increasingly inhibited over time, particularly if the hydrates start to lose water).

5. SIZE EFFECT OR STRUCTURAL EFFECT ?

A recurrent question with concrete is that of the size effect. For the physicist, a size effect is most often only a secondary phenomenon, which he has difficulty eliminating from his tests, or that systematically biases the measurements he makes on real objects, but generally does not prevent study of the main physical phenomenon he is seeking, first and foremost, to understand and describe: he generates explanatory models (i.e. at first qualitative). If, exceptionally, he wishes to quantify a size effect as such, it will be, for example, to reveal the fractal character of an object (which describes nothing more, it should be noted, than the geometry of its structure, but constitutes even so one of the possible explanations of a scale effect). For the engineer, the situation is somewhat different: he must decide, and for that he calculates, dimensions, checks that the stresses nowhere exceed certain values, etc.; he therefore needs quantitative models. And in these models, the consequences of size effects must remain moderate and, most important of all, bounded.

Laboratory experiments have two practical limitations: one concerns the size of the test object, the scale of the structural elements tested, the size of the specimens of material; and the other the duration of the tests and the age of the material. For the material concrete, different mechanisms (continuation in the very long term of the hydration of the cement, therefore of the hardening of the concrete, slowness of drying and of the resulting structural effect) make the influence of the size of the parts and the age of the material large. Analysis and checking of the safety of the structures, evaluation of their life, and management of their maintenance therefore call for two

types of extrapolations of the available experimental data: extrapolation of the laws of evolution to the long term, and extrapolation of the scale laws to large thicknesses.

Except in cases (rare) where exchanges of moisture are prevented, the shrinkage and creep of concrete are greatly affected by the size of the parts, because they are linked to the drying of the material, the duration of which varies roughly as the inverse of the square of the thickness (in practice, between the wire netting elements of some types of bridges and dams, the thicknesses range from a few centimetres to tens of metres, and the corresponding drying times span four orders of magnitude!). It then ceases to be sure that the ultimate values will be identical (especially since they cannot be determined, without extrapolation, by experiment).

Quantitatively, therefore, it is impossible to speak of a secondary effect.

Naturally, these extrapolations are based on physical laws (of diffusion) that relate the durations to the square of the thicknesses. But two findings restrict the scope of these laws:

1. depending on the water content, the movements of water are primarily in the liquid phase (DARCY type) or primarily in the gaseous phase (FICK type), with a very gradual transition from one to the other [ACKER, 1992];
2. skin cracking, which is probably very important in shrinkage tests, is very different in creep tests.

In these conditions, it is possible to wonder whether providing models, or constitutive laws, parameterized by the size of the parts and the mean ambient humidity meets all the current needs of the engineer. These laws are effectively very useful for checks of the global behaviour of structures (the evaluation of losses of prestress, in particular, for which they were developed and are, moreover, satisfactory), but say nothing about local behaviour, in particular skin cracking, and yet better mastery of this behaviour would be appreciated.

Consider the case of a massive structure. Typically 1 metre thick, which is not rare in large civil engineering structures. Laboratory tests have clearly shown that drying acts for a long time only to a small depth, and that the difference in stresses between the core and the skin of the concrete can be considerable [ACKER, 1990]. In these structures, this has two consequences:

1. the skin stresses are not representative of the mean stresses and analysis of them by strain measurements or the interpretation of cracking can lead to substantial errors;
2. calculations that do not take this effect of drying into account can not be used for the analysis of non-through cracking of the concrete, nor for the determination of skin reinforcements.

Should we not also attempt to provide engineers models that could help them to deal with these questions ? This calls for the development of constitutive laws in which the water content is a variable.

6. THE RILEM CREEP TEST

The RILEM draft recommendation for the creep test of concrete is based on three basic ideas:

1. the choice of slender cylindrical specimens to eliminate edge effects, especially large in tests of drying shrinkage;
2. the possibility of reconstituting, over a rather long period, the behaviour of a massive part from the experimental data obtained with and without drying, respectively;

3. the utility of being able to perform quasi-instantaneous loading.

6.1 Slender cylindrical specimens

Theoretical analyses [WITTMANN, 1980] and experimental analyses [ABDUNUR, 1989] of creep and drying shrinkage tests have clearly shown the importance of the heterogeneity of water content within the specimens during almost the whole duration of these tests. In addition to the fact that, near the ends of the specimen, the water content fields are affected by the edge effect (which can be eliminated by sealing the ends), it is clear that the sections cease to be plane in this zone (even with this sealing). It is therefore important that the longitudinal strains be measured only in the central part, between two right sections more than 1.5 diameter from the ends, according to SAINT-VENANT.

Furthermore, in the case of shrinkage, it is known that the zone near the surface is located, by reference to direct tensile tests performed at imposed strain, beyond the stress peak, and it is nearly certain that the specimens are cracked on the perimeter. If there is cracking, it may be amplified in a specimen having a square section, because of stress concentration near the edge. This leads to preferring specimens having a circular section. Another advantage of the latter is to allow a more powerful numerical simulation (axisymmetrical calculation).

Moreover, it is clear that if the depth of this cracking is large, it can be affected by the edge effect over a length greater than one specimen diameter. For drying shrinkage, it is therefore prudent to measure the strains on a base more than one specimen diameter from the ends.

6.2 Combine tests with and without drying

In structures of medium and large thickness, drying is a relatively shallow phenomenon for a very long time. For a concrete of average strength (and thus permeability), the depth affected at the end of 15 years is less than 20 cm. Now all the tests show a large difference, both in shrinkage and in creep, between the behaviours that occur during drying and those that occur in the absence of any exchange of moisture.

In these conditions, the question the engineer faces is: is it more realistic to model the behaviour of the structure by extrapolation from experimental results obtained on small specimens (by statistical regression on the thickness parameter) or to treat the structure as a multi-layer composite? In this latter approach, the internal layer, at least up to a certain age (an age that can be estimated from the square of the thickness), is exposed to the conditions of tests without drying, while both surface layers experience conditions close to those of tests with drying. It should be noted that this latter approach also provides information about the transverse distribution of the stresses in the structure.

Such an approach can not, of course, solve all problems, and remains to be extended and validated. But in the absence of a quantitative explanation of PICKETT's paradox, it can already be used to deal pertinently with some problems.

Finally, the (small) section of the specimens tested makes it possible to hold that the experimental shrinkage and creep values obtained under these two extreme conditions bracket the behaviours in service.

6.3 Quasi-instantaneous loading

Current technology makes it possible, either with the oil-air accumulator or by electronic servocontrol, to perform quasi-instantaneous loading of the specimen (non-instantaneous however to avoid dynamic effects in the apparatus and in the specimen). The record of the applied force and

of the strain of the specimen in the course of loading shows that the initial creep rate is not infinite and allows fine separation of the instantaneous and delayed strains of the specimen (Fig.7).

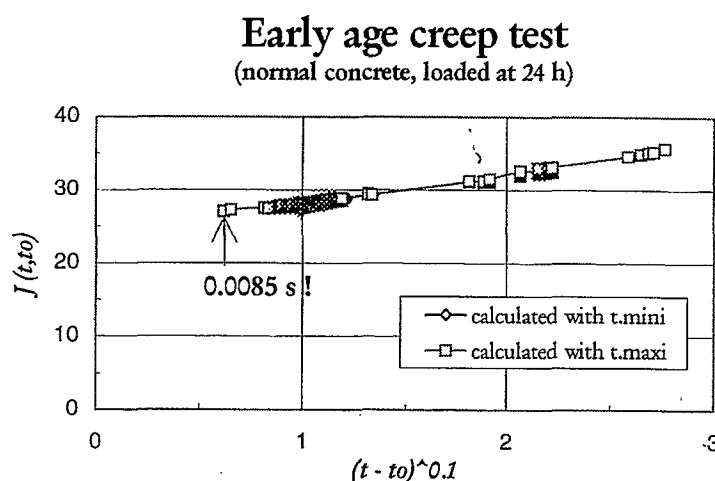


Fig.7: Creep strain measured until a few microseconds with a loading frame equipped by a flat jack and an oil-air accumulator separated by a valve allowing an quasi instantaneous loading.

The first benefit of this procedure is to eliminate any need for correction (always difficult to standardize and to make objective) of the start of the test. Moreover, such a correction requires choosing a constitutive law, which may contradict the very objective of the tests.

The second benefit is to be able to provide the value of the instantaneous strain modulus of the material measured under the same conditions as the creep. This measurement (which will probably be systematically different from those made in accordance with recommendations specific to this property) makes it possible:

1. to detect a loading anomaly, if the value found is too far from the measured or estimated value of the modulus;
2. to eliminate the experimental fluctuations on the value of the force actually applied to the specimens of a given series;
3. to better interpret the creep results (some atypical values are due to the aggregates, and this should be apparent in the modulus).

Of course, the possibility of providing the instantaneous strain in no way alters the requirement of providing the experimental results, and above all the models, in terms of total strains [BAZANT, 1988].

7. CONCLUSIONS

Creep tests of concrete must be rigorously standardized, because creep is a major fact of the mechanical behaviour of the material, depends on many factors, and is very sensitive to the conditions of preservation. The need to establish robust and usable data bases leads to fixing a certain number of the parameters of the test. However, the various uses engineers can make of it, and the type of results they need, may be quite varied.

The recommendations for such a test must therefore be both precise and suited to the variety of engineering needs today. The draft of subcommittee RILEM TC 107-CSP has been prepared in this spirit. Many questions are still unanswered, in particular the question of the PICKETT effect.

8. REFERENCES

- ABDUNUR C., ACKER P., MIAO B. (1989) *Superficial Shrinkage of Concrete: Evaluation and Modeling*, in Proceedings IABSE Symposium on Durability of Structures, LISBON, p.157-162.
- ACKER P. (1988) *Comportement mécanique du béton : apports de l'approche physicochimique*, Rapport de recherche des LPC n°152, LCPC, Paris, 120 p.
- ACKER P., MAMILLAN M., MIAO B. (1990) *Drying and Shrinkage of Concrete: The case of Massive Parts*, in *Serviceability and Durability of Construction Materials* (Ed. B.A. SUPRENANT), ASCE, NEW YORK, p.1072-81.
- ACKER P., MORANVILLE-REGOURD M. (1992) *Physicochemical Mechanisms of Concrete Cracking*, in *Materials Science of Concrete II* (Ed. J.P. SKALNY), AMERICAN CERAMIC SOCIETY, p.149-183.
- ASTM (1987) *Standard Test Method for Creep of Concrete in Compression* (designation: C512-87).
- BASTIAN G., KHELIDJ A. (1995) *Propriétés thermophysiques d'un béton fraîchement coulé*, BULL. LIAISON LABO. P. et Ch, n°200, nov.-déc., p.25-35.
- BAROGHEL BOUNY V. (1996) *Texture and moisture properties of ordinary and high-performance cementitious materials*, in *Béton, du matériau à la structure*, Proceedings of RILEM Symposium.
- BAZANT Z.P., RAFTSHOL W.J. (1982) *Effect of Cracking in Drying and Shrinkage Specimens*, CEMENT AND CONCRETE RESEARCH, Vol.12, p.209-226.
- BAZANT Z.P. (1986) *Material Models for Structural Creep Analysis*, Fourth RILEM International Symposium on Creep and Shrinkage of Concrete: Mathematical Modeling, Chapter 2, NORTHWESTERN UNIVERSITY, USA.
- BAZANT Z.P., WITTMANN F.H., KIM J.K., ALOU F. (1987) *Statistical Extrapolation of Shrinkage Data — Part I: Regression*, ACI MATERIALS JOURNAL, Vol.34, p.20-34.
- BAZANT, Z.P. (1988) *Mathematical Modeling of Creep and Shrinkage of Concrete*, JOHN WILEY & Sons, LONDON.
- BAZANT Z.P., CAROL I. (1993), *Creep and shrinkage of concrete*, E & FN SPON, 934 p.
- BOULAY C., PATIÈS C. (1993) *Mesure des déformations du béton au jeune âge*, MATERIALS & STRUCTURES, Vol.26, n°159, Juin, p.308-314.
- BRESSON J. (1982) *La prévision des résistances des produits en béton*, Proc. Colloque International RILEM sur le Béton jeune, Vol.1, Editions AENPC, Paris, p.111-115.
- COUSSY O. (1995) *Mechanics of porous continua*, John Wiley & Sons, 455 p.
- CRASSOUS J., CHARLAIX E., GAYVALLET H., LOUBET J.L. (1993) *Experimental Study of a Nanometric Liquid Bridge with a Surface Force Apparatus*, LANGMUIR, Vol.9, N°8, p.1995-1998.
- GRANGER L., TORRENTI J.M., ITHURRALDE G. (1993) *Delayed behaviour in concrete nuclear power plant containments: analysis and modeling*, in *Creep and shrinkage of concrete*, Proceedings of the RILEM Symposium, p.751-756.
- GUENOT-DELAHAIE I. (1997) *Contribution à l'analyse physique et à la modélisation du fluage propre du béton*, LPC Report 0A24, 144 p.
- HUA C., ACKER P., EHRLACHER A. (1995) *Analyses and models of the autogenous shrinkage of hardening cement paste*, CEMENT & CONCRETE RESEARCH, Vol.25, n°7, Juin, p.1457-1468.
- LAPLANTE P. (1993) *Propriétés mécaniques des bétons durcissants. Analyse comparée des bétons classiques et à très hautes performances* (Mechanical Properties of Hardening Concrete. Comparison OPC/VHSC), ENPC PhD.

- LAPLANTE P., BOULAY C. (1994) *Evolution du coefficient de dilatation thermique du béton en fonction de sa maturité aux tout premiers âges*, MATERIALS & STRUCTURES, Vol.27, n°174, p.596-605.
- LE ROY R. (1996) *Déformations instantanées et différées des bétons à hautes performances*, LPC Report, OA22, 372 p.
- THELANDERSSON S., MÅRTENSSON A., DAHLBLOM O. (1988) *Tension Softening and Cracking in Drying Concrete*, MATERIALS & STRUCTURES, Vol.21, p.416-424.
- TORRENTI J.M., ACKER P., PIAU J.M. (1992) *Numerical Simulation of Concrete Hydration: Thermal and Mechanical Effects*, Third International Workshop on Behaviour of Concrete Elements under Thermal and Hygral Gradients, WEIMAR.
- TORRENTI J.M., DE LARRARD F., GUERRIER F., ACKER P., GRENIER G. (1995) *Numerical simulation of temperatures and stresses in concrete at early ages: the French experience in Thermal cracking in concrete at early ages*, Proceedings of the RILEM Symposium, E & FN Spon, p.281-288.
- TROST H. (1978) *Kriech- und Relaxationsversuche an sehr altem Beton*, Deutscher Ausschuss für Stahlbeton, ERNST & Sohn, BERLIN, Heft 295, p.3-27.
- ULM F.J., BAZANT Z.P. (1997) *Modeling of creep and viscous flow mechanisms in early-age concrete*, ASCE ENGINEERING MECHANICS, submitted.
- WITTMANN F.H., ROELFSTRA P.E. (1980) *Total Deformation of Loaded Drying Concrete*, CEMENT & CONCRETE RESEARCH, Vol.10, p.601-610.
- WITTMANN F.H., BAZANT Z.P., ALOU F., KIM J.K. (1987) *Statistics of Shrinkage Test Data*, CEMENT, CONCRETE & AGGREGATES, Vol.9, n°2, p.129-153.

Prediction of Concrete Creep and Shrinkage: Past, Present and Future

By Zdeněk P. Bažant¹

ABSTRACT: The first part of the paper summarizes various aspects of the prediction of concrete creep and shrinkage to be discussed in the conference lecture. They include the theories of physical mechanism, prediction models, constitutive equations, computational approaches, probabilistic aspects, and research directions. The second part then presents two new prediction models. One of them deals with the approximate prediction formulae for pore relative humidity distributions, required for realistic creep and shrinkage analysis, and the other deals with the extrapolation of short time measurements of creep and shrinkage into long times.

1 Introduction

A long time has elapsed since the first observations of concrete shrinkage in the previous century and the discovery of concrete creep at the beginning of this century (Hatt 1907). Much research has been devoted to this complex problem ever since. However, despite major successes, the phenomenon of creep and shrinkage is still far from being fully understood, even though it has occupied some of the best minds in the field on cement and concrete research and materials science—Glanville, Dischinger, Troxell, Pickett, L' Hermite, Arutyunian, Aleksandrovskii, Powers, Hansen, Rüsch, Neville, Trost, Dilger, Wittmann, Hilsdorf, Müller, Huet, to name but a few. The present lecture will attempt to review the highlights of the past successes, explain some basic physical mechanisms and mathematical concepts, appraise our current capabilities and suggest some profitable future research directions and applications. Due to time and space limitations, the review will be far from exhaustive. Also, it will be flavored by the previous studies at the writer's institution.

The present brief paper will give in the first part a brief summary of the main points to be discussed in more detail in the lecture. In the second part, one new and one recent mathematical developments will be presented in some detail.

2 Review of Basic Results and Issues

Correct mathematical prediction of concrete creep and shrinkage inevitably requires understanding of the physical mechanism. It is generally accepted that drying shrinkage is caused by capillary tension, solid surface tension, and withdrawal of hindered adsorbed water and interlayer water from cement gel. Further shrinkage, called autogeneous, is further produced by

¹Walter P. Murphy Professor of Civil Engineering and Materials Science, Northwestern University, Evanston, IL 60208.

chemical volume changes (which could be negative, i.e. expansive) and self-desiccation. As for creep, many mechanism causing creep or influencing it have been proposed and studied:

1. Plastic flow.
2. Consolidation theory.
3. Load-bearing hindered adsorbed water.
4. Bond breakage in slip and its reformation
5. Nonlinear deformations and cracking as a contribution to Pickett effect.
6. Solidification theory for short-term aging (Bažant and Prasannan 1989).
7. Microprestress of creep sites in cement gel microstructure, causing the Pickett effect and long-term aging (Bažant, Hauggaard, Baweja and Ulm 1997).

The early mathematical models were formulated with a view to facilitate structural analysis. But computers made it possible to use any type of model, and thus the recent modeling could focus on representing the experimental data as closely as possible. The following prediction models have been proposed, although those numbered 1–3 have been superseded by newer ones:

1. Dichinger-Glanville theory, or rate-of-creep model (or theory of aging).
2. Updated Dischinger model or rate-of-flow model.
3. Arutyunian-Maslov model.
4. Double power law and log-double power law for basic creep.
5. BP and BPKX models and, as the latest version, the B3 model.

The first three models attempt a certain simplification of structural analysis. In this regard, the simplest methods, widely used, are:

- Effective modulus method (much simpler than Dischinger methods yet not involving a larger error)
- Age-adjusted effective modulus method (AAEM).

Formulation of a comprehensive prediction model is a very difficult task. In view of the limited knowledge we possess, the task of model formulation does not have a unique answer. Probably different models can describe the current knowledge equally well. However, they cannot be very different because a model acceptable today must not only fit the existing data (Müller, RILEM data bank), but should also conform to the mathematical consequences of several well established physical phenomena, including:

1. Activation energy theory of bond ruptures (temperature dependence of aging and of creep viscosities).
2. Diffusion theory, particularly its simple asymptotic properties for initial and final drying or shrinkage.
3. Modeling of cracking due to residual stresses in the cross section as a mechanism of apparent shrinkage reduction.
4. Solidification theory, particularly the fact that aging is only an apparent feature and must be caused by solidification—deposition of unstressed layers of hydration products on the pore walls.
5. Microprestress, which causes additional apparent long-term aging that cannot be explained by volume growth of hydration products.
6. Effect of fracture growth on apparent creep (the nonlinear part of creep is probably nothing but the effect of time-dependent crack growth).

In detail, see RILEM TC-107 (1995) Guidelines.

Aside from aging, the most difficult aspect of creep is the humidity variation, particularly the drying creep effect, also called the Pickett effect. A number of mathematical models have been proposed to describe it:

1. Pickett's (1943) model with creep nonlinearity.
2. Microdiffusion of hindered adsorbed or interlayer water and changes of disjoining pressure (manifested as stress-induced shrinkage).
3. Shrinkage reduction due to tensile cracking (Wittmann, 1970's) or by tensile strain softening (Bažant and Wu, 1974).
4. Microprestress of highly localized creep sites in cement gel caused by humidity (and temperature) changes.

Combination of the last two appears to provide the proper predictive model.

Among prediction models one must distinguish:

- True constitutive equations, describing the behavior of a small representative volume of concrete, and
- Models for the approximate overall (mean) behavior of the cross section of a long member.

The latter models are inevitably much more complicated in their form, because they must also characterize the solution of the boundary value problem of humidity distributions, residual stresses and cracking. However, the former models are much more difficult to identify from test data because their fitting to data involves an inverse boundary layer problem.

With the availability of finite element programs, the practice should shift from models for cross section behavior to the direct use of constitutive equation. This of course means splitting

the cross section into a number of finite elements. Only this approach can satisfy the hope for good predictions.

Computational approaches of various types have been developed:

1. One-step approximate solutions using the age-adjusted effective modulus method.
2. Step-by-step solution according to the integral-type creep law based on the principle of superposition.
3. Step-by-step solution according to a rate-type creep model based on the Kelvin or Maxwell chain.

The last approach gives most realistic results, because only the rate-type model allows physically sound incorporation of the effects of varying pore humidity and temperature on creep and aging.

Considerable strides have been made in the probabilistic modeling, which is very important because of high statistical variability, and in micromechanics of the effect of concrete composition on creep and shrinkage (e.g., Granger, 1995). Nevertheless, the best way to achieve good long time predictions is to conduct short-time tests on the given concrete and then extrapolate them, taking into account the physics.

For future research, the following avenues seem most promising and important:

1. Updating of long-term predictions on the basis of short-time measurements, with the use of probabilistic concepts.
2. Incorporation into structural analysis the solutions of pore humidity and temperature distributions in the cross section.
3. Mastering the interaction of creep with fracture (Bazant, 1993, 1995).
4. Micromechanical modeling and use of composite material theories for predicting creep and shrinkage from the properties of constituents.
5. Improved thermodynamical theory for the effects of pore water and temperature.
6. Nonlinear triaxial creep at high stress, especially taking into account time-dependent fracture and damage growth.
7. Improved, physically-based, probabilistic modeling of creep and shrinkage.
8. Creep and shrinkage of high strength and special concretes.
9. Means to reduce shrinkage and, for some applications, creep (the stress relaxation due to creep is sometimes beneficial).

3 Two New Mathematical Models

3.1 Explicit Approximate Formulae for Predicting Pore Humidity Distributions

Realistic prediction of the effects of creep and shrinkage in concrete structures exposed to drying environment requires the calculation of the distributions of relative humidity in the pores of concrete at various times. Although it is not difficult to solve the problem numerically by finite difference or finite element solutions of the nonlinear diffusion equation for concrete drying (e.g., Bažant and Najjar, 1972, Xi et al. 1996, Bažant, ed., 1988, Bažant and Raftshol, 1982, Bažant and Kim, 1991), simple explicit formulas are desired by structural analysts.

One very simple formula was presented by Parrott (1991). However a close examination shows that this formula is oversimplified. It was compared only to an extremely limited set of data, and does not agree with the broader experimental evidence (e.g., Bažant and Najjar, 1972, Xi et al., 1995?). Also this formula does not conform to the asymptotic behavior for very short and very long times, which should be easy to satisfy by an explicit formula. Furthermore, since the water loss is approximately proportional to the drop in the average relative humidity in the pores, and the drying shrinkage is approximately proportional to the water loss, the average humidity obtained from the formula should evolve in time similarly as shrinkage, for which plentiful data are available and a rather accurate prediction model has been developed (Bažant and Baweja, 1995).

It is possible, as will now be shown, to develop an improved simple formula that exhibits correct asymptotic behaviors, agrees better with the measurements of pore relative humidity, and also agrees better with the shrinkage prediction formula. We consider a drying process that may be approximately considered as one-dimensional in space. The cross-section may be that of a wall limited by two parallel planes. As an approximation, rectangular or square cross-sections, as well as a cube and prism can be treated similarly using cylindrical or spherical coordinates.

The average relative humidity in the pores is defined as

$$\bar{h}(t) = \frac{1}{D} \int_0^D h(x, t) dx \quad (1)$$

in which t = time, D = thickness of cross-section. Because the change of average humidity is approximately proportional to the average shrinkage in the cross-section, the shrinkage prediction formula in Bažant and Baweja (1985) indicates that

$$\frac{\varepsilon_{sh}(t)}{\varepsilon_{sh\infty}(h_e)} = \frac{w_0 - \bar{w}(t)}{w_0 - w_{\infty}(h_e)} = \frac{h_0 - \bar{h}(t)}{h_0 - h_e} - \tanh \xi, \quad \xi = \sqrt{\frac{t - t_0}{\tau_{sh}}} \quad (2)$$

in which h_0 = initial relative humidity in the pores, assumed to be uniform (usually between 95% and 100%), h_e = environmental relative humidity, ε_{sh} = average shrinkage strain in the cross section, $\varepsilon_{sh\infty}$ = final value of shrinkage strain corresponding to h_e , w_0 = initial specific evaporable water content in concrete, \bar{w} = average specific water content, w_{∞} final water loss

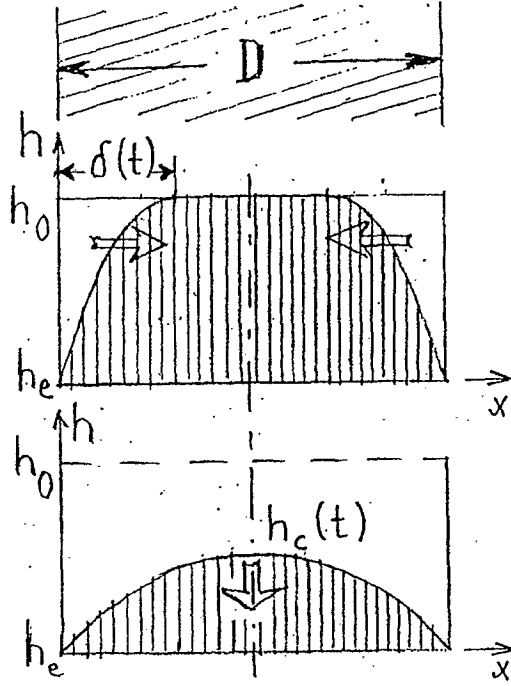


Figure 1: Approximate parabolic profiles of pore humidity in the first and second stages of drying of a wall, and time evolution of average humidity or shrinkage.

corresponding to h_e , and t_0 = initial time at the start of exposure to drying environment, $t - t_0$ = duration of drying, τ_{sh} = shrinkage or drying half-time, which is expressed as

$$\tau_{sh} = k_t (k_s D)^2 \quad (3)$$

Here D is generally defined as the effective cross-section thickness, $D = 2v/s$, where v and s are the volume and the surface of the structural member. D must be given in inches, and t, t_0 in days. The parameter k_t can be predicted from the empirical expressions $k_t = 190.8 t_0^{-0.08} f'_c{}^{-1/4}$ days in.⁻² in which f'_c = average uniaxial compression strength which must be given in psi.

The tangent-hyperbolic function in (2) (Fig. 1 right) satisfies two basic asymptotic properties, which are exhibited by the solutions of the nonlinear diffusion equation (Bažant and Kim, 1991a,b):

$$\text{for } t - t_0 \ll \tau_{sh}: \quad \tanh \xi = \xi - \frac{1}{3}\xi^3 + \frac{2}{15}\xi^5 - \dots \approx \xi \quad (4)$$

$$\text{for } t - t_0 \gg \tau_{sh}: \quad \tanh \xi = 1 - 2(e^{-2\xi} - e^{-4\xi} + e^{-6\xi} - \dots) \approx 1 - 2e^{-2\xi} \quad (5)$$

Thus, the function $\tanh \psi$ is justified as a simple interpolation between these two opposite asymptotic behaviors. There are other functions that can match these asymptotic behaviors, but they are more complicated. The pore humidity distributions at various times can be approximately assumed as power curves, given by the expression

$$\text{for } x \leq \delta(t): \quad h(x, t) = h_c(t) - [h_c(t) - h_e] \left(1 - \frac{x}{\delta(t)}\right)^\gamma;$$

$$\text{for } \delta(t) \leq x \leq D : \quad h(x, t) = h[\delta(t), t] \quad (6)$$

(see Fig. 1); γ = empirical constant. For linear diffusion theory, the profiles can be closely approximated as parabolas, in which case $\gamma = 2$. Due to the nonlinearity of diffusion in concrete, consisting primarily in the fact that the diffusivity greatly decreases with the decrease of humidity (about 20 times as the humidity drops from 0.95 to 0.7), the optimum value of exponent $\gamma > 2$. Usually the best fit is obtained for $\gamma = 3$ or 4. Parameter δ represents the depths of penetration of the drying front. After the drying fronts from the opposite surfaces meet, $\delta = D/2 = \text{constant}$ and parameter h_c represents the pore humidity in the center of the thickness of the cross section. Before that, h_c represents also the humidity at the front of drying, i.e., $h_c = h_0$.

As is well known from exact diffusion solutions, the drying process can be divided in two stages: during the first stage, the drying front advances, which continues until the drying fronts meet in the center of the cross section. During that stage, the humidity profiles are scaled horizontally, i.e., are being transformed by affinity in the horizontal direction with respect to a vertical axis on the surface (Fig. 1 left). During the second stage, the humidity profiles are being scaled down, transferred by affinity in the vertical direction with respect to a horizontal axis (see Fig. 1 middle).

To obtain an expression for parameters $\delta(t)$ and $h_c(t)$, we may substitute (5) into the averaging integral 1, and match the result to the average humidity obtained from Eq. (2). After various algebraic rearrangements, one obtains the formulas in the following algorithm for predicting the pore humidity distributions at various times t .

$$1. \quad \delta(t) = \frac{\gamma+1}{2} D \tanh \frac{t-t_0}{\tau_{sh}}, \quad h_c(t) = h_0 \quad (7)$$

$$2. \quad \text{If } \delta(t) \leq D/2, \text{ go to 5} \quad (8)$$

$$3. \quad \delta(t) = D/2 \quad (9)$$

$$4. \quad h_c(t) = h_e + \left(1 + \frac{1}{\gamma}\right) (h_0 - h_e) \tanh \sqrt{\frac{t-t_0}{\tau_{sh}}} \quad (10)$$

$$5. \quad \text{Evaluate } h(x, t) \quad (11)$$

3.2 Improvements of Prediction Based on Short-Time Measurements

Close prediction of the future creep and shrinkage is impossible without short-time measurements on the given concrete. Since this is a very important problem, a recently published model (Bažant and Baweja 1995) taking into account the coupling with water diffusion will now be described.

An important advantage of the B3 Model compliance function $J(t, t')$ (Eq. 7, p. 359, and 15, p. 363, in Bažant and Baweja, 1995) is that all the free parameters for creep with elastic deformation, that is, q_1, q_2, q_3, q_4, q_5 , are contained in the formulas linearly. Therefore, linear regression based on the least-square method can be used to identify these parameters from test data, so as to minimize the value of the coefficient of variation of the deviations of model prediction from the available data points, $\bar{\omega}_{all}^2$. The linearity also applies to parameter $\epsilon_{sh\infty}$

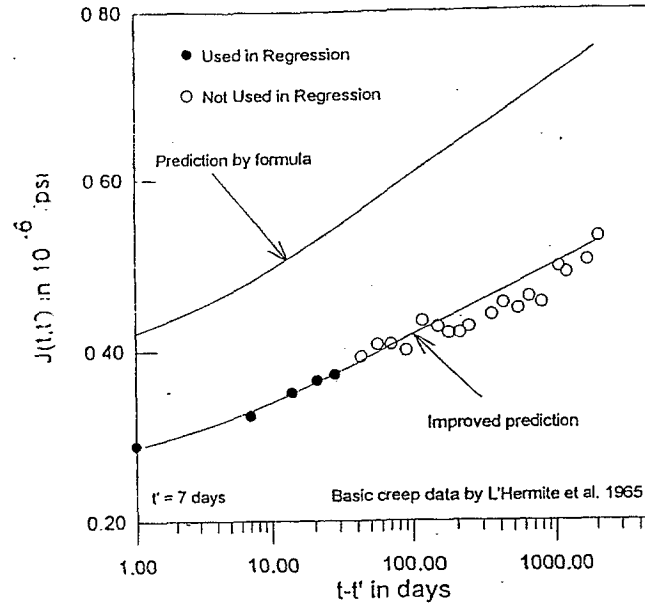


Figure 2: Example of improving the creep prediction by the use of short-time test data.

for shrinkage. Thus the only nonlinear parameter of the entire formulation is the shrinkage half-time τ_{sh} .

The largest source of uncertainty of creep and shrinkage prediction model is the dependence of model parameters on the composition and design strength of concrete. This uncertainty can be greatly reduced by carrying out short-time measurements on the given concrete and adjusting the values of the same model parameters accordingly. Carrying out measurements of at least short-time creep and shrinkage (of duration 1–3 months) is important especially for special concretes such as high strength concretes. Various types of admixtures, superplasticizers and pozzolanic ingredients used in these concretes have been found to have a significant effect on creep and shrinkage of concrete. Empirical formulas for the effects of all these ingredients on the model parameters would be very difficult to formulate because of the great variety of additives and different combinations used. Compared to other models, including the original BP Model, the solidification theory which is the basis of the present model has the advantage that the adjusted values of model parameters except C_0 can be easily obtained by linear regression of the short-time test data.

To illustrate the procedure, consider now the data for creep at drying by L'Hermite et al., for which the present formulae for the effect of composition and strength do not give a good prediction, as is apparent from Fig. 2. We now pretend we know only the first 5 data points for the first 28 days of creep duration, which are shown by the solid circles. We consider the updated compliance function in the form

$$J(t, t') = p_1 + p_2 F(t, t') \quad (7)$$

in which p_1 and p_2 have the role of updated parameters q_1 and q_2 , and

$$F(t, t') = C_0(t, t') + C_d(t, t', t_0) \quad (8)$$

This function is evaluated according to the model, using the formulae for the effect of composition parameters and strength. If the data agreed with the form of the present model B3 exactly, the plot of $J(t, t')$ versus $F(t, t')$ would have to be a single straight line for all t, t' and t_0 . The vertical deviations of the data points from this straight line represent errors which are regarded as random and are to be minimized by least-square regression. So we consider the plot of the known (measured) short-time values $Y = J(t, t')$ (up to 28 days of creep duration) versus the corresponding values of $X = F(t, t')$, calculated from model B3, and pass through these points the regression line $Y = AX + B$. Then the slope A and the Y -intercept B of this line give the values of p_1 and p_2 that are optimum in the sense of the least-square method; $A = p_2$ and $B = p_1$. According to the well-known normal equations of least-square linear regression, $p_2 = [n \sum (F_i J_i) - (\sum F_i)(\sum J_i)] [n \sum (F_i^2) - (\sum F_i)^2]^{-1}$ and $p_1 = \bar{J} - p_2 \bar{F}$ where subscripts $i = 1, 2, \dots, n$ label the known data points, n is their total number, $\bar{F} = \bar{F}(t, t')$, $\bar{J} = \bar{J}(t, t')$, \bar{J} = mean value of all the measured J and \bar{F} = mean value of all the corresponding F . Obviously, the improvement of long-time predictions achieved by short-time measurements is in this example very significant. The well-known formulae of linear regression also yield the coefficients of variation of p_1 and p_2 , which in turn provide the coefficient of variations of $J(t, t')$ for any given t and t' .

For planning of short-time creep measurements, note that prediction improvement based on short-time data is more successful if the creep measurements begin at very short times after loading (and likewise for shrinkage, if the measurements begin immediately after the stripping of the mold). The reason is that the creep curves are known to be smooth through the entire range from 0.0001 s to 30 years. In our example, the first reading was taken as late as 1 day after loading, as is often done, and therefore we needed up to 28 days of creep data for prediction improvement. In a similar example using a different formulation it was shown that if the first reading is taken as soon as possible after loading (within 1 minute) and about six readings are taken in the first two days of load duration a similar improvement can be achieved using those readings only. Thus the duration of short time test could be reduced if readings are begun immediately after loading. Anyhow for reliable prediction over five years of creep duration, short-time tests of at least 28 days duration (with the first reading immediately after loading and further readings equally spaced on the logarithmic scale for creep duration in hours) are recommended.

The shrinkage predictions, too, can be improved on the basis of the measurements of the given concrete. However, an important limitation has recently been noted (Bažant and Baweja, 1993, 1995). The updating based only on short time measurements of shrinkage values is not possible unless the measurements extend into rather long times, at which the shrinkage curves begins to level off on approach to the final value. The reason is the special nonlinear form of the shrinkage formulae arising from the diffusion nature of the problem. If the time range of shrinkage measurements is not sufficiently long, the problem of fitting the shrinkage formula in Eqs. (9)–(12), p. 360, of Bažant and Baweja (1995) to the measured strain values is an ill-posed problem. In other words, very different values of parameters $\epsilon_{sh\infty}$ and τ_{sh} can give almost equally good fits of short-time data, as shown in Fig. 3 (taken from Bažant and Baweja, 1993). This is true not only for the present model B3 formulae (which in this case are the same in the BP and BP-KX models) but also for all other shrinkage formulae, including the Ross' hyperbola used in the ACI model (this formula does not give a good shape of the shrinkage curves and

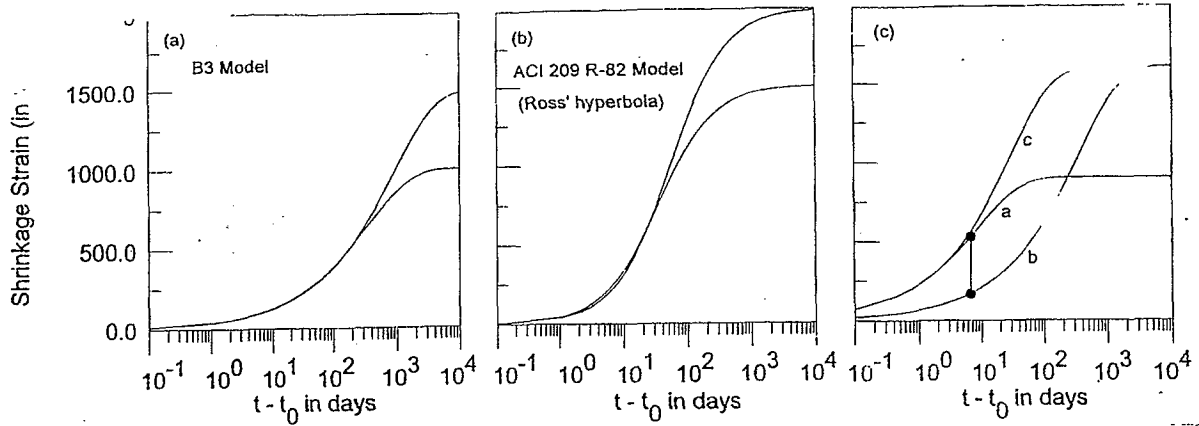


Figure 3: Examples of shrinkage-time curves giving nearly the same initial shrinkage but very different final values Left: B3 Model and Right: ACI 209 Model.

disagrees with the asymptotic forms for short and long times required by the RILEM Committee Guidelines. The problem is clear from Fig. 3 in which two shrinkage curves according to the present model or the ACI model, corresponding to very different parameter values, are shown to nearly coincide for a long period of time. If the data do not reach beyond the time at which the two curves shown in Fig. 3 begin to significantly diverge, there is no way to determine the model parameters unambiguously.

From such plots it must be concluded that a reliable determination of the final value of shrinkage would require, for 6 in. (15 cm) diameter cylinders, measurements of at least 5 years duration, which is unacceptable for a designer. Even with a 3 in. (7.5 cm) diameter cylinder, this would exceed 15 months. Increasing the temperature of the shrinkage tests to about 50° C would not shorten these times drastically and would raise further uncertainties due to the effect of temperature. A greater increase of temperature would change the shrinkage properties so much that inferences for the room temperature would become questionable. Significant acceleration of shrinkage would require reducing the thickness of the shrinkage specimen under about 1 in. (2.54 cm), but in that case the specimens would have to be saw-cut from larger specimens and the three-dimensional composite interaction between the mortar matrix and the aggregate pieces will very be different from bulk concrete.

Assume first that τ_{sh} is known. The updated values of shrinkage prediction, labeled by primes, are considered as follows:

$$\epsilon'_{sh} = p_6[\epsilon_{sh}(t, t_0)]_{\tau_{sh}} \quad (9)$$

in which ϵ_{sh} are the values predicted from the present model B3 based on the value of τ_{sh} , and p_6 is an update parameter. Consider that values ϵ^*_{shi} at times t_i have been measured. Let ϵ_{shi} be the values predicted for these times by the present model B3. The optimum update should minimize the sum of square deviations of the updated model from the data, that is

$$S = \sum_i \Delta_i^2 = \sum_i (p_6 \epsilon_{shi} - \epsilon^*_{shi})^2 = \text{Min} \quad (10)$$

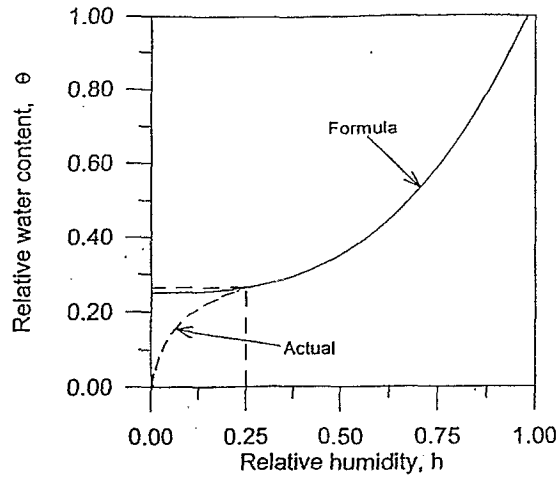


Figure 4: Relative water content of concrete versus relative humidity h in equilibrium.

A necessary condition of minimum is $dS/dp_6 = 0$. This yields the condition $\sum_i (p_0 \epsilon_{sh_i} - \epsilon_{sh_i}^*) \epsilon_{sh_i} = 0$. From this the value of the update parameter is calculated as

$$p_6 = \frac{\sum_i \epsilon_{sh_i} \epsilon_{sh_i}^*}{\sum_i \epsilon_{sh_i}^2} \quad (11)$$

Next consider the practical case, in which τ_{sh} is not known in advance. To circumvent the aforementioned ill-posedness of the shrinkage updating problem, the following idea was recently proposed by Bažant and by Bažant and Baweja (1995). It has been known for a long time that shrinkage strains are approximately proportional to the water loss, denoted as Δw . The water loss can be easily measured simultaneously with shrinkage tests. Now, an important point to realize is that the final value $w_\infty(0)$ of water loss at complete drying (corresponding to zero relative humidity) is easily determined by heating the test specimen to 100° C after the conclusion of the short-time test. Using the approximately known shape of the desorption isotherm shown in Fig. 4, one may then estimate the final water loss $\Delta w_\infty(h)$ corresponding to drying at humidity h ;

$$\Delta w_\infty(h) \approx 0.75 \left[1 - \left(\frac{h}{0.98} \right)^3 \right] \Delta w_\infty(0) \quad (12)$$

This equation satisfies the condition that there is no water loss for $h \approx 0.98$ (in water immersion, $h = 1$, there is water gain). For $h < 0.24$, this equation is invalid, but such low humidities are usually not of interest.

Because Eqs. (9), (10) and (12) on p. 360 of Bažant and Baweja (1995) were derived from diffusion theory, assuming proportionality to water loss, the evolution of water loss with time should approximately follow the same equation as (10), p. 360 of Bažant and Baweja (1995), that is

$$\frac{\Delta w}{w_\infty} = \tanh \sqrt{\frac{t - t_0}{\tau_{sh}}} \quad (13)$$

This equation is easily rearranged to a linear form

$$t - t_0 = \tau_{sh}\psi, \quad \text{with } \psi = \left[\tanh^{-1} \left(\frac{\Delta w}{w_\infty} \right) \right]^2 \quad (14)$$

Now consider that at times t_i of shrinkage measurements the values of water loss Δw_i and the corresponding values of ψ_i have been determined. The optimum value of τ_{sh} must minimize the sum of square deviations, i.e.

$$S = \sum_i [\tau_{sh}\psi_i - (t_i - t_0)]^2 = \text{Min} \quad (15)$$

A necessary condition of minimum $dS/d\tau_{sh} = 0$. This yields the linear equation $\sum_i [\tau_{sh}\psi_i - (t_i - t_0)]\psi_i = 0$. From this, the desired updated value of τ_{sh} is:

$$\tau_{sh} = \frac{\sum_i (t_i - t_0)\psi_i}{\sum_i \psi_i^2} \quad (16)$$

Based on this value one may then use Eq. (7) to obtain the updating parameter p_6 for the shrinkage values as indicated before.

An example of the updating procedure, using shrinkage data of Granger measured at LCPC for the concrete of the Civaux nuclear power plant containment, is shown in Fig. 5.

It should be noted that although the relationship of water loss and shrinkage underlying the foregoing equations is reasonably well established and widely accepted, a direct check of this updated procedure has not yet been made. The proposed method deserves deeper accuracy evaluation.

Acknowledgement: Partial financial support from National Science Foundation under grant MSS-911476 to Northwestern University is gratefully acknowledged. Additional partial support has been received from the Center for Advanced Cement-Based Materials at Northwestern University.

4 Chronological Partial Bibliography and References

- Troxell, G.E., Raphael, J.E. and Davis, R.W. (1958). "Long-time creep and shrinkage tests of plain and reinforced concrete". *Proc ASTM* 58, 1101-1120.
- Aleksandrovskii, S.V. (1959). "On thermal and hygrometric properties of concrete related to heat and moisture exchange (in Russian), Akad. Stroit. i Arkhitektury USSR (Moscow), Nauchno-Issled. Inst. Betona i Zhelezobetona (NIIZhB) Issled. Svoistv Betona, Zhelezob. Konstr., Trudy Inst., No. 4, 184-214.
- Carslaw, H.S. and Jaeger, J.C., (1959). "Conduction of heat in solids", 2nd ed., *Oxford University Press*, London (p. 97).
- Abrams, M.S., and Monfore, G.E. (1965). "Application of a small probe-type relative humidity gage to research on fire resistance of concrete, *Journal of the Portland Cement Association Research and Development Laboratories*, Vol. 7, No. 3, pp. 2-12 (PCA Bulletin 186).
- Abrams, M.S., and Orals, D.L., (1965). "Concrete drying methods and their effect on fire resistance, in: *Moisture of materials in relation to fire tests*, STP No. 385, 57-32, publ. by American Society of Testing Materials (PCA Bulletin 181).
- Keeton, J.R. (1965). "Study of creep in concrete, Technical reports R333-I, R333-II, R333-III" (U.S. Naval civil engineering laboratory, Port Hueneme, California).

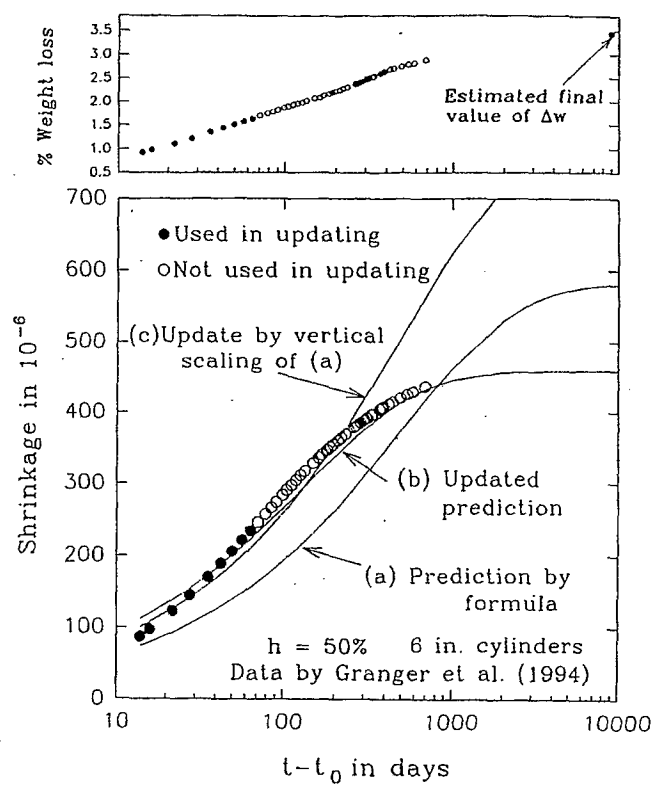


Figure 5: Updating of long-term shrinkage prediction using short-term measurements at LCPC reported by Granger (1995).

- L'Hermite, R.G. Mamillan, M. Lefèvre, C. (1965). "Nouveaux résultats de recherches sur la déformation et la rupture du béton *Ann. Inst. Techn. Bâtiment Trav. Publics* 18(207-208), 323-360.
- Wallo, E.M., Yuan, R.L., Lott, J.L., Kesler, C.E. (1965). "Sixth progress report on prediction of creep in structural concrete from short time tests". T & AM report No. 658, Department of theoretical and applied mechanics, University of Illinois at Urbana.
- Hansen, T.C. and Mattock, A.H. (1966). "Influence of size and shape of member on the shrinkage and creep of concrete", *ACI J.* 63, 267-290.
- Hughes, B.P., Lowe, I.R.G., and Walker, J. (1966). "The diffusion of water in concrete at temperatures between 50 and 95° C, *British Journal of Applied Physics*, Vol., 17, 252-263.
- Browne, R.D. (1967). "Properties of concrete in reactor vessels", in Proceedings of Conference on Prestressed Concrete Pressure group C (Institution of Civil Engineers London, pp 11-31.
- Hancox, N.L. (1967). "A note on the form of the rate of drying curve for cement paste and its use in analyzing the drying behavior of this material, *RILEM Bulletin*, No. 36, 197-201.
- Hannant, D.J. (1967), "Strain behaviour of concrete up to 95°C under compressive stresses" in Proceedings of Conference on Prestressed Concrete Pressure group C (Institution of Civil Engineers London, pp 57-71.
- Helmuth, R.A., and Turk, D.H. (1967). "The reversible and irreversible drying shrinkage of hardened portland cement and tricalcium silicate paste, *Journal of the Portland Cement Association Research and Development Laboratories*, Vol. 9, No. 2, 8-21 (PCA Bulletin 215).
- Abrams, M.S., and Gustaferro, A.H. (1968). "Fire endurance of concrete slabs as influenced by thickness, aggregate type, and moisture, *Journal of the Portland Cement Association Research and Development Laboratories*, Vol. 10, No. 2, pp. 9-24 (PCA Bulletin 223).
- Hanson, J.A., (1968). "Effects of curing and drying environments on splitting tensile strength, *American Concrete Institute Journal*, Vol. 65, 535-543.
- L'Hermite, R.G. and Mamillan M. (1970). "Influence de la dimension des éprouvettes sur le retrait" *Ann. Inst. Techn. Bâtiment Trav. Publics* 23 (270) (1970) 5-6.
- Bazant, Z.P. (1972). "Prediction of concrete creep effects using age-adjusted effective modulus method." *American Concrete Institute Journal*, 69, 212-217.
- Bazant, Z.P., and Najjar, L. J. (1972). "Nonlinear water diffusion in nonsaturated concrete." *Materials and Structures* (RILEM, Paris), 5, 3-20.
- Rostasy, F.S., Teichen, K.-Th. and Engelke, H. (1972). "Beitrag zur Klärung des Zusammenhangs von Kriechen und Relaxation bei Normal- beton", Amtliche Forschungs- und Materialprüfungsanstalt für das Bauwesen, Heft 139 (Otto-Graf-Institute, Universität Stuttgart, Strassenbau und Strassenverkehrstechnik.
- Bazant, Z.P., Carreira, D., and Walser, A. (1975). "Creep and shrinkage in reactor containment shells." *Jour. Struct. Div.*, Am. Soc. Civil Engrs., 101, 2117-2131.
- Kommendant, G.J., Polivka, M., and Pirtz, D. (1976). "Study of concrete properties for prestressed concrete reactor vessels, final report Report No. UCSESM 76-3 to General Atomic Company (Department of Civil Engineering, University of California, Berkeley).
- Bazant, Z.P. and Panula, L. (1978). "Practical prediction of time dependent deformations of concrete". Parts I-VI *Materials and Structures* 11 (1978) 307-316, 317-328, 425-434, 12 (1979) 169-183.
- Takahashi, H., Kawaguchi, T. (1980). "Study on Time-Dependent Behaviour of High Strength Concrete (Part 1) - Application of the Time-Dependent Linear Viscoelasticity Theory of Concrete Creep Behaviour", Ohbayashi-Gumi Research Institute Report, No.21, pp.61-69.
- ACI committee 209 (1982). "Prediction of creep, shrinkage and temperature effects in concrete structures,(ACI 209-82)," *American Concrete Institute* Detroit, 108 pp.
- Bazant, Z.P., and Raftshol, W. J. (1982). "Effect of cracking in drying and shrinkage specimens." *Cement and Concrete Research*, 12, 209-226; Disc. 797-798.

- Neville, A.M., Dilger, W.H. and Brooks, J.J. (1983), "Creep of plain and structural concrete", Construction Press, London and New York.
- Bazant, Z.P., and Chern, J.C. (1985), "Concrete creep at variable humidity: constitutive law and mechanism". *Materials and Structures* 18, 1-20.
- Wittman, F.H. Bazant, Z.P., Alou, F., Kim, J.K. (1987), "Statistics of shrinkage test data", *Cem., Conc. Aggreg.* 9 (2), 129-153.
- RILEM Committee TC-69 (1988). "Creep analysis of structures" (principal authors Z.P. Bazant and O. Buyukozturk), *ibid.*, 217-273.
- RILEM Committee TC 69 (1988). (Z. Bazant, Chairman and princ. author), "State of the art in mathematical modeling of creep and shrinkage of concrete," in *Mathematical Modeling of Creep and Shrinkage of Concrete*, ed. by Z.P. Bazant, J. Wiley, Chichester and New York, 1988, 57-215; and in prelim. form: "State-of-art report on creep and shrinkage of concrete: mathematical modeling," Preprints, *Fourth RILEM International Conference on Creep and Shrinkage of Concrete*, 1986, ed. by Z.P. Bazant, 41-80.
- RILEM Committee TC 69 (1988). (Z. Bazant, Chairman), "State of the art in mathematical modeling of creep and shrinkage of concrete," in *Mathematical Modeling of Creep and Shrinkage of Concrete*, ed. by Z.P. Bazant, J. Wiley, Chichester and New York, 1988, 57-215.
- RILEM TC69 (1988). "Conclusions for structural analysis and for formulation of standard design recommendations", Chapter 6 in *Mathematical Modeling of Creep and Shrinkage of Concrete*, ed. by Z.P. Bazant, John Wiley and Sons, Chichester and New York; reprinted in *Materials and Structures* (RILEM, Paris) 20, 395-398.
- Bazant, Z.P. and Prasannan, S. (1989). "Solidification theory for concrete creep: I. Formulation, and II. Verification and application", *ASCE J. of Engg. Mech.* 115(8), 1691-1725.
- Brooks, J.J. (1989). "Influence of mix proportions, plasticizers and superplasticizers on creep and drying shrinkage of concrete", *Magazine of concrete research* 41 (148), 145-153.
- CEB-FIP Model Code, (1990), Design Code, Thomas Telford.
- Bazant, Z.P., and Kim, Joong-Koo (1991). "Consequences of diffusion theory for shrinkage of concrete." *Materials and Structures* (RILEM, Paris) 24 (143), 323-326.
- Bazant, Z.P., Kim, Joong-Koo, and Panula, L. (1991). "Improved prediction model for time-dependent deformations of concrete: Part 1-Shrinkage." *Materials and Structures* (RILEM, Paris) 24 (143), 327-345.
- Bazant, Z.P. and Kim, Joong-Koo. (1991). "Consequences of diffusion theory for shrinkage of concrete" *Materials and Structures* 24, 323-326.
- Bazant, Z.P. and Kim, Joong-Koo. (1991). "Improved prediction model for time dependent deformations of concrete Part 1-Shrinkage *Materials and Structures* 24 (1991), 327-345, Part 2-Basic Creep *ibid* 24 409-42, Part 3-Creep at drying *ibid* 25(1992), 21-28, Part 4-Temperature effects *ibid* 25(1992), 84-94.
- Parrott, L.J. (1991). "Factors influencing relative humidity in concrete", *Magazine of Concrete Research*, 43 (No.154, March) 45-52.
- Bazant, Z.P. Panula, L., Kim, Joong-Koo, and Xi, Y. (1992). "Improved prediction model for time dependent deformations of concrete: Part 6-Simplified Code-type formulation" *Materials and Structures* 25, 219-223.
- Brooks, J.J. (1992). "Preliminary state of the art report: Elasticity, creep and shrinkage of concretes containing admixtures, slag, fly-ash and silica-fume" ACI committee 209.
- Bazant, Z.P. (1993). "Current status and advances in the theory of creep and interaction with fracture." Proc., *5th International RILEM Symposium on Creep and Shrinkage of Concrete (ConCreep 5)*, held at U.P.C., Barcelona, September, ed. by Z.P. Bazant and I. Carol, E & FN Spon, London, 291-307.
- Bazant, Z.P., and Xi, Y. (1993). "Stochastic drying and creep effects in concrete structures." *J. of Structural Engineering*, ASCE, 119 (1), 301-322.
- Bazant, Z.P., Xi, Y., and Baweja, S. (1993). "Improved prediction model for time dependent

- deformations of concrete: Part-7 Short form of BP-KX model, Statistics and extrapolation of short-time data." *Materials and Structures* 26, 567-574.
- Carol, I. and Bažant, Z.P. (1993). "Viscoelasticity with aging caused by solidification of non-aging constituent." *ASCE J. of Engg. Mech.* 119 (11), 2252-2269.
- Gardner, N.J. and Zhao, J.W. (1993). "Creep and shrinkage revisited", *ACI Materials Journal* 90, 236-246.
- Tsubaki T. (1993). "Sensitivity of factors in relation to prediction of creep and shrinkage of concrete" in Creep and Shrinkage of Concrete, Proceedings of fifth international RILEM symposium, Barcelona, Spain, 611-622.
- Bažant, Z.P. (1994). "Creep and thermal effects in concrete structures: A conspectus of some new developments." Proc., *Computational Modelling of Concrete Structures (EURO-C)*, held at Innsbruck, Austria, March, Pineridge Press, 461-480.
- Xi, Y., Bažant, Z.P., and Jennings, H.M. (1994). "Moisture diffusion in cementitious materials: Absorption isotherms." *Advanced Cement Based Materials* 1, 248-257.
- Xi, Y., Bažant, Z.P., Molina, L., and Jennings, H.M. (1994). "Moisture diffusion in cementitious materials: Moisture capacity and diffusivity." *Advanced Cement Based Materials* 1, 258-266.
- Bažant, Z.P. (1995). "Creep and Damage in Concrete." *Materials Science of Concrete IV*, J. Skalny and S. Mindess, Eds., Am. Ceramic. Soc., Westerville, OH, 355-389.
- Bažant, Z.P., and Baweja, S. (1995), in collaboration with RILEM Committee TC 107-GCS, "Creep and shrinkage prediction model for analysis and design of concrete structures - model B3" (RILEM Recommendation). *Materials and Structures* (RILEM, Paris) 28, 357-365; with Errata, Vol. 29 (March 1996), p. 126.
- Bažant, Z.P., and Baweja, S. (1995). "Justification and refinement of Model B3 for concrete creep and shrinkage. 1. Statistics and sensitivity." *Materials and Structures* (RILEM, Paris) 28, 415-430.
- Bažant, Z.P., and Baweja, S. (1995), in collaboration with RILEM Committee TC 107-GCS, "Creep and shrinkage prediction model for analysis and design of concrete structures - model B3" (RILEM Recommendation). *Materials and Structures* (RILEM, Paris) 28, 357-365; with Errata, Vol. 29 (March 1996), p. 126.
- Bažant, Z.P., and Baweja, S. (1995). "Justification and refinement of Model B3 for concrete creep and shrinkage" *Materials and Structures* (RILEM, Paris) 28, 415-430.
- Granger, L.P., and Bažant, Z.P. (1995). "Effect of composition on basic creep of concrete and cement paste." *ASCE J. of Engrg. Mechanics* 121 (11), 1261-1270.
- RILEM Techn. Com. TC-107 (1995) (Z.P. Bažant and I. Carol, main authors), "Guidelines for characterizing concrete creep and shrinkage in structural design codes or recommendations." *Materials and Structures* 28, 52-55.
- Bažant, Z.P., and Baweja, S. (1996). "Short form of creep and shrinkage prediction model B3 for structures of medium sensitivity" (Addendum to RILEM Recommendation TC 107-GCS). *Materials and Structures* (Paris) 29 (Dec.), 587-593.
- Bažant, Z.P., and Kaplan, M.F. (1996). *Concrete at High Temperatures: Material Properties and Mathematical Models* (monograph and reference volume). Longman (Addison-Wesley), London 1996 (412 + xii pp.).
- Bažant, Z.P., Hauggaard, B., Baweja, S. and Ulm, F.-J. (1997). "Microprestress-solidification theory for aging and drying creep of concrete." *J. of Engrg. Mech. ASCE* 123, in press.

ASSESSMENT OF CREEP METHODOLOGIES FOR PREDICTING PRESTRESSING FORCES LOSSES IN NUCLEAR POWER PLANT CONTAINMENTS

By Laurent GRANGER¹, Zdenek BITTNAR² and Tibor JAVOR³

Members of RILEM TC-MNL

Methodology for Life Prediction of Concrete Structures in Nuclear Power Plants /
*Méthodologie pour la prévision de la durée de vie des structures en béton dans des
centrales nucléaires*

¹ : EDF SEPTEN, Civil-Engineering Division, Villeurbanne, FRANCE

² : Czech Technical University, Prague, CZECH REPUBLIC

³ : Expertcentrum, Bratislava, SLOVAKIA

RESUME :

Ce travail a été réalisé dans le cadre du groupe RILEM TC-MNL (Méthodologie pour la prévision de la durée de vie des structures en béton dans les centrales nucléaires). Il a pour but de proposer une analyse et des réflexions afin d'améliorer la façon dont la prédiction des pertes de précontrainte liées aux déformations différées du béton est réalisée dans le domaine des enceintes de centrales nucléaires. Nous précisons tout d'abord les données du problème, les spécificités du nucléaire ainsi que l'état des connaissances dans le domaine du comportement différé du béton. Puis, après avoir présenté l'expérience théorique et expérimentale acquise par EDF dans ce domaine, nous présentons une approche simplifiée, basée sur des résultats expérimentaux et permettant de prédire le niveau de perte de précontrainte auquel on peut raisonnablement s'attendre sur structure. Cette méthode s'appuie essentiellement sur la façon dont on peut transposer des résultats obtenus sur éprouvette en laboratoire à un mur d'enceinte de centrale nucléaire de forte épaisseur.

ABSTRACT :

This contribution has been realised as part of RILEM TC-MNL work (Methodology for Life Prediction of Concrete Structures in Nuclear Power Plants). Its aim is to analyse and propose certain recommendations in order to improve the way the prediction of prestressing forces losses due to the delayed behaviour of concrete is performed in the nuclear containment field. First of all, we give a short state of the art of the delayed behaviour of concrete (in particular the limits of today's knowledge) and we try to point out the particularities of the nuclear field. After introducing EDF's experience in this domain, both theoretical and experimental, we present a simplified approach, experimentally based, allowing to predict the level of prestress losses that can be expected on a containment. This method relies on the possibility of transposing laboratory results obtained on 16 cm diameter samples to a thick containment wall.

NOTATIONS :

t	Current time
t_p	Age of concrete prestressing
t_d	Age at which the concrete starts drying
σ	Stress applied to the concrete element
ϵ	Total strain of the concrete
E_b	Young's modulus of concrete
ν	Poisson's ratio (around 0.16 for creep predictions)
ϵ_{as}	Autogeneous Shrinkage strain (measured on a non-drying and non-loaded specimen)
ϵ_{ds}	Drying Shrinkage strain (measured on a drying and non-loaded specimen)
ϵ_{bc}	Basic Creep strain per MPa (measured on a non-drying and loaded specimen)
ϵ_{dc}	Drying Creep strain per MPa (measured on a drying and loaded specimen)
R	Average drying radius of the structure defined by : $R = \frac{1}{S} \iint_S d(x, \partial S) dS$ where $d(x, \partial S)$ is the distance of each point of the section to the external media. $R = \text{Radius} / 3$ for a cylinder and $R = \text{Thickness} / 4$ for a wall

1. INTRODUCTION

A large number of nuclear power plant (NPP) containments throughout the world are made of prestressed concrete. Depending on the technology used to ensure the leaktightness of the structure, there can be one or two containments and this containment can be either unlined or lined with a metallic or with a composite liner.

In any case, these structures are very thick (in the order of 100 and up to 120 cm for the 1300 MWe PWR French reactor vessel) to ensure the leaktightness function of the containment. Finally, they are usually biaxially prestressed since they are designed to withstand, in the event of a hypothetical accident, an internal pressure of the order of 0.5 MPa.

The first thing to be noticed is that this kind of thick structure is not very conventional in the civil engineering field. Indeed, the largest concrete part (a beam for example) of a long span bridge or tall building has usually a surface / perimeter ratio of less than 15 cm compared to 60 cm in the case of a 120 cm thick containment. As a consequence, a certain number of regulations, developed historically mainly for bridges or buildings, may not be well adapted for nuclear containments since they may not satisfactorily take into account the scale effect on creep and shrinkage.

Moreover, there can be two different policies concerning the structural maintenance of the level of prestressing of the containments depending on the technology chosen to prevent the corrosion of the tendons :

- Some countries like France, have a grouted tendon policy to prevent any fluid circulation at the contact of the tendons and thus ensure good protection against corrosion (there are moreover two other advantages : grouted tendons will pick up stresses a lot faster (due to friction between the grout and the tendons) and they ensure that a locally damaged tendon will still carry loads in another part of the structure). In this case, apart from a few tendons that are usually not grouted, visual and mechanical inspections are not possible. This is usually replaced by a very precise monitoring of the structure (strain gauges, invar wires, thermocouples, stress cells etc.). Thus, knowing the concrete strain, as a function of time (since once the monitoring device is installed, each measurement is not very expensive), some corrections are performed to get rid of thermal effects and a diagnosis is made allowing a short prediction over the following 5 or 10 years depending on the age of the containment. Its major drawback is that any repair is very difficult to perform and would certainly have a very high cost.
- In the second case (USA for example), the tendons are ungrouted and the prestress cables are injected with a protective grease. A visual inspection of some of the tendons is always possible every 5 or 10 years as part of an ageing management program to control their integrity and their degree of corrosion. Moreover, a direct mechanical inspection of some of the tendons (with a certain stochastic procedure) is also possible to determine the global tension loss in time and to compare it to its design value. This is of course a direct and very precise method of measurement of the concrete prestressing level. Its cost does not however permit a high frequency of measurements. Finally, in the event of corrosion trouble (that may happen more often), any tendon can be replaced and some prestressing can be added if the stress loss is too great. Furthermore, this operation can be done while the plant is still in operation.

In both cases, prediction of the time behaviour of concrete (creep and shrinkage) is very important because of its potential impact on the prestress level that in turn affects the leak-tightness and the structural integrity of the containment.

Finally, in both cases, even if the tendons are not grouted, any repair is a very difficult and costly operation and that could be avoided by a better evaluation of the

risks of using a particular concrete and by developing methodologies of assessment of the prestressing forces losses.

2. CREEP AND SHRINKAGE PREDICTION OF CONCRETE

Concrete is an ageing viscoelastic material. But this is true to the extent that creep and shrinkage of a particular concrete can be up to 2 to 6 times its elastic strain (which is quite a lot compared with steel for example).

When a particular containment is designed, the concrete is not already known and its delayed behaviour is usually evaluated (knowing only its design strength) by using regulations of the country ([3, 8] in the case of France) and sometimes international standards like CEB FIP code [9] or better international recommendations like in [5] when the mix design is already known. But although regulations give a fairly good average approximation of the delayed behaviour on a large number of concretes tested, they can significantly underestimate a particular concrete. Even very complex and powerful models like the BP-KX model [4] (for normal concrete only) proposed by Bazant are not sufficient to avoid the need for experimental measurement (direct or indirect) on the concrete that will be used *in situ* if more precise estimations are required (in this case, some parameters of the mode can be fitted on short time experimental results).

The fundamental reason for this is that, unlike steel, the physico chemical mechanisms at the origin of creep and shrinkage of concrete [11, 24] are not yet entirely understood (mainly concerning creep).

Shrinkage is nowadays fairly well identified. Hydration of cement is mainly responsible for autogeneous shrinkage [21], heat generation during hydration is responsible for thermal shrinkage together with the simultaneous increase of the mechanical properties of concrete due to hydration (ageing) [25], and drying is responsible for drying shrinkage (with the same mechanisms as for autogeneous shrinkage due to capillary tensions) [10, 22].

For concrete creep, things are much more difficult. What is now sure is that the four mechanisms that have been identified for shrinkage (hydration, heat generation, drying, ageing) play an important role in the creep process [1, 11]. Furthermore, cracking is an apparent mechanism that is involved in the drying creep process but does not explain all of it [15]. In fact, even though some very interesting theories have been put forward, the intrinsic origins of basic creep and drying creep have not yet been experimentally identified.

Furthermore, even if some of the main variables influencing the delayed behaviour of concrete are known [4, 23] such as water/cement ratio, silica-fume/cement ratio, aggregate content, maximum compactness of the aggregate skeleton [13, 18], humidity, temperature, time at loading and geometry of the specimen tested, some other parameters such as the shape of the aggregates, their mineralogy, the type of cement and its compatibility with the additives are only empirically understood. This will lead, most of the time to a half empirical formulation of the delayed behaviour of concrete which can hardly take into account all the driving parameters of creep and shrinkage.

The difficulty of predicting over a long period is not only due to poor knowledge of the physico chemical origins. In this TC, our goal is certainly not to perform fundamental research on creep and shrinkage of concrete but we have to be aware of the difficulties encountered in the modelling of the delayed behaviour of concrete. Among the difficult points, the following are of particular interest :

- The size effect of the drying part of creep and shrinkage will be very great on a thick structure such as a nuclear containment since the drying time of a structure is proportional to the square of its diameter (cf. § 4) [20].
- The lack of long and reliable experimental creep and shrinkage data on a period longer than 10 years. The direct consequence is that it will always be difficult to extrapolate the experimental curves in the long run. Some authors propose a curve that reaches an asymptote in the long run [1], others are more inclined to propose a curve equivalent to $\ln(t)$ [4]. Even if it is difficult to admit, we must be aware that most of the time, the theoretical predictions that can be made are not fully scientifically based. This is easily understandable. As long as the physico-chemical origins of creep and shrinkage are not clearer, it will always be difficult to extrapolate experimental data and any judgement will be unsure unless it has been previously verified experimentally on a similar time period. Unfortunately, the prediction of the behaviour of concrete is still a summary of a "large-scale and clever data fitting" either with mathematical curves proposed in the regulations or even by "rules of the tube" like "the strain velocity is divided by x every y years" !
- The lack of knowledge of the ageing process of creep. The containment is usually prestressed between 1 and 3 years. This is quite late compared to other structures where the concrete is prestressed at the early age (between 1 week and 3 months). Some very promising developments have been proposed recently in the solidification theory [6], but this theory still does not satisfactorily take into account in a physical way the loadings at very late age.
- The lack of biaxial creep results since Poisson's ratio plays an important role in the calculation of biaxial creep.
- The difficulty of experimental procedures (humidity, temperature and stress control are difficult to ensure, the price of the equipment is quite high and the experiments are very long).
- Interference of creep and shrinkage with cracking at the skin of concrete. This interaction (mechanical and drying coupling) is very difficult and is still a very important research issue.

All these difficulties explain the low level of confidence of a prediction at 50 years of a particular regulation formula and the necessity of an experimental monitoring of the containment together with an experimentally based ageing management program of the stress level of the containment.

3. THE IMPORTANCE OF CREEP AND SHRINKAGE TESTS

We have previously seen that the prediction of the behaviour of concrete in a thick structure such as a nuclear containment and over a very long period of time was particularly difficult and that it was not possible to rely completely on a half empirical prediction.

The assessment of the prediction of prestressing forces losses could therefore possibly rely on experimental tests on the particular concrete used. These tests, performed according to international recommendations proposed by many experts and summed up in RILEM in reference [2], could be systematically associated with mechanical tests and loss of weight tests in order to qualify the behaviour of the concrete used more completely.

These tests should be performed at the beginning of the construction of the plant on the concrete that will be used, or preferably, on different proposed concrete mixes before the choice of the final concrete mix.

The experimental data will therefore be very useful for various purposes such as :

- Comparison of the experimental data with regulations used to design the containment which will enable these regulations to be improved and the kinetics of the creep and shrinkage curves used in the design calculations to be modified.
- Choice or modification of the concrete mix like in the EDF Civaux II nuclear power plant (France) where a high strength / high performance concrete [12] has been selected for the second plant, ensuring a much lower creep together with a better leaktightness (0,19 % per day of the volume of the containment at 0.53 MPa) due to higher compactness and lower heat generation at setting.
- Choice of the right level of prestressing when the experimental results are higher than the design values like in the EDF Civaux I nuclear power plant. This is possible since prestressing of the structure starts only after 1 to 3 years.
- Choice of a monitoring frequency as early as possible for a particular containment whose concrete is known to have an important delayed behaviour.
- Assessment of the ageing management diagnosis when the behaviour of the concrete is already known in the laboratory.

4. EDF EXPERIENCE

4.1. PRESENTATION OF THE FRENCH 1300 MWE PWR REACTOR

The reactor building of a 1300 MWe nuclear power plant consists of 2 concentric containments (**Figure 1**). The inner containment, biaxially prestressed, from 90 to 120 cm thick, is designed to withstand an internal pressure of 0.5 MPa, which leads to a mean initial prestress of 8.5 MPa along zz and 12.0 MPa along $\theta\theta$. The outer containment, designed to withstand external hazards, is made of reinforced concrete. The construction of the containment lasts 5 years ; the prestressing begins at the end of the 2nd year and takes 1 year, in a complex site staging.

In an accident condition, the tightness of the structure depends mainly on the residual prestress of the concrete. But the devices for surveillance of delayed strains (wire strain gauges, Invar wires, etc.) reveal strain kinetics that regulation models [3, 8, 9], fail to incorporate in a satisfactory manner.

To improve the "management" of the set of power stations, through a better evaluation of their life, EDF undertook in 1992 a vast programme of study [16] with a view to predicting the true creep behaviour of the containments. This study includes many shrinkage and creep tests on concretes reconstituted in the laboratory, together with numerical modelling with a view to prediction of the *in situ* strains in 40 years.

In this paragraph, we will present the modelling that was developed in the finite element code CESAR in LCPC (Paris, France). In § 5, we give a simplified analysis that has been validated in details in [16] and that give a good idea of the delayed strains in the long term obtained in the finite element computations. More details can be found in [16, 19].

4.2. MODELLING OF THE DELAYED BEHAVIOUR OF CONCRETE

An elastic calculation, by finite elements, in which the structure is subjected to an external pressure (simulating the prestress), shows that in the part remote from discontinuities, $15\text{ m} < z < 45\text{ m}$, the shaft is deformed as an infinite cylinder, not

constrained by the dome or the foundation raft. This calculation is used to validate the material approach, chosen over a relatively cumbersome numerical calculation of the whole structure.

As usually, we shall distinguish drying creep from basic creep and drying shrinkage from endogenous shrinkage according to the commonly accepted definitions [11]. The engineering model we propose, of the equivalent continuum type, is based on a very simple principle : each physico-chemical component receives specific numerical treatment.

- As for the linear thermo-elastic strain, $\underline{\varepsilon}_e$, we write, conventionally :

$$\underline{\varepsilon}_e = \frac{1+\nu}{E} \underline{\sigma} - \frac{\nu}{E} \text{tr}(\underline{\sigma}) \underline{1} + \alpha \Delta T \underline{1} \quad (1)$$

- The basic creep is modelled as a function of the relative humidity h (% RH) and temperature T (K). The creep function J_{bc} , taken from [9], is then :

$$J_{bc}(t, t_c, h, T) = \frac{1}{E_0} + h \frac{T - 248}{45} \cdot \frac{28^{0.2} + 0.1}{t_c^{0.2} + 0.1} \Phi_{bc}(t_{eq}, t_c = 28, h = 1, T = 20^\circ) \quad (2)$$

$$t_{eq}(t) = \int_{s=t_0}^t \exp\left(-\frac{U_c}{R} \left(\frac{1}{T(s)} - \frac{1}{293}\right)\right) ds \quad (3)$$

The viscoelastic constitutive law we use makes it possible to take the temperature and humidity history into account. If, at time t_n , the stress, the strain, the temperature, and the humidity, assumed constant over a time interval, are known, the strain for $t \in [t_n, t_{n+1}]$ is found by writing:

$$\varepsilon_n(t) = \varepsilon_{n-1}(t) - \sigma_{n-1} J_{bc}(t, t_n, h_{n-1}, T_{n-1}) + \sigma_n J_{bc}(t, t_n, h_n, T_n) \quad (4)$$

This formulation, which corresponds to an unloading and complete reloading, then indeed satisfies the elementary criteria of continuity.

- The drying shrinkage ε_{ds} is taken as proportional to the weight loss $(\frac{\Delta P}{P})$ [1, 11, 16] :

$$\varepsilon_{ds}(t) = k \left[\left(\frac{\Delta P}{P} \right)_t - \left(\frac{\Delta P}{P} \right)_0 \right] \quad (5)$$

The term $k(\frac{\Delta P}{P})_0$ results from the fact that the shrinkage induces skin micro-cracking of the material by blocked strain (rarely visible to the naked eye).

- The drying creep ε_{dc} results from the sum of an intrinsic creep (int) proposed by Bazant and a structural effect (str) linked to the drying shrinkage :

$$\Delta \varepsilon_{dc}^{int} = \lambda \sigma |\Delta h| \quad \varepsilon_{dc}^{str} = k F(\sigma) \left[\left(\frac{\Delta P}{P} \right)_{load} - \left(\frac{\Delta P}{P} \right)_0 \right] \quad (6)$$

where $(\frac{\Delta P}{P})_{load} \leq (\frac{\Delta P}{P})_0$ is the weight loss that has already occurred at the age of loading. $F(\sigma)$ is a function of the stress and is given by :

$$\sigma \leq 0 \Rightarrow F(\sigma) = 0 \quad 0 \leq \sigma \leq 15 \Rightarrow F(\sigma) = \frac{\sigma}{15} \quad 15 \leq \sigma \Rightarrow F(\sigma) = 1 \quad (7)$$

The total delayed strain ε_{tot} is then found by adding together the different contributions:

$$\varepsilon_{tot}(t) = \varepsilon_e(t) + \varepsilon_{ds}(t) + \varepsilon_{bc}(t) + \varepsilon_{dc}^{int}(t) + \varepsilon_{dc}^{sr}(t) \quad (8)$$

It should be noted that only the basic creep must follow the constitutive law established in (4).

As for the sequencing of the calculations, a thermal calculation is performed first of all. It is followed by a calculation of hygral diffusion (transient, non-linear) in which the coefficient of hygral diffusion is a function of the water content $C(\underline{x},t)$ and of the temperature $T(\underline{x},t)$ given by the previous calculation :

$$\frac{dC}{dt} = \text{div}(D(C,T)\underline{\text{grad}}(C)) \quad (9)$$

Finally, a 3rd calculation, viscoelastic, uses the foregoing results and calculates, at each time step, the total delayed strain at each point of integration of the mesh. Note that the fact of linking the three calculations in this order presupposes some conventional decoupling hypothesis between the various delayed strains (9). The main physical parameters of the model are then determined from the results of the experimental programme, mechanical tests, a weight loss test, and a complete test of delayed behaviour (autogenous shrinkage, total shrinkage, basic creep, and creep at 50 % RH).

The results of the various simulations are given in **figure 2**, which shows the breakdown of the various delayed strains calculated on a laboratory sample of 16 cm diameter.

4.3. SIMULATION OF STRAINS ON CONTAINMENT

When the various parameters of the model have been determined, it is possible to predict the results on a structure (**figure 3**) from the staging of prestressing and the boundary conditions (in temperature and humidity) and compare the simulations performed with measurements made *in situ* over a period of 10 years (**figure 4**).

The study of the containment is limited to study of an annulus 6 m high and 120 cm wide calculated in axisymmetry. To model the initial prestress, the test body is subjected to a constant pressure along e_{zz} of $p_{zz} = 8.5$ MPa and a constant pressure along e_{rr} calculated as follows $p_r = \frac{\sigma_{\theta\theta}}{R_{ext}} = \frac{12}{24} = 0,5$ MPa to model the prestress along $\theta\theta$.

5. SIMPLIFIED PREDICTION OF PRESTRESS LOSSES

As introduced in § 4, we will now present a simplified analysis that has been validated in [16] (on 6 different French NPP of the same type with 6 different concrete mixes) giving a good idea of the delayed strains obtained in the long run in the finite element computations. More details can be found in [16, 19].

When some experimental points have been obtained in laboratory, a simple and accurate theoretical prediction can be proposed. Indeed, the kinetics of the drying part of creep and shrinkage (which represents around 60 to 70-% of the delayed strains) is a lot faster on a small laboratory sample than in a 100 cm thick wall. This method was developed and validated in [16] on 6 different (but of the same type) French nuclear power plant showing 6 different concrete mixes.

Each of the delayed strains are determined on the experimental data obtained in laboratory, for example at 28 days at a temperature of 20°C and relative humidity of 50 %. The total strain of the sample tested in laboratory is equal to :

$$\varepsilon(t) = \varepsilon_{\text{shrinkage}}(t, t_d) + \frac{\sigma}{E_b(t_p)} + \sigma \varepsilon_{\text{creep}}(t - t_p, t_d) \quad (10)$$

This corresponds to the sum of the shrinkage strain, elastic strain and creep strain.
with :

$$\begin{aligned} \varepsilon_{\text{creep}}(t - t_p, t_d) &= \varepsilon_{bc}(t - t_p, t_d) + \varepsilon_{dc}(t - t_p, t_d) \\ \varepsilon_{\text{shrinkage}}(t, t_d) &= \varepsilon_{as}(t) + \varepsilon_{ds}(t - t_d) \end{aligned} \quad (11)$$

with the natural assumption that $t_p \geq t_d$.

In order to maximise (and thus ensure a small conservatism) the measured drying creep strain, it is even proposed to use $t_p = t_d$ for the laboratory experiments. Indeed, when the concrete starts drying before loading, the creep strain is reduced [11].

If we then want to translate these equations onto the containment, the strain at time t can be computed by equation (12) where $t_p \cong 7$ days corresponds to the day when the concrete is demolded and $t_p \cong 1$ or 2 years to the age of the concrete when the prestressing begins.

$$\begin{cases} \varepsilon^{zz}(t) = \varepsilon_{\text{shrinkage}}(t, t_d) + \frac{\sigma^{zz} - \nu \sigma^{tt}}{E_b(t_p)} + (\sigma^{zz} - \nu \sigma^{tt}) \varepsilon_{\text{creep}}(t - t_p, t_d) \\ \varepsilon^{tt}(t) = \varepsilon_{\text{shrinkage}}(t, t_d) + \frac{\sigma^{tt} - \nu \sigma^{zz}}{E_b(t_p)} + (\sigma^{tt} - \nu \sigma^{zz}) \varepsilon_{\text{creep}}(t - t_p, t_d) \end{cases} \quad (12)$$

where σ^{tt} and σ^{zz} are the initial prestressing of concrete in order to maximise the concrete strain. ν is the Poisson's ratio and can be taken between 0.15 (which ensures a small conservative margin) and its elastic value (generally close to 0.2).

In equation (12), $\varepsilon_{\text{shrinkage}}$ and $\varepsilon_{\text{creep}}$ are given by :

$$\begin{aligned} \varepsilon_{\text{shrinkage}}(t, t_d) &= \varepsilon_{as}(t) + \varepsilon_{ds}(\lambda(R)(t - t_d)) \\ \varepsilon_{\text{creep}}(t - t_p, t_d) &= \varphi(T)V(t_p)\varepsilon_{bc}(t - t_p, t_d) \\ &\quad + \psi(T)[\varepsilon_{dc}(\lambda(R)(t - t_p), t_d) - \varepsilon_{bc}(\lambda(R)(t - t_p), t_d)] \end{aligned} \quad (13)$$

where the functions $\lambda(R)$, $V(t_p)$, $\varphi(T)$, $\psi(T)$ are respectively the drying size effect function, the ageing function for basic creep and two functions of the temperature to take into account the acceleration of the kinetics of basic creep and drying of concrete at a temperature different from the laboratory temperature (supposed to be equal to 20°C). They can be defined as follows but other types of function can be found in the literature or adjusted on particular experimental data :

$$\lambda(R) = \left(\frac{R_{\text{laboratory}}}{R_{\text{containment}}} \right)^2$$

$$V(t_p) = \frac{0.1 + (28)^{0.2}}{0.1 + (t_p^{\text{prestressing}})^{0.2}} \quad (14)$$

$$\varphi(T) = \psi(T) = \frac{T + 25}{45}$$

From this, a direct estimation of the loss of prestressing can then be computed according to equation (15) which gives a system where $\Delta\sigma_b^{zz}(t)$ and $\Delta\sigma_b^{tt}(t)$ are the two unknowns.

$$\begin{cases} (\Delta\varepsilon_b^{zz}(t) =) \frac{\Delta\sigma_b^{zz}(t) - \nu\Delta\sigma_b^{tt}(t)}{E_b} + \varepsilon_{\text{delayed}}^{zz}(t) = \frac{B^{zz}}{A^{zz}E_s} \Delta\sigma_s^{zz}(t) \\ (\Delta\varepsilon_b^{tt}(t) =) \frac{\Delta\sigma_b^{tt}(t) - \nu\Delta\sigma_b^{zz}(t)}{E_b} + \varepsilon_{\text{delayed}}^{tt}(t) = \frac{B^{tt}}{A^{zz}E_s} \Delta\sigma_s^{tt}(t) \end{cases} \quad (15)$$

A and B correspond to the steel section and to the concrete section respectively. E_s is the Young's modulus of steel and E_b is the Young's modulus of concrete.

This calculation is performed without any coupling between the stress of the tendons and the delayed strains of concrete in order to maximise the prestress loss. Since the prestress loss is around 10 to 15 %, this simple calculation can be considered as accurate enough as demonstrated in [16, 17]. This calculation does not take into account the loss of prestress due to steel relaxation which can be added afterwards in a very simple way.

Furthermore, it is interesting to keep in mind an idea of the value of $\lambda(R)$. If the experimental data in laboratory are obtained on a 16 cm diameter sample $R_{\text{laboratory}} = \frac{8}{3}$ and if the containment is 100 cm wide $\left(R_{\text{containment}} = \frac{100}{4} \right)$, we will have :

$$\lambda(R) = \left(\frac{8}{3} \cdot \frac{4}{100} \right)^2 = \frac{1}{87.9} \quad (16)$$

The direct consequence is that an experimental time period of one year for the drying part of the delayed behaviour of concrete will be "equivalent to" 87.9 years for the containment. Of course, this is true as long as the same mix design has been used in situ and in laboratory, which is sometimes difficult to ensure.

6. CONCLUSION

The goal of RILEM TC-MNL is not to give a complete state of the art of creep and shrinkage of concrete since it has already been done before in various occasions by very famous experts. However, our goal is to analyse the actual practices and in particular, their limits.

Most of the time, creep and shrinkage are viewed as consequences of a certain level of strength or modulus of concrete. People that are in charge of the choice of the concrete must now understand that the delayed behaviour of concrete is part of their duties and that it is possible to constitute a concrete mix with a low creep and shrinkage strain and not only a strength and a slump.

Most of the time, designers rely on not-so-well-tested regulations or recommendations to evaluate the prestress forces losses. This is not always sufficient in our opinion and a more experimentally based ageing management program is necessary when nuclear safety is concerned.

In structural calculations, the behaviour of concrete is taken into account in accordance with regulations that give an average response for the material. It should however be recalled that the delayed strains of a particular concrete (for a given range of strengths) can be rather far from the tendency indicated by the regulation. For sensitive industrial applications, it is therefore recommended that a study of the delayed behaviour of the concrete used should be undertaken when the building of the structure is started. In the case of nuclear containments, the shrinkage and creep results obtained in the laboratory are used to judge the delayed strains to come and therefore the life of the structure.

Finally, what we propose is a systematic experimental program on the concrete that will be used or that is intended to be used. Thus, with a low cost program (for less than \$US 20,000), lots of results will be available on the concrete and theoretical extrapolations, experimentally based, can be proposed. Whatever the technology chosen for the construction of the containment, this will reduce the risk of problems and the costs of maintenance of concrete prestressing.

However, the phenomena of delayed strains can be investigated only by relatively long tests (2 years) ; for other applications, this time is sometimes incompatible with construction site planning. If it is desired to guard against the hard-to-control influence of the constituents (aggregates, binder), the use of a high-performance concrete (compatible with the design criteria of the structure), one that is particularly good in terms of shrinkage and creep [12], can help to substantially reduce the risks related to losses of prestress.

ACKNOWLEDGEMENTS :

The authors would like to express their gratitude to Mr Costaz (EDF), Prof. Acker (LCPC), Prof. Torrenti (CEA) and to Dr. Naus (Chairman of RILEM TC-MNL).

REFERENCES

- [1] Acker P. (1988) 'Comportement mécanique du béton : apports de l'approche physico-chimique', Rapport de recherche LPC n°152.
- [2] Acker P. (1993) 'Recommendations for measurement of time dependant strains of concrete loaded in compression', Proceedings of the 5th International RILEM Symposium on 'Creep and Shrinkage of Concrete' (ConCreep5), RILEM TC-107, Subcommittee. 4.
- [3] BAEL (1991) 'Règles techniques de conception et de calcul des ouvrages et constructions en béton armé suivant la méthode des états limites', Fascicule 62 de CCTG, French code for reinforced concrete.
- [4] Bazant Z. P., Kim J. K. (1991) 'Improved prediction models for time dependant deformations of concrete : Part 1 to 6', Materials and Structures, 25, 219-223.
- [5] Bazant Z. P., Xi Y. P., Baweja S. (1993) 'Preliminary guidelines and recommendations for characterising creep and shrinkage in structural design codes', Proceedings of the Fifth International RILEM Symposium on 'Creep and Shrinkage of Concrete' (ConCreep5), TC 107, Subcommittee 1.
- [6] Bazant Z. P., Prasannan S. (1989) 'Solidification theory for concrete creep. Part I : Formulation ; Part II, Verification and application', J. Engng. Mech., Vol. 115, pp. 1691-1725.
- [7] Bazant Z. P., Xi Y., (1994) 'Drying creep of concrete : constitutive model and new experiments seperating its mechanisms', Materials and Structures, 27, pp. 3-14.
- [8] BPEL (1991) 'Règles techniques de conception et de calcul des ouvrages et constructions en béton précontraint suivant la méthode des états limites', Fascicule 62 de CCTG, French code for prestressed concrete.
- [9] CEB FIP model (1990) General task group n°9, Evaluation of the time behaviour of concrete.
- [10] Coussy O. (1994) 'Mechanics of porous continua', J. Willey & sons.
- [11] ConCreep4 (1986) Proceedings of the Fourth International RILEM Symposium on 'Creep and Shrinkage of Concrete : Mathematical Modelling', Z. P. Bazant and F. H. Wittmann Editors, Evanston, USA.
- [12] de Larrard F., Ithurralde G., Acker P., Chauvel D. (1990) 'High-Performance Concrete for a Nuclear Containment', 2nd Int. Conf. on "Utilisation of HSC", Berkeley, ACI SP, pp. 121-127.
- [13] de Larrard F., Le Roy R. (1992) 'Relation entre formulations et quelques propriétés mécaniques des bétons à hautes performances', Materials and Structures, 25, pp. 464-475.
- [14] Granger L., Torrenti J.-M., Diruy M. (1994) 'Simulation numérique du retrait du béton sous hygrométrie variable', Bull. liaison Labo. P. et Ch., 190, mars-avr., pp. 57-64.
- [15] Granger L., Acker P., Torrenti J.-M. (1995) 'Discussion of "Drying creep of concrete : constitutive model and new experiments separating its mechanisms" by Z. P. Bazant and Y. Xi', Materials and Structures, 27, pp. 616-619.
- [16] Granger L. (1995) 'Comportement différé du béton dans les enceintes de centrales nucléaires - analyse et modélisation', PhD thesis of *Ecole Nationale des Ponts et Chaussées* (France).

- [17] Granger R., Le Roy R. (1995) 'Le problème des déformations différées du béton précontraint et du béton armé : fluage combiné du couple acier béton', Bull. liaison Labo. P. et Ch., 197, mai-juin, pp. 13-18.
- [18] Granger L. Bazant Z. P. (1995) 'Effect of composition on basic creep of concrete and cement paste', J. of Engng Mech., ASCE, 121 (11), pp. 1261-1270.
- [19] Granger L., Torrenti J.-M. (1995) 'Evaluation of the lifespan of a nuclear PC vessel in terms of delayed behaviour and loss of prestress', IABSE Symp. on Extending the lifespan of structures, San-Francisco, pp. 1411-1416.
- [20] Granger L., de Larrard F., Torrenti J.-M., Acker P. (1995) 'Thoughts about drying shrinkage : scale effects and modelling', Accepted for publication in Materials and Structures.
- [21] Hua C. (1995) 'Analyse et modélisation du retrait d'autodessiccation de la pâte de ciment durcissante', Etudes et recherches des Laboratoires des Ponts et Chaussées, Série ouvrages d'art, OA 15.
- [22] Lassabatère T. (1994) 'Approche thermo-poro-hydromécanique en milieu non saturé, application au retrait de dessiccation du béton', PhD thesis of *Ecole Nationale des Ponts et Chaussées* (France).
- [23] Le Roy R. (1995) 'Prévision des déformations instantannées et différées des bétons à hautes performances', PhD thesis of *Ecole Nationale des Ponts et Chaussées* (France).
- [24] Neville A. M., Dilger W. H., Brooks J. J. (1981) 'Creep of plain and structural concrete', Construction Press, Longman Group Ltd, England.
- [25] Torrenti J.-M., Paties C., Piau J.-M., Acker P., de Larrard F. (1992) 'La simulation numérique des effets de l'hydratation du béton', Colloque Stru Co Me, Paris.

Figure 1 : Simplified diagram of containment and prestress for the French 1400 MWe PWR of the N4 series.

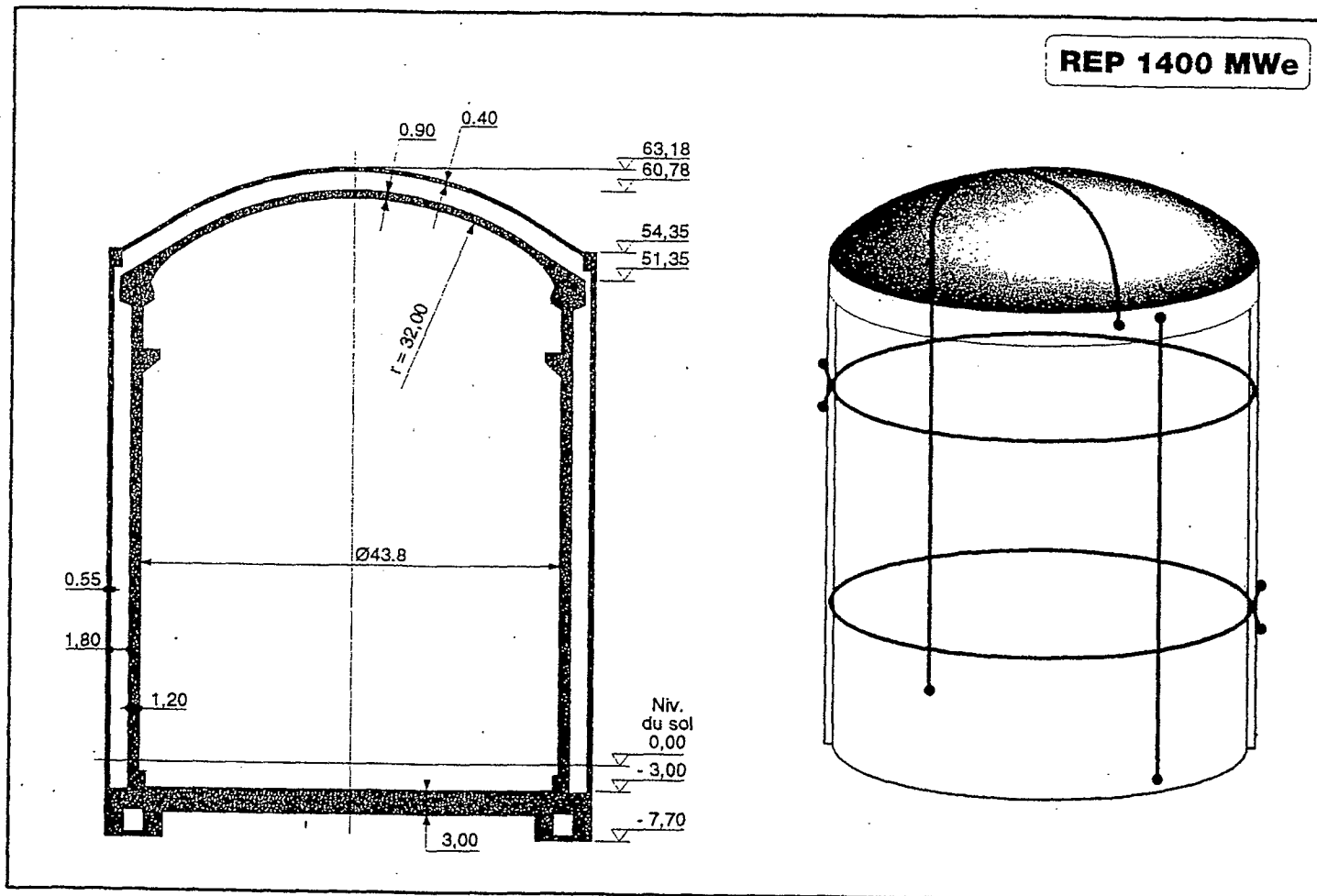


Figure 2 : Breakdown of delayed strains of Paluel on specimen \varnothing 16 cm.

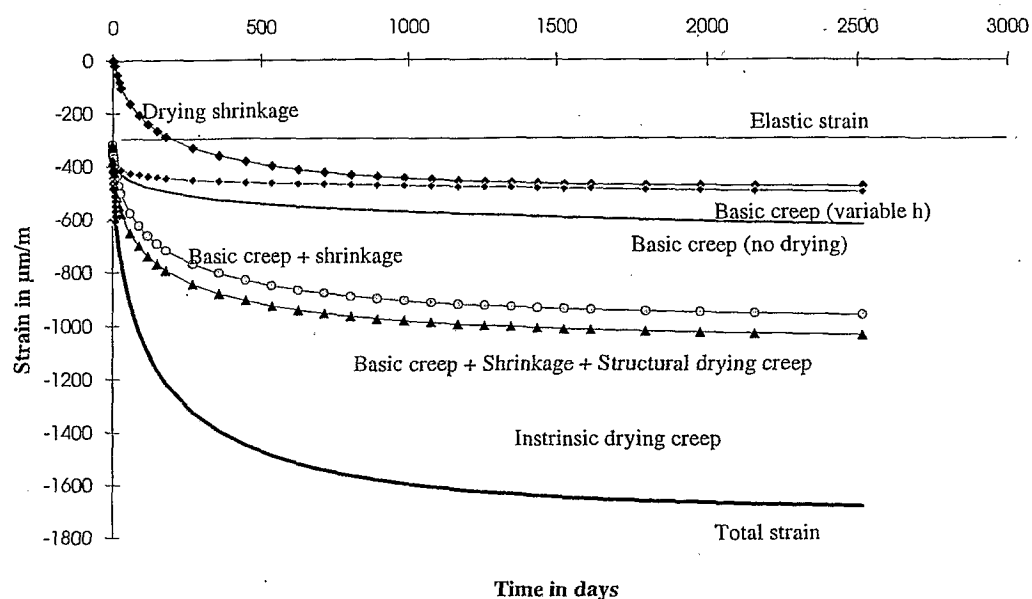


Figure 3 : Simulations of Paluel containment for a constant initial prestress.

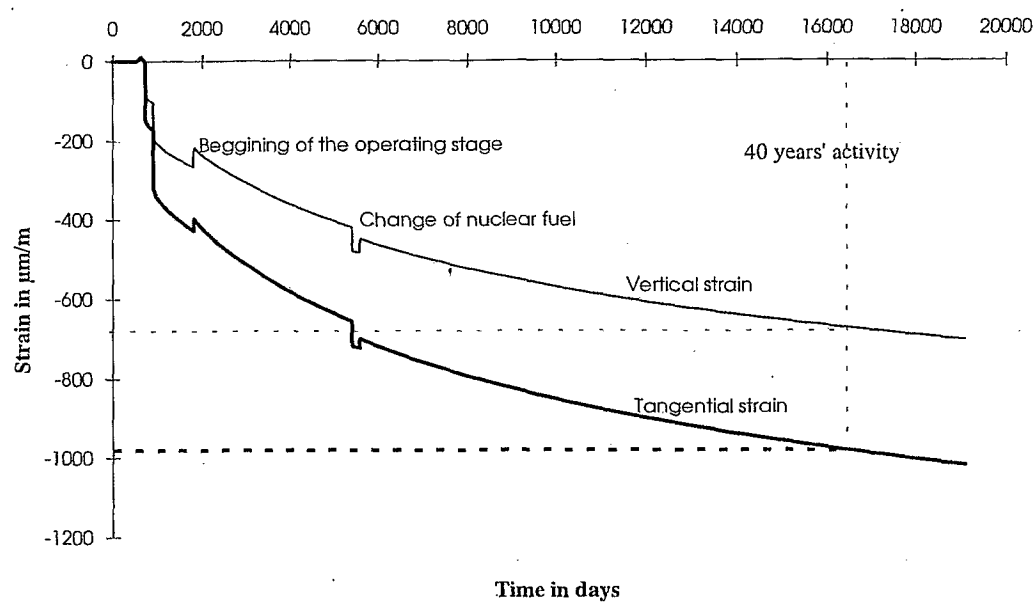
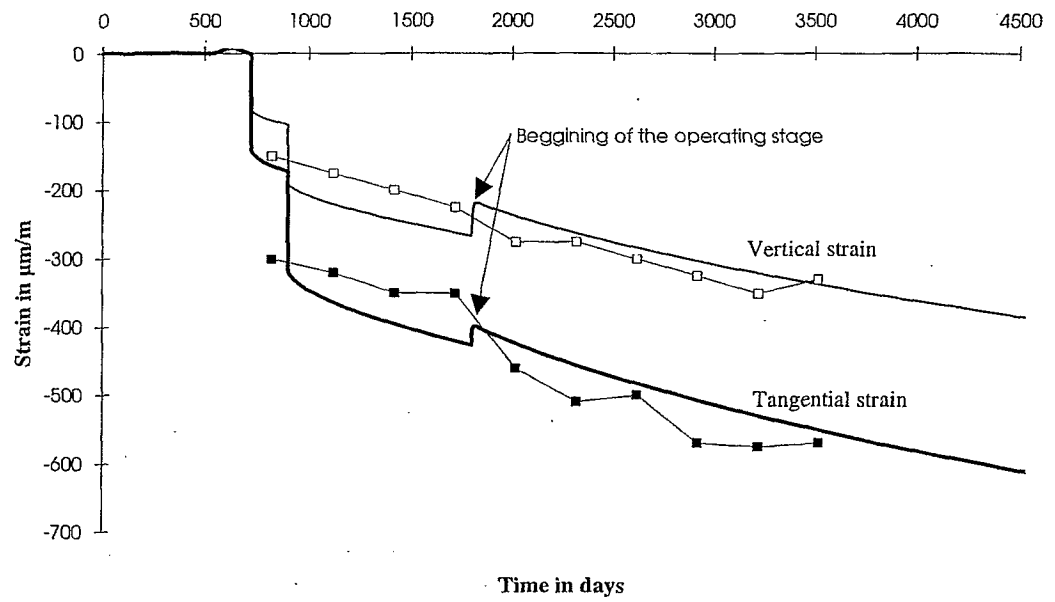


Figure 4 : Comparison between simulations and *in situ* measurements over a 10-year period.



PRESTRESS BEHAVIOUR IN BELGIAN NPP CONTAINMENTS

*Paper presented at the joint WANO-PC/OECD-NEA workshop on
prestress loss in NPP containments, Poitiers 25-26 August 1997.*

AUTHORS : L. de Marneffe, Principal Engineer,
BELGATOM, Technical Department, Civil Works Branch
Avenue Ariane 7, B1200 Brussels
Tel : 32-2- 7738148 Fax : 32-2-7738970

Ph. Simoens, Section Manager,
BELGATOM, Quality Assurance,
Avenue de l'Industrie 1, B4500 Tihange
Tel : 32-85-243087 Fax : 32-85-243079

L. Imschoot, Engineer,
BELGATOM, Technical Department, Civil Works Branch
Avenue Ariane 7, B1200 Brussels
Tel : 32-2- 7739862 Fax : 32-2-7738970

ABSTRACT

In each Belgian NPP prestressed containment building, prestress behaviour is monitored by a double system, as required in regulations :

- lift-off of several grease-injected tendons (other tendons are cement grouted);
- strain deformation of concrete.

The paper emphasizes the monitoring system and presents an interpretation of the measurements made during a period of some 20 years.

Due to the degradation of several devices, the re-instrumentation of one containment is under way. The paper describes this re-instrumentation and the related difficulties.

1. Introduction

Located at the centre of Europe, Belgium generates about 60% of her electricity in Nuclear Power Plants. Seven PWR plants are shared among 2 sites (fig 1): Tihange, on the river Meuse, and Doel, near the North Sea on the river Scheldt.

Table 1 summaries of the main characteristics of each plant.

TABLE 1 - BELGIAN NUCLEAR POWER PLANTS		
	<u>Power</u>	<u>Year of First Operation</u>
Doel 1-2	2*392 MW	1975
Doel 3	970	1982
Doel 4	1001	1985
Tihange 1	962	1975
Tihange 2	960	1983
Tihange 3	1015	1985

2. Presentation of Belgian NPP containments

2.1 General design

Belgian NPP Reactor Buildings were all designed with :

- an inner containment able to withstand the pressure and energy releases which would result in the unlikely event of an accident such as a pipe break;
- an outer containment providing protection against external hazards such as an aircraft crash;
- between both containments, an annular space ensuring that any radioactivity released from the inner containment would not leak to the environment.

2.1.1 Doel 1-2

The twin NPPs of Doel 1-2 have a spherical steel containment inside a reinforced concrete building (fig 2.1).

As these containments are not prestressed, we will not further discuss Doel 1-2 in this paper.

2.1.2 Other Plants

The containments of the five other NPPs have the same classical lay-out (fig 2.2) :

- an inner prestressed concrete containment covered on the inside with a steel liner (6 mm);
- an annular space;
- an outer reinforced concrete containment.

The containments of Doel are founded on sand through piles (fig 2.1 and 2.2). The containments of Tihange are founded directly on rocks (fig 2.3 and 2.4).

Table 2 gives the main dimensions of each containment.

TABLE 2 - MAIN DIMENSIONS OF BELGIAN NPP CONTAINMENTS (m)				
	Doel 3-4	Tihange 1	Tihange 2	Tihange 3
Inside Diameter	21.25	21	21	21
Wall Thickness	0.85	0.7	0.8	0.8
Annular Space	2.9	2	2.4	3
External Wall	1.2	0.5	1.2	1.3
Dome Inside Radius	32.8	30.5	33.3	33.3
Wall Height	48	51	55	63

2.2 Safety criteria

All containments were designed according to the requirements of U.S. rules, among other :

- ASME III Division 2 CC 3000 "Concrete Containments" for the design of the shell and the liner.
- Regulatory Guide 1.90 - "Inservice Inspection of prestressed concrete containments with grouted tendons" which defines the instrumentation for monitoring the prestress level.

Procedures were recently updated to take into consideration the requirements of ASME XI (1992) Subsections IWE and IWL for the inservice inspection of liners and prestressed concrete.

2.3 Prestressing

Containments were built using the technology of cement grouted tendons. Nevertheless, to comply with the regulations, 3 tendons of each group were grease- injected with the purpose of monitoring their load by lift-off.

Table 3 gives the main characteristics of the prestress layout of each containment.

Freyssinet's prestress system was used. Tendon ultimate capacities range from 3000 kN to 10000 kN according to the evolution of the technology, the most recently built containments being prestressed with the most powerful tendons.

TABLE 3 PRESTRESS LAYOUT				
<u>Cylinder Vertical Prestress</u>				
- Doel 3-4	:	from ring to basement gallery		
- Tihange 1	:	from ring to basement gallery		
- Tihange 2-3	:	from ring to ring, through U tubes at base slab level		
<u>Cylinder Hoop Prestress</u>				
	<u>Butresses</u>	<u>Tendon Length</u>	<u>Ultimate Tendon Capacity</u>	
- Doel 3-4	:	2	360°	10000 kN
- Tihange 1	:	5	270°	3000 kN
- Tihange 2	:	4	270°	3000 kN
- Tihange 3	:	3	360°	10000 kN
<u>Dome Prestress:</u>				
	<u>Frames</u>	<u>Ultimate Tendon Capacity</u>		
- Doel 3-4	:	3 frames at 120°	10000 kN	
- Tihange 1	:	3 frames at 120°	3000 kN	
- Tihange 2	:	3 frames at 120°	6000 kN	
- Tihange 3	:	3 frames at 120°	6000 kN	
<u>Base Slab Prestress</u> : The base slabs of the 3 units of Tihange are slightly prestressed as shown on fig 2.5.				

3. Inservice inspection

3.1 Monitoring design

At the design stage, monitoring devices were included to follow-up the evolution of the prestress along the years:

- lift-off devices for several greased tendons of each containment;
- strain measuring devices or loads cells (see table 4).

This instrumentation corresponds to RG 1.90 : prestress behaviour is evaluated from the monitoring results. Full internal pressure tests, with corresponding deformation monitoring are not required.

TABLE 4 - CONCRETE STRESS/STRAIN MONITORING DEVICES

Doel 3	:	78 pressure cells + 70 strain gauges + 33 C.W. strain gauges
Doel 4	:	78 pressure cells + 108 strain gauges + 90 C.W. strain gauges
Tihange 1	:	203 vibrating wires
Tihange 2	:	240 vibrating wires
Tihange 3	:	232 vibrating wires + 80 pressure cells

3.2 Ageing management programme

An Inservice Inspection Program was implemented for each containment. The program was updated recently to follow the evolution in regulations, i.e. to include the requirements of the IWE and IWL Subsections of ASME XI (1992).

The programs include :

- visual inspection of prestressed concrete and liner;
- lift-off of grease injected tendons;
- measurement of strain (stress) in the concrete.

Let us mention also the use of test beams at Tihange 2 in order to follow the long term behaviour of the prestress material itself. These beams are 5 m long, contain one tendon with its anchorage, are prestressed and grouted. They are stored in environmental conditions similar to those of the containment shell. At intervals of several years, a beam is cut and its materials examined in a laboratory.

3.3

Lift-off

Lift-off is a mechanical process: Two bearing plates are installed at the end of a grease injected tendon. Jacks and wedges are inserted between the plates (fig 3.1). When the pressure is injected in the jacks, the distance between bearing plates is modified.

A curve is drawn showing the evolution of this distance as a function of the load in the jacks (fig 3.2). The curve has an inflexion point (Point A) :

- for a small pressure in the jacks, wedges remain stressed; the system is stiff (AB domain);
- for higher values of the pressure, wedges are unstressed and can be removed; the load is transferred directly in the tendon; the system is more deformable (AC domain).

A tangent to curve AC is drawn at point A (tangent AD). Its intersection with the ordinate axis is deemed to give the current load in the tendon.

There are several ways to measure the displacement between bearing plates :

- micrometer reading for several values of the pressure in the jacks ; or
- injecting pressure in the jacks until it is possible to insert a calibrated gauge between bearing plates (this is repeated for several thickness of the gauge); or
- injecting pressure in the jacks to move the bearing plate, then inserting a calibrated gauge, releasing the pressure to block the gauge and reading the pressure at the manometer. (This is repeated for several thickness of the gauge).

Anyway, this mechanical procedure is quite lacking in accuracy. Indeed, if the theoretical curve is bi-linear (fig 3.2), actual curves can be continuous (see fig 3.3) and their graphical interpretation very difficult.

3.4

Strain monitoring

Strain monitoring of concrete is performed with 4 kinds of devices :

- vibrating wires cast in concrete. Electromagnetic excitation allows the measurement of their natural frequency. Indeed, a variation of the strain in the concrete induces a variation of the strain of the tensioned wire and thus of its natural frequency.

A typical distribution of the devices in the structure is :

- * 15 % in the base slab,
- * 43 % in the cylinder in the horizontal direction,
- * 17 % in the cylinder in the vertical direction,
- * 10 % in the dome,
- * 15 % around large penetrations.

At each location, vibrating wires are installed near each face of the concrete so as to be able to evaluate bending strains.

- electric strain gauges cast in the concrete. A modification of the strain in the concrete induces a modification of the resistivity of the gauge.
- pressure cells. They are small flat jacks cast in the concrete. A measurement requires to put the cell under pressure again.
- strain gauges for civil works at the face of concrete. Pairs of brackets are glued to the concrete, each separated by 30 cm. The variation of their distance is monitored with a portable micrometer.

3.5 Prestress behaviour

All the measurements done so far confirmed the good behaviour of the prestress.

For example, fig 3.4 shows the evolution of the load in a tendon of a dome. It is in accordance with the expected evolution estimated at the design stage. The estimation was done according to the material parameters of the FIP-CEB code of the seventies .

Fig 3.5 shows the evolution of the strain in the domes of Tihange 2 and 3. The two domes have a similar design, but the second was cast 5 years after the first. They show a similar behaviour with a long term evolution lower than theoretically foreseen. The curves give the mean values of the results of several vibrating wires in the domes.

4. Problems related to prestress monitoring

4.1 Lift-off

Several difficulties were experienced with the lift-off procedure. Indeed, for several tendons, the load in the jacks has reached the yield load of the tendon while the wedges were not yet freed from the bearing plates.

Those difficulties can be explained by geometrical particularities (fig 4.1) :

- the geometry of the containment and the layout of the tendons imposed a slight curve of the duct a few meters behind the bearing plate;
- the tendon is made of strands. Each strand was threaded in the duct, one after the other. The first strand took the best location in the duct, the next had more difficulties to find a path, and the last took only what was possible.

As a consequence, a kind of "knot" exists in the tendon, a few meters behind the bearing plate. This is of no consequence when the tendon is stressed for the first time. But now, each time the lift-off procedure is applied, the knot is tightened harder and does not seem to release. The extra deformations applied with the lift-off procedure correspond to extra strains in the first meters of the tendon.

The interpretation of available data shows that :

- obviously, the tendon is currently highly stressed;
- it is not possible now to measure by lift-off the exact value of the current load;

- if, in the future, the current load in the tendon is reduced due to creep and relaxation, it will then be possible to remove the wedges again and to proceed with a correct measurement of the load;
- there is a possibility that a strand may break during the lift-off procedure. Instruction was given to lift-off operators to avoid excessive pressure in the jacks.

One way to overcome this difficulty would be to replace this mechanical procedure by new permanent devices such as special vibrating wires or electrical strain gauges. The advantages of this would be the ability to monitor permanently and with precision the load in the tendon without applying extra strains to the steel.

4.2 Strain measurement

Table 5 shows the performance of each kind of device.

TABLE 5 - DEVICES PERFORMANCE			
<u>Vibrating Wires</u>			
	<u>Total</u>	<u>Operative</u>	
Tihange 1 :	203	124 (61%)	after 20 years
Tihange 2 :	240	212 (88%)	after 15 years
Tihange 3 :	232	213 (91%)	after 10 years
<u>Pressure Cells</u>			
	<u>Total</u>	<u>Operative</u>	
Doel 3 :	78	0	after 15 years
Doel 4 :	8	0	after 12 years
Tihange 3 :	80	39 (48%)	after 10 years
<u>Strain Gauges</u>			
	<u>Total</u>	<u>Operative</u>	
Doel 3 :	70	43 (61%)	after 15 years
Doel 4 :	108	94 (87%)	after 12 years

Vibrating wires are robust. Electrical strain gauges have also a good performance.

The result is not so good where pressure cells are concerned: more and more of these devices are defective. That is the reason why a replacement program is under way concerning the containment of Doel 3.

5. Re-instrumentation at Doel 3 NPP

5.1 New devices

146 new vibrating wires are fitted to the inner containment at Doel 3. Indeed, following the experienced robustness of vibrating wires cast since more than 20 years in the concrete of Belgian containments, it was decided to use the same kind of device for the re-instrumentation project.

These strain gauges (fig 5.1) consist of cylindrical housing containing a tensioned wire, electromagnetic excitation and pick-up coils. Watertight sliding heads, to which the vibrating wire and mounting blocks are attached, terminate both ends of the gauge. The heads offer minimal resistance to movement in the longitudinal direction of the gauge. They are secured to the mounting brackets which are screwed-glued at the face of the concrete.

5.2 Interpretation

These new devices are the origin of an interpretation problem. Indeed, they will give information with regard to further concrete strain evolution, with a reference "zero" strain recorded the day of their installation. If we want an estimation of the total strain, i.e. including strain evolution from construction time up to date (fig 5.2), it is necessary to correlate, as far as possible, new measures with measures coming from old devices.

This correlation is partly possible. Indeed, fig 5.3 shows the evolution of the strain in a dome measured according to two procedures: strain gauges inside the concrete and hand measurement at the faces. Let us notice the seasonal variation of the hand measured curve (theoretical thermal correction is applied to the values of the curve). This seasonal variation does not appear for the strain inside the concrete. Nevertheless, there is a fair correlation between the two curves.

Furthermore, if we look at the strains measured in a section during a pressurisation test (fig 5.4), we notice a good correlation of flexure strains with the strains measured at the face of the concrete.

As a consequence, we are preparing a correlation procedure between new and old devices :

- where possible, new devices will be located as near as possible to old devices;
- current strain at the location of new devices will be estimated by interpolation from available data from adjacent devices in the concrete (where possible);
- a new reference strain ("zero" strain) will be measured at the installation of each new device;
- the total strain evolution due to concrete creep and steel relaxation equals the sum of those two values.

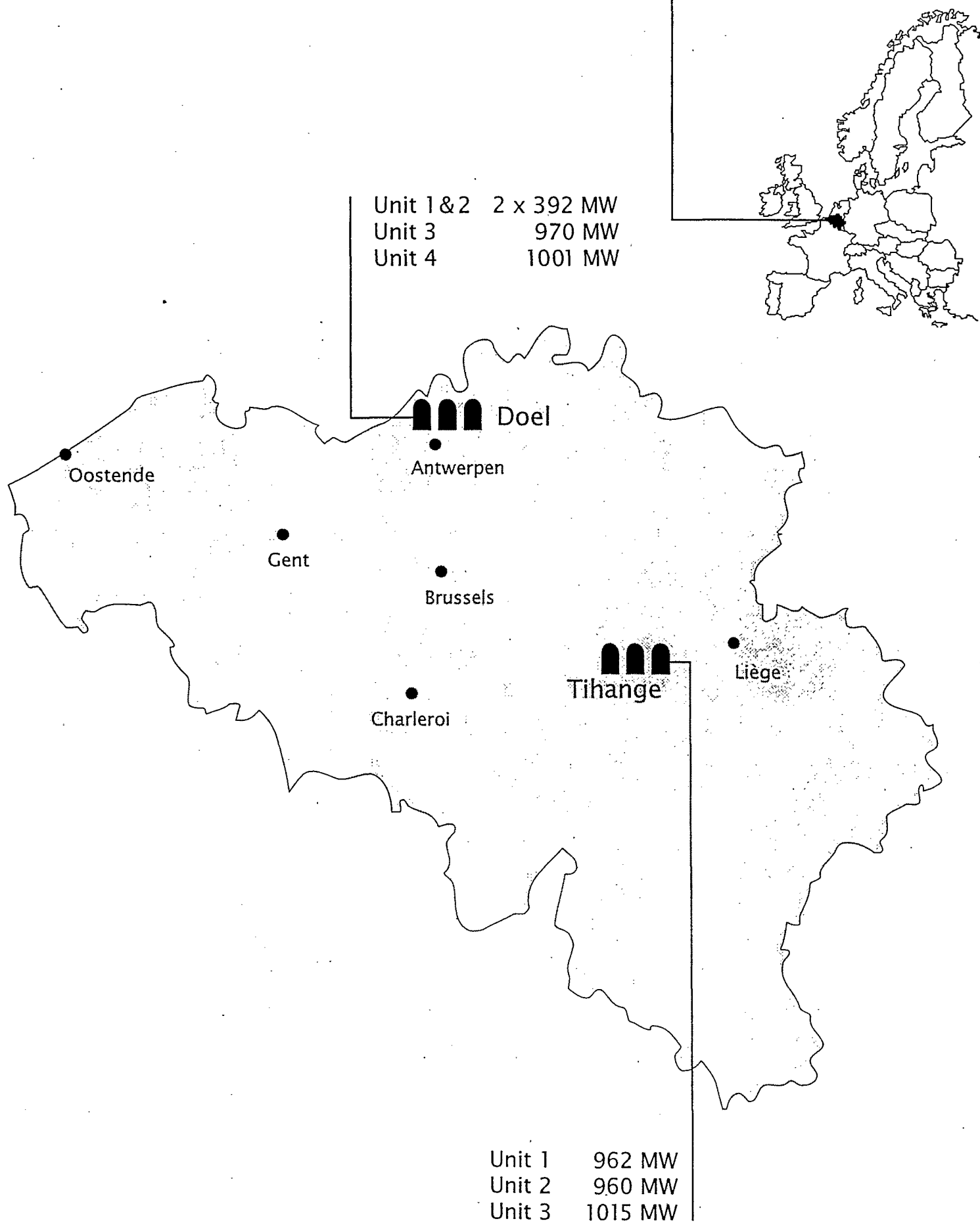
6. Conclusions

Up to now, Belgian NPP containments show a correct behaviour: time evolution of concrete and prestress is slower than anticipated.

Vibrating wires appear to be robust devices. Meanwhile, due to deficiency of pressure cells, a re-instrumentation project is under way for the Doel 3 NPP.

For the future, it is expected that a "new generation" of measuring devices will be available which would be robust, cheaper and more accurate.

Nuclear Power Plants in Belgium



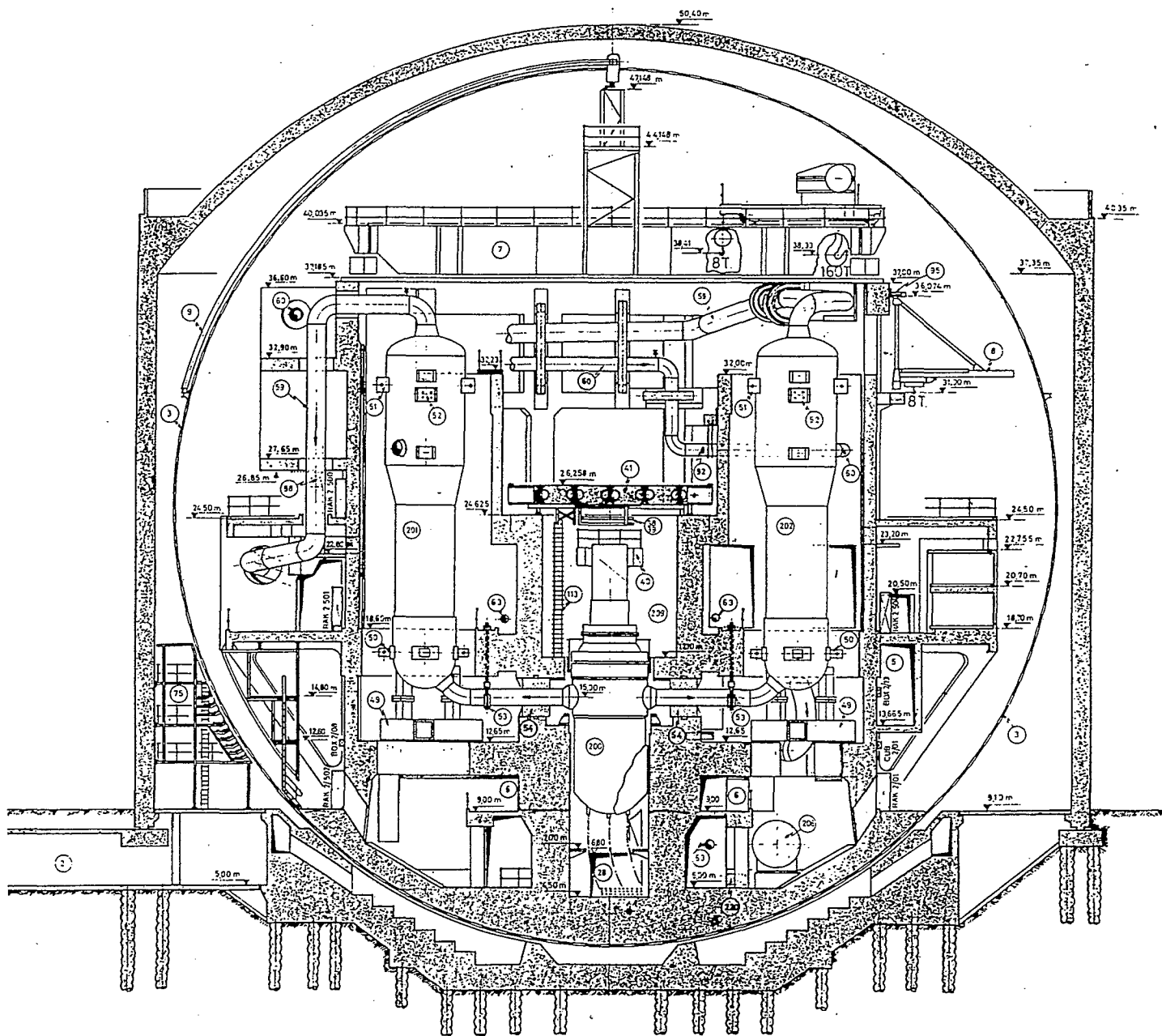


Fig. 2.1 DOEL 1-2 : REACTOR BUILDING

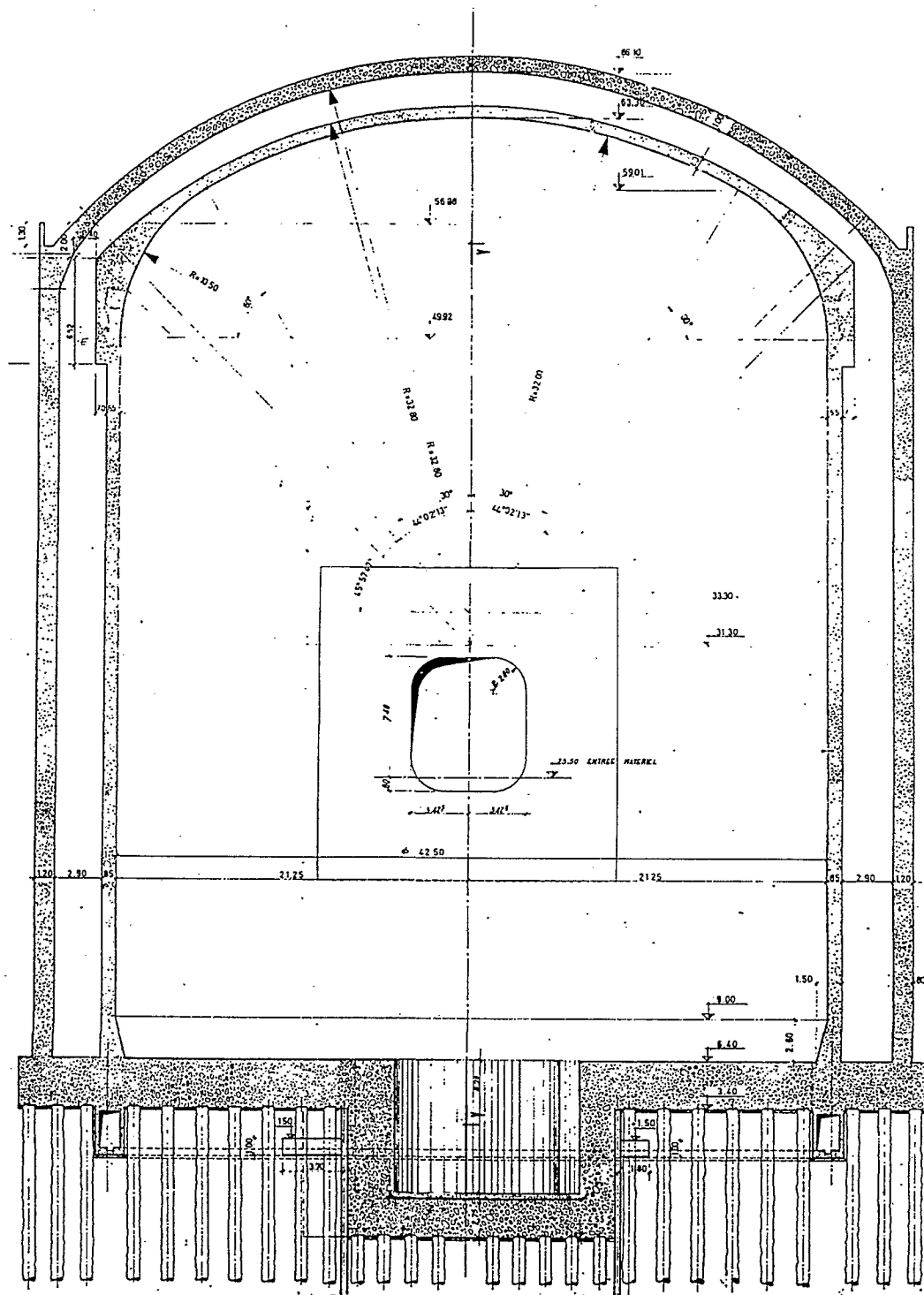


Fig. 2.2 DOEL 3 : REACTOR BUILDING

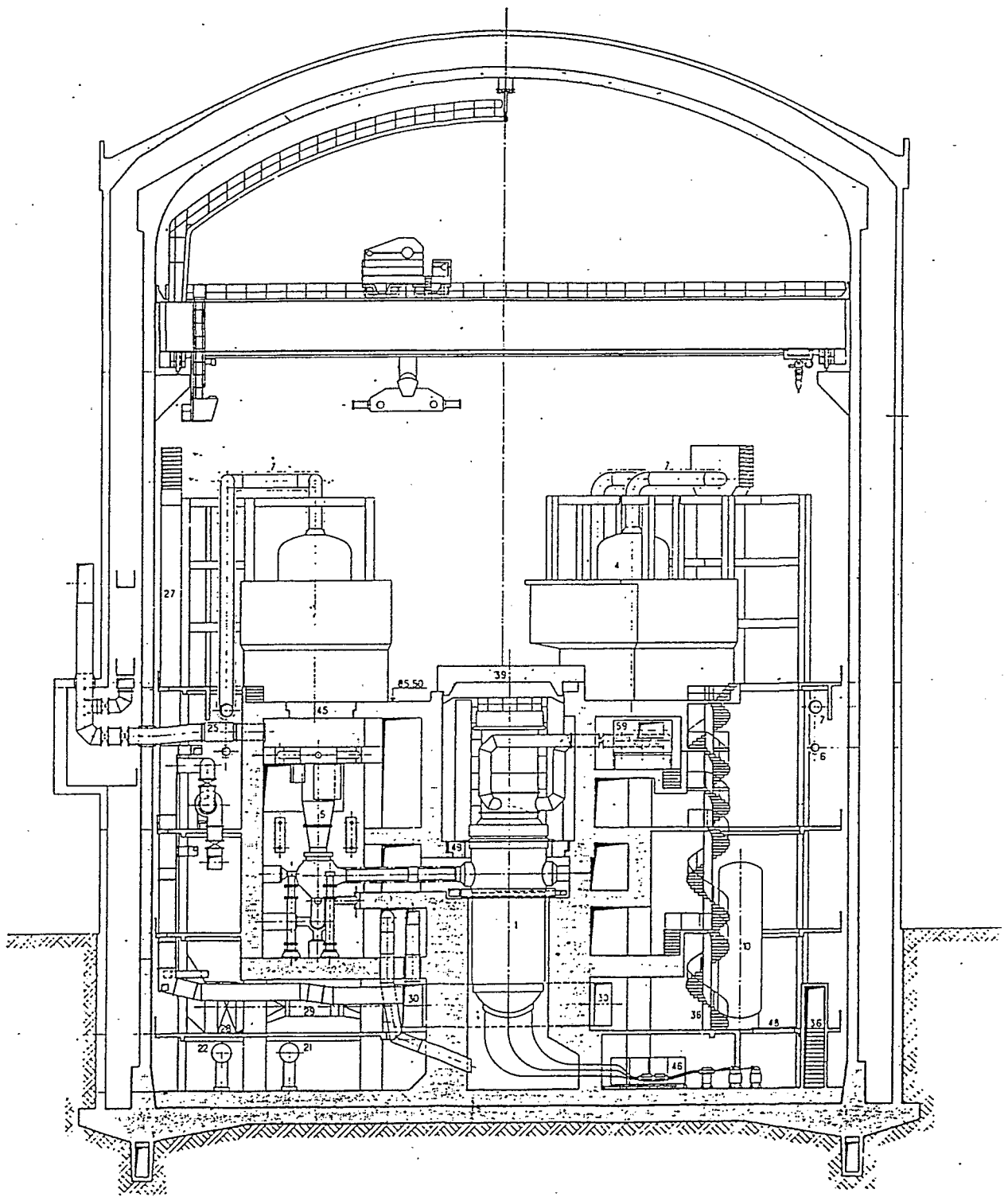


Fig. 2.3 TIHANGE 1 : REACTOR BUILDING

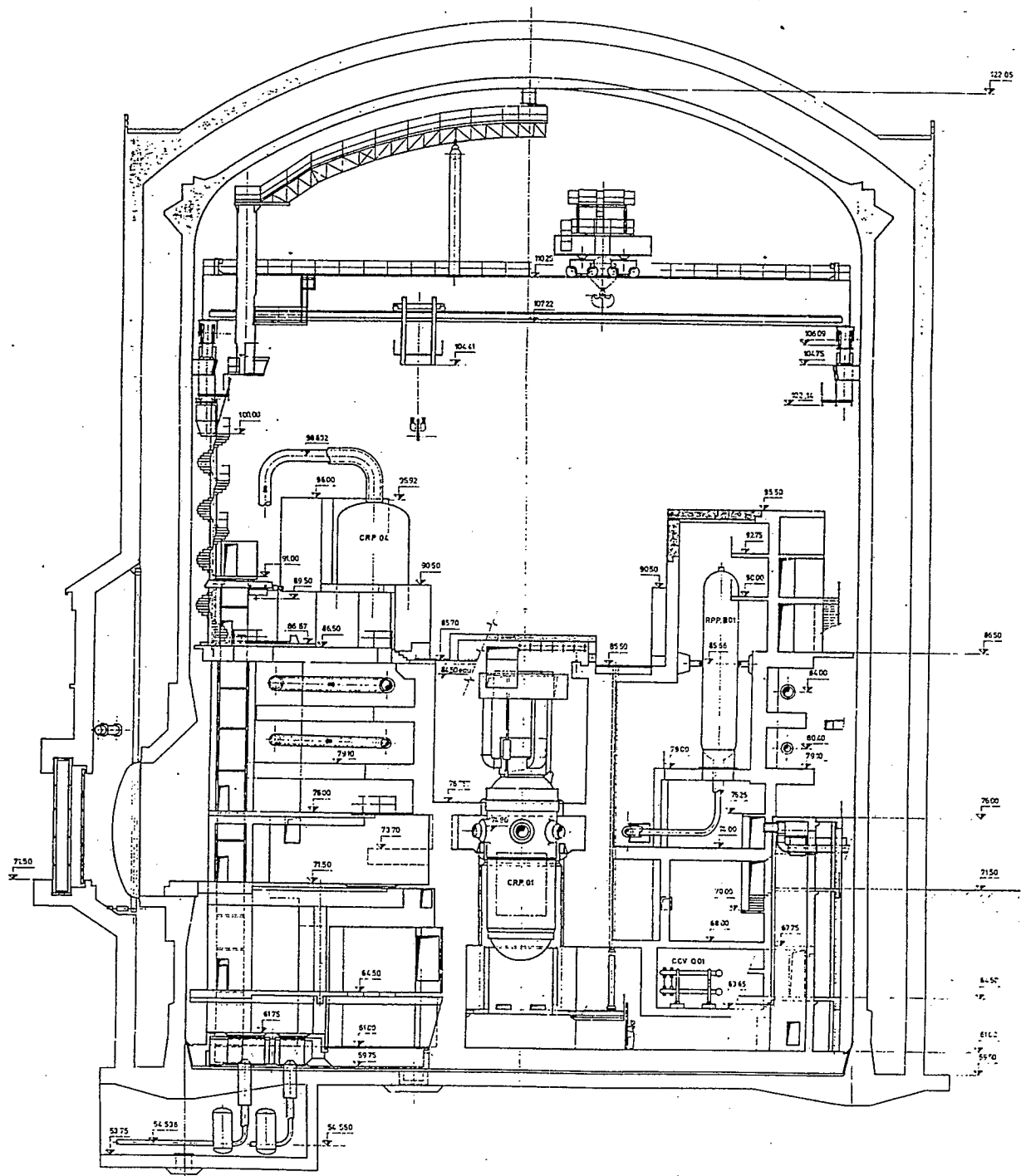


Fig. 2.4 TIHANGE 2 : REACTOR BUILDING

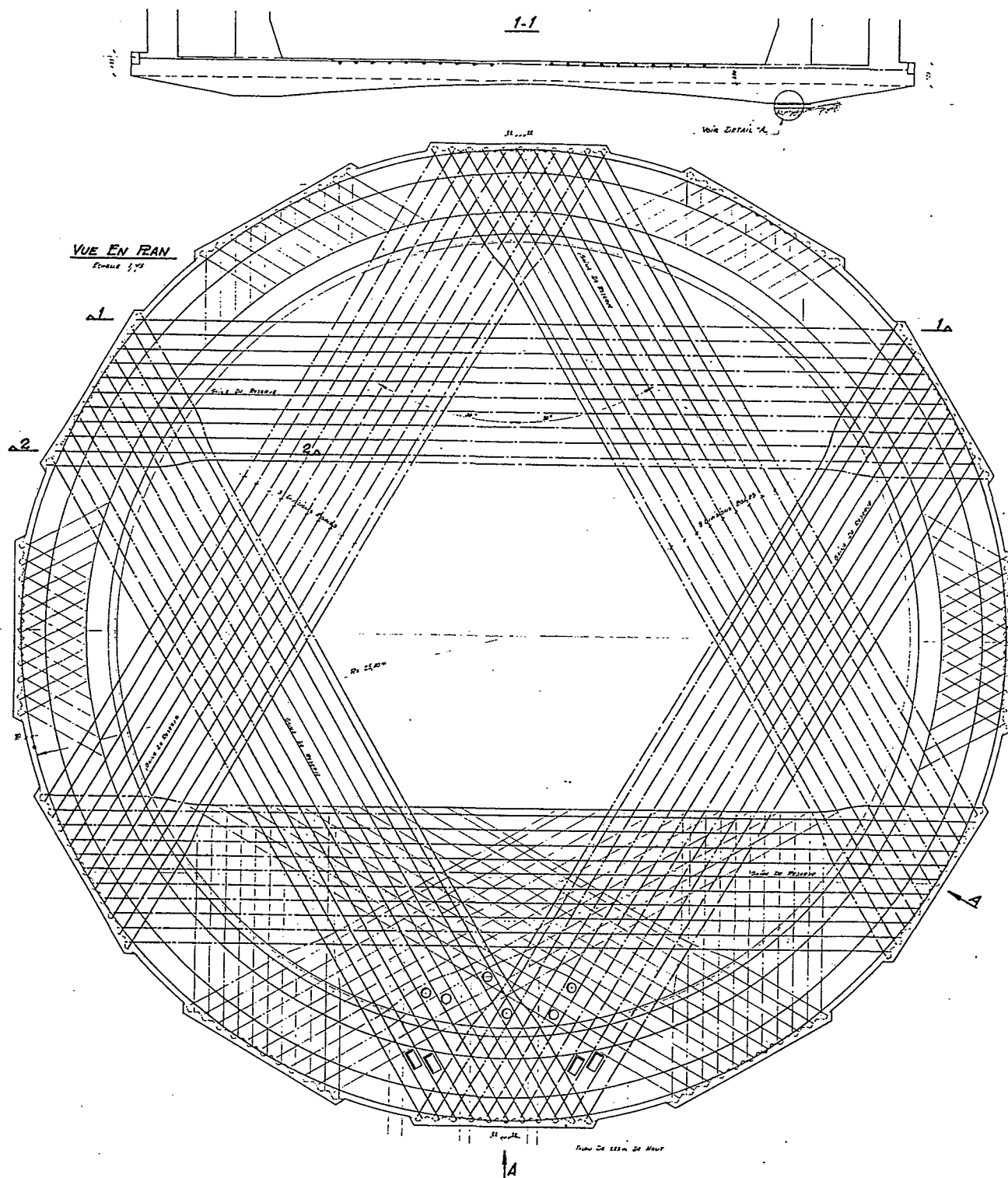


Fig. 2.5 TIHANGE 2 : BASESLAB PRESTRESS

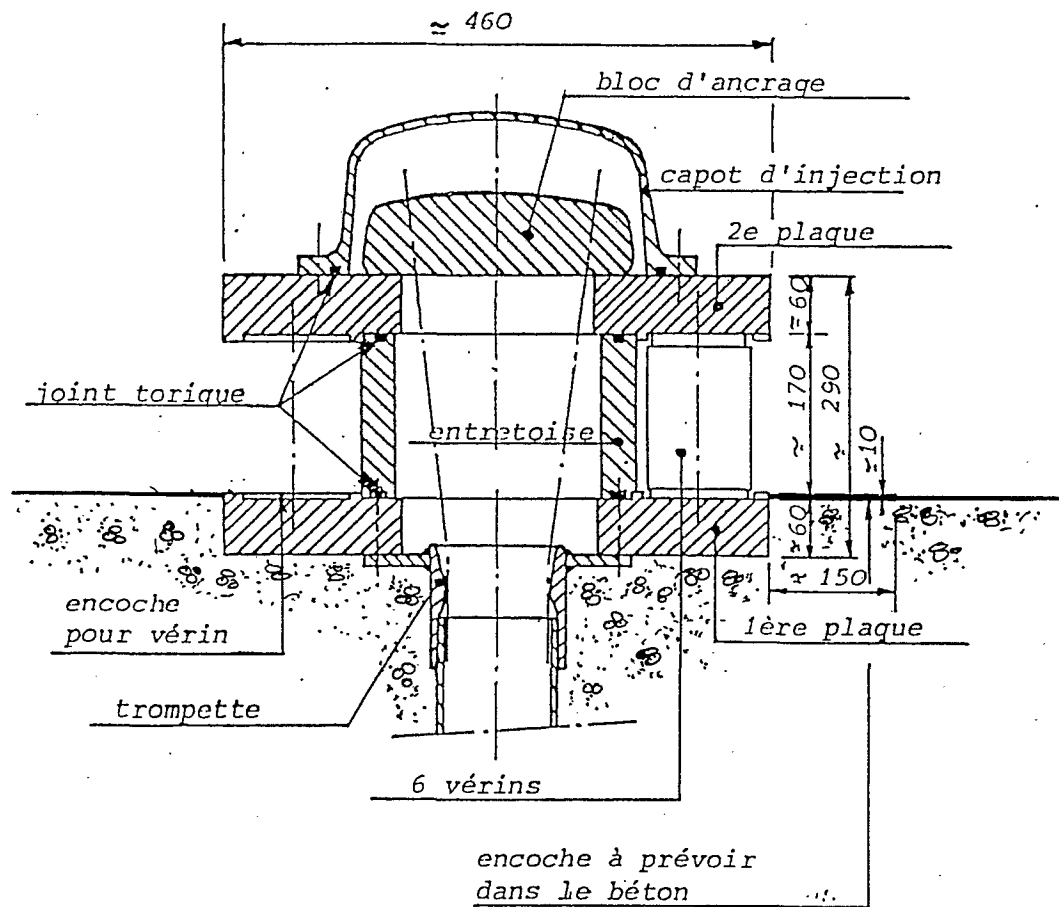


Fig 3.1 - LIFT - OFF BEARING PLATES

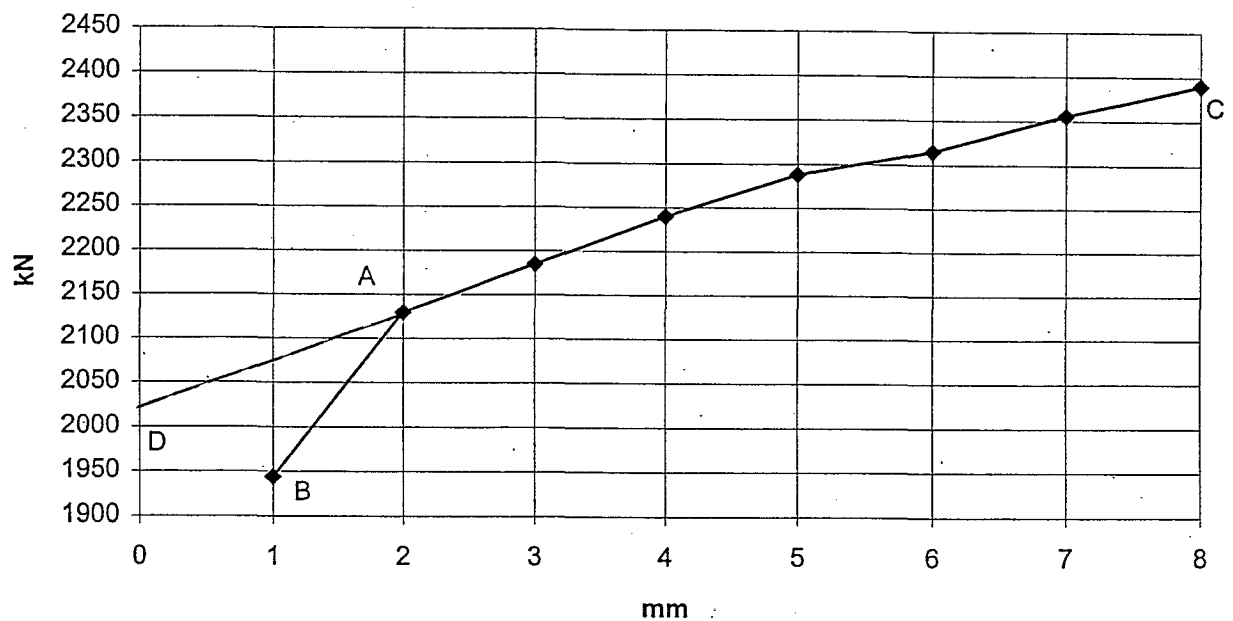


Fig 3.2 LIFT - OFF OF TENDON T2 - D2M- 92

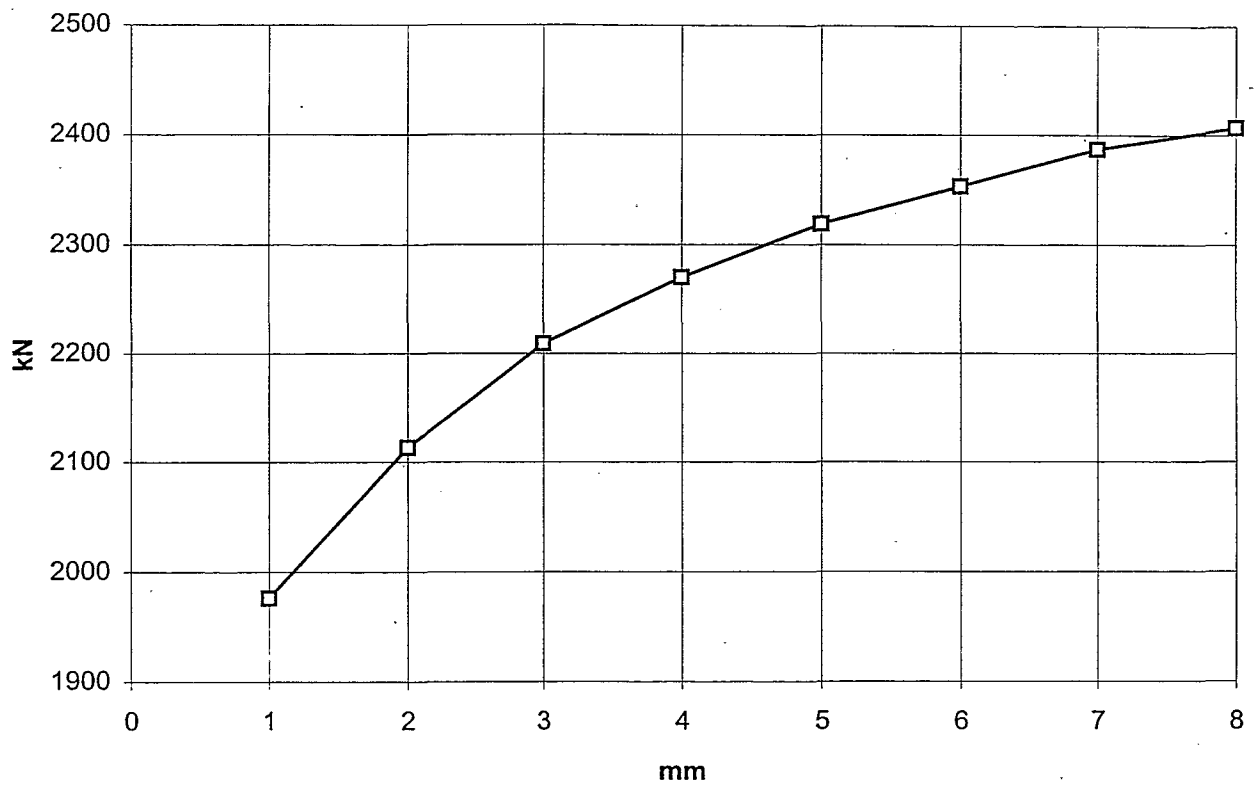


Fig 3.3 LIFT - OFF OF TENDON T2 - V149A - 92

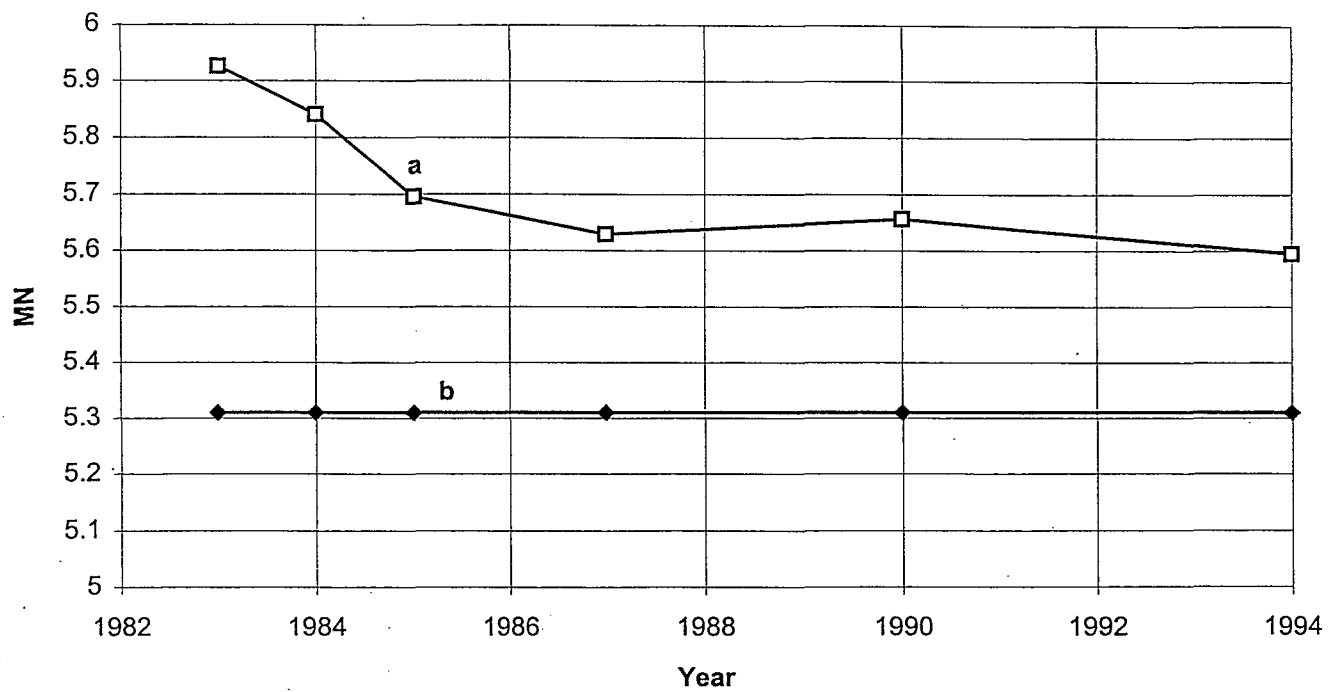


Fig 3.4 a) EVOLUTION OF TENDON LOAD DOEL 4 DOME
b) ESTIMATED LOAD AFTER 40 YEARS

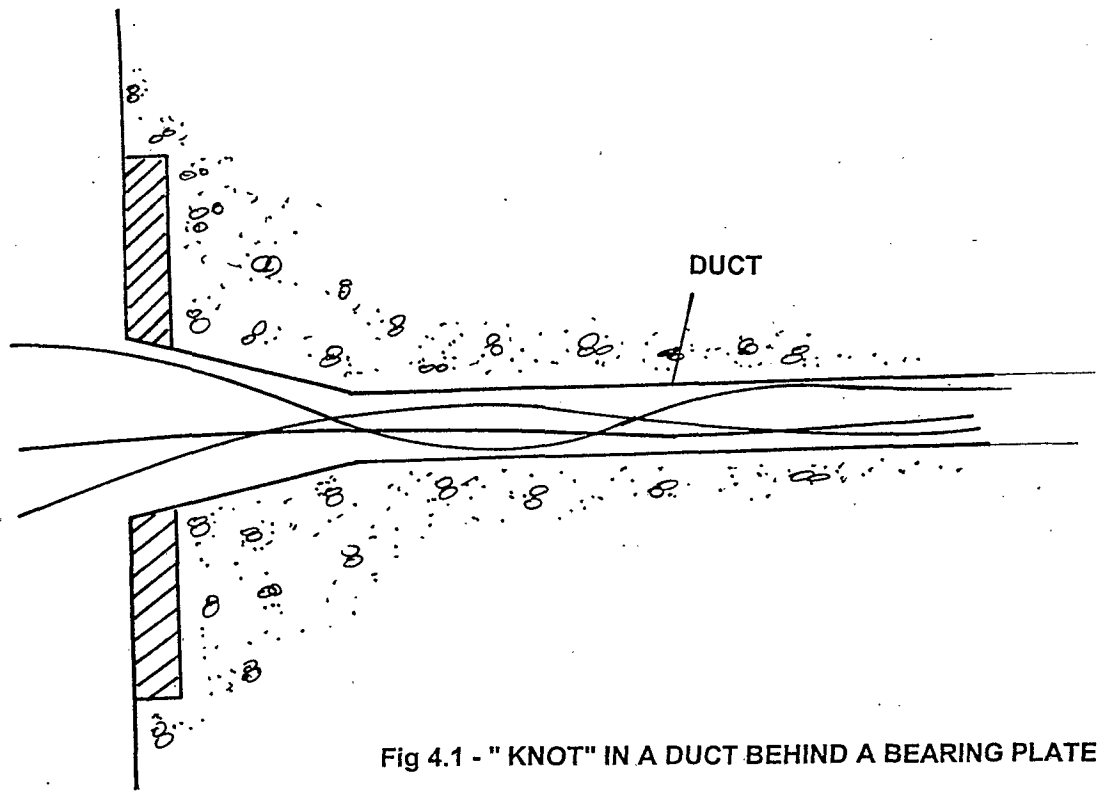


Fig 4.1 - " KNOT" IN A DUCT BEHIND A BEARING PLATE

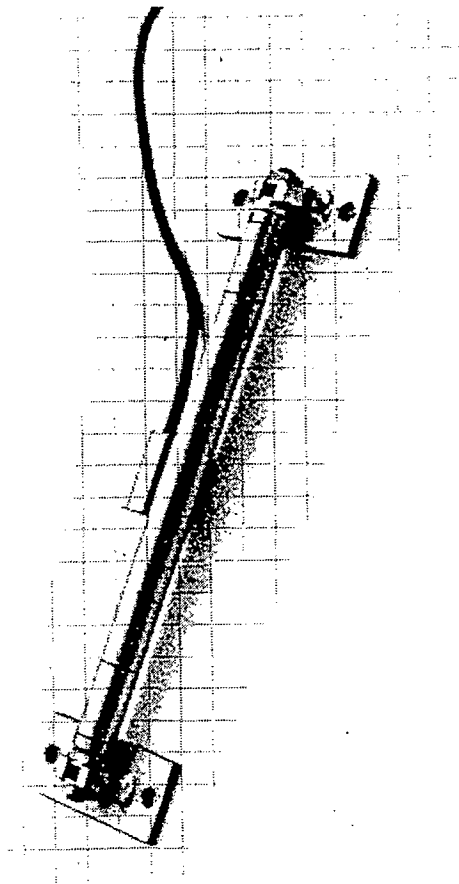


Fig 5.1 - VIBRATING WIRE FOR RE - INSTRUMENTATION

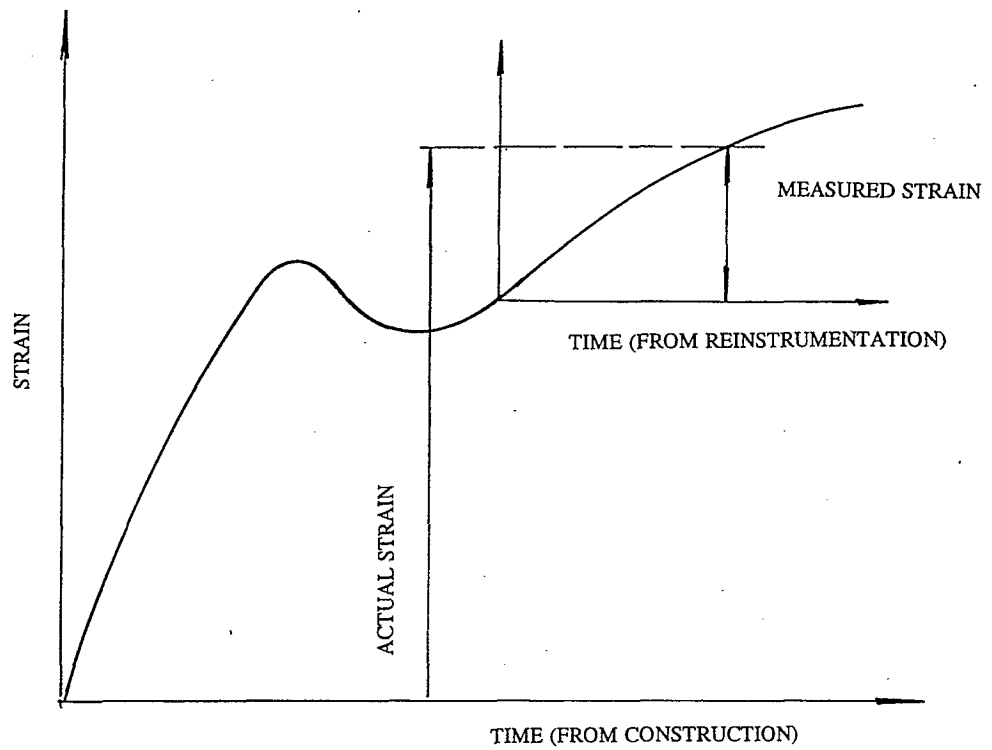


Fig 5.2 EVOLUTION OF STRAIN IN CONCRETE
ACCORDING TO ORIGINAL AND
NEW MEASURING DEVICES

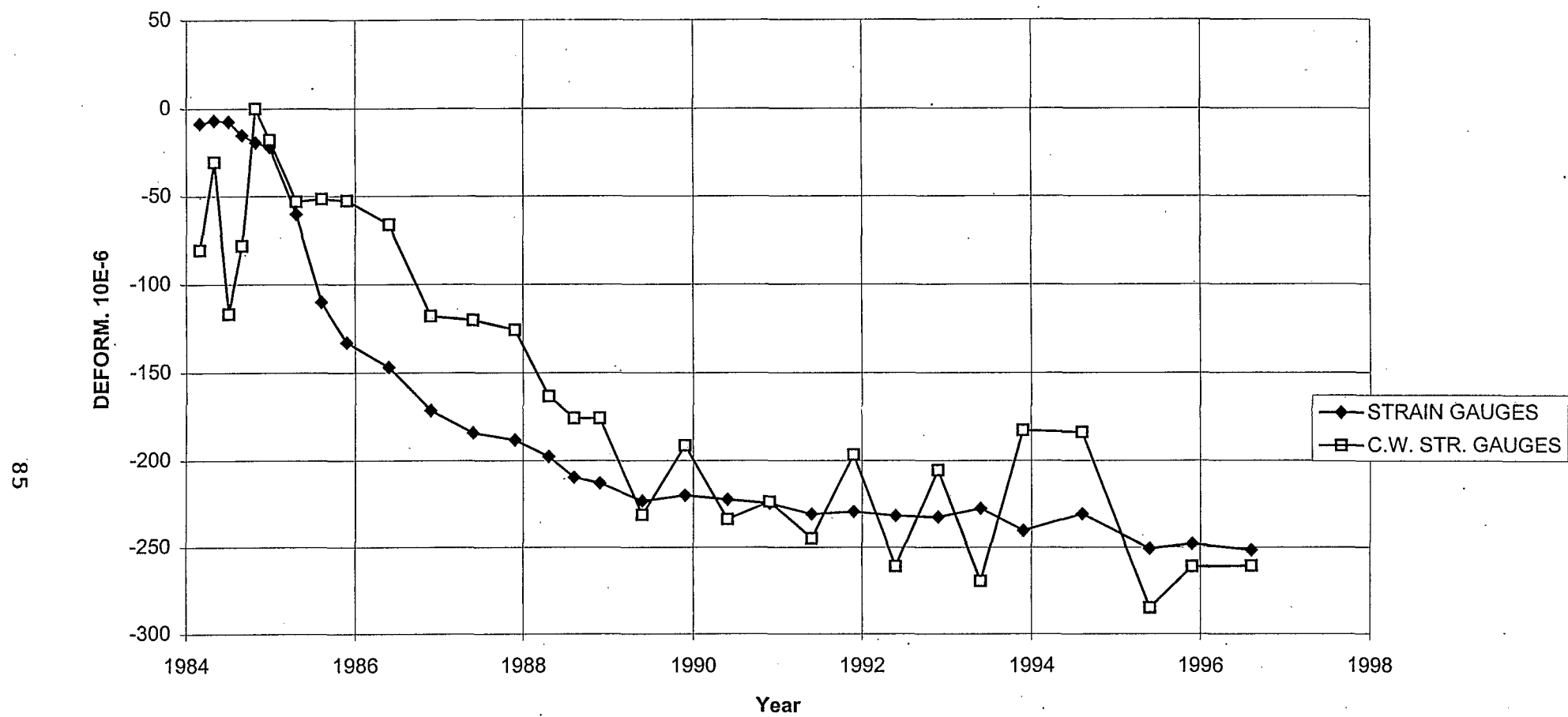


Fig 5.3 - EVOLUTION OF STRAINS IN DOEL 4 DOME

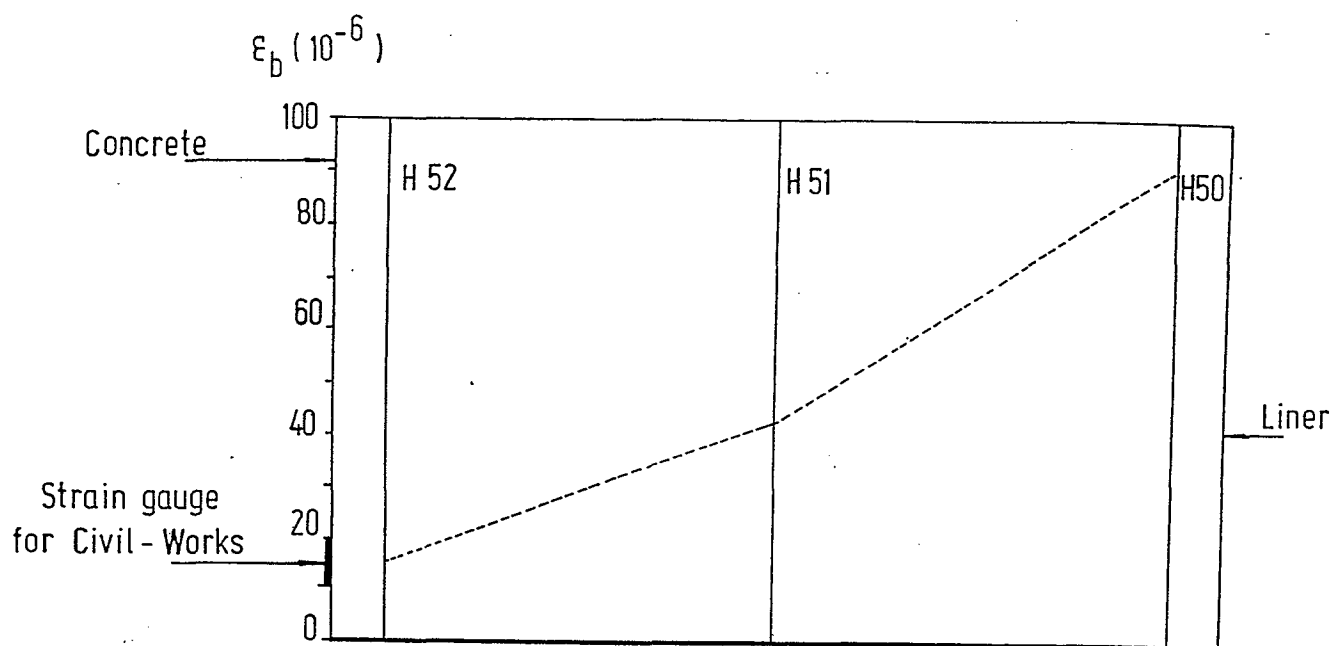


Fig 5.4 PRESSURISATION TEST
EVOLUTION OF STRAIN ACROSS A SECTION
STRAIN GAUGES H50, H51 and H52
+ STRAIN GAUGE FOR CIVIL - WORKS

JOINT WANO-PC/OECD-NEA WORKSHOP ON PRESTRESS LOSS IN NPP
CONTAINMENTS
POITIERS, FRANCE 25, 26 AUGUST 1997

PRESENTATION OF GENTILLY 2 NPP CONTAINMENT

Nelson Garceau - Hydro Québec

ABSTRACT

The paper describes in details the plant significant features and the concrete containment life management including ageing related problems and remedies applied. A synopsis is presented below. Gentilly 2 NPP is a PHWR CANDU 6 nuclear power plant with a net 600 MW (680 MW gross) capacity, located in the province of Quebec, Canada and owned by Hydro-Quebec.

The plant was constructed during the years 1973-78 and went in operation on 1983. To date, Gentilly 2 has an operating record of 84.2% of disponibility factor combined at a reactor power factor of 80.2%. The containment concrete is 18 years old from the date the concrete was cast. During 15 years operations, the plant was shutdown every year for maintenance and repairs including the periodic reactor building leak rate test.

The containment is a 35 Mpa (5000 psi) concrete cylinder with a dome roof, resting on a concrete base slab. It is reinforced and prestressed structure with an inside diameter of 41.4 meters and a wall thickness 1070 mm for the cylinder wall and 610 mm for the dome. The base slab have a thickness of 1524 mm resting on a subbase of various thickness and both separated by a membrane. BBR was selected as prestressing system, with independant cables in the containment base slab, cylinder and dome. All cables are grouted.

The interior face of the containment has applied an epoxy as original liner to provide leak tightness and a surface easy to decontaminate. The liner has been replace by a new one, which is an organic liner. Strain gauges were embedded in the concrete with readings in 2 directions at each location, to provide a confirmation of the acuracy of the design at the time of the commissionning, during the pre-operational pressure test. The same gauge can provide an insight into the concrete ageing process at each subsequent high pressure lesk rate test. The design allowable leak rate is 0.5% of free volume in 24 hours, at the accident pressure of 124 Kpa (18 psi).

According to Canadian regulations, for obtaining/renewing the operating licence, prove is required that the actual leak rate is below the allowable rate of 0.5% V/D. The leak rate is periodically measured, at maximun of 3 years (usually) interval, as specified in the operating licence and is performed accordingly to CAN/CSA-N287.7. Over the 15 years of operation, 7 containment leak rate tests were performed and the results recorded. The variation of the leak rate, a sign of ageing, is discussed in this paper, as well as the remedies applied to reduced it.

The construction method of the containment concrete was slipforming to avoid construction joint. The major construction joints were at the base slab/cylinder joint, cylinder/dome (the ring beam) at the top, (the 2 air locks are embedment parts, not a joint) and the 2 temporary openings left in the cylinder structure for access of large equipement like calandria, or steam generators.

The non-conformances during construction and which had an impact on the containment ageing process are also discussssed in the paper. Finally the ageing management program is described, including inspection and testing. Under testing are presented the results of the periodic high pressure leak rate tests performed and the low pressure test performed at full power, of the lift-off and of the test beams tests, as part of monitoring of the ageing of the concrete and prestressing cables respectively. Where remedial actions were applied, the method used and results obtained are described.

Containment Structure Monitoring And Prestress Losses

Experience from DAYA BAY Nuclear Power Plant

XuYao Zhang

Guangdong Nuclear Power Joint Venture Corporation

Abstract

This article describes the main characteristics of containment structure, the devices of containment deformation monitoring, especially about measurement method, data treatment and result assessment of the tendon relaxation.

Key words: Containment, monitoring, device, tendon, relaxation

1 Introduction

Guangdong Nuclear Power Station(GNPS), which was owned by Guangdong Nuclear Power Joint Venture Corporation, is located in DAYA BAY, Shenzhen city, Guangdong province, China. There are two PWR units, the capacity of each is 984MW. In 1994, the project construction for GNPS was completed, and then, unit 1 commenced commercial operation on February 1, unit 2 on May 7 in 1994 respectively.

GNPS has been a member of the World Association of Nuclear Operators(WANO) since 1991. During 1994, GNPS established twinning relationship with Ulchin Nuclear Power Plant(South Korea), Tricastin Nuclear Power Plant(France) and Gravelines Nuclear Power Plant(France).

2 Presentation of GNPS containment

- Main characteristics of the containment

Dimensions

— External diameter

38.80m

--- Overall height (including the dome and the base mat)	66.40m
--- Cylindrical Wall thickness-normal section	0.90m
--- Base mat thickness-standard section	3.50m
--- Dome thickness-standard section	0.80m

Prestressing (for unit 1& unit 2)

Ensured by cables type "STUP 19T15" (design section:2641mm²,maximum tension at anchorage: 8855KN), it was distributed as follows:

--- Horizontal prestressing and tensioned at both ends	: 274 cables, covering 3/4 of the circumference of the vessel
--- Vertical prestressing case	: 212 cables tensioned at their upper end only in the normal case
--- Dome prestressing	: 162 cables in three groups and tensioned at both ends
--- Foundation	: granite
--- Design relative internal pressure	: 4.2 bar
--- Construction period (unit 1)	: September 1987 to May 1990
--- Prestressing (unit 1)	: May 1990 to November 1991
--- Pre-commissioning strength test(unit 1)	: January 1993

3 Monitoring devices

As the reactor building containment is a particularly important safety-related structure, it is vital to monitor its behaviour in time(in normal or exception operating conditions, for instance on an earthquake) and during certain construction or operation phases. So, the containment of Guangdong Nuclear Power Plant have been fitted out with monitoring instrument in order to measure structural deformations of the containment during the construction and during the life of Nuclear Power Plant. This monitoring instruments mainly consist of

- Acoustic strain gauges
 - 52 TELEMAT-Type C110 for unit 1
 - 24 TELEMAT-Type C110 for unit 2
- Thermocouple
 - 36 CORECL jacketed thermocouple-type K for unit 1

21 CORECL jacketed thermocouple-type K for unit 2

--- Pendulum

12 direct pendulum as instruments on four vertical generating lines for each unit

--- Hydraulic leveling pots

13 pots set in the base mat for unit 1 and 9 pots set in the base mat for unit 2

--- Dynamometers

4 dynamometers measure the force of four vertical tendons (only for unit 1)

These instruments mentioned above monitor the base mat, the containment wall and the dome. As behaviour of prestressing tendons is homogeneous in both units, monitoring of certain cables to assess their relaxation with time is only executed in unit 1. In construction and operation, the entire containment monitoring period is three months. All items have also been executed on strength and leaktightness tests every 10 years.

4 Monitoring & data treatment for prestress losses

The force of four vertical tendons is measured by using four dynamometers. These dynamometers were installed in unit 1, fitted to the lower ends of four vertical tendons. These vertical tendons were protected against corrosion by a viscous material (grease of type TRACTA 1391 manufactured by CONDA S.A. or approved equivalent) which allows free movement of strands in the rigid duct.

The readings are gotten with mini-frequencymeter through an eight-channel switching box to which the individual 18-core cables are brought out.

The dynamometers measure the force of four vertical measuring tendons as following:

-- No. 18 at 349.722 grades

-- No. 54 at 249.722 grades

-- No. 90 at 149.722 grades

-- No. 126 at 49.722 grades

The force in the tendon is calculated by

$$F = K8 \sum (N^2 - N_0^2) \times 9.8 \times 10^{-6}$$

where

F: force in tendon (expressed in KN)

N: frequency measured (in dHz)

No: frequency at initial time (in dHz)

K8: CV8 type calibration coefficient

Here is an example of results obtained for four vertical tendons. First, we measured the readings of four vertical tendons with mini-frequencymeter by using dynamometer on site, then, calculated the force for each tendon, after that, we calculated the force variation for each tendon in relation to the force of initial measured on May 1993, therefore, we have determined the force variations with time, i.e., prestress losses. Here below are the test results from May 1993 to October 1996.

Date	Tendon Number	Force variation (KN) (unit 1)			
		126	90	54	18
27/05/93		0	0	0	0
26/08/93		51	-2	-14	22
25/11/93		124	19	16	32
23/02/94		153	19	12	35
22/06/94		189	11	8	47
13/09/94		220	9	6	48
06/12/94		243	245	11	53
14/03/95		249	18	22	29
07/06/95		-42	3	22	-102
21/09/95		229	1	25	-9
06/03/96		228	-142	34	0
10/07/96		222	-3	313	23

From above-mentioned, except in a few instances, the tendon force variations with time are essentially linear, the prestress losses are not significant.

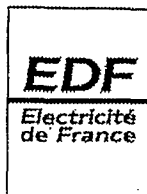
5 Conclusion

As Guangdong Nuclear Power Plant is a new plant, only a few tests for monitoring containment structure deformations were performed. By this time, we do not encountered the problems for containment deformations, such as creep of concrete, relaxation of the tendons, corrosion and so on. Up to now, the containments of Guangdong Nuclear Power Plant have

experienced pressure test two times which showed a good behaviour, for instance, a good reversibility of the characteristics, the linear variation of the strain and the displacements versus pressure, the comportment of containment structure conforming to the design, etc. All of these verify that containments of Guangdong Nuclear Power Plant are in good condition . We will continue working on it to assess and predict prestress losses for the purpose of assessing and predicting life of containment concrete structure.

Reference

1. Containment instrumentation system for periodic test (EAU)
PG017EAU001EREM45GN--PG017EAU013EREM45GN



PRESTRESS LOSSES IN NPP CONTAINMENTS - THE EDF EXPERIENCE

Authors : E. MARTINET (EDF-DTG), P. GUINET (EDF-SEPTEN)

H.ROUSSELLE (EDF-EPN), L.GRANGER (EDF-SEPTEN)

ABSTRACT

Electricité de France's set of nuclear power plants currently (1997) comprises 58 pressurized water reactor units.

As for the plant containments, the series-oriented policy resulted in the construction of two types of structure:

- the 900 MW containments (Fessenheim, Bugey, CP1 and CP2 series) consist of a single prestressed concrete wall which withstands the effects of pressure in the event of accident and external hazards such as plane crash. Leaktightness is ensured by a 6mm thick metal liner;
- the 1300 and 1450 MW containments (P4, P'4 and N4 series) have a double wall: the prestressed-concrete inner wall withstands accident pressure, and the reinforced-concrete outer wall withstands external hazards. Any leakage is collected and treated in the inter-wall space, which is kept depressurised.

The cables used to prestress containments are injected with cement grout, so cannot be retensioned; and irreversible phenomena are all the more detrimental to the structures.

For this reason, a specific surveillance program has been implemented to provide the best possible data on structure behaviour and changes; as a result, we are able to check that the leakrate and residual-prestress level will meet safety criteria throughout the forecast plant lifespan of 40 years.

This program is supplemented by R&D studies, in order to improve our understanding of the phenomena and create models to predict the behaviour of the prestressed concrete.

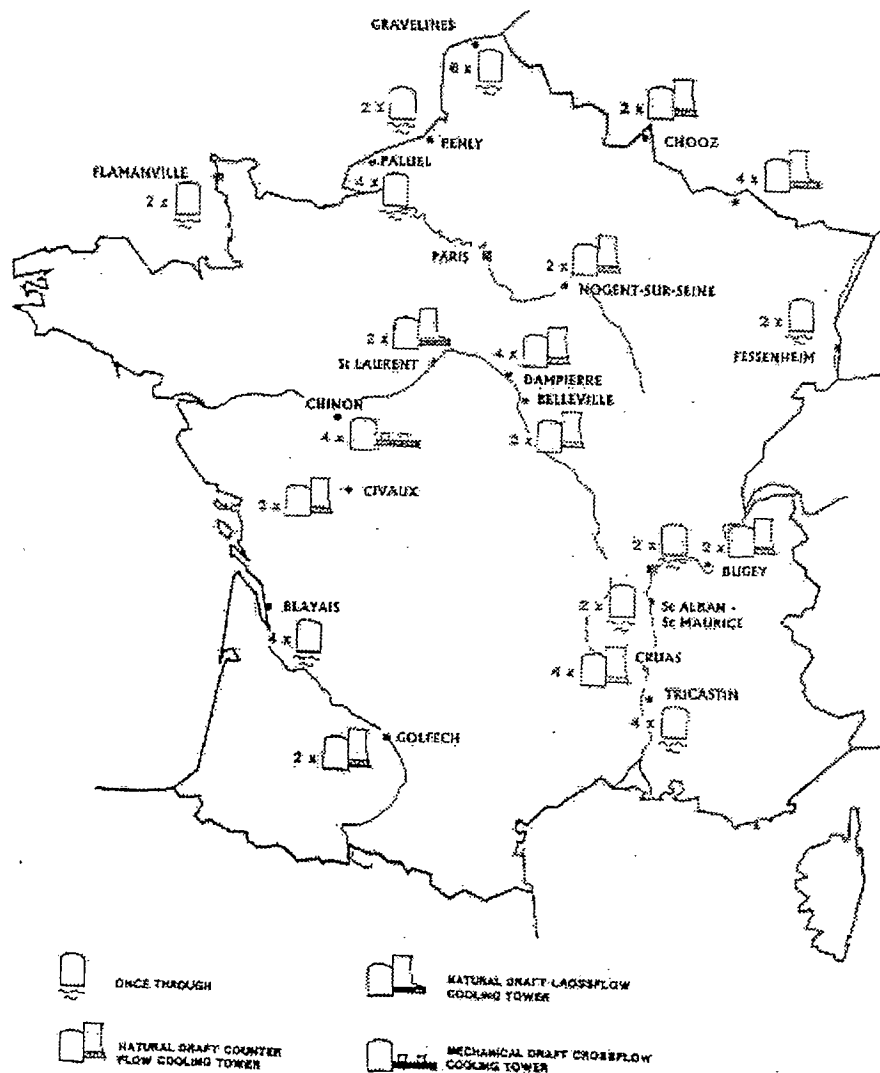
The results gathered so far show that the behaviour of the NPP containments is generally satisfactory. However, lifespan forecast studies indicate that two or three containments are liable to fall below the acceptable level of minimum residual stress after 40 years' service.

The test results should help us acquire a better grasp of these phenomena.

1. INTRODUCTION

Electricité de France's set of nuclear power plants currently (1997) comprises 58 pressurized water reactor units (see map below).

FRENCH PWR PLANTS





This programme was launched in 1970 with the plants at Fessenheim and Bugey, whose six units were commissioned between 1977 and 1979.

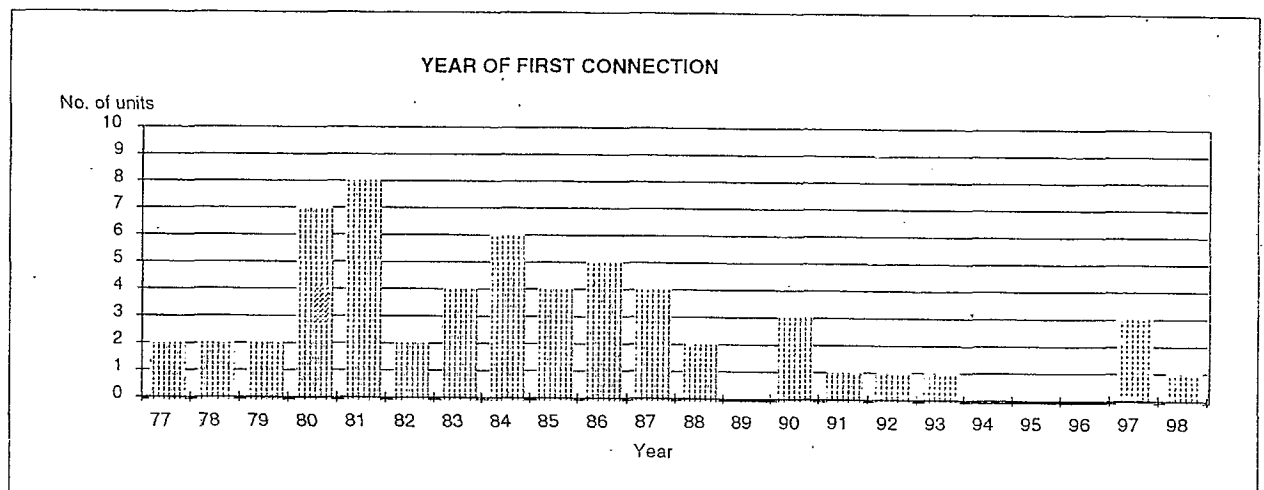
Following the construction of these two plants, which can each be considered a prototype, EDF standardised its units by implementing a series-oriented policy. The following facilities (see tables below) have been brought into service:

- 18 900 MW units CP1 series from 1980 to 1985
- 10 900 MW units CP2 series from 1981 to 1987
- 8 1300 MW units P4 series from 1984 to 1986
- 12 1300 MW units P'4 series from 1986 to 1993

The four units of the N4 series (1450 MW) are scheduled for connection to the grid in 1997 and 1998.

Series	Site	No. of units	Power	Date of first connection to grid					
				unit 1	unit 2	unit 3	unit 4	unit 5	unit 6
CP0	FESSENHEIM	2	880	Apr-77	Oct-77				
"	BUGEY	4	"		May-78	Sept-78	Mar-79	July-79	
CP1	DAMPIERRE	4	890	Mar-80	Dec-80	Jan-81	Aug-81		
"	GRAVELINES	6	910	Mar-80	Aug-80	Dec-80	June-81	Aug-84	Aug-85
"	TRICASTIN	4	915	May-80	Aug-80	Feb-81	June-81		
"	BLAYAIS	4	910	June-81	July-82	Aug-83	May-83		
CP2	St LAURENT	2	915	Jan-81	June-81				
"	CHINON	4	905	Nov-82	Nov-83	Oct-86	Nov-87		
"	CRUAS	4	915	Apr-83	Sep-84	May-84	Oct-84		
P4	PALUEL	4	1330	June-84	Sep-84	Sep-85	Apr-86		
"	St ALBAN	2	1335	Aug-85	July-86				
"	FLAMANVILL E	2	1330	Dec-85	July-86				
P'4	CATTENOM	4	1300	Nov-86	Sep-87	July-90	May-91		

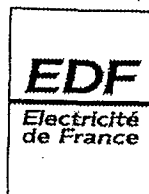
"	BELLEVILLE	2	1310	Oct-87	July-88				
"	NOGENT	2	1310	Oct-87	Dec-88				
"	GOLFECH	2	1310	June-90	June-93				
"	PENLY	2	1330	May-90	Feb-92				
N4	CHOOZ	2	1455	Jan-97	Apr-97				
"	CIVAUX	2	1450	Oct-97	Nov-98				



As for the plant containments, the series-oriented policy resulted in the construction of two types of structure:

- the 900 MW containments (Fessenheim, Bugey, CP1 and CP2 series) consist of a single prestressed concrete wall which withstands the effects of pressure in the event of accident and external hazards such as plane crash. Leaktightness is ensured by a 6mm thick metal liner;
- the 1300 and 1450 MW containments (P4, P'4 and N4 series) have a double wall: the prestressed-concrete inner wall withstands accident pressure, and the reinforced-concrete outer wall withstands external hazards. Any leakage is collected and treated in the inter-wall space, which is kept depressurised.

Section 2 below outlines the evolution of the structures' dimensional features, and particularly the increase in prestress tensions. This was made possible by using cables of larger section, thus permitting a correlated reduction in the required number of cables.



To protect the cables against corrosion, EDF opted to inject the sheaths in all the containments with cement grout (except the cables fitted with load cells). This provision minimizes the consequences of a cable rupture, but prevents cable retensioning or replacement should they be necessary. For this reason, a specific surveillance program has been implemented to provide the best possible data on structure behaviour and changes; as a result, we are able to check that the leakrate and residual-prestress level will meet safety criteria throughout the forecast plant lifespan of 40 years.

The results are regularly (at least every two years) sent to the French Safety Authority and to its technical support teams, who carry out analysis and, if necessary, request additional data or studies from EDF when deviations or single points are detected.

We will now present the structures' main features, the applicable safety criteria, the surveillance principles, and the processing methods used and principal results.

Drawing on experience feedback, one chapter will be devoted to the main problems identified and the solutions that will (or could be) chosen to solve them.

We shall also describe the Research and Development programmes under way, with the results already obtained and those expected in the future.

2. THE CONTAINMENT

2.1. Safety criteria

The safety criteria focus on acceptable leakrates of air and of steam/air mixture; to respect these criteria, the structure must have a minimum degree of residual compression.

For the single-wall containments (900 MW), the acceptable leakrate (steam/air mixture) is 0.3%/day in the event of a LOCA and 0.162%/day (air) of the air mass inside the containment. This criterion is verified during the type A tests.

For the double-wall containments (1300/1400 MW), the overall leakrate is 1.5%/day in the event of a LOCA and 1%/day (for air) of the air mass inside the inner containment. The outer wall is deemed to be leaktight if its leakrate at 3 mbar negative pressure is less than 1%/day of the air mass contained in the volume delimited by the inner covering of the outer wall.

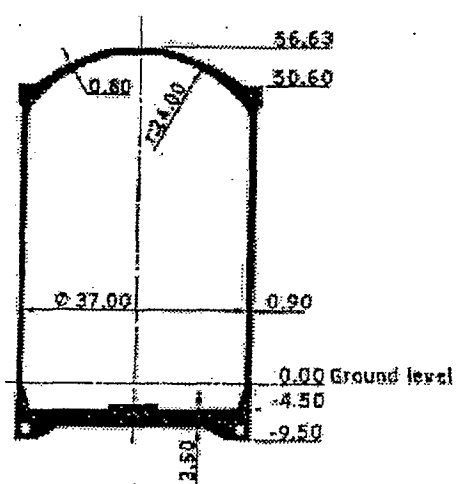
Coupled with the above criteria are criteria concerning the concrete's residual compression, which must be at least 1 Mpa in the standard section (of the double-wall containments) and 0 Mpa for the single-wall containments.

Obviously, these two categories of containment must withstand an external hazard of the "missile" type.

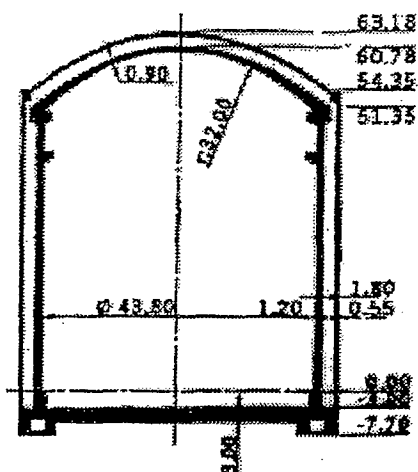
2.2. Main features of the containments

The two charts and table below summarize the main features, with regard to geometry and prestress, of the containments of the French NPP set.

FEATURES OF THE CONTAINMENTS



PWR 900 MW



PWR 1400 MW

Type of containment	900 MW type			1300 MW type		
	CP0	CP1/2 (except Cruas)	Cruas	P4	P'4	N4 (CHOOZ B *)
Outside diameter (m)	38.70	38.80	39.20	46.80	46.20	46.20
Total height, dome and basemat included (m)	63.50	65.40	64.50	66.50	65.20	60.78
Basemat thickness, in standard section (m)	6.00	3.50	3.00	3.00	2.80	3.00
Cylindrical-wall thickness, in standard section (m)	0.85	0.90	1.10	0.90	1.20	1.20
Dome thickness, in standard section (m)	0.75	0.80	0.90	0.95	0.82	0.82
Inter-wall thickness (m)	-	-	-	2.00	1.80	1.80
Type of prestressed cable	12T15	19T15	37T15	37T15	37T15 36T16	36T16 37T16
Max. anchoring tension (kN)	2400	3855	7650	7650	7650 7630	7630 7858
Cable cross-section (mm ²)	1668	2641	5143	5143	5143 5400	5400 5550
Number of horizontal cables in cylindrical wall	402	274	125	119	122	134
Number of vertical cables in cylindrical wall	368	212	182	51	57	60
Number of gamma cables	0	0	0	120	98	112
Number of cables in dome	288	162	102	0	18	0

(*) The prestress value at CIVAUX is slightly greater than at CHOOZ B.



With the exception of four cables in the first unit on each site, which are fitted with load cells and injected with wax or grease, all the cables are injected with grout after tensioning.

2.3. General principles of containment surveillance

Surveillance of the containments involves monitoring their leakrate and mechanical behaviour.

The compatibility of each containment's leakrate with the criteria defined in §2.1 is verified during each containment test, by measurements carried out by EDF's General Technical Division (DTG).

In one test, the containment is filled with dry air to accident pressure. The pre-operational test is performed at the end of containment construction; the test is reperformed during the first fuel-reloading operation, and then every ten years.

In this test, for the 900 MW type containments, the total leakrate is measured at the containment's design-basis pressure, by calculating the change in the dry-air and water-vapour weights contained in the reactor building when subject to different pressure levels.

For the double-wall containments, verification of containment efficiency requires, in addition, evaluation of leaks not collected by the inter-wall space, which are called non-transiting leaks.

Monitoring of the containment's mechanical behaviour currently starts during the construction phase: in particular, this makes it possible to detect changes in the structure during concreting and the various phases of prestressed cable tensioning. The main purpose of the monitoring is to verify prestress integrity and the durability of the concrete's mechanical characteristics, using results from measurements performed on the monitoring system.

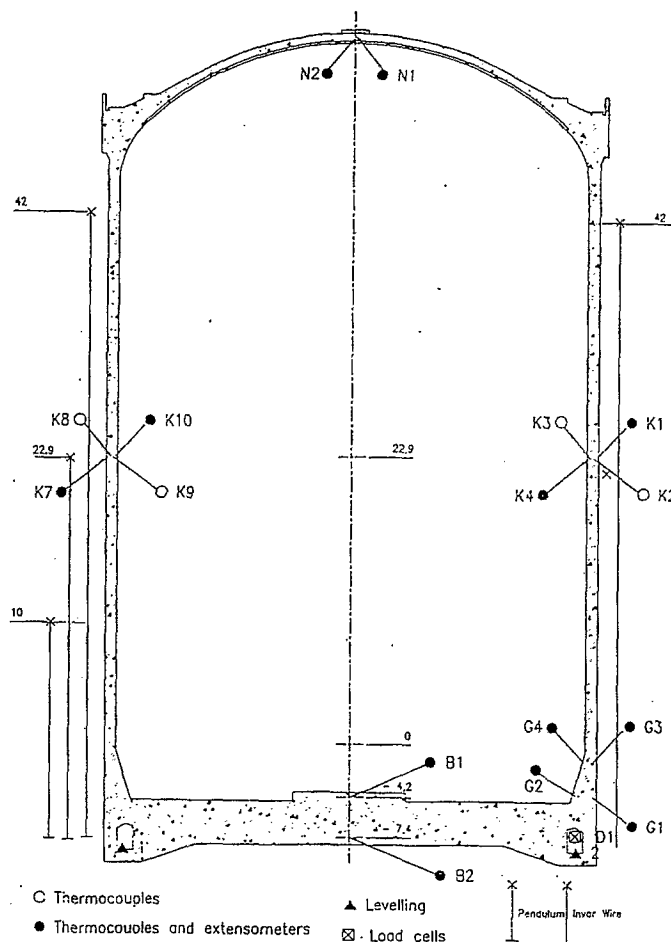
In addition, overall movements of the containment and its differential settlements with the peripheral buildings are monitored by topographical measurements.

To achieve the objectives outlined above, the monitoring system permits inspection of:

- *the containment's thermal state*, using measurements from the thermocouples, in order to check on the scope of the thermal gradients in the wall and to correct the other measured magnitudes of the reversible effects caused by variations in temperature;
- *the residual prestress level* by direct means, using load cells that measure the prestress tension of the four vertical cables on the first unit on each site;

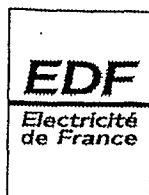
- *the range of shrinkage/creep phenomena* by means of the corrected values of the reversible effects (temperature and pressure) of the displacements measured by the pendulums and Invar wires, and of the deformations measured by the vibrating-wire extensometers. These values also make it possible to determine *the residual prestress level* by taking account of the theoretical relaxation of the prestressing cables.
- the subsidence and tilt of the containment, using direct levelling measurements.

The number of devices, and their disposition and distribution, were defined so as to allow, for a standard plant unit, inspection of the essential dimensional variations of the containment (diameter, height) and those of the special areas (basemat, dome, gusset) which may take large forces (see chart below).



The first unit in each plant series is equipped with extra instrumentation to consolidate the initial design reports and monitor certain specific containment areas, such as those located near the steam penetrations and the personnel and equipment hatches.

The first unit on each site has more instrumentation than a standard unit too, particularly for inspection of the site geology's impact on basemat behaviour.



The setup of the monitoring systems makes it possible to cross-check the results from different sensors:

- variations in diameter calculated using the pendulum measurements with the tangential deformations of the extensometers at mid-barrel level;
- variations in height of the Invar wires with the vertical deformations of the extensometers at mid-barrel level;
- prestress losses measured with the load cells and calculated from the vertical deformations at mid-barrel level;
- containment tilt determined by direct levelling and calculated using pendulum measurements.

Up until the first operating test, the monitoring-system measurements are performed monthly, and subsequently every three months. This timetable may be changed should it be necessary to better characterise certain phenomena affecting the containment; if the monitoring system is refurbished; or if negative drift in the chronological measurement series is highlighted.

Also, for the particularly close monitoring required by some containments, a remote measurement system has been developed; this allows the entire monitoring system to be remotely checked.

Generally speaking, plant personnel take the programmed measurements themselves; and, using the PANDA software, they make an initial analysis of the raw measurements, which involves transposing the reading obtained into the physical magnitude of the phenomenon being measured.

After validation, the measurement is sent to EDF-DTG within the scope of its mission to manage the monitoring-system database and to monitor the behaviour of EDF's large civil-engineering structures.

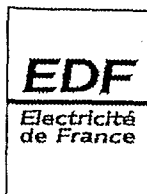
The raw measurement is then reduced to identical temperature and pressure conditions by applying the statistical model of behaviour.

Structural change is then assessed using shimming strips sized from the corrected measurements of the reversible phenomena; the structure's behaviour can thus be ensured to be normal. If a difference in relation to the known behaviour is observed, a further measurement series is done on the entire monitoring system in order to confirm the difference and identify its origin.

In addition to this regular monitoring, EDF-DTG writes a two-yearly report on each containment, which in particular details changes in irreversible shrinkage/creep phenomena and permits an assessment of the integrity of the structure's prestress.

There are five users of the report:

- the structure's owner, within the framework of regulatory monitoring



- the French Safety Authority (DSIN) and its technical support teams
- EDF's Nuclear Plant Operations centre (EPN), in order to define maintenance operations at series level and operating plant set level
- EDF's Basic Design Department (SEPTEN), in its capacity as designer, for the feedback on the analysis of the containments' theoretical behaviour
- EDF-DTG, as part of its mission to monitor structure behaviour.

2.4. Monitoring-system data processing

At this level, a distinction should be made between the processing of the results obtained during containment testing and those collected during each periodic measurement series.

The results obtained from the monitoring-system during strength tests must allow verification of the linearity and reversibility of the displacements and deformations induced by variations in the containment's internal pressure. In addition, the scope of the measured phenomena is compared to the theoretical values and to those that may have been obtained during the previous tests.

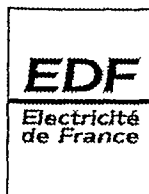
In addition, Young's modulus and Poisson's ratio are calculated from the tangential and vertical deformations measured in the standard section of the barrel.

To complement these measurements, a visual inspection of the external facing is performed each time the 900 MW type containments are tested. This inspection makes it possible to identify, prior to testing, the degree of deterioration of the structure and to monitor how its cracks evolve under the effect of variations in pressure.

Regarding the periodic measurements, experience shows that the raw measurements recorded on the structure result, in a first approximate analysis, from superposing of three main states:

- a state corresponding to a long-term irreversible change in the phenomenon in time t , a change that may tend to slow down over several years (concrete shrinkage and creep, relaxation of prestressed cables) or continue at a roughly constant rate.
- a state corresponding to a spatial distribution, in the structure, of the temperatures, a distribution that can be represented by the characteristic temperature of q thermal zones $\theta_1, \theta_2, \dots, \theta_q$.
- a state corresponding to the elastic effect of the internal pressure P .

The latter two states, which are related to temperature and pressure, are reversible.



These three types of influence have been shown by experiment to be independent; this makes it possible to use a containment-behaviour model in which every result from a raw measurement can be expressed according to three independent functions: f_1 function of time, f_2 function of temperature, and f_3 function of pressure:

$$M_b = A + f_1(t) + f_2(\theta) + f_3(P) + \varepsilon$$

where A is a constant which takes into account the arbitrariness of the phenomenon-measurement scale and ε represents experimental measurement errors and the effects of any other secondary cause neglected by simplification.

Using the algebraic expressions chosen for the laws $f_1(t)$, $f_2(\theta)$ and $f_3(P)$, the measurement results are statistically processed; this method, by minimising the sum of the ε^2 's, makes it possible to calculate the functions $f_1(t)$, $f_2(\theta)$ and $f_3(P)$ and to apply the model thus obtained to any further measurement. We can then calculate the corrected value of the pressure and temperature influences, which is called the value with identical pressure and temperature conditions. This is expressed by:

$$M_c = M_b - f_2(\theta) - f_3(P)$$

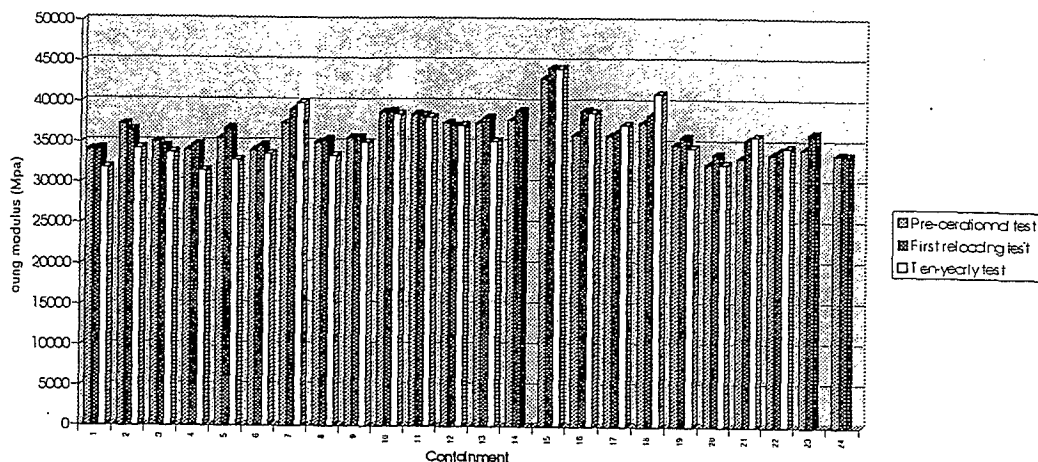
This expression characterises the effect of time on changes in the material's mechanical properties, and therefore on the maintaining of the integrity of the prestress force.

2.5. Main results obtained from the containment monitoring system

The results obtained from the 150 mechanical-strength tests performed up to now have shown behaviour in line with expectations. Deformations and displacements due to variations in internal pressure are actually linear and reversible, and their scope is similar to that forecast in the design reports.

The characteristic values of Young's moduli and Poisson's ratios, deduced from deformations at mid-barrel level, remain remarkably homogeneous for each containment from test to test (see chart below). This stability of results over time shows that the structure's behaviour is not modified by the effects of the shrinkage and creep observed since the end of construction.

Young's modulus of 900 MW containments (Mpa)

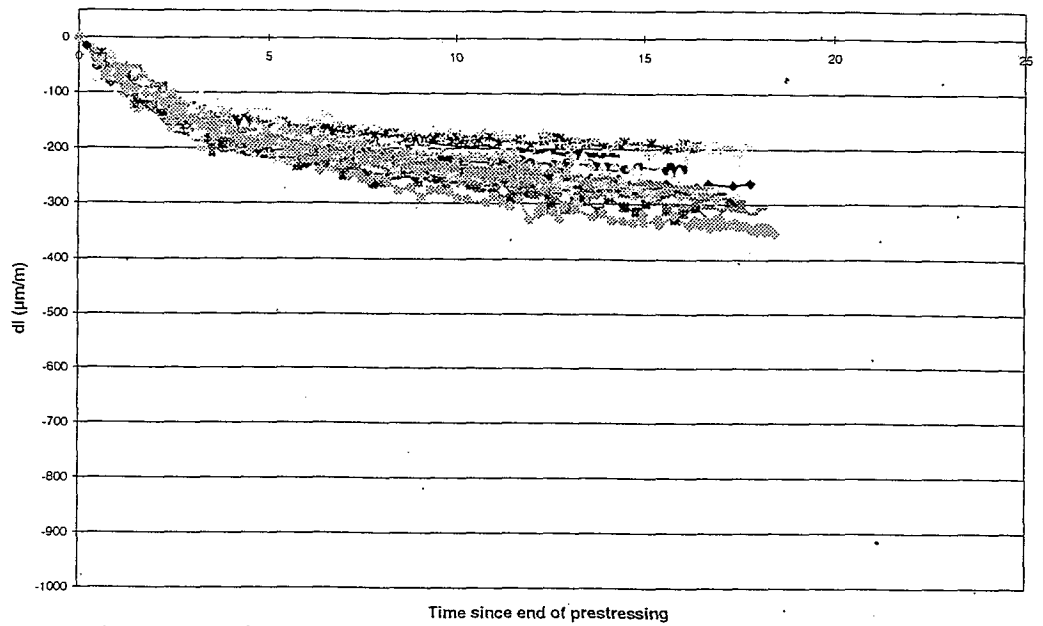


The size of the periodic surveillance database compiled from a set of 58 containments, monitored for an average of about 17 years, makes it possible - among other things - to conduct comparative studies of the different units in the same series and to define, by experiment, the standard mean behaviour.

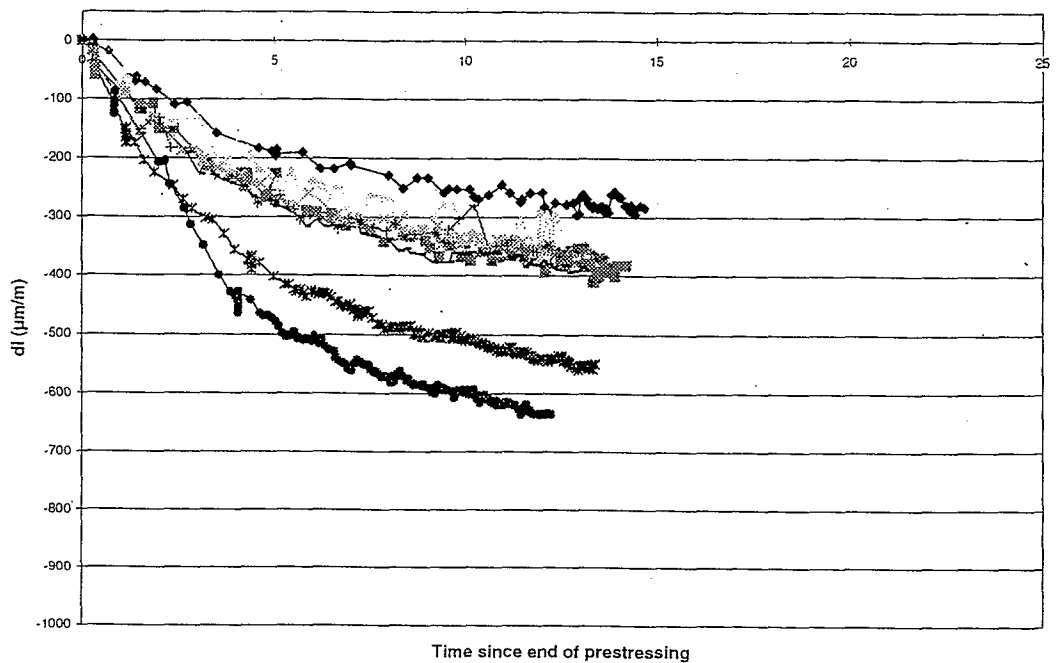
This experiment in monitoring highlighted, in the first years following the construction containments, those whose changes required special surveillance; this requirement gave rise to the remote measurement system.

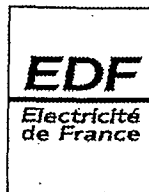
In addition, this monitoring experiment has illustrated how time-delayed deformations can vary between units in the same series by about 30 to 50% from the series' standard mean behaviour (see charts below). This value, which is related to different concrete compositions but also to local conditions of implementation and operation, reflects the difficulty in predicting *a priori* the scope of changes in the containment concrete, and emphasizes the usefulness of experimental monitoring of these changes (see section 3).

Vertical deformation at mid-barrel of CP1-2 series



Vertical deformation at mid-barrel of P4 series





The time zone of the measured deformations nevertheless shows that the effects of shrinkage and creep can be represented by a graph of the slowed-down exponential type, and that most of these effects are observed during the first 8 to 10 years in structures' lives.

Monitoring measurements are also put to good use through containment lifespan studies, which are based on these experimental measurements and on the forecast future behaviour of containments in order to ensure that the residual prestress level will be maintained for the 40 years of the structure's forecast lifespan.

3. PRESTRESS-RELATED PROBLEMS

- The cables used to prestress containments are injected with cement grout, so cannot be retensioned; and irreversible phenomena are all the more detrimental to the structures.

A brief reminder: three phenomena result in tension loss in prestressed cables, and therefore in loss in the residual compression of the structural concrete. These are: shrinkage and creep of the containment's material, and the relaxing of the prestressed cables.

Although cables are known to relax at relatively low temperatures (10-50°C), shrinkage and especially creep in such structures are quite difficult to assess over the long term (40-50 years). These irreversible phenomena affect the reactor buildings of France's NPP set with varying acuteness, depending on the specificity of each structure.

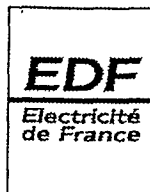
In addition, there is the local problem of cracking of the extrados of the 900 MW wall, which, unlike the inner wall of the double containments, is subject to external hazards.

- The first 900 MW units (FESSENHEIM) have been operating for nearly 20 years, and the first 1300 MW units (PALUEL) for 10 years. Experience feedback shows that:

- overall, prestress loss in the 900 MW containments has been slightly greater than initially anticipated; however, the margins required to maintain "0" compression are adequate in the event of a LOCA.

- cracking of the containment extrados in the critical structural zones is insignificant.

- prestress loss in the double-wall containments is substantially greater than initially anticipated, reaching 45% for the P4 series (FLAMANVILLE) and 30% for the P'4 series (BELLEVILLE). However, the criterion of 1 Mpa residual compression in the standard section is respected in the event of a LOCA. During type A tests, these containments (CHOOZ, CATTENOM) exhibit cracking round the equipment hatch.



- The notion of tension drop, and consequently of residual-compression drop, is important only with regard to the phenomena of concrete traction and cracking, because these can cause the LOCA-induced leakrate to rise. Given that the cables cannot be retensioned (see previous paragraph), EDF has undertaken a programme called "Projet Durée de Vie" (Project Lifespan). In this project, each containment is assessed with regard to the current estimate of 40 years. The project requires regular monitoring of each structure and the carrying-out of design reports based on a planned service life of 40 years.

Resistance to external hazards is not brought into doubt because the containment is practically free from cracking; we can conclude that the structure has not been weakened.

- In general terms, inspection of the outer wall provides assurance with regard to external hazards. In the event of cracking, repairs can be carried out. As for the prestress, a combination of irreversible-change monitoring and periodic design reports makes it possible to track the structure's ageing process.

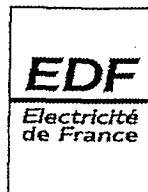
- For the future:

- through Project Lifespan, EDF is ensuring that containments respect design criteria;

- lift-off has been validated at CIVAUX and FLAMANVILLE; this technique provides the tension values of certain cables and consequently permits calculation of relaxation, taking into account shrinkage and creep phenomena;

- the composite liners that will be validated on the MAEVA mock-up can be used locally (equipment hatch, ribs, dome/barrel connection) to restore leaktightness.

Nevertheless, with regard to the 1300/1400 MW units, although a drop in the concrete's residual compression can cause the overall leakrate to rise, we should remember that only direct leaks (i.e. not passing through the inter-wall space) harm the environment, and that this type of leakage is very small and well within the criteria in force for the 900 MW series.



4. RESEARCH AND DEVELOPMENT

4.1. Introduction

We have seen previously that EDF had to justify to the French Safety Authority the containment's capacity to ensure a leak rate which, in accident conditions, is less than 1.5%/24hrs of the total fluid mass (air/steam mixture) in the containment. It must be pointed out that this aspect is far more constraining than the requirement of simple mechanical stability, because a leaktightness criterion calls for severe control of the degree of concrete cracking. To justify this leak rate experimentally, each containment periodically undergoes a lifesize test (before plant startup, at first reloading, then every 10 years) : a dry air test at 20°C and design-basis pressure, called the containment pressure test.

With time, prestress losses caused by the concrete's delayed behavior (shrinkage + creep) reduce the mechanical loading the structure is able to withstand. But these losses also result in larger cracks in the concrete - cracks whose thermal origin is inherent in the thickness of the structure and its construction process, and which are therefore inevitable. In case of accident, the prestressing must ensure minimum compression of the concrete so as to keep all existing cracks "closed". The concrete's tensile strength is not considered during design ; this offers an additional margin of a few MPa's with regard to the structure's bearing capacity, though probably not for leaktightness, because when the concrete is in traction the pre-existing cracks grow, and the leaktightness threshold is quickly exceeded.

Moreover, the containment instrumentation systems show delayed concrete deformation which the regulatory design models do not satisfactorily take into account with regard to kinetics, dispersion and asymptomatic value. So, with the goal of improving French NPP set "management" via better lifespan evaluation, EDF launched in 1992 a 3-year study program [10] designed to anticipate the actual creep behavior of existing containments. The study, which was financed within the larger framework of the "Lifespan Project" (or "*Projet Durée de Vie*" in French), permitted numerous shrinkage and creep tests on concretes reconstituted in-laboratory, and a physico-chemical analysis and numerical modeling of delayed concrete deformation, with the aim of making a 40-year forecast of prestress losses *in situ*. For more details on this work and its results, please refer to [10, 13].

In many respects, these delayed-deformation problems are similar to those found in bridges: prestress loss, excessive deflection over time, redistribution of forces in hyperstatic structures.

In addition, a number of new problems arise regarding equipment hatches. The hatches, following the strain of the concrete over time makes them difficult to reclose after a unit outage: gaps, related to the elastic return motion of the hatch when opened, appear at the flanges and bolting.



4.2. Difficulties hindering progress

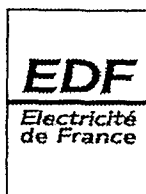
Without going into the details of modeling, it is useful to list the main difficulties the modeler and the engineer face when addressing the problem of delayed deformation.

An as-yet incomplete understanding of the physico-chemical phenomena that cause delayed concrete behavior [1, 6, 10], particularly basic creep and drying creep [4, 12]. As a result, we are often obliged to extrapolate from the experimental results [2] of a creep test with no real scientific basis ; and with many cases and authors, the study is reduced to "super-smoothing graphs". Indeed, in this case, extrapolation is meaningful only in fields where it can be validated by experiment.

Regulations that are adequate for conventional structures but are hardly applicable to structures that are as complex and sensitive as nuclear power plants. In the case of delayed strains, the models currently being developed most often propose empirical expressions based on a large number of results in the literature. These types of model, although they give very good results in most cases, do not shield the designer from the occasional surprise, especially when he is designing very particular concretes such as those of Flamanville or Paluel NPPs. These two concretes have similar compositions (only the aggregate mineralogy differs) but their delayed behavior is very different. In fact, these models are truly reliable only in the field in which they were developed, and offer no guarantee (i.e. by error control) in other domains. In addition, the desire to include in these models all current knowledge on concrete-formulation parameters [11], as well as theoretical considerations on scale effects, leads sometimes to highly complex expressions which, ultimately, are difficult to use.

The models mentioned above can be compared to the BPEL [5] (French best-practice document for prestressed concrete design). This document, on the contrary, opted from the outset for great simplicity of use but passed over many essential parameters : it assumes for example that creep and shrinkage deformation are the same for all concretes (except the HPCs) ! In addition, the BPEL document can be criticised for disregarding the physics of the phenomena. It makes no distinction between endogenous deformations and those related to drying (only a single formula is proposed for shrinkage and for creep), even if the deformations caused by drying exhibit a very marked scale effect for large-thickness walls [1, 6]. Lastly, its ageing function (a function of the material's age) and its dependence on the thickness of the structure are well suited to structures having the order of magnitude of a building column loaded within 28 days, but are less suited for thick structures, prestressed at an age of 2 years. In the case of thick structures, it is practically impossible, in laboratory conditions, to perform experiments on the structure's scale. It is therefore necessary to perform "theoretically" the transitions (laboratory specimen behavior) \Leftrightarrow (in situ behavior of concrete in the structure) \Leftrightarrow (overall deformation of the structure). In fact, the existence of such diverse models and philosophies hides a real lack of knowledge about the complex physical-chemical phenomena that cause delayed deformation.

Difficulties related to the industrial nature of the study and particularly to the type of loading studied on a containment :



- the biaxial (tangential/vertical) nature of the prestress ;
- a late loading age of about 2 years ;
- complex loading (mean duration: about 1 year) ;
- thermal coupling (temperature gradient between the intrados and extrados) ;
- effect of structure outside standard sections (restraint by basemat or dome).

4.3. Current outlook for R&D in the mid-term

In the mid-term, research on delayed concrete deformation is likely to focus on the effect of a biaxial stress field specific to the containment, and on the eternal question of deformation's physico-chemical origins [3], given that work must be conducted both on ordinary concretes and on the HPCs [8] of future units.

The obvious partners in France are the LCPC for the mechanical (modeling/coupling) and physical-chemical aspects; and the LMDC in Toulouse, which will concentrate more on interface phenomena, electronic microscopy, aggregate mineralogy, etc... No one doubts, however, that the problems related to reclosure of the equipment hatches are - also - likely to require a number of more technological research programmes.

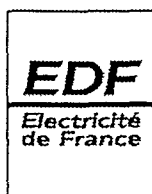
5. CONCLUSION

Concrete - this material that is viscoelastic, fragile when stretched, heterogeneous, porous and out-of-balance - still holds many secrets [9, 14] (the 1993 conference in Barcelona [7] devoted exclusively to creep, where over a hundred papers were given, is proof of this). But to avoid painting too black a picture, we should remember that, for conventional civil-engineering applications, the regulations as they stand are perfectly adequate! Only particularly innovative applications - thick, exceptional or unusually sensitive structures - may require more in-depth thinking and more careful justification.

This is one of the reasons why the containments of EDF's NPP set are subject to attentive monitoring, supplemented by R&D studies, in order to improve our understanding of the phenomena and create models to predict the behaviour of the prestressed concrete.

The results gathered so far show that the behaviour of the NPP containments is generally satisfactory. However, lifespan forecast studies indicate that two or three containments are liable to fall below the acceptable level of minimum residual stress after 40 years' service.

The test results should help us acquire a better grasp of these phenomena.



6. BIBLIOGRAPHY

- [1] Acker P. (1988) "Comportement mécanique du béton : apports de l'approche physico-chimique", **Rapport de recherche LPC** n° 152.
- [2] Acker P. (1993) "Recommendation for measurement of time dependent strains of concrete loaded in compression", in [7], pp. 849-858.
- [3] Baroghel-Bouny V. (1994) "Caractérisation microstructurale et hydrique des pâtes de ciment et de béton ordinaire et à hautes performances", **Thèse de Doctorat de l'ENPC**.
- [4] Bazant Z. P. (1993) "Current status and advances in the theory of creep and interaction with fracture", in [7], pp. 291-307.
- [5] **BPEL** (1991) "Règles techniques de conception et de calcul des ouvrages et constructions en béton précontraint suivant la méthode des états limites", fascicule 62 du CCTG, Règlement français.
- [6] ConCreep 4 (1986) **Creep and shrinkage of concrete: Mathematical modeling**, Proc. of the 4th RILEM Int. Symp., Bazant Z. P. Editor, Evanston, USA.
- [7] ConCreep 5 (1993) **Creep and shrinkage of concrete**, Proc. of the 4th Int. Rilem Symp., Barcelona, Z. P. Bazant Editor, E & FN Spon.
- [8] de Larrard F., Ithuralde G., Acker P., and Chauvel D. (1990) "High-Performance Concrete for a Nuclear Containment", 2nd Int. Conf. on Utilization of HSC, Berkeley, ACI SP, pp. 121-127.
- [9] Freysinnet E. (1993) **Un amour sans limite**, Editions du Linteau, Paris.
- [10] Granger L. (1995) "Comportement différé du béton dans les enceintes de centrales nucléaires : analyse and modélisation", **Thèse de Doctorat de l'ENPC**.
- [11] Granger L., Bazant Z. P. (1995) "Effect of composition on basic creep of concrete and cement paste" *J. of Mech. Engng.*, ASCE, 121 (11), pp. 1261-1270.
- [12] Granger L. (1995) "An insight in the reduction of drying shrinkage due to skin micro-cracking", 2nd Int. Conf. on **Fracture Mechanics of Concrete and Concrete Structures**, F. H. Wittmann Editor, Zurich, pp. 1493-1502.
- [13] Granger L., Torrenti J.-M. (1995) "Evaluation of the lifespan of a nuclear PC vessel in terms of delayed behavior and loss of prestress", IABSE Symp. on **Extending the lifespan of structures**, San Francisco, pp. 1411-1416.
- [14] Toutlemonde F., Granger L. (1995) "Maîtriser la rupture du béton : améliorations du matériau, progrès de la modélisation, exemples industriels", *Revue de métallurgie et cahiers techniques d'information*, Série Science et génie des matériaux, 92, pp. 285-301.
- [15] Rousselle H. (1993) "Comportement mécanique des enceintes de confinement des centrales d'EDF", *Journées d'étude de l'ENPC des 9 et 10 décembre 1993*.

**JOINT WANO-PC/OECD-NEA WORKSHOP ON
PRESTRESS LOSS IN NPP CONTAINMENTS**

**PRESTRESS FORCE MONITORING
ON THE THTR PRESTRESSED CONCRETE REACTOR VESSEL DURING 19 YEARS**

by F. Stangenberg, M. Borgerhoff, K. Schimmelpfennig

ABSTRACT

The prestressed concrete pressure vessel (PCPV) of the THTR (Thorium High Temperature Reactor) nuclear power plant (NPP) in Hamm-Uentrop, Germany, has the advantage of most other nuclear prestressed concrete structures that prestress forces have been monitored from 1976 to 1995 during erection, commissioning, test operating and decommissioning of this plant.

Over this whole period, 30 prestressing force transducers installed at anchor heads of 10 horizontal and 10 vertical ungrouted tendons have been monitored as well as a large number of concrete strain transducers, strain gauges at steel components, thermocouples and resistance thermometers.

The authors' company had been commissioned by the authorities to act as experts reviewing the monitoring results periodically in order to check whether the PCPV structure behaves as designed. Therefore we have analysed the mechanical behaviour of the structure with consideration of pressure and temperature history, concrete creep and shrinkage influenced by mass concrete conditions and temperatures as well as stress relaxation of tendons over this whole period and compared computational results with the results of periodical measurements.

Results of these measurements – mainly prestressing forces – are shown in comparison with the values over 19 years time as predicted by the analysis. The monitoring devices are described, and problems encountered with some transducers, which required partial exchange, are discussed. Conclusions about predictability of prestress loss and on the feasibility of this kind of monitoring for indicating the proper behaviour of a prestressed concrete vessel or containment structure are drawn.

1. INTRODUCTION

Beforehand it has to be pointed out that the subject of this paper is no NPP secondary containment in the general sense, but a reactor vessel integrating primary and secondary functions. Nevertheless, this large cylindrical prestressed concrete structure is an important part of a nuclear plant and – mainly because of its prototype character – equipped with an extensive measuring instrumentation including a number of prestressing force transducers, which have been monitored over the whole period of the vessel life from erection until decommissioning of the NPP. For that reason however, it fits the purpose of this workshop to approach and experience about assessment of the prediction of prestress losses, which should not be essentially different between a containment and a prestressed reactor vessel.

This reactor vessel is the prestressed concrete pressure vessel (PCPV) of the 300 MWe THTR (Thorium High Temperature Reactor) prototype NPP in Hamm-Uentrop, Germany. This plant has been manufactured in the seventies by a working combine under the leadership of Krupp Company. The THTR-NPP is owned by the Hochtemperatur-Kernkraftwerk GmbH, Hamm, Germany, a subsidiary company of the Vereinigte Elektrizitätswerke Westfalen AG, Dortmund, Germany. This plant started its test operation in 1985 and has been shut down for the purpose of the scheduled revision on September 29th, 1988. It has been decommissioned finally on September 1st, 1989. After the following periods of inactive operation and discharge of the reactor core, the plant meanwhile has passed into the state of safe inclusion.

The former senior manager of the authors' firm, Prof. Zerna, at that time had been ordered by the building authorities to check the structural documents, to carry out the site supervision and to make several expert assessments on this behalf, including supervision of the pressure test and evaluation of the measurements concerning the prestressed concrete structure of the reactor vessel. After the pressure test, the review of the monitoring results, which had to be carried out periodically in order to check whether the PCPV structure behaves as designed, has been done by the authors' firm. This work has been completed in 1995, that means 19 years after the prestressing of the PCPV.

2. DESCRIPTION OF THE PCPV AND ITS MONITORING DEVICES

The well known shape of the THTR PCPV is illustrated as a reminder by a photo of a demonstration model in Fig. 1, showing a section through the vessel walls and the primary circuit components. The pebble bed core, two of the six steam generators, one of the six gas blowers and the arrangement of the prestressing tendons in the concrete walls can be recognized.

The technical data of the THTR-PCPV have already been mentioned in a number of publications. So, only the most important data are repeated here. The main dimensions are (cf. Fig. 2):

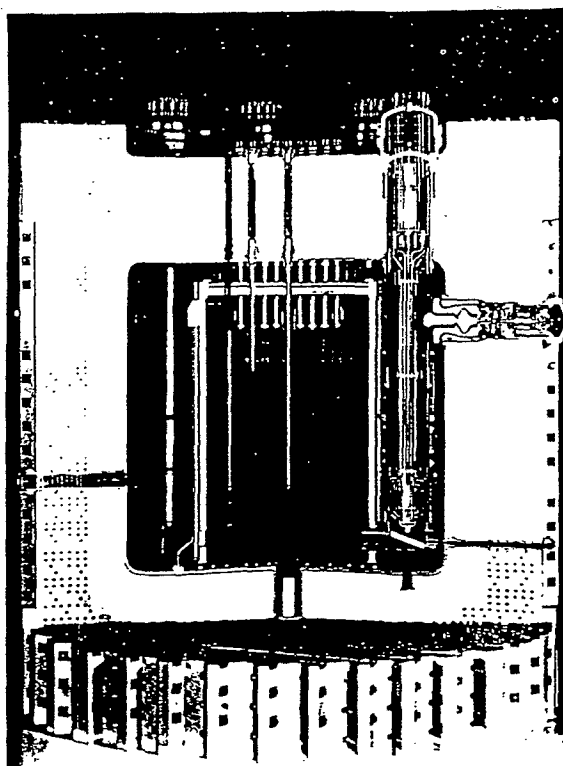


Fig. 1 Model of the THTR-PCPV

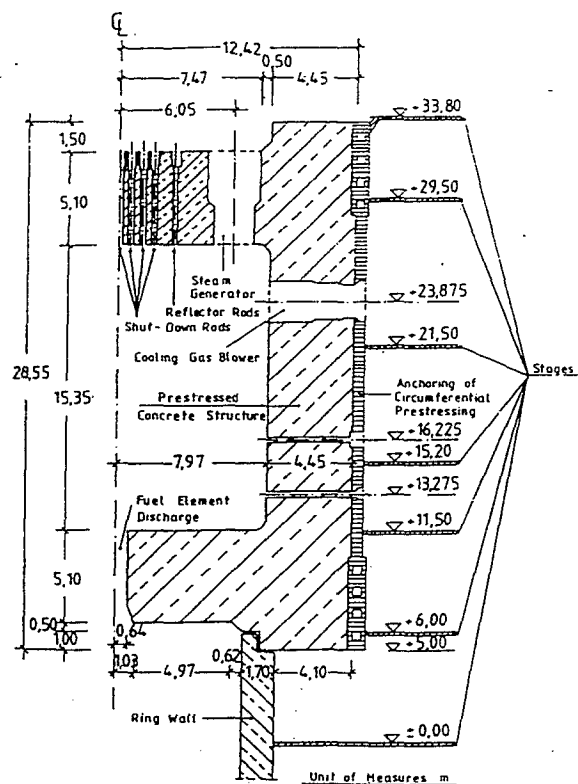


Fig. 2 Section through THTR-PCPV

- external diameter: 24.8 m,
- internal diameter: 15.9 m,
- cylinder wall thickness: 4.5 m,
- external height: 28.5 m,
- internal height: 15.4 m,
- thickness of the slabs: 5.1 m.

The prestressing system consists of 292 vertical and 560 circumferential, buttress anchored tendons of the BBRV system, each with a bearing capacity of about 9000 kN. Operational design values are the normal operating pressure of 39.2 bar and the normal concrete temperature at the inner surface of about 45 °C. The proof pressure has been 46.1 bar.

The THTR-PCPV is instrumented with a great number of measuring devices, namely

- 452 concrete strain transducers (vibrating wire gauges), predominantly arranged in three radial wall sections,
- 30 prestressing force transducers installed at the anchor heads of tendons which are not grouted like the others but filled with the grease "Astrolan",
- 437 strain gauges fixed at steel components of the vessel,
- 305 thermocouples fixed at steel components of the vessel,
- 234 resistance thermometers embedded in concrete.

3. EVALUATION OF THE MEASUREMENT RESULTS

3.1 GENERAL

Measurements of all devices listed in chapter 2 have been recorded periodical-ly since start of prestressing. The evaluation of these measurements is based on a comparison of predicted and measured values. The calculations of the vessel history have been carried out mainly by use of an axisymmetric model of the PCPV. For the purpose of providing comparative values for measured values of gauges in not axisymmetric vessel areas, these calculations are supplemented by use of existing 3D analysis results.

3.2 PREDICTION OF CONCRETE STRAINS AND PRESTRESSING FORCES

The calculation of the mechanical behaviour of the PCPV in its lower half has been performed by use of an axisymmetric model of its prestressed concrete structure. In the hatched areas of the mesh of the computation model depicted in Fig 3., the reduced stiffness due to large penetrations is taken into account by introducing a fictitious modulus of elasticity.

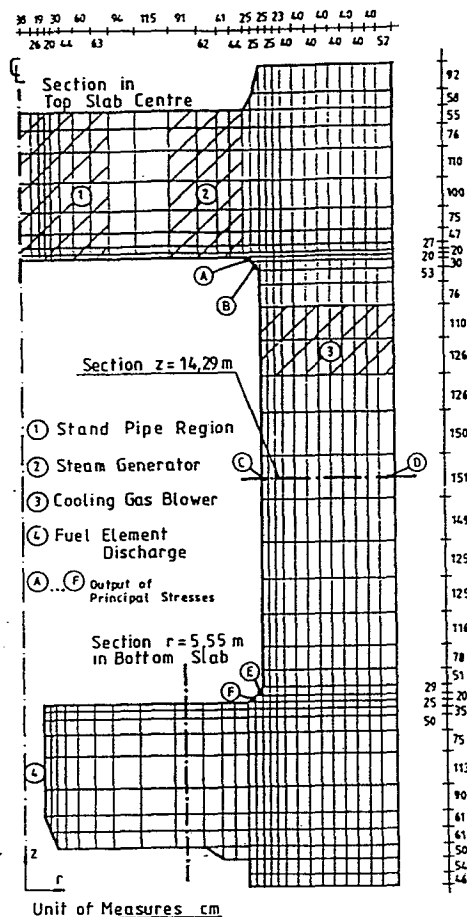


Fig. 3 Axisymmetric Computation Model of THTR-PCPV

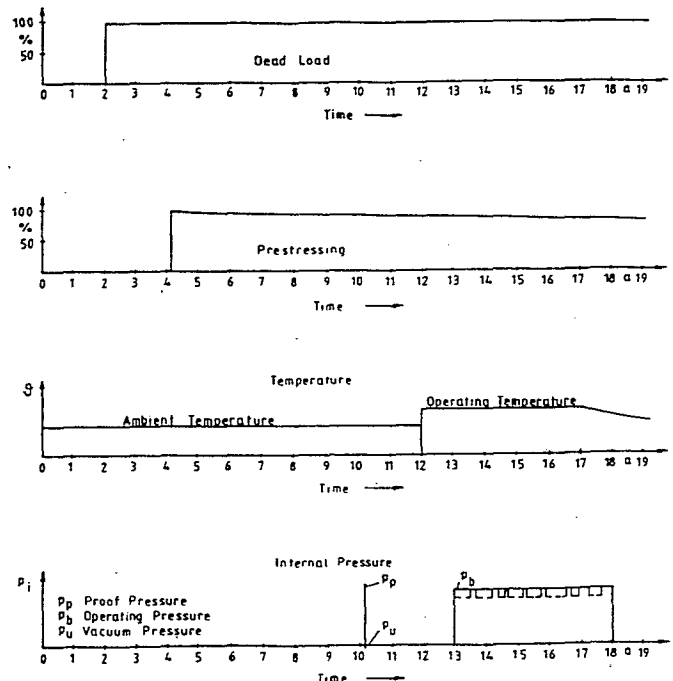


Fig. 4 Idealized Load History of THTR-PCPV

The characteristic value of the modulus of elasticity of the concrete is $E = 40000$ MPa. The creep behaviour is taken into account by use of a fictitious modulus of elasticity which is defined to be the reciprocal value of the time and temperature dependent specific creep strain. Shrinkage of concrete is assumed to develop in affinity to concrete creep. The wires of the tendons consist of hot-rolled SIGMA-St 1420/1570 prestressing steel. The time dependent relaxation predominates the applied prestressing forces. Further changes of the prestressing forces due to concrete creep are regarded in the analysis.

A realistic calculation of stresses and deformations of the PCPV at certain points of time based on the time dependent material behaviour required the load history until that time to be taken into account. The idealized load history of the THTR-PCPV is depicted in Fig. 4. In this sense, the single loadcases deadload, prestressing, operation temperature, internal pressure and shrinkage are analysed considering the different creep times, and afterwards are superimposed according to the law of linear superposition.

3.3 COMPARISON OF PREDICTED AND MEASURED VALUES

3.3.1 CONCRETE STRAINS

Since the concrete strains are not the essential subject of this report, only one selected diagram with comparative values of calculated and measured strains inside the vessel walls shall be shown here. In Fig. 5, the tangential strains near the inner surface of the cylinder wall at the height of the vessel equator are plotted versus time. The time axis of the diagram is defined to be the interval since the midst of the prestressing period, that is October 10th, 1976. The measured values are plotted as crosses. The calculated values are linked by straight lines resp. dotted lines. The following conclusions can be drawn from the comparison of the calculated and measured strains.

The absolute values of the calculated strains initially show a distinctly stronger increase than the measured strains. That means that the capacity of creep is overestimated by the used design creep law. The reason for these differences has been found to be the dependence on the age of concrete at first loading, which has been already about two years on an average at time of prestressing, and which is not taken into account by the design creep law.

The peak at day 2170 is caused by the pressure test. The measured strain differences agree well with those calculated by elastic calculation. The statistical evaluation of all gauges in undisturbed vessel regions indicates that the actual modulus of elasticity at time of the pressure test has increased up to about 13 % higher than the specified 90 days' value, that is 45000 MPa.

The strain behaviour after final shut-down of the reactor has been calculated with and without consideration of reverse creep of concrete after unloading. But the comparison with the measured strains shows no indication for reverse creep after unloading from internal pressure.

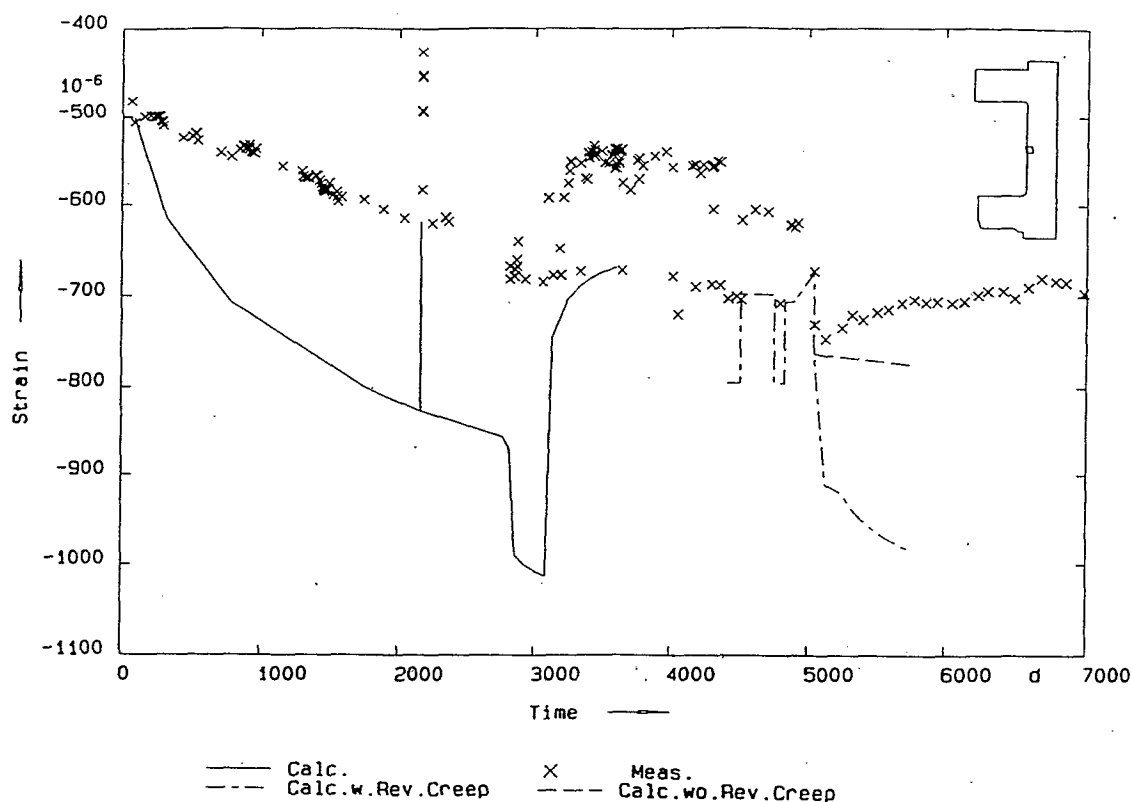


Fig. 5 Measured and Calculated Tangential Concrete Strains
Gauge No. 1254, $r = 8.26$ m, $\phi = 210^\circ$, $z = 14.07$ m

3.3.2 PRESTRESSING FORCES

The 30 prestressing force transducers are installed at 10 vertical and 10 horizontal circumferential tendons. Each monitored vertical tendon is equipped with 1 transducer since the vertical tendons are prestressed only from one end. The horizontal tendons have transducers at both anchors. Table 1 contains the prestressing force transducers in numerical order of the anchor head numbers. The group number in the last column of Table 1 distinguishes the transducers relating to their performance during measurement history. This topic will be treated on in section 3.4.

The measured and calculated prestressing forces of some selected tendons are depicted vs. time in the Fig. 6 to 11. The measured values are plotted as crosses. The calculated values are linked by straight lines. The dotted curves characterize the tolerances due to the effects of measuring inaccuracies. They result from the addition of different influences quantified as follows:

- 1 % of the measured value due to the influence of the measuring facility,
- 2.5 % of the measured value due to deviation from linearity,
- 300 kN due to the influence of the installation of the transducers under site conditions.

The abscissa unit is the time in days since the midst of the prestressing period.

Tendon Type	Anchor Head No.	Gauge No.	Group No.
Horizontal Tendons	5.9.1	542 + 543	B 2
	5.9.2	501	A 1
	8.3.1	506	A 2
	8.3.2	530 + 531	B 2
	23.3.1	508	A 2
	23.3.2	509	A 1
	24.5.1	510	A 2
	24.5.2	549 + 521	B 1
	38.2.1	526	A 1
	38.2.2	527	A 2
	39.6.1	545 + 546	B 1
	39.6.2	547 + 548	B 1
	55.2.1	524	A 1
	55.2.2	525	A 2
	61.6.1	512	A 1
	61.6.2	517 + 518	B 2
	75.1.1	502	A 1
	75.1.2	515 + 511	B 1
	76.9.1	500 + 513	B 2
	76.9.2	505	A 2
Vertical Tendons	32	532 + 533	B 1
	39	522	A 1
	45	516	A 1
	148	534 + 535	B 1
	153	523	A 1
	161	537 + 544	B 2
	168	514	A 1
	252	519	A 1
	261	538 + 539	B 1
	266	540 + 541	B 1

Table 1 Anchor Heads with Prestressing Force Transducers

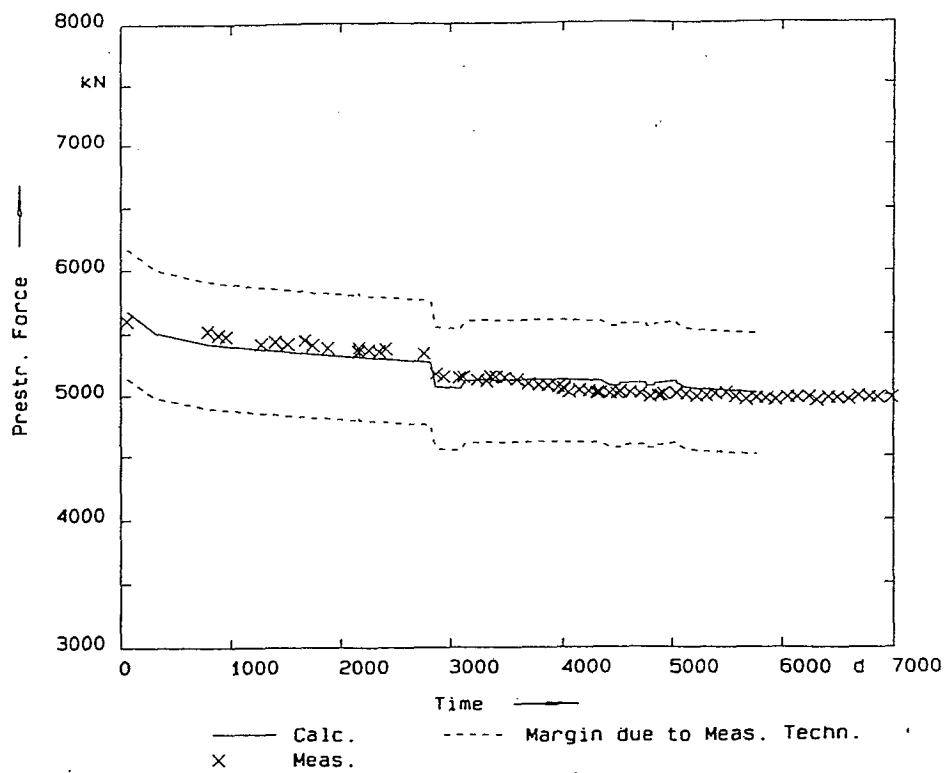


Fig. 6 Measured and Calculated Prestressing Forces
Gauge No. 508, Anchor Head No. 23.3.1

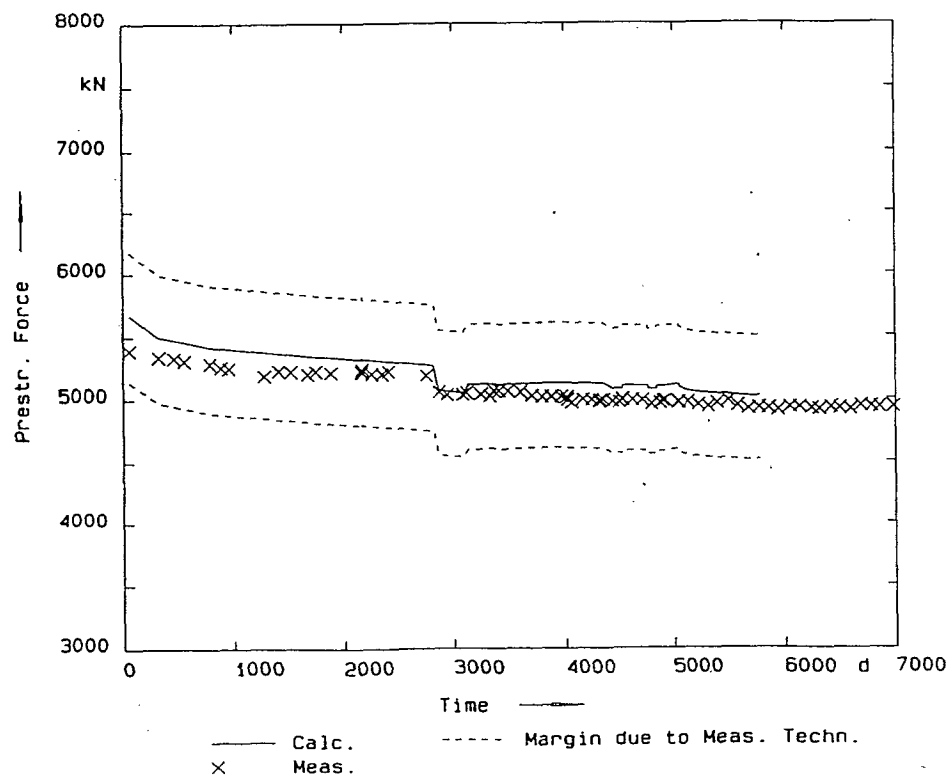


Fig. 7 Measured and Calculated Prestressing Forces
Gauge No. 509, Anchor Head No. 23.3.2

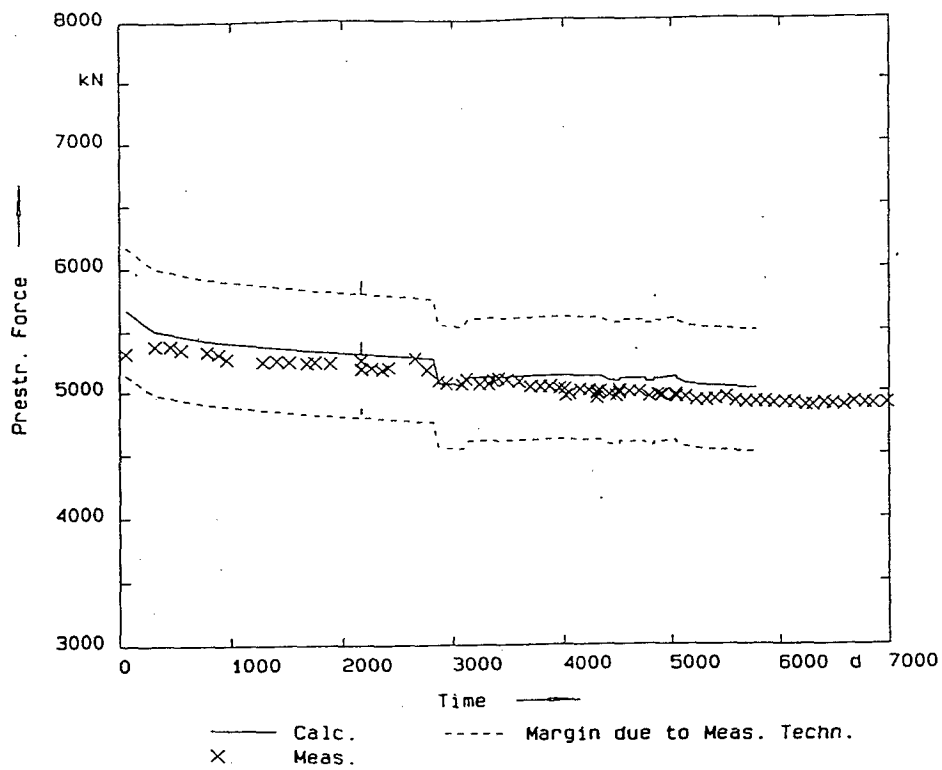


Fig. 8 Measured and Calculated Prestressing Forces
Gauge No. 526, Anchor Head No. 38.2.1

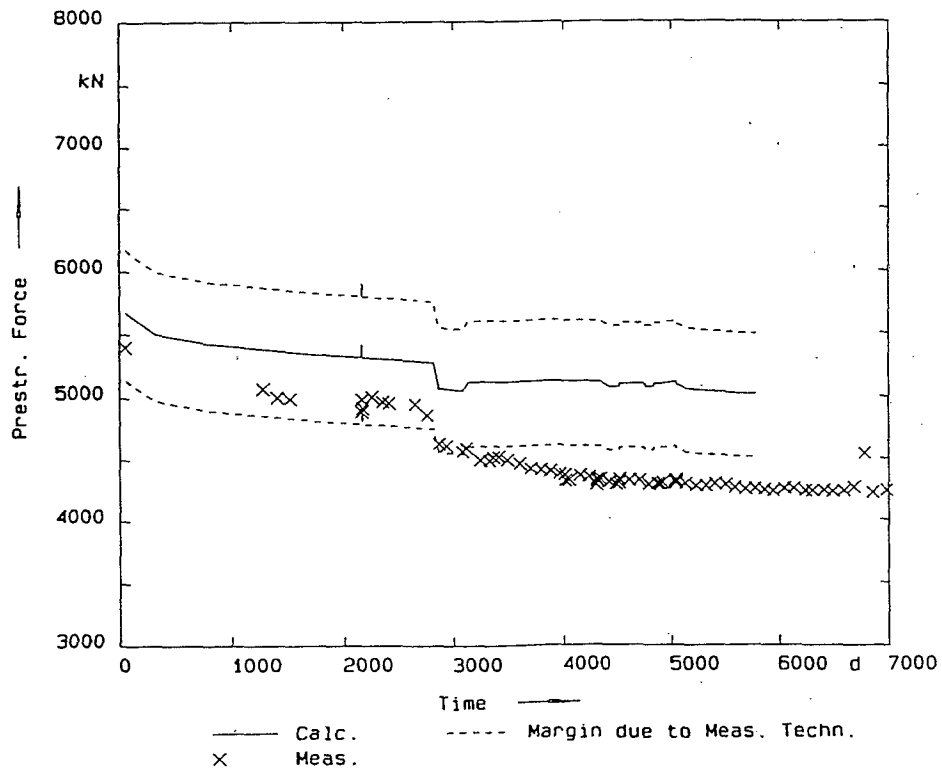


Fig. 9 Measured and Calculated Prestressing Forces
Gauge No. 527, Anchor Head No. 38.2.2

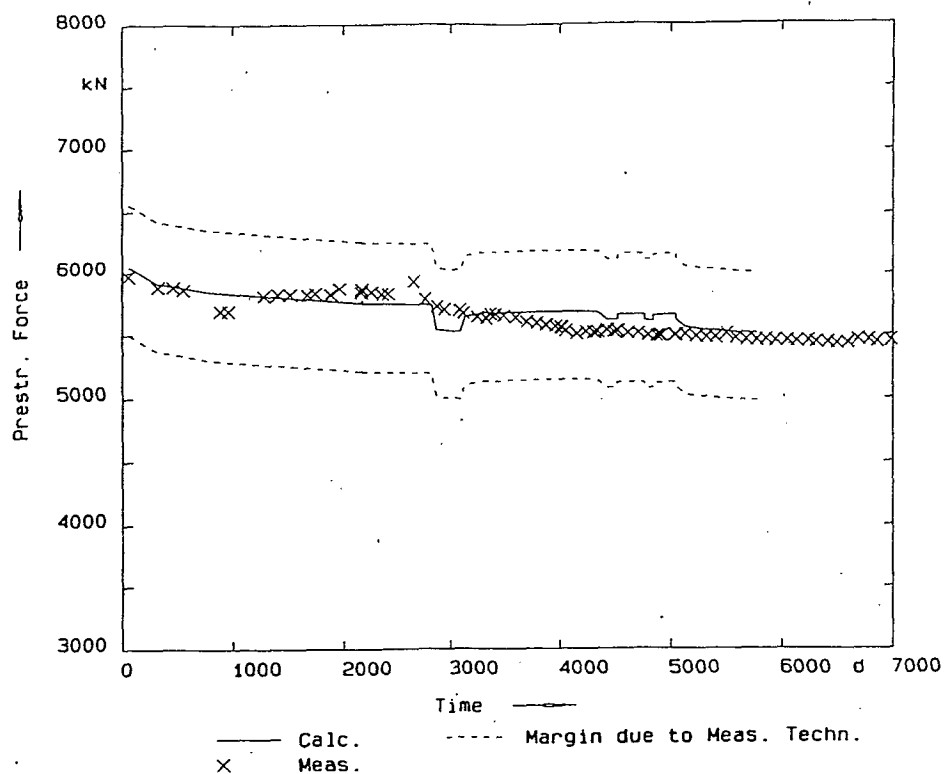


Fig. 10 Measured and Calculated Prestressing Forces
Gauge No. 532 + 533, Anchor Head No. 32

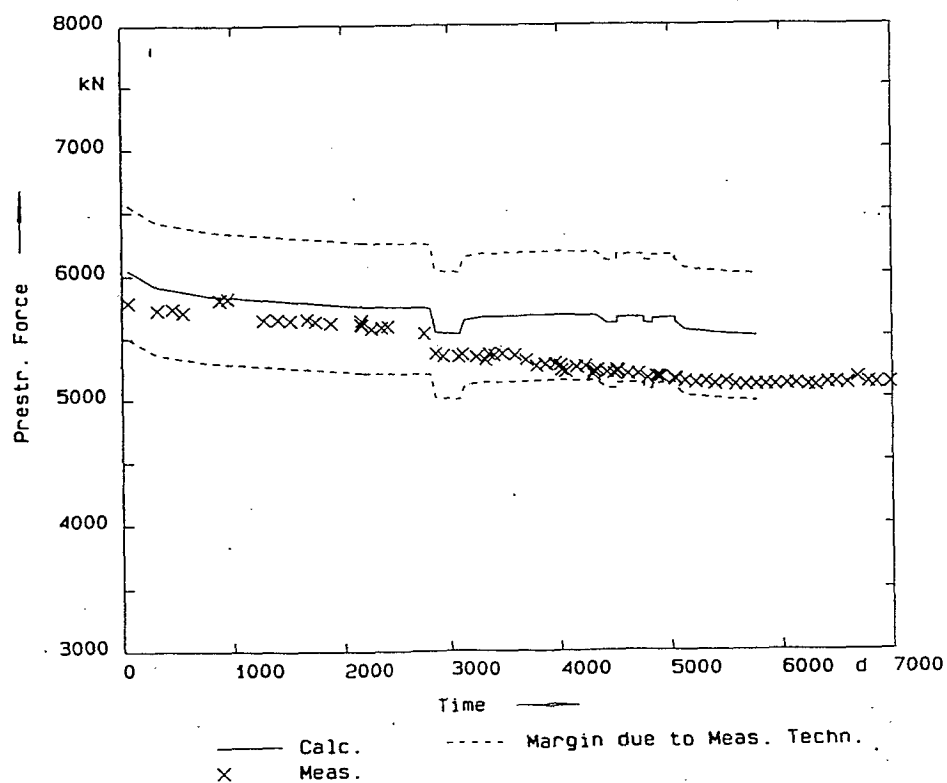


Fig. 11 Measured and Calculated Prestressing Forces
Gauge No. 522, Anchor Head No. 39

The groups established in Table 1 are defined dependent on their performance until exchange of 13 of 30 force transducers (cf. section 3.3) as follows:

- | | |
|----------------|--|
| Group No. A 1: | not exchanged transducers, faultless or only short-term breakdown without effect on the measured values, |
| Group No. A 2: | not exchanged transducers with long-term breakdown or malfunctions due to penetrated humidity, |
| Group No. B 1: | exchanged transducers with subsequent faultless function, |
| Group No. B 2: | exchanged transducers with subsequent deviating measured values. |

The following conclusions can be drawn from comparing measured and calculated prestressing forces:

- Except a small number of tendons, the imagined connecting line between the first two measuring crosses takes a course which is less decreasing than the calculated function. This confirms the assessment made in section 3.3.1 that the initial creep deformations of the concrete – approximately in the first two years – are substantially lower than calculated by use of the design creep law of the THTR concrete.
- After this initial period, the measured and calculated prestressing forces mainly proceed parallel with mostly small deviations.
- As expected, the increase due to internal pressure is negligible in comparison with the losses of force due to concrete creep, shrinkage and steel relaxation.
- 43 % of all force transducers have transmitted measurements with similarly good agreement of calculated and measured prestressing forces as shown in Fig. 6, 7, 8 and 10. At 13 % of the transducers, prestressing forces have been measured which run out of the lower margin. In all these cases it concerns transducers of the groups A 1 and A 2 of Table 1, that are the unexchanged transducers. Fortunately, it can be concluded from the measurements at the opposite anchor head that the tendon is all right, cf. Fig. 8 and 9. Hence, the assessed deviations must be connected with defaults of measuring. The left over transducers have transmitted measuring results, which remain within the tolerable limits (see Fig. 11 as an example).

3.3 PROBLEMS ENCOUNTERED WITH MEASURING DEVICES

Concerning problems which have occurred relating to the measurements, the following remarks concentrate on the prestressing force transducers.

In March, 1982, 13 of the 30 transducers have been exchanged. These can be distinguished in Table 1 by double gauge numbers. The double numbers reveal that instead of the original undivided steel cylinders between anchor heads and

bearing plates carrying the strain gauges, two half-shells had to be installed. The exchange has become necessary because of different reasons as follows:

- failure of the internal bridging branch,
- unexplicable measured values and
- varying insulation resistance.

On the opportunity of the exchange of the transducers, the prestressing forces of the concerning tendons have been checked. These measurements have shown that the true prestressing forces measured by the jack are all higher than recorded by the force transducers.

Predominantly in the years 1977 and 1978, a certain number of the unexchanged transducers showed malfunctions due to penetrated humidity which could have been eliminated by drying.

4. CONCLUSION

This paper deals with monitoring of 20 tendons of the presented THTR-PCPV by use of 30 prestressing force transducers over a period of 19 years.

Considering this long period, these transducers have shown a good performance as a whole. 13 transducers have been exchanged providently in 1982. After that time, only one transducer completely has failed. On the other hand, 80 % have transmitted prestressing forces within the tolerable limits. The 4 transducers with measuring default values only applied to tendons equipped with 2 transducers. So, the opportunity remained referring to the recordings of the opposite transducer of the same tendon.

Accordingly, during the whole time of monitoring the prestressing force transducers have been a safe instrument for the purpose of assessing the mechanical behaviour of the PCPV with respect to its design.

NUCLEAR POWER PLANT CONTAINMENT DESIGN
EVOLUTION AND INDIAN EXPERIENCE

BY

A.S. WARUDKAR *

1. **Introduction**

Nuclear Power was ushered in India in 1969 with the commissioning of Tarapur Atomic Power Station (TAPS) comprising two boiling water type reactors. This Station was set up on a turn-key basis by M/s. General Electric Company. Further Indian Nuclear Power Programme is essentially based on Pressurised Heavy Water Reactors (PHWRs) using natural uranium as fuel and heavy water as moderator.

History of Indian containments starts with the use of Steel containment with cylindrical shell capped with steel dome for one of its research reactor.

However construction of India's first indigeneously engineered nuclear power containment and reactor building started in 1963 with Presurised Heavy water Reactor in Rajasthan. Today, eight reactors of this type are already in operation and six are under construction.

* Chief Engr. (Civil), Nuclear Power Corporation, India

The number, age, location and type of NPP owned by India are indicated in Table-1.

Primary responsibility for design, engineering, construction, commissioning and operation of these power stations rested on Power Projects Engg. Division of Department of Atomic Energy (DAE) Government of India till 1987. However after Sept. 1987 this responsibility is with Nuclear Power Corporation, Public Sector Company (Govt. of India Enterprise).

Atomic Energy Regulatory Board (AERB) was formed in 1983 by Govt. of India. One of the functions of the AERB is to ensure compliance by DAE and Non-DAE installations of Safety codes and standards during construction/commissioning / operation stages.

2.0 Evolution of Indian Containments upto Kaiga/TAPP 3-4 Projects

The Indian PHWR Containments have been evolved over a period of time from the time of its first application at Rajasthan Atomic Power Project (RAPP-1&2). RAPP Containment (sketch 1) has R.C. Wall and prestressed concrete dome. Its dome had design features which were common to the French Containments at that time, such as construction of single barrier using prestressing to achieve uncracked concrete barrier and use of Polyvinyl Paint on inner surface as an additional leak-tight

membrane to serve as flexible liner. The common design basis was "working stress method" that was internationally used at that time for design of concrete structures in general and prestressed concrete structures in particular.

The next containment at Madras Atomic Power Project (MAPP) (sketch 2) adopted prestressed concrete wall and dome cast monolithically for the inner containment and introduced the outer containment wall in reinforced rubble masonry enclosing the inner wall but not the dome portion, thus introducing concept of double containment. The Inner Containment was designed on the same philosophy as that of RAPP dome. The addition of outer wall, enables retrieval of leakages passing the first barrier of I.C. Wall by trapping the same within the annular space from where it could be released to environment in a controlled manner. Creation of partial vacuum for this purpose establishes the net flow of air from outside towards annular space thus eliminating direct escape of radioactive leakages from I.C. Wall to environment altogether. The outer wall, being a low pressure system was required to be only nominally leak-tight.

The containment of Narora (NAPP) (sketch 3) and Kakrapar (KAPP) were designed incorporating the improvement of

providing total outer enclosure in reinforced concrete with R.C. dome. The outer containment protects the inner containment from rain, wind, solar radiation and corrosive atmosphere. It also provides protection to reactor from external missiles like aircraft crash, wind borne missiles in cyclones. The Inner containment is roofed over by cellular flat concrete slab in two tiers with bottom tier fully prestressed and top tier in reinforced concrete. The same basic approach has been adopted for next series of containments at Kaiga 1&2, RAPP 3&4, (sketch 4) TAPP 3&4 (sketch 5) except that in these containments the Inner Containment has prestressed concrete dome as a roof which is cast monolithically with the wall, since the steam generators have been taken inside of Inner Containment. These containments have openings in both inner and outer domes to facilitate lowering of steam generators during their installation and future replacement.

3.0 General design philosophy

The basic approach is to evaluate the highest load intensities likely to be encountered during the various stages such as construction, normal operations, accidental situations and testing etc. In addition to normal live loads, and ambient temperature loads containment is mainly designed for internal pressure and temperature rise due to postulated design basis accident. Also environmental loads due to wind having return period of

1000 years and earthquake with return period of 1000-10000 years are considered in design. The prestressing forces, although treated as external loads in the analysis are actually introduced in the structure as the design solution with the intention of controlling the tensile stresses to avoid any through cracking of concrete.

In order to evaluate the response of the structure subjected to various loads, methods of linear elastic analysis are used. The response of the structure under various load combinations is obtained by using principle of superposition.

Achieving required leaktightness is considered as the prime design aim. The inner containment is expected to restrict the leakage within 0.3% of the enclosed volume per hour.

The design of containments from RAPP, MAPP, NAPP and KAPP were based on 'Working Stress Method' of design. The design philosophy adopted for containments from Kaiga onwards is a 'Limit State Philosophy' as per French Code RCC-G where responses of the containment for both the "limit state of servicability" and "limit state of strength" are checked under various load combinations. The permissible stresses at servicability limit state

are limited to a value within which the overall structural response to the service loads is more or less elastic and linear. The safety margins in strength are checked by ultimate load checks.

Salient design parameters of the containment are indicated in Table 2.

4.0 Arrangement of prestressing

All prestressing cables used are bonded type tendons. For initial containments at RAPP/MAPP, wire system was used for prestressing. In the containment at NAPP and KAPP 12T13 system with ultimate capacities of cable of 220T was used. To take care of increased design pressure, in the containments at Kaiga/RAPP 3&4/TAPP 3&4, Wall and dome of inner containment are prestressed with 19K13 type high tensile strands with ultimate capacity of 355T. This system consists of 19 strands of 12.7mm nominal diameter to form one cable. Cables are either prethreaded or postthreaded through duct hole of 80mm dia made out of sheathing manufactured from spirally wound lead coated m.s. strips of 0.5mm thickness. The space between the cable and the duct hole is grouted immediately after stressing the cable.

In a typical containment, I.C. wall is prestressed by horizontal ring cables spaced approximately at 270mm centre along its height. In vertical direction cable spacing is approximately 370mm alternatively spaced at

inner and outer face of wall. Some of the vertical cables are anchored at top of the ring beam at one end and in the soffit of the stressing gallery (in foundation raft) at other end.

In the case of Kaiga/RAPP 3&4/TAPP 3&4, the inner dome is prestressed by orthogonally placed cables in two layers, generally spaced at 450mm centre and in closely spaced bands near S.G. opening, they are generally spaced at about 225mm c/c. Some of the dome cables and vertical cables in wall are combined to form inverted J shape cables.

5.0

Structural integrity & Leaktightness test

Performance of the containment subjected to internal pressure load is checked prior to commissioning. The pressure is applied by means of compressed air in steps. Initially at low pressure (such as 0.2 bar, 0.4 bar etc.) extensive checks are made for locating any leakages from embedded parts or from construction joints or any other areas by making use of soap solution applied on external surfaces. The major leaks from internal surfaces are located by using smoke test. These leakage points are repaired by reapplying polysulphide caulking compound or repairing by epoxy mortar caulking. The leakage paths are grouted using low viscosity epoxy formulation.

After initial repairs, the main leak-tightness test is taken up. The pressure is increased in pre-determined steps and leakage rates measured.

The leakage is measured at full specified pressure for leak testing. This should be within allowable limits. Also correlation between leakage rates at low pressures and that at full pressure are established to facilitate periodical qualification of the containment.

During the progress of this test, the structural response of the containment is measured at pre-determined locations. The overall structural deformations (deflections) as well as local strains are measured and compared with the theoretically estimated values. The overall response upto proof testing pressure is expected to be more or less elastic and linear. The structural integrity tests have shown the behaviour more or less as predicted in all containments so far tested. It has been possible to keep leak rates from inner containments within allowable limits after carrying out necessary repairs.

6.0 In-service inspection

In-service inspection of containment covers the following activities:

- 1) Visual inspection of the containment.

- 2) The inspection of embedded surface mounted permanent instrumentation,
- 3) Inspection of external surfaces including the dome
- 4) Inspection around components and penetrations.

Visual inspection will assess the damage (if any) to the containment surface and surface coating during operation due to dropping of loads, or damage due to ageing effects etc. Special visual inspection is arranged in case of accidents like fire, if any. Platforms are provided in the annular space at various levels to provide access to the outer surface of the IC Wall to facilitate visual inspection.

Leakage of rain water/ground water into stressing gallery or containment is monitored and corrective action taken. Caulking compounds, polyurathene seals used around penetrations or at the construction joints are also inspected periodically.

In containments from Kaiga onwards periodical monitoring instruments for determining the general stress levels in prestressed concrete walls/dome are planned, with the help of embedded strain gauges.

7.0 Instrumentation

The appropriate instrumentation for monitoring structural behaviour during prestressing, and during proof testing of containment are provided. These generally

consist of penduli, invar wires, vibrating wire strain gauges, surface mounted electrical strain gauges, mechanical demec gauges, strain gauges for measuring thermal strains etc.

8.0 Problems related to prestressing

The problem is faced by the designer in calculating the long term losses due to prestressing due to creep, relaxation, shrinkage, due to wide variation in results obtained using different codal formulations.

For one of the containment, the authors organisation worked out the long term losses using various codal formulations and the comparison of the same is indicated in Table 3. From the table, large variation is noted in the long term losses in prestressing.

The relaxation losses mainly depend on whether normal relaxation or low relaxation strands are used. The codal values are for 20° C temperature during relaxation test. The upward corrections to be applied to these specified values for other values of operating temperatures in the containment are varying. Some codes are silent about this correction. Also the laws of extrapolation of relaxation losses from the test data of 100/1000 Hrs. tests to life period of structure are also varying from manufactures to manufacture and from one code to other.

In the containment, though the tendons are prestressed at 80% of ultimate tensile strength (UTS) of the tendon, the sustained load in the tendons after instantaneous losses is less than 70% of UTS. In view of this it would be appropriate to consider relaxation loss corresponding to 70% of UTS as initial stress.

Creep is also reported to be affected significantly by ambient temperature.

9.0 Research and Development Work

a) Scale model test

As early as 1975, 1:12 scale model of the containment of MAPP-1 was made at Structural Engg. Research Centre, Madras.

The model was designed as a direct true scale model (stress scale factor equal to unity).

Concrete of the prototype was modelled by micro concrete in the model, untensioned reinforcement by annealed steel wires, and prestressing cables by prestressing wires of 4mm and 2mm. Major openings in the containment were also simulated in the model. Instrumentation was provided to measure deflections, prestress strains and temperature measurement.

The model was subjected to internal pressure loading upto 16 psi pressure.

It was observed from the experimental results that theoretical analysis could predict the behaviour of the

dome reasonably well. It was also noted that ribs, openings and thickenings around openings have considerable influence on the behaviour of wall in their neighbourhood and axisymmetric analysis should take into account these effects.

b) **Anchorage zone stress**

In 1979, field measurements of strains in the reinforcement and stresses in the concrete in the anchorage zone of a segment of containment wall, under construction at NAPP were made. Thirty two load cells were placed in two layers on either side of the cable. Similarly some of the reinforcement bars placed in the anchorage zone were fixed with 10mm strain gauges. The strains in the steel and concrete were measured during hardening period of the concrete and later strains in the containment shell were measured during prestressing and destressing of the cable. These observations helped the designer to gain confidence in detailing of reinforcement in the anchorage zone.

c) **Development of prestressing system**

In RAPP 1&2/MAPP containments wire system (12 ϕ 7/12 ϕ 8) was used. With a view to reduce congestion and increase cable spacing in NAPP and KAPP, 12T13 system (220T UTS) was developed and used. To take care of increased design pressure of Kaiga/RAPP 3&4 containments, 19K13 system (355 T UTS) was developed and used.

All these development works have given impetus to indigenous prestressing industry. For future containments use of higher capacity systems with UTS of 500/750 T is proposed and as these capacity system are not readily available in India, development work is in progress.

d) Ultimate pressure capacity

Though the internal pressure rise in the containment due to all postulated accidents are considered in the present design, the stray possibility of pressure going beyond design value is not ruled out. To examine safety implications for such eventuality, ultimate strength of the containment is planned to be determined by non-linear analysis. This work is taken up as development work. This is also proposed to be verified by conducting experiments on scale model of prestressed containment.

e) Secondary effects

The shrinkage, creep and fracture energy tests are being conducted for the concrete mix being used in the Kaiga containments. These test results would enable to compare the prestress losses as worked out using formula given in national code.

f) **Long term monitoring**

In earlier containments upto and including KAPP containment, there were no instruments embedded in the prestressed concrete containment for monitoring its long term behaviour. However the leaktightness of containment and its structural integrity was assessed based on periodical pressure testing of containment at reduced design pressure.

In containments from Kaiga onwards, the appropriate instrumentation is provided for monitoring structural behaviour during prestressing, during structural integrity test at full design pressure and thereafter at regular interval during the life of containment. Vibrating wire strain gauges (24 Nos.) will be embedded in the containment, ring beam and wall. Concrete specimens will also be cast for measurement of shrinkage and creep strains over the life period of the containments.

Conclusion

Nuclear containment is important safety structure. In India it has undergone modifications and improvements during design of every new plant with a view to improve safety features. This may continue as more and more experience from construction and operational feed back from previous reactors is obtained.

References :

1. Indian Nuclear Power Programme with PHWRS - NPCIL Publication - Sept. 1992
2. Evolution of Indian Containments and Future Trends in Design & Construction - by Mr. N.N. Kulkarni - Workshop on Structures for NPP Reactor Technology IIT, Madras 1987
3. Perspectives from a Developing Country - by Mr. C.R. Alimchandani - Technorama - July 1992.

TABLE 1

NUCLEAR POWER PLANTS IN INDIA

Station/ Project	TYPE	Rated capacity	Year of criticality
TAPS 1&2	BWR	2x160	1969
RAPS 1&2	PHWR	100/200	1972/80
MAPS 1&2	PHWR	2x220	1983/85
KAPS 1&2	PHWR	2x220	1992/93
<u>UNDER CONSTRUCTION</u>			Expected Criticality
KAIGA 1&2	PHWR	2x220	1999/1998
RAPP 3&4	PHWR	2x220	1998/1999
TAPP 3&4	PHWR	2x500	2004/2005

TABLE NO. 2

SALIENT DESIGN PARAMETERS

	RAPP 1&2	MAPP 1&2	NAPP 1&2	KAPP 1&2	Kaiga 1&2	RAPP 3&4	TAPP 3&4
Type	Single Containment	?	?	Double Containment	?	?	?
1.Design pressure kg/cm ²	0.42	1.16	1.25	1.25	1.73	1.73	1.44
2.Test pressure kg/cm ²	0.53	1.44	1.44	1.44	1.73	1.73	1.44
3.Pre-stressing system	12ø7	12ø8	12T13	12T13	19K13	19K13	19K13
4.Cable UTS (Tonnes)	74	92	220	220	355	355	355

TABLE NO 3(a)

COMPARISON OF DEFERRED LOSSES. USING VARIOUS CODAL FORMULATIONS

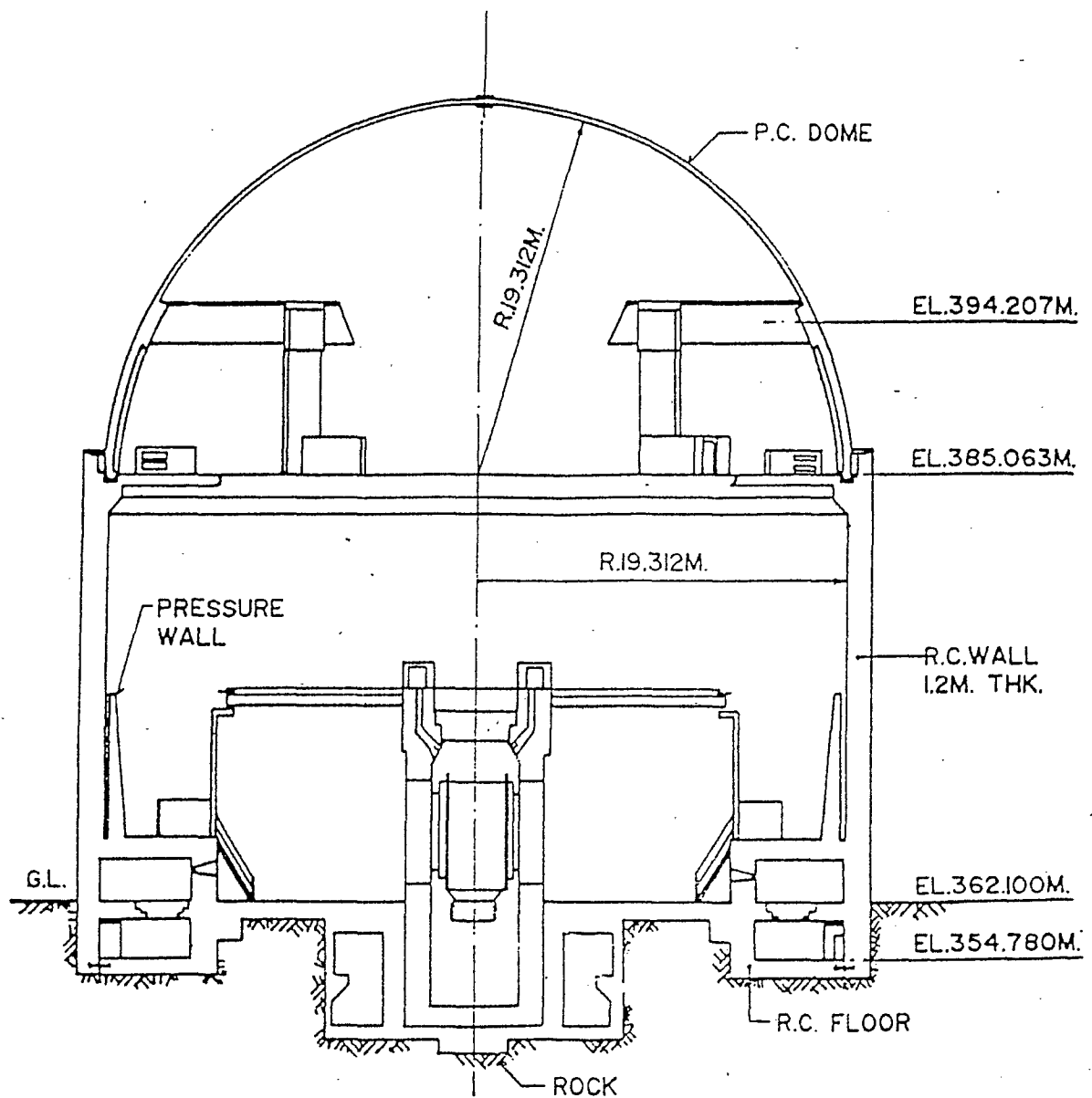
CODES	App. Temp.	SHRINKAGE		CREEP	
		FORCE	%LOSS	FORCE	%LOSS
BPEL-83	20deg	6.26	2.61	27.44	11.43
BIS-1343	27deg	3.52	1.63	15.27	6.36
ACI-209		1.80	.75	8.93	3.72
CIB-FIP	20deg	14.26	5.94	17.05	7.10
AUS-3600	20deg	5.88	2.45	13.50	5.63

TABLE NO. 3(b)

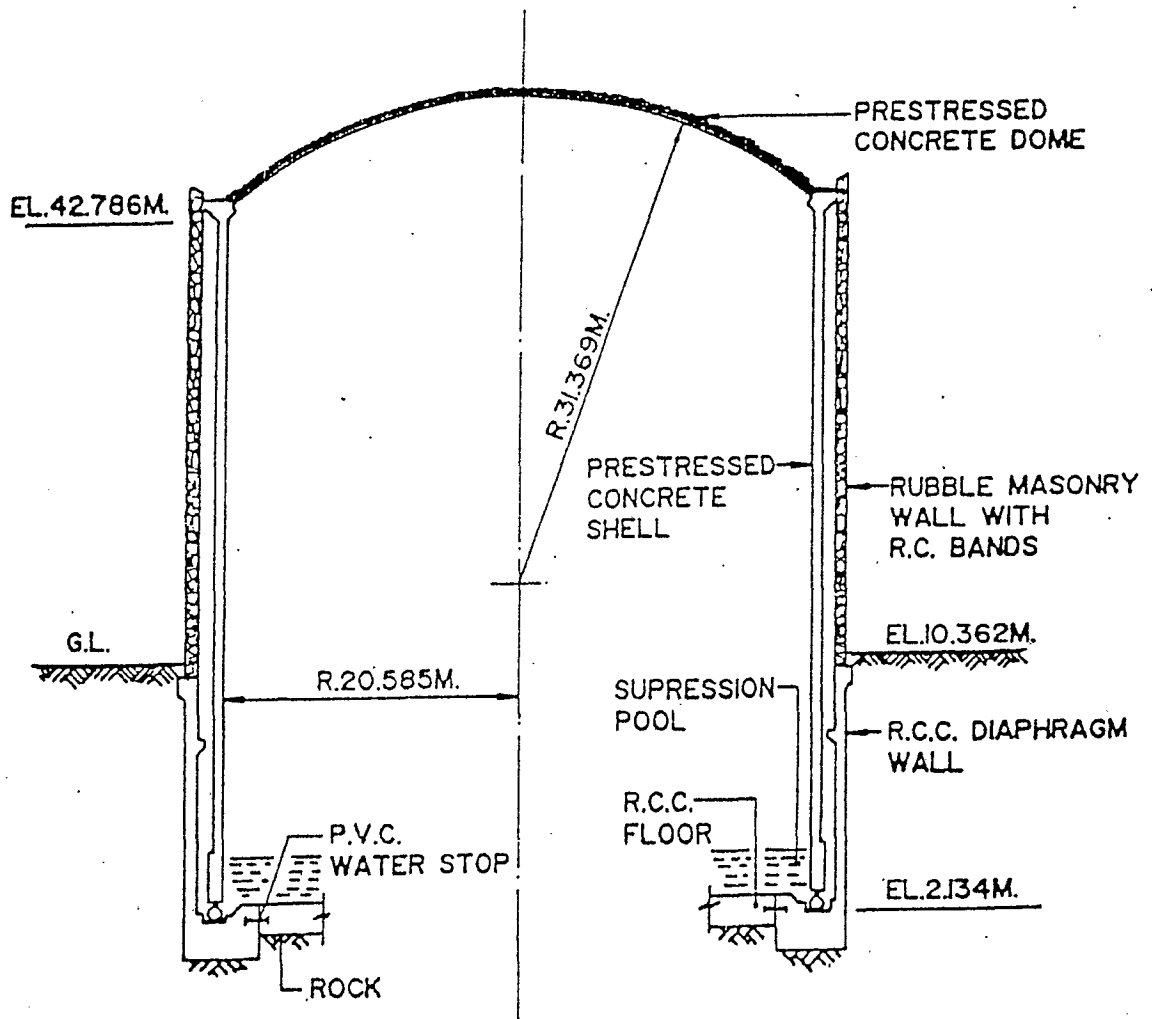
CODES	App. Temp.	RELAX(LOW)(50 YR)			TOTAL		REMARKS
		FORCE	%LOSS	1000	FORCE	%LOSS	
BPEL-83	20deg	6.67	2.78	2.50*	40.21	16.75	
	40deg	19.32	8.05	5.00	52.86	22.03	
		4.11	1.71	1.54**	37.65	15.69	
		11.90	4.96	3.08	45.44	18.93	
BIS-1343	27deg	No Spec.			36.07	15.03	
ACI-209		No Spec.					
CIB-FIP	20deg	18.00	7.50	2.50*	49.30	20.54	No temp. effect recommended
AUS-3600	20deg	8.64	3.60	2.50*			Ref.Design of Prestressed conc. Gilbert & Mickleborough
	40deg	17.28	7.20	5.00	36.66	15.28	

* Guaranteed Value of relaxation loss at 1000 Hours as a percentage of initial tension, at 20°C (As per BIS Code)

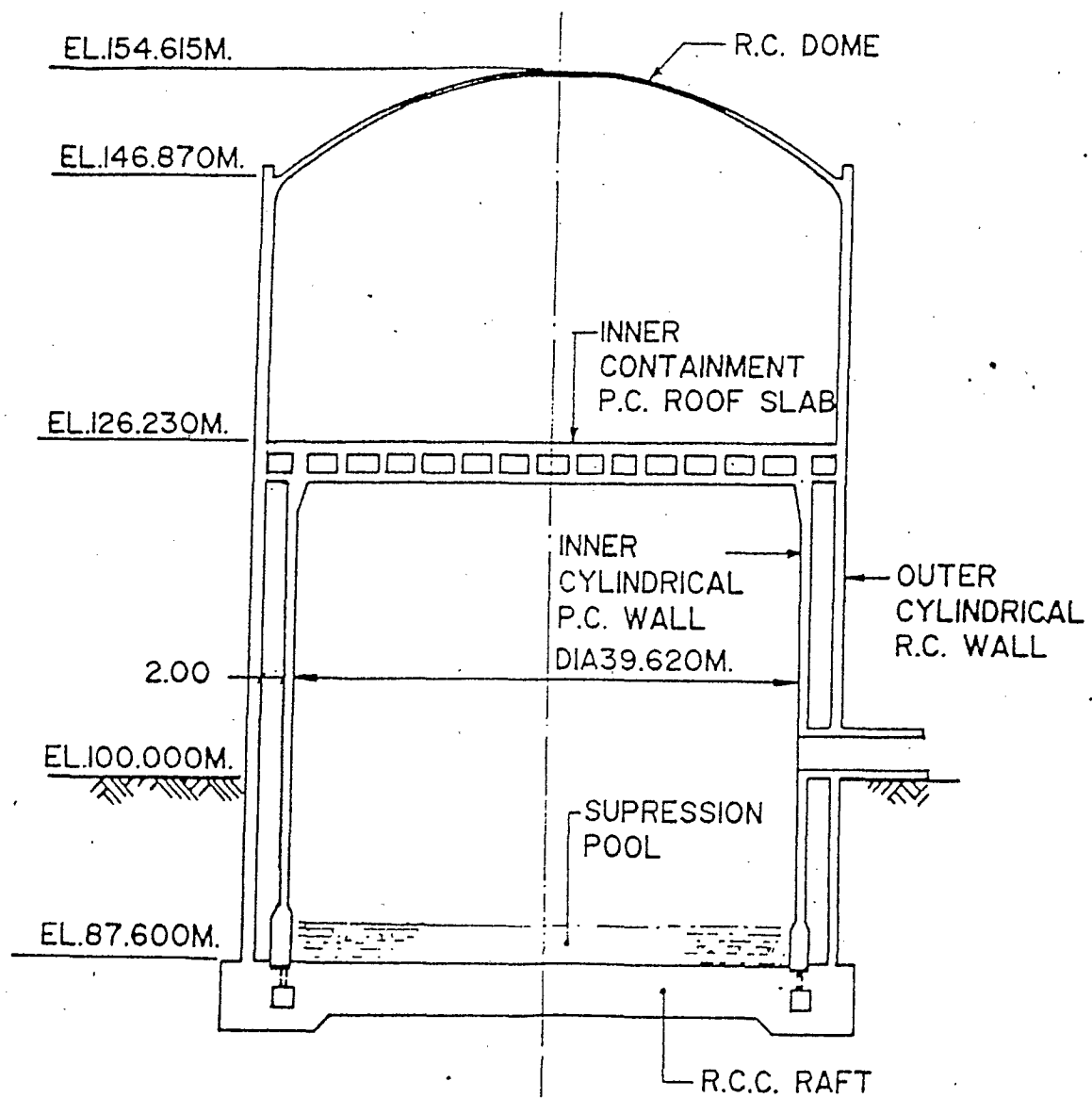
** -do-
(From test results of one of the supplier)



RAPP CONTAINMENT
(SKETCH No. 1)

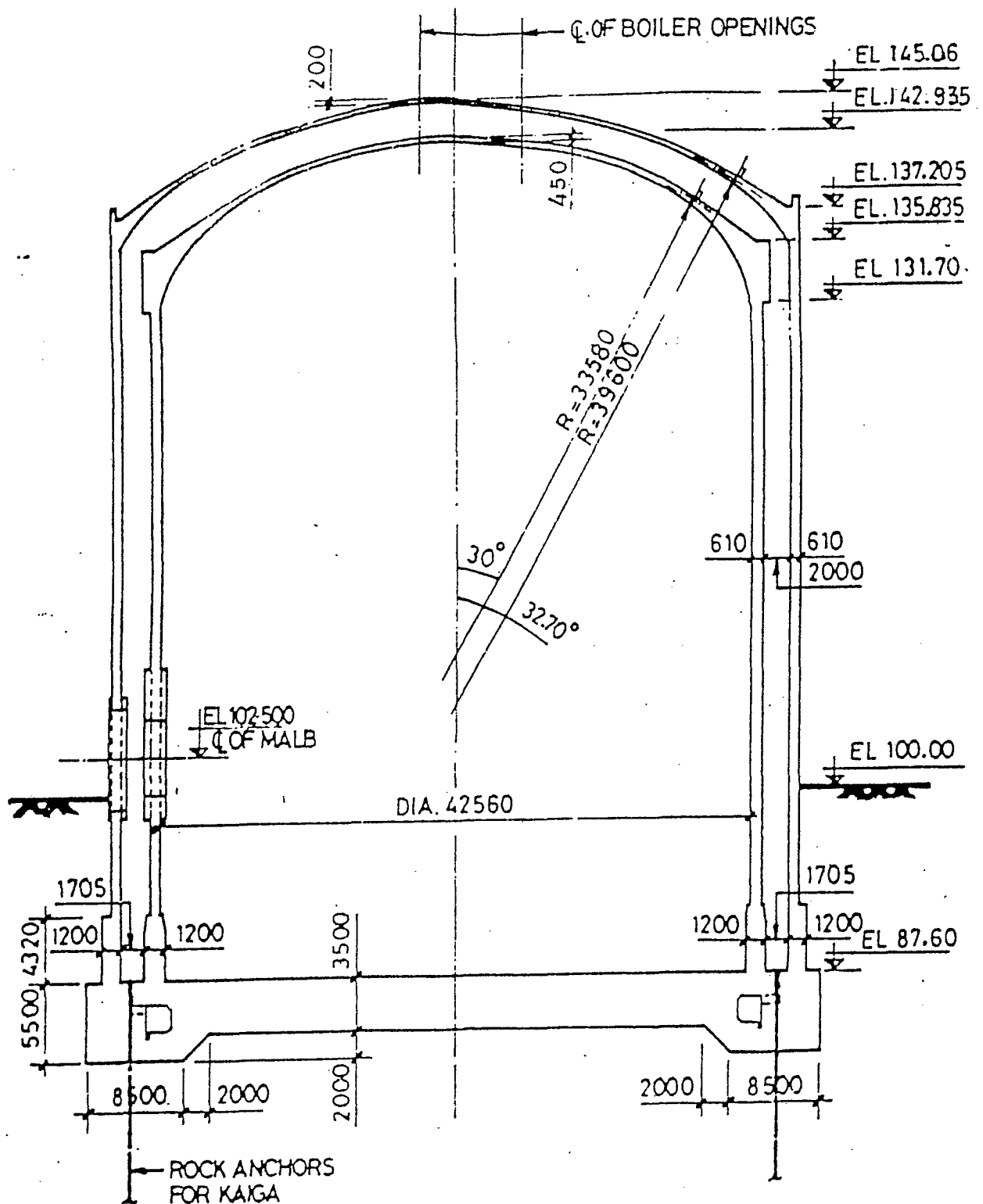


MAPP CONTAINMENT
 (SKETCH No. 2)



NAPP CONTAINMENT

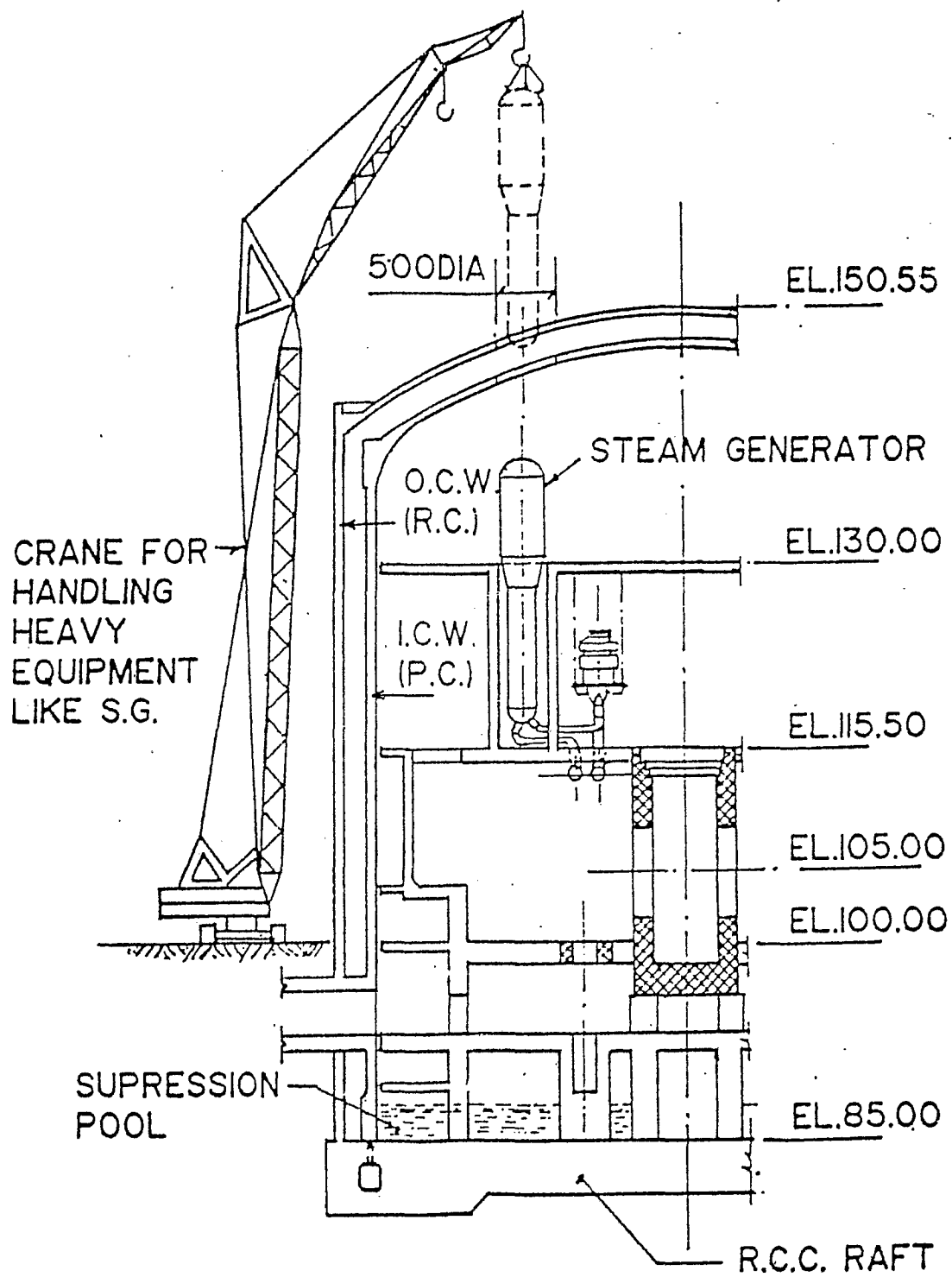
(SKETCH No.3)



GENERAL ARRANGEMENT OF CONTAINMENTS

KAIGA 1,2

(SKETCH No. 4)



500 MW_e STRUCTURE

(SKETCH No. 5)

In-service inspections and R&D of PCCVs in Japan

Watanabe, Yukio, Kawai, Ikurou
The Japan Atomic Power Co., Tokyo, Japan

Kowada, Akira, Akita, Shodo
The Kansai Electric Power Co., Inc., Osaka, Japan

Itou, Yoshitetsu, Sono, Youichi
Kyushu Electric Power Co., Fukuoka, Japan

Koyanagi, Mitsuo, Yamamoto, Mikio
Obayashi Corporation, Tokyo, Japan

25, 26 August, 1997

In-service inspections and R&D of PCCVs in Japan

Contents

1. INTRODUCTION

2. SIT/ISI PRACTICE IN JAPAN

2.1 *Outline of PCCVs*

2.2 *SIT/ISI Practice*

3. ISI PRACTICE

3.1 *Inspections and tests*

3.2 *Results of inspections and tests*

4. PRACTICE ON STRAIN MEASUREMENT

4.1 *Measuring method of concrete strain*

4.2 *Results of measured concrete strain*

5. EVALUATION METHOD ON RESIDUAL TENDON FORCES

5.1 *Method of measuring tensile force in tendons*

5.2 *Evaluation method of tendon tensile force*

5.3 *Measured results of tendon tensile force*

6. CONCLUDING REMARKS

1. INTRODUCTION

In Japan, Tsuruga Unit No.2 (GT-2), Ohi Unit No.3/4 (KON #3 & KON #4), and Genkai Unit No.3/4 (QGN #3 & QGN #4) power stations adopt the prestressed concrete containment vessel (PCCV).

Since the PCCV was introduced from the U.S., the in-service inspection test (ISI) to confirm the structural integrity was basically put into practice in conformity to the Regulatory Guide 1.35 of U.S. NRC.

Experimental and analytical examinations are enforced at ISI to improve the reliability of the evaluation method on structural integrity which is the same as when the series of planning, drafting, enforcement tests to confirm structural reliability were performed when PCCV was introduced.

As a result, the present evaluation method on structural integrity was confirmed to be quite reliable.

In this paper, the ISI practice in Japan is introduced together with some results of the series of experimental studies enforced to improve the reliability of the evaluation method.

2. SIT/ISI PRACTICE IN JAPAN

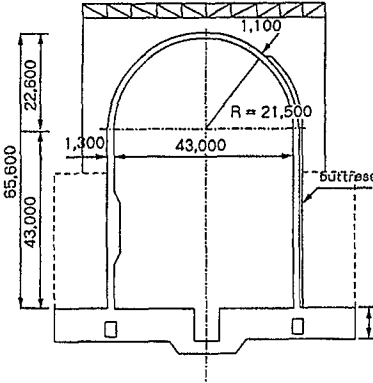
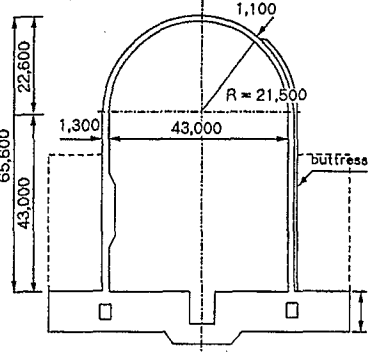
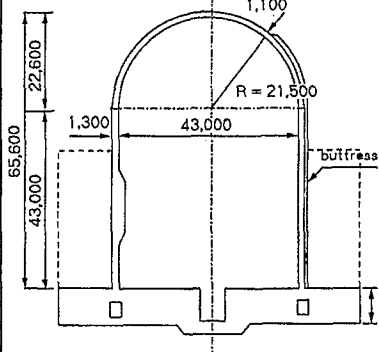
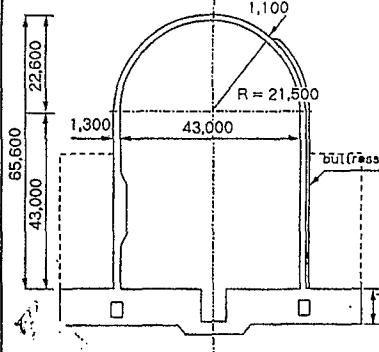
2.1 *Outline of PCCVs*

Since the operation of the GT-2 in 1987, 5 power stations with PCCV are now under operation.

Outline of PCCV is shown in Fig.1 and tendon model of KON #3 & KON #4 is shown in Photo 1. The basic dimensions of the 5 PCCVs are almost the same, where the inner diameter 43.0m and the height 64.5m, a 1.3m thick cylindrical wall of 21.5m inner radius and a 1.1m thick hemispherical dome with 6.4mm steel liner covering the whole inner surface. The other dimensions for each power plant differ little, the thickness of the basemat 8.0m through 11.1m, number of buttresses 2 or 3, the prestressing system being BBRV or VSL though all are 1000t class, and the concrete strengths are 420kg/cm^2 or 450kg/cm^2 .

2.2 *SIT/ISI practice*

The ISI is enforced to verify the structural function of the PCCV as well as the unbonded tensioning system to be sufficient, and to confirm the safety of the nuclear power station. Up to now, GT-2 has completed its third ISI, and the second for KON #3 & KON #4 and QGN #3 its first. Fig.2 shows the ISI enforcements.

Owner	The Japan Atomic Power Co.	The Kansai Electric Power Co.	Kyusyu Electric Power Co.	
Power plants (Year of commercial operation)	GT-2 (1987)	KON#3 (1992) KON#4 (1993)	QGN#3 (1994)	QGN#4 (1997)
Type of reactor (Output capacity)	PWR (1,160MWe)	PWR (1,180MWe)	PWR (1,180MWe)	PWR (1,180MWe)
Dimensions				
Nos. of buttresses	3	2	3	2
Tendon capacity	1,000t Class	1,000t Class	1,000t Class	1,000t Class
Prestressing system (Unbonded type)	BBRV	VSL	BBRV	BBRV
Standard concrete strength (kg/cm ²)	420	450	420	420

※The broken line shows the RC structure of REB.

Fig.1 Outline of PCCVs in Japan

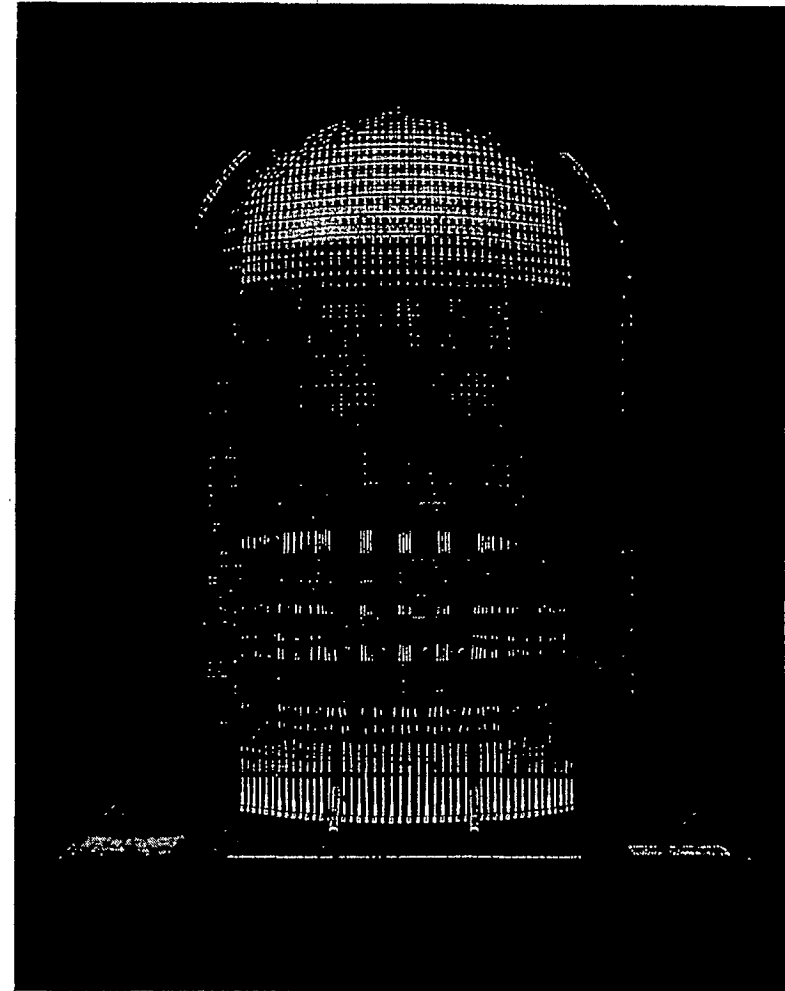
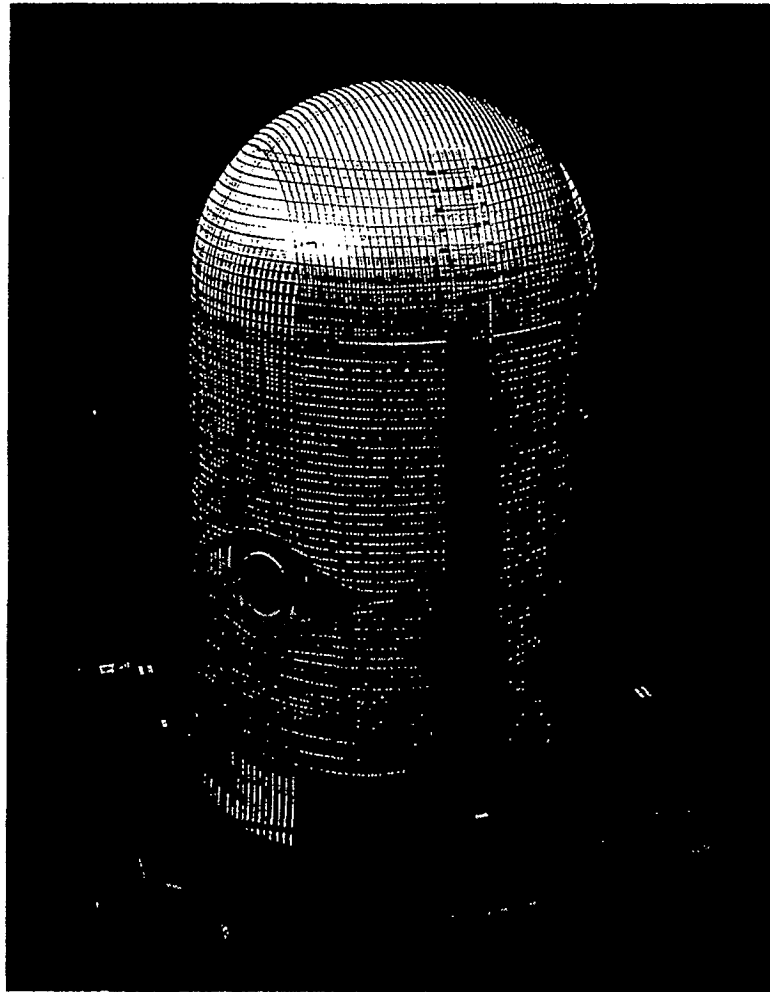


Photo.1 Tendon Model of KONG#3 and KONG#4
(Vertical tendons at $@2^\circ$, Hoop tendon of cylinder at $@450\text{mm}$)

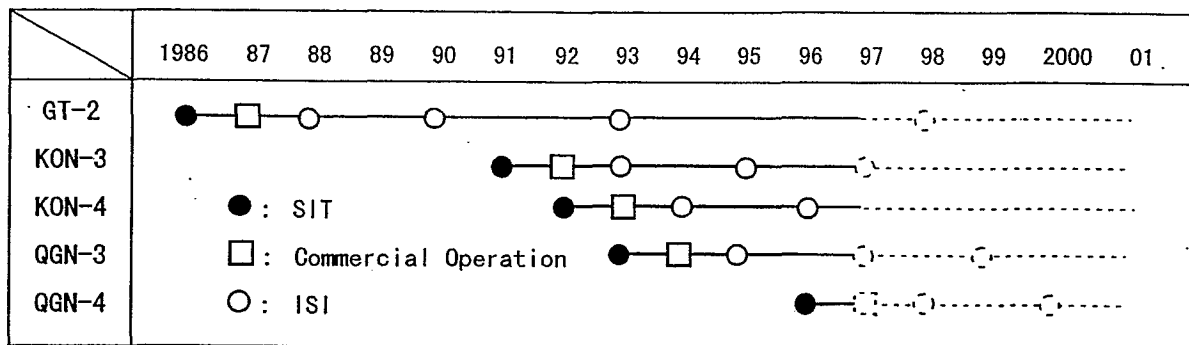


Fig.2 Schedule of ISI (In-service Inspection) on PCCVs

3. ISI PRACTICE

3.1 Inspections and tests

Inspections and tests shown in Table 1 are items enforced at ISI which is in conformity to the Regulatory Guide 1.35 of U.S. NRC.

The ISI is enforced in the 1st (No.1 ISI), 3rd (No.2 ISI) and 5th (No.3 ISI) years after commercial operation and the rest are undecided.

The total tendon of containment is divided into 2 groups, inverted-U tendons and hoop tendons then 4% of the tendon (at least 4 specimens) from each group are chosen randomly for testing. At least 1 specimen from each group should be tested from the first ISI throughout the plant life to clarify its history by comparing its past observed data.

Table 2 shows the numbers of specimen chosen for ISI at each power plant.

Table 1 Items of Inspection

	Items of Inspection/Test	Criterion for Judgement
1	Visual inspection of exposed concrete	• Should not have widespread cracks, spalling and stains showing corrosion of rebar.
2	Visual inspection of the anchoring portion of tendon and its surrounding concrete	• Should not have serious corrosion and cracks at the anchoring portion. • Should not have remarkable change from previous test results at the surrounding concrete portion.
3	Examination and testing of extracted grease	• Cl^- , NO_3^- , S^- should not exceed 10ppm. • Water content should not exceed 10% • Neutralization rate should not be below 50% of the value at initial setting.
4	Inspection on lift-off force of tendon	• Should be above the required design value. • Should not deviate the calculated target value.
5	Inspections and tests on newly injected grease	• Same as extracted grease for chemical tests, though the neutralization rate should not be below 35mgKOH/g. • The volume of newly injected grease should meet the amount of removed grease.

Table2 Numbers of Specimens (No.1,No.2,No.3 ISI Tests)

Plant	Number of Buttresses	Group	Number of Tendons	Number of Specimens	Notes
GT-2	3	Inverted U Tendon	90	4	
		Hoop Tendon	162	7	2 are chosen from dome portion
KON#3 KON#4	2	Inverted U Tendon	90	4	
		Hoop Tendon	108	5	1 are chosen from dome portion
QGN#3	3	Inverted U Tendon	90	4	
		Hoop Tendon	165	7	2 are chosen from dome portion
QGN#4	2	Inverted U Tendon	90	4	
		Hoop Tendon	110	5	1 are chosen from dome portion

3.2 Results of inspections and tests

Results of inspections and tests were nearly the same for each power plant. Results of the No.3 ISI at GT-2 are as below as representative. Photo.2 ~ Photo.11 are photographs taken at the ISI.

i. From the visual inspection of the exposed concrete, cracks, chipping, rust, and grease leaks were not detected.

Detailed visual inspection on limited areas showed small changes compared to the previous examination results, with its maximum crack width being 0.2mm.

ii. The filling conditions for the grease at the anchoring portion was satisfactory. And there was no abnormality such as discoloration of grease to be observed. All examination items on chemical tests for grease satisfied the allowable limits.

iii. Visual inspection on the anchorage detected no abnormality such as cracks or corrosion of the buttonheads, anchor heads and the same for the shim and bearing plate as well. All the inspected tendons had no broken or missing wires.

iv. From the visual inspection on the concrete surrounding the anchoring portion were cracks to be found where most of them being 0.2mm ~ 0.25mm but none were abnormal.

v. Measurements of all examined tendons at the lift-off test were large enough compared to the expected required design measurements. It is obvious that the tendon has enough residual tensile force for No.3 ISI.

vi. All the inspection items at the chemical tests for the newly injected grease satisfied the

allowable limit. The volume of newly injected grease is the same as the removed grease.

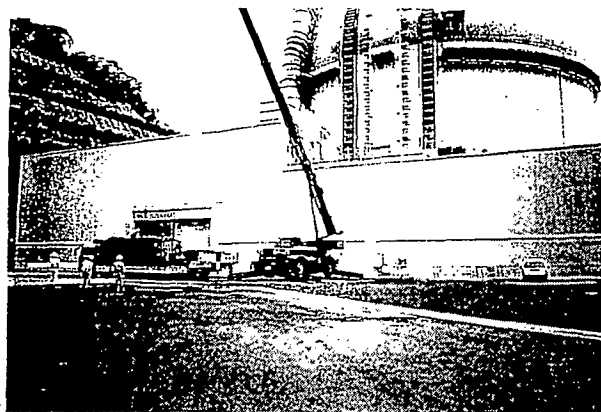


Photo.2 Delivering of ISI machines (KON#4)



Photo.3 Inspection of Grease Caps Inside T/G (QGN#3)



Photo.4 Condition of Grease Right after The Removal of Grease Cap (QGN#3)

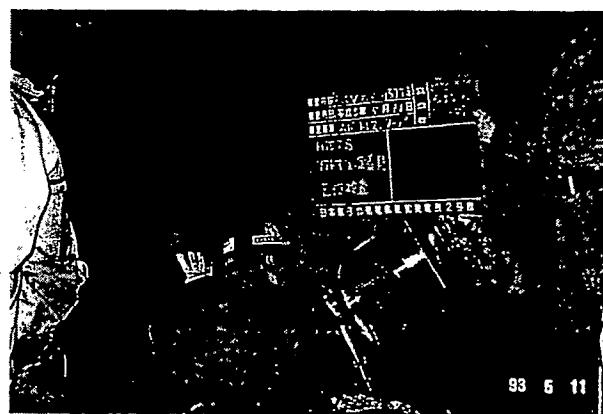


Photo.5 Visual Inspection on BBRV Steel Wires of Hoop Tendon (GT-2)

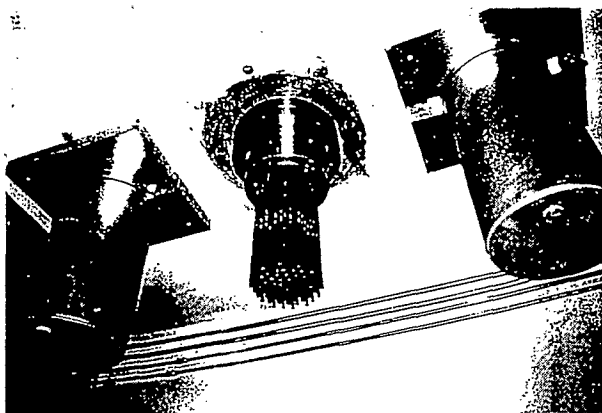


Photo.6 Visual Inspection on VSL Wire Strands of Inverted U Tendon (KON#4)



Photo.7 Lift-Off Test at Inverted U Tendon (GT-2)



Photo.8 Lift-Off Test at Hoop Tendon (KON#4)

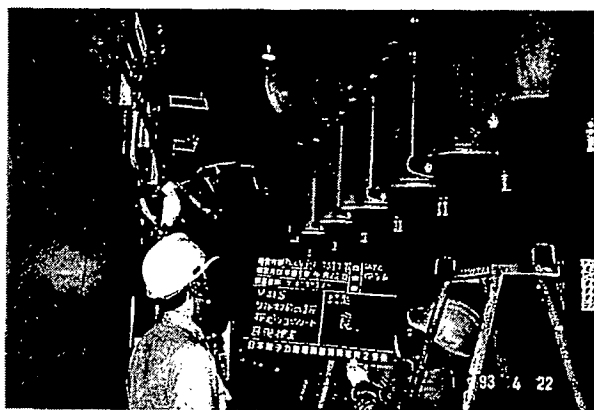


Photo.8 Visual Inspection on T/G Concrete Surface (GT-2)

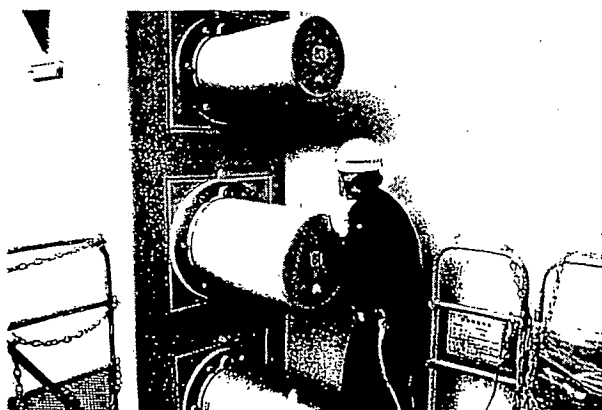


Photo.10 Visual Inspection on Surrounding Concrete of Hoop Tendon (KON#4)

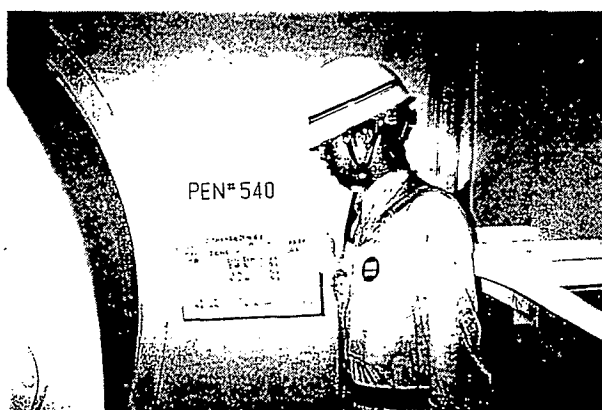


Photo.11 Visual Inspection on Surrounding Concrete of Opening (QGN#3)

4. PRACTICE ON STRAIN MEASUREMENT

4.1 *Measuring method of concrete strain*

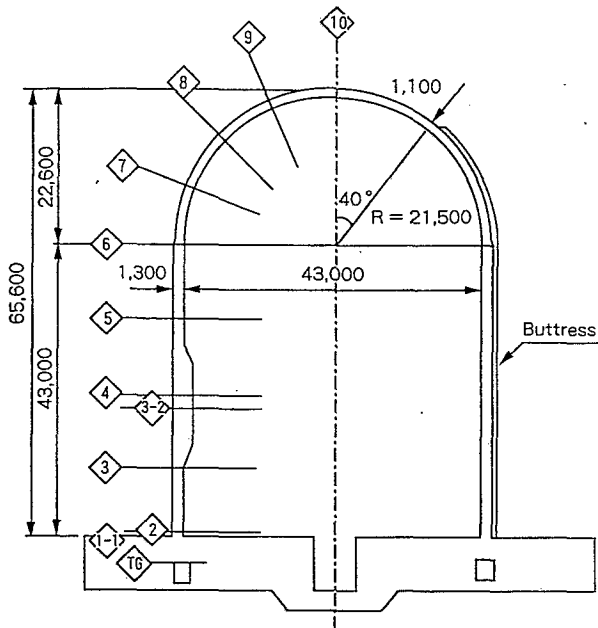
Strains and temperatures of the concrete were measured periodically 2 ~ 4 times a year (in summer and winter if 2 times a year) at the PCCV in subject.

Fig.3 shows the points measured for each PCCV. As for KON #3, Table 3 ~ Table 6 and Fig.4 shows the details of the points for measuring strain and temperature of concrete. Fig.5 and Fig.6 shows the strain gauge containing a thermocouple, and detailed location respectively.

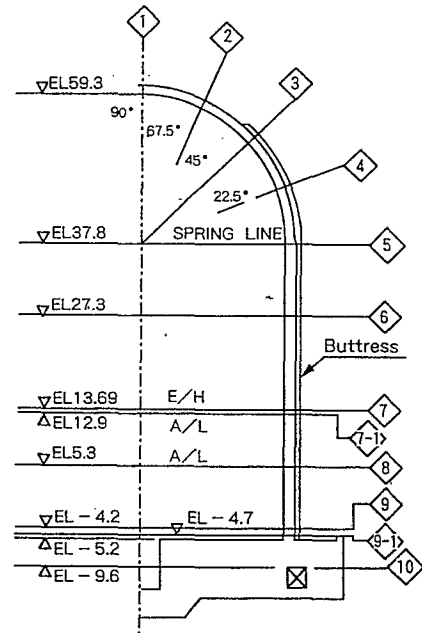
The strain was measured by four strain gauges embedded in both sides of the concrete wall for longitudinal/circumferential direction per one measurement section.

Since the measurements from this rebar strain gauge and concrete strain gauge showed good agreement at the SIT, evaluation is made using rebar strain considering it as concrete strain.

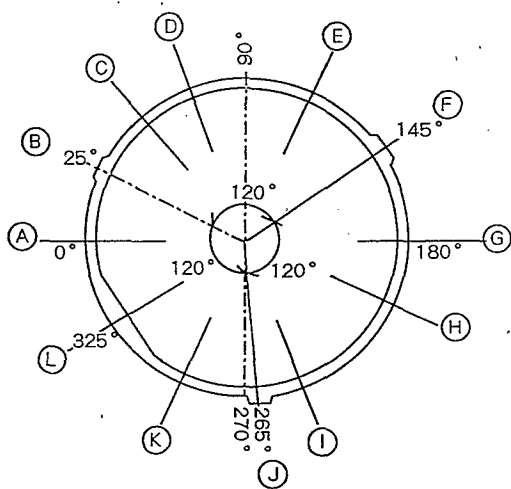
Furthermore, each strain measure contains thermal strain. This thermal strain has an adverse effect on the evaluation of concrete creep and shrinkage strain. Therefore, temperature at 3 ~ 5 points for each measuring section were measured and used to estimate the approximate thermal strain which were eliminated from the measured strain. However, the obtained thermal strain here corresponds to the thermal bending stress due to the change of temperature throughout the section. In other words thermal stress was calculated with the thermal incline under the assumption that the cylindrical shell maintains its shape. Therefore the thermal stress due to external restriction at the discontinuous parts of the structure is not taken into account. Thermal strain is eliminated from the strain measurements used here and are converted to membrane strain in the longitudinal and circumferential directions at each section.



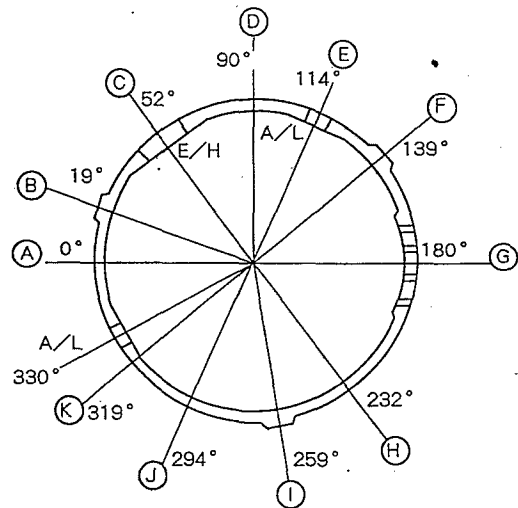
(1) Vertical Section
(GT-2, KON#3, KON#4)



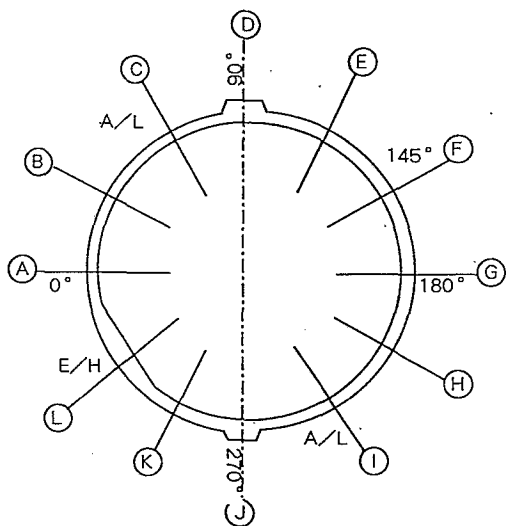
(4) Vertical Section
(QGN#3, QGN#4)



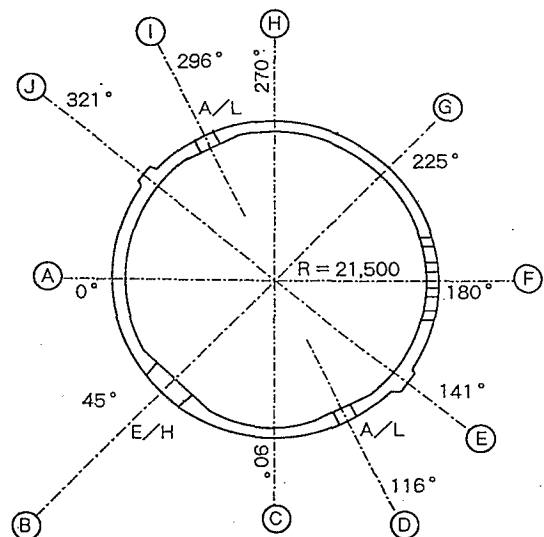
(2) Horizontal Section (GT-2)



(5) Horizontal Section (QGN#3)



(3) Horizontal Section (KON#3, KON#4)



(6) Horizontal Section (QGN#4)

Fig.3 Location of Measurement for Strain

Table 3 Strain Measuring Location

Horiz. Loc.	A	B	C	D	E	F	G	H	I	J	K	L
Vert. Loc.	0°	30°	60° A/L 62°	90° Buttress	120°	150°	180°	210°	240° A/L	270° Buttress	300°	360° E/H
10 Elevation Angle 90°												○
9 67.5°								○				○
8 45.0°		○		○		○		○		○		○
7 22.5°								○				○
6 EL60.1		○		○		○		○		○		○
5 EL48.0								○				○
4 EL35.8	○	○		○	○	○	○	○	○	○	○	⊙ E/H
4-1 EL35.2			⊙ A/L									
3 EL27.6				○				○				○ *
2 EL18.1				○				○				○
1 EL17.1		●		●		●		●		●		●
T62 EL16.7												□
T61 EL12.6												□

Note) ○ : General Parts (Inner and Outer Vertical/Horizontal Bars) 4pts. each $4 \times 34 = 136$
 ⊙ : Around Openings (See Fig. 4) $24(E/H) + 8(A/L) = 32$
 ● : Bottom of cylindrical wall (Inner and Outer Vertical Bar) 2pts. each $2 \times 6 = 12$
 □ : Upper Part of T/G 2pts. each $2 \times 2 = 4$
 * : Results Shared with Those Surrounding E/H

Total 184 Points

Table 4 Temperature Measurement Location

Horiz. Loc.	A	B	C	D	E	F	G	H	I	J	K	L
Vert. Loc.	0°	30°	60° A/L 62°	90° Buttress	120°	150°	180°	210°	240° A/L	270° Buttress	300°	360° E/H
10 Elevation Angle 90°												● ₁
9 67.5°								○				○
8 45.0°		● ₁		○		● ₁		● ₁		○		● ₁
7 22.5°												○
6 EL60.1		● ₁		○		● ₁		● ₁		○		● ₁
5 EL48.0												○
4 EL35.8	○	● ₂		○	○	● ₁	○	● ₂	○	○	○	E/H See Table 5
4-1 EL35.2			A/L See Table 5									
3 EL27.6				○				● ₂				● ₂ *
2 EL18.1				○				○				○
1 EL17.1		○		○		○		● ₂		○		● ₂
T62 EL16.7												○
T61 EL12.6												○

Note) ○ : Rebar Strain Gauge (Containing a Thermocouple)
 ●₂ : A Rebar Strain Gauge and 2 Thermocouples
 ●₁ : A Rebar Strain Gauge and 3 Thermocouples
 * : Results Shared with Those Surrounding E/H

Table 5 Around E/H

	324° -3.48m	324° +3.48m	338°	344°
39.28		○		
35.8	○	E/H P540	● 2	○
32.32		● 2		
30.4		● 2		

(See Fig. 4)

Table 6 Around A/L

	62° -1.722m	324° +1.722m
36.972		○
35.2	○	A/L P520
33.428		● 2

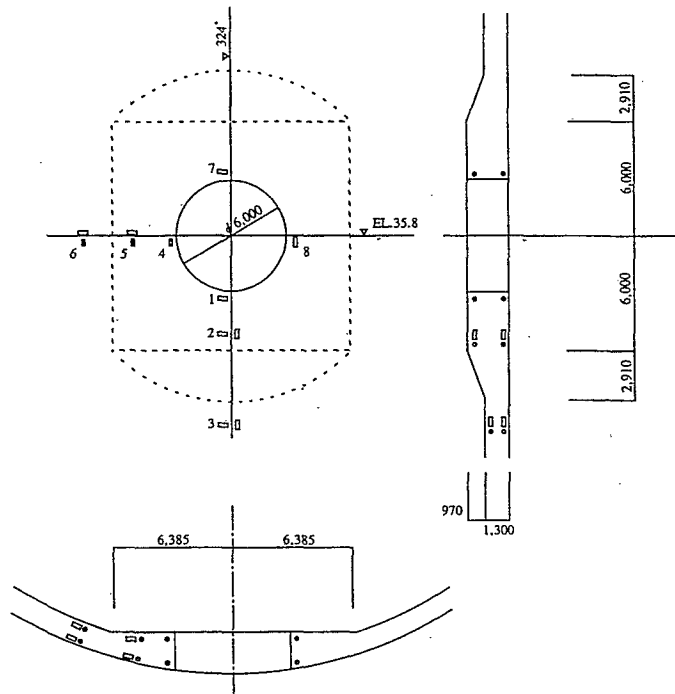


Fig. 4 Location of Measurement for Strain around E/H

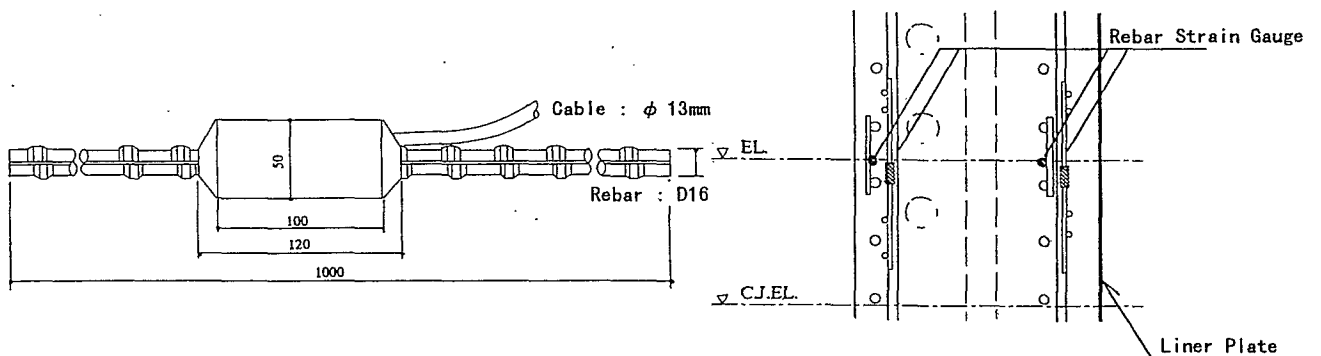


Fig. 5 Rebar Strain Gauge
(Containing a thermocouple)

Fig. 6 Location of Rebar Strain Gauge

4.2 Results of measured concrete strain

Fig.7 ~ Fig.13 shows the representing examples of concrete strain under long-term behavior. The horizontal axis is effective age t of concrete since casting, and the vertical axis is the change of strain ϵ since the beginning of SIT.

As can be seen from these figures, strain measurement has a fluctuating characteristic. Strain is small in summer and large in winter at portions besides in the circumferential direction at the bottom of cylindrical wall (sec.2 as Fig.13). On the other hand strain in the circumferential direction at the bottom of cylindrical wall is large in summer and small in winter.

Such characteristics can be observed from all PCCV strain measurements.

The reason for this periodical fluctuation of the strain measurement is assumed to be due to the change of humidity in winter. It is known from the past research that concrete creep and drying shrinkage themselves are dominated by the environmental factors particularly the relative humidity. The fluctuating character of strain is also known to be influenced by the relative humidity. The results of long-term behavior tests at concrete slabs enforced in a room which does not have steady temperature and humidity shows the relative humidity to fluctuate between 40% and 80% during winter and summer causing direct influence on the strain and deformation of concrete slabs.

Therefore the calculation was made under the condition that the PCCVs should be influenced by the fluctuation of seasonal humidity.

Creep and shrinkage of concrete are calculated by basic eqs.(1) which has been used for designing PCCVs in Japan.

$$\left. \begin{aligned} \phi(t, t_0) &= \phi_{d0} \cdot \beta_d(t - t_0) + \phi_{f0} \cdot (\beta_f(t) - \beta_f(t_0)) \\ \epsilon_s(t, t_0) &= \epsilon_{s0} \cdot (\beta_s(t) - \beta_s(t_0)) \end{aligned} \right\} \text{eqs.(1)}$$

where;

- $\phi(t, t_0)$: creep factor
- ϕ_{d0} : basic creep factor for delayed elastic strain
- ϕ_{f0} : basic creep factor for flow strain
- $\beta_d(t)$: function of effective days after loading ($t - t_0$)
- $\beta_f(t)$: function of effective age t
- $\epsilon_s(t, t_0)$: drying shrinkage strain
- ϵ_{s0} : basic shrinkage strain factor
- $\beta_s(t)$: function of effective age t
- t : effective age of concrete at calculation
- t_0 : effective age of concrete at prestressing

In eqs.(1), basic creep factor for flow strain ϕ_{f0} and basic shrinkage strain factor ϵ_{s0} is

dominated by relative humidity. Though the design method does not consider the periodical fluctuation, here ϕ_{f0} , ε_{s0} considers the relative humidity fluctuation within seasons.

$$\left. \begin{aligned} \phi_{f0} &= 1.8 + 0.18 \sin\left(2\pi(t - t_0^*)/365 \cdot C\right) \\ \varepsilon_{s0} &= 225 + 18 \sin\left(2\pi(t - t_0^*)/365 \cdot C\right) \end{aligned} \right\} \text{eqs.(2)}$$

where;

t_0^* : effective age since concrete casting to the first Oct.

C : coefficient of effective age

Therefore the relative humidity is set at 70% for GT-2 , KON #3 & KON #4 and 80% for QGN #3 considering the quality of paint. Both ϕ_{f0} and ε_{s0} are considered to fluctuate sinusoidally $\pm 10\%$.

With this method the calculated strain measurement shows very good correspondence with the measured concrete strain as shown in Fig. 7 ~ Fig. 12.

On the other hand, shown in Fig. 13, circumferential strain indicates an opposite tendency at the bottom of cylinder. In other words, strain increase in summer and decrease in winter. It is judged that this behavior is caused by the thermal stress due to restraint of basemat on radial deformation of cylindrical wall. This stress is defined as thermal stress due to external restraint forces, which is closely related to increase of average temperature of wall. As this thermal stress is dominated by boundary condition at the bottom of cylindrical wall, in a strict manner, basemat temperature also influences thermal stress. Furthermore external restraint forces (boundary forces) basically consists of out-of-plane bending force and transverse shear force acting on the boundary of the cylindrical wall and foundation mat. And such external restraint forces influences only a small area and rarely on position of Sec.3 as Fig.10. Moreover, at the position of Sec.2 as Fig.13, external restraint force has very small influence on longitudinal membrane stress and is large on the circumferential membrane stress.

The amount of thermal stress due to external restraint was roughly calculated (accuracy of calculation was limited by lack of data for basemat temperature) using the increment of measured temperature data at the bottom of cylinder. Comparison of the sum of calculated creep, shrinkage and thermal strain with the measured concrete strain were made showing good agreement, as in Fig.13. Though only the results at sec.2 of KON #3 is shown here, similar results were obtained from other PCCVs.

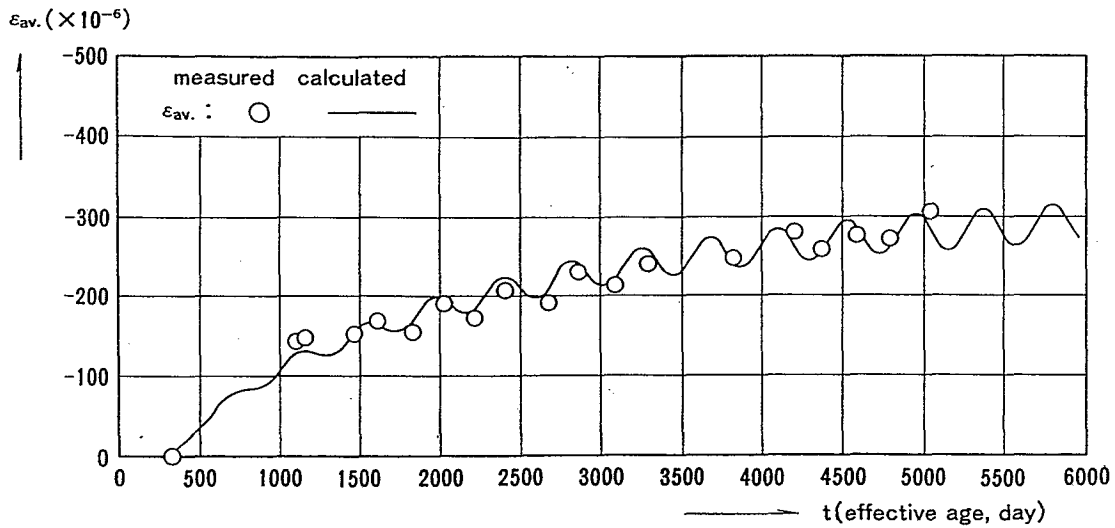


Fig.7 Long-Term Behavior of Concrete Strain
(Sec.10-9 in Dome ;Tsuruga Unit No.2)

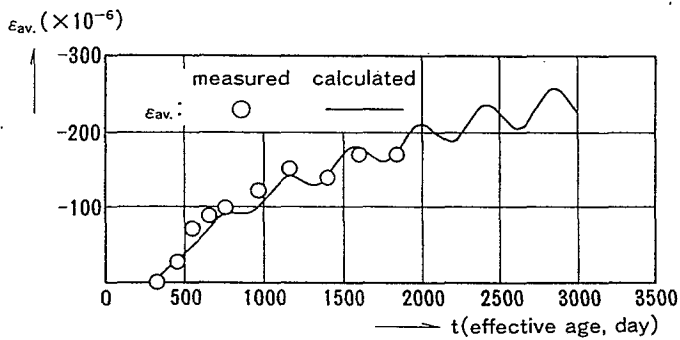


Fig.8 Long-Term Behavior of Concrete Strain
(Sec.8 in Dome ;Ohi Unit No.3)

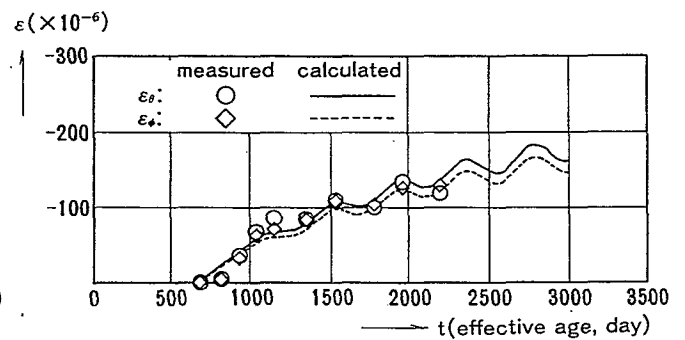


Fig.9 Long-Term Behavior of Concrete Strain
(Sec.6 at Spring-Line ;Ohi Unit No.3)

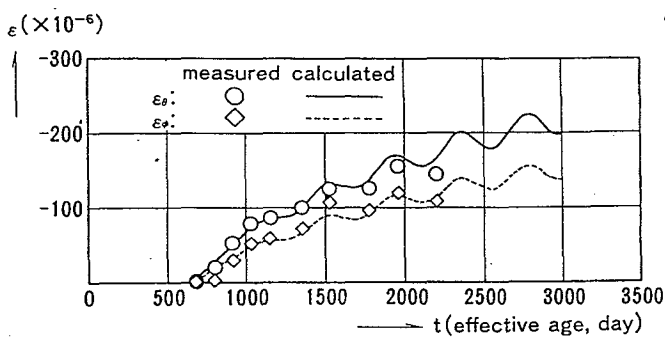


Fig.10 Long-Term Behavior of Concrete Strain
(Sec.5-3 in Cylindrical Wall ;Ohi Unit No.3)

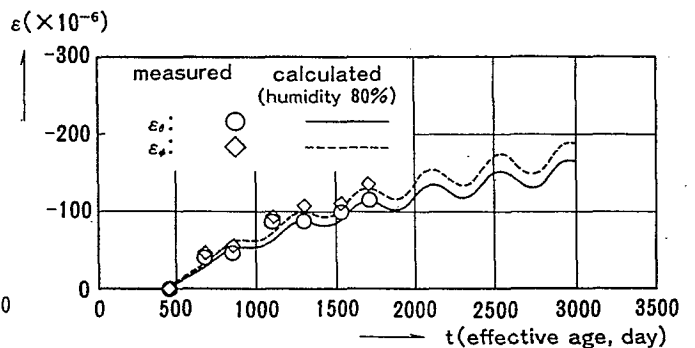


Fig.11 Long-Term Behavior of Concrete Strain
(Sec.3 in Dome ;Genkai Unit No.3)

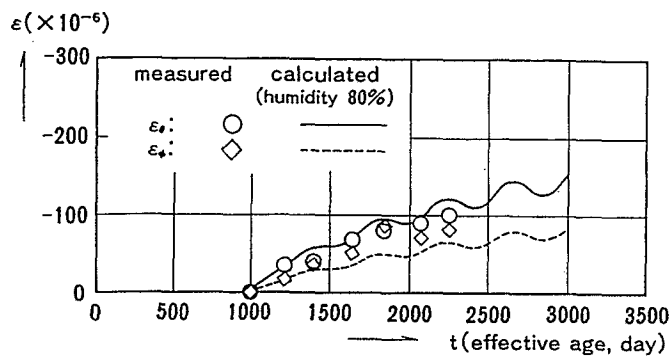


Fig.12 Long-Term Behavior of Concrete Strain
(Sec.6 in Cylindrical Wall ;Genkai Unit No.3)

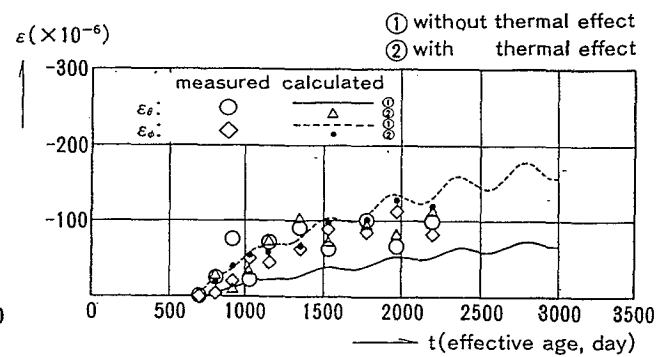


Fig.13 Long-Term Behavior of Concrete Strain
(Sec.2 in Cylindrical Wall ;Ohi Unit No.3)

5. EVALUATION METHOD ON RESIDUAL TENDON FORCES

5.1 Method of measuring tensile force in tendons

Lift-off force is measured separately at the field anchorhead side and the shop anchorhead side (D side and N side for VSL). After the jack and pressure inverter is set, the jack loading is increased until enough gap for the filler gauge (0.6mm thick) is made. Next the filler gauge is set one in the right and another in the left as Fig.14, then the jack loading is removed.

Jack loading is increased once again when the filler gauge is pulled by hand, then the jack loadings are read at the removal of each right and left filler gauge. This is repeated until the difference of the maximum and minimum values match the required value for 3 continuing measurements, then the average of the 3 measurements are considered as the lift-off force at the tendon end.

Fig.15 and Fig.16 shows the tendon arrangements at each PCCV.

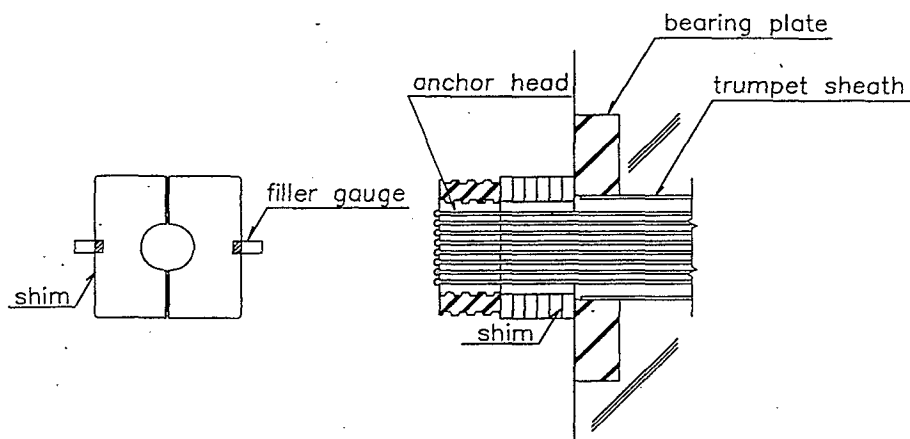
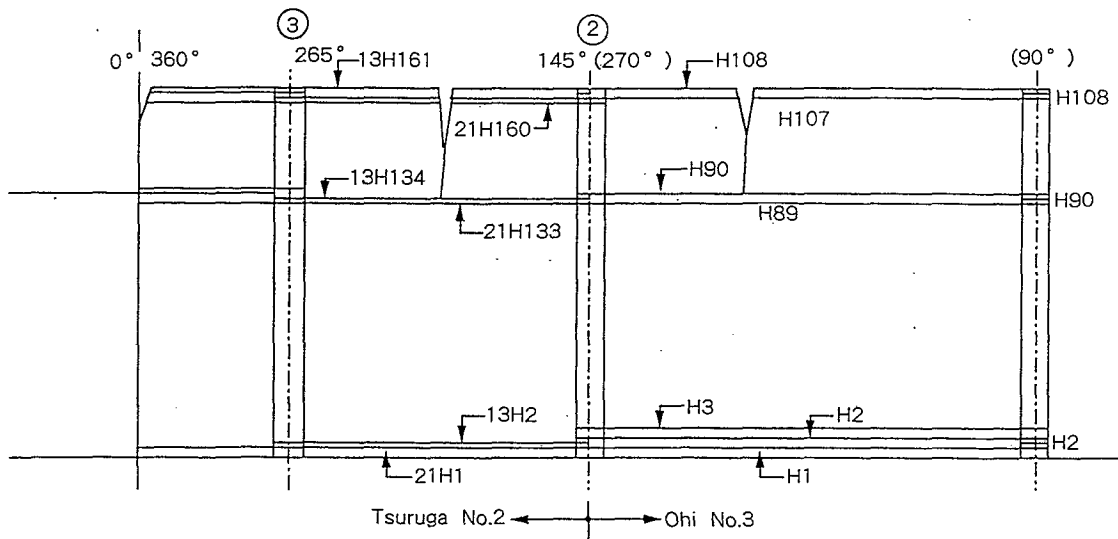
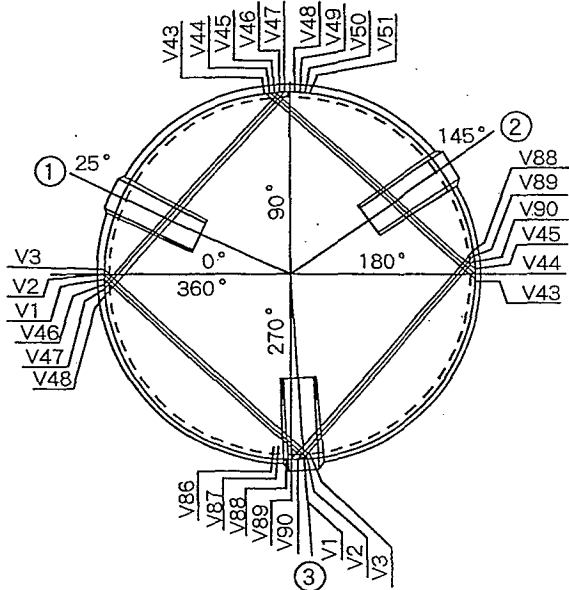


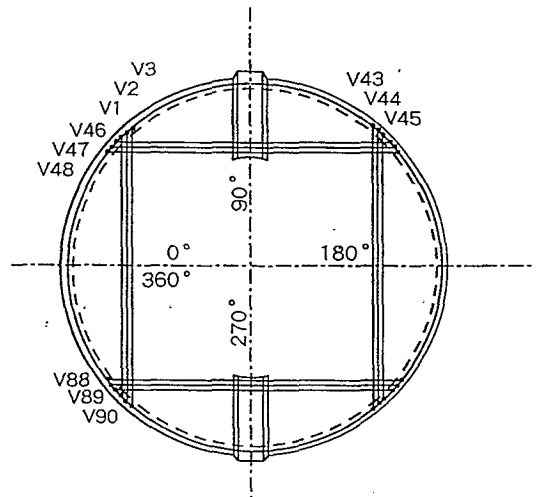
Fig.14 Filler Gauge



(1) Hoop Tendons (GT-2, KON#3)

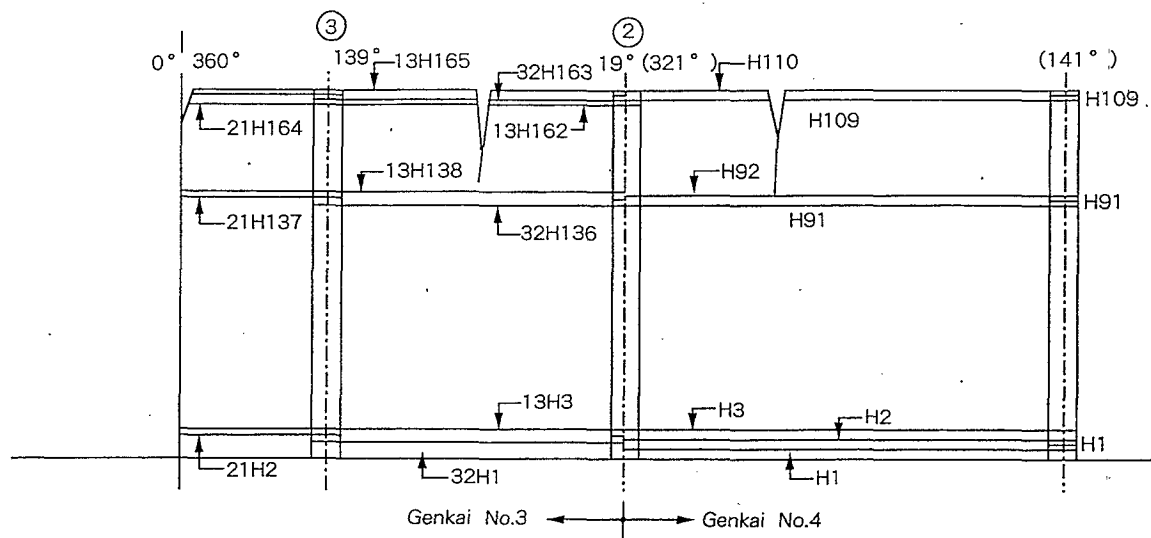


(2) Inverted U Tendons (GT-2)

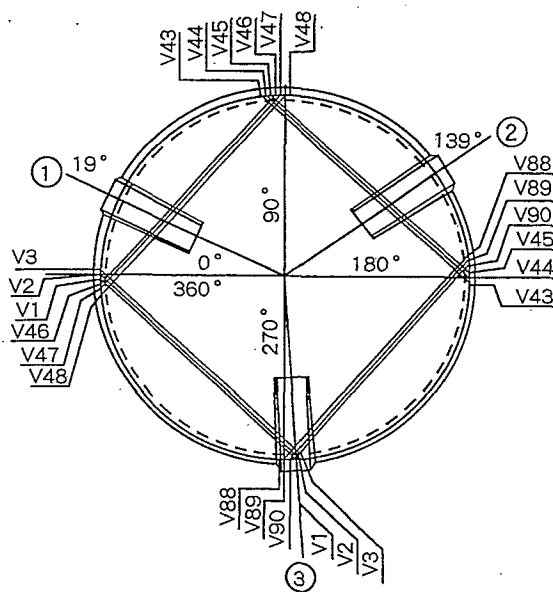


(3) Inverted U Tendons (KON#3)

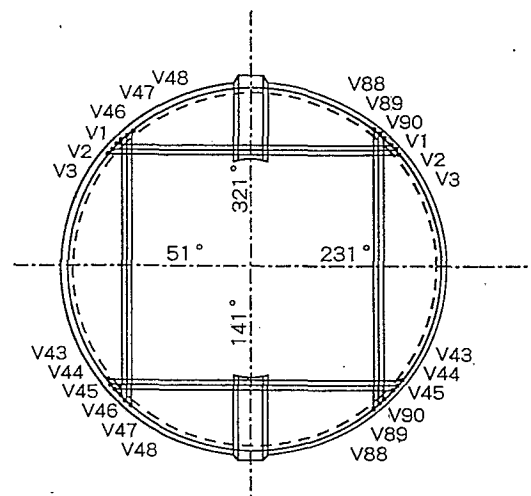
Fig.15 Tendon Arrangements (GT-2, KON#3, KON#4)



(1) Hoop Tendons (QGN#3, QGN#4)



(2) Inverted U Tendons (QGN#3)



(3) Inverted U Tendons (QGN#4)

Fig.16 Tendon Arrangements (QGN#3, QGN#4)

5.2 Evaluation method of tendon tensile force

Measurement results of tendon force are read from lift-off tests as mentioned before. Therefore the measurements can be understood as the tensile force (residual force) at tendon ends rather than the average tensile force along the entire tendon. Nevertheless if the loss of tendon tensile force is equal anywhere along the tendon as in Fig.17, the loss of tensile force measured at the lift-off test can be understood as the average tensile force loss.

Basically this loss of tensile force is influenced by elastic deformation loss (ΔF_1) of concrete due to tensioning of tendon, relaxation loss (ΔF_2) due to relaxation of tendon, creep loss (ΔF_3) due to concrete creep and shrinkage loss (ΔF_4) due to concrete shrinkage. Besides ΔF_1 , 3 factors $\Delta F_2 \sim \Delta F_4$ are time dependent.

Therefore, the calculations are made by subtracting the total loss (Δ), which is the sum of $\Delta F_1 \sim \Delta F_4$ from the lock-off force.

Table 7 ~ Table 11 shows the measurement results and calculation results of lift-off test at the representing tendon of each PCCV.

Table 8 (results of GT-2) is an example of each calculated loss of tensile force used to calculate the residual tensile force mentioned above. ΔF_3 and ΔF_4 are values which consider the influences by seasonal change.

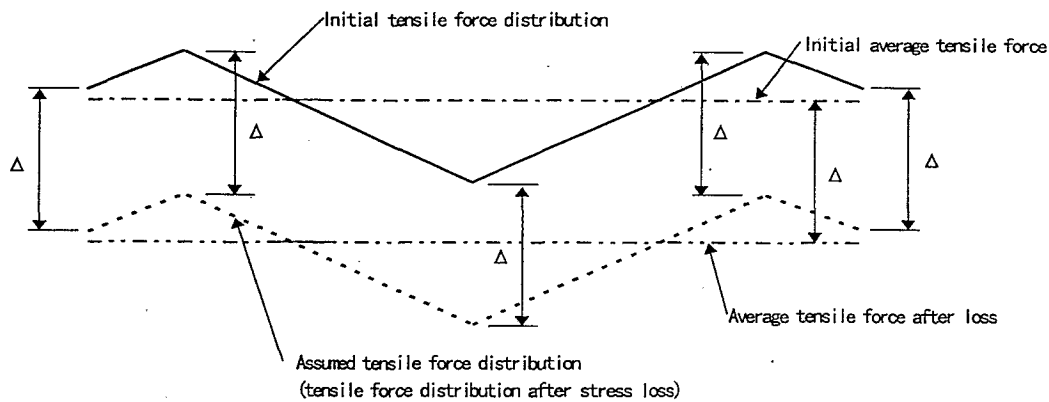


Fig.17 Assumed Tensile Force Fluctuation of Tendon
(Δ shows the average tensile force loss throughout the tendon)

a. Loss due to elastic deformation (ΔF_1)

$$\Delta F_1 = E_p \cdot A_p \cdot \Delta \varepsilon$$

where;

E_p :Young's modulus of tendon

A_p :sectional area of tendon

$\Delta \varepsilon$: results of FEM (considering influences by each tendon tensioning)

b. Loss due to relaxation of tendon (ΔF_2)

$$\Delta F_2 = \Gamma(t) \cdot F_0 \cdot \left\{ 1 - 2 \times (\Delta F_3 + \Delta F_4) / F_0 \right\}$$

where;

$\Gamma(t)$:relaxation coefficient of tendon
(by Larson-Miller method)

ΔF_3 :creep loss

ΔF_4 :shrinkage loss

c. Loss due to creep (ΔF_3)

$$\Delta F_3 = E_P \cdot A_P \Delta \varepsilon_{CREEP}$$

where;

E_P :Young's modulus of tendon

A_P :sectional area of tendon

$\Delta \varepsilon_{CREEP}$:from formulas below

$$\Delta \varepsilon_{CREEP} = \phi_{cr} \cdot (\sigma_c - \nu_c \sigma_\theta) / E_e \dots \dots \dots \text{inverted-U tendon}$$

$$\Delta \varepsilon_{CREEP} = \phi_{cr} \cdot (\sigma_\theta - \nu_c \sigma_c) / E_e \dots \dots \dots \text{hoop tendon}$$

where;

ϕ_{cr} :creep coefficient

$$\phi_{cr} = \phi_{d0} \cdot \beta_d(t - t_0) + \phi_{f0} \cdot \{\beta_f(t) - \beta_f(t_0)\}$$

$$\phi_{d0} = 0.4$$

$$\phi_{f0} = 1.8 + 0.18 \sin(2\pi(t - t_0^*) / 365 \cdot C)$$

where;

t_0^* :effective age since concrete casting to the first Oct.

C : coefficient of effective age

$$t_0, t = \{ \Sigma(T + 10) \cdot \Delta t' \} / 30$$

- $\Delta t'$:total days where temperature is T°C
 $c\sigma_\phi$:longitudinal stress results from FEM analysis
 $c\sigma_\theta$:circumferential stress results from FEM analysis
 E_e :equivalent Young's modulus
 ν :Poisson's ratio

d. Loss due to shrinkage (ΔF_4)

$$\Delta F_4 = E_p \cdot A_p \cdot \Delta \varepsilon_s$$

where;

$\Delta \varepsilon_s$:shrinkage strain

$$\Delta \varepsilon_s = \varepsilon_{s0} \cdot \{ \beta_s(t) - \beta(t_0) \}$$

$$\varepsilon_{s0} = 225 + 18 \sin(2\pi(t - t_0^*) / 365 \cdot C)$$

where;

t_0^* :effective age since concrete casting to the first Oct.

C : coefficient of effective age

5.3 Measured results of tendon tensile force

Table 7 shows the measurement/calculation ratio which was 0.97 ~ 1.01 for the No.1, 0.98 ~ 1.05 for the No.2, and 0.97 ~ 1.03 for the No.3 ISI test results of GT-2.

The measurement results and calculations indicated good agreement taking into account the errors of the lift-off measurements being $\pm 2.0\%$ of the introduced force.

Table 9 and Table 10 shows the comparison of measurement results from lift-off test and calculations at KON #3 and KON #4.

The results here were obtained using the previous method. The measurement/calculation ratio was 0.99 ~ 1.04 for the No.1 and 1.01 ~ 1.03 for the No.2 ISI test thus measurement and calculation results indicating good agreement.

Detailed studies are made with these results.

As history test tendon, 4 tendons H37, H102, H141, V23 for GTN-2, 3 tendons H45, H101, V29 for both KON #3 and KON #4 were chosen.

The elastic deformation (ΔF_1) varies largely being 1.7~ 31.7^t. Although this is about 5%

of the residual tendon force, the calculation results of residual force and ISI measurements indicated relatively good agreement. In other words, ΔF_1 is quite reliable.

When the No.1 ISI lift-off measurement of the history test tendon is set as standard and the fluctuation characteristics of tensile force from it is in object, elimination of affects due to elastic deformation is possible. Here, the No.1 ~ No.3 ISI fluctuation characteristics of tensile force are studied using 4 history test tendons of GTN-2.

Tendon	meas.	cal.	meas./cal.
H37	622	614	1.01
H102	627	621	1.01
H141	639	637	1.00
V23	653	652	1.00

Here ;measurements are from No.3 ISI lift-off test

;calculations are from calculated residual tensile force obtained from No.1 ISI lift-off measurements eliminating calculated tensile force loss.

As from above, measurements and calculations indicate good agreement and this is the same when ΔF_1 is eliminated.

Therefore, not only ΔF_1 but $\Delta F_2 \sim \Delta F_4$ are quite reliable.

Table 11 shows the comparison of lift-off measurements and calculations on representing tendons at QGN #3.

The strain measurements at QGN #3 are generally small compared to those of GTN-2 and KON #3 & KON #4.

Therefore the environmental factor of relative humidity is set at 80% when ΔF_3 and ΔF_4 are calculated for the mid-cylindrical portion and above. However, ΔF_1 and ΔF_2 of this portion and $\Delta F_1 \sim \Delta F_4$ of the portions below this is obtained by the same method as GTN-2, and KON #3 & KON #4.

The lift-off measurement and calculation ratio is between 0.99 and 1.02 indicating quite good agreement.

As from above, lift-off measurements and calculations obtained from No.1, No.2, No.3 ISI tests at GTN-2, No.1, No.2, ISI tests at KON #3 & KON #4 ,and No.1 ISI test at QGN indicated good agreement, therefore the fluctuation of tendon force can be predicted quite accurately.

Actually the lift-off measurements are forces read from the anchoring end of the tendon and the calculations responds to the fluctuation amount of the average tendon force. Additionally among the lift-off measurements, there are tendons whose amount of tensile force between the both ends of a buttress to be large and there are also forces that increases which should decrease.

This is assumed to be caused by the redistribution of tensile force being non-uniform due to friction.

Heated tendon tests on a solid concrete cylinder with tendons wound around (see 14th SMIRT, H01/6) were enforced to understand the influences of redistribution of tensile force.

The test specimen is shown in Fig.18 and examples of calculations using friction theory equation which considers tendon slip and the test values are shown in Fig.19 and Fig.20. The calculations and test values indicate good agreement. Assumptions on tendon force of existent PCCVs were made using this equation which explained the fluctuation of force at local portions, and also confirmed the influence of residual tendon force to be small as the influences by redistribution of force at tendon ends were 2 ~ 3% of the introduced force.

Table 7 Lift-off Test Results of Tendon in Tsuruga Unit No.2

Tendon No.			T ₀	No. 1 ISI			No. 2 ISI			No. 3 ISI		
				①	②	① / ②	③	④	③ / ④	⑤	⑥	⑤ / ⑥
		Av.	meas.	meas.	cal.		meas.	cal.		meas.	cal.	
Cylinder Hoop Tendon	H5	Av.	691	653	657	0.99	-	-	-	-	-	-
	H10	Av.	690	-	-	-	-	-	-	650	638	1.02
	H25	Av.	699	-	-	-	654	641	1.02	-	-	-
	H37	Av.	689	627	625	1.00	632	617	1.02	622	612	1.02
	H44	Av.	689	-	-	-	630	622	1.01	-	-	-
	H54	Av.	690	-	-	-	-	-	-	633	638	0.99
	H58	Av.	682	644	639	1.01	-	-	-	-	-	-
	H86	Av.	693	-	-	-	-	-	-	616	619	1.00
	H102	Av.	689	634	650	0.98	636	642	0.99	627	637	0.98
	H115	Av.	686	-	-	-	641	631	1.02	-	-	-
Dome Hoop Tendon	H119	Av.	692	636	655	0.97	-	-	-	-	-	-
	H141	Av.	697	649	668	0.97	650	660	0.98	639	656	0.97
	H150	Av.	679	-	-	-	631	632	1.00	-	-	-
	H157	Av.	687	-	-	-	-	-	-	651	635	1.03
Inverted U Tendon	H161	Av.	690	631	647	0.98	-	-	-	-	-	-
	V16	Av.	687	655	665	0.98	-	-	-	-	-	-
	V23	Av.	691	661	660	1.00	663	654	1.02	653	651	1.00
	V31	Av.	688	-	-	-	655	650	1.01	645	646	1.00
	V50	Av.	693	-	-	-	-	-	-	652	644	1.01
	V56	Av.	688	655	654	1.00	-	-	-	-	-	-
	V63	Av.	686	-	-	-	681	653	1.04	666	650	1.03
	V82	Av.	690	-	-	-	677	646	1.05	-	-	-
	V85	Av.	693	663	663	1.00	-	-	-	-	-	-

Note 1; T₀ : Lock-off force of tendon
T₁, T₃, T₅ : Lift-off force at 1st, 3rd, 5th year ISI respectively (tonf)
Av. : Average tensile force of S and F side anchoring ; tonf

Table 8 Items of Tensile Force Loss of Tendon in GT-2

		Meas.	Calculated Values															
			Lock-Off	No.1 ISI T ₁				② Calculated Residual Tensile Force	No.2 ISI T ₂				④ Calculated Residual Tensile Force	No.3 ISI T ₃				⑥ Calculated Residual Tensile Force
				Cal. Each Loss of Tensile Force					Cal. Each Loss of Tensile Force					Cal. Each Loss of Tensile Force				
				ΔF ₁	ΔF ₂	ΔF ₃	ΔF ₄		ΔF ₂	ΔF ₃	ΔF ₄	ΔF ₂		ΔF ₃	ΔF ₄			
Cylinder Hoop Tendon	H5	691	1.7	7.7	20.6	3.9	657	-	-	-	-	-	-	-	-	-		
	H10	690	7.4	-	-	-	-	-	-	-	-	-	8.2	27.9	8.9	638		
	H25	699	17.3	-	-	-	-	8.0	25.6	6.8	641	-	-	-	-	-		
	H37	689	31.7	7.7	20.6	3.9	625	8.0	25.6	6.8	617	8.2	27.9	8.9	612	-		
	H44	689	27.0	-	-	-	-	8.0	25.6	6.8	622	-	-	-	-	-		
	H54	690	6.9	-	-	-	-	-	-	-	-	-	8.2	27.9	8.9	638		
	H58	682	11.1	7.7	20.6	3.9	639	-	-	-	-	-	-	-	-	-		
	H86	693	29.3	-	-	-	-	-	-	-	-	-	8.2	27.9	8.9	619		
	H102	689	6.8	7.7	20.6	3.9	650	8.0	25.6	6.8	642	8.2	27.9	8.9	637	-		
	H115	686	21.0	-	-	-	-	-	8.0	18.9	6.8	631	-	-	-	-	-	
	H119	692	10.4	7.7	15.3	3.9	655	-	-	-	-	-	-	-	-	-		
Dome Hoop Tendon	H141	697	2.9	7.9	13.9	4.6	668	8.2	17.6	8.0	660	8.4	19.1	10.5	656	-		
	H150	679	6.8	-	-	-	-	8.2	24.5	8.0	632	-	-	-	-	-		
	H157	687	6.3	-	-	-	-	-	-	-	-	-	8.4	26.7	10.5	635		
	H161	690	11.8	7.9	19.4	4.6	647	-	-	-	-	-	-	-	-	-		
Inverted U Tendon	V16	687	-0.1	8.0	10.7	3.9	665	-	-	-	-	-	-	-	-	-		
	V23	691	8.7	8.0	10.7	3.9	660	8.2	13.3	6.8	654	8.4	14.4	8.9	651	-		
	V31	688	10.2	-	-	-	-	-	8.2	13.3	6.8	650	8.4	14.4	8.9	646		
	V50	693	17.4	-	-	-	-	-	-	-	-	-	8.4	14.4	8.9	644		
	V56	688	11.1	8.0	10.7	3.9	654	-	-	-	-	-	-	-	-	-		
	V63	686	4.5	-	-	-	-	-	8.2	13.3	6.8	653	8.4	14.4	8.9	650	-	
	V82	690	16.1	-	-	-	-	-	8.2	13.3	6.8	646	-	-	-	-	-	
	V85	693	7.6	8.0	10.7	3.9	663	-	-	-	-	-	-	-	-	-		

Note : T₀ : Lock-off force of tendon (Average tensile force of S and F side anchoring ; tonf)

T₁, T₃, T₅ : Lift-off force at 1st, 3rd, 5th year ISI respectively (tonf)

ΔF₁ : Elastic deformation (tonf)

ΔF₂ : Relaxation of tendon (tonf)

ΔF₃ : Creep (tonf)

ΔF₄ : Shrinkage (tonf)

ΔF₁ : Elastic deformation (tonf)

Calculated residual tensile force ②~④ are results of lock-off measurements subtracted by total calculated loss.

Table 9 Lift-off Test Results of Tendon in Ohi Unit No.3

Tendon No.			T ₀	No. 1 ISI				No. 2 ISI			
			meas.	① meas.	② cal.	① / ②	③ meas.	④ cal.	③ / ④	⑤ meas.	⑥ cal.
Cylinder Hoop Tendon	H10	Av.	673	634	639	0.99	—	—	—	—	—
	H18	Av.	675	—	—	—	644	632	1.02	—	—
	H24	Av.	672	634	625	1.01	—	—	—	—	—
	H29	Av.	682	—	—	—	652	640	1.02	—	—
	H45	Av.	672	650	637	1.02	640	630	1.01	—	—
	H71	Av.	675	646	630	1.03	—	—	—	—	—
	H81	Av.	675	—	—	—	649	634	1.02	—	—
Inverted U Tendon	H101 (Dome)	Av.	672	640	641	1.00	651	634	1.03	—	—
	V18	Av.	692	679	667	1.02	—	—	—	—	—
	V29	Av.	692	658	659	1.00	661	653	1.01	—	—
	V40	Av.	681	—	—	—	651	646	1.01	—	—
	V56	Av.	686	662	650	1.02	—	—	—	—	—
	V63	Av.	689	—	—	—	666	659	1.01	—	—
	V80	Av.	667	655	632	1.04	—	—	—	—	—
	V86	Av.	667	—	—	—	637	623	1.02	—	—

Table 10 Lift-off Test Results of Tendon in Ohi Unit No.4

Tendon No.			T ₀	No. 1 ISI				No. 2 ISI			
			meas.	① meas.	② cal.	① meas.	② cal.	③ meas.	④ cal.	③ meas.	④ cal.
Cylinder Hoop Tendon	H10	Av.	678	658	644	1.02	—	—	—	—	—
	H18	Av.	679	—	—	—	—	646	638	1.01	—
	H24	Av.	678	639	632	1.01	—	—	—	—	—
	H29	Av.	679	—	—	—	—	653	638	1.02	—
	H45	Av.	676	641	642	1.00	—	654	635	1.03	—
	H71	Av.	675	639	630	1.01	—	—	—	—	—
	H81	Av.	675	—	—	—	—	648	639	1.01	—
Inverted U Tendon	H101 (Dome)	Av.	673	663	642	1.03	—	657	635	1.03	—
	V18	Av.	698	663	673	0.98	—	—	—	—	—
	V29	Av.	698	640	665	0.96	—	663	660	1.00	—
	V40	Av.	685	—	—	—	—	657	650	1.01	—
	V56	Av.	684	639	649	0.98	—	—	—	—	—
	V63	Av.	688	—	—	—	—	668	659	1.01	—
	V80	Av.	679	638	644	0.99	—	—	—	—	—
	V86	Av.	674	—	—	—	—	645	631	1.02	—

Table 11 Lift-off Test Results of Tendon in Genkai Unit No.3

Tendon No.			T ₀	No. 1 ISI			
			meas.	① meas.	② cal.	① meas.	② cal.
Cylinder Hoop Tendon	H15	Av.	688	650	647	1.00	—
	H58	Av.	685	641	634	1.01	—
	H62	Av.	690	649	652	1.00	—
	H86	Av.	690	652	652	1.00	—
	H126	Av.	685	646	645	1.00	—
	H153 (Dome)	Av.	696	664	659	1.01	—
	H164 (Dome)	Av.	699	660	669	0.99	—
Inverted U Tendon	V8	Av.	630	614	609	1.01	—
	V23	Av.	634	613	607	1.01	—
	V55	Av.	646	631	622	1.01	—
	V68	Av.	635	620	608	1.02	—

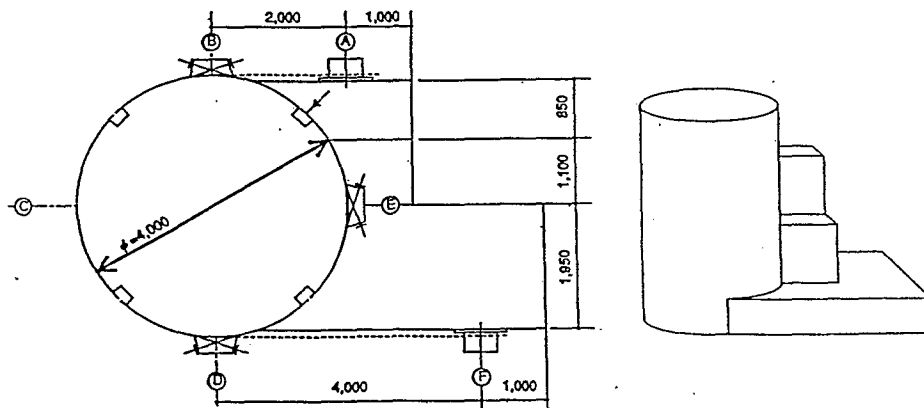


Fig.18 Test Specimen

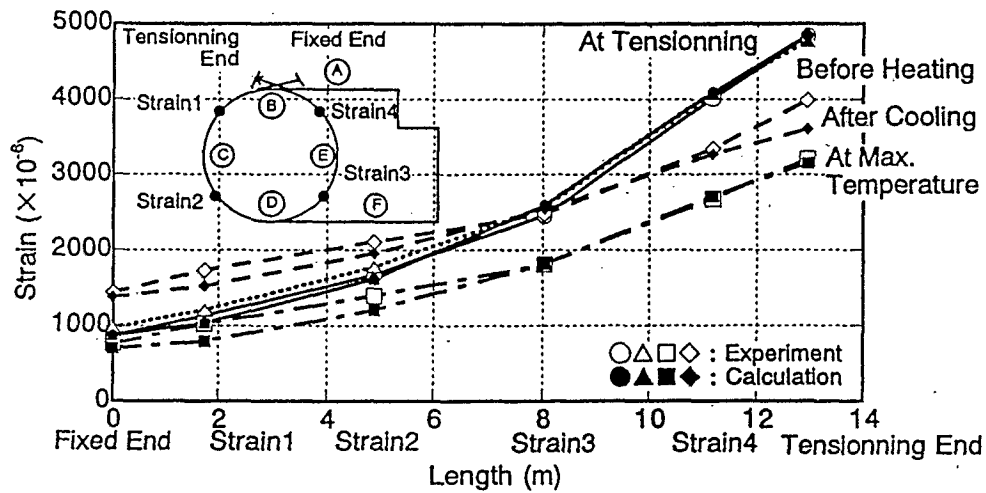


Fig.19 Strain Distribution of Tendon(H5.0-2.2)

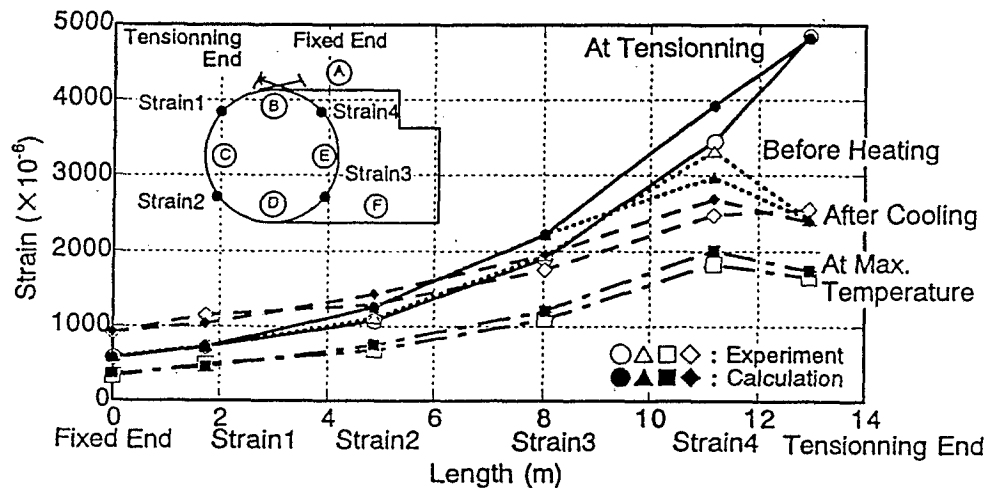


Fig.20 Strain Distribution of Tendon(H5.0-4.1)

6. CONCLUDING REMARKS

The following remarks are made from the results of strain measurements in PCCVs, lift-off tests on tendons, and studies of tests on redistribution of force in tendons.

- i. Although the fluctuating characteristics of creep and shrinkage of PCCV are influenced by the seasonal environment factors (humidity in particular), the design method does not consider its effects. But calculation by design method and measurement results basically agrees well, therefore the correspondence of the two is judged to be quite good.
- ii. Comparison of the measurement results on tendon tensile force loss (lock-off force subtracted by lift-off force) and calculation results (elastic deformation, relaxation of tendon, creep, and shrinkage losses) were made but the judgement on their relations were difficult.

On the other hand the measurement results on residual force (lift-off force itself) and calculation results (lock-off force subtracted by the calculated loss mentioned above) indicated good agreement, with their difference settling within the range of error.

iii. Where tendon forces are not uniform in the longitudinal direction, temperature change or deformation of the structure redistributes the tensile force throughout the tendon. However the effects on the evaluation of residual tendon force by the redistribution of tensile force were confirmed to be small.

iv. Considering the affects by measurement errors and redistribution of tensile force, the measurement results of residual tendon force and calculations indicated excellent agreement, thus the residual force in tendon was confirmed to behave in the predicted manner. Therefore integrity evaluation by ISI tests with strain measurements in subject may be enforced without problem.

REFERENCES

- 1) A. Kato, T. Abe, Y. Sono, T. Yamaguchi and M. Yamamoto, (1997). Study on the tensile force redistribution of heated tendon, Transaction of the 14th SMIRT, H01/6
- 2) M. Ozaki, T. Abe, Y. Watanabe, A. Kato, T. Yamaguchi and M. Yamamoto, (1995). A prediction method for long-term behavior of prestressed concrete containment vessels, Transaction of the 13th SMIRT, vol.H, PP 143-148
- 3) S. Tamura, Y. Watanabe, A. Kato, T. Yamaguchi, etc. (1991), A Delayed phenomena Evaluation of prestressed concrete containment vessel at Tsuruga Unit No.2 power station, transaction of the 11th SMIRT, vol.H, PP 305-310
- 4) M. Yamamoto & T. Yamaguchi, 1996, Numerical study on redistribution of tendon under high temperature. Summaries of Technical Paper of Annual Meeting AIJ B-2:1079-1080
- 5) M. Yamamoto, A. Kato, K.Sakurai, K. Kiyohara, T. Yamaguchi, etc. 1995, Study on Redistribution of Tendon Forces under High Temperature. Summaries of Technical paper of Annual Meeting, AIJ B-2:1025-1026

Dr. Alex G. Miller
OECD-NEA
Nuclear Safety Division
Le Seine St-Germain
12 bd des Iles
F-92130 ISSY-LES-MOULINEAUX
FRANCE



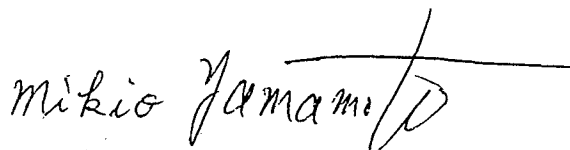
Mikio Yamamoto
Deputy General Manager
Engineering Dept.
Nuclear Facilities Division
Obayashi Corporation
3-7 Nishi-shinjuku, Shinjuku-ku
Tokyo, 163-10 Japan
TEL:+81-3-5323-3559
FAX:+81-3-5323-3550

2 Oct. 1997

Dear Dr. Miller,

Here I am sending you a copy of the answers to the questionnaires about WANO/OECD workshop paper entitled "In-service inspections and R&D of PCCVs in Japan". I have sent a copy to you by fax but I am sending this to you again in case it has not reached you.

Yours Sincerely,


Mikio Yamamoto

The answers to your queries concerning the OECD/WANO paper are as follows.

- Q.1 In section 3.2 results, para v, it is stated that measurements of all examined tendons at the lift-off test were large enough compared to the expected design requirements.
- A.1 Fig.1 shows the predicted design value and Fig.2 shows the relations of the measured values and predicted design values. As in Fig.2, the lift-off force sufficiently exceeds the required design value. Also the lift-off force is scattering. This scattering largely derives from the scattering of lock of force.
- Q.2 In section 6 conclusions, para iv, it is stated that ... indicated excellent agreement, thus the residual force in tendons was confirmed to behave in the predicted manner.
- A.2 The ratio of measured values to calculated values of residual tendon force is 1.05 at maximum. (see Table 7 in p22)
The evaluation on the influences by tensile force redistribution at actual PCCV was made based on the evaluation formula in the papers of 14th SMIRT (H01, Study on the tensile force redistribution of heated tendon). As a result the influences by this was found to be 2~3% of the average tensile force. Since the measurement error of lift-off force is 2%, the total of effect due to redistribution and measurement error is 4~5% which corresponds to the ratio of 1.05 mentioned above.
Therefore, the conclusions written in paragraph 4 in chapter 6 Conclusions is made.

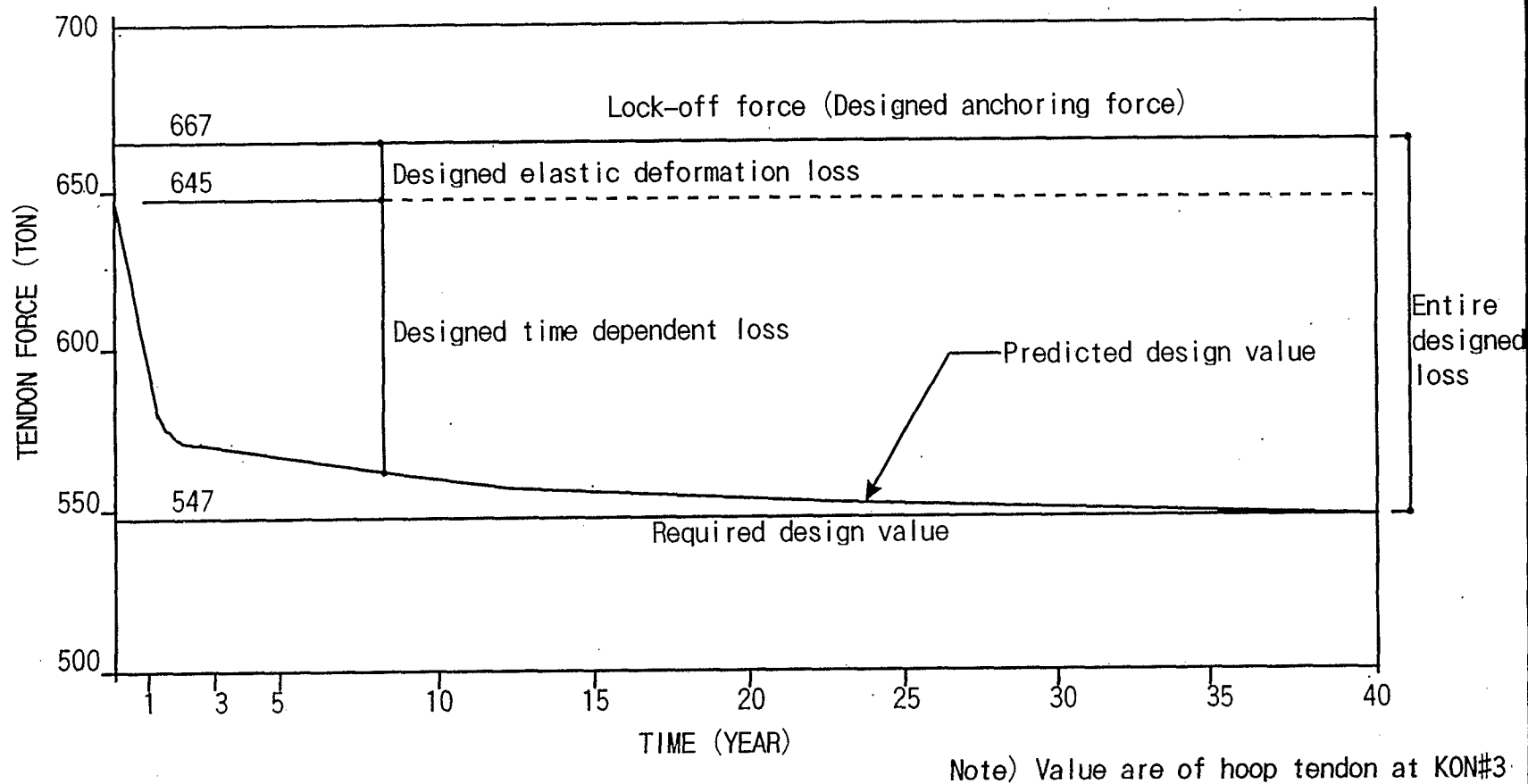


Fig.1 Graph of Predicted Design Value

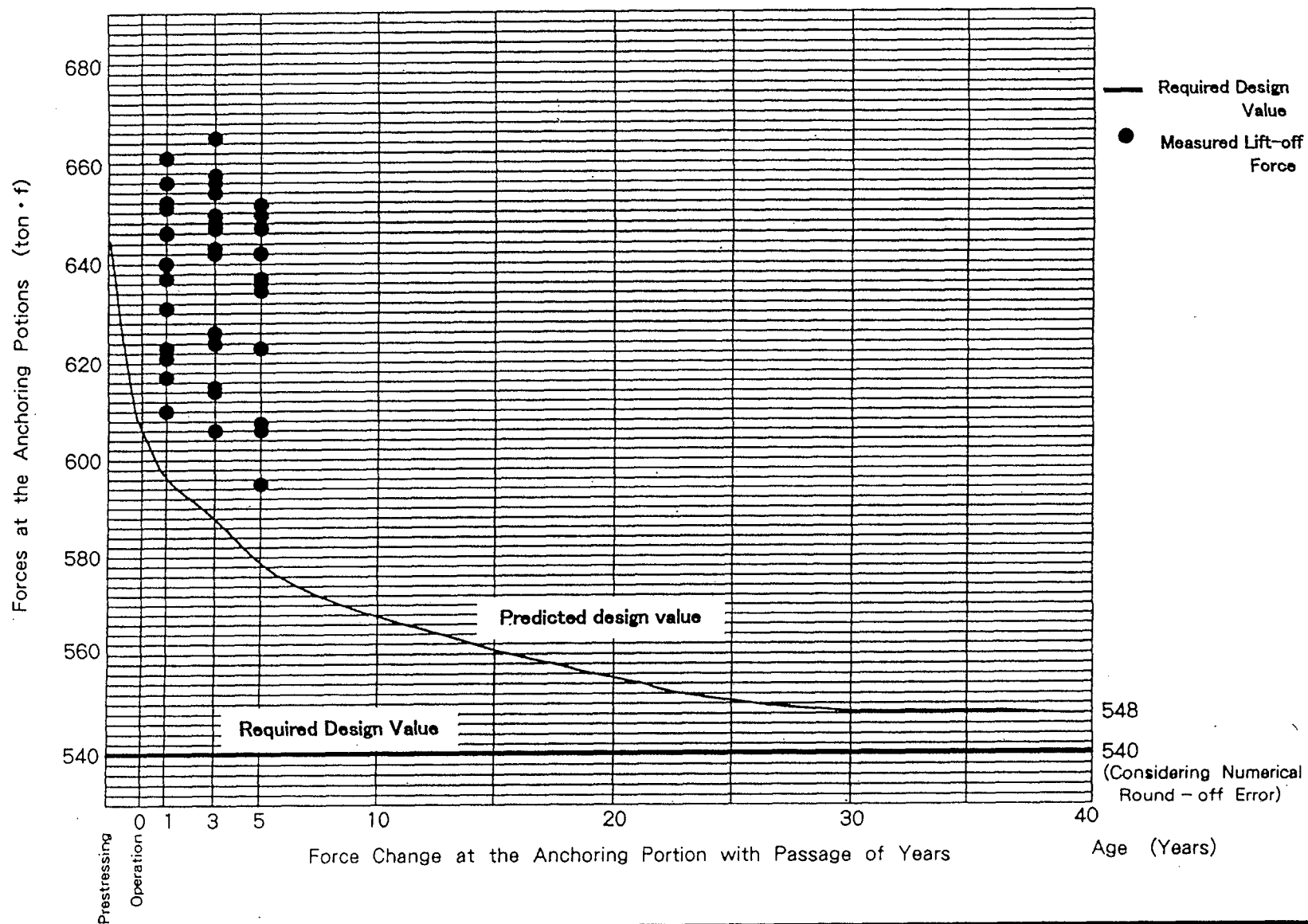


Fig.2 Lift-off Force of Hoop Tendon (3 Buttressed)

Supplementary explanation on Answer 2.

Fig.3 and Fig.4 shows the calculated distribution of tensile force at relative temperature change of 80°C and relative partial temperature change of $\pm 30^{\circ}\text{C}$ due to solar radiation at actual PCCV respectively. Table 1 shows the ratio of tensile force at tendon end against initial force.

The temperature of 80°C is measured when grease was injected after the anchoring of tendon. The temperature changes at normal operation is about $20^{\circ}\text{C} \sim 30^{\circ}\text{C}$. Therefore, the ratio of tensile force at about $20^{\circ}\text{C} \sim 30^{\circ}\text{C}$ against initial force is $1/4$ of it at 80°C . In this way the ratio of tensile force at the temperature of about 30°C is $2 \sim 3\%$ against normal temperature changes as well as against partial temperature changes.

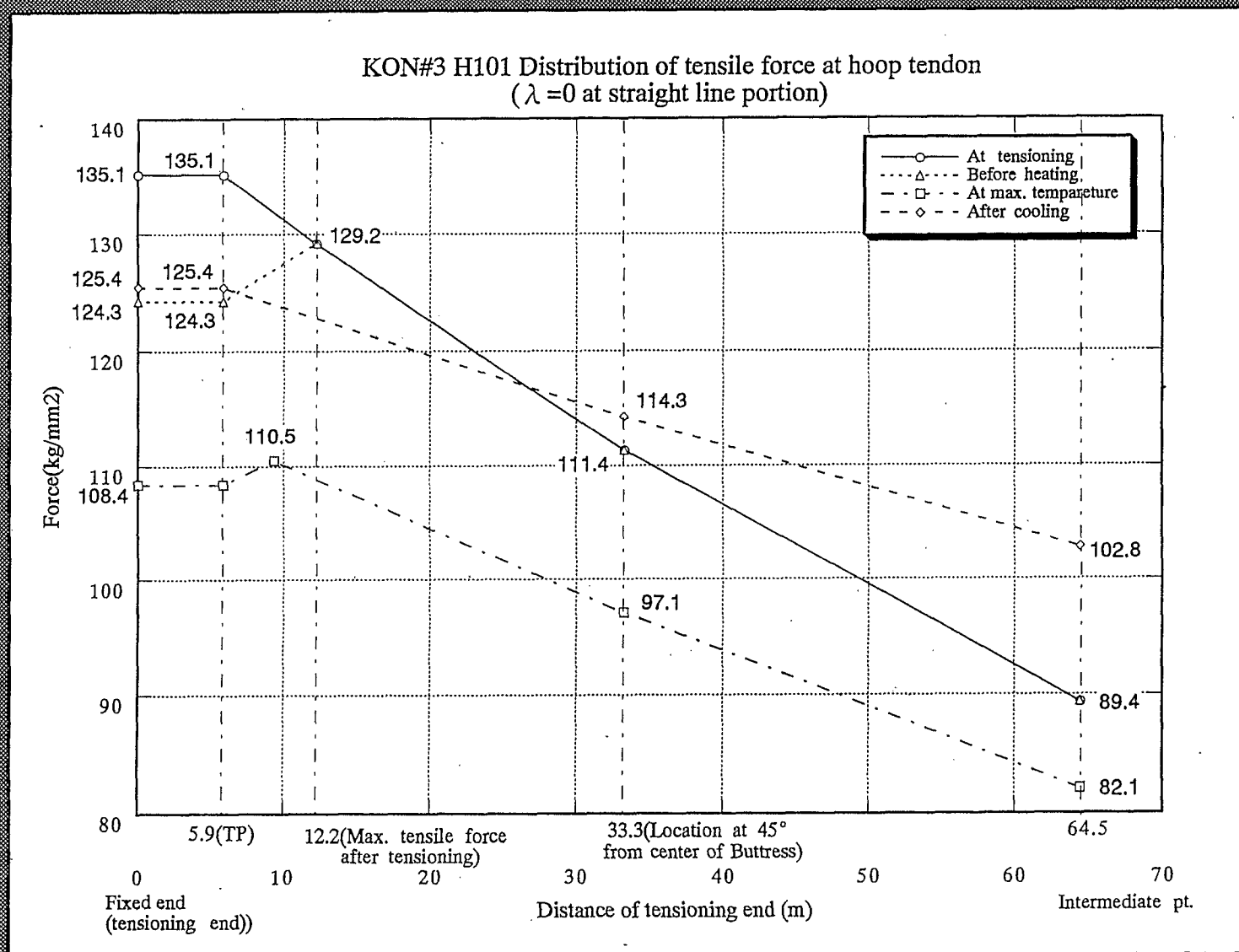


Fig.3 KON#3 H101 Distribution of tensile force at hoop tendon
($\lambda = 0$ at straight line portion)

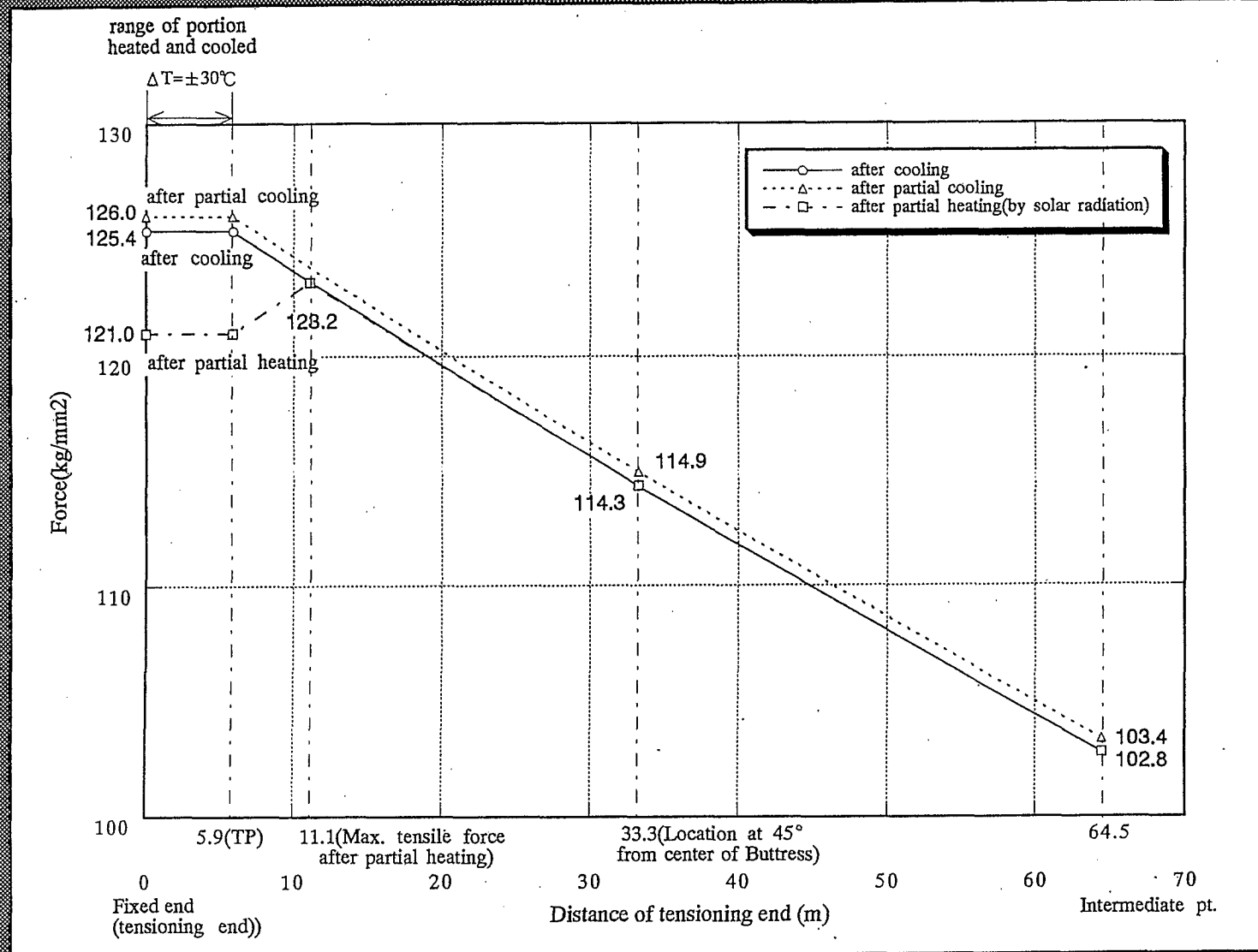


Fig.4 KON#3 H101 Distribution of tensile force at hoop tendon
 $\mu = 0.067$ (partial heating)

Table 1 Influence of redistribution of tensile force

		tensile force at tendon end (kg/mm ²)	ratio against initial force
80°C uniform heating	before heating	124.3	—
	under max. heat	108.4	-13%
	after cooling	125.4	+1%
± 30°C partial heating	before heating	125.4	—
	under max. heat	121.0	-4%
	maximum cooling	126.0	+0.5%

COMPARISON OF GROUTED AND UNGROUTED TENDONS IN NPP CONTAINMENTS

Munir Ahmad*

**CHASHMA NUCLEAR POWER PROJECT
PAKISTAN ATOMIC ENERGY COMMISSION**

* Munir Ahmad is Principal Engineer in Chashma Nuclear Power Project, Pakistan Atomic Energy Commission.

COMPARISON OF GROUTED AND UNGROUTED TENDONS IN NPP CONTAINMENTS

**Munir Ahmad
Principal Engineer
Chashma Nuclear Power Project
Pakistan Atomic Energy commission
P. O. Box 1133 Islamabad, PAKISTAN
Ph. 0092 51 920 5600
Fax 0092 51 921 7864**

**WORKSHOP ON PRESTRESS LOSSES IN NPP
CONTAINMENTS, POITIERS FRANCE, 25-26 AUGUST 1997**

ABSTRACT

Containments of nuclear power plants are prestressed by post-tensioned prestressing systems using grouted or ungrouted tendons. Cement grout is normally adopted for protection of tendons from corrosion in case of grouted tendon systems. This practice has widely been followed in France and for all the plants of French origin. On the other hand, ungrouted (greased) tendon systems were used for prestressing of containments of American nuclear power plants. Both the practices carry advantages over each other. Grouted tendons, once grouted, are not available for direct inspection and can't be replaced after they are grouted while greased tendons can be directly inspected after installation and may be replaced if required. The author has discussed in this paper all the details of grouted and ungrouted tendons, including their advantages and disadvantages over each other. In addition, inservice inspection techniques normally followed for both the categories have been briefed. The question, whether to follow grouted or ungrouted tends to become more a philosophical than a technical one because both the practises have produced good results. It can possibly be commented that desired results in each case can be obtained through proper detailing, improved construction practices and using more refined material constituents which require further research and development.

1.0 GENERAL

Ordinary concrete is weak in tension and cracks when subjected to tensile stresses. Tensile stresses are always carried by steel reinforcement while all or most of the compressive stresses are taken by concrete. During the development of tensile stresses, fine (hairline) cracks are developed in the concrete as a result of strains in the steel reinforcement. These cracks, although not visible and not dangerous from structural point of view, rather affect the leak tightness capability of containment structure. In case of loss of coolant accident (LOCA) and test conditions, very high tensile stresses are developed in the containment structure due to high over pressures. To overcome these high tensile stresses and to ensure the leak tightness during the test and accident conditions, containments are normally prestressed. The prestressing is established in such a way that the compressive stresses implied by the prestressing system are higher than the tensile stresses developed due to over pressure. In this way, leak tightness of the containment structure is ensured by keeping it under compressive state throughout the operating and accident conditions.

Prestressing is of two types; pre-tensioning and post-tensioning. When a member is fabricated in such a way that the tendons are stretched and each end is anchored to the concrete section after the concrete has been cast and has attained sufficient strength to safely withstand the prestressing force, the member is said to be prestressed by post-tensioning. In post-tensioning, during pouring of concrete, a mortar tight metal tube or flexible metal hose is provided. This metal tube is referred to as the sheath or the duct (or also called tendon sleeve) and remains in the structure. The tendon cables are threaded through the sleeves and, after tensioning, are anchored at both ends.

2.0 PROTECTION OF PRESTRESSING TENDONS

Prestressing plays a vital role in ensuring the structural integrity of the prestressed concrete containment throughout its life which is normally 40 years. Since the tendons and their end anchorages are fabricated from high-strength and high-hardness materials, they are susceptible to stress corrosion and hydrogen embrittlement. The tendons and the load-bearing hardware are, therefore, protected from the corroding environment by filling the tendon ducts/sleeves with some suitable material. Two types of tendon protection is normally followed.

- i. Grouting or bonded protection.

- ii. Greasing or unbonded protection.

2.1 GROUTING OR BONDED PROTECTION

For bonding of tendons to the concrete after tensioning, cement grout is injected, which also serves to protect the steel against corrosion. Entry for the grout into the cable way is provided by means of holes in the anchorage heads and cones, or the tendon ducts. The grout can be injected at one end of the member until it is forced out of the other end. For longer members, it can be applied at both ends until it is forced out at a centre vent.

An advantage of grouting, in addition to providing corrosion protection, is that a well-designed and well-constructed grouted tendon system provides a degree of bond between the tendons and the surrounding concrete. This bond, in turn, helps the anchorage system to resist the fluctuating stresses that arise after construction of the structure. Unlike greased tendons, grouted tendons are not available for direct inspection after they are grouted. It is, therefore, essential that the proposed grout and grouting procedure be thoroughly evaluated before it is used in the construction of containment structure.

The effectiveness of Portland cement as a deterrent to the corrosion of steel was evidenced by its performance history in prestressed concrete for more than 50 years. A review of the durability performance of post-tensioned tendons in conventional civil engineering structures showed that incidents of corrosion were small and related to either ill-conceived detailing, poor construction practices or the presence of contaminants in the grout. This performance history was supplemented by extensive tests conducted to ensure adequate penetration of grout through long vertical and curved hoop tendon ducts.

2.1.1 Basic Characteristics of Grout

The grout and its constituents should have following characteristics in general.

- The grout (whether freshly mixed or hardened) should not cause chemical attack on prestressing elements through its interaction with the material of the tendon steel, material of the anchorage system or material of the duct.
- The grout shall have proper fluidity.

- Water cement ratio of grout shall be strictly controlled.
- The grout shall completely fill the duct on hardening.
- Portland cement used in the grout shall conform to the requirements of ASTM C150 or the equivalent standards.
- The grout shall make permanent bond with the cable and the duct.
- The physical properties of grout shall satisfy the requirements of Article 2243.2 of ACI 359 (ASME Sec. III Div. 2) or the equivalent standards.
- Water used in the grout shall not contain any ingredients harmful to the prestressing steel/system or the grout. Water contaminated (1 ppm) with hydrogen sulphide (sulphide ion) is not recommended. It shall conform to Article CC 2223.2 of ACI 359 (ASME Sec. III Div. 2) or other relevant codes.
- Acceptable admixtures may be used if tests have demonstrated that their use improves the properties of grout, e.g., increases workability, reduces bleeding, prevents water separation when pumped at high pressure, entrains air, expands the grout, or reduces the shrinkage. The quantities of harmful substances should be kept to a minimum. Use of calcium chloride is not allowed.
- The pH value of the grout at the inlet and outlet of the tendon duct shall be strictly controlled as prescribed by the applicable codes and standards.
- The quantities of different harmful substances (chlorides, nitrates, sulphates, sulphides, etc.) added individually for each constituent and expressed as parts per million of water in over all grout composition shall be within the limits prescribed by the codes.

These are brief requirements for the grout and the constituent materials. Detailed specifications may be prepared following relevant codes and standards.

Effective corrosion protection of prestressing system can be provided by Portland cement grout if appropriate precautions are taken to eliminate the potential source of corrosion. To this end, close quality control is necessary for each constituent of the grout, the tendon material, and the tendon duct material and the method of mixing and pumping the grout and ensuring that the tendon is surrounded from end to end with qualified

grout. In addition, special care is required to avoid separation of cement and water between wires of tendons; and the upper part of the vertical ducts and at the upper side of hoop ducts at the big openings.

2.2 GREASING OR UNBONDED PROTECTION

Although the significant use of organic petroleum based corrosion protection compounds (greases) is a more recent development than the use of Portland cement grout, it has gained prominence in prestressed containments all over the world because of the relative ease with which the tendon can be inspected. Additional advantages include:

- Tendons can be physically inspected if required after they are tensioned and greased.
- Encapsulation (if applied) provides a comprehensive reduction in the friction factor, thus permitting the use of longer tendons, a less number of buttresses and anchorages.
- Tendons can be relaxed, re-tensioned and replaced if required.
- Grease products are directly purchased in bulk from manufacturers and not prepared like the grout at site, assuring a better quality control in the manufacturing process.

The petroleum based filler greases have evolved over the years to better attune the products to the application of unbonded (greased) tendons in prestressed containments. Initially the products was a sheathing filler containing polar wetting agents, rust prevention additives, microcrystalline waxes, and proprietary constituents formulated to be water displacing, self-heating and resistance to electrical conductivity. The next generation of materials was formed by adding a plugging agent to increase the low flow point of the products to keep them from seeking loose sheathing joints and flowing into hairline cracks. A subsequent refinement incorporated a light base number to provide alkalinity for improved corrosion protection. Additional modifications have produced the current generation of products that are formulated to:

- Increase the viscosity without sacrificing pumpability.
- Raise the congealing point.
- Increase the resistance to flow through sheathing joints.

- Increase water displacing characteristics.
- Raise the base number to provide higher reserve alkalinity.
- Increase the resistance to electrical conductivity.

Visconorust 2090P-4 duct filler is a scientifically compounded petroleum based corrosion preventive designed for bulk application. It is composed of complex additive-petroleum system to exclude air and water from tendon surfaces. This system preferentially wets the tendon by the action of polar agent, displaces moisture, provides a high reserve alkalinity, and forms a moisture transmission barrier of micro-crystalline wax reinforced by a laminar in organic structure. It has been adopted as duct filler for protection of tendons from corrosion in almost all the NPPs in Spain and most of the NPPs in the United States.

3.0 MONITORING OF GROUTED AND UNGROUTED TENDONS

The prestressing system of a prestressed containment is a principal strength element of the structure. Since the ability of the containment to withstand the events postulated to occur during life time of the structure depends on the functional reliability of the structure's principal strength element, any significant deterioration of the prestressed element due to corrosion may present potential risk to the public safety. In addition, some of the design parameters (prestress losses due to concrete creep/shrinkage and relaxation of steel) are assumed at the design stage. Hence, a system is must which should include procedures to detect any corroding of prestressing steel and also provide a quantitative means of verifying the design assumptions regarding the volumetric changes in concrete and relaxation of steel.

3.1 MONITORING OF GROUTED TENDONS

The performance history of grouting was supplemented by extensive tests conducted to ensure adequate penetration of grout through curved hoop and long vertical tendons. The regulators, however, were concerned about not being able to positively check the integrity of the grouted post-tensioned system throughout the service life of the structure. As a result of discussions and public meetings, the United States Nuclear Regulatory Commission (US NRC) developed two regulatory guides; RG 1.90 and RG 1.107. RG 1.107 provides recommendations for the qualification of

cement grout and defines limitations, while RG 1.90 provides two distinct approaches for inservice inspection of prestressed containment with grouted tendons. Although, the intent of these actions was to thoroughly scrutinise grout material, its installation and to periodically check the status of prestressed containment with grouted tendons, these actions did not encourage the use of grouted tendons in the prestressed containments in the United States because only 2 out of 41 prestressed containments have grouted tendons.

Monitoring program as recommended by US NRC RG 1.90 is described as follows.

a) Force Monitoring of UngROUTED Test Tendons

According to RG 1.90, nine test tendons (3 vertical + 3 hoop + 3 dome) are left ungrouted and protected from corrosion by oil, grease or any other corrosion protection medium. The changes observed in these tendons are not intended to represent the changes due to environmental or physical effects with respect to corrosion. Instead, these tendons are used as reference to evaluate the creep or shrinkage and relaxation of tendon steel. Prestress force in these tendons is monitored by applying load cells.

b) Monitoring of Grouted Tendons

There are two alternatives for monitoring of grouted tendons and any one can be followed.

Monitoring of prestress level (Alternative A)

In this alternative, the prestress level in the containment wall and dome is directly monitored by installing stress meters and/or strain gauges. There are two ways of installing the stress meters or the strain gauges.

- i. Stress meters or strain gauges are embedded in the concrete or applied on the steel rebar. This is a preferable way because of comparatively easy installation with less chances of damage to the gauges.
- ii. Strain gauges may be fixed directly on the prestressing tendons. This method is more sophisticated and difficult one.

and the gauges may be damaged during threading, tensioning and grouting of tendons.

The main advantage of alternative A is that after establishment of this system, only the system software/hardware is required and containment can be monitored without entering into it. However, these strain gauges, once embedded, can't be replaced or re-calibrated. This inspection is carried out at 1, 3 and 5 years after Initial Structural Integrity Test (ISIT) and every 5 years thereafter.

Monitoring of deformation under pressure (Alternative B)

Testing the prestressed containment under pressure can provide means of assessing integrity of containment by evaluating the elastic behaviour of the structure. Any significant decrease in stiffness of the structure due to loss of prestress would result into higher deflections or cracking. This inspection is similar to the ISIT and similar instrumentation is required. The comparison of the condition and deformation of structure during monitoring by pressure testing and ISIT could provide a real basis for evaluating the functionality of the structure.

Apparently this method seems to be simple when compared with alternative A. However, installation of temporary instrumentation and support system is very laborious and an exclusive shutdown of at least two weeks for each pressure test is required which is highly uneconomical. If adopted, pressure testing is recommended to be carried out at 1, 3, 7, 13, 20, 27, 33 and 39 years after ISIT.

It is generally advised to adopt alternative A initially and shift to alternative B if results of alternative A, at any stage of plant operation, are found to be unreliable due to possible defects and damages to the embedded strain gauges.

c) Visual Examination

A visual examination program is established for structurally critical areas (discontinuities, penetrations, heavily loaded areas, etc.) and end anchorages of prestressing tendons.

There seems to be little experience on the monitoring program of RG 1.90 in the United States because there are only three containments in the United States which have grouted tendons. In France, almost all the

containments have grouted systems and follow a bit simple monitoring program which consists of:

- i. Leave only four vertical tendons ungrouted, fill them with grease and apply load cells/lift-offs to monitor the prestress force.
- ii. Perform pressure test at design pressure after every 10 years.

The French practice is rather simple when compared to that recommended by RG 1.90. However, monitoring of some greased tendons in each case requires part of the overall efforts required for monitoring of ungrouted tendons.

There are some prestressed containments in different countries with all tendons grouted and none greased. These can only be monitored through pressure testing and visual inspections.

3.2 MONITORING OF GREASED TENDONS

An inservice inspection program for prestressed containment with greased tendons should include:

- Direct monitoring of prestress force.
- Removal and inspection of end anchorage assemblies.
- Relaxing, inspecting and testing of tendon wires/strands.
- Examination of grease.
- Re-tensioning of tendons.

US NRC RG 1.35 establishes an inservice inspection program which may be applied to all containments with greased tendons regardless of plant geographical location. The prestressing force in the tendons may be checked by lift-offs or other equivalent tests to discover any brittle, damaged or broken wires. Any eventual decrease in the prestressing force is due to the simultaneous time dependent factors such as:

1. Stress relaxation;
2. Temperature variation of the wire;
3. Shrinkage, creep, and temperature deformation in the concrete;

4. Differential thermal expansion and contraction between the concrete and the tendon; and
5. Reduction in cross section of the wire, including possible fracture due to corrosion.

A lift-off test does not differentiate in the effects of these factors, and corrosion, the factor of greatest concern, can't be isolated. Therefore, tolerance limits for the loss of prestressing force including effects of possible corrosion are to be established and inservice program is oriented to determine whether the limits are exceeded. It is important to note that only gross deterioration of the prestressing loss is detected. It may also be kept in mind that repeated load checking on a tendon is likely to cause the lift off load to drop below that of a previously unchecked tendon.

According to RG 1.35, inservice inspection is carried out at 1, 3 and 5 years after ISIT and every five years thereafter. Inservice inspection program as recommended by RG 1.35 is briefed as follows.

a) Selection of Tendon Samples

Inspection samples for first three inspections are selected as follows.

Typical containment

Six dome tendons (two located in each 60° family), five vertical tendons (randomly/representatively distributed) and similarly ten hoop tendons.

Hemispherical dome containment

About 4 % of U tendons but not less than 4.
4 % of hoop tendons but not less than 9.

If initial three inspections indicate no problem with the prestressing tendons, the samples for subsequent inspections may be decreased.

b) Visual Examination

Tendon anchorage assembly hardware (such as bearing plate, anchor plate, stressing washers, shims, wedges, and buttonheads, etc.) of all the selected tendons are to be visually inspected.

c) Monitoring Tests

Tendons selected for inspection should be subjected to lift-off or other equivalent tests to monitor the loss of prestress force. One tendon from each group should be removed for testing and examination over the entire length to determine if evidence of corrosion or other deleterious effects are present. Tensile test may also be performed keeping in view the possibility of stress cycling. A detailed examination of grease and its intended function including influence of temperature variations may be carried out.

It is evident that following the inspection program of RG 1.35, many of the tendons will not be monitored during the life time of the plant. It is, therefore, proposed that containments with ungrouted tendons may be subjected to a pressure test at design pressure at least after every 10 year to evaluate the overall structural response of the containment.

4.0 SUMMARY

1. Containments of nuclear power plants are prestressed by post-tensioned prestressing systems while the tendons and load bearing components are protected from corroding environment by filling the tendon ducts/sleeves with cement grout or grease. Both ways of protecting the tendons are equally popular.
2. In case of ungrouted (greased) tendons, grease is purchased directly from the market or the manufacturer while in case of grouted tendons, an additional set up for preparation of grout is required throughout the prestressing activity.
3. Grouted tendons are not available for direct inspection after they are grouted and can't be relaxed and replaced if required, while greased tendons can be directly inspected, relaxed and replaced if required.
4. An advantage of grouting, in addition to providing corrosion protection, is that a well-designed and well-constructed grouted tendon system provides a degree of bond between the tendons and the surrounding

concrete. This bond, in turn, helps the anchorage system to resist the fluctuating stresses that arise after construction of the structure.

5. There must be an inservice inspection program to monitor the changes in the tendons due to time dependent prestress losses and due to environmental/physical changes due to corrosion. US NRC regulatory guides RG 1.90 and RG 1.35 recommend inservice inspection programs for containments with grouted and ungrouted tendons, respectively. These may be fully adopted or formulated with slight modifications. No specific inservice inspection is compulsory; however, it should be established to represent the whole prestressing system and should be approved by the concerned regulatory authority.
6. It is evident that following the inspection program of RG 1.35, many of the tendons will not be monitored during the life time of the plant. It is, therefore, proposed that containments with ungrouted tendons may be subjected to a pressure test at design pressure at least after every 10 year to evaluate the overall structural response of the containment.
7. Ungrouted tendon system looks more reliable due to possibility of direct inspection and flexibility of replacing the tendons. This is only an option and may be possible but a difficult end solution. On the other hand, the properly grouted systems, even where grout with obviously high water cement ratio, provide excellent protection to the prestressing steel. Corrosion of sheath or tendon wires is always related to the chlorides or other harmful substances in the grout. When tendons are properly grouted, the performance of post-tensioned prestressing system is predictable and excellent.
8. End anchorages of grouted tendons are embedded in secondary concrete because there is no question of their removal while in case of ungrouted tendons, due to possibility of replacement of tendons, any architectural treatment or environmental protection should be removable without damage to the end anchorages. Further more, access provisions are to be considered in the layout and design/installation for all end anchorages of the ungrouted tendons.
9. In both the tendon systems, gross prestress losses (loss due to creep/shrinkage of concrete + loss due to relaxation of steel + loss due to physical effects of corrosion) can be monitored directly or indirectly. However, it is not possible to isolate these losses quantitatively. It is, therefore, very important to evaluate the upper and lower tolerance limits of expected prestress losses in both cases i.e., in grouted and ungrouted tendon systems.

10. Since the grouted tendons can't be directly inspected and replaced after they are grouted, there must be a strict quality control / assurance program to keep the harmful substances (like chlorides, sulphates, sulphides, nitrates, etc.) within the acceptable limits.
11. A few tendons are normally recommended to be left ungrouted for direct inspection in the containments with grouted tendons. This requires part of overall inspection efforts required for inspection of containments with ungrouted tendons.
12. The question, whether to follow grouted or ungrouted tends to become more a philosophical than a technical one because both the practises have produced good results. It can possibly be commented that desired results in each case can be obtained through proper detailing, improved construction practices and using more refined material constituents which require further research and development.

REFERENCES

1. T. Y. Lin and Paul Zia; Design of Prestressed - Concrete Structural Members.
2. Arthur H. Nelson; Design of Prestressed Concrete.
3. W. Thorpe, Simon Carues Ltd. Stockport England and F. E. Speck, Bureau BBR Ltd., Zurich, Switzerland; BBRV Post-Tensioning Systems as Applied to Reactor Containments and Prestressed Concrete Vessels.
4. J. Irving, J. R. Smith, D. McD. Eadie, I.W. Hornby; Experience of Inservice Surveillance and Monitoring of Prestressed Concrete Pressure Vessels for Nuclear Reactors.
5. Morris Schupack; Durability Study of a 35-Years-Old Post-tensioned Bridge (ACI Concrete International, Feb. 1994)
6. US NRC RG 1.35 (Rev. 2, 1976); Inservice Inspection of Ungrouted Tendons in Prestressed Concrete Containment Structures.
7. US NRC RG 1.107 (Rev. 1, 1977); Qualifications for Cement Grouting for Prestressing Tendons in Containment Structures.
8. US NRC RG 1.90 (Rev. 1, 1977); Inservice Inspection of Prestressed Concrete Containment Structures with Grouted Tendons.

9. J. C. Bertel, Freyssinet International; M. Pousse, Advisor to GPN; E. Faure, EDF/Cemete; G. Ithurralde, EDF/Septon; "The French Nuclear Containment Contributions of Prestressing in Cost Saving on the Projects".
10. ACI 359-89; Code for Concrete Reactor Pressure Vessels and Containments (ASME Sec. III Div. 2).

PRESTRESS LOSSES IN CONTAINMENT OF VVER 1000 UNITS

Maliavine V.P - Atomenergoproekt

1. FOREWORD

In the report are presented results from 20 years experience of AEP in the field of monitoring and analysis of the stress state of containments aimed at controlling the prestress level of the reactor building of units operating in the Russian Federation for 18 years.

Three of them concern the initial and modernised types (unit 5 in Novovoronezhskaya NPP, unit 1 and 2 in Kalininskaya NPP, respectively located in the vicinity of Voronezh and Tver), the four remaining units being of the unified series (unit 1, 2, 3, 4 of Balakovskaya NPP) located close to the town Balakovo.

Containment buildings are considered as constructions belonging to the safety class 2, according to PNAE G-1-011-89 rules, to seismic category 1 according to PNAE G-5-006-87 rules and protection against radiation is ensured by the functional equipments and systems located inside them, in agreement with PIN - 5.6.

To control the variations of the stress/strain state (SSS) of the containment, in construction phases as well as when they are normally operating, they are fitted with a monitoring system.

When they are normally operating checking of the prestress level is obtained by regular measurements of the stress/strain state parameters by means of the monitoring system, in the scope of scheduled control works.

Since plants have been operating, such controls on the prestress system have been carried out from 2 to 7 times in the above mentioned containments.

Control of the fulfilment of the criteria necessary to allow normal operating of containments, as regards prestress level and stress state, is carried out by the NPP Direction with the participation of specialists and with Safety Authorities.

2. DESCRIPTION OF THE CONTAINMENTS OF REACTOR BUILDINGS

Prestressed concrete containments of reactor building of VVER 1000 Units designed by AEP have the form of a vertical cylinder, with an internal diameter of 45 m, based on foundation construction and capped by a gently sloped spherical dome (figure 1).

Zone of connection of cylinder with the supporting slab is strengthened by a gusset, zone of connection of dome with the cylinder is ensured (is strengthened) by the dome belt. thickness of cylinder walls is 1,2 m, thickness of dome in its central part - 1,1 m. Containment has a liner

with a thickness of 8 mm and special anti-corrosion coating. Prestressing system consists in two systems - prestressing system of cylinder and prestressing system of dome. The first system has an helicoidal pattern of prestressed tendons, the second has an orthogonal pattern. Ducts of the first system are positioned in three layers in the thickness of wall close one to the other. The external and the internal layers contain the left-hand entry of the helicoidal line, the median layer contains the right-hand entry of the helicoidal line. Ducts of the second system are positioned in two layers in the thickness of dome. Directions of each layer are perpendicular one to the other [7].

Concrete used for shell is heavy weight concrete with increased strength grade B30 (M 400), frost- resistance (F 150), water-tightness (W4) [8]. For reinforcement are mainly used hot-rolled reinforcement bars of grade of A-III with physical yield point, design strength is of 365 MPa [8].

For prestressed tendons high-strength carbon steel of grade B-II, diameter 5 mm, assembled in bundles shall be used. Design tensile strength of the bundle shall be determined as rupture load identified by testing of a sample batch with 0,95 confidence divided by a (safety) coefficient 1,6 [4, 8].

Containments of the first type (first generation) have a height of nearly 64 m, and there is no external constructions around them (figure 1a.)

Foundation of containment is drum shaped and consists in two reinforcement slabs bound by columns and walls. Total amount of tendons is 256 among which 184 - in the cylinder and 72 - in the dome. Ducts in the cylinder have an inclination of $35^{\circ}15'$ relatively to horizontal direction. One end of the tendon (reinforcement element) located in the cylindrical part of containment is fixed on the upper part of the dome belt, the other is fixed in the gallery under the bottom slab of the containment and consequently each tightening anchor is installed after every other one. Dome ducts are located in planes passing through the centre of the dome's spherical surface [7]. Anchoring of the end of each tendon (reinforcement element) is carried out in lower part of the dome belt from opposite sides. At present time, 5 units with containment of this type are in operation.

Containments of second type (second generation) are placed in central-symmetrical position in surrounding constructions which are 66 x 66 m in dimensions and rest on a single box type foundation construction. Reactor Building is disconnected from contiguous buildings by antiseismic joints. Height of a containment is nearly 54 m (figure 1b). Total amount of tendons is 132, among which 96 - in the cylinder and 36 - in the dome.

Ducts in the cylinder have an inclination of $35^{\circ}.05'$ relatively to horizontal direction. Tendons are set in an helicoidal-loop pattern with anchoring of both ends of each tendon on the top of the dome belt and bent under the containment bottom slab. In the dome, tendons are arranged in an orthogonal-loop pattern with anchor installed on one side of lower part of dome belt and bent on the opposite side (figure 2, [7]). At present time, 14 units with containments of this type are in operation.

Containments of these two types were designed to take into account the following basic actions and conditions [19] :

- a design accident (LOCA) : maximum internal relative pressure in containment of first and second types P_{Loca} respectively 3,636 bars and 4,04 bars and temperature

- + 150°C ; accident (LOCA) is assumed to occur once in the entire lifespan equal 40 years;
- internal pressure for pre-operating testing P_{test} (calculated accident pressure) is equal to 1,15 P_{Loca} , i.e. respectively 4,19 bars and 4,646 bars ;
- seismic effects - maximum design earthquake (MDE) - level 7 on a scale MSK-64;
- impact of external air wave with intensity of 3 kg per cm² and compression phase up to 1 s ;
- effects of normal operating conditions minor accident, etc.

Prior to commissioning containment shall be tested for strength under pressure equal to 1,15 P_{Loca} and for tightness - under design pressure [5]. While in operation the containment shall be tested periodically for tightness under a pressure of 0,707 bars [5, 7].

Containment prestressing value has been established with a condition of no membrane tensile stress in typical zones of containment under strength test pressure.

Level of concrete prestressing according to the national codes and standards [6] is limited to 0,65 of design resistance of concrete, that is in the frame of the linear theory of creep. At the beginning of prestressing strength of concrete should not be less than 50 % (of the strength) of the selected class of concrete and no less than 90 day strength of the concrete of the project. Prestress losses in a tendon are determined primarily in accordance with codes and standards [6] and with regard to results of large-scale test. Total prestress losses in a tendon were calculated for a design service life of 40 years with provision for losses to account for relaxation of stresses in the wire, shrinkage and creep of concrete. Value of losses are in a range of 15 % to 30 % [8].

In the project, prestressing of containment is carried out successively in several stages with specific phasing [9, 10]. The nominal controlled force in the jack after completing tension of a tendon and minimum controlled effort allowed during in operation period must follow regulations.

To prestress containment double-strand tendons were developed by institute "Orgenergostroy". The tendon consists of 442 and 450 smooth high-strength parallel wires of class B-II, 5 mm in diameter with design prestressing force of 1000 tons (10 MN). Technology of tendon manufacturing uses the method of continuous twisting between two fixed steps. Anchoring is performed with help of conical anchors with threaded fixing upon completion of prestressing, polyethylene tubes (PVP, type CL) 225 mm in diameter are used as ducts. Tendons are installed in polyethylene ducts with use of gun greasing without injection of the ducts, which allows at any time in case of necessity to re-tension or replace tendons [7].

During construction and operation the regular measurement of controlling parameters of the stress/strain state (SSS) of containment by means of monitoring system and visual inspection of concrete containment structures will be carried out . As measurement devices measuring (wire) transducers (MT) are used, which are installed in the containment during its erection and measure temperatures and strains of concrete , stresses in reinforcement bars and displacements (deflection) of the cylinder wall. The gauges (MT) are placed as "measurement

rosette" in the most critical zones of containment : the connection zone of the cylindrical wall with the supporting slab and dome, in typical zones - mid height of the cylinder and central zone of the dome and along 4 meridian lines (figure 3). Additional gauges were placed for measurement of normal static stresses at soil interface under foundation slab and to measure liner's strains. The quantity of installed gauges in containments of first generation ranges from 381 to 197, for second generation - from 372 to 160 [11]. The estimation of the stress state of containment is carried out on the basis of measurements made during the erection, prestressing, acceptance test and operation [11].

Periodically - annually in the first 5 years, then once per 5 years, the technical state of prestressing system shall be checked during scheduled checking -preventive works [7, 12] : the prestress level of tendons is checked selectively ; existence of corrosion ; complete unloading and tensioning of 2 tendons in the cylinder and 1 - in the dome ; dismantling of 2 tendons in the cylinder and 1 - in the dome.

Should any defector decrease of prestress in concrete be detected, tendon shall be re-tensioned to design value or replaced, if required [9, 12].

Thus, the control of the prestress level of containment is carried out by two independent methods -direct, by measurements of residual tendon tension on its ends by means of hydrojacks during scheduled checking preventive works (CPW) - and indirect, by regular measurement of parameters of the containment SSS by means of MT (gauges) of automatical systems for control (ASC), in typical zones of containment, during the whole period of operation.

Criteria for estimation of SSS and prestress level of containment during operation, or during realisation CPW are the following design and standard requirements [3....12] :

- values of compressive stress in concrete in containment typical zones calculated on measurement increments of SSS parameters (stresses in reinforcement bars and strains in concrete) induced by its prestress, should not be , during operation , less then the absolute value of tension stress in concrete caused by test pressure only;
- value of tension stress in the reinforcement bars of non typical zones of containment should not exceed design resistance limit in longitudinal and transverse reinforcement;
- width of cracks openings on external surfaces of containment concrete in operational period should not exceed 0,3 mm;
- prestress losses in containment should not exceed the design value, but average value of tension of tendons on their end should be not less than design one.

Conclusion about operational suitability of containment relatively to its prestress level with the prediction of prestress losses and both recommendations for volume and terms of next check are established on the basis of results of CPW.

The prediction of prestress losses is carried out for prestressing tendons :

- at their end taking into account their service life and residual prestress measured by means of hydrojacks;

- in typical zones of a containment on the basis of value of concrete strains measured by gauges of ASK ; herewith predicted value of concrete strains is calculated on the basis of the equations obtained from regression method (trend) or analysis of the rate of strains increments obtained from long term measurements.

During erection of a containment slump of concrete mix, density and strength of concrete at the age of 28 days, 60 days and 90 days are checked. Strength property of the concrete used for works is checked on control samples at the beginning of prestressing and at acceptance tests.

The representatives of the General Designer of concrete containment structure and prestressing tendons shall be on site during the realisation of containment prestressing, its acceptance tests and first CPW. They together with representatives of the NPP Direction and Safety Authorities RF make the conclusion on operational suitability of the containment on the basis of its prestress level and its SSS and on serviceability of prestressing tendons with recommendation for maintaining their design level.

The Construction of the 3 containments of the first type was completed in from 1978 to 1985, of the containment of the second type - in 1984...1989. Prestressing of containments was carried out respectively from 1979 to 1986 and from 1985 to 1990 , acceptance tests - accordingly in 1979...1986 year and 1985..1992 year. The duration of erection of first type containments was 1,8. to 6,7 years, containments of second type - 1 to 1,9 years. Duration of prestressing of the first type containments - 1,7 to 4 months, containments of second type - 1 to 4 months. 6 to 7 CPW were carried out in containments of the first type containments, 2 to 5 CPW - in containment of the seconde type. At the beginning of containment prestress the age of concrete in typical zones was for the cylinder/dome - 365/90 to 808/366 days for containments of the second type - 272/50 to 583/40 days.

The average value of cubes strength on control samples of concrete of containment gave :

- for the first type at the age of 28 days - 33,6 to 37,1 MPa with coefficient of variation 14 to 16 %;
- for the second type at the age of 28 days - 40 to 41,2 MPa with coefficient of variation 11 to 12,4 %; at the age of 60 and 90 days - 43,8 MPa and 45,6 MPa.

Prism strength , elasticity modulus creep, Poisson's coefficient and linear thermal expansion for the concrete of two containments of the first type were determined.

According to data from NIS Hydroproject [14, 15, 16], characteristics of concrete samples from these containments at the age of 28 days and temperature 20°C were :

- prism strength - 32,2 MPa and 33,0 MPa;
- elasticity module - 36720 MPa and 37500 MPa;
- creep of concrete under stress level (0,3 to 0,4) R_{prism} for 100 day loading $2,55 \cdot 10^{-5}$ 1/MPa and $4 \cdot 10^{-5}$ 1/MPa;
- Poisson's coefficient - 0,19;
- coefficient of thermal expansion $0,98 \cdot 10^{-5}$ 1/degree C.

The prestressing system of containments had tendon with an average section of 135...140 mm, value of tendon tension is 9,6...9,9 MN. Tendons for 2 containments of the second type of construction 1987...1989 used stabilised wire.

The acceptance tests of containments are carried out within 1,5..12 months from the completion of their prestressing. Test pressure rises in 6 steps for containments of the first type and 5 steps -second type with 2 hours duration intermediate steps. The results of tests have confirmed construction integrity and elastic behaviour containments [11].

According to results of first carried out CPW the average value of prestress losses on the measured residual tensions in tendons which have been checked were [17] :

- in 3 containments of the first type during operation 3,9..9,7 years - 21 % ... 28 %;
- in 4 containments of the second type during operation 1,6..2,2 years
 - 10 % ...21 %;
- and in containments with stabilised wire tendons for a period 1,6...1,9 years
 - 10 % - 14 %.

Following gauge readings of monitoring system heterogeneity of the stress/ strain state on perimeter of containments has been noticed in some containments of the first generation, caused basically by the influence of erection period . In non typical zones of these containments tension strains of concrete and stresses in reinforcement bars appeared. Readings of "shrinkage cones" testify for practical lack of shrinkage strains of concrete in mid part of the wall of containment in operation. In this period temperature of concrete in these zones did not exceed 40°C [11, 17].

For the prediction of prestress losses of tendon tension in typical zone of containment , computational formulas are established on the history of concrete loading and linear theory of creep and equations of regression (trend) are used. The trend equation are calculated by a method of the least squares for gauges located in typical zones of 3 containments of the first type and measuring stress of reinforcement bars and concrete strains, on long-term (5... 9 years) monitoring.

The computed expressions of compressive stress variations in the reinforcement bars σ_s and relative strains of concrete ε_b as a function of time t from completion of containment prestressing look like (figure 4) :

$$\begin{aligned}\sigma_s(t) &= at^n \\ \varepsilon_b(t) &= at^n \\ \varepsilon_b(t) &= a + b \ln t\end{aligned}$$

where a , b , n - factors, selected on the basis of statistical processing of the measured readings for each gauge.

The trend equation enable to estimate the effect of concrete creep on the level of prestress in typical zones, actual creep deformation of concrete, and to predict the prestress losses, term and volume of tendon retensioning works [11].

In containments of the first series, after 5...6 years of operation average rate of prestress losses has not exceeded 3...4% per one year after 8....9 years - 1...2 %.

Inspection of concrete containment structures was carried out on 6 containments of the second type, thus 5 of them were in operation 4...9 years and 1 - before prestressing [18,19]. For an estimation of physical-mechanical properties of containment concrete, the methods of determination of strength on samples picked out from constructions and mechanical non destructive control methods - method of elastic jump (Schmidt's method), tear with split and ultrasonic method were used.

With results of containment monitoring and experimental researches, the basic materials for development of the program on management of ageing containment construction materials were gathered [20].

3. MAIN ISSUES OF THE CONTAINMENT PRESTRESS

As regards of containment prestress according to results of measured data we can notice an excess of the value of actual prestress losses compared to design (values) in containments of first generation.

In prestress of containments, arises the problem of the differences between the design value for prestress losses compared to actual ones, mainly due to the relaxation of the wires used for tendons and to creep of concrete in containments of the first series

To solve this problem the rheological properties of wires of prestressing tendons and concrete have been studied under loads applied for many years

The excess of prestress losses is explained, first of all, by the use of calculation formulas based on investigations made for drying concrete (for which creep practically stops trough 3...4 years) and for high-strength wires, relaxation of which practically stops in 1000 hours.

According to results carried out in NIIZB, the prediction of stress losses from relaxation of high-strength wire $\Delta\sigma_{\text{ref}}^t$ for a long period of time (30 and more years) at 20°C temperature and initial stresses σ_{sp} is suitably defined by formula [21] :

$$\Delta\sigma_{\text{rel}}^{t,20} = \Delta\sigma_{\text{rel}}^{t,1000} [0,3 + 0,135 (\lg t)^{1,5}]$$

$$\Delta\sigma_{\text{rel}}^{t,1000} = a (\sigma_{\text{sp}} / \sigma_u - b) \sigma_{\text{sp}};$$

where

$\Delta\sigma_{\text{rel}}^{t,1000}$ - stress losses during 1000 hours with an initial level of tensioning σ_{sp} ;

σ_u - temporary resistance of a wire to break , MPa ;

$a = 0,4; b = 0,5$ for wires and strands with low temperature tempering;

$a = 0,17; b = 0,55$ for the stabilised wires;

With the proposed formulas in 10 years the value of losses in wire will be almost 1,8 times the value of stress losses for 1000 hours, and for a period from 10 years to 30 years - they will

increase only by 12,8 % and reaching 14,3 %. Thus stress losses of in the stabilised wire are almost 3,3 times smaller than for prestressing wire obtained through low temperature tempering.

From results of 17 years investigation in NIIES [16] on concrete samples kept at constant moisture content from containment of unit 5 of Novovoronskaya NPP, loaded at the age of 28 days with a loading level $0,4 R_{prism}$ and temperature 20°C , the basic creep comes to an end at 10 year. Average value of creep $C(t)$ within the first year was $3,64 \cdot 10^{-4} \text{ MPa}^{-1}$, in 10 years - $6,39 \cdot 10^{-5} \text{ MPa}^{-1}$, that is 1,75 times more, in 15 years - $6,55 \cdot 10^{-4} \text{ MPa}^{-1}$, that is 2,5 % more, than in 10 years and 1,8 times more than in 1 year.

The analysis of results of comparison of known expressions for the description of long-term creep of concrete with time - logarithmic (C1), power (C2), hyperbolic (C4) and hyperbolic with powered argument (C5), proposed by ACI with the experimental data obtained by Cэke has shown that the more exact prediction up to 20...25 years are given by the formula (C5). Thus it is proposed for the factors in this formula, to use empirical values from experiment. The recommended expression for the predicting long-term creep of concrete of a class B30 $C(t)$, loaded in the age of 28 day with a level loading $0,4 R_{prism}$, has of the form (figure 5, [16]):

$$C(t) = C_{\infty} \frac{t^n}{a_n + t^n}$$

where C_{∞} creep of concrete corresponding to long-term (17 years) loading.

On the basis of value of creep and stresses in concrete is carried out calculation of the increment of concrete strains and prestress losses of containment for the design period [13.22].

The results obtained have confirmed the necessity to use stabilised wires for tendons and have allowed to define procedure of the regular control of prestressing level of containment on the basis of periodic checking of the residual values of tendon tensions by scheduled CPW and regular measurements of the stress/strain parameters by means of the monitoring system.

Thanks to obtained data the use of stabilised wire for tendons and the increase of quality of concrete essentially have reduced prestress losses of containment of more recent constructions.

The prediction of average value of prestress losses during operation unit is carried out on the basis of:

- analysis of the measured values of residual tendon tension;
- adjusted equation for concrete strains;
- results of the investigation carried out on rheological properties of concrete and prestressed wire.

To assess containment predicted prestress level, monthly gauge readings of the monitoring system are carried out together with an estimation of kinematics of its changes.

4. CRITERIA AND DOCUMENTS

For the stress/strain state and the control of the level of prestress of containments, construction codes are used at the design stage :

- construction codes and rules for concrete and reinforcement structures [6] ;
- standards in nuclear engineering [2...5] ;
- documents of the prestressing system [10, 12] ;
- recommendations for the monitoring of stress/strain state of containment of VVER 1000 NPP [13] ;
- results of measured data and research studies [15, 16, 17, 21, 22] .

Norms and methodological documents of the above mentioned type are in a development stage which take into account results of containment monitoring and experimental researches of subject.

5. CONCLUSION

The 18-year's operational experience in prestressed containments with helicoidal prestress pattern without injection in the cylinder and orthogonal prestress pattern without injection in the dome confirms that the rules which have been developed and the design of the monitoring system allows to reliably control the prestressing level of containments and support their operational suitability regarding their design prestress level.

Specificity of containments with helicoidal prestress pattern without injection, influence of wire relaxation and creep of concrete on containment prestress losses for their entire lifespan have been studied and corresponding measures have been taken.

For the NPP containments belonging to future new series orthogonal prestress pattern without injection has been considered, together with the use of high strength strands and concrete with improved rheological characteristics.

6. REFERENCES

1. Общие положения обеспечения безопасности атомных станций (ОПБ-88). ПНАЭ Г-1-011-89. Госатомэнергонадзор СССР, Энергоатомиздат М., 1990 .
2. ПНАЭ Г-5-006-87 Нормы проектирования сейсмостойких АЭС. М., 1989
3. Нормы строительного проектирования АС с реакторами различного типа. Правила и нормы в атомной энергетике. Пин АЭ-5.6, Минатомэнерго СССР, 1986.
4. Нормы проектирования железобетонных конструкций локализирующих систем безопасности атомных станций. ПНАЭ Г-10-007- 90, Госпроматомнадзор СССР, 1991.
5. Правила устройства и эксплуатации локализирующих систем безопасности атомных станций. ПНАЭ Г-10-021-90, Госатомэнергонадзор СССР, М., 1990.
6. Строительные нормы и правила. Бетонные и железобетонные конструкции. СНиП 2.03.01-84, М., 1985.
7. Белохин С.Л., Кричевский А.З. Опыт проектирования, строительства и эксплуатации преднапряженных железобетонных защитных оболочек. Working material Technical Committee on Severe Accident Containment Design Bases Organized by the International Atomic Energy Agency and Held in Moscow, USSR. 17...21 October 1988. Reproduced by the IAEA. Vienna, Austria, 1989, p. 44...59.

8. Кляницкий В.И., Белохин С.Л. Основные положения расчета железобетонных защитных оболочек на статические и температурные воздействия. Working Material. Technical Committee on Severe Accident Containment Design Bases Organized by the International Atomic Energy Agency and Held in Moscow, USSR, 17...21 October 1988. Reproduced by the IAEA, Vienna, Austria, 1989, p. 99...111.

9. Титарников В.П., Беркович В.М., Малышев Б.К., Ноздрин Г.И., Таранов Г.С. Проектные основы защитных оболочек АЭС с реакторами типа ВВЭР при учете тяжелых аварий. Working Material. Technical Committee on Severe Accident Containment Design Bases Organized by the International Atomic Energy Agency and Held in Moscow, USSR, 17...21 October 1988. Reproduced by the IAEA, Vienna, Austria, 1989, p. 1...9.

10. Комплект технологических карт на преднапряжение защитной оболочки АЭС с реакторами ВВЭР-1000. Органергострой. М., 1990

11. Малявин В.П., Нефедова Г.Н., Котлов В.М., Царев А.П., Блинов И.Ф., Шехтер Е.М. Натурные испытания защитных железобетонных оболочек АЭС на прочность. Working Material. Technical Committee on Severe Accident Containment Design Bases Organized by the International Atomic Energy Agency and Held in Moscow, USSR, 17...21 October 1988. Reproduced by the IAEA, Vienna, Austria, 1989, p. 156...166.

12. Инструкция по техническому обслуживанию системы преднапряжения защитных оболочек головной серии и модернизированной конструкции для АЭС с энергоблоками ВВЭР-1000. ОЭС, М., 1989

13. Разработка рекомендаций по методам контроля НДС строительных конструкций защитной оболочки АЭС нового поколения, АЭП., М., 1991.

14. Блинов И.Ф., Нефедова Г.Н., Шехтер Е.М. Прочность железобетонных защитных оболочек АЭС по данным натурных наблюдений. Информэнерго, М., 1987.

15. Рекомендации по учету ползучести бетона при определении напряженно-деформированного состояния бетонных сооружений. П-795-83. Гидропроект, М., 1984

16. Выбор и обоснование зависимости для описания многолетней ползучести бетона строительных конструкций АЭС. НИИЭС. Коган Е.А. М., 1993.

17. Заключение АЭП по оценке НДС и уровня обжатия защитных оболочек АЭС с ВВЭР-1000 на основе показаний КИА системы АСК НДС и результатов КНР СПЗО

18. Определение физико-механических и реологических характеристик бетона защитной оболочки шестого энергоблока Запорожской АЭС, ДИСИ, Д., 1992

19. Определение фактических прочностных и деформационных характеристик бетона защитных оболочек эксплуатирующихся энергоблоков Запорожской АЭС, ДИСИ, Д., 1992

20. Program for Nuclear Plant Ageing Research. US-USRR Joint Coordinating Committee for Civil Nuclear Reactor Safety. W.6.12 meeting. Moscow, June 17...21, 1991

21. Мамедов Т.И. Оценка потерь напряжений в высокопрочной проволочной арматуре от релаксации при нормальной температуре. Бетон и железобетон. 1990, стр. 27...29

22. Проектирование железобетонных конструкций. Справочное пособие. Будевельник, К., 1990

23. Беляничев А.К., Бердичевский Л.А., Клоницкий М.Л., Книжник Г.Г. Перспективы проектирования защитных оболочек реакторных отделений атомных станций. Working Material. Technical Committee on Severe Accident Containment Design Bases Organized by the International Atomic Energy Agency and Held in Moscow, USSR, 17...21 October 1988. Reproduced by the IAEA, Vienna, Austria, 1989, p. 67...83.

24. Project VVER 1000. AES-92. Conception de L'enceinte. Dossier Technique. ATOMENERGOPROJECT-E.D.F./C.L.I. KL N 645

Типы конституционных обидчиков с 1993-1999

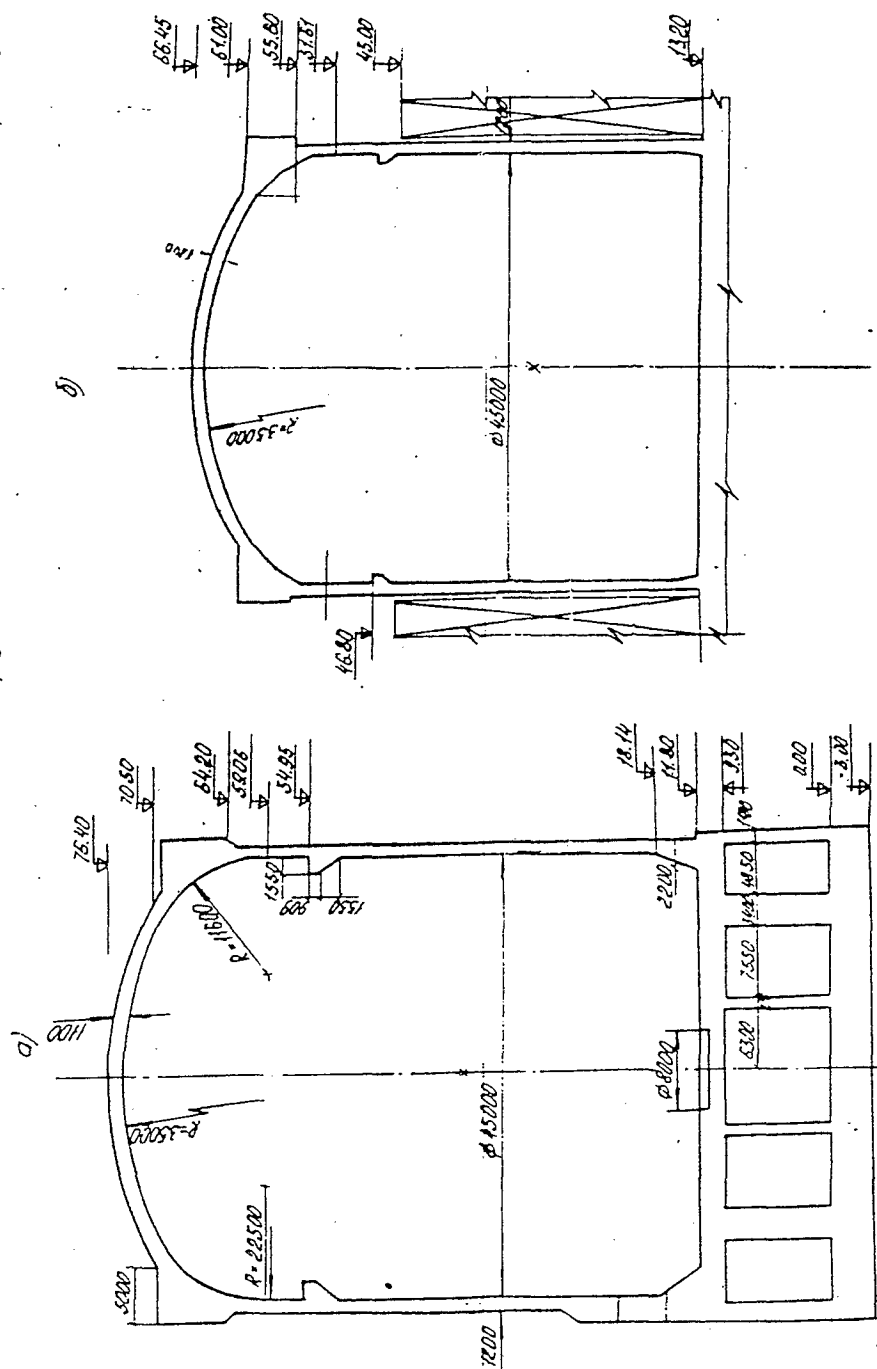


FIG. 1

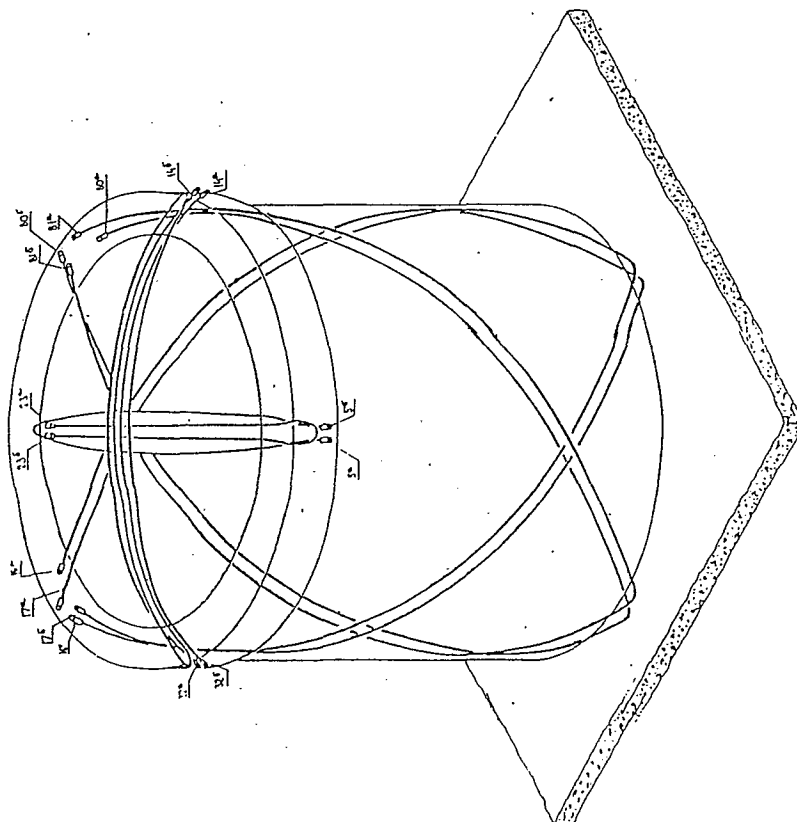
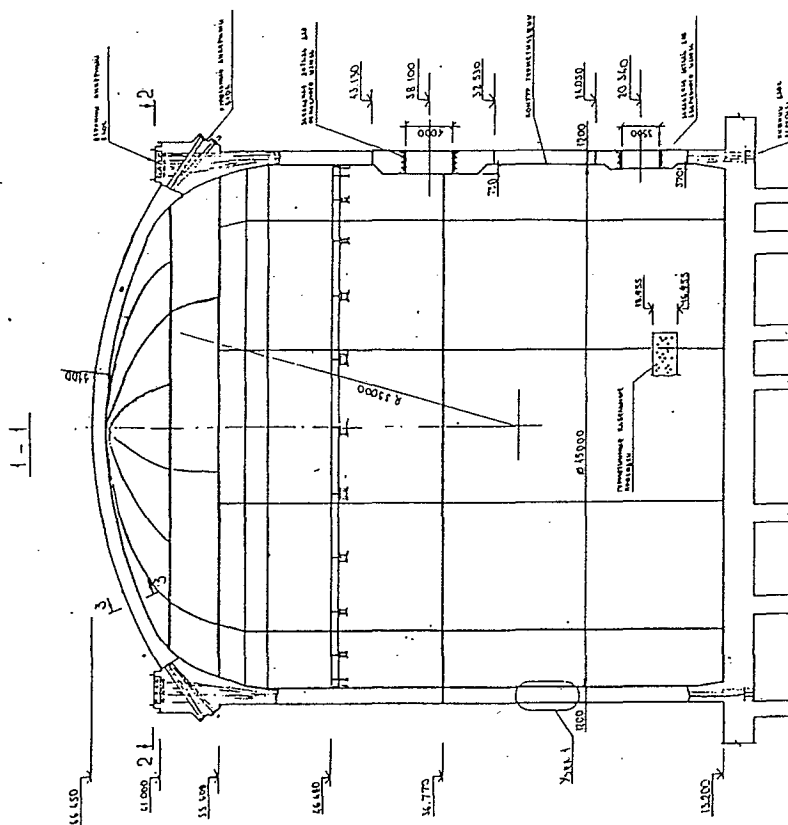


FIG. 2

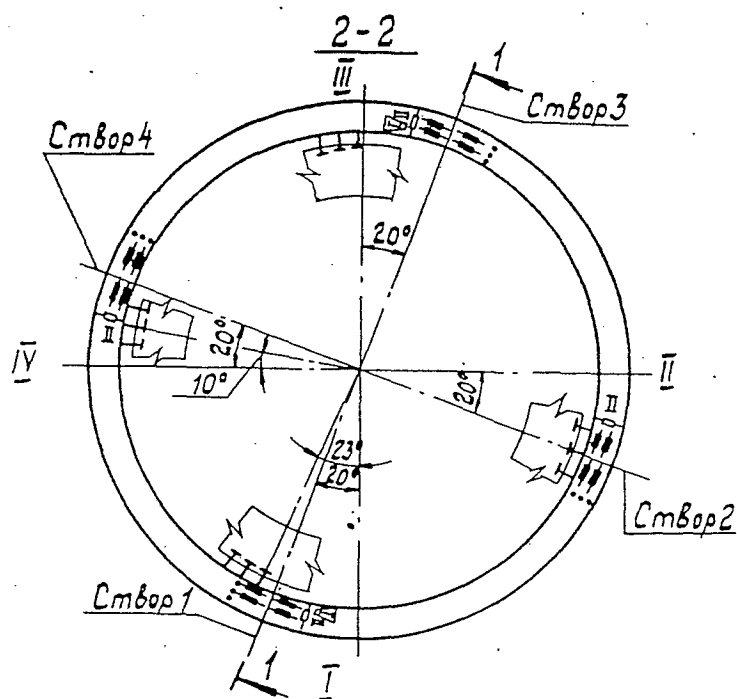
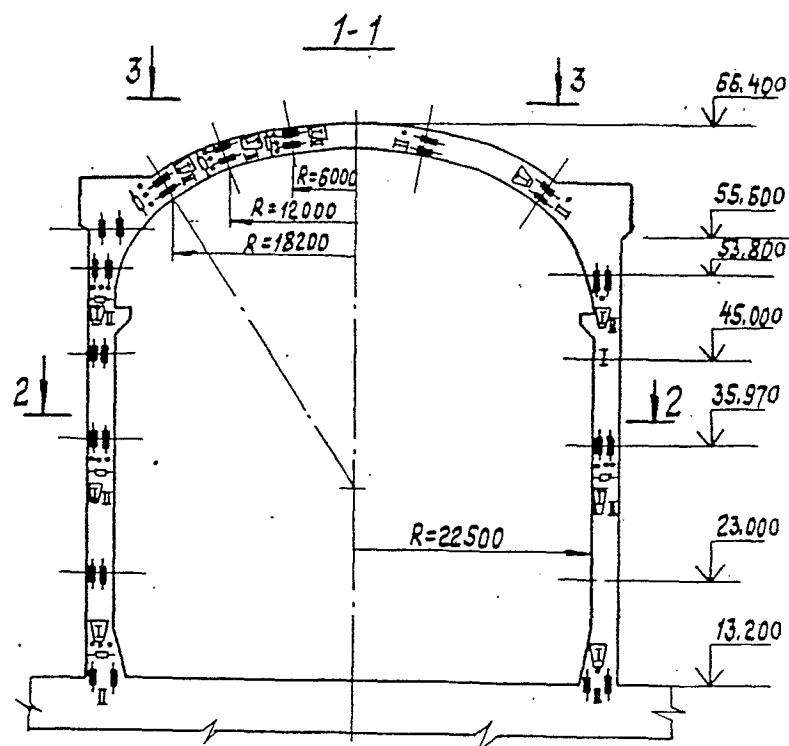
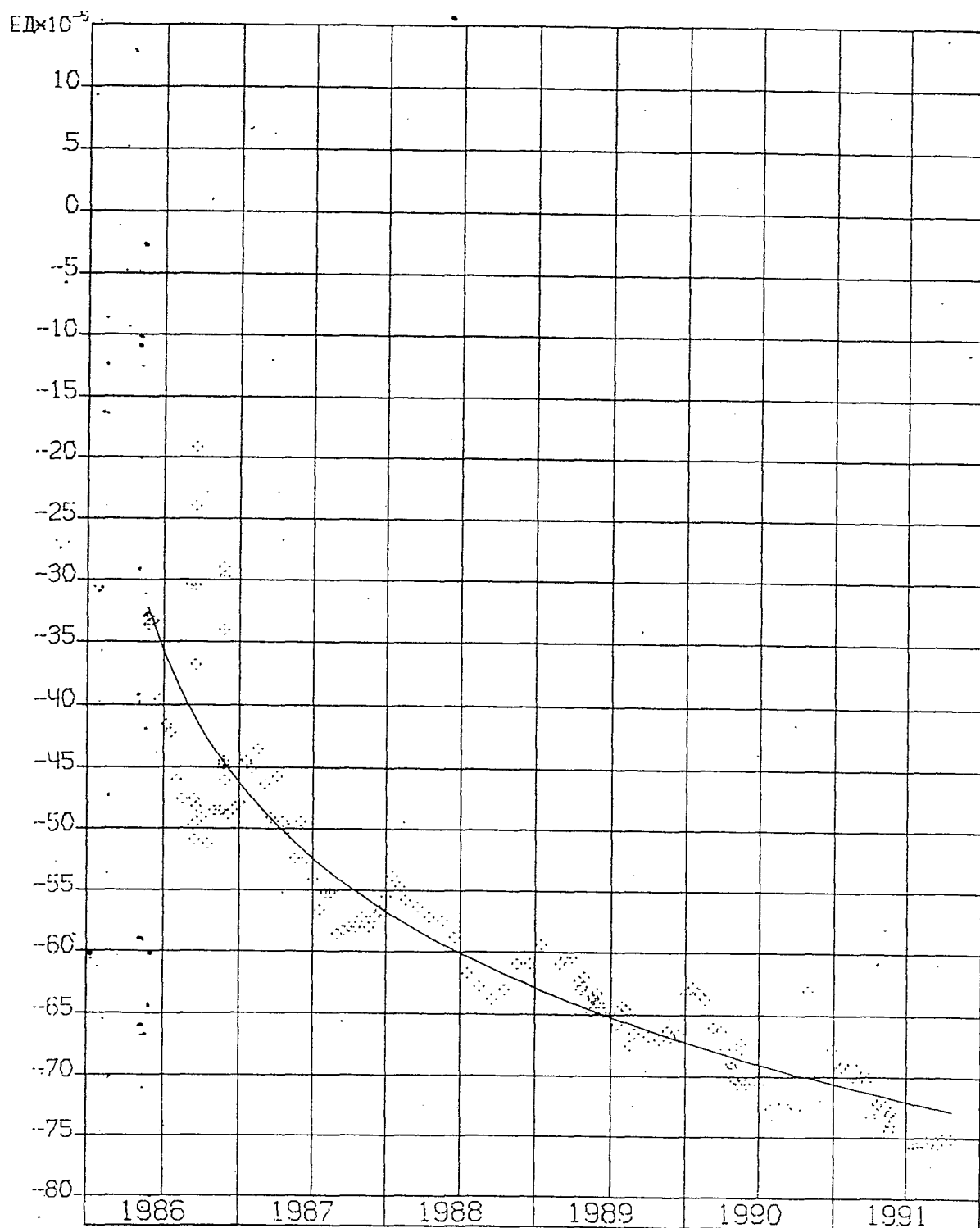


Fig.3

АПРОКСИМИРУЮЩАЯ ЗАВИСИМОСТЬ (ТРЕНД) ИЗМЕНЕНИЯ ВО ВРЕМЕНИ
ВЕЛИЧИНЫ КОЛЫЦЕВЫХ ДЕФОРМАЦИЙ В БЕТОНЕ ЦИЛИНДРА
ЗАЩИТНОЙ ОБОЛОЧКИ РО-2 КЛНАЭС



2401

Fig.4

Сравнение экспериментальных значений меры ползучести с расчетными по разным формулам
(ПВ АЭС, $\tau = 28$ сут.)

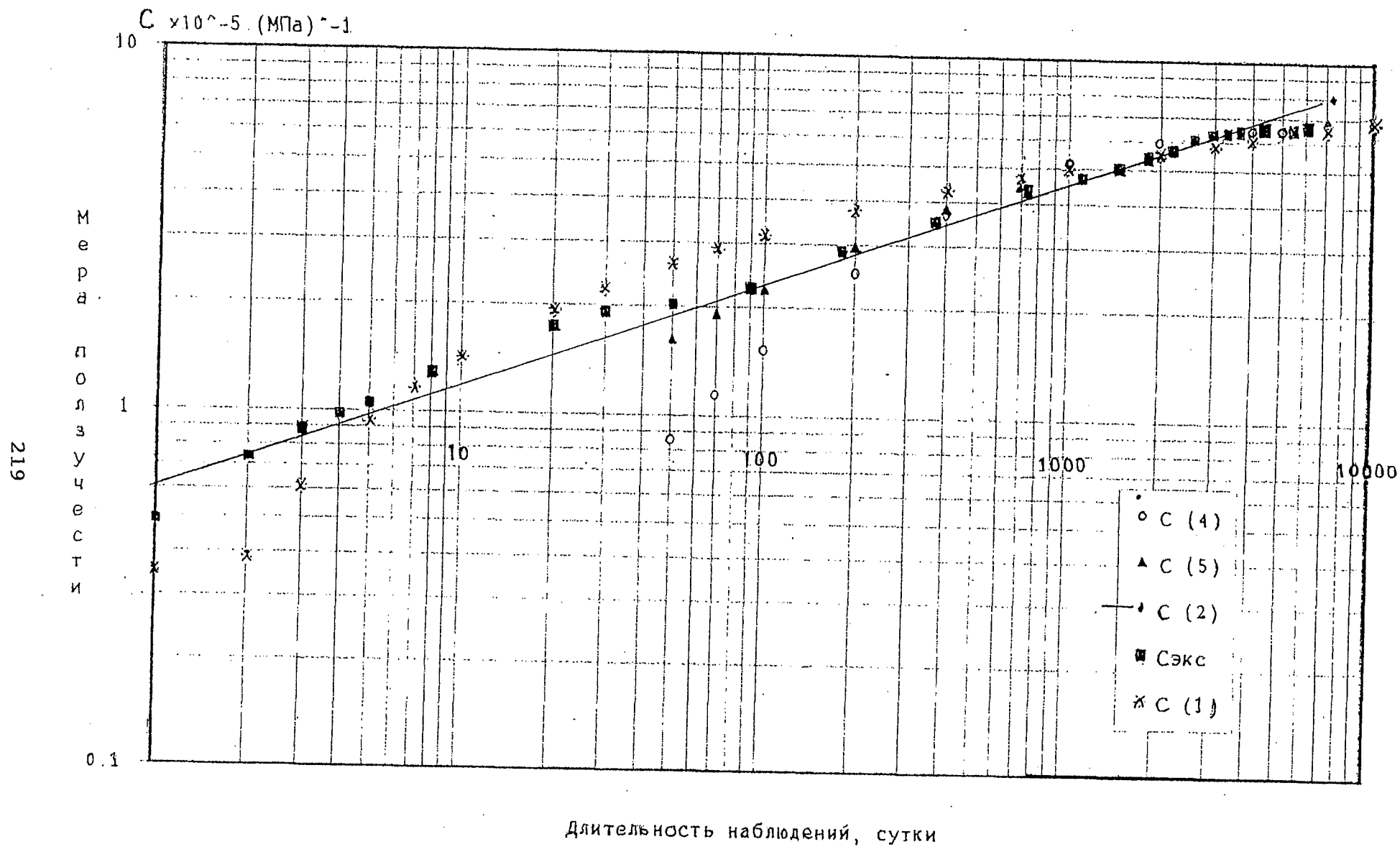


Fig.5

25-26 AUGUST 1997 JOINT WANO-PC/OECD-NEA WORKSHOP ON
PRESTRESS LOSS IN NPP CONTAINMENTS

Title:

**PRESTRESSING IN NUCLEAR POWER PLANTS
ANCHOR LIFT-OFF MEASURING SYSTEM FOR 37 T 15 TENDONS**

Authors:

Víctor Vives M., Asoc. Nuclear Ascó (España)

Luis Ubalde S. , Asoc. Nuclear Ascó (España)

ABSTRACT

The Asco Nuclear Power Plant is composed of two 930 MW PWR units. The external wall of the Containment Building in each unit is made of prestressed concrete. The Pre-stressing System, a Freyssinet technology using 37 T 15 tendons, is the non-adhering type (sheathing is filled with grease). This technique allows to verify the design conditions of the prestressing design directly through the tendons by means of periodical inspections carried out during the whole life of the structure. These inspections take place three times in the first five years and afterwards, once every five years. One of the objectives of these inspections is to measure the prestressing force that the type 37 T 15 tendons apply on the structure.

The measurement of the force is made by the same KC 1000 jack used in the pretensioning with a capacity of 1000 ton which acts on the tendon anchorage, increasing the outside tendon tension progressively up to reaching the block anchorage lift-off from its support plate. The lift-off force applied by the jack is the internal tension developed by the tendon. The problem is to determine the exact moment when the tendon anchorage block "lift-off" takes place.

In the 80's decade, the anchorage block lift-off was determined by inserting thin shims. The insertion of one of these shims between the support plate and the anchorage block indicated the separation. Simultaneously, the necessary force applied by the jack to overcome the tendon compressive action on the structure was registered. This force, extrapolated to a zero separation, was assumed to be acting on the anchorage. This procedure had the inconvenience presented by the lack of accuracy in determining the physical phenomena.

The system used at the present to measure the lift-off force consists basically in taking continuous elongation and jacking force data by means of a computerized system. The present work describes this new system, resulting from 15 years of experience in measuring the lift-off forces in the prestressing system.

Finally, as a conclusion, the experience in using this new measurement system for all the horizontal tendons in Asco N.P.P. Unit I is summarized. Satisfactory results were obtained in relation to reliability and accuracy of the measurements carried out. The new measurement system allowed to minimize the existent errors in the traditional methods (use of shims for detecting the lift-off).

GENERAL DESCRIPTION.

The Ascó Nuclear Power Plant is located on the right bank of the Ebro river in the province of Tarragona, about 30 Km from the Mediterranean sea. In this site, there are two identical units of PWRs, each of 930 MW nominal power. Unit I construction was completed in 1981 and Unit II in 1983.

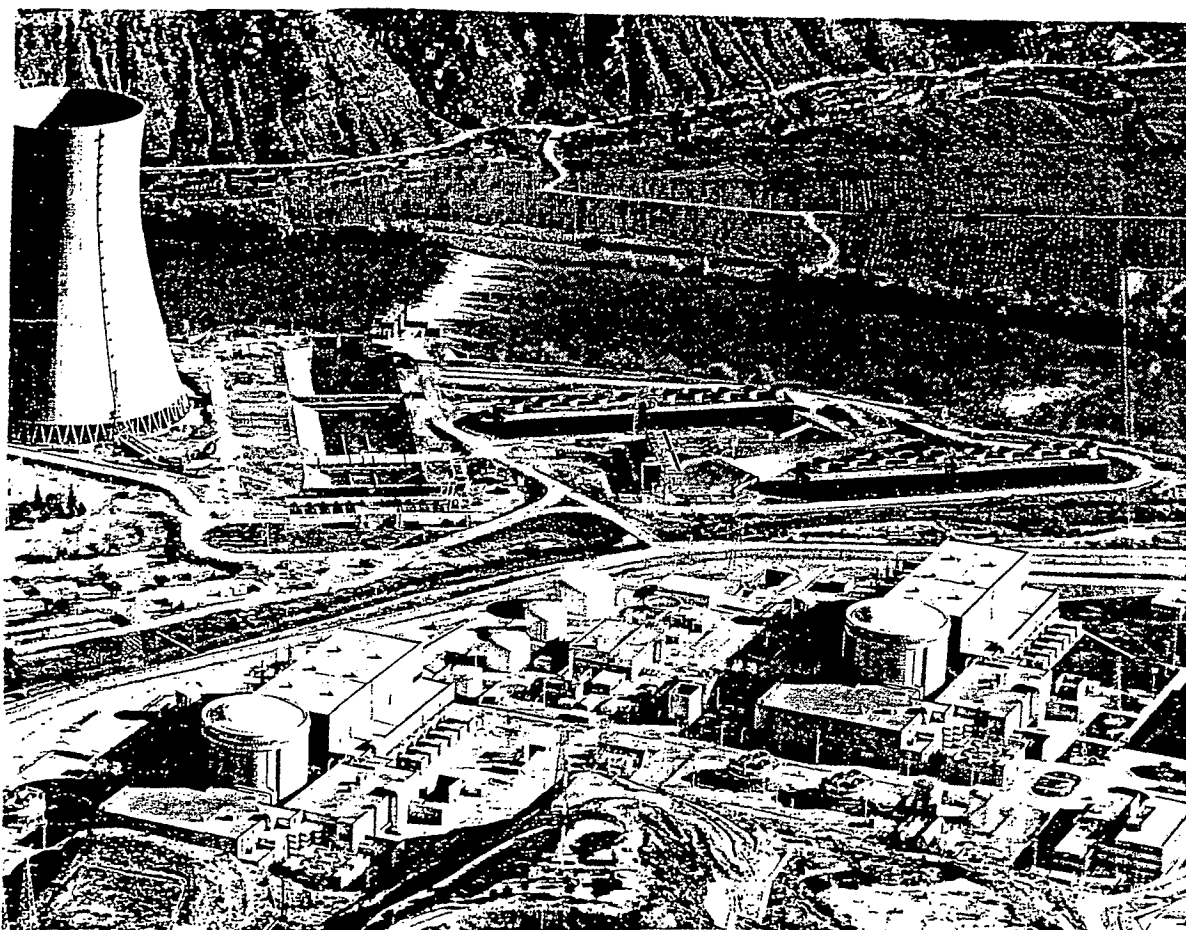


Figure 1. Plan View of the Location and Disposition of the Power station.

The NSSS is of Westinghouse design and is enclosed by a single shell Containment Building. It is a post-tensioned prestressed reinforced concrete structure with a metallic interior liner plate of 6,5 mm thickness.

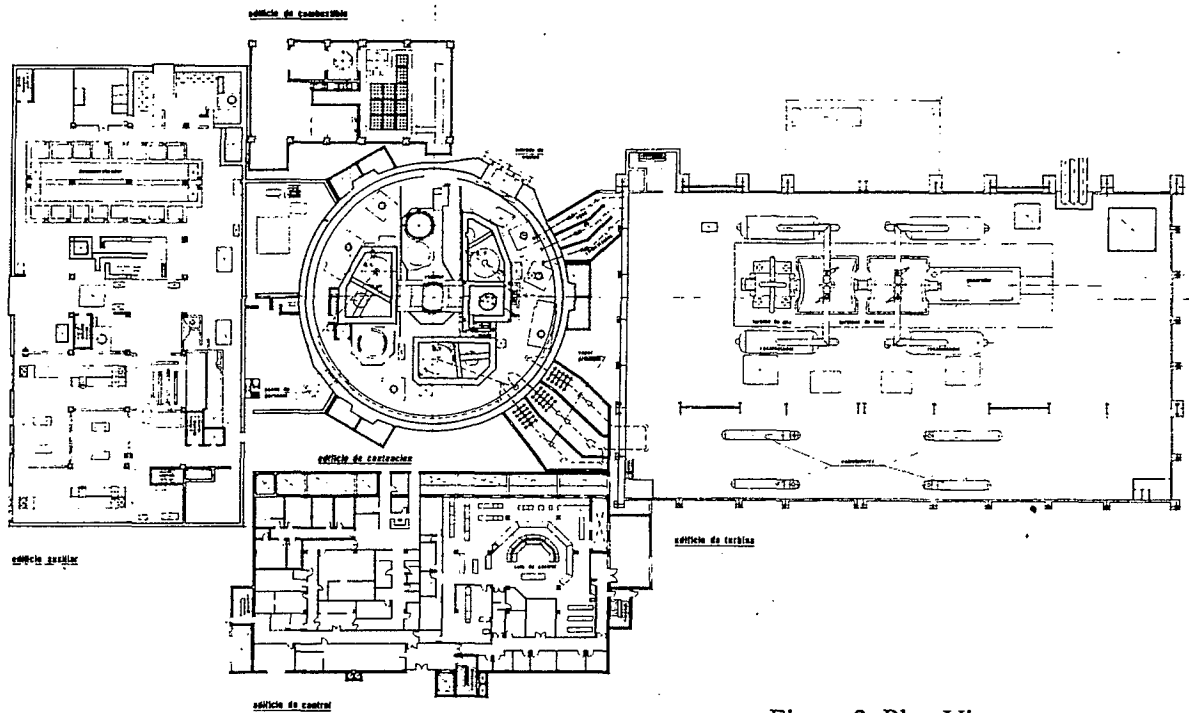
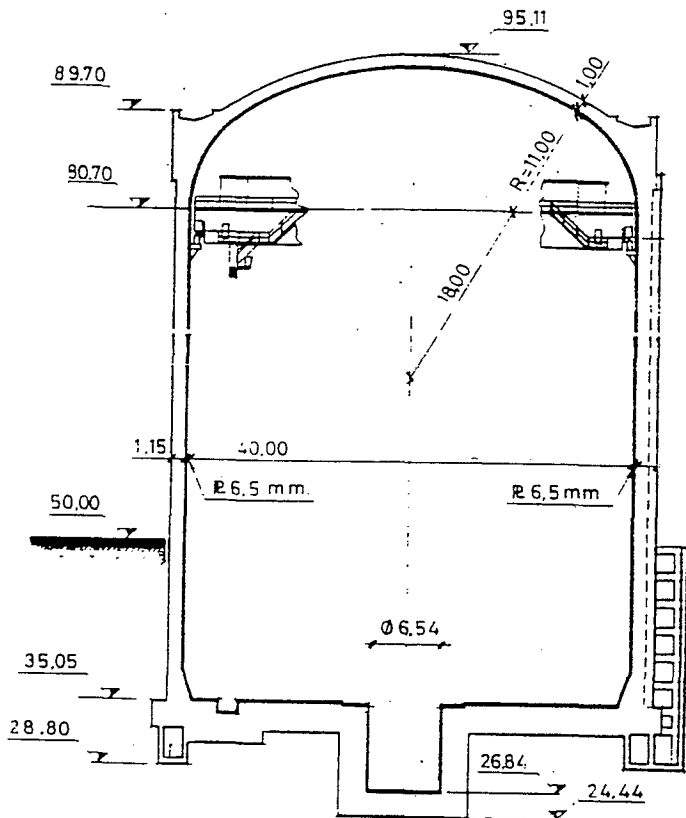


Figure 2. Plan View



Containment Section

The Containment Building wall is a vertical cylinder of 40 m interior diameter and 1,15 m thickness, with three buttresses that serve as anchorage for the horizontal tendons of the post-tensioning system. The dome is spherical torus of 1,00 m thickness with a ring girder at its spring line at the top of the wall. This ring girder serves as anchorage for the dome and the vertical tendons. The base of the building is a reinforced concrete mat without prestress of 2,75 m thickness, with a cavity at the center to house the lower part of the reactor. The total height from the top of the basemat to the dome it is 60 m. The interior volume of the Containment is about 60.000 m³.

DESCRIPTION OF THE POST-TENSIONING SYSTEM

The post-tensioning system of the Containment Building of ASCO N.P.P. is of non-adherent tendons (the sheathings are filled with grease) of 37 T 15 anchorage type by Freyssinet. The system is formed by three families of tendons: Horizontal, Vertical and the Dome. There are 132 Horizontal tendons, each of which covers $\frac{2}{3}$ of the perimeter. They provide a minimum average compression in the concrete wall of 930 Ton/m² in the most critical section for the life time of the plant. There are 122 vertical tendons extending from a tendon gallery located under the basemat to the ring girder located at the spring line of the dome. The minimum compression that they should provide is 470 Ton/m² of the wall. There are a total of 84 Dome tendons, distributed in 3 groups each oriented at 120° with respect to the others. In each group, there are 28 parallel tendons. They provide should a minimum compression in the concrete of 460 Ton/m² at the most critical section of the dome. In Fig. 3 shows the disposition of the tendons.

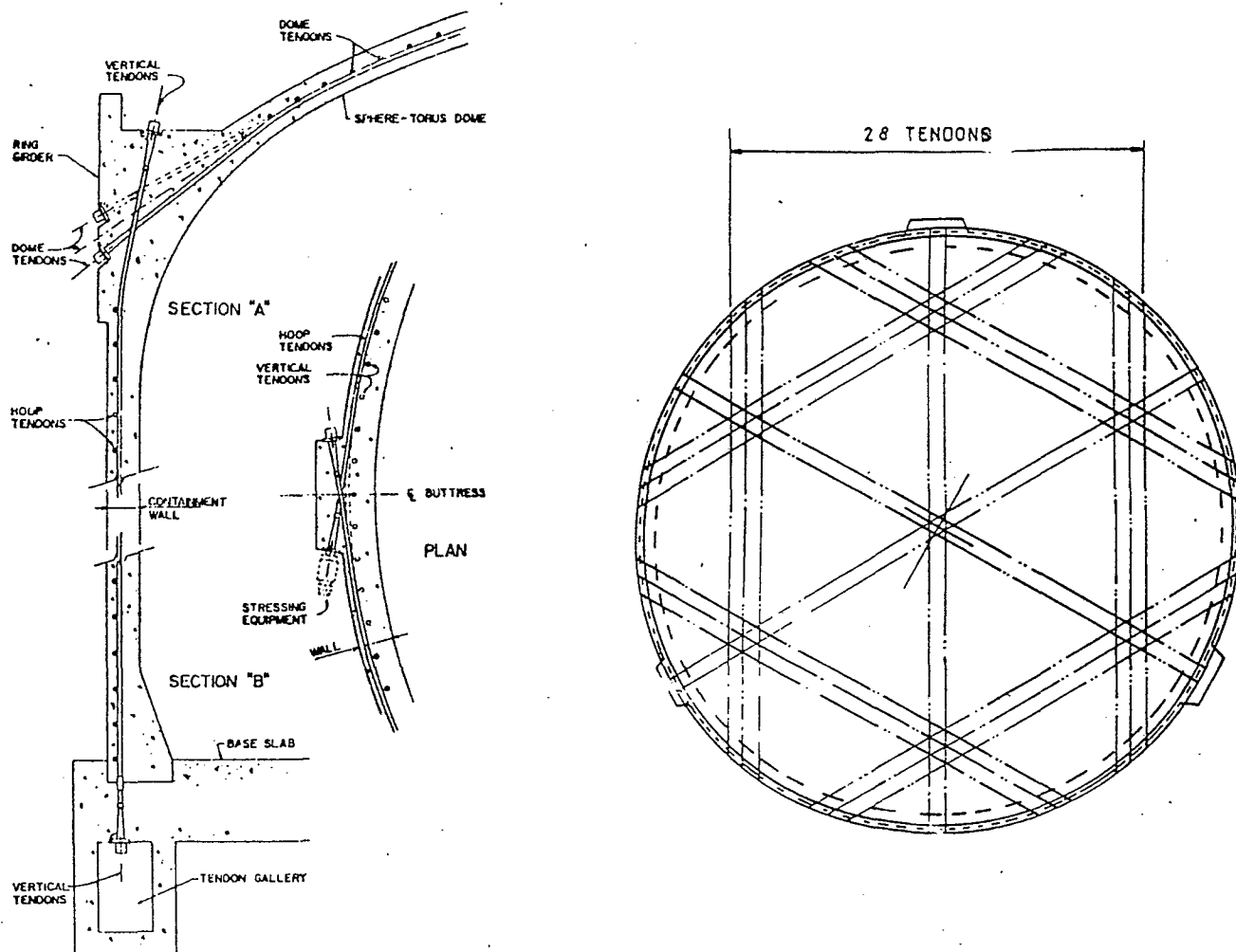


Figure 3. Disposition of the tendons

As shown in Figure 4, each tendon is composed of a sheathing, a trumpet and a bearing plate, embedded in the concrete during the construction, and of a tendon of 37 strands with their corresponding wedges anchoring to the anchor block, as the removable part installed later on. The tendon, after tensioned, is left with a minimum of 80 cm of extension from the anchor block, to be able to perform the lift-off operations afterwards. A cap filled with grease covers this extending part of the tendon, to protect it.

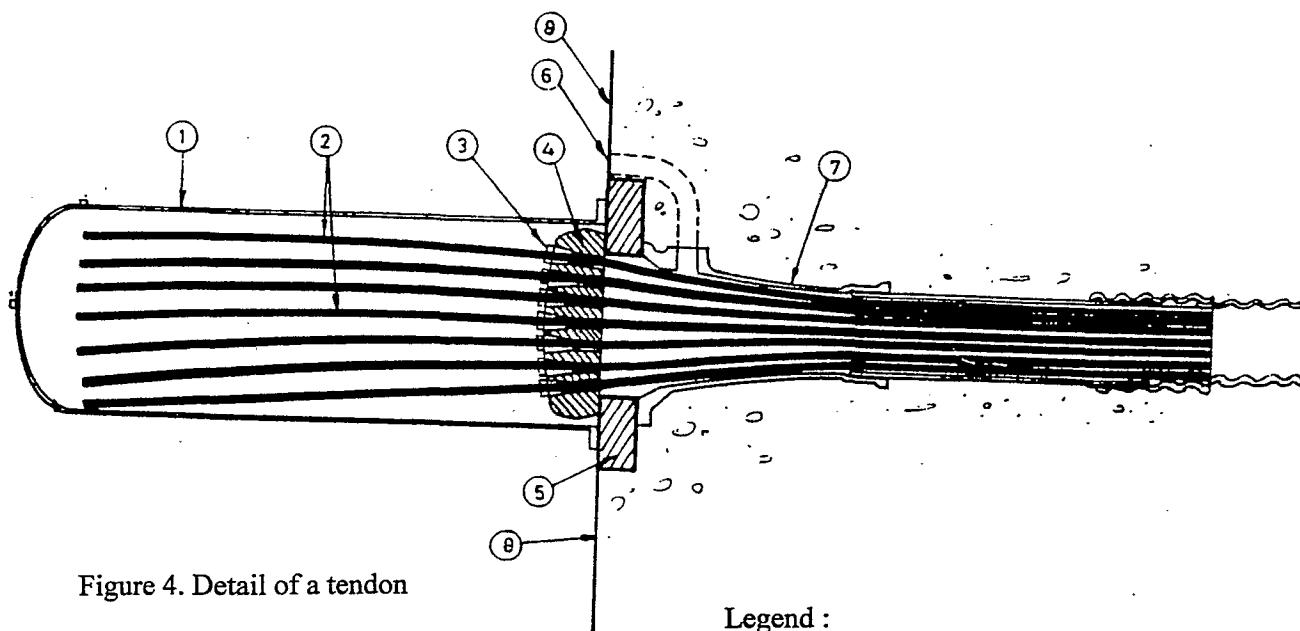


Figure 4. Detail of a tendon

Legend :

- 1.- Grease cap
- 2.- External tendon
- 3.- Wedges
- 4.- Anchor block
- 5.- Bearing plate
- 6.- Filler fitting
- 7.- Trumpet
- 8.- Concrete surface

The cable has a guaranteed ultimate tensile (G.U.T.) strength of 25.400 Kg/mm² and it is made up of 7 wires; its elasticity module is of 19.500 Kg/mm². The sheathing is injected with a special grease to allow the movement of the tendon when it is necessary (for a lift-off measurement or for the extraction of a strand, or for retensioning) and also for the protection of the tendon system during the life time of the plant.

The sheathing of the tendons is performed by placing one by one the 37 strands, after which the tendon is tensioned to the 80% of its G.U.T. This tensioning originally was made without the use of the new technique of "initial equal tensioning", nor the "hydraulic wedge gripping". This difference in the technique should be noted, since the original technique produces a state of asymmetric tension that causes a slight inclination and torsion in the measuring jack during the lift-off, as will be seen further ahead.

SURVEILLANCE OF THE POST-TENSIONING SYSTEM

The U.S. Regulatory Guide 1.35, basis of the design of the post-tensioning system, requires periodic surveillance of the system to verify that the conditions of the design are maintained during the life of the plant. These campaigns of surveillance are performed three times during the first five years of the plant, and then once every five years afterwards during the remaining life time of the plant.

The main aspects that are evaluated in each one of these surveillances are:

- Selection of a representative sample of the tendon population, in the case of ASCO N.P.P. of 5 horizontal tendons, 4 vertical and 4 dome, to verify that the prestress tension is within the limits foreseen in the design. One tendon of each family (horizontal, vertical and dome) it is always kept the same in all surveillances.
- Overall evaluation of the state of stress of the tendons based on the results obtained and its extrapolation to forecast its future tendency to assure that the stress level is maintained within the limits of the design calculation until the next surveillance.
- Selection of a tendon from each family to detension totally and to extract a strand for a detailed analysis of corrosion and ultimate strength.
- Visual inspection of the anchors and of the surface of the concrete in their vicinity. Analysis of the tendon protection grease.

OBJECTIVE OF THIS WORK

One of the operations of surveillance, measuring the prestress tension that the tendons impart on the structure, is the objective of this work. The classic system employed in the eighties to measure this force is described and it is compared with the computerized system that is in use currently at the ASCO N.P.P. In measurement of the prestress tension, the same KC-1000 jack normally used for tensioning the tendons is used. The force measured is that transmitted by the anchor block to the structure. This is the only place of the tendon accessible from the exterior, without having to use instrumentation embedded in the concrete or bonded to the tendon. The force measured is compared to the value forecasted in the calculation for the evaluation.

MEASUREMENT OF THE PRE-TENSIONING FORCE

The forecast of the anchor force is obtained by a calculation process that incorporates the uncertainties; on the other side, the measurement of the anchor force is a complex operation. The purpose is to determine the magnitude of the force that the tendon transmits to the bearing plate; the tensioning jack is the only device which will make possible the measurement of this force in an anchor block under tension.

The measurement of this force in the case of ASCO N.P.P is done by KC-1000 jack of 1000 ton capacity, acting on the tendon anchor. The extending part of the tendon is inserted in the jack which grips the ends of the strands as shown in the Fig. 5. Afterwards, the tension on the extension of the tendon is increased progressively until the anchor block lifts-off from the bearing plate. The lift-off tension applied by the jack is the force that the tendon imparts on the structure. The problem is to determine the exact moment in which the lift-off of the block takes place.

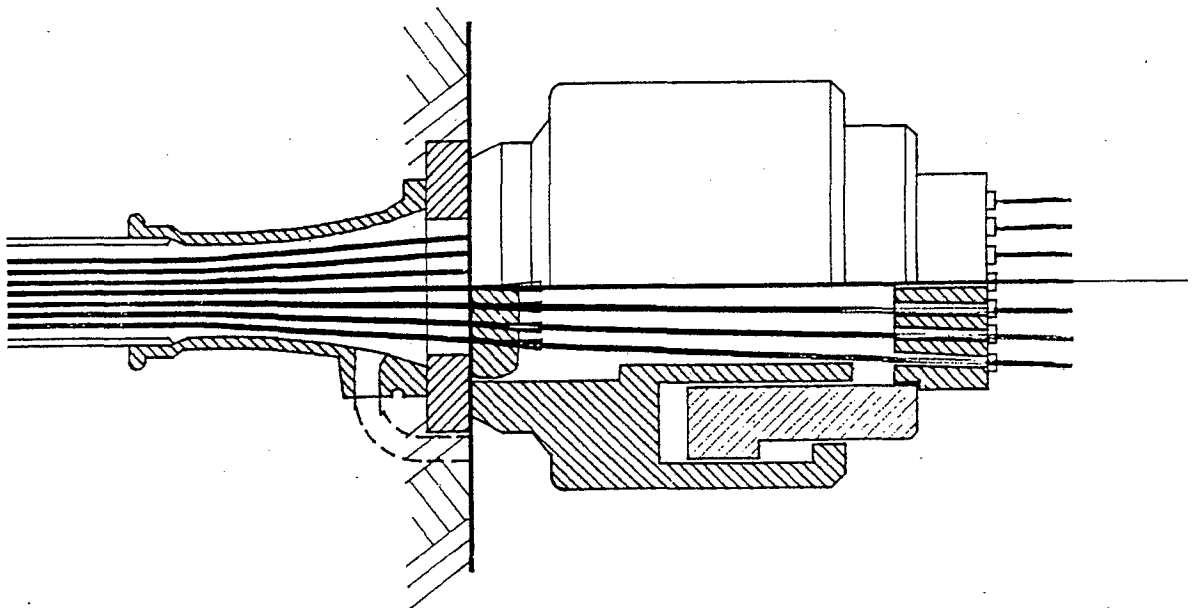


Figure 5. Positioning of the Jack

CLASSIC SYSTEM

In the decade of the 80's, the lift-off of the anchorage block was determined by means of shims of 1, 2 and 3 mm. of thickness. The jack to measure the "lift-off" has 3 symmetrically positioned openings at its end to permit seeing the lift-off. In reality, due to interferences, it was not usually possible to measure with the shims through these openings. The entrance of each one of these shims between the bearing plate and the anchor block indicated the separation in mm. At the same time, the force applied by the jack was visually read off and manually registered. This force extrapolated to zero separation was adopted as the actual lift-off of the anchor. See Fig. 6.

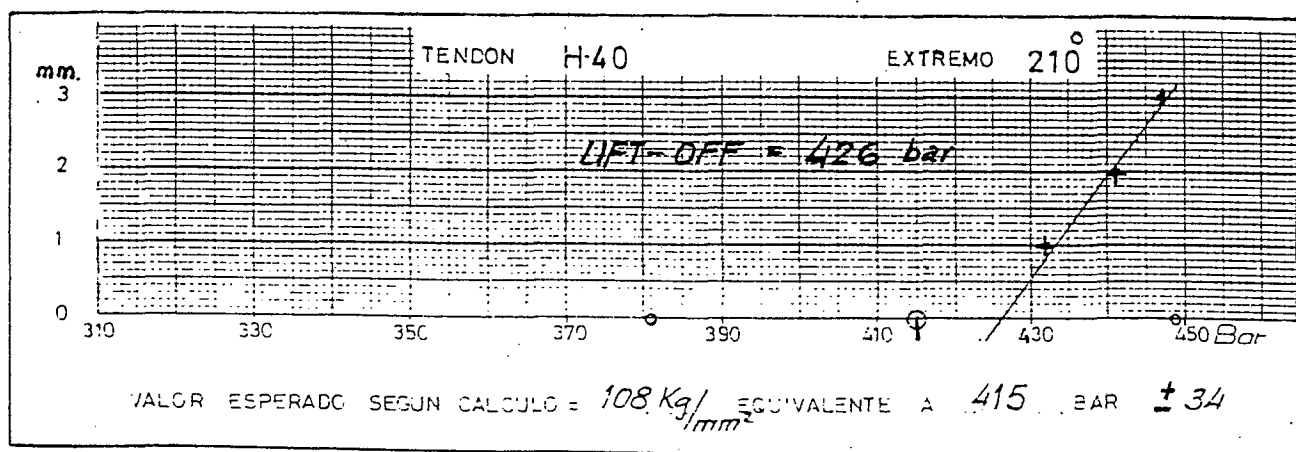


Figure 6. Graph 1, 2, 3.

Establishing the "lift-off" force in this manner is not very precise, since in reality the block doesn't lift off simultaneously in all its perimeter but rather it detaches producing a movement made up of a rotation and a translation with respect to the bearing plate, while it is necessary to measure at least in 3 points to determine a plane. It must be observed that the center of gravity of the forces of the strands doesn't coincide with the geometric center of the anchorage, because of the differences in the forces in each one of the strands (the initial tensions, the lengths and the entrances of wedges of each strand are different, and therefore, the final force in each are also different). This phenomenon makes it difficult to determine the exact moment of the lift-off, and therefore, the force that produces it.

Also, the Classic System introduces important errors of measurement because of the imprecisions of the operator himself who visually establishes the moment at which he should introduce the shim between the block and the support plate and to read off and register the corresponding force.

COMPUTERIZED SYSTEM OF MEASUREMENT

The current system consists mainly of data register on a continuous basis for deformation and pressure, by means of a computerized data acquisition system (D.A.S.).

A GOMETRICS model DPM-9000/500 pressure measuring gauge with a DRESSER model K8-MV-100-700 transducer applied to the hydraulic circuit of the KC-1000 jack , transmits the analogical signal to the D.A.S. Simultaneously, three Penny+Giles model HLP 129 SA1/100 extensometers are attached to three of the 37 strands of the tendon, at equal distance on the perimeter, for measuring strains, and send their analogical signals to the D.A.S. An outline of the installation is shown in the Fig. 7.

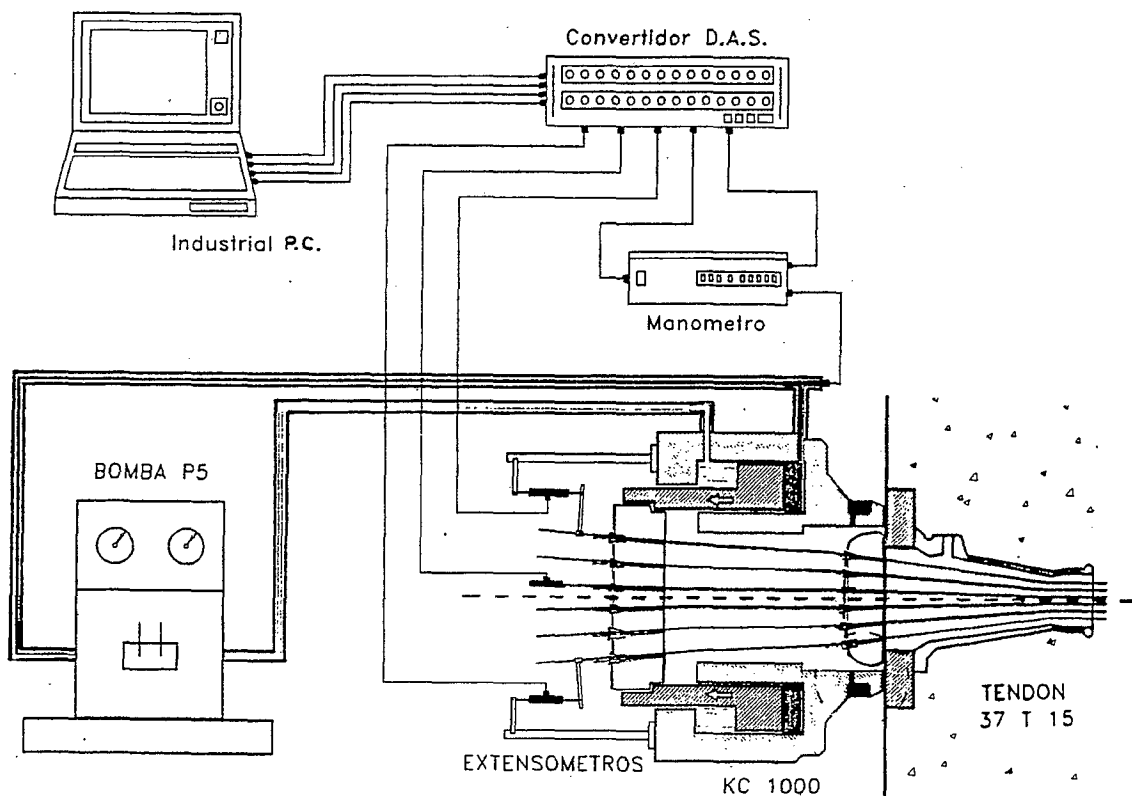


Figure 7. Outline of the Installation of D.A.S.

Both signals, pressure and strain, go from the D.A.S., which feeds the instruments and transforms the signals from analogical to digital, to the PCMCIA installed on the computer. This computer is loaded with the appropriate program to store and to process of approximately 10.000 data produced during each operation of lift-off.

DETERMINATION OF "LIFT-OFF" FORCE

The program makes a selection of the data obtained "before" (Fig. 8) and "after" the lift-off (Fig. 9), and establishes graphically the correlation between the force and the displacement by means of two lineal regressions, one for the lower part of the graph ("before") representing the phase where the lift-off has still not taken place and the other for the upper part ("after") representing the phase with the block now lifted-off.

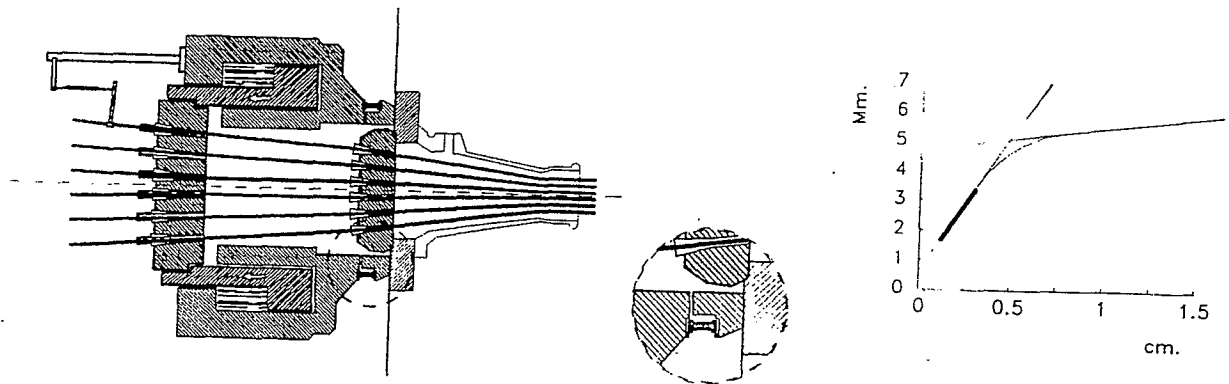


Fig. 8 " before" the lift-off

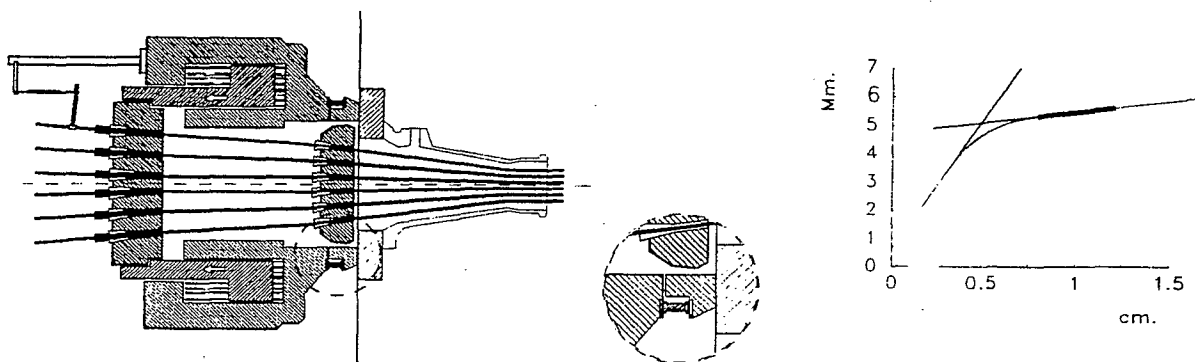


Fig. 9 "after" the lift-off

The transition line between the two straight segments corresponds to the gradual lift-off of the anchor block, a process which is neither instantaneous nor defined with absolute exactitude because of the existing bearing between the anchor block and the bearing plate and also the eccentricity of the resulting prestress force, as mentioned before. The lift-off force is defined as the intersection of the prolongation of these two straight segments, representing the elastic elongation of the strands before and after the lift-off. The calculation of this intersection provides the force corresponding to the lift-off. See Fig. 10.

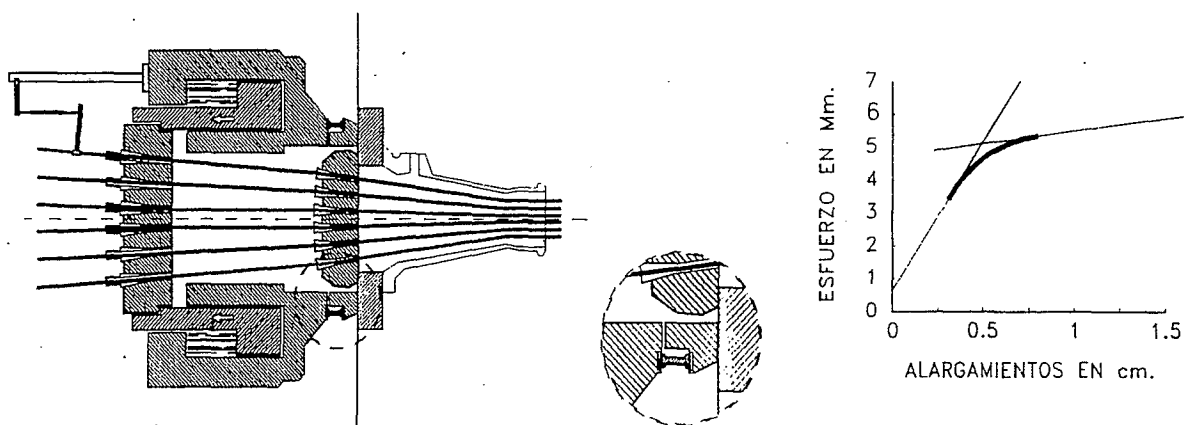


Fig. 10. Transition line

The program finally prints the results with the graphics of both of the straight lines, calculating their slopes, origins terminations, and the coefficient of correlation of the lineal regression made. These data are used to engineering assessment of the reliability of the calculations made. See Fig. 11.

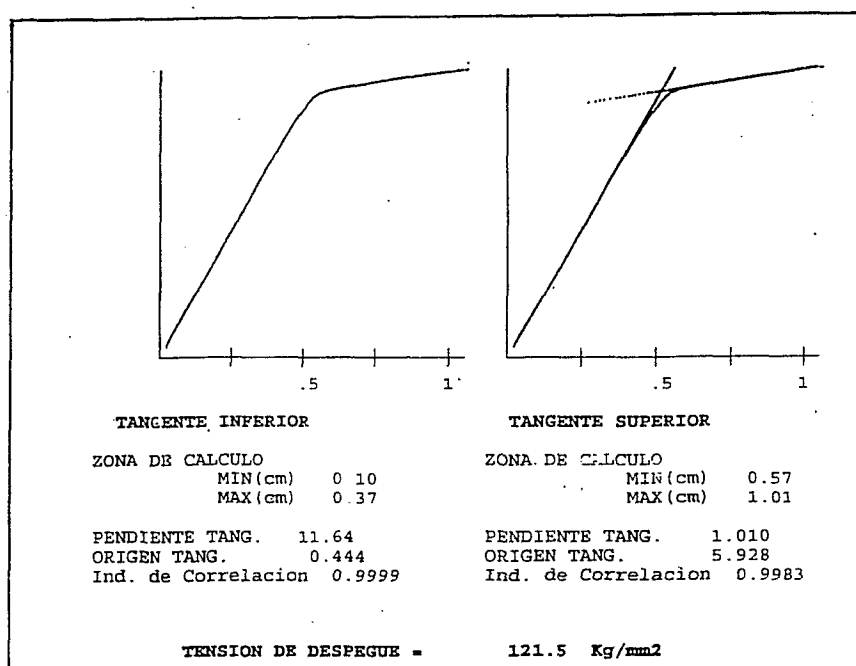


Fig. 11 Results with the graphics

CONCLUSIONS

This new measurement system has been tested and used on all the horizontal tendons of ASCO Unit I N.P.P. during the last surveillance campaign, obtaining satisfactory results with the reliability and the precision of the measurements taken, and permitting minimizing the errors associated with the traditional methods using shims to detect the lift-off and visually reading the corresponding pressure.

Prof. J.Klimov

State Research Institute of Building Construction, Kiev, Ukraine,

Monitoring of Stressed-Strained State and Forces in Reinforcing Cables of Prestressed Containment Shells of Nuclear Power Plants

Abstract

The paper presents a general analysis for the results of the stressed-strained state monitoring of containments and forces in reinforcing cables during 10...15 years period of studies.

The paper also presents data concerning the laws of changes of forces in cables providing for tightenings performed while containments are in service, theoretical assessment and analysis of the effect of different factors on the value of forces drop in cables, the background of the developed technique on prediction of forces drop in cables in time.

The developed technique for assessment of a stressed-strained state according to indications of a control instrumentation (special sensors, installed in the containment body at the erection stage) is set forth. The results of the stressed- strained state monitoring of containments in the form of the laws as to changes of stresses in nonprestressed circular and meridian reinforcement, concrete strains in circular and meridian directions were quoted. The design assessment according to the developed technique on the level of concrete compression of the containment and forces drop in cables while in service was obtained by indications of the control instrumentation.

The results of monitoring made it possible to ascertain a real pattern and laws of change of a stressed-strained state and forces in reinforcing cables of containments and also to use the data obtained for prediction of corresponding processes at a subsequent operation.

Introduction

Nowadays 10 power units of Nuclear Power Plants with water-moderated reactors and with a localising safety system in the form of containments of prestressed reinforced concrete are operated in the Ukraine. Lifetime of these containments is from 2 to 15 years. Serviceability of a containment and its capability to perform corresponding functions for the localization of accidents are estimated on the basis of stressed-strained state monitoring results of a containment body and forces in reinforcing cables of a prestress system carried out and at erection and while in service. Monitoring of the containment body stressed-strained state is performed by means of a special automated system based on indications of transducers (string transducers) installed at erection stage and measuring stresses in prestressed reinforcement and strains of concrete. Monitoring of the forces in reinforcing cables includes measurements of forces in the cables at the stage of control-preventive work. The paper presents a general analysis for the results of monitoring of stressed-strained state of containments and forces in reinforcing cables over a period of 10-15 years.

Principle Structural-and-Technological Conceptions For Containments and Characteristic Properties of Monitoring

A containment of Nuclear Power Plants is a vertical reinforced concrete cylinder of 53.25 m high with an internal diameter 45.0 m, thickness of the wall 1.2 m, closed on top by a sloping spherical dome of 1.1 m thick and close to the ground by a reinforced concrete foundation slab of 2.4 m high (Fig. 1). The containment has a sealing metallic facing 8 mm thick from the internal side. The containment is made of monolithic reinforced concrete with an actual compression strength in the order of 36.0 ... 40.0 MPa. The containment is reinforced with nonprestressed reinforcement 20...40 mm in diameter of class A-III, arranged at exterior and interior surfaces of

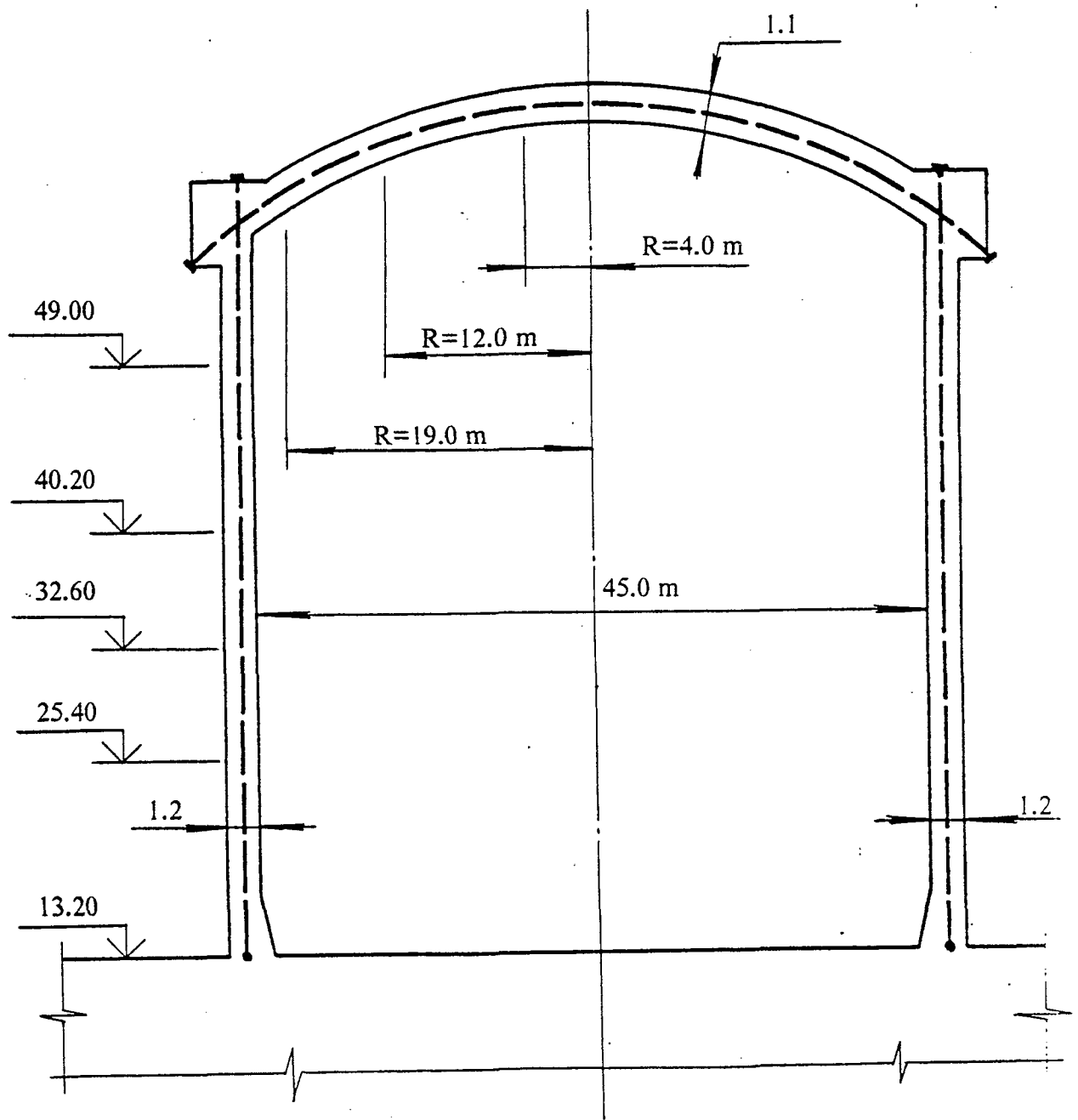


Fig. 1. Structural diagram of the containment and places of arrangement of the control instrumentation

the cylinder and the dome in circular and meridian directions and besides with constructional reinforcement in a radial direction. Percentage of reinforced in middle portions of cylindrical and domed parts of the containment accounted for 0.4...0.8 and near conjugation joints 1.25...1.5.

The containment is built of prestressed reinforced concrete. Compression of the containment is carried out by means of a set of reinforcing cables (Fig. 2) consisting of 450 high-strength stabilized wires 5 mm in diameter with the following main performance data: ultimate strength $\sigma_u = 1800...1820$ MPa; yield strength $\sigma_{0.2} = 1700...1730$ MPa; modules of elasticity $E_s = 2 \cdot 10^5$ MPa; relative elongation at rupture $\delta_{100} = 4.0$ %; stress relaxation in 1000 hours at stress level $\sigma_s = 0.7 \sigma_u$ - 2.5...3.0%. Reinforcing cable diameter in a middle section constitutes 135...140 mm, the length ranges from 95 to 110 m in the domed part of the containment and between 175 and 190 m in the cylindrical part of the containment. There are special means on ends of a cable for tightening and anchorage.

Lay-out of reinforcing cables in the cylindrical part is helical with inclination angle $35^\circ 15'$ to a horizontal surface and the lay-out of reinforcing cables in the domed part is orthogonal in two mutually perpendicular directions (Fig. 3, 4). Cables are set in polyethylene duct tubes, arranged in three rows along cylinder wall thickness and in two rows intersecting at right angle the dome. In all, 96 cables are arranged in the cylindrical part of the containment and - 36 cables are arranged in the domed part of it.

Tightening of reinforcing cables at the stage of erection of the containment is carried out by means of hydraulic jacks step-by-step up to the attainment of the force equal to 9000-10000 kN. A particular feature of adopted constructive solution of containment lies in the fact that in order to support the specified level of the elastic compression of concrete the technological regulations of operation provide for carrying out so-called a control-preventive work during which the real force in reinforcing cables is determined, its additional tightening up to a specified level is carried out, and the exchange of the defective cables also takes place. Force in a cable during testing is determined by working liquid pressure in the hydraulic system of a jack at the moment of an anchor nut breaking off, measured to an accuracy of about 0.5%.

Monitoring of the stressed-strained state of containments in the process of construction and operation is performed by means of a special automatic test set, that is by means of string measuring transducers. A string force transducer is used for the determination of force in nonstressed reinforcement, a string transducer of linear strains is used for the determination of concrete strains, a temperature transducer is used for the determination of temperature of concrete. String transducers are installed by groups in four vertical ranges at five levels along the height of the cylinder and at three levels along the height of the dome (Fig. 5). At this, forces (stresses) in circular, meridional and radial reinforcements are measured by means of force transducers (range of measurement is up to 200 kN in compression and up to 280 kN in tension with an error of $\pm 2\%$) relative strains in meridian and circular directions are measured by means of strain transducers (range of measurement is $0.5 \cdot 10^{-3}...2 \cdot 10^{-3}$ with an error of $\pm 2\%$), the temperature of concrete at surfaces and in mean section of the containment body is measured by means of temperature transducers (range of measurement is $-20...+60$ C° with an error of $\pm 2\%$).

Analysis of General Rules Concerning of Forces in Reinforcing Cables. Fundamental Points of Forces Prediction Technique.

The basic diagram for monitoring of forces and production operations performed as to reinforcing cables in all containments in service may be presented as follows. Tightening of reinforcing cables at containments erection stage was made according to a special technique step-by-step during 2.5...3 months. While the containments were in service, testing of forces and tightening of cables had been carried out with a specified periodicity within the scope of control-preventive after works. The first testing of forces in all cables of the cylinder and the dome was performed within 3...6 years of the tightening. For all this, as a rule, the tightening was carried out

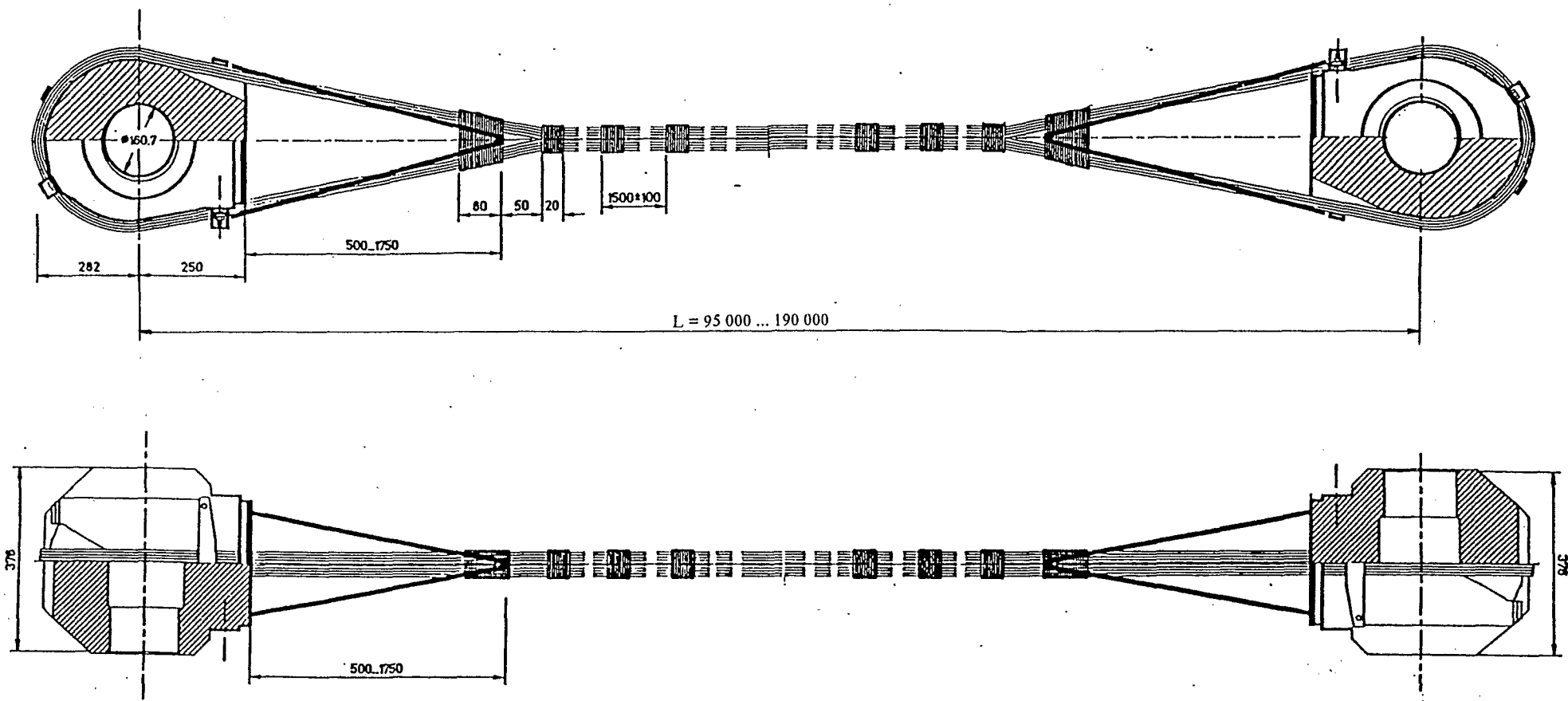


Fig. 2. General view of the reinforcing cable

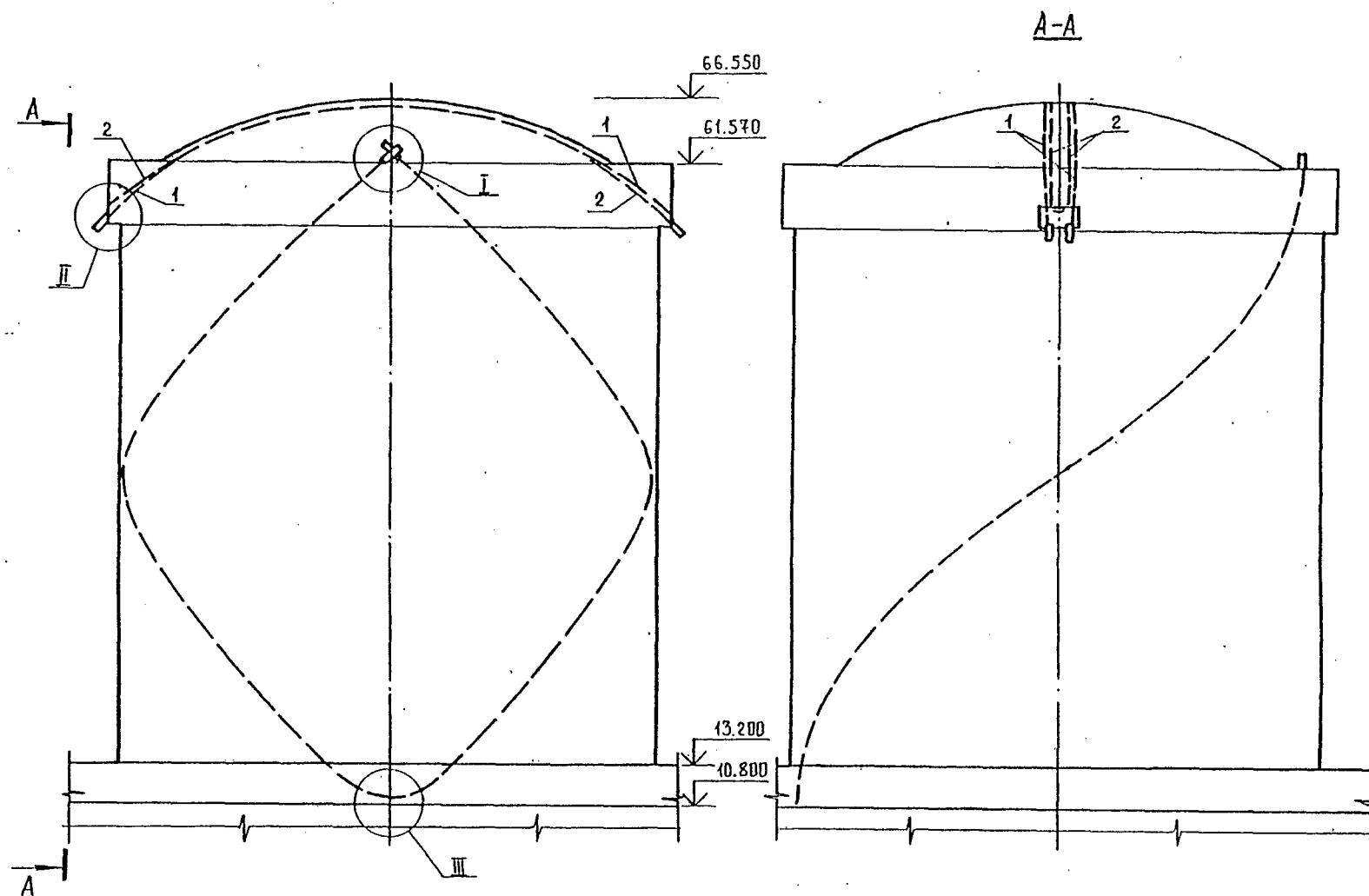


Fig. 3. Diagram of placement of the reinforcing cables in containment
(I-III - anchorage joints, 1, 2 - two cables of dome)

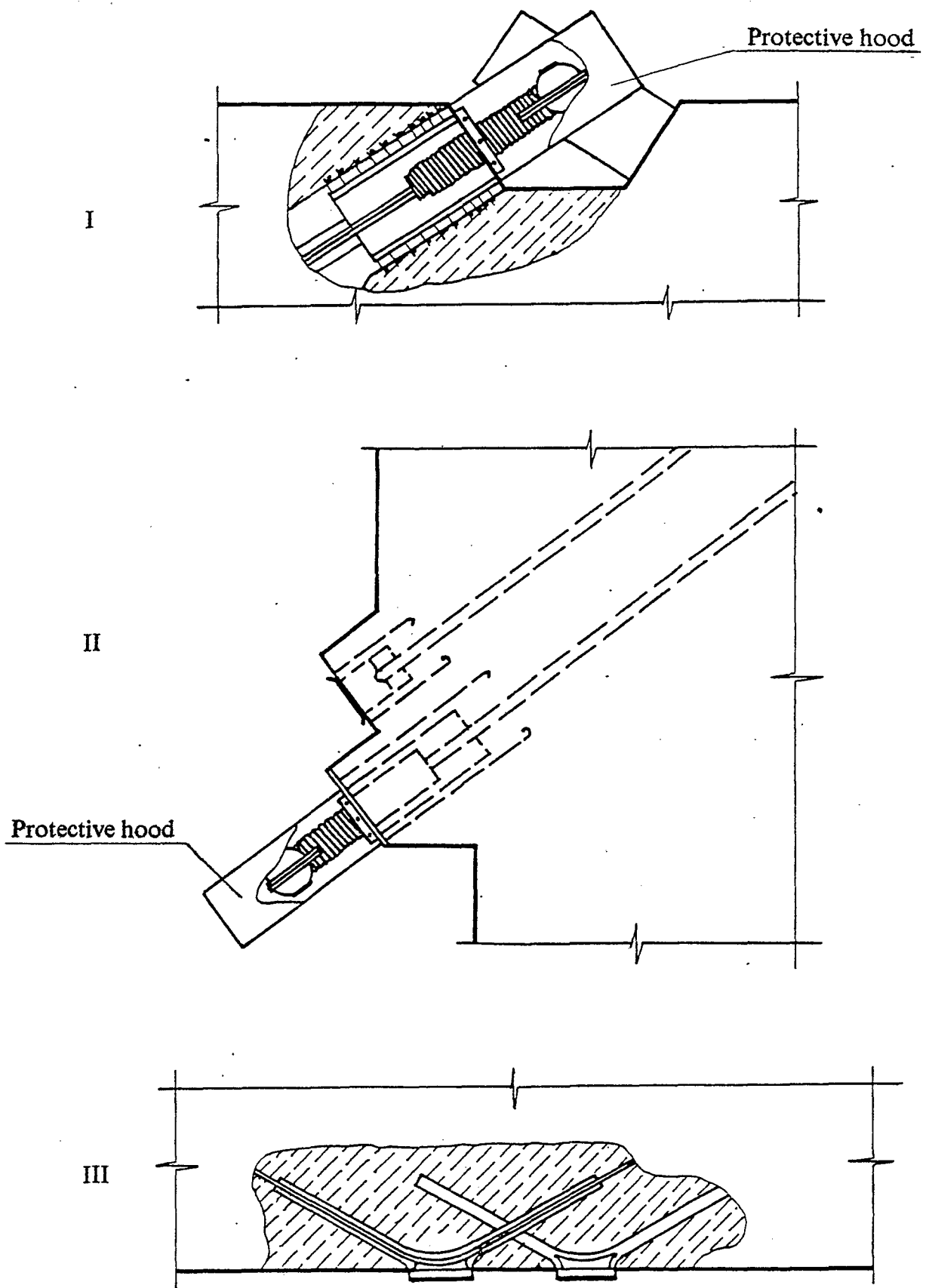


Fig. 4. Anchorage joints

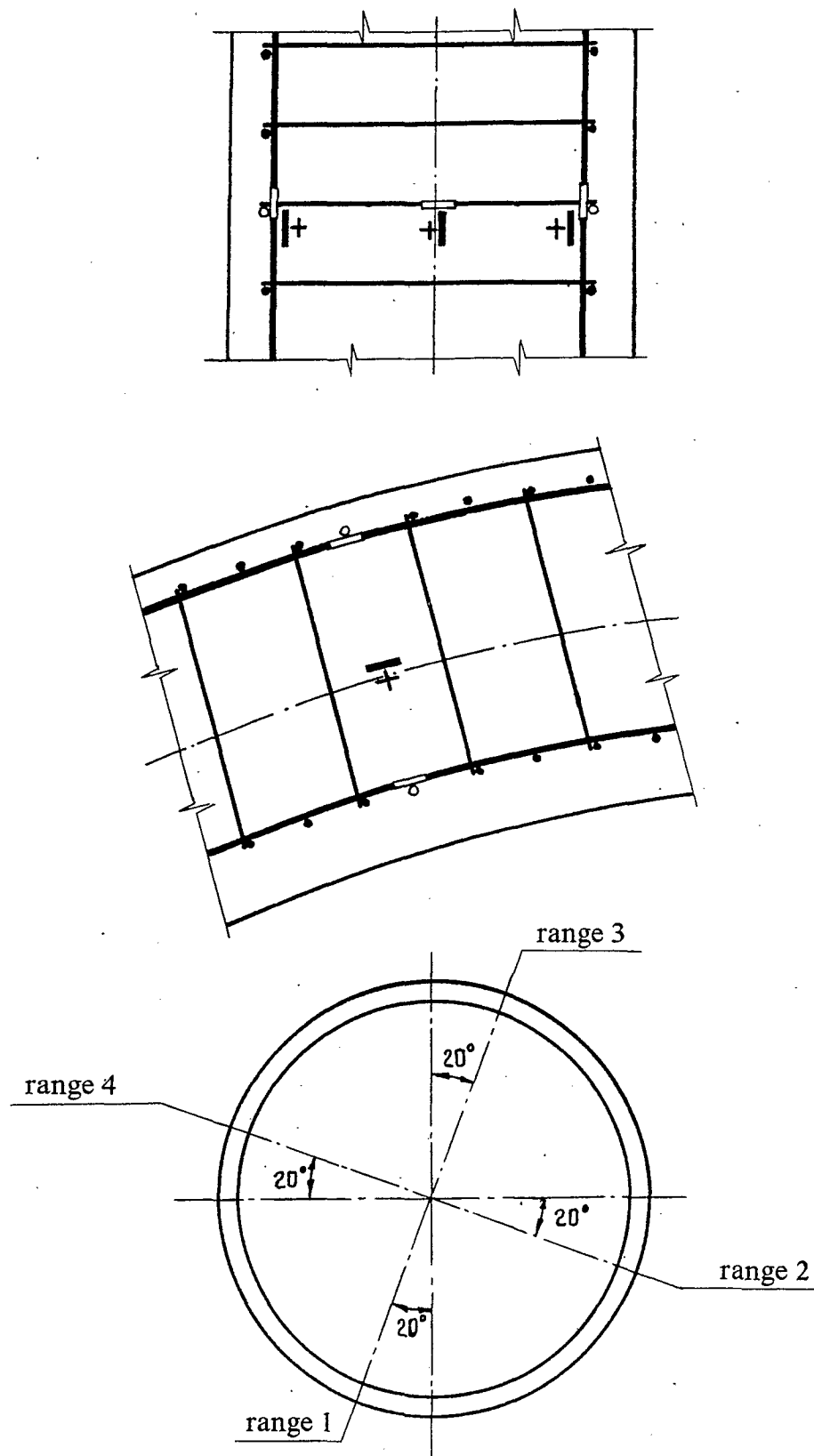


Fig. 5. Diagram of placement of a control instrumentation in the containment body :
 o, □, ≡ - string measuring transducers of circular, meridian and radial
 directions reinforcement
 +, | - string measuring transducers of circular and meridian directions
 on concrete.

either to the given force of all cables or selectively, only of those cables, in which the maximum decrease of force was indicated. The second testing of forces in cables was performed after 3...5 years. For all this, and also while in subsequent service, the random testing of forces and tightening of cables were predominantly practiced. The following testing of forces and tightening of cables were carried out after 1...3 years. Replacement of separate cables was made in a number of cases after testing of forces.

Generalization, processing and the analysis of monitoring results permitted to ascertain general rules concerning changes of forces in reinforcing cables. The results of the corresponding analysis for the containment being in service during more than 12 years are given below as an example permitting to visualize as much as possible the general pattern of changes concerning forces in cables while in use.

The results of the statistical processing data of the first testing (within 4.7 years after tightening) of forces in cables of the cylinder and the dome are given in figures 6 and 7 in the form of: - distribution of relative forces in cables under control (a); - graphical representation of forces drop values in cables (b); - distribution of forces in drop cables (c). Mean values of forces drop, root-mean-square deviation and coefficient of variation for cables of the cylinder and the dome constituted correspondingly: 25.08%, 6.01% and 0.239; 24.11%, 4.68% and 0.195. All cables of the cylinder and dome were tightened up by 8.25...25.3 %. For all this, mean values forces increase in cables of the cylinder and the dome were close to each other and accounted for about 18%.

The following (second) testing of forces in all cables of the cylinder and dome was carried out after 4.3 years. The results of data processing obtained are given in figures 8 and 9. For all this, mean of values forces drop, root-mean-square deviation and coefficient of variation for cables of the cylinder and the dome constituted correspondingly: 6.88%, 5.26% and 0.768; 6.33%, 6.57% and 1.03. As appears from the comparison between figures 6, 7 and 8, 9 and also values of statistical characteristics given above, the observed decrease of forces drop intensity in cables in time was accompanied by the increase of spread in drop values. So, there were cables in the cylinder and dome of the container the forces drop in which was not registered during the second testing, where as such a drop in separate cables constituted 23.3...33.3 %.

So long as later on testing and tightening of cables were carried out selectively, the following analysis was performed with reference to groups of cables. The cables which underwent the same production operations in time (testing and tightening) were united into a group. Three groups of cables in the cylinder and two groups of cables in the dome were singled out in the containment in question.

Experimental dependencies for changes of mean forces in the singled out groups of cables of the cylinder and dome over the whole period of service are given in figures 10 and 11. While in service, group 1 cables of the cylinder (fig. 10a) and the dome (fig. 11a) were tightened up once (during the first testing), subsequently, only testing of forces was performed in cables of these groups. Group 2 cables of the cylinder (fig. 10b) were tightened up twice after the testing. Group 3 cables of the cylinder (fig. 10c) and group 2 cables of the dome (fig. 11b) were tightened up twice after the testing of forces.

As follows from the analysis of fig. 10a and fig. 11a, the forces drop in cables of the cylinder and the dome, tightening up once, come about according to the law, which is close to the linear one. For all this, over 8 years after tightening, mean values of forces drops in cables of cylinder and dome accounted for 8.25 % and 9.76% , that corresponded to the forces drop intensity 1.03 % per year and 1.22 % per year.

It is necessary to take into account in analysis of general concerning changes of forces in cables of other groups, that their tightening was in many respects forced and it was defined as a need for provision of minimum allowable level for compression of the containment. As far as the data analysis, concerning the containment at issue and also other containments in service, showed, the effectiveness of cables tightenings from the point of view of the containment compression decreased with the increase of the number of cables tightenings. So, during the last testing of forces in group 3 cables of the cylinder and group 2 cables of the dome which were tightened up thrice while in service, the mean value of forces drop over the year constituted correspondingly 2.67 %

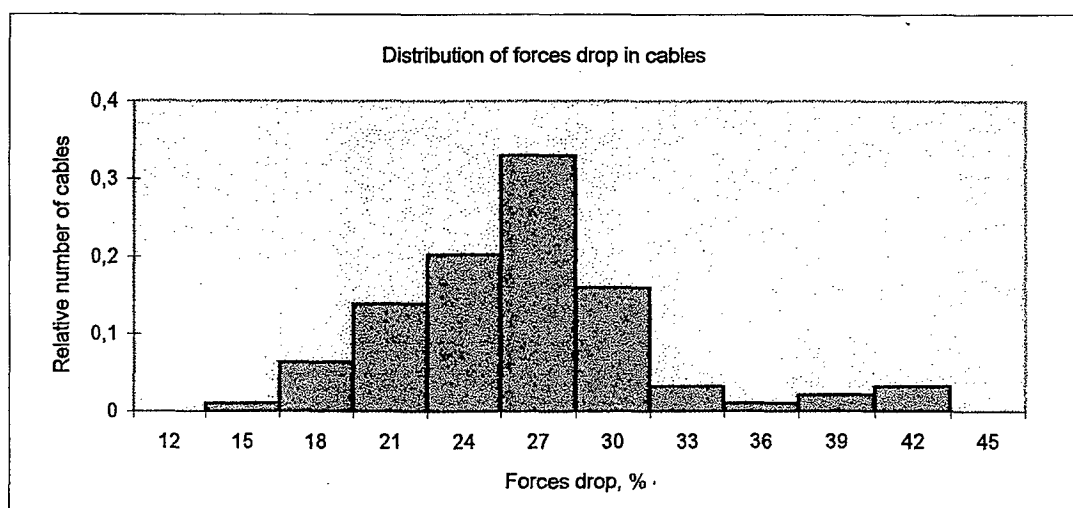
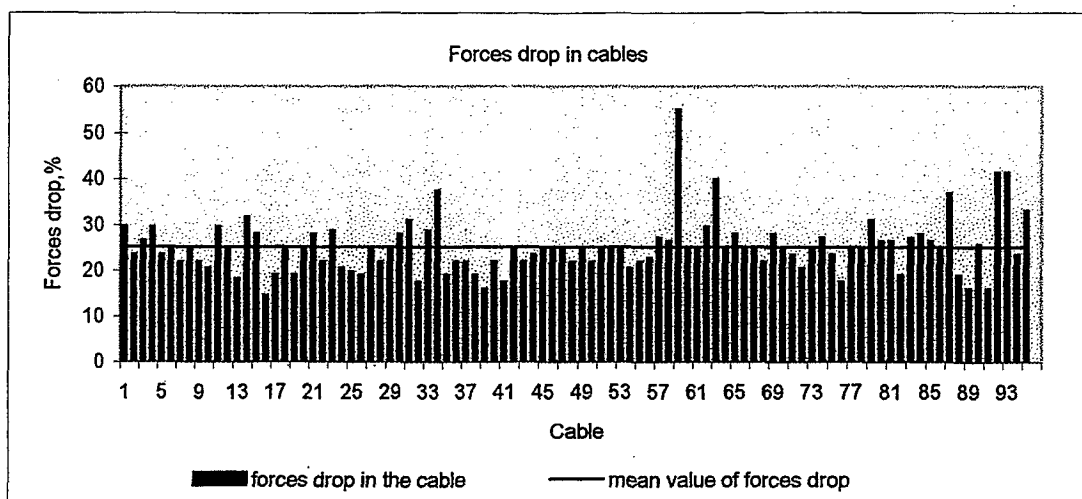
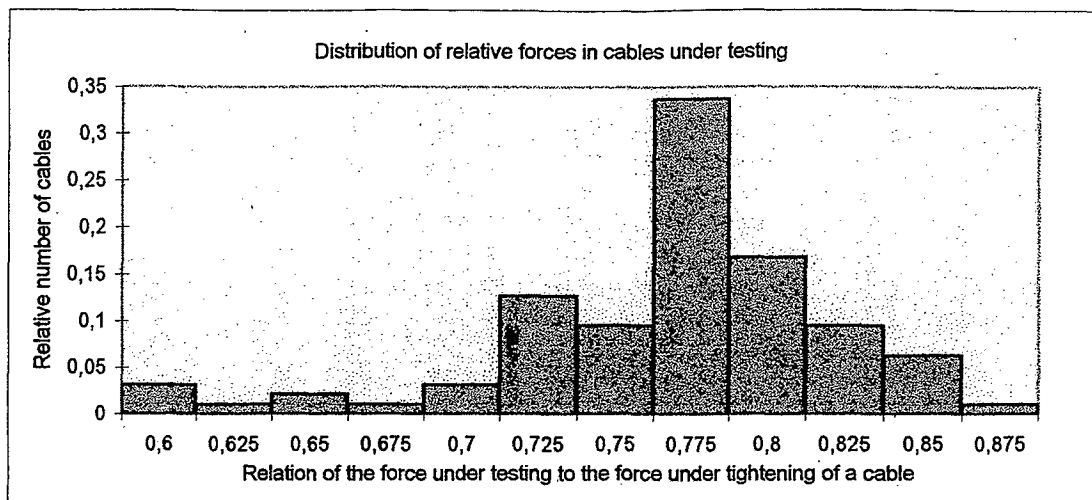


Fig.6. Results of the first testing of forces in reinforcing cables of the cylinder.

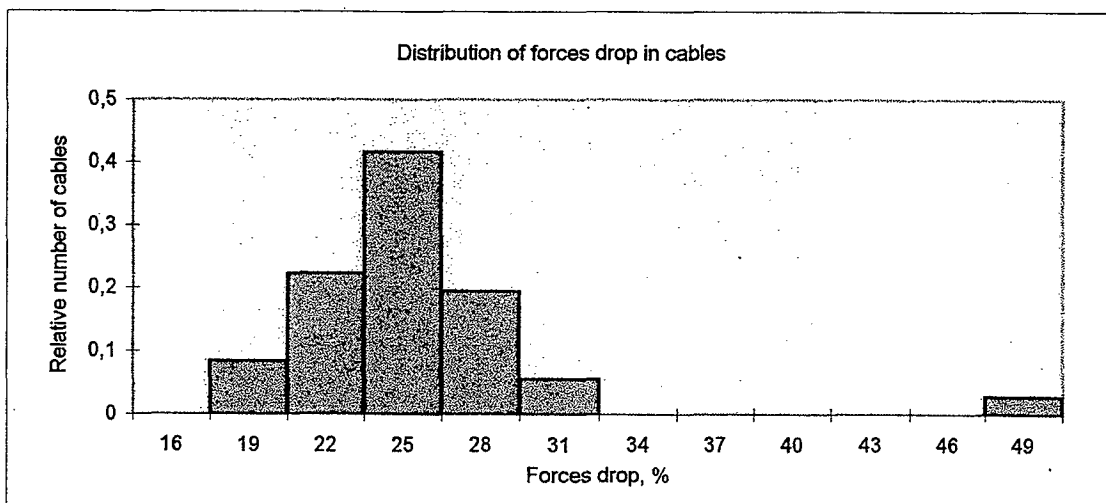
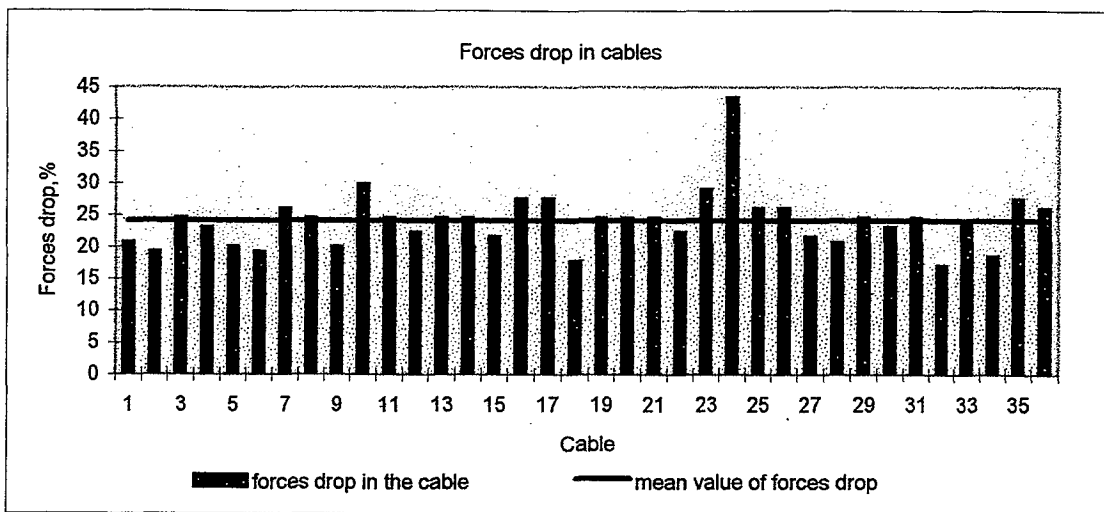
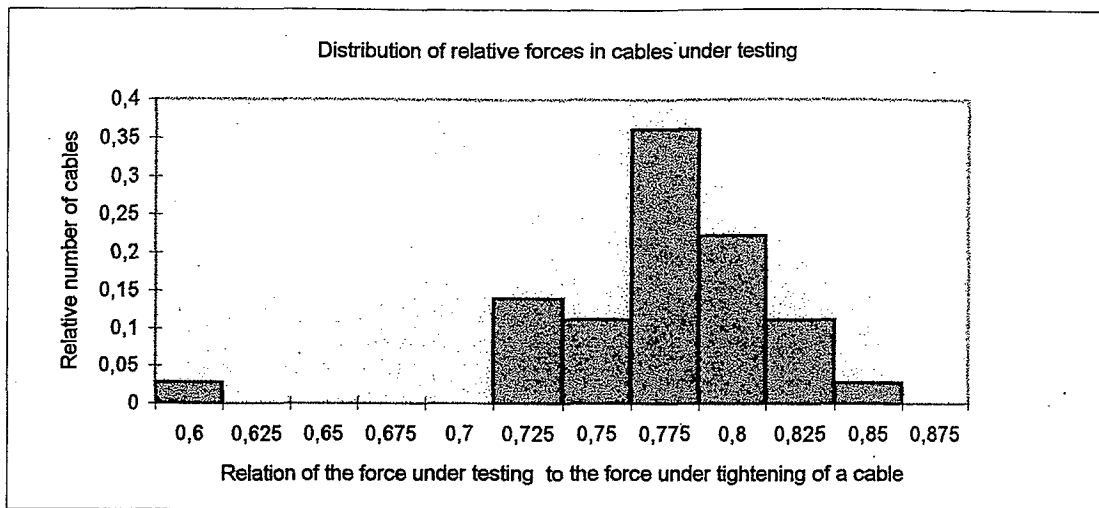


Fig. 7. Results of the first testing of forces in reinforcing cables of the dome.

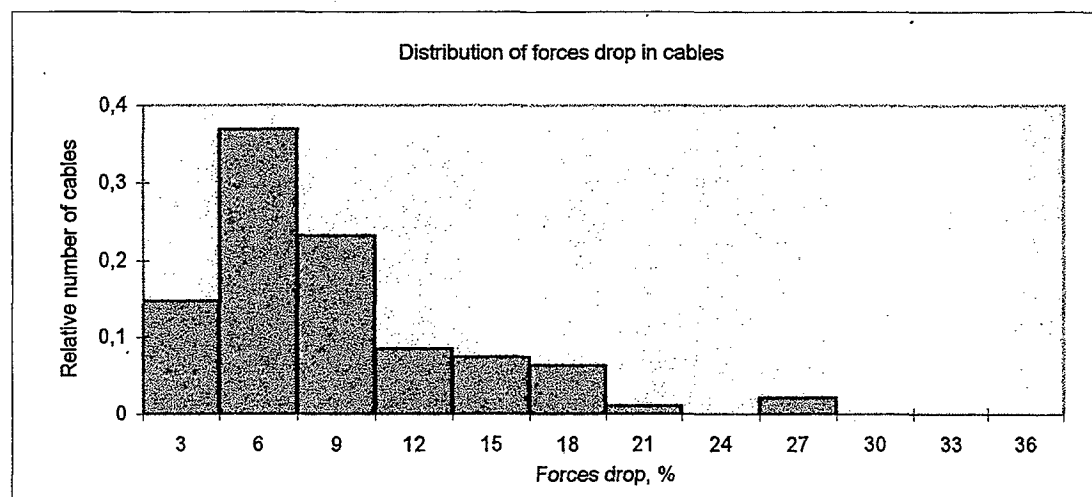
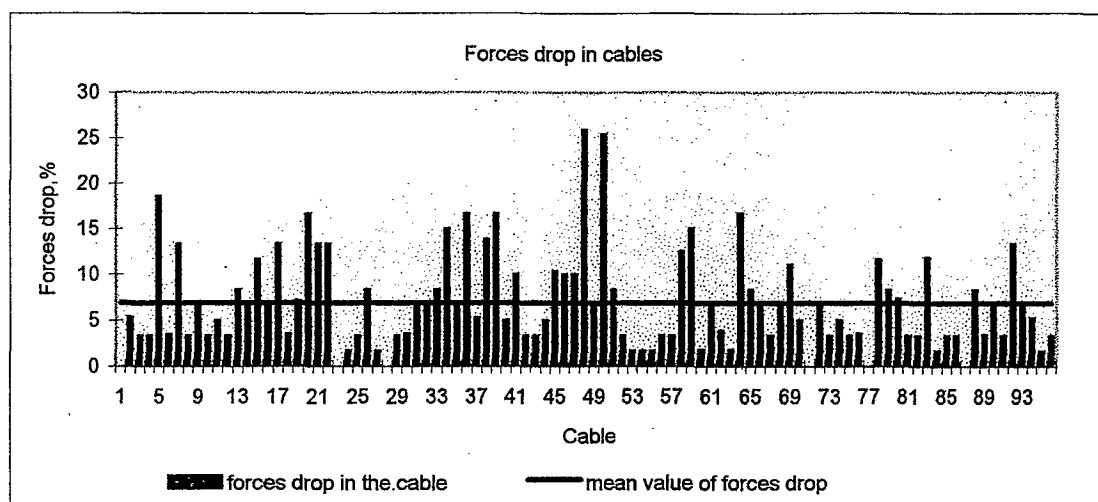
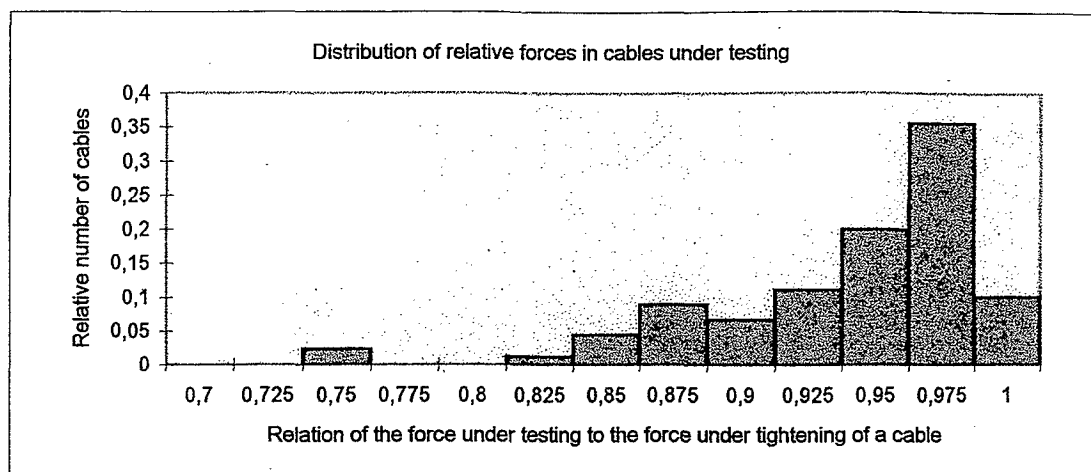


Fig.8. Results of the second testing of forces in reinforcing cables of the cylinder.

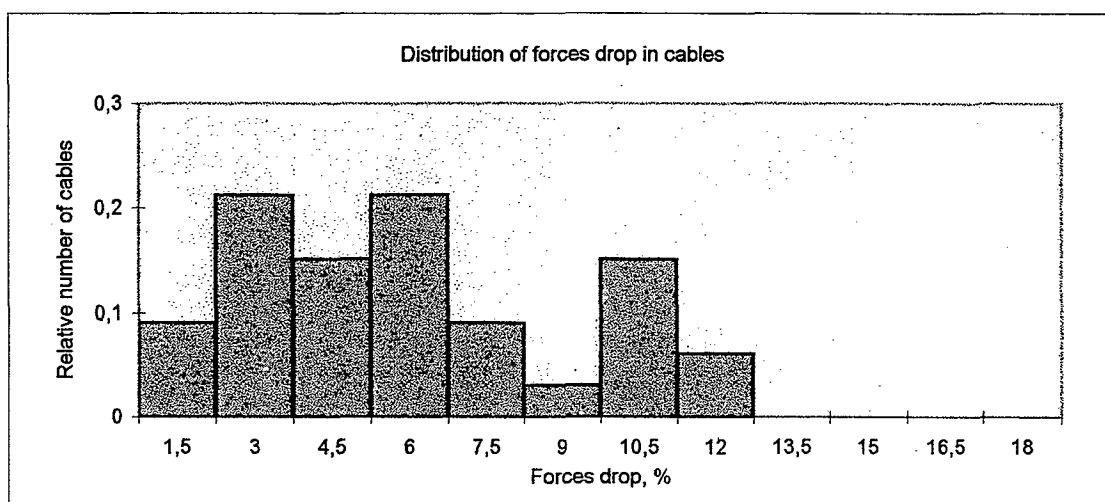
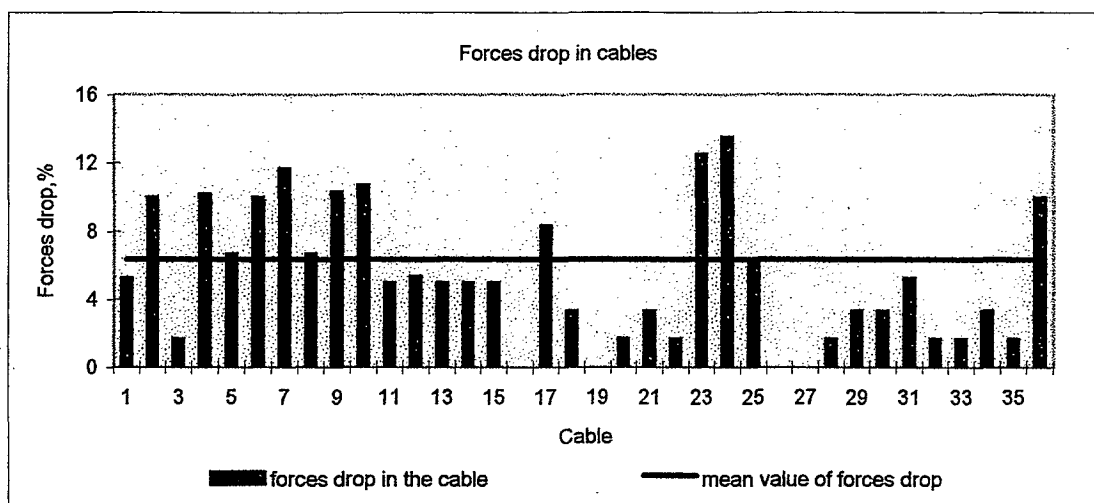
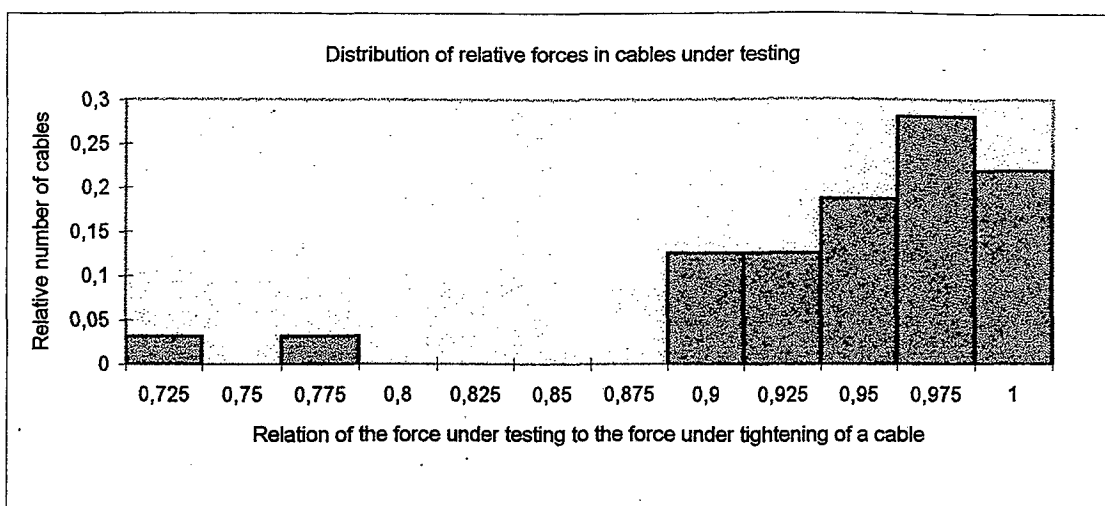
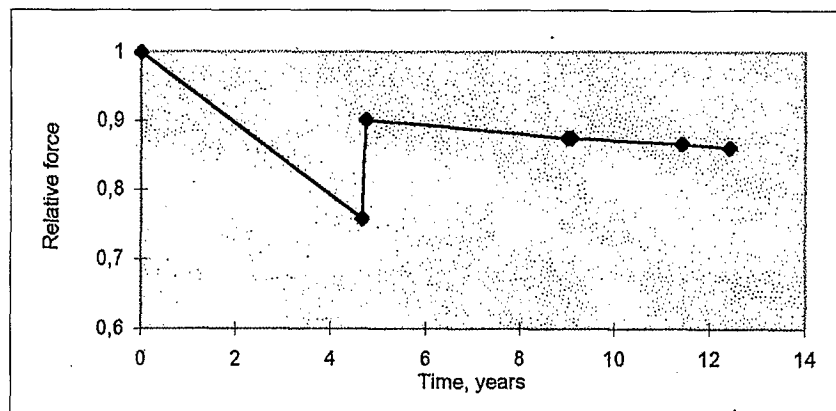
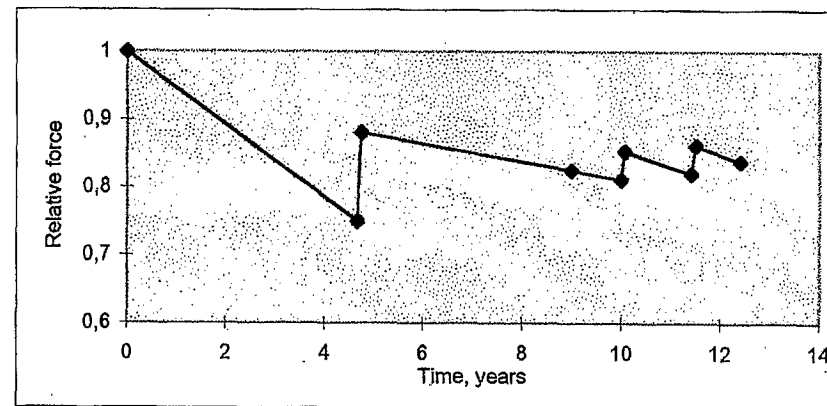


Fig. 9. Results of the second testing of forces in reinforcing cables of the dome.

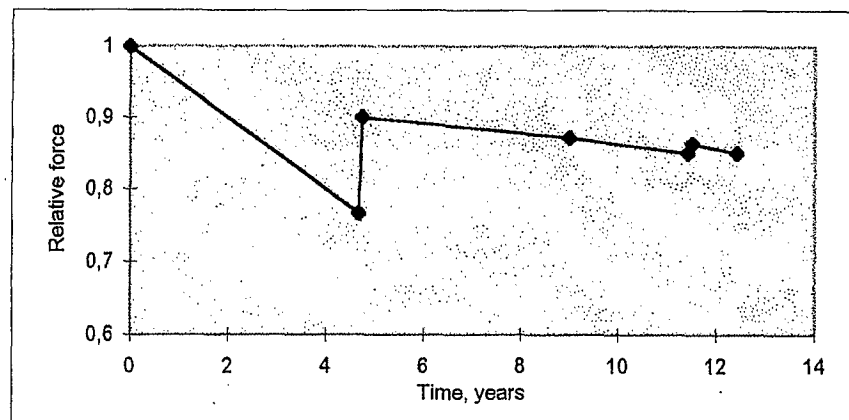


a

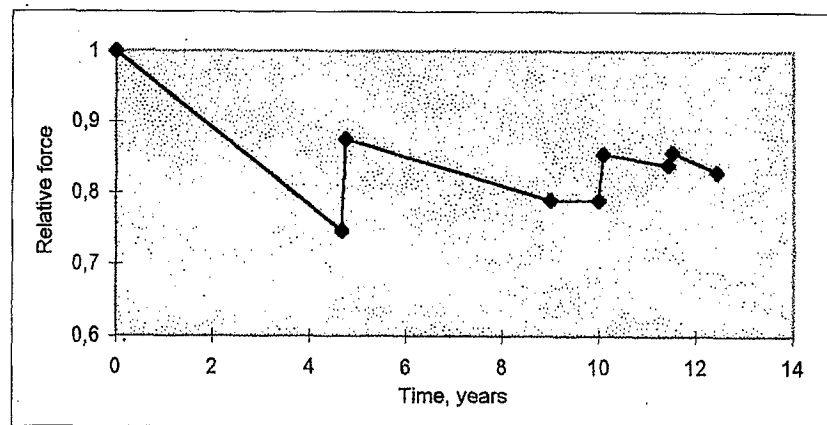


B

Fig.10. Change of mean relative forces in reinforcing cables of groups 1 (a) and 3 (b) of the cylinder.



a



B

Fig.11. Change of mean relative forces in reinforcing cables of groups 1 (a) and 2 (b) of the dome.

and 3.44 %.

The results of the monitoring performed were assumed as a basis for the technique developed to predict forces in cables. The aim of this technique consisted in assessment of a compression level of the containment in reference to the given instant in order to assign the data for conducting of works on forces testing and, if it is necessary, for tightening of cables.

Development of the technique was carried out on the basis of the results of statistic data processing concerning general rules as to changes of forces in cables and calculation estimation of factors having the most pronounced effect on forces drop in cables.

The following factors in calculation estimation were referred to the number of the most significant ones: concrete creep; stress relaxation in wires of a cable; elastic compression of concrete induced by staging of tightening at compression stage or by tightening of cables at the stage of carrying out of control-preventive works. It was assumed to estimate the rest of factors, first of all representing the specific character of the structural concept adopted as to force transfer onto concrete (crushing of concrete under support slabs, shear reinforcing meshes in the zone of anchorage and cable bend), the effect of which is difficult to take into account by calculation, integrally. The effect of these factors in quantitative aspect was estimated according to difference between the real value of forces drop and the total design value of forces drop due to concrete creep, stress relaxation in wires of a cable and staging of cables tightening.

The time interval from tightening of a cable up to the moment of carrying out of the first forces testing was considered in order to estimate the greatest in quantitative aspect effect of all factors enumerated and also to receive the real pattern of forces change in cables. For all this, a mean value of forces drop in a cable by the moment of termination of the containment compression on the whole (2-3 month after tightening) and a corresponding forces drop by the first testing (after 4.7 years in the containment in question) was estimated by way of calculation.

The basic design diagram of forces changes in cables from the moment of tightening to the first testing of forces is given in figure 12, where the corresponding forces are designated as follows: N_{st} - real value of a force in a cable after tightening at the stage of compression; N_p - design value of a force drop in a cable induced by an elastic compression of concrete (staging of tightening); N_{rel} - design value of a force drop in a cable induced by stress relaxation in wires of a cable; $N_{cr,1}$ и $N_{cr,t}$ - correspondingly, design value of a force drop in a cable due to concrete creep by the moment of the containment compression in general and by the moment of the first testing; N_{loc} - design value of a force drop in a cable from the moment termination of the containment compression up to the first testing, induced by integrally estimated factors; N_{con} - real force in a cable during the first testing.

Force loses in a cable of the cylinder due to elastic compression of concrete by the moment of termination of the containment compression were determined on the basis of a design diagram, given in figure 13. For all this, the most unfavorable case was considered, when tightening of five side-by-side situated cables had been carried out following tightening of the cable at issue.

Force loses in a cable due to elastic compression were determined proceeding from the compatibility of concrete deformations and deformations of the cable at issue along the axis of the latter by a formula:

$$N_p = \varepsilon_s E_s A_c = \varepsilon_b E_s A_c = \frac{\sigma_b}{E_b} E_s A_c = \sigma_b \alpha A_c, \quad (1)$$

where

σ_b - stresses in concrete along the axis of the cable in a question at tightening of five side-by-side situated cables, calculated on the basis of the design diagram in figure 13;

$\alpha = E_s / E_b$ - relationship of elastic modulus of wires of a cable to the initial elastic modulus of concrete;

A_c - cross-section area of a cable.

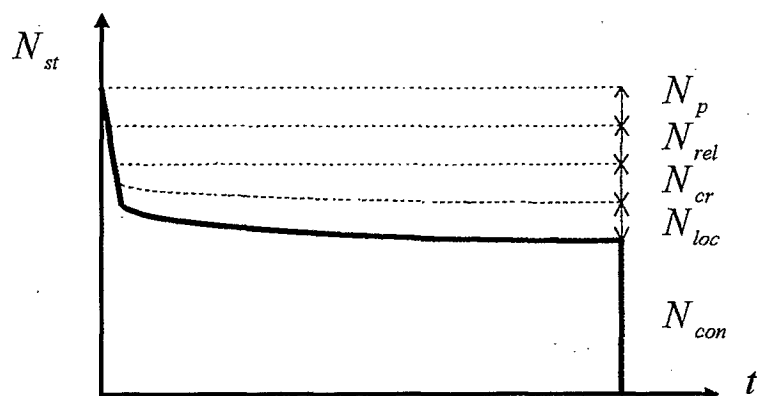


Fig. 12. The basic design diagram of forces changes in cables from the moment of tightening to the first testing of forces

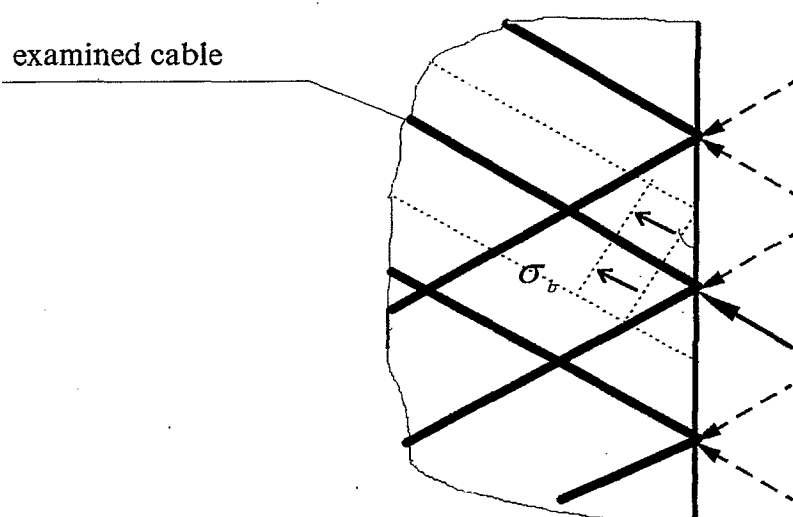


Fig.13. For the determination of forces drops in reinforcing cables because of elastic compression of concrete.

Corresponding dependence for cables of the dome too was obtained in much the same way, supposing that after the cable in question, tightening of two side-by-side situated cables was performed.

Force loses value in a cable from stress relaxation in wires was adopted on the basis of

analysis of the results of corresponding testings of wire. Force loses value in a cable from the relaxation was assumed as equal to 3 %, by the moment of termination of the containment compression. Subsequent losses of stresses from the relaxation in view of their small value were not taken into account at calculations.

Force loses in a cable due to concrete creep were determined on the basis of a design conception alternative of the creep theory - up-dated theory of ageing, proceeding from compatibility of deformations of concrete and the cable along the axis of the latter.

$$N_{cr} = \varepsilon_s E_s A_c = \varepsilon_{b,cr} E_s A_c = \varepsilon_b \varphi_t \zeta E_s A_c = \frac{\sigma_b}{E_b} \varphi_t \zeta E_s A_c = \sigma_b \varphi_t \zeta \alpha A_c, \quad (2)$$

where σ_b - stress in concrete along a axis of the cable during compression of the containment, calculated at corresponding values of forces, geometric dimensions and spacings between cables in the cylinder and the dome;

φ_t - limiting (maximum at $t \rightarrow \infty$) value of creep characteristic, calculated by a formula:

$$\varphi_t = C \cdot E_b \xi_1 \xi_2 \xi_3, \quad (3)$$

here C - concrete creep rate;

E_b - modulus of concrete elasticity ;

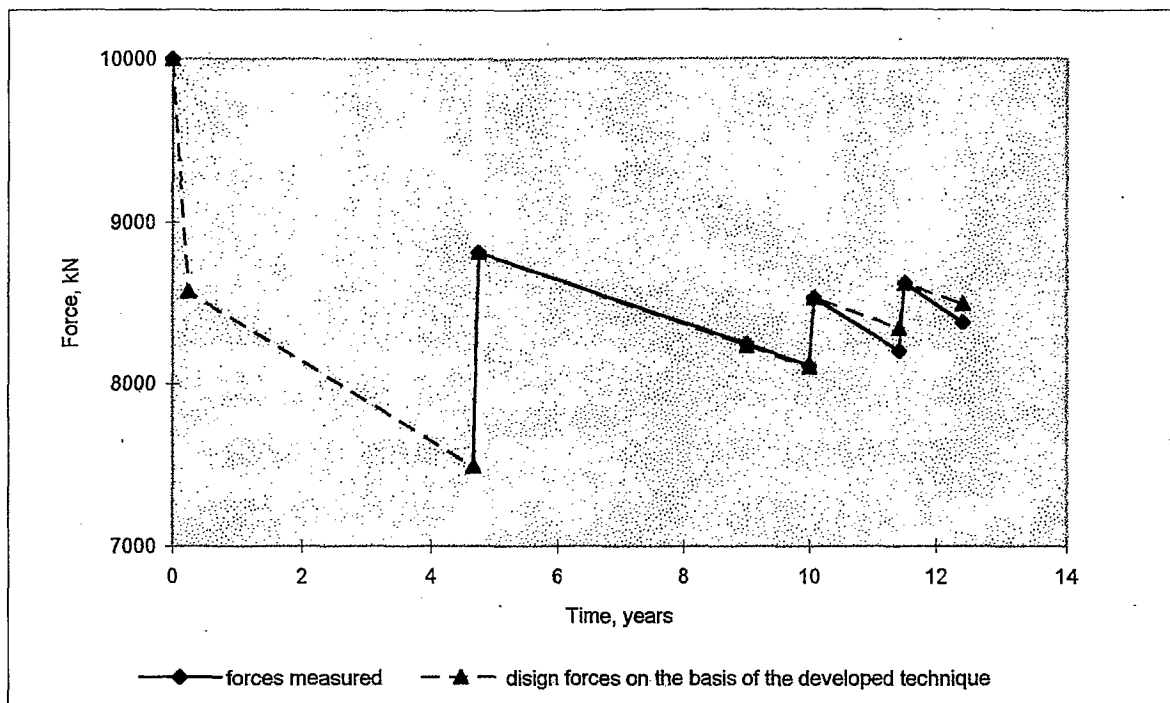
ξ_1, ξ_2, ξ_3 , - coefficients, correspondingly taking account of age of concrete at the moment of compression, open, unit surface of concrete and relative humidity of environment;

ζ - coefficients, taking account of losses from creep by the given instant after tightening of a cable, adopted as equal to 0.64 by the moment of the containment compression in general and 0.96 by the moment of the first testing of a force (for the containment at issue - 4.5 years).

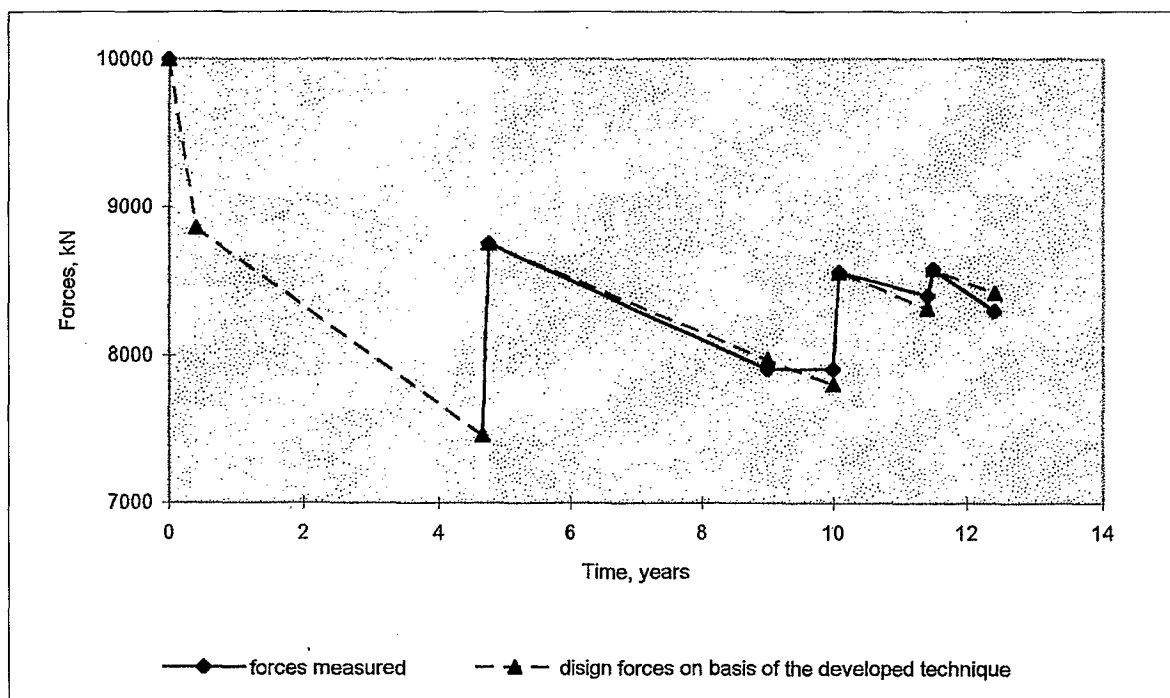
As a result of calculations performed, it was ascertained, that by the moment of termination of the containment compression the total design forces drop in cables of cylinder constituted 14.4%, of which 5.17% were induced by the staging of tightening 3% by stresses relaxation in wires and 6.23% by concrete creep. The total design forces drop in cables of the dome by the moment of termination of compression accounted for 11.48%, of which 3.6% were induced by the staging of tightening, 3% by stresses relaxation in wires and 4.88 % by concrete creep. The total design forces drop by the moment of the first testing constituted in cables of the cylinder 17.52% and in cables of the dome 13.93%, that was induced by the increase of forces losses from concrete creep up to 9.35% and 73.5% correspondingly.

As appears from a fore-cited the real forces loss in cables of the cylinder and the dome of the containment in question by the first testing accounted for 25.08% and 24.11% . Thus, the value of force losses attributed to integrally estimated factors N_{loc} , over 4.7 years constituted in the cylinder 8.56 % and in the dome - 10.18 %. It corresponded to the intensity of forces drops by 1.53% per year in cables of the cylinder and by 2.13 % per year in cables of the dome.

The analysis of the numerical values obtained as to forces drop, induced by the effect of the factors singled out, showed, that neither concrete creep nor stress relaxation in wires may be the cause of such a considerable forces drop in cables after the first tightening, registered during subsequent testings (fig. 10, 11). It is obvious, that in the given case, the forces drop is the consequence of the factors effect, reflecting the specific character of the structural concept for force transfer onto concrete and estimated integrally by us. In general this assumption is confirmed by the satisfactory agreement between design and experimental laws of forces change in group 3 cables of the cylinder and group 2 cables of the dome, given in figure 14. Design dependencies of forces change in cables after the first and subsequent tightenings are plotted with the assumption of the fact, that the intensity of forces drop, caused by integrally estimated factors, remains constant and is equal to the values calculated above (1.53% per year in cables of the cylinder and



a



B

Fig.14. Change of mean forces in cables of group 3 of the cylinder (a) and group 2 (b) of the dome while in service according to the results of measurements and calculation on the basis of the developed technique.

2.13% per year in cables of the dome) for the interval of time from the termination of the containment compression to the first testing of forces. As is obvious from figure 14, there are certain discrepancies after the second and the third tightenings of cables. For all this, the increase of the forces drop intensity may be explained by an additional crushing of concrete in the zone of anchorage and bend of cables at the increase of forces.

A statistical approach for development of the technique on prediction of forces in cables was applied in conditions established, when it is rather difficult to explain the laws of forces change in cables by calculation, while the containment is in service, and the accuracy of forces measurement in testing is comparable with the very drop value. The following points of this approach were adopted as salient ones:

- prediction of forces is formed for each cable of the containment with due account of its belonging to a certain group separated from cables of the cylinder and the dome;
- formation of groups is carried out on the principle of unification of cables which underwent while in service just the same production operations (testing, tightening) in time;
- change of forces in a cable from the moment of tightening up to the first testing of forces is described by calculation on the basis of the technique given above;
- prediction of forces in a cable beginning from the first tightening is performed proceeding from the linear law of change of forces in time;
- intensity of forces drop in cable is determined on the basis of data concerning forces drop in two last testings but not more than a mean value of intensity as to the group, to which belongs the cable in question;
- in cases, when a random testing of forces in cables of a group was carried out, the intensity of forces drop in cables, the testing of forces in which was not performed, is assumed as equal to the mean value of the group.

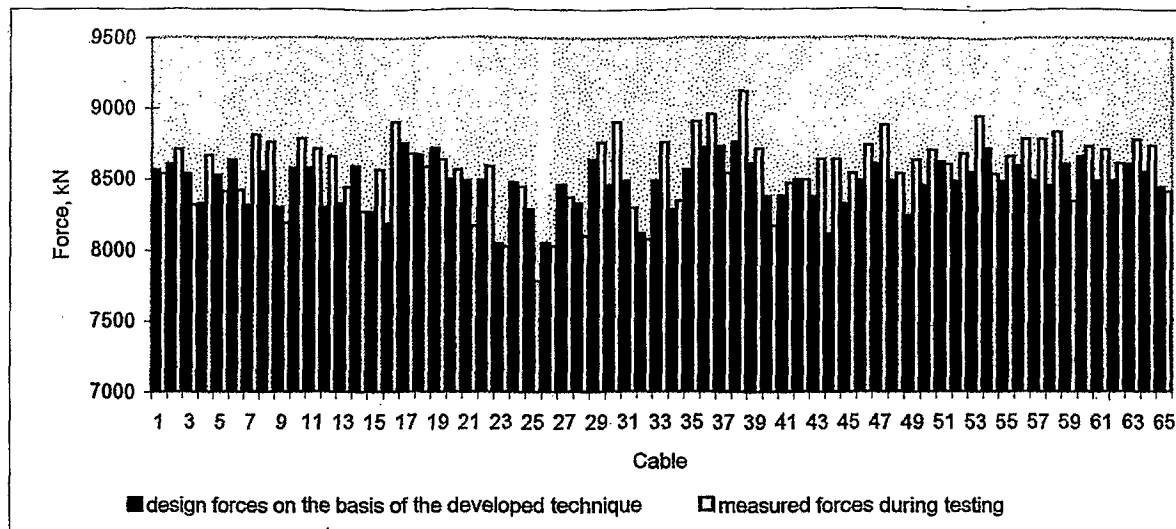
Predictions of changes of forces in containments in service were formed and monitoring results processing was carried out according to the technique developed, which side-by-side with the points enumerated also included a number of other particular points. For all this, the accuracy of the predictive determination of forces at comparison with the results of the testing, performed in 1997, proved to be quite satisfactory (fig. 15).

Technique and Results of assessment of Strained State of Containments According to Indications of Control Instrumentation

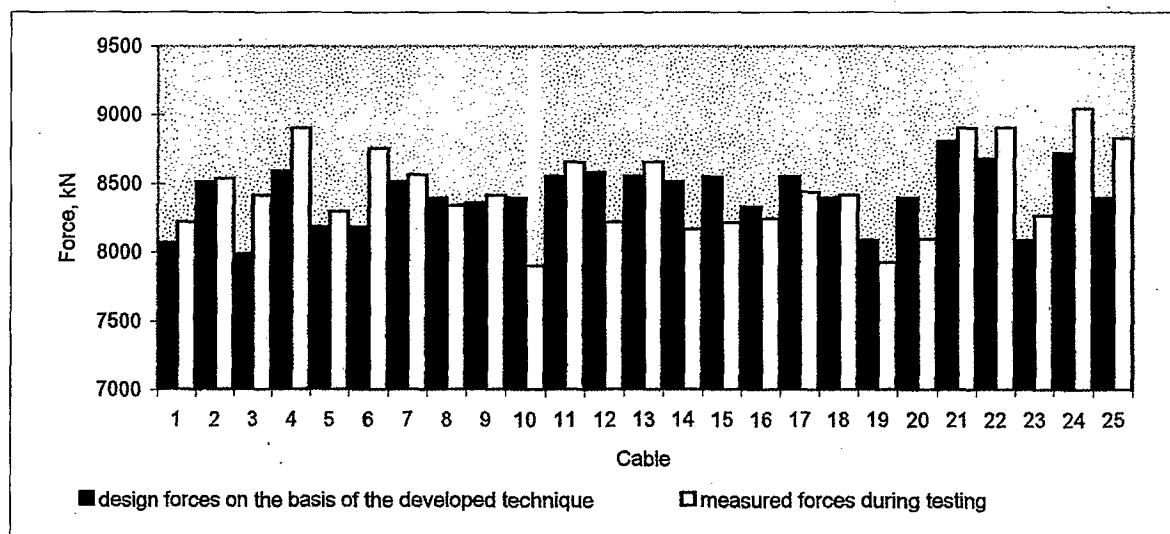
The technique submitted below is based on the results of the up-to-date studies of the theory of reinforced concrete in the field of taking into account influences of long-duration processes. The technique is directed toward solving a specific problem i.e. the assessment of stressed-strained state of containments according to indications of a control instrumentation, takes into account structural features, conditions of loading and maintenance.

The technique is based on the following initial preconditions:

- in general, the stressed-strained state of a containment is assessed according to the stressed-strained state in ranges, where a control instrumentation is installed; a part of the containment 1000 mm wide with an axial arrangement of the control instrumentation segregated by two plane vertical sections passing to the vertical axis of symmetry of the containment is assumed as a reference section of the range;
- stressed-strained state of the range is determined by stresses in meridional and circular nonprestressed reinforcements disposed at exterior and interior surfaces of the containment, by stresses in a radial nonprestressed reinforcement, by meridian and hoop stresses in concrete at exterior and interior surfaces and along the axis of the containment;
- stresses in reinforcement and concrete at a given instant of time are calculated as an algebraic sum of increments of corresponding stresses at the following stages of time: stage 1 - from the beginning of concrete placement to the instant of compression of the containment; stage 2 - compression of the containment; stage 3 - from putting in operation to the first testing of forces; stage 4 - an additional compression of the containment during tightening of cables after testing of



a



b

Fig.15. Comparison of design and measured forces in cables of the cylinder (a) and the dome (b) during control in 1997.

forces; stage 5 - between proceeding and subsequent testing of forces (tightening and testing; stage 6 - an additional compression of the containment during tightening of cables after conducting of a subsequent testing of forces (subsequent control- preventive works); stage 7 - from the last testing of forces (tightening) of cables to the given instant of time;

- concrete, nonprestressed reinforcement and wires of reinforcing cables work within the limits of an elastic range of corresponding structural diagrams at the tightening of reinforcing cables.

- increments of stresses in meridional and circular reinforcements are determined directly according to indications of corresponding transducers;

- increments of stresses in concrete at short-term loading (application of the own weight at the 1-st stage, compression of concrete at the stage of construction and subsequently during tightening of cables, stages 2, 4, 6 etc., correspondingly) are calculated according to increments of strains, measured by means of linear strain transducers; increments of strains in concrete at a long-term loading (stages 1, 3, 5, 7 etc.) are calculated according to experimental values of increments of corresponding stresses in a nonprestressed reinforcement on the basis of the technical alternative of the creep theory.

- decrease of the force in reinforcing cables is determined in non-instant zones of the cylindrical (at the mark 32.600) and dome-shaped (with radius 0...9 m) parts of the containment proceeding from the compatibility (equality) of strains of concrete and cable along the axis of the latter;

- forces drop in cables at internals between the previous and subsequent testings is determined proceeding from the compatibility of deformations of concrete and a cable along the axis of the latter.

The following initial preconditions are used at determination of stresses in concrete: concrete is considered as a homogeneous isotropic material; there is a linear dependence between elastic strains arbitrarily conforming to a short-term loading and stresses; there is also a linear dependence between creep strains and stresses; principle of superposition is followed concerning creep strains; absolute values of elastic strains and creep strains do not depend on alternating stresses; elastic strains and creep strains of concrete are distributed along the height of cross sections according to the linear law; forces developing in concrete and nonprestressed reinforcement at a long-term action of a load refer to the category of their own and become mutually balanced.

In the light of the adopted initial preconditions stresses in nonprestressed reinforcement $\sigma_{s,t}$ and concrete $\sigma_{b,t}$ at exterior and interior surfaces of containments at a specified instant of time t are calculated by formulae:

$$\sigma_{s,t} = \sum \Delta \sigma_{s,i} ; \quad (4)$$

$$\sigma_{b,t} = \sum \Delta \sigma_{b,i} . \quad (5)$$

Increments of stresses in concrete at a preliminary compression of the containment (stage 2) and tightening of reinforcing cables in the process of performing of control-preventive works (stages 4,6 etc.), which are regarded as single-stage acts, are calculated by the formula:

$$\Delta \sigma_{b,i} = \Delta \varepsilon_{b,i} E_b . \quad (6)$$

Increments of stresses in concrete at exterior $\Delta \sigma_{b,i}^{ext}$ and interior $\Delta \sigma_{b,i}^{int}$ surfaces of the containment at a long-term loading (stages 1, 3, 5 etc.) are in a normal section in question (Fig. 16), from the joint solution of balance equations of longitudinal forces and bending moments

about the axis passing through the center of gravity of concrete:

$$\Delta N_{p,i} + \Delta N_{s,i}^{ext} + \Delta N_{s,i}^{int} + \Delta N_{b,i} = 0 ; \quad (7)$$

$$M_{b,i} - \Delta N_{s,i}^{ext} z_s^{ext} + \Delta N_{s,i}^{int} z_s^{int} = 0 . \quad (8)$$

where $\Delta N_{s,i}^{ext}$ - increment of an axial force in nonprestressed reinforcement stage in question is calculated by the formula :

$$\Delta N_{s,i}^{ext} = \Delta \sigma_{s,i}^{ext} A_s^{ext} ; \quad (9)$$

$\Delta \sigma_{s,i}^{ext}$ - increment of stresses in reinforcement at the stage in question according to indications of a corresponding force transducer :

A_s^{ext} - area of reinforcement in a reference normal section;

$\Delta N_{s,i}^{int}$ - increment of an axial force in nonprestressed reinforcement disposed at the interior surface of the containment at the stage in question is calculated by the formula :

$$\Delta N_{s,i}^{int} = \Delta \sigma_{s,i}^{int} A_s^{int} ; \quad (10)$$

$\Delta \sigma_{s,i}^{int}$ - increment of stresses in reinforcement at the stage in question according to indications of a corresponding force transducer :

A_s^{int} - area of reinforcement in a reference normal section;

$\Delta N_{b,i}$ - increment of force in concrete at the stage in question is calculated by the formula :

$$\Delta N_{b,i} = 0,5(\Delta \sigma_{b,i}^{ext} + \Delta \sigma_{b,i}^{int})bh ; \quad (11)$$

$\Delta \sigma_{b,i}^{ext}$ - increment of stresses in concrete on the level of reinforcement, disposed at the exterior surface of the containment;

$\Delta \sigma_{b,i}^{int}$ - increment of stresses in concrete on the level of reinforcement, disposed at the interior surface of the containment;

$M_{b,i}$ - bending moment created by the force in concrete about the axis passing through the center of gravity of the concrete section.

The value $\Delta N_{p,i}$ in (7) reflects the decrease of the containment body level in the direction at issue in time as a result of the force drop in cables. Proceeding from the preconditions assumed, the $\Delta N_{p,i}$ value is according to measured values of stresses increments $\Delta \sigma_{s,i}^{ext}$ and $\Delta \sigma_{s,i}^{int}$:

$$\Delta N_{p,i} = 0,5(\Delta \sigma_{s,i}^{ext} + \Delta \sigma_{s,i}^{int})A_c h / l, \quad (12)$$

where l - is a distance between axes of cables.

The value $\Delta N_{p,i}$ for cables of the dome according to (12) determined a value of forces drop between the previous and the subsequent testing. The value of corresponding forces drop in

cables of cylinder was determined as a resultant of forces $\Delta N_{p,i}$ according to (12) in meridian and circular directions to the axis of a cable.

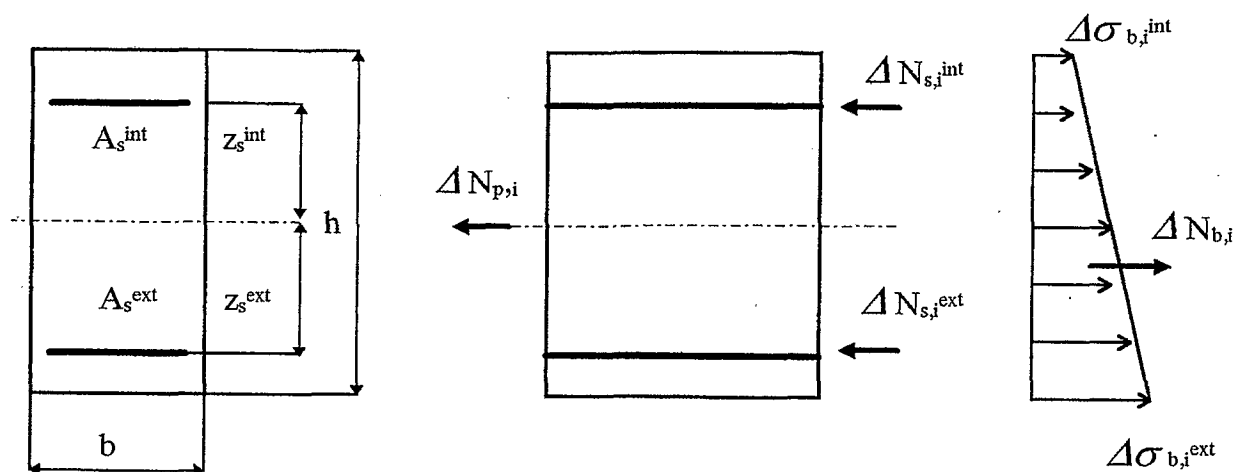


Fig.16. Determination of stress increments in concrete of containment during long-duration loading.

The processing of the obtained experimental data according to the afore-cited technique, their generalization and analysis made it possible to receive the following picture of the stressed-strained state of the containments and principle mechanisms of its change in the process of construction and operation.

Mean durability of the containment erection constitutes from 12 to 18 months and up to the moment when compression begins (stage 1) the total picture of the stressed-strained state, reflecting actions of the empty weight and long-term processes in concrete, was characterized by the following parameters. Concrete of the cylindrical and the domed parts of a containment is in conditions of the flat stressed state "compression-tension" (compression in the meridian direction, tension in the circular direction): meridian compressive stresses in concrete of the cylinder at the level of the foundation plate constituted 1.7-1.8 MPa, and at the level of the carrier ring of the dome - 0.9-1.2 MPa, reducing in the limits of the cylinder height practically linearly; circular tensile stresses in concrete of the cylinder accounted for approximately 0.1-0.2 MPa; meridian compressive stresses along the height of the dome decreased from 0.6-0.8 MPa practically to zero values, and circular tensile stresses at this constituted 0.4-0.7 MPa. Compressive stresses in meridian and circular reinforcement of the containment up to the moment when the compression begins constituted correspondingly: cylinder - 15.5-40.7 and 3.5-19.2 MPa and 3.5-19.2 MPa; dome - 2.8-17.5 and 3.7-22.9 MPa.

Tightening of reinforcing cables (stage 2) causes increments of compressive stresses in concrete and nonprestressed reinforcement of the containment body, the values of which constituted: meridian and circular stresses in concrete of the cylinder - 3.5-5.4 and 6.5-11.2 MPa; meridian and circular stresses in concrete of the dome - 4.2-9.1 and 4.1-10.3 MPa; meridian and circular reinforcement of the cylinder - 22.6-77.9 and 36.5-73.8 MPa; meridian and circular reinforcement of the dome - 26.6-95.0 and 20.0-87.5 MPa.

Thus, before the operation concrete of the containment was in conditions of the flat stressed state "compression-compression" with the following values of stresses: cylinder - meridian 4.4-6.4 MPa, circular 6.3-11.6 MPa; dome - meridian - 3.5-10.5 MPa, circular 4.4-10.2 MPa.

Stressed-strained state of the containment while in service was characterized by the increase of compressive stresses in non-prestressed reinforcement and the growth of concrete strains which was accompanied by the drop of compressive stresses in concrete at intervals of time between

tightenings.

Graphs of stresses change, during 12-year period of studies, in nonprestressed reinforcement (a), strains (b) and stresses in concrete (c) are given in figure 17 at the most characteristic zones of the containment i.e. the middle part of the cylinder height (membrane zone) and the middle part of the dome. The laws of change in corresponding parameters had a close nature also in other containments with a lesser period of service.

Data concerning stresses in nonprestressed meridional (a) and circular (b) reinforcement for height of the cylinder and the dome immediately after compression and 12 years of service are given in figure 18. For all this, in general, stresses in reinforcement increased by 1.6...2.1 fold and their maximum values constituted 150...184 MPa in the central zone of the dome and 140...153 MPa in the membrane zone of the cylinder.

Strains of concrete while in service increased by 1.7...2.8 fold. Growth of strains at intervals of time between tightenings of reinforcing cables was accompanied by the drop of stresses in concrete and during tightenings by the increase of stresses in concrete. For all this, the proportion of concrete strains induced by the tightening of cables did not exceed 8...12 % of the total strain increment from the moment of termination of the containment compression.

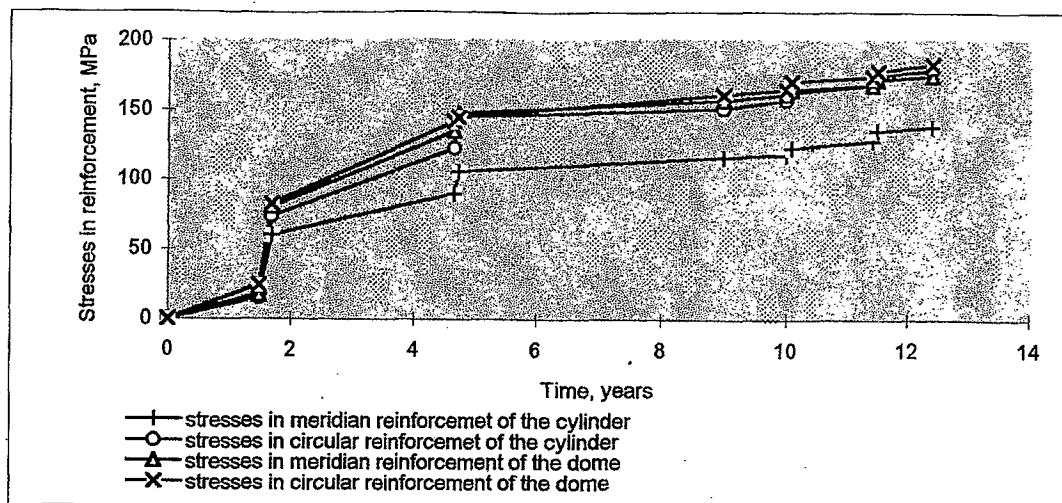
The quantitative assessment of a concrete creep characteristic was given according to the results of concrete strains measurements processing while in service. The ϕ_t value was determined as a relation of concrete strains in a membrane zone of the cylinder in a circular direction by the moment of the first tightening of cables to corresponding concrete strains by the moment of termination of the containment compression. The ϕ_t value, determined in such a way, constituted 1.4...1.6 in 4.7 years after tightening of cables, that satisfactorily corresponded to the calculated theoretical values of the creep characteristic according to (3).

The drop of stresses in concrete from the moment of termination of the containment compression (fig. 17, c) with due accounted of tightenings of reinforcing cables performed, constituted: 6...8.5% in the cylinder in a meridian direction and 3.5...6.3% in a circular direction; 8-10% in the dome in a in a meridian direction and 5..7.6% in a circular direction. For all this, the level of compression during the whole term of service in accordance with safety requirements provided an integrity of the containment body (absence of cracks) at design accident conditions, among which the effect of an excess internal pressure 0.46 MPa was a prevailing one.

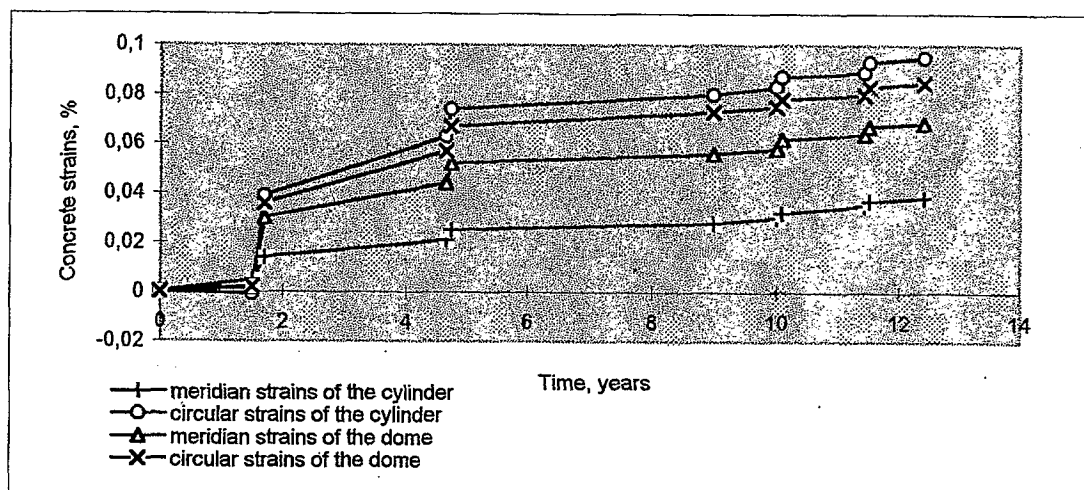
Calculation according to the technique developed makes it also possible to determine forces drop values in reinforcing cables while in service on the basis of indications of the most consistently working sensors on reinforcement. The forces drop value in cables of the dome was determined according to (12) and the forces drop value in cables of the cylinder was determined by analogy as a projection of a forces drop resultant in meridian and circular directions on to the axis of a cable. Forces drop values in cables according to the results of testings at the stage of control-preventive works performed, and determined by indications of sensors were given in table 1. Satisfactory agreement between the values given permits to use indications of sensors for the integral criterion of forces drop in reinforcing cables at time intervals between testings of forces.

Table 1

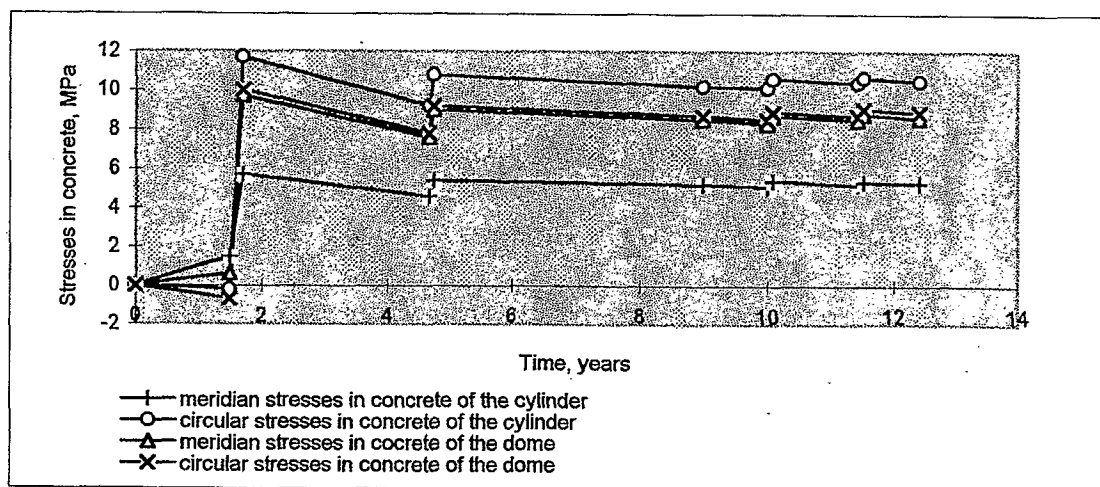
Disposition of sensors (fig. 1.)	Mean values of forces drop in reinforcing cables from the moment of termination of the containment compression, %			
	t = 4.7 years (the first testing)		t = 9.0 years (the second testing)	
	according to testing data	according to design to indications of sensors	according to testing data	according to design to indications of sensors
Cylinder mark level 32.6	6.63	8.56	6.88	5.75
Dome R = 4.0	9.45	10.18	6.76	6.33



a



b



c

Fig. 17. Change of stresses in nonprestressed reinforcement (a), strains (b) and stresses (c) in concrete of the containment.

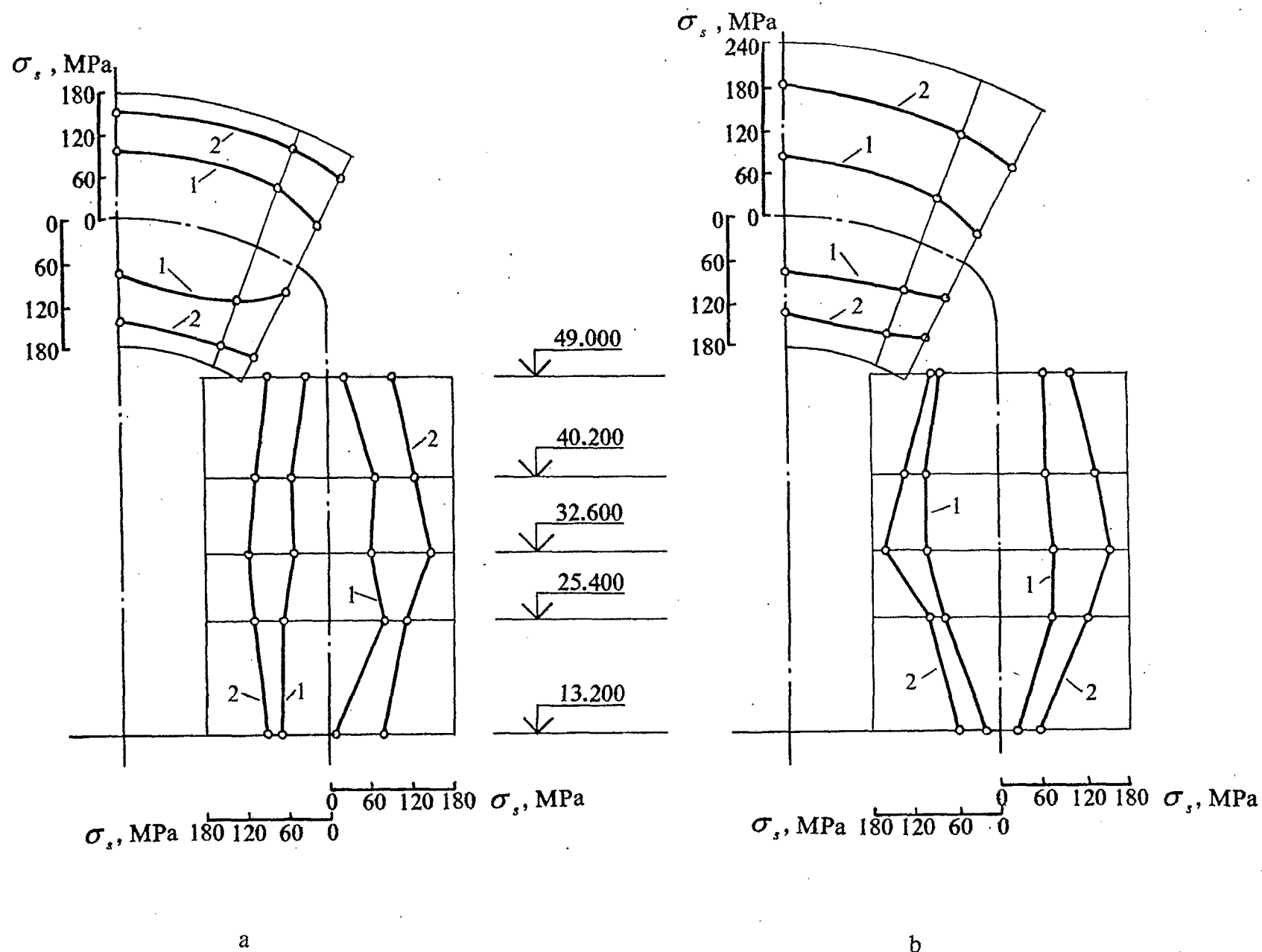


Fig. 18. Data concerning stresses in nonprestressed meridional (a) and circular (b) reinforcement for height of the containment (1 - the moment of the termination of the containment; 2 - after 12 years of service)

Conclusions

Generalization and analysis of the afore-cited results of monitoring permit to come to the following conclusions concerning the principle laws for changes of forces in reinforcing cables and stressed-strained state of containments while in service.

As it was to be expected, the most considerable forces drop in reinforcing cables occurs during the first years of service. The value of forces drop in cables after 4...5 years of service constituted on the order of 23...28 % of the tightening force at the stage of the containment compression. As the design analysis showed, the losses mentioned were not only the result of the factors which are as a rule taken into account (concrete creep, stress relaxation in wires of cable, elastic compression of concrete at the stage of compression) but also of a complex of other factors, representing first of all the specific character of a structural conception adopted for the force transfer on to concrete. For all this, the effect of the latter remains pronounced enough may reach 20...25 % even if to allow for a possible error in determination of forces losses due to creep, relaxation and elastic compression. Subsequently, forces drop in cables takes place according to the law relative to the linear one with the intensity on order of 1.03...3.44 % per year, inspite of tightenings performed. From the stand point of the encasement compression, the efficiency of each subsequent tightening decreases, as the intensity of forces drop in cables increases at this.

A probabilistic approach may be used for prediction of forces drop in cables, the realization of which within the scope of a specially developed technique permits to-determine with a necessary accuracy forces in cables to the specified moment of time.

Stressed-strained state of the containment while in service was characterized by the increase of compressive stresses in non-prestressed reinforcement and the growth of concrete strains which was accompanied by the drop of compressive stresses in concrete at intervals of time between tightenings. For all of this, as a result of more than 12 years period of studies of instrumentation indications, it was ascertained the following: stresses in non-prestressed reinforcement increased 1.6...2.1 times and their maximum values reached 180...240 MPa; concrete strains increased 1.7...2.8 times, when the portion of strains induced by tightening of cables did not exceed 8...12 %; the drop of stresses in concrete from the moment of termination of encasement compression accounted for 3.5...10 %. Values of stresses in concrete were calculated according to indications of sensors on the basis of a specially developed technique, also permitting to evaluate integrally by indications of sensors the value of forces drop in reinforcing cables while in service.

The results of monitoring made it possible to ascertain a real pattern and laws of change of a stressed-strained state and forces in reinforcing cables of containments and also to use the data obtained for prediction of corresponding processes at a subsequent operation.

**CSNI PRINCIPAL WORKING GROUP No.3 ON INTEGRITY OF COMPONENTS
AND STRUCTURES**

**JOINT WANO-PC/OECD-NEA WORKSHOP ON PRESTRESS LOSS IN NPP
CONTAINMENTS**

**Held at Civaux NPP, Poitiers, France
25 - 26 August 1997**

Hosted by Electricite de France

**LONG TERM IN-SERVICE MONITORING OF PRE-STRESSING IN MAGNOX
PRE-STRESSED CONCRETE PRESSURE VESSELS**

D W Twidale, Magnox Electric plc.

LONG TERM IN-SERVICE MONITORING OF PRE-STRESSING IN MAGNOX PRE-STRESSED CONCRETE PRESSURE VESSELS

SUMMARY

The paper describes the Oldbury and Wylfa PCPVs and their prestressing details, outlines the safety case for these reactor vessels and the in-service surveillance programme which underpins it and of which the prestressing tendon monitoring programme is a part. The long term results from in-service tendon load monitoring are given.

Measured vessel concrete strains, obtained from embedded vibrating wire strain gauges both on and off power are compared against the predicted values obtained from Finite Element analysis to give a measure of the composite performance of both prestressing and concrete.

The tendons and the vessel concrete have performed as originally envisaged and a good correlation is observed between measured and predicted vessel strains.

LONG TERM IN-SERVICE MONITORING OF PRE-STRESSING IN MAGNOX PRE-STRESSED CONCRETE PRESSURE VESSELS

D W Twidale, Magnox Electric plc.

1. Introduction

Magnox Electric is wholly owned by the UK Government and operates six nuclear power stations each with two reactors. Four of the stations have steel reactor pressure vessels and two have prestressed concrete pressure vessels. Magnox Electric is also decommissioning three steel pressure vessel power stations, one each in England, Wales and Scotland.

Of the four prestressed concrete pressure vessel (PCPV) reactors operated by Magnox the two at Oldbury in Gloucestershire are of the thick walled vertical cylinder type, and the two at Wylfa on the island of Anglesey in North Wales are of spherical internal shape with ribbed exterior. The earliest vessel at Oldbury was stressed in 1966. Pre-stressing is in all cases unbonded with in-service anchorage loads being in the range 1649 kN to 5600 kN.

The paper describes the Oldbury and Wylfa PCPVs and their prestressing details, outlines the safety case for these reactor vessels and the in-service surveillance programme which underpins it and of which the prestressing tendon monitoring programme is a part. The long term results from in-service tendon load monitoring are given.

Measured vessel concrete strains, obtained from embedded vibrating wire strain gauges both on and off power are compared against the predicted values obtained from Finite Element analysis to give a measure of the composite performance of both prestressing and concrete. The tendons and the vessel concrete have performed as originally envisaged and a good correlation is observed between measured and predicted vessel strains, with stable trends for at power compressive creep strains being established.

2. Oldbury PCPVs - Vessel and Prestressing Details

Figure 1 shows a sectional elevation through the PCPV. Each vessel is essentially a vertical closed cylinder with minimum external diameter 32.62m and height 31.29m. The reactor core and boilers are contained in a central cavity of diameter 23.5m and height 18.31m. Minimum side wall thickness is 4.56m and the top and bottom caps are 6.29m and 6.69m respectively. The vessel is constructed in high strength concrete with a steel liner as the pressure boundary and is prestressed by means of prestressing tendons arranged in two principal systems, one approximately helical within the wall of the vessel and extending from top to bottom, the other approximately rectilinear within the top and bottom slabs and extending from wall to wall. Each tendon has a guaranteed ultimate tensile strength of 273 tons and is unbonded and within a duct allowing the tendon to be inspected, tested and replaced if necessary. Each tendon is anchored at the ends of its duct. Figure 2 shows the general arrangement of prestressing tendons.

There are in total 3315 helical tendons in 22 layers of cables arranged alternately clockwise and anticlockwise, each spanning 130° of twist of the helix and tensioned from stressing

galleries at the top and bottom. The tendons are diverted around the various penetrations and anchored with Freyssinet anchorages which comprise of male and female fluted cones between which the twelve strands are individually trapped.

There are nominally 600 top slab tendons in 20 layers and 472 bottom slab tendons in 16 layers arranged at right angles. The tendons all contain 12 strands, each strand consisting of seven wires.

3. Wylfa Vessel and Prestressing Details

The Wylfa vessels have a spherical internal shape of 29.26m and are lined with a 20mm steel liner anchored to the vessel wall to ensure gas tightness. The external surface of the vessel is a stepped structure, consisting of three cylindrical surfaces of 21.64m, 31.19m and 35.96m diameter. The stepped structure design helps to partly retain a uniform wall thickness whilst providing horizontal and vertical surfaces for anchoring the prestressing tendons.

Situated around the vessel circumference at 22.5° intervals are 16 vertical ribs, each 2.44m square in plan. They are in three groups- the main group attaching to the outer cylindrical vessel surface, with two smaller groups attaching to the middle cylindrical surfaces above and below the equator. Their purpose is to contain the hoop prestressing tendons and their anchorages. Figures 3 and 4 show a sectional elevation and plan of the vessel.

The Wylfa prestressing system is a modified version of the Freyssinet 12/06" system (ie 12 strands per tendon each of 0.6 inch diameter) which uses 36 strands of stabilised high tensile steel rather than 12. This is formed into a hexagonal cross section of 4.2 inch maximum diameter passing through 5.5 inch internal diameter steel ducts. The majority of tendons follow the curvature of the vessels inner surface except where deviating to anchor on the vessels outer surface. At their anchorage points each tendon sub-divides into 3 "cables" of 12/0.6" strands that anchor separately on a common anchor block.

Each vessel is prestressed by 1338 tendons which were tensioned to an end load of approximately 615 tonf (6128 KN) before their anchorage and consequent transfer of load to the vessel. Each tendon has a GUTS of 820 tonf (8170 KN) and they are recognised as being arranged in five main groups, ie, Top Cap containing 218 tendons and Bottom Cap containing 208 tendons in 5 layers:- Meridional tendons, a "great circle" system of 480 tendons in vertical planes through the vessel barrel:- Rib Vertical Tendons which are the eighth and outermost layer of the meridional group, the 48 rib verticals passing vertically through the main ribs of the vessel to anchor at the top and bottom ends, and finally the Hoop Tendons an external system of 384 tendons in approximately horizontal planes passing through and anchored on the vessel ribs.

4. Safety Criteria

The overall structural integrity of the PCPVs is provided by the joint action of the structural strength of the concrete used and the prestressing system; the latter maintains the PCPV structure under compression during normal operation and under fault conditions. Monitoring of the long term condition and integrity of the prestressing tendons and the condition of the concrete forms the basis of the safety case for continued operation of the PCPV's.

4.1 PCPV Safety Case Requirements

Monitoring of the concrete vessel and its prestressing system is focused on those aspects of structural integrity which contribute most to the pressure vessel safety case, both during normal operation and during fault conditions.

Potential threats to the safe operation arise from adverse loading or non standard operational regimes that may be applied to the structure eg;

- (i) excessive internal reactor gas pressure
- (ii) loss of prestress over a significant area
- (iii) regions within the PCPV at high temperature

A multi legged safety case outlined below provides defence in depth against each of the possible threats to safe operation. The in service monitoring must ensure that each aspect is adequately covered.

4.2 Pressure effects

The PCPVs are protected against over-pressurisation faults by a number of factors;

- 1) operator action in response to alarms or measured data
- 2) automatic reactor trip on high pressure
- 3) automatic operation of safety relief valves
- 4) elastic response of the PCPV up to design pressure and progressive type failure thereafter
- 5) Ultimate Load Analysis (ULA) shows a Factor of Safety in excess of 2.5 for Oldbury and 2.65 for Wylfa and a "gas in cracks" Factor of Safety of 2.13 for Oldbury and 1.745 for Wylfa compared to the 2.5 and 1.5 figures respectively required by BS 4975 (Reference 1).

4.3 Loss of Prestress

Loss of prestress occurs during the life of the station at an exponentially reducing rate with time and reduces the capacity of the PCPV to resist the internal gas pressure and erodes the margins calculated from the ULA. The process is well understood and monitored with the volume of data accumulated over station life confirming the rate of loss model.

Tendon prestress is also affected by the temperature of the tendon material; ie under a fixed displacement loading condition an increase in tendon temperature leads to a reduction in the applied prestress. Therefore overheating of the tendons would also lead to a reduction in the prestress applied to the PCPV.

Protection against loss of prestress is afforded by;

- 1) regular monitoring of residual tendon loads and condition of anchorages
- 2) adjustment of tendon loads if the residual load falls below that calculated from the ULA. Tendons can be replaced and/or their prestress load reset to the design value.
- 3) tendons operate in the elastic regime ie, they are loaded to 75% of their guaranteed ultimate tensile strength which gives a margin on performance before yield and creep rupture occurs.

4.4 Temperature effects

Bulk concrete temperature limits are set at around 65°C for Oldbury and 40°C for Wylfa but the vessel concrete will withstand temperatures well in excess of those likely to be experienced during normal operation.

Temperatures in excess of 65°C could be experienced by the concrete due to breakdown of insulation on the hot face of the liner, loss of cooling to the liner by the Pressure Vessel Cooling System (PVCS), or due to leakage of gas through the main or penetration liners. Any of these postulated events would lead to a physical change in the concrete with change in its material properties and could also affect the prestressing.

Overheating of PCPV concrete is guarded against by a multiplicity of factors such as monitoring of the PVCS inlet and outlet temperatures and operator action or automatic reactor trip to shut of the primary heat source. The large specific heat capacity of the concrete and its poor thermal conductivity also gives immunity to short term thermal excursions.

The prestressing itself is protected to some extent in that the large mass flow rate coolant gas leaks required to initiate prestressing tendon damage would be detected by operators and there is also redundancy in the prestressing system.

5. The In-Service Surveillance Programme

The Nuclear Site Licence conditions under which Magnox are the Licensee require that the PCPVs be inspected on a regular basis to support the main legs of the safety case outlined above. The statutory maintenance period is currently 2 years for Wylfa and 3 years for Oldbury although interim inspections based on a 2 year period are also carried out at Oldbury. The maintenance inspection covers 9 areas as follows;

5.1 Concrete Surface

The external concrete surface of the pressure vessel, where accessible, is examined visually to record the presence or propagation of any cracks or other defects or evidence of water leakage. Particular attention is paid to areas surrounding penetrations.

5.2 Tendon Anchorages

A sample consisting of a minimum of 1% of all anchorages is inspected. The exposed parts of male and female cones, bearing rings, shims and their supporting concrete are examined to detect defects, corrosion, mechanical damage, slippage or cracking and spalling of the supporting concrete. During the course of the residual load checks, the anchorage components are disturbed. These anchorages plus those associated with a further three tendons at Oldbury, or 2 strands from 8 tendons at Wylfa, nominated for corrosion sampling are inspected.

5.3 Tendon Load Checks

Tendon load checks are carried out to measure the residual anchorage load in a representative selection of tendons, usually 1% of all tendons. The sample size has been chosen to try to give a reliable estimate of the true mean and standard deviation of the tendon loads. In practice each sample is a different percentage of the total in its group. For Oldbury however the total sample of 44 represents just over 1% of the total number of tendons. Individual results and the mean load for each group are compared to the design minimum mean load. (For Oldbury this is 1694kN (170 tons)). The results of the load checks are presented in graphical form such that current and past trends can be compared with design expectations and the maximum permissible limits for loss of load. The results for Oldbury R1 are given at Figures 5 to 7 and those for Wylfa R1 are given at Figures 8 to 12.

At Oldbury two slightly different types of strand have been used, about 85% is British Ropes stress relieved strand, the remaining 15% is Somerset Wire stabilised strand which has better creep properties due to the introduction of a small amount of plastic strain at a suitable temperature during the final stages of manufacture. At the time of construction it was estimated that the creep relaxation of the Somerset Wire strand over the life of the station would be about 10% compared with 17% for the British Ropes strand and this difference is apparent from the load checks carried out (Figs. 5 & 7). Stabilised strand was used for all subsequent UK vessels.

In all other respects the load performance of the prestressing has followed the predicted performance with the only deviations being those to be expected from the tolerances inherent in load cell and jack calibration and in the "trap, free" measurement procedures used in the earlier lift-off testing.

A statistical examination by Irving in August 1975 (Reference 2) of the first eight years tendon load check results at Oldbury R1 predicted mean values at June 1997 after 30 years operation that are remarkably close to the values recorded in the June outage this year viz:

Location Oldbury R1	Actual Mean Load June 1997	1975 Extrapolation of Mean Load at 30yrs, June 1997	Tolerance on Extrapolated Load (plus or minus)
Top Cap	1805 kN, 181 Tons	179.3 Tons	4.5 Tons
Helicals	1786 kN, 179 Tons	180.3 Tons	8.0 Tons
Bottom Cap	1826 kN, 183 Tons	180.7 Tons	2.3 Tons

5.4 Corrosion Examination

Strands are removed and inspected for signs of deterioration in their protective coating and for underlying corrosion or mechanical damage. Lengths of strand are tested to determine mechanical properties such as strength or ductility.

5.5 Vibrating Wire Strain Gauges

The strain behaviour of the PCPVs is routinely monitored using a strain gauge logger connected to embedded vibrating wire strain gauges (VWSG's).

The strain gauges are read at monthly intervals at least and at 5 yearly intervals the readings are compared with a theoretical strain analysis which takes account of time-temperature dependent tendon relaxation and concrete creep.

5.6 Vessel Temperatures

The Pressure Vessel temperature records are examined in order that any general or local fluctuations, which have exceeded the equivalent permissible values, can be assessed.

5.7 Main Reactor Coolant Loss

The results of leakage rate tests from the PCPV are examined for the operational period and an assessment is made the significance for the vessel structure of main gas circuit leakage where this leakage cannot be explained by deficiencies in the circuit external to the vessel.

5.8 Vessel Settlement and Tilt

Vessel settlement and tilt are measured to ensure that design considerations related to control rod insertion and vessel internal support structures are not compromised.

5.9 Vessel Cooling Water System Loss

Routine visual inspections of tendon anchorages and pipework penetrations are carried out in order to detect evidence of water leaks.

6. Long Term Comparison of Vessel Predicted and Actual Results

The structural performance of each vessel is reviewed at five yearly intervals. Most recently a three dimensional finite element study (Reference 3) has been carried out on the Oldbury containment to allow comparison of the actual stresses and strains recorded over time with those computed from the date of transfer of prestress up to 40 years of operation. The 3D model used included the boiler loading slot and the gas circulator penetrations, these being the major penetrations in the vessel but by exploiting symmetry the mesh was confined to a 45° slice of the vessel, from one circulator centre line to a line midway between circulators.

The finite element calculations allowed for concrete creep, tendon relaxation, gravity loads, gas pressure history and thermal gradients. Finite element strain predictions were compared with readings from 37 vibrating wire strain gauges taken both on and off load. The data used were generally specific to Reactor 1, but the conclusions are also applicable to R2, which is of almost identical design, and has a similar operating history.

Computed gauge strains were noted at the end of the fifteenth station outage ($t=11016$ days), and at the end of the period of normal operation preceding this ($t=10972$ days). These

strains were compared with the measured off load and on load strains to produce scatter plots (Figures 13 & 14). An ideal correlation would show all points on the $y = x$ line in the plots. In reality a good correlation is obtained if most points lie within the plus or minus 200 microstrain bands. Figures 13 and 14 show good overall agreement between current measured and predicted gauge strains, both on and off load.

The strain plots show that at the great majority of locations, radial axial and hoop strains are compressive, and becoming more so with time. The rate of compression tails off early in the reactor lifetime, so that from the present to 40 years operation, creep strain components are predicted to change by around 15 microstrain on average.

7. Problems with the PCPVs and Prestressing

There have been very few problems with either the concrete vessels or the prestressing. The original design and safety cases have remained robust throughout the station lifetimes and will prove adequate for 40 years plus of safe operation.

Current predictions, based on a plot of 95% confidence limit of mean load, indicate that the Oldbury R2 Top Horizontal Tendons (600 No.) may require reshimming within 10 years but this activity can be undertaken with the reactor on load. All other tendon groups are indicating adequate loads.

Oldbury has experienced a small number of PVCW leaks which have wetted tendons but investigation has shown that in all cases the effect on the tendons has been negligible.

At Wylfa current data also indicates that reshimming will not be required to gain 40 year life although again this can be undertaken with the reactor on load if required.

In 1971 pitting corrosion was discovered in some of the Wylfa Hoop Tendons, possibly due to the presence of chlorides. Subsequent investigation has shown that the pit depth no longer appears to be increasing with time and is not critical.

Wylfa R1 experienced a PVCW leak earlier this year which has wetted some tendons. Attempts to seal the leak during the recent station outage failed but since the leak was within the limits of the system make up and no corrosion of embedded components or tendons is taking place the vessel has been returned to service.

8. Conclusions

In conclusion the PCPV safety cases are robust and remain in line with the original design intent and original safety cases produced in the 1960's.

Tendon lift off data obtained from the surveillance programme continues to confirm the design assumptions and support the load loss/ time model.

The composite action of the concrete and the prestressing systems continues to act as the original designers predicted and as predicted by more modern methods of analysis.

The long term behaviour of the unbonded prestressing systems at both Oldbury and Wylfa has been excellent.

References

- 1 British Standards Institution 1990 "BS Specification for Prestressed Concrete Pressure Vessels for Nuclear Engineering" BSI London . BS 4975. 1990.
- 2 Central Electricity Generating Board, "Oldbury Power Station, An Assessment of Prestressing System Check Loads And Their Relation To Design Predictions And Limits" J Irving , August 1975
- 3 Magnox Electric Plc. " A 3-D Finite Element Analysis of the Oldbury Prestressed Concrete Reactor Pressure Vessels", A J Carter, January 1997.

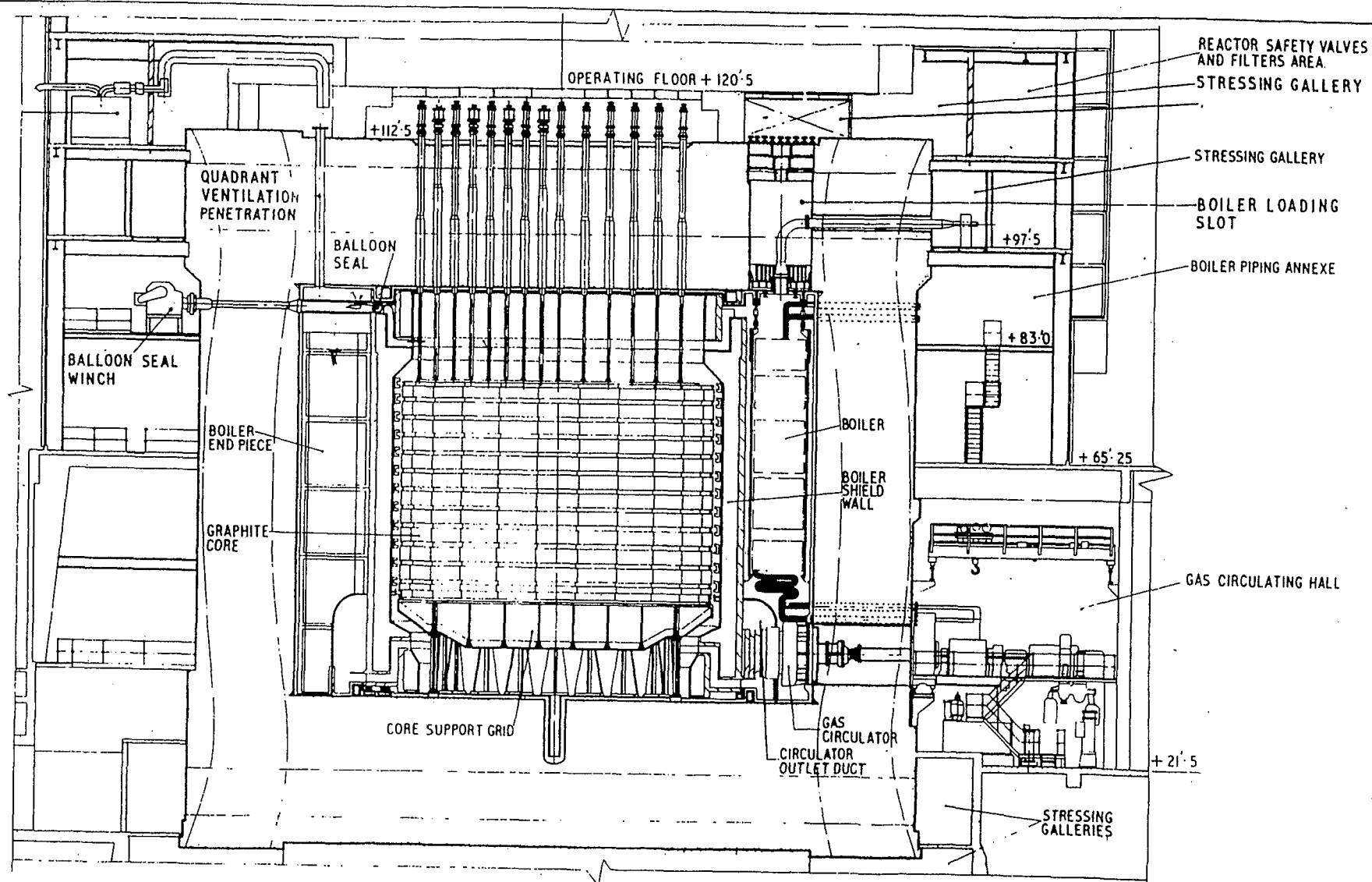
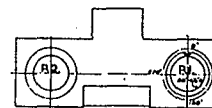


FIG.1

OLDBURY P.S.—ARRANGEMENT OF REACTOR UNIT.

OLD/21/23/4106
OLD/21/23/4107
OLD/21/23/4109
OLD/21/23/4108
OLD/21/24/4100
OLD/21/22/4101



KEY PLAN

[illegible]

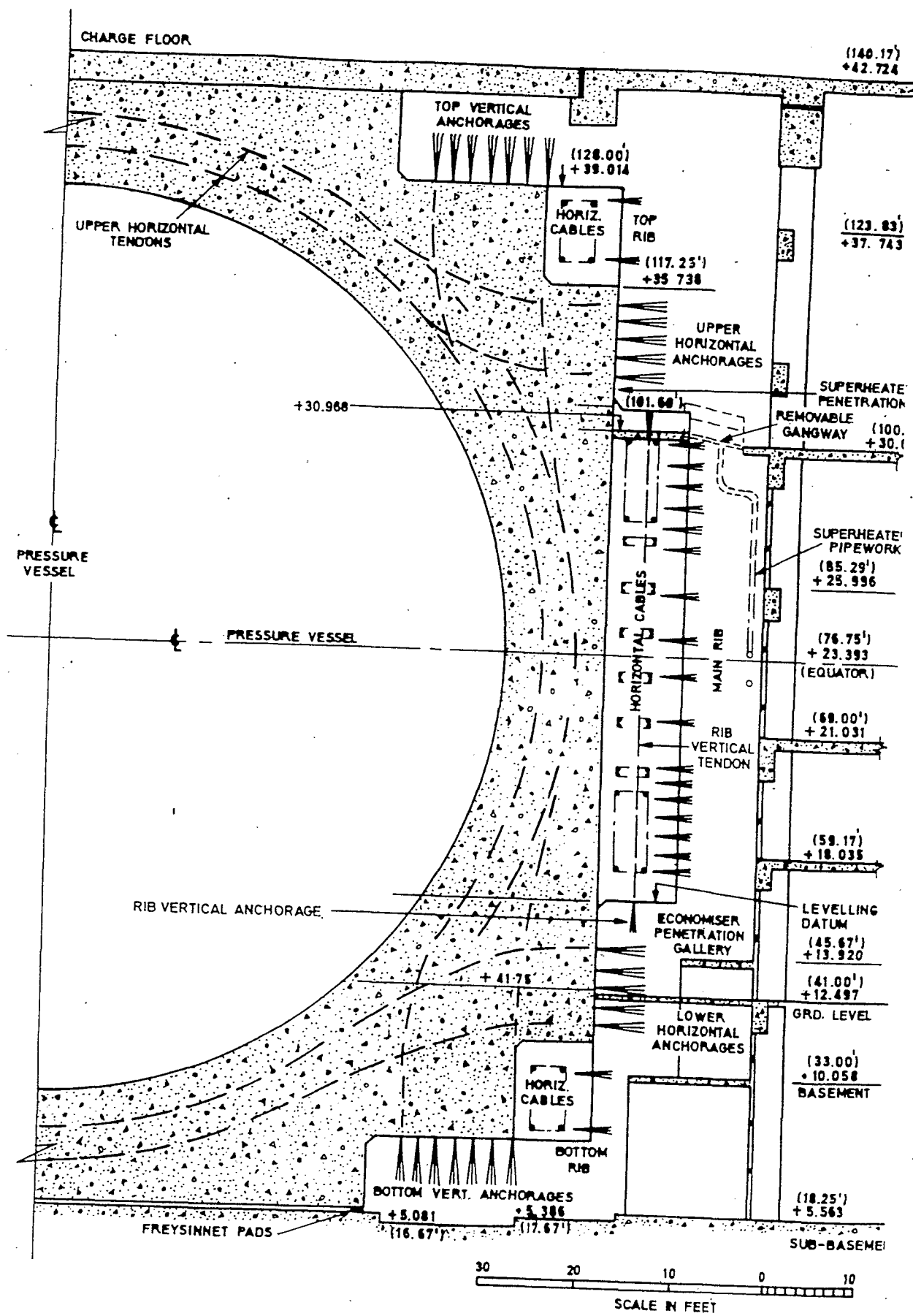


FIG.3

WYLF A P.S.—SECTION THRO' PRESSURE VESSEL.

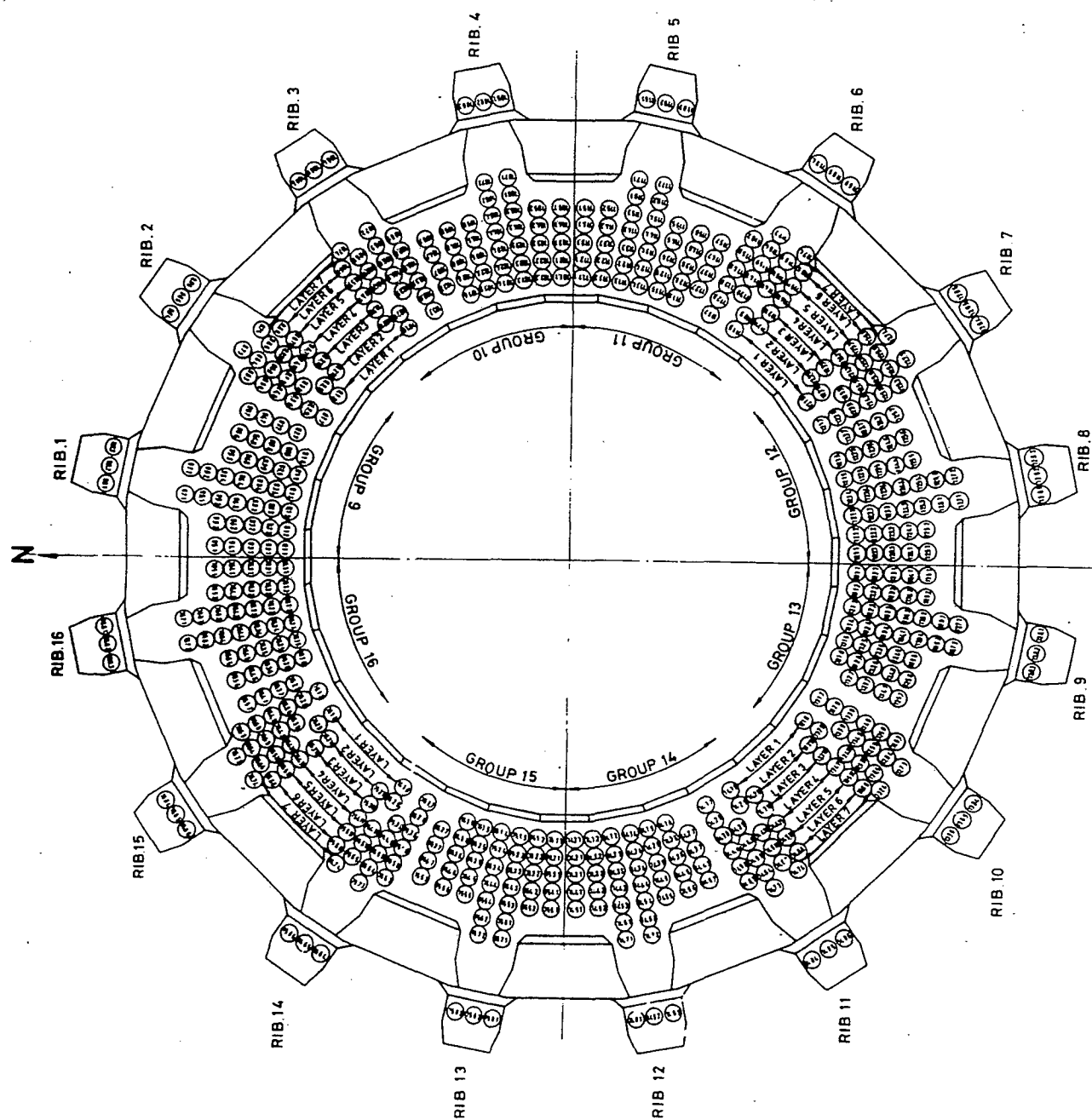


FIG. 4 WYLFA P.S.—LOCATION OF TENDONS.

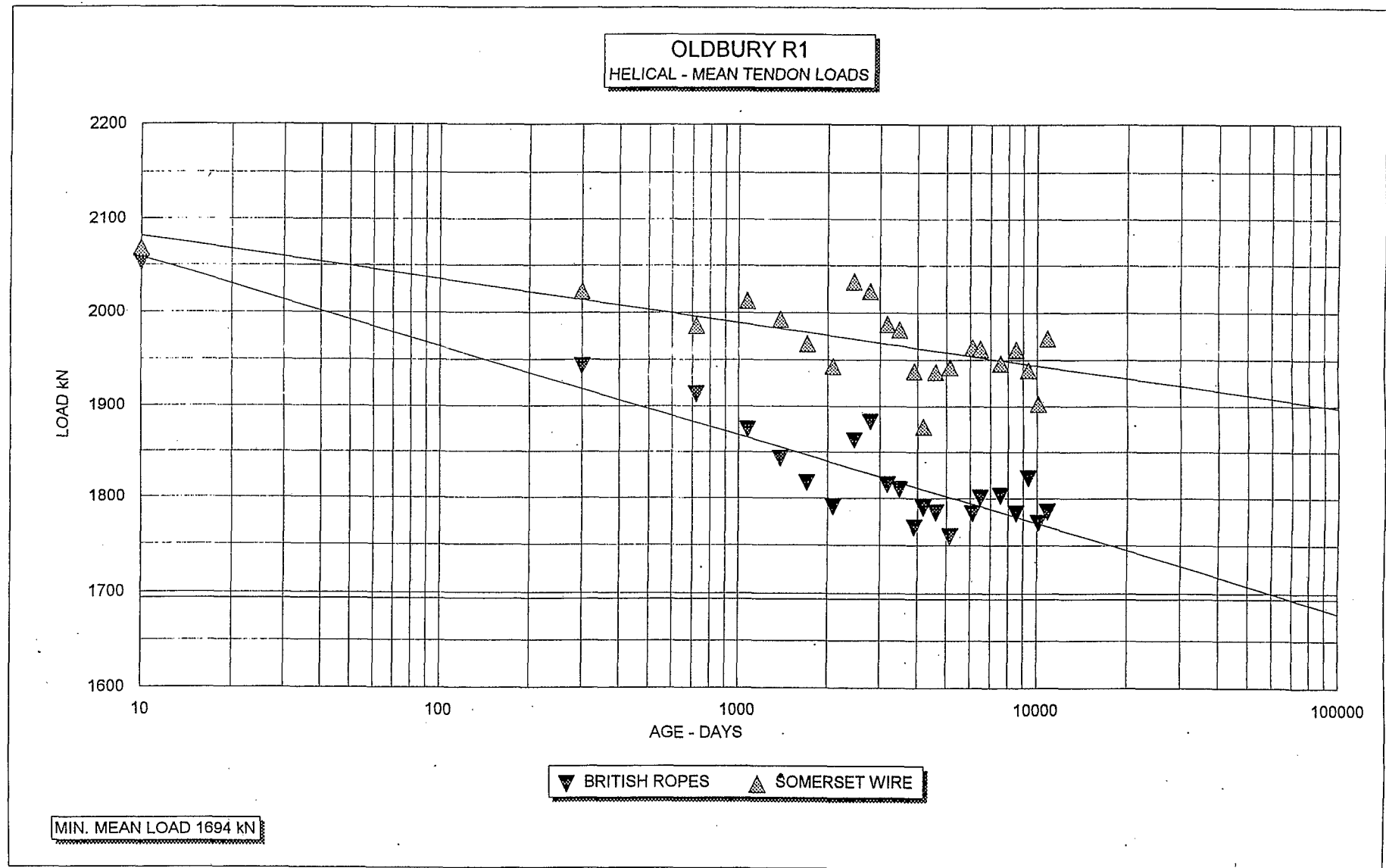
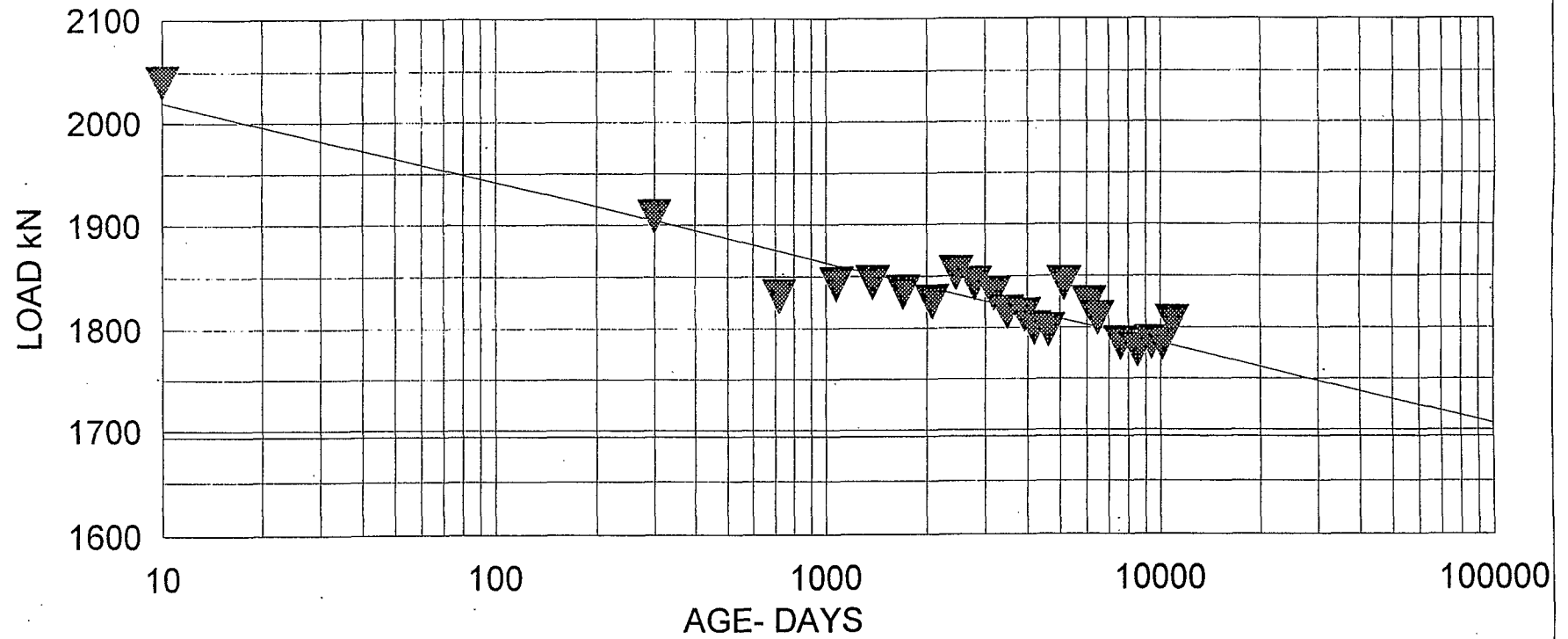


Figure 5

OLDBURY R1
TOP SLAB - MEAN TENDON LOADS



▼ BRITISH ROPES

MIN. MEAN LOAD 1694 kN

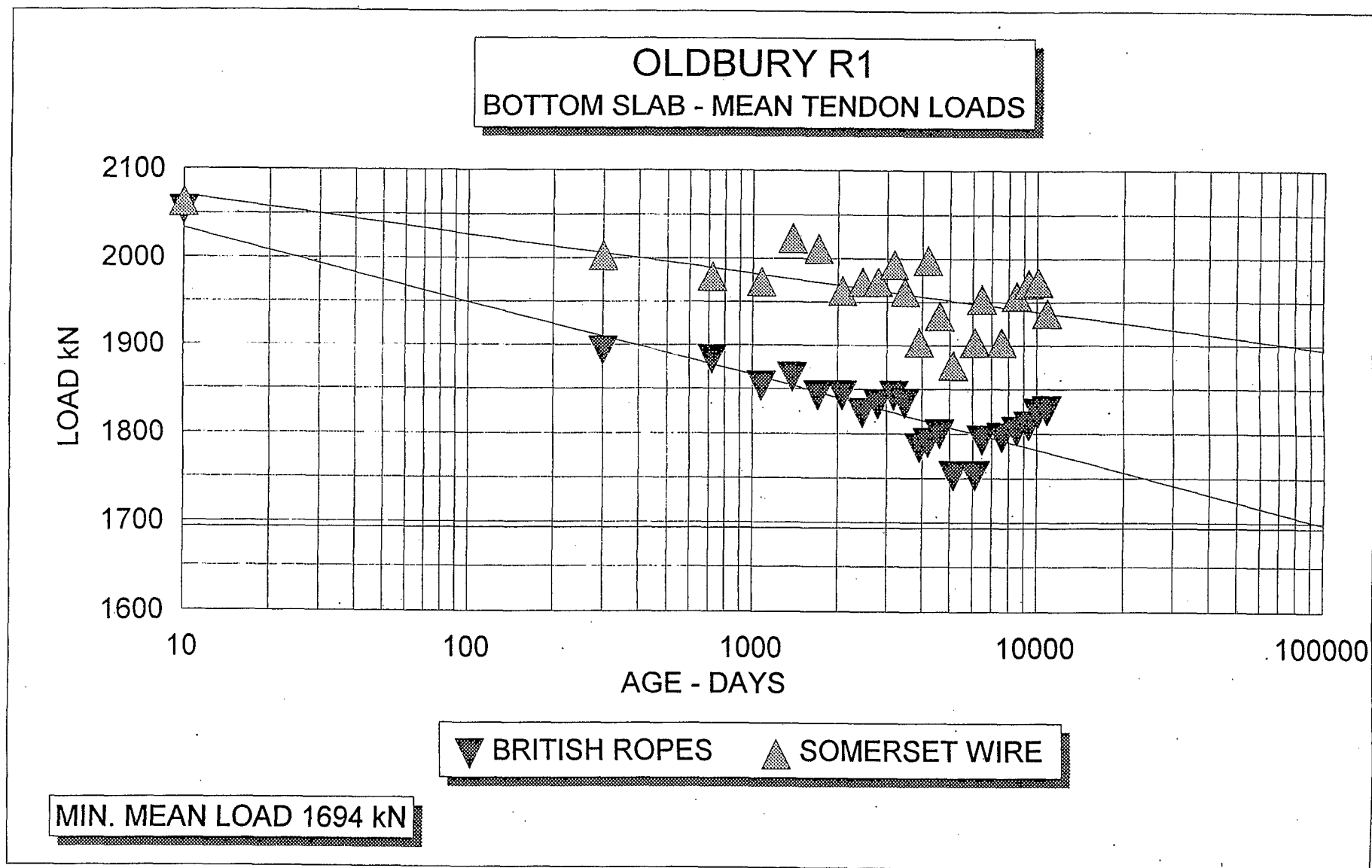
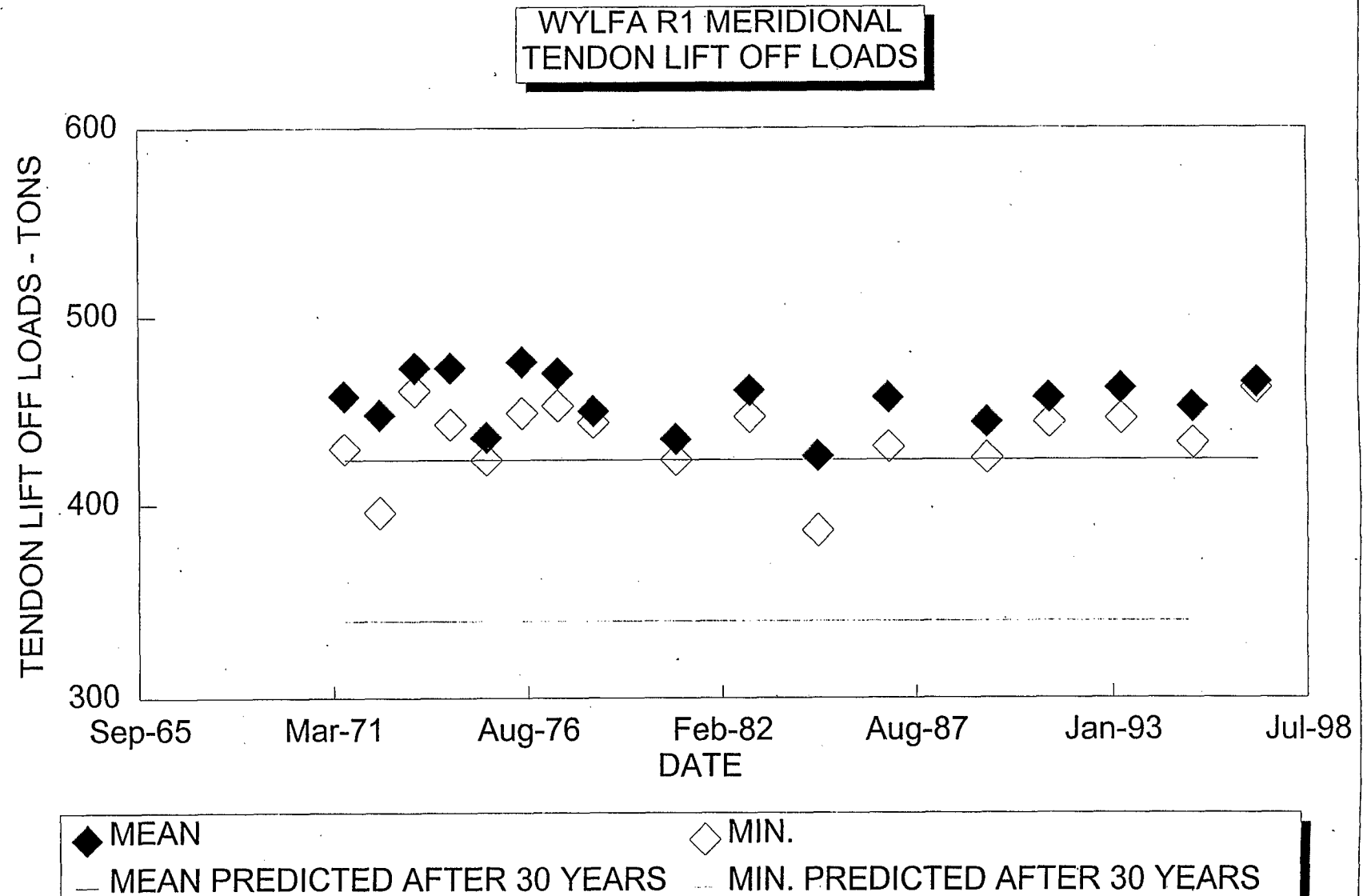
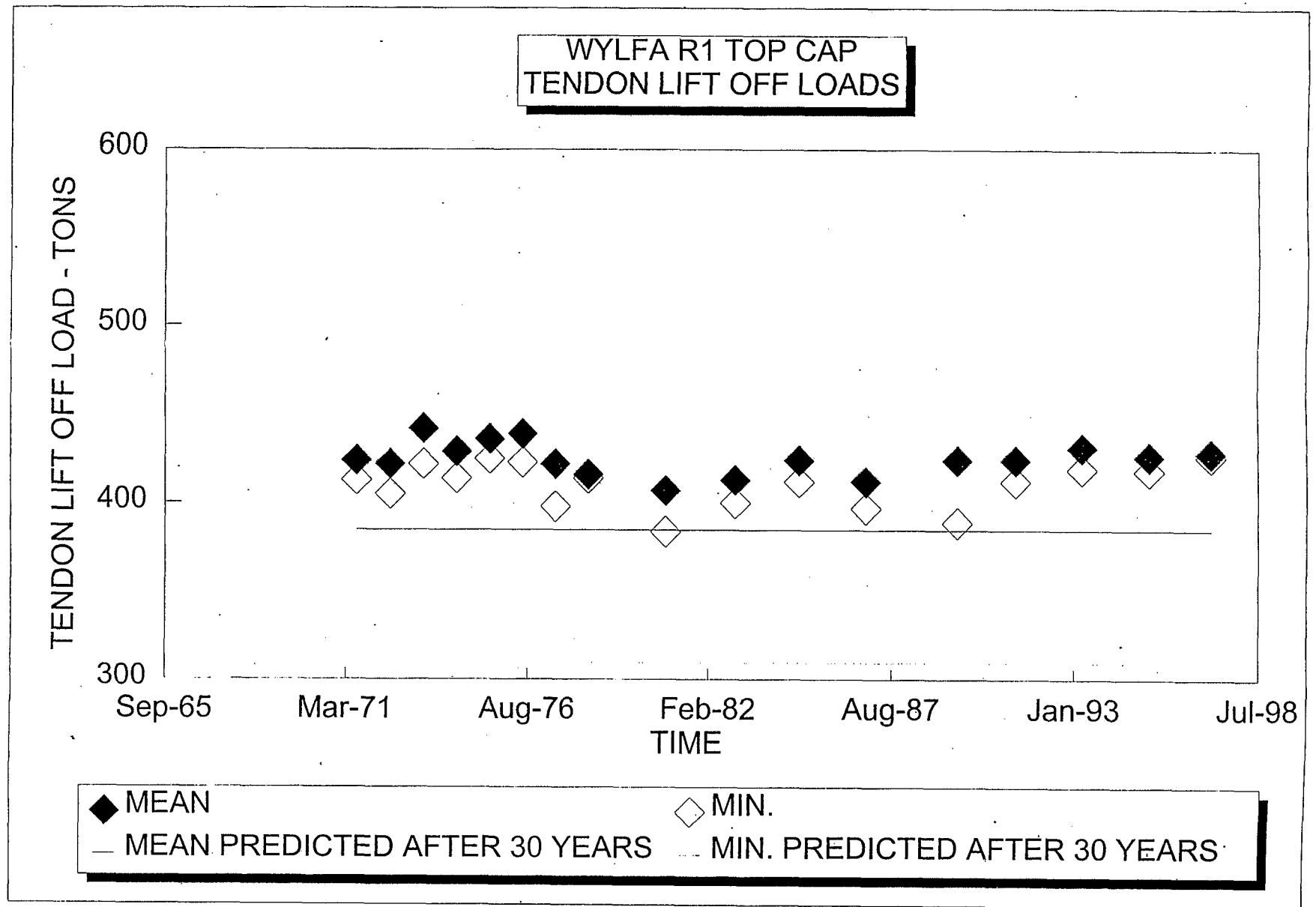
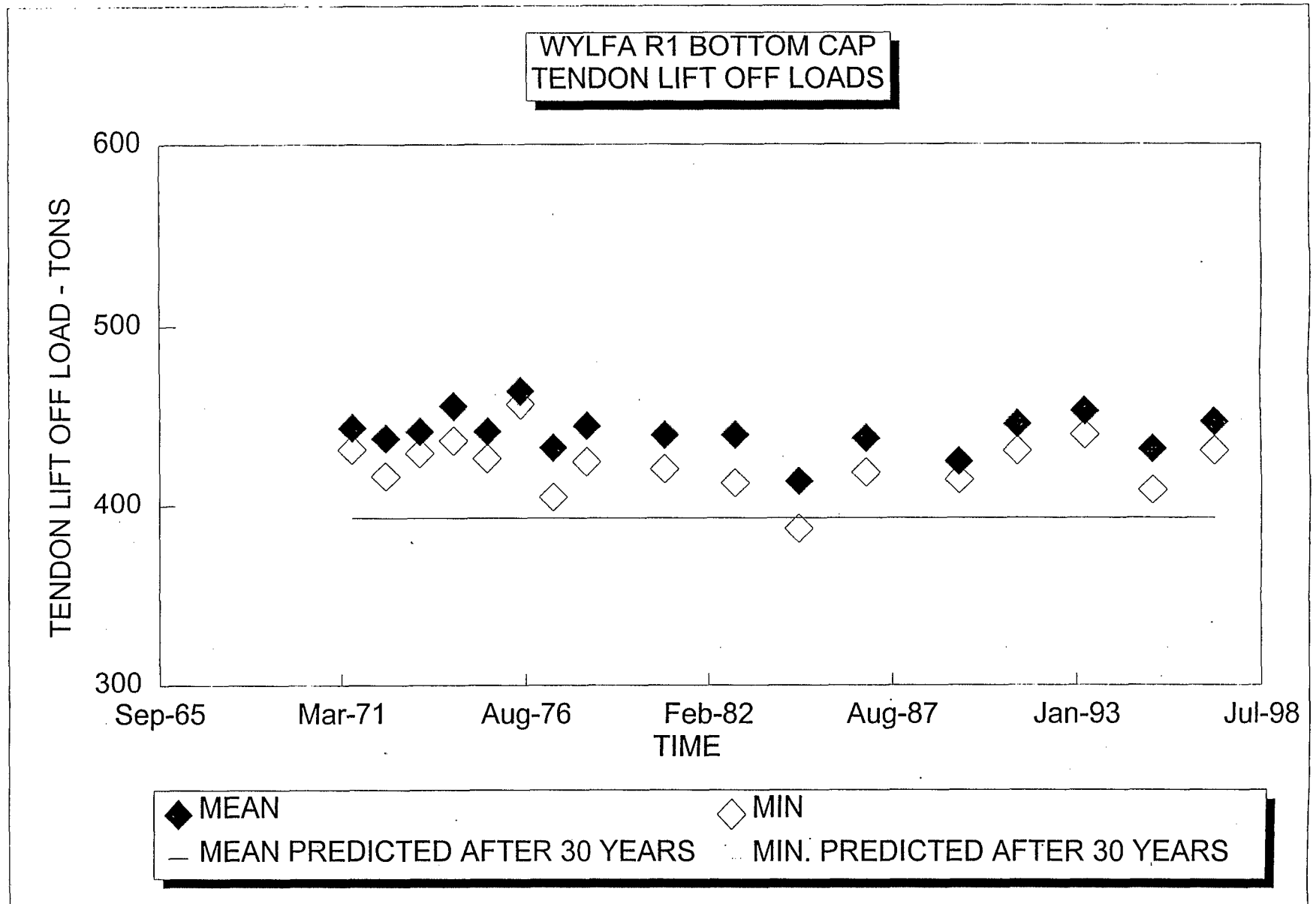
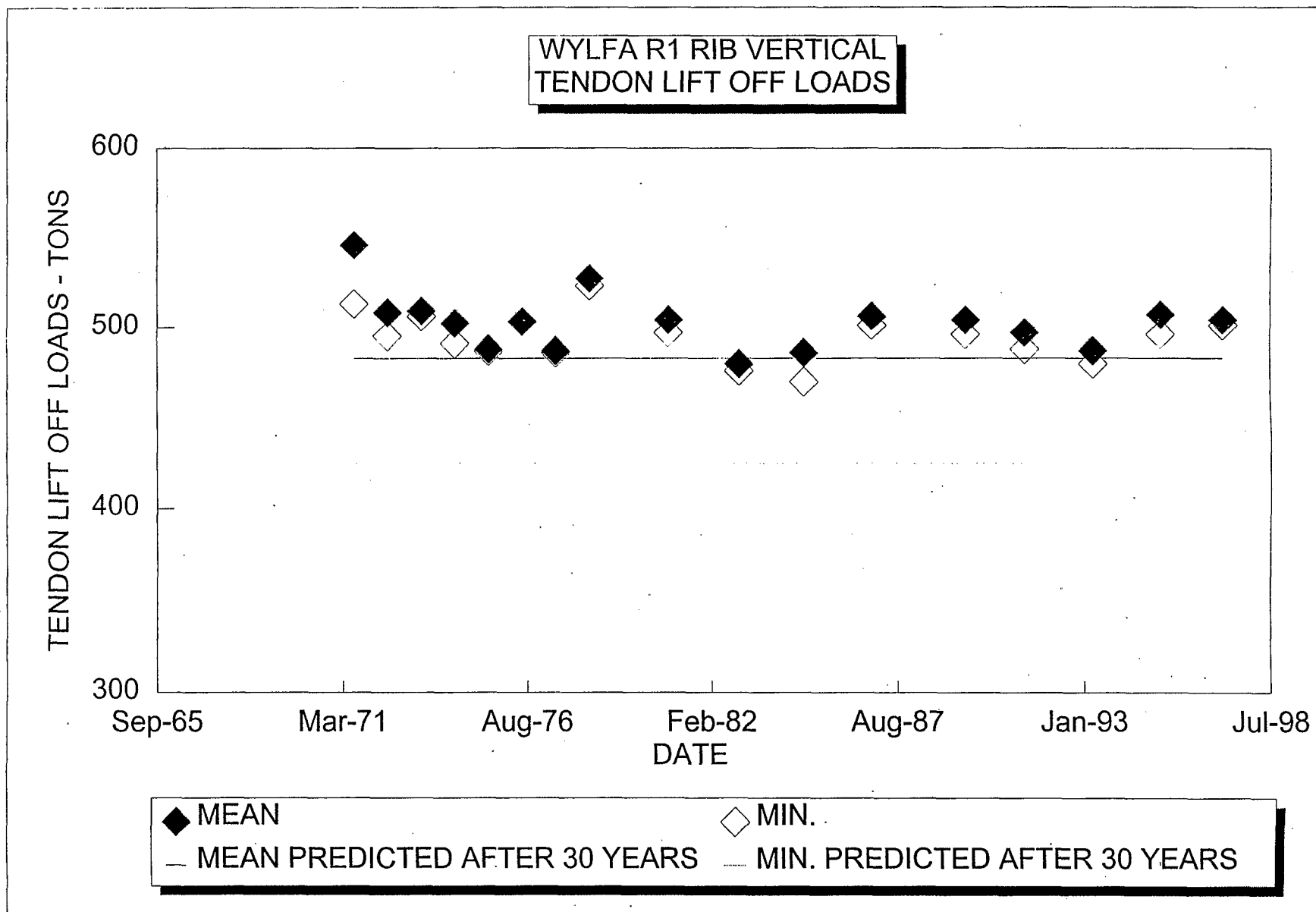


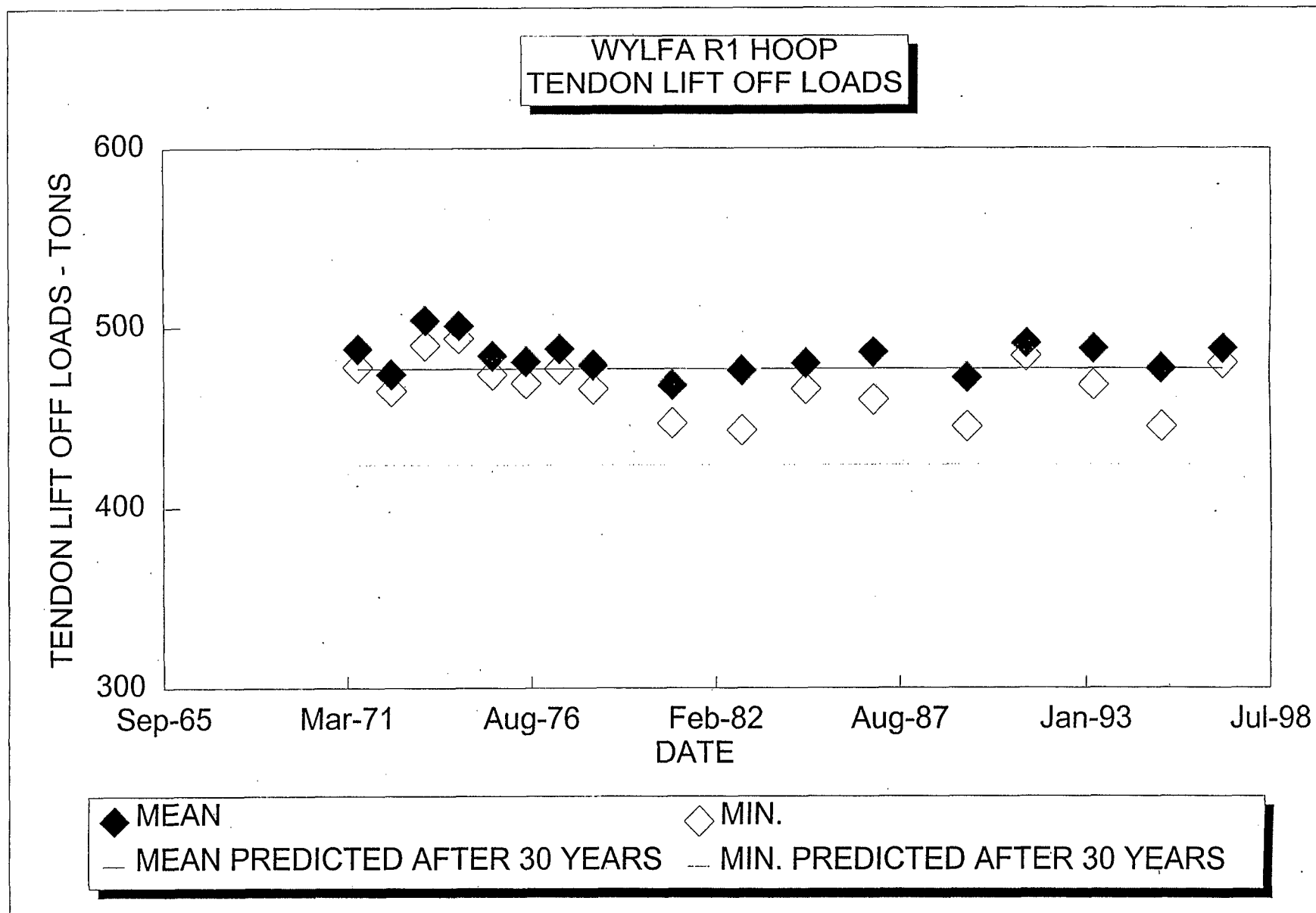
Figure 7



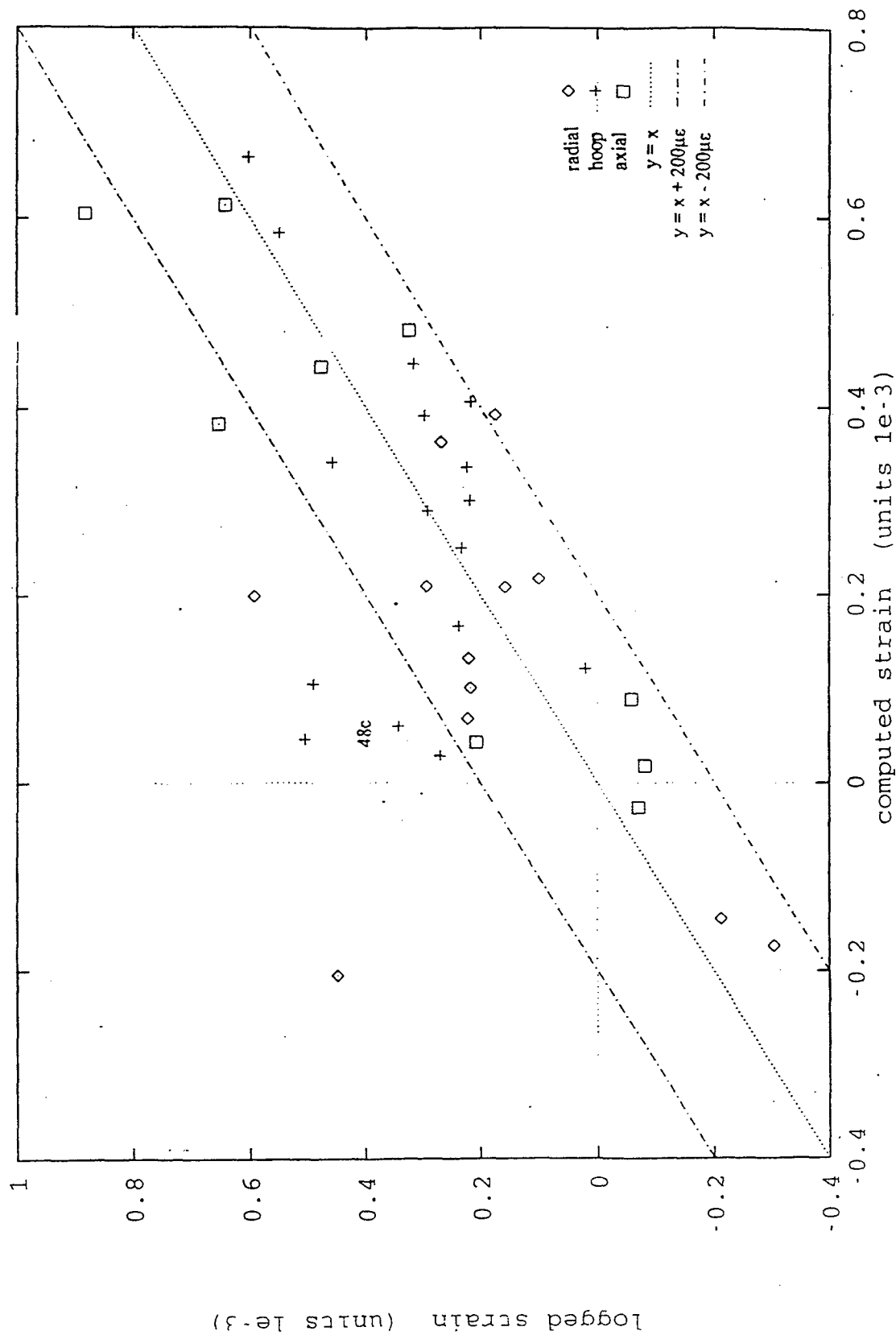








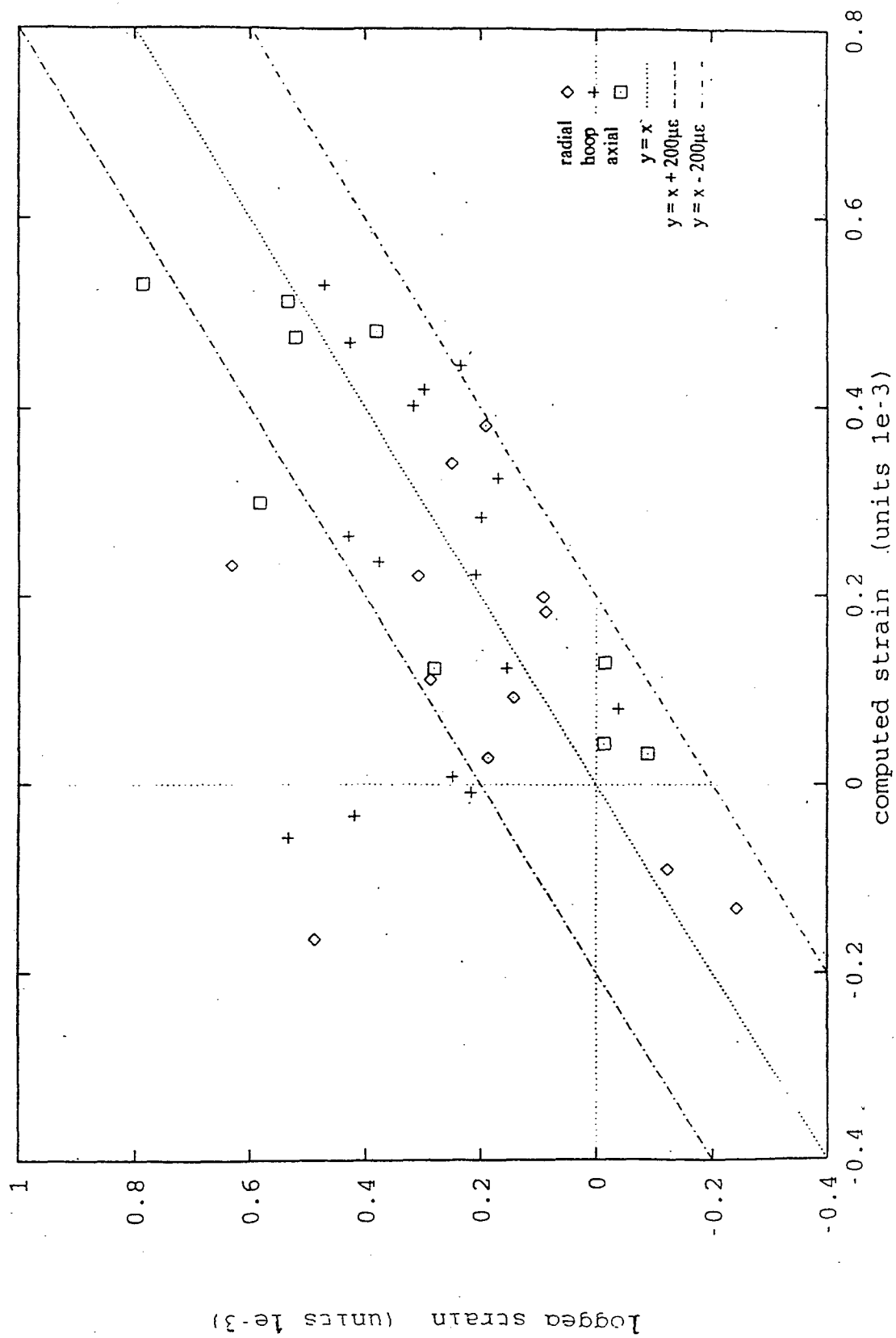
Oldbury



Reactor 1 off-load strains (current operation).

FIG. 13

Oldbury



Reactor 1 on-load strains (current operation).

FIG. 14.

CSNI PRINCIPAL WORKING GROUP No. 3 ON INTEGRITY OF COMPONENTS AND
STRUCTURES

JOINT WANO-PC/OECD-NEA WORKSHOP ON PRESTRESS LOSS IN NPP CONTAINMENTS

Held at Civeaux NPP, Nr. Poitiers, France
25 - 26 August 1997

Hosted by Electricité de France (EDF)

Paper for Presentation:-

**THE MEASUREMENT OF UNBONDED TENDON LOADS
IN PCPV AND PRIMARY CONTAINMENT BUILDINGS**

by

J Irving¹, M S Hinley² & D McCluskey³

¹ Multi Design Consultants Ltd., Stockport, Cheshire, UK
² Multi Design Consultants Ltd., Stockport, Cheshire, UK
³ Scottish Nuclear Ltd., East Kilbride, UK

THE MEASUREMENT OF UNBONDED TENDON LOADS IN PCPV AND PRIMARY CONTAINMENT BUILDINGS

SUMMARY

The Paper describes work undertaken as part of a study conducted for the Licensees of all commercial nuclear generating stations in the United Kingdom. The scope included researching the records of prestressing tendon load measurements held by the Licensees which encompassed 18 prestressed concrete pressure vessels (PCPV) for gas cooled reactors and one primary containment for PWR; the historical record contains more than 300 reactor-years of data.

The main purpose of the study was to assess the validity of specified calibration and measurement techniques used by the Licensees or their contractors to establish jacking and residual anchorage loads in the post construction period. This included existing lift-off measurement techniques such as feeler gauge insertion and displacement transducer systems allied to graphical analysis of jack load versus displacement to determine the residual anchorage load. The second stage was to assess the designer's assumptions regarding long term creep and relaxation effects in the light of all available load checks since construction to determine whether the original design was adversely affected as a result of the current assessment of tendon load distributions.

The Paper includes summaries of the results of the assessment of historical load check data, load measurement methods and derived residual anchorage loads. Conclusions are made regarding the validity of design assumptions for anchorage and residual tendon loads and their implications for future load measurements.

THE MEASUREMENT OF UNBONDED TENDON LOADS IN PCPV AND PRIMARY CONTAINMENT BUILDINGS

by

J Irving, M S Hinley & D McCluskey

1. INTRODUCTION

All the nuclear power stations which are the subject of this Paper were originally constructed and operated by the Central Electricity Generating Board (CEGB) in England and Wales or the South of Scotland Electricity Board (SSEB) in Scotland. Since the privatisation of the electricity supply industry in 1990 there have been several changes in the ownership of individual stations culminating in the separation of nuclear power generation into a government controlled public company, Magnox Electric plc (MEP), responsible for the operation and decommissioning of the nine older gas-cooled magnox reactor stations with a total capacity of about 2.8 GW and a private company, British Energy (BE), acting as the holding company for Nuclear Electric Ltd (NEL) and Scottish Nuclear Ltd (SNL), responsible for the operation of the seven advanced gas-cooled reactor (AGR) stations and the Sizewell B pressurised water reactor (PWR) station. The stations operated by NEL in England and Wales have a total capacity of about 7.8 GW while those operated by SNL in Scotland have a total capacity of about 2.6 GW.

The location, type and date of completion of civil engineering construction of the first prestressed concrete pressure vessel (PCPV) or the prestressed concrete containment (PCC) at each station are shown in Fig. 1. The earlier steel pressure vessel magnox reactor stations operated by MEP are not shown. Apart from Sizewell B, which has a single reactor, all stations have two reactors.

2. DESIGN AND SAFETY CRITERIA

The design criteria for PCPV are embodied in British Standard Specification BS 4975 (Ref. 1). In summary, the criteria require the prestressing system to maintain the concrete structure in a generally compressive state within specified permissible stress limits for all normal operating and frequent fault conditions. In addition, the effects of infrequent and limiting fault conditions and specified hazards must be examined.

To ensure an adequate safety margin over the design gas pressure an ultimate load analysis, supported by scale model tests (typically 1/10th scale), is required to demonstrate that at ambient temperature the vessel can withstand a substantially greater pressure (normally 2.5 times design pressure). In this analysis the steel liner is assumed to remain intact and it is not intended to demonstrate a precise margin against a realistic accident condition. To demonstrate the tolerance of the vessel to liner leakage, a further calculation is required to cover the case of a failed liner where gas pressurisation of cracks in the concrete is assumed but without any heating of the tendons. In this hypothetical situation an ultimate pressure of 1.5 times design pressure is normally required. Periodic monitoring is also required to enable any liner leakage to be detected

The design criteria for PCC were adapted for UK conditions (Ref. 2) from the ASME III Division 2 Boiler and Pressure Vessel Code (Ref. 3). The load cases to be considered, their combination and

factoring are generally similar to ASME III with one important addition, namely, an ultimate load condition similar to that for PCPV. In this case the ultimate load analysis, again supported by a 1/10th scale model test, is required to demonstrate that at ambient temperature the containment can withstand an internal pressure of at least 2.0 times the design pressure.

On completion of construction all PCPVs were required to undergo a proof pressure test (PPT) to a pressure of 1.15 times design pressure which must demonstrate that the structural behaviour is in good agreement with design predictions and that measured strains and deformations show linear responses to pressurisation and depressurisation. A similar test was required for the PCC, known as the structural overpressure test (SOT), to 1.15 times design pressure as well as an integrated leak rate test (ILRT) at the accident pressure in which it must be demonstrated that a leak rate of no more than 0.1% by volume per day can be achieved.

3. PRESTRESSING SYSTEMS

The contractual arrangements for the majority of the period during which PCPVs were constructed in the UK encouraged competition between up to three separate nuclear consortia. The result was that a wide range of designs were built each with unique geometry and different prestressing systems. It is not possible, therefore, in the space allotted for this Paper to illustrate all the design features of the myriad types of vessel and containment in existence. However, the AGR vessels are shown in Figs. 2 and 3 and the remainder will be briefly described below. Details of the prestressing systems employed in each vessel and containment are given in Table 1. All the prestressing systems are post-tensioned and ungrouted with an oil, grease or wax based lubricator and corrosion inhibitor applied during installation of the tendons in their steel lined ducts.

Individual descriptions of each design are given below

3.1. Oldbury on Severn

Each of the two PCPV is a vertical cylinder of prestressed concrete with an internal diameter of 23.5 m and an internal height of 18.3 m. The cylinder wall is 4.6 m thick, and the top and bottom slabs are 6.7m thick. Two principal tendon systems are employed, one helical within the wall thickness, the other horizontal within the end slabs.

In the wall, over the extent of the internal height of the vessel, the helical layers are arranged in balanced clockwise and anti clockwise layers to minimise horizontal torque. The layers are inclined at 45° to the horizontal at the centre of gravity of the tendon system. The idealised path of each tendon is constructed by horizontal and radial projection of the appropriate notional helix on to a barrelled surface within the wall thickness. Over the height of the end slabs the tendons follow straight lines from tangent points to the anchorages. To comply with design requirements 3320 tendons are distributed through 22 circumferential layers leaving 40 spare ducts which were provided in case of construction blockages.

The barrelling provides additional favourable concrete compressive stresses. The tangential tendon sections increase the spacing to accommodate the required anchorage pitch in the top and bottom stressing galleries.

The helical tendon anchorages are set very close to the idealised positions, but in the wall the tendons are required to deviate from their ideal paths to avoid numerous penetrations. The friction losses in the actual structure are therefore higher than would arise in the idealised system.

The 20 and 16 horizontal layers of tendons in the top and bottom slabs emerge normally from the concrete surface and are arranged so that alternate layers are orthogonal. The top slab tendons are deviated to avoid the boiler access openings and the charge and control standpipe penetrations.

The helical tendon anchorages are grouped so that access can be obtained from two permanent stressing galleries, one at the top and one at the bottom anchorage face. Two more circumferential galleries at appropriate levels give access to the horizontal tendon anchorages in the top and bottom slabs.

The entire anchorage is proud of the concrete surface and is arranged so that a specially designed stressing jack can be used at any time to lift the anchorage off the bearing plate without upsetting the grip on the tendon between the male and female cones. A calibrated jack can therefore be used to give a measure of the residual anchorage load and shims can be inserted between the anchorage and the bearing plate to adjust the tendon load in the event of relaxation

3.2. Wylfa

The internal surface of each of the two prestressed concrete pressure vessels is spherical with a diameter of 96 ft (29.3 m). The external surface is generally cylindrical and is stepped at the top and bottom of the vessel to maintain as near as possible a uniform wall thickness. The minimum vessel wall thickness is 11 ft (3.4 m) at the equator and bottom pole of the vessel. At the top pole of the vessel the concrete thickness is increased to 12 ft (3.7 m) to afford a measure of compensation for the high degree of perforation by standpipe penetrations. A series of 16 vertical ribs, each 8 ft (2.4 m) square in plan, is symmetrically disposed around the external cylindrical surfaces to carry the external hoop prestressing tendons and their anchorages. At each position there being one "Main Rib" and, inset above and below this rib, a "Small Rib".

Each vessel is prestressed by 1338 tendons, each having a guaranteed ultimate tensile strength (GUTS) of 820 tonf (8170 kN). The tendons are categorised into five main groups, viz.:-

(1) Top Cap Tendons

An orthogonal small circle system of 218 tendons, in 5 layers, passing through the standpipe zone. These tendons are anchored around the upper surface of the vessel barrel.

(2) Bottom Cap Tendons

A similar orthogonal system of 208 tendons anchored around the lower surface of the vessel barrel.

(3) Meridional Tendons

A "great circle" system of 480 tendons in vertical planes through the vessel barrel, anchored in flat surfaces near the top and bottom of the vessel.

(4) Rib Vertical Tendons

Forming the eighth and outermost layer of the Meridional group of tendons, the 48 rib. verticals pass vertically through the Main Ribs of the vessel to anchor on their top and bottom ends.

(5) Hoop Tendons

An external system of 384 tendons, in approximately horizontal planes, pass through and are anchored onto the vessel ribs. 256 of these tendons pass through the Main Ribs and are therefore known as Main or Large Hoop, the remaining 128 tendons are associated with the inset small ribs and are designated "Small Hoop". Each tendon is anchored on a vessel diameter.

The prestressing system is a development of the Freyssinet 12/0.6 in system, similar to that used at Oldbury but with a refined anchor cone system. Each tendon consists of 36 stabilised strands of 0.6 in (15.2 mm) diameter, which divide at the ends into three cables of twelve strands for separate anchorage against a single anchorage block attached to the face of the vessel. The three pairs of cone anchorages, together with the common anchor block which spans the 'trumpet' at the end of the tendon duct comprise an anchorage assembly.

In general, flexible ducts are provided to house the tendons but horizontal ducts in the ribs are made from rigid mild steel tubes.

3.3. Dungeness B

Each of the two vessels, shown in Fig. 3, is a vertical cylinder of prestressed and reinforced concrete with an internal diameter of 20 m and an internal height of 17.7 m. The cylinder wall is 3.8 m thick, and the top and bottom slabs are 6.2 m and 6.0 m thick.

The prestressing system is the Birkenmaier, Brandestini, Ros and Vogt (BBRV) buttonhead system, manufactured under licence by Simon Carves Ltd. The UK licence for the BBRV system is now held by Multi-BBRV, the sister company of Multi Design Consultants Ltd. There are 384 vertical tendons, 366 circumferential barrel tendons, and 108 circumferential tendons in each of the top and bottom caps

Each prestressing tendon consists of 163 parallel, cold drawn, stress relieved and stabilised steel wires of 0.276 inch (7 mm) diameter. The wires were treated with rust inhibiting coatings during manufacture, and with additional coatings on-site. Each tendon was loaded to nominally 80% of the Guaranteed Ultimate Tensile Strength (GUTS) of 975 tonf (9,715 kN) for a design lock-off load of nominally 75% GUTS, i.e. 731 tonf (7,286 kN). Some circumferential tendons (48 in total) were prestressed to only 16% GUTS as these are designed to contribute solely to the ultimate load capacity of the PCPV.

3.4. Hinkley Point B and Hunterston B

Each of the four PCPV, as shown in Fig. 2, is a vertical cylinder of prestressed concrete with an internal diameter of 18.9 m and an internal height of 19.4 m. The cylinder wall is 5 m thick, the stepped top slab is 5.5/7.1/ 8.5 m thick and the bottom slab 7.5/7.8 m thick. All the prestressing tendons are arranged in a single helical system within the wall thickness.

In the wall the helical layers are arranged in balanced clockwise and anti clockwise layers to minimise horizontal torque. In the wall, over the complete height of the vessel between the top and bottom anchorage surfaces, the tendon geometry is based on notional clockwise and anticlockwise helices which are inclined at 36° 45' to the horizontal at the centre of gravity of the tendon system.

The underside of the vessel base slab which extends beyond the foundation plug contains up to 16 alternately clockwise and anti clockwise circumferential rows of anchorages incorporated into 76 precast concrete beams forming permanent shuttering for the in-situ slab above.

The arrangement of tendons results in their anchorages being grouped so that access to most tendons can be obtained from the two permanent stressing galleries, one at the top and one at the bottom anchorage face.

The anchorage system consists of 7 individual barrel and wedge anchors. The anchors transmit their load to the PCPV concrete through a square bearing plate and a cast steel type trumpet unit connected to a mild steel, seam welded, tendon duct. Detensioning spacers are fitted under each barrel to allow detensioning of individual strands without applying excessive additional load. Every strand can be individually shimmed to increase the residual anchorage load without regripping by the permanent wedges. The central strand is fitted with a dummy barrel to facilitate access.

3.5. Hartlepool and Heysham 1

The vessels, as shown in Fig. 2, have two distinctly different prestressing systems as a consequence of the podded boiler design which precludes the use of circumferential tendons within the walls. The vessels have no major penetrations exiting from the outer face of the walls.

The first or circumferential prestressing system is provided by 0.2 inch (5 mm) diameter high tensile steel wire wound under controlled tension into channels formed in precast units which make up the outer vertical face of the pressure vessels using a winding technique in which up to 35 layers of wire, each about 10 km long, were wound under tension into 20 separate channels encircling the outer face of the wall. Each of the 700 layers is individually anchored at both ends with barrel and wedge anchors. Access to the wire winding channels is somewhat restricted by the framework and removable panels of the mini-annulus insulating screen.

The eight boiler closure unit plugs are circumferentially prestressed using a similar system but with smaller diameter wire.

The second or longitudinal prestressing system comprises 272 tendons each made up of 28 strands of 0.7 inch (18) mm diameter Dyform strand (7 wires per strand) each tendon being contained in a steel duct of 152 mm internal diameter. The tendons have essentially straight paths apart from the inner row of 40 tendons which curve round the bottom corner to anchorages in the base slab soffit. At the tendon anchorages the strands are splayed out and individually anchored by wedges in a bearing plate which transmits the tendon load into a cast steel 'trumpet' which is embedded in the vessel concrete. The anchorages are set at a minimum spacing of 600 mm. The curved tendons are stressed from both ends and the vertical tendons from one end only.

3.6. Heysham 2 and Torness

As shown in Fig. 3, the four vessels at Heysham 2 and Torness are similar to the Hinkley Point B and Hunterston B vessels. The provision of improved internal access to the boilers and a new arrangement of gas baffle necessitated an increase in the internal dimensions from 18.9 to 20.25 metres diameter and from 19.4 to 21.9 metres height. The working pressure was also marginally increased from 3.86/4.14 to 4.15/4.42 N/sq mm. Due in part to these requirements, the number of tendons increased from 2750 at Hinkley/Hunterston to 3744 at Heysham/Torness.

The prestressing system is similar to that at Hinkley B and Hunterston B as described earlier.

3.7. Sizewell B

The primary containment is a prestressed reinforced concrete cylindrical structure with a hemispherical dome lined on the inner surface with mild steel plate of 6 mm thickness. The internal diameter is 45.7 m and the height to the dome springline is 41.76 m. The vertical wall below the springline has a thickness of 1.3 m while the dome roof is 1.0 m thick. The heavily reinforced base slab is not prestressed and is generally 3.85 m deep. The internal design pressure is 0.345 MPa.

Prestress is applied in the meridional direction by 74 'up and over' tendons each of 11,100 kN ultimate load capacity. These tendons are anchored at equal distances on the underside of the base within the annular prestressing gallery, run vertically up the wall and cross the dome on 'small circles' forming an orthogonal pattern. Circumferential prestress is applied by 107 hoop tendons starting near the bottom of the cylinder wall and extending to a 45° angle over the dome. The hoop tendons are anchored on three equi-spaced vertical buttresses at 120° to each other with each tendon passing through 240° between the anchored ends. The tendon pattern is modified as necessary to accommodate the large number of penetrations through the containment wall.

The prestressing system employed is the Freyssinet/PSC 35 K 15, in which each tendon comprises 37 strands of 15.2 mm diameter. Each strand is made up of seven wires compacted and stabilised by heat treatment under tension. Anchorage is achieved by the use of tapered wedges with teeth to grip the strands located in similarly shaped holes in a special bearing plate. The tendons are housed in spirally wound ungalvanised mild steel ducts of 130 mm internal diameter. Corrosion protection is provided by a grease filler which was injected into the tendon ducts on completion of prestressing.

4. MONITORING AND REPORTING PROCEDURES

The Nuclear Site Licence Conditions enforced by the Regulating Authority, HM Nuclear Installations Inspectorate (NII) of the UK's Health and Safety Executive require the owner to undertake monitoring and periodic inspection of each PCPV.

The surveillance programme is carried out on a regular basis, generally at intervals of 14 to 36 months for each vessel. A statement on the structural condition of the vessel has to be provided by a suitably qualified and experienced Chartered Engineer (known as the Appointed Examiner) prior to raising power and prior to reactor start-up following each statutory outage. The minimum programme, as required by Ref. 1, consists of the following items:-

1. tendon load checks to measure residual force at the anchorage;
2. tendon anchorage examinations to detect signs of deterioration;
3. tendon corrosion examinations to detect signs of deterioration;
4. concrete surface examinations to monitor and assess the significance of any cracking and the general condition of the concrete;
5. foundation settlement surveys.

The following are also listed in Ref. 1 as items which may be included in the inspection report for supporting information:-

- (a) survey of readings of vibrating wire strain gauges embedded in the concrete and their correlation with theoretical predictions;

- (b) survey of vessel concrete and liner temperature readings and their compliance with the operating rules for the vessel;
- (c) main reactor coolant leakage summaries;
- (d) PCPV deflection surveys, if carried out;
- (e) a review of operating history for the period under consideration.

The Station Maintenance Schedules incorporate all the items listed above as well as a requirement to review instances of pressure vessel cooling water leakage emanating from within the PCPV (e.g. from pipework embedded in the concrete).

The great benefit of the statutory requirements outlined above is that the Appointed Examiner reports provide an excellent and detailed source of data on the performance of unbonded prestressing systems over a period of nearly 30 years. Indeed, the majority of the results which are presented in this Paper are extracted from Appointed Examiner reports and their supporting documentation.

Similar arrangements exist for the PCC at Sizewell B but, since the Licensing Conditions require the plant to be licensable in its country of origin (the USA), the surveillance programme is based closely on the requirements of ASME XI (Ref. 4) so there are some differences in the criteria from those in place for PCPV.

Ageing management is therefore achieved through the application of Maintenance Schedules drawn up for each station defining the requirements and responsible persons for regular inspections, "walk-downs", testing, assessment and reporting. Tendon load measurement and corrosion examinations are the principal items in the programme for ensuring that each vessel continues to be fit for service.

4.1. Tendon Load Measurement

The residual anchorage load is measured using the jack to apply steadily increasing load to the free end of the tendon until the anchorage component 'lifts off' the bearing surface. The method of detecting the lift off point, hence the associated residual anchorage load, varies from system to system. A summary of the procedures employed on each vessel is given in Table 2.

The results of the residual anchorage load checks are assessed against the level of force, as determined by the design analysis, required to ensure that stresses and deformations of the vessel and its components remain within the minimum permissible service levels defined by the applicable codes, specifications and standards. For the purpose of the Paper, this is referred to as the minimum design level of average residual anchorage load.

4.2. Tendon Examinations

A number of tendons are destressed and strands extracted for examination and testing to determine the condition of the tendons in terms of corrosion attack, material and mechanical property deterioration or damage.

The results are assessed in terms of the design requirements for a minimum ultimate load capacity against increasing internal pressure. In the case of corrosion, particularly surface pitting attack, the extent and depth of any pits found on withdrawn strands are assessed against permissible limits determined from extensive laboratory testing of strand and wire with natural and artificially induced surface defects.

The permissible levels are set conservatively for PCPVs with a history of tendon corrosion identified during their construction period. By using sampling statistics to determine the probable population density and extremes of corrosion in the tendons based on the evidence accrued from successive examinations, assurance can be obtained that the safety margins represented by the ultimate load factor are not jeopardised.

5. RESULTS OBTAINED FROM THE MONITORING PROGRAMME

The results obtained from tendon residual load monitoring are illustrated in Figs. 4 to 13 for the first completed PCPV at each station and the Sizewell B PCC. The graphs are based on the mean of all anchorage lift-off load checks undertaken on the vessel at each periodic examination. The ratio of the sample mean residual load to the maximum initial load at prestress is plotted against elapsed time in days from the mean date of prestressing operations. Each graph shows the minimum design anchorage load as defined in Section 4.1 above. Notable features of the results are discussed below.

The longest record is that from Oldbury covering over 27 years of operation as shown in Fig. 4. This is the only station with two different types of prestressing material; stress relieved from British Ropes (BR) and low relaxation from Somerset Wire (SW). The latter type of low relaxation steel has been employed, from various manufacturers, on all subsequent vessels. It is clear that the low relaxation material has superior relaxation properties with residual loads remaining above 88% of initial load compared to 84% for the stress relieved material.

The Hunterston B vessel was subject to reshimming operations to increase prestressing loads at the top anchorages in 1977 and this is evident from the results shown in Fig. 8 before 1200 days and after 1500 days.

The results for Hartlepool and Heysham 1 shown in Figs. 9 and 10 respectively are based on a re-assessment of applied jack loads. It was discovered in 1987 that the jacking force indicated by the then primary method of measurement, the load cell mounted within the rear of the jack, was not in agreement with the force indicated by the hydraulic pressure on the ram. Although the load cell calibrated within specification (plus or minus 1%) when tested off the jack, the indicated load when mounted in the jack was of the order of 15% higher than that actually applied as calculated from the hydraulic pressure times ram area. As a result all previous prestressing and load checking operations were reassessed based on the recorded hydraulic pressures and the applicable procedures for all further prestressing operations now use jack pressure as the primary load measurement system.

The data from all stations were combined to provide the summary graphs shown in Figs. 14 and 15. A least squares regression analysis of the residual load ratio versus log of time in days gave the best fit and 95% two tailed confidence limits shown in both the figures. It can be seen that the data are remarkably consistent and that, with reasonable confidence the 10,000 day residual load should lie between about 80% and 90% of the maximum initial prestressing anchorage load. This is in line with design predictions.

Reference back to Figs. 4 to 13 demonstrates that residual anchorage loads remain above the minimum design loads for each vessel.

6. PROBLEMS RELATED TO PRESTRESSING

Few major problems have been encountered with prestressing systems. Concerns have arisen from pitting corrosion encountered during the construction phase caused by storage of made up tendons on site for lengthy periods under conditions of high humidity and a marine salt atmosphere. Where such corrosion was found the affected tendons were replaced with new material. Efforts have also been made, on the basis of research and experience, to use suitable corrosion inhibiting treatments and protective greases or waxes combined with ensuring a low humidity environment (<65% RH) within the prestressing ducts during construction and operation of the vessels.

Anchorage examinations have revealed a small number of instances of missing and cracked buttonheads or slippage of Freyssinet anchorages which have been disturbed by destressing, replacement of strands and restressing. During in-service inspections, wire breaks have occurred occasionally close to the anchorage when load checking or when regripping strand to destress a tendon.

An unusual number of strand breakages occurred during routine testing of materials prior to installation in the Heysham 2 and Torness PCPVs. These were diagnosed as brittle fractures in some batches of material delivered to site. As a result, samples from each batch of strand were subjected to testing prior to threading into the tendon ducts. Subsequent in-service inspections have not revealed a higher than expected incidence of wire or strand breakages.

The data obtained from periodic load checking has confirmed that the design predictions of losses due to creep of concrete, steel relaxation and thermal effects were conservative. The predictions of creep and relaxation were based on experimental data required under the specification. Considerable additional theoretical analysis and laboratory testing were undertaken by the CEBG and its successor companies which supplemented that supplied by the contractors as part of the original contract and served as supporting information for beyond design basis studies of PCPV and PCC behaviour.

Unexpectedly low residual loads have been found at the top anchorages of the Hinkley B and Hunterston B PCPVs. Where appropriate, reshimming to the initial maximum anchorage load has been undertaken. However, as discussed and illustrated in Sections 4 and 5 above, the residual anchorage loads on all vessels have remained above the design minimum load.

Some problems have been encountered with load measurement and calibration of jacks for high capacity (>8,000 kN) multi-strand systems. These were dramatically brought to light during periodic load checking of the Hartlepool and Heysham 1 PCPVs. After a painstaking and lengthy investigation it was concluded that the load cells incorporated in the jacks gave false (high) indications of the true load being applied by the jack based on calibrations of the load cells on certified test machines after removal from the jacks.

The solution was to reassess past prestressing and load check operations based on the recorded jack hydraulic pressure and ram area, allowing for friction losses determined by testing the complete jack-load cell-anchorage-tendon system on a test rig.

Calibration rigs had already been employed at other stations, notably Wylfa, Oldbury and Dungeness B where few problems have arisen other than the need to upgrade instrumentation and methods. It is under consideration that the methods used at the latest station, Sizewell B, should change over to using jack pressure as the primary method of load measurement with secondary confirmation provided by the jack load cell.

7. RESEARCH AND DEVELOPMENT

Under the same overall programme as the study reported here, research work has been undertaken on the performance of the corrosion protection applied to prestressing tendon strand. This included a review of the systems used and an assessment of their performance in typical environments. It was concluded that tendons which remained dry would not suffer degradation due to corrosion. The extent of any corrosion on tendons which had been wetted would depend on the exposure duration, water chemistry and the corrosion protection which had been applied. A current project involves sampling and testing service-aged corrosion protection materials to confirm their continued satisfactory performance. The samples are obtained from the tendons withdrawn from the PCPVs during the statutory inspections described earlier. Another current project is investigating the creep behaviour of prestressing steel at temperatures in the range 160 °C to 200 °C.

Work has been carried out in the past for CEGB and NEL on the creep of prestressing steel at temperatures from 200 °C to 260 °C, investigating the creep behaviour and failure of the wire. This work supported studies into the effects of reactor coolant gas coming into contact with prestressing tendons under fault conditions.

Corrosion of prestressing tendons is a potential problem area which is monitored. Examinations of tendons withdrawn from operating PCPVs have revealed no significant instances of corrosion. Studies on this subject have been carried out in the past, determining the effect of corrosion on load capacity and mechanical properties of prestressing tendon steel. At present, no further research work is being undertaken on this topic.

8. CONCLUSIONS

The performance of the unbonded post tensioned prestressing systems in eighteen PCPVs and the single PCC designed, constructed and operated in the United Kingdom over the last 30 years has generally been excellent and has met the requirements of the relevant codes and standard specifications.

A number of isolated incidents have occurred in which shortcomings have been found in the mechanical performance or material condition of components but these have not affected either the serviceability or the safety of the vessel concerned.

In general, apart from the small number of exceptions noted, the design predictions of loss of prestressing force have been found to be conservatively overestimated when compared to measurements of residual anchorage load. Analysis of the results presented in this paper shows that the reduction in residual load is proportional to the logarithm of time. At an elapsed time of 10,000 days after initial prestress, the mean residual anchorage load can be expected, with 95% confidence, to lie between about 80% and 90% of the maximum initial anchorage load.

Experience has shown that load measurement using load cells built into the jacks of high capacity (>8,000 kN) multi-strand systems may be unreliable even where off-jack load cell calibrations indicate good accuracy. It has been found that calibration of load measurement in these cases is best carried out using a test rig and that the primary measurement should be derived from the hydraulic pressure and jack ram area with the load cell acting as a secondary confirmation of measured load.

ACKNOWLEDGEMENTS

The Authors wish to thank Nuclear Electric Ltd, Scottish Nuclear Ltd and Magnox Electric plc for permission to publish this Paper.

REFERENCES

1. British Standards Institution 1990 "BS Specification for Prestressed Concrete Pressure Vessels for Nuclear Engineering". BSI London. BS 4975:1990.
2. Davies D R, Richardson C & Roberts A C 1995 "Power Station Design". Proc. Inst. Civ. Engrs., Sizewell B Power Station Supplement to Civil Engineering, Vol. 108, Special Issue 1, Feb. 1995.
3. ASME 1985 "The ASME Boiler and Pressure Vessel Code". Section III, Rules for Construction of Nuclear Power Plant Components.
4. ASME 1992 "The ASME Boiler and Pressure Vessel Code". Section XI, Sub-Section IWL, Requirements for Class CC Concrete Components of Light-Water Cooled Plants.

TABLES

1. Details of prestressing systems.
2. Methods of anchorage residual load measurement

FIGURES

1. Locations of UK nuclear power stations with PCPV or PCC.
2. Plans and sectional elevations of Hartlepool (& Heysham 1) and Hinkley Point B (& Hunterston B).
3. Plans and sectional elevations of Heysham 2 (& Torness) and Dungeness B.
4. Oldbury PCPV R1 - Residual anchorage loads.
5. Wylfa PCPV R1 - Residual anchorage loads.
6. Dungeness B PCPV R21 - Residual anchorage loads.
7. Hinkley Point B PCPV R3 - Residual anchorage loads.
8. Hunterston B PCPV R3 - Residual anchorage loads.
9. Hartlepool PCPV R1 - Residual anchorage loads.
10. Heysham 1 PCPV R1 - Residual anchorage loads.
11. Heysham 2 PCPV R7 - Residual anchorage loads.
12. Torness PCPV R1 - Residual anchorage loads.
13. Sizewell B PCC - Residual anchorage loads.
14. Summary of all PCPV & PCC data against log(time).
15. Summary of all PCPV & PCC data against time.

Station	Prestressing System Supplier	Anchorage Type	Tendon Type	Wire/Strand Type		Tendon Layout		Tendon Strength [GUTS or CUTS]	Remarks
				Supplier	Material Type	Group	Number of Tendons		
Oldbury-on-Severn	PSC	Freyssinet	12 No. 0.6 in ϕ 7-wire strand	British Ropes (85% of total)	Stress Relieved	Top Slab Wall Helical Btm Slab	600 3320 474	273 ton (2720 kN)	Single Cavity Magnox Reactor Vessel
				Somerset Wire (15% of total)	Low Relaxation Stabilised	Total	4394		
Wylfa	PSC	Freyssinet	3 x 12 = 36 No. 0.6 in ϕ 7-wire strand	Somerset Wire	Low Relaxation Stabilised	Top Slab Meridional Hoop Rib Vertical Btm Slab	218 480 384 208	820 ton (8170 kN)	Single Cavity Magnox Reactor Vessel
						Total	1338		
Dungeness B	BBRV	Buttonhead	163 No. 0.276 in ϕ parallel wires	Johnson & Nephew	Low Relaxation Stabilised	Top Slab Wall Hoop Wall Vertical Btm Slab	108 342 384 108	975 ton (9715 kN)	Single Cavity AGR Vessel
						Total	942		
Hinkley Point B & Hunterston B	CCL	Individual Strand Barrel & Cone Wedge	7 No. 0.7 in ϕ 7-wire Dyform strand	Bridon	Low Relaxation Stabilised	Helical	2750 & 2816	260 ton (2581 kN)	Single Cavity AGR Vessel
						Total	2750 & 2816		
Hartlepool & Heysham 1	Longitudinal - CCL	Multistrand Cone Wedges in Bearing Plate	28 No. 0.7 in ϕ 7-wire Dyform strand	Bridon	Low Relaxation Stabilised	Vertical in Wall	272	1040 ton (10,360 kN)	Multi Cavity AGR Vessel with Podded Boilers
	Circumferential - TWC Wire Wound System	Individual Layer Barrel & Cone Wedge	Each layer is 31,900 ft (9,730 m) of 0.2 in ϕ wire wound on at 119/120 turns per layer	Johnson & Nephew	Low Relaxation Stabilised	External wall surface has 20 channels each with 33/35 layers	Total No. of Layers is at least 700 per vessel	3.46 ton (34.4 kN) each wire	
Heysham 2 & Torness	CCL	Individual Strand Barrel & Cone Wedge	7 No. 18 mm ϕ 7-wire Compact strand	GKN	Low Relaxation Stabilised	Helical	3744	2660 kN (267 ton)	Single Cavity AGR Vessel
						Total	3744		
Sizewell B	PSC	Multistrand Cone Wedges in Bearing Plate	37 No. 15.2 mm ϕ 7-wire Compact strand	Somerset Wire	Low Relaxation Stabilised	Vertical Hoop	74 107	11,100 kN (1151 ton)	Cylindrical, hemispherical domed PWR primary containment
						Total	181		

Note: GUTS = Guaranteed Ultimate Tensile Strength CUTS = Characteristic Ultimate Tensile Strength

Table 1 - Details of Prestressing Systems

Station	System Supplier	Load Measurement and Maintenance	Lift-off Detection Technique	Primary Load Measurement System	Secondary Load Measurement System	System Calibration Method
Oldbury-on-Severn	PSC	Lifting of complete cone pair Insertion of shims between female cone and bearing plate	Feeler gauge insertion	Jack ram pressure	None	Calibration rig with short tendon length and jack assembly
Wylfa	PSC	Lifting of complete cone pair Insertion of shims between female cone and bearing plate Carried out simultaneously with three jacks, one on each anchorage	Graphical method using displacement transducers	Jack ram pressure	Instrumented shimming feet	Calibration rig with short tendon length and jack assembly
Dungeness B	BBRV	Lifting of anchorage assembly block Insertion of shims under pull ring	Graphical method using displacement transducers	Strain meter on jack pulling rod	Jack ram pressure	Calibration rig with short tendon length and jack assembly
Hinkley Point B & Hunterston B	CCL	Lifting of barrels from bearing plate using single strand jack Insertion of shims under wedge barrel	Feeler gauge insertion	Jack load cell	Jack ram pressure	Load cell assembly on single strand
Hartlepool & Heysham 1	Longitudinal - CCL	Lifting of bearing plate from anchorage using multi-strand jack Insertion of shims under bearing plate	Graphical method using displacement transducers	Jack ram pressure	Load cell in jack	Calibration rig with short tendon length and jack assembly
	Circumferential - TWC Wire Wound System	Load cells under saddle in built-in change of load cell unit on three channel windings	Not applicable	Removable load cell	G String devices	Full scale mock up during design phase
Heysham 2 & Torness	CCL	Lifting of barrels from bearing plate using single strand jack Insertion of shims under wedge barrel	Feeler gauge insertion	Jack load cell	Jack ram pressure	Load cell assembly on single strand
Sizewell B	PSC	Lifting of complete anchorage Insertion of shims between anchorage and bearing plate	Graphical method using displacement transducers	Load cell in jack	Jack ram pressure	Jack assembly calibrated in laboratory test house machine Change of primary measurement system under consideration

Table 2 - Methods of Anchorage Residual Load Measurement

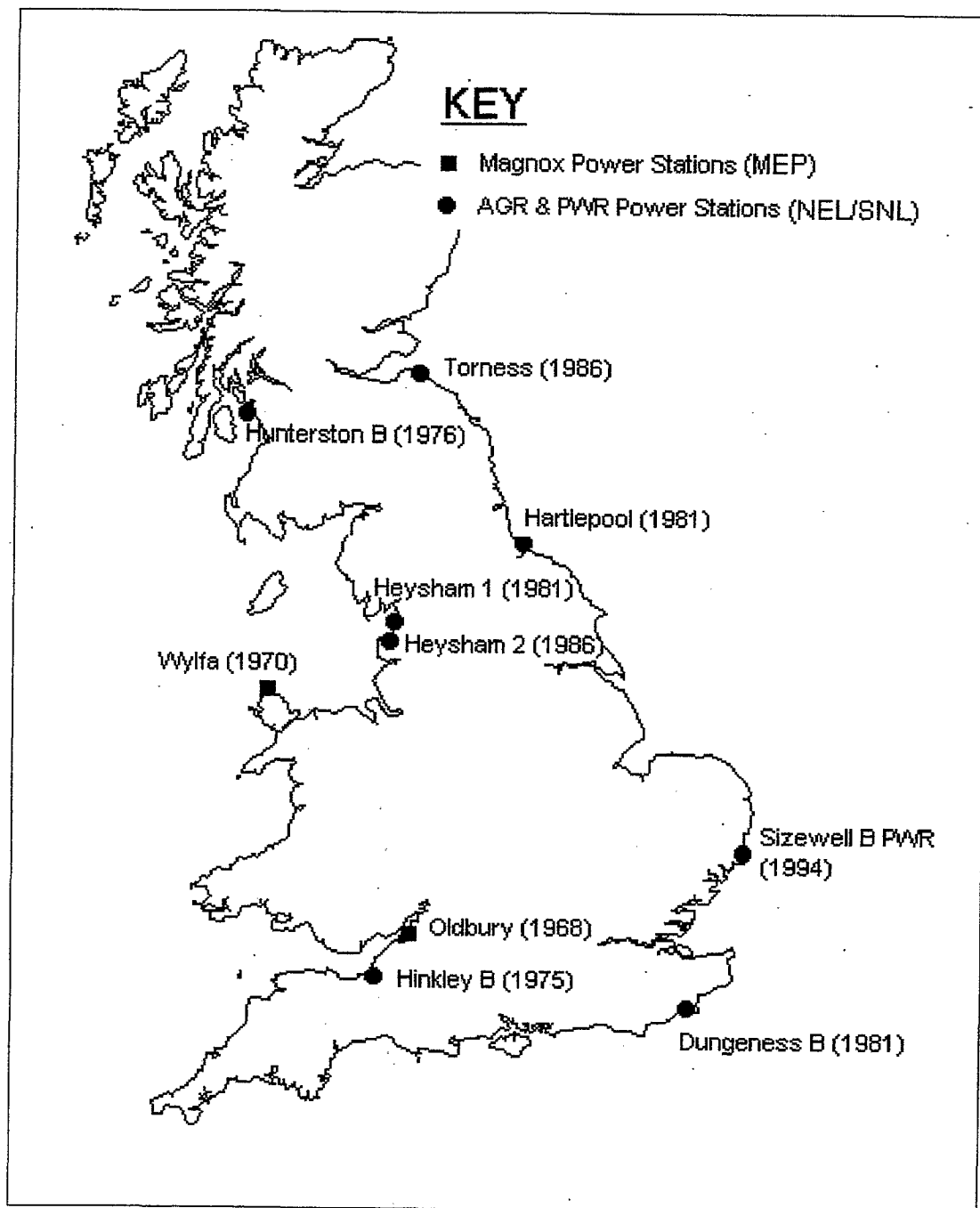


Figure 1 - Locations of UK nuclear power stations with PCPV or PCC.
 Date of completion of civil construction given in brackets ()

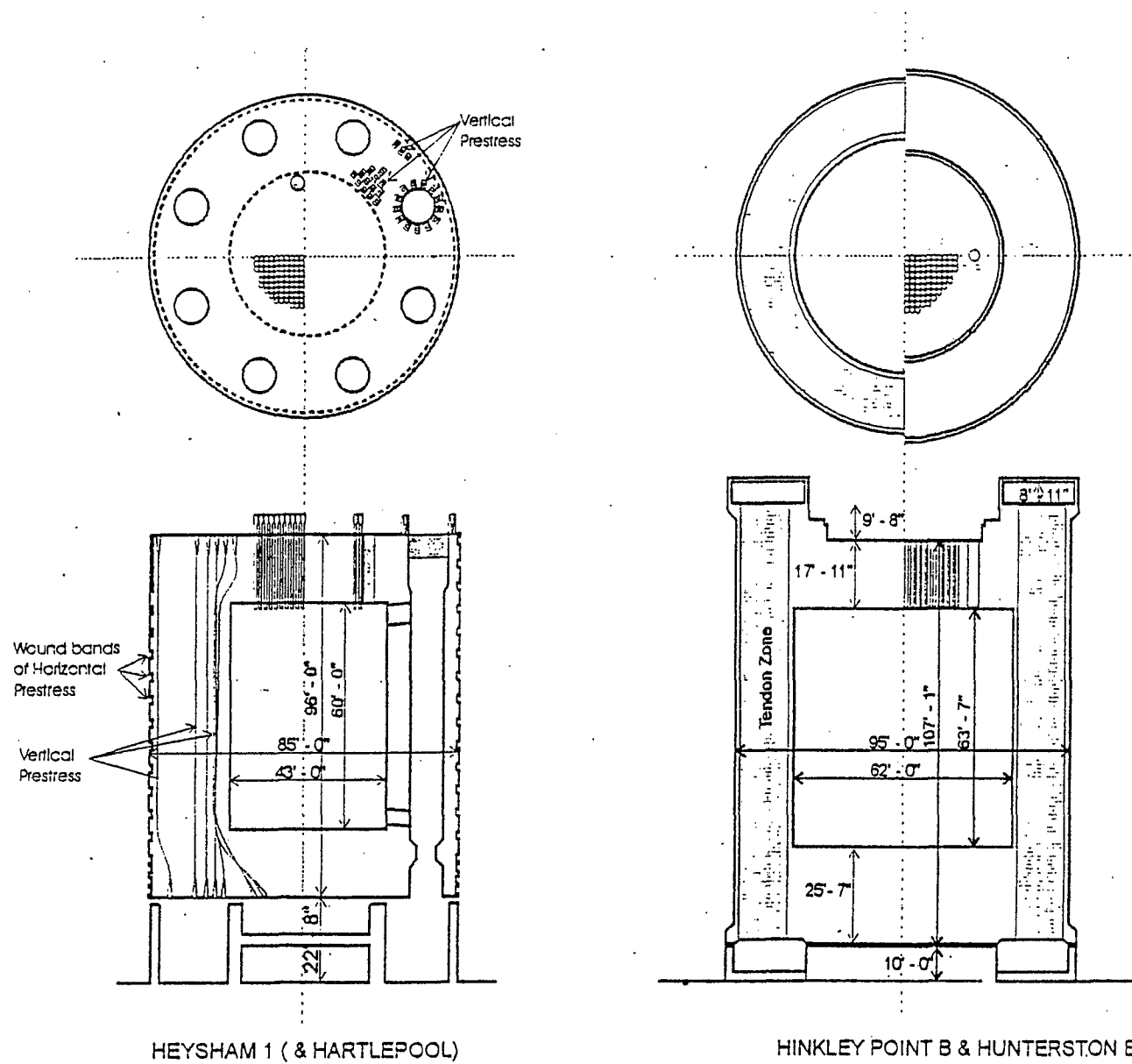


Figure 2 - Plans and sectional elevations of Hartlepool (& Heysham 1) and Hinkley Point B (& Hunterston B)

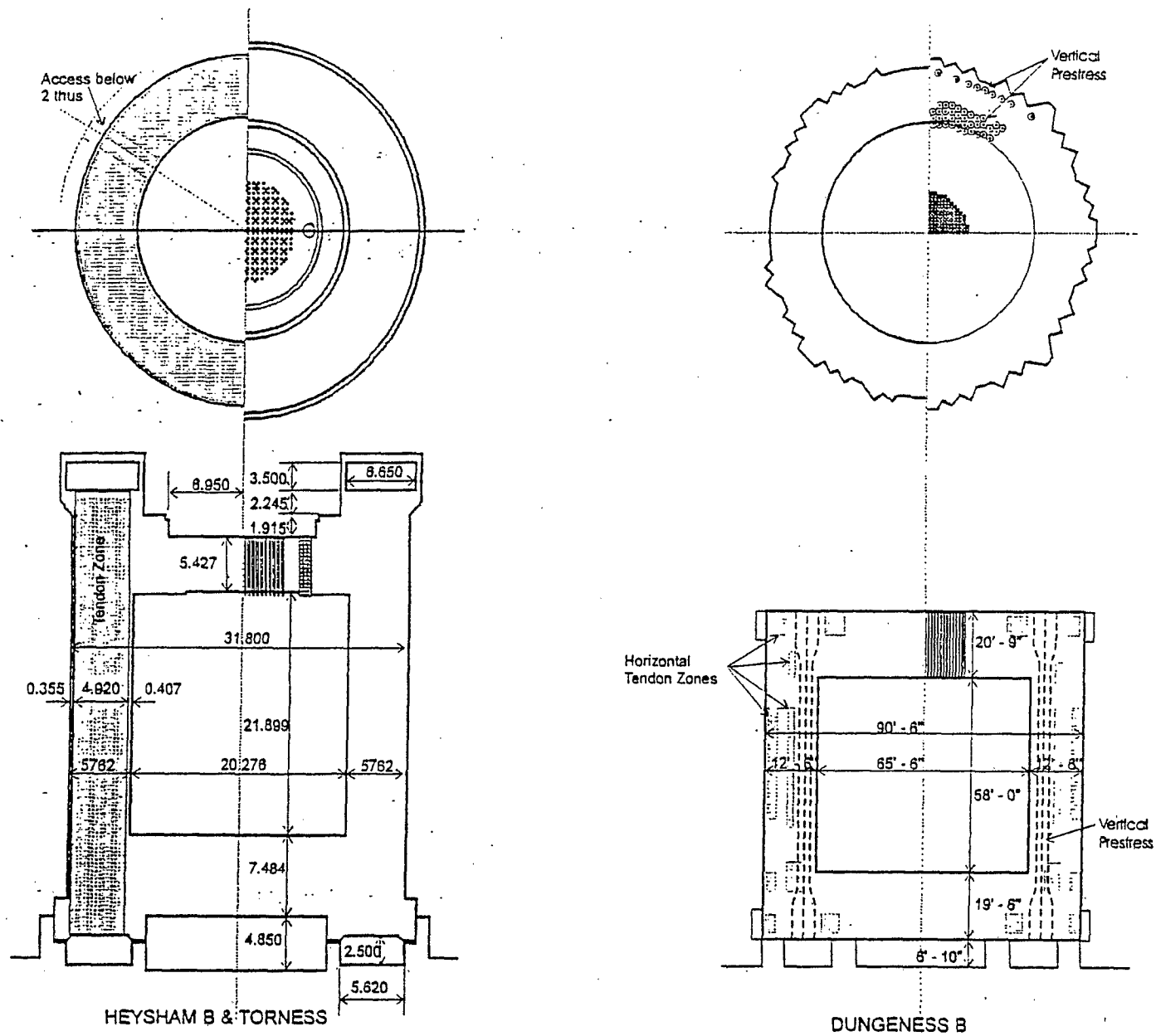
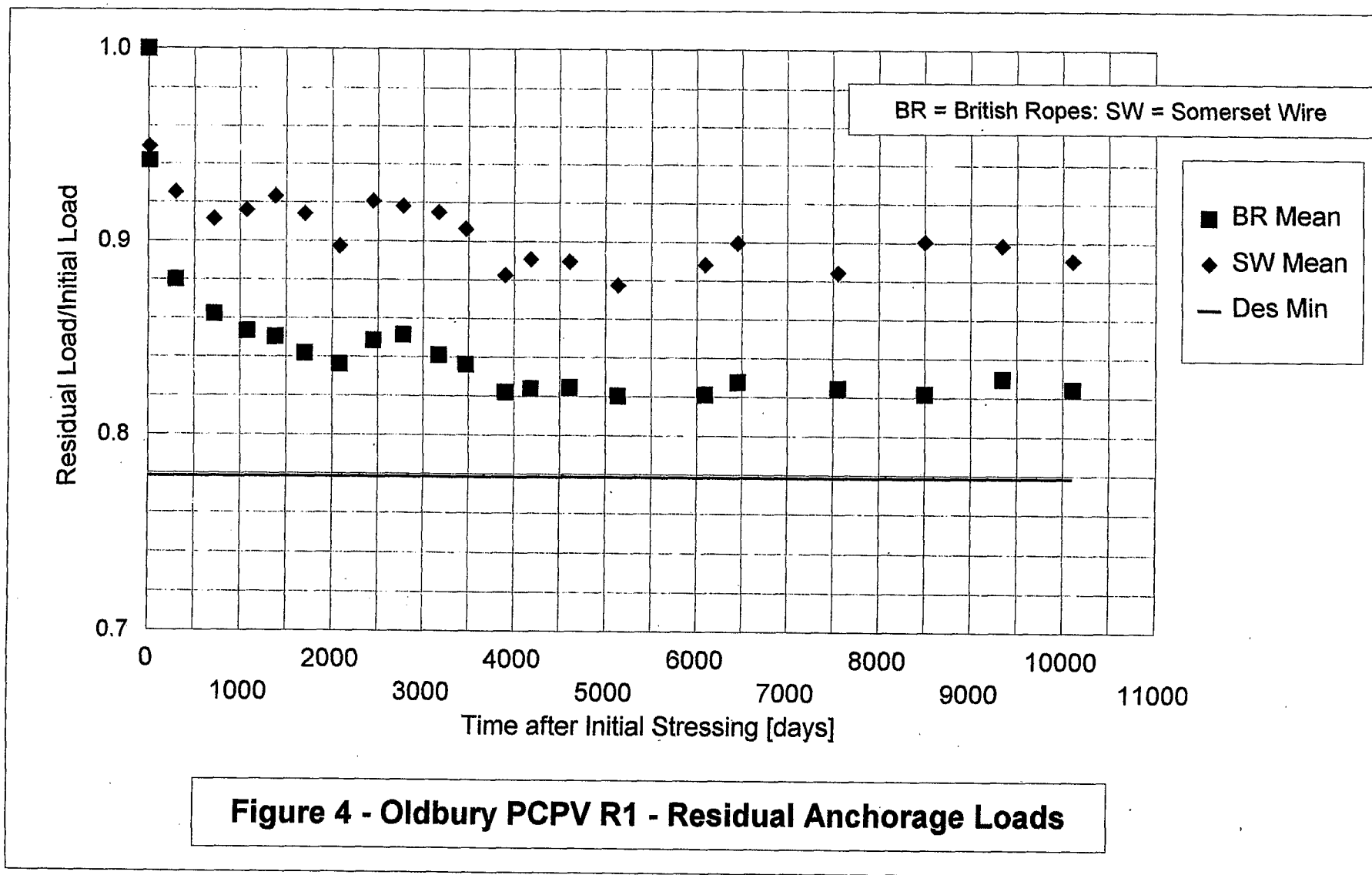


Figure 3 - Plans and sectional elevations of Heysham 2 (& Torness) and Dungeness B



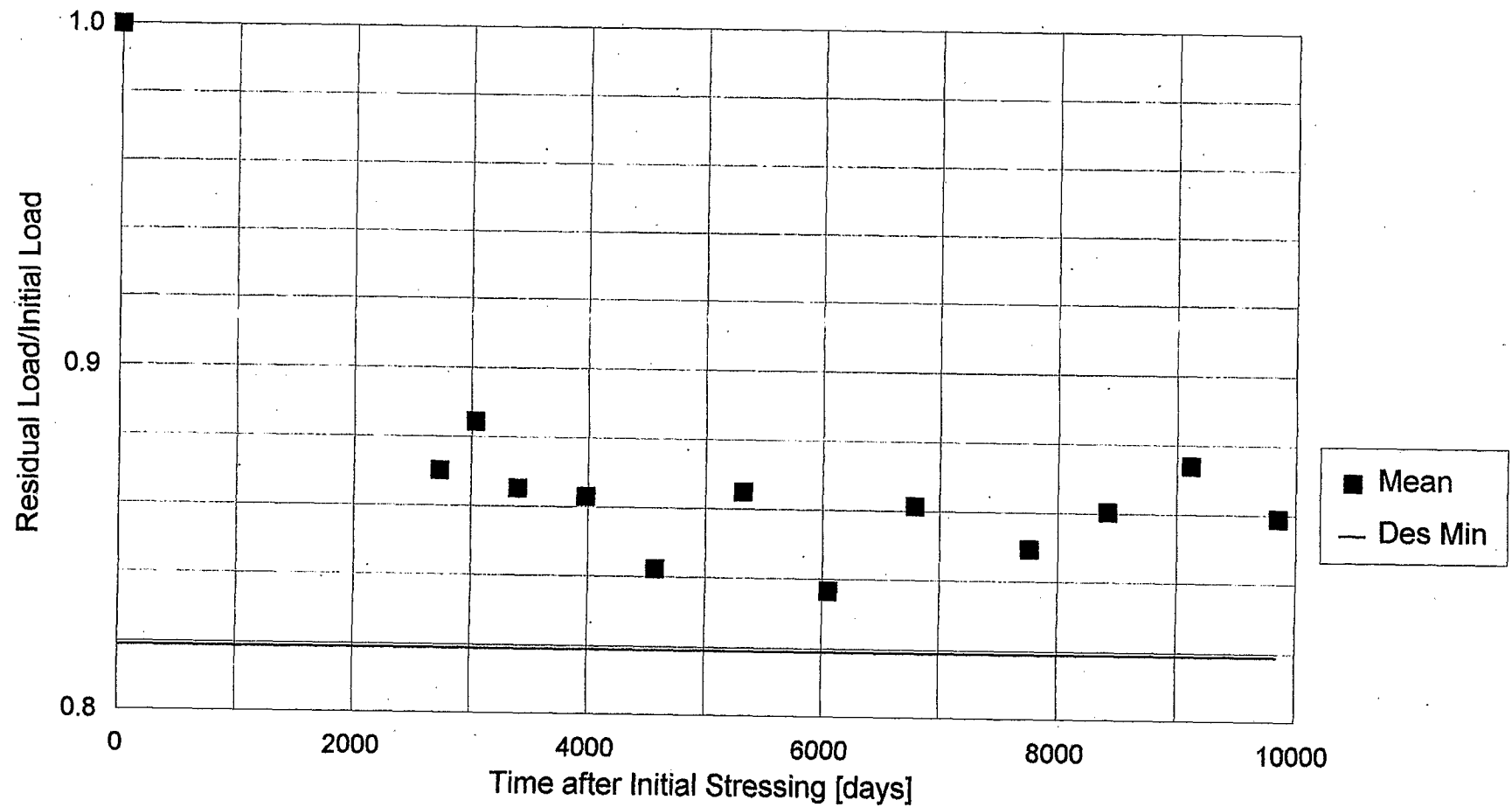


Figure 5 - Wylfa PCPV R1 - Residual Anchorage Loads

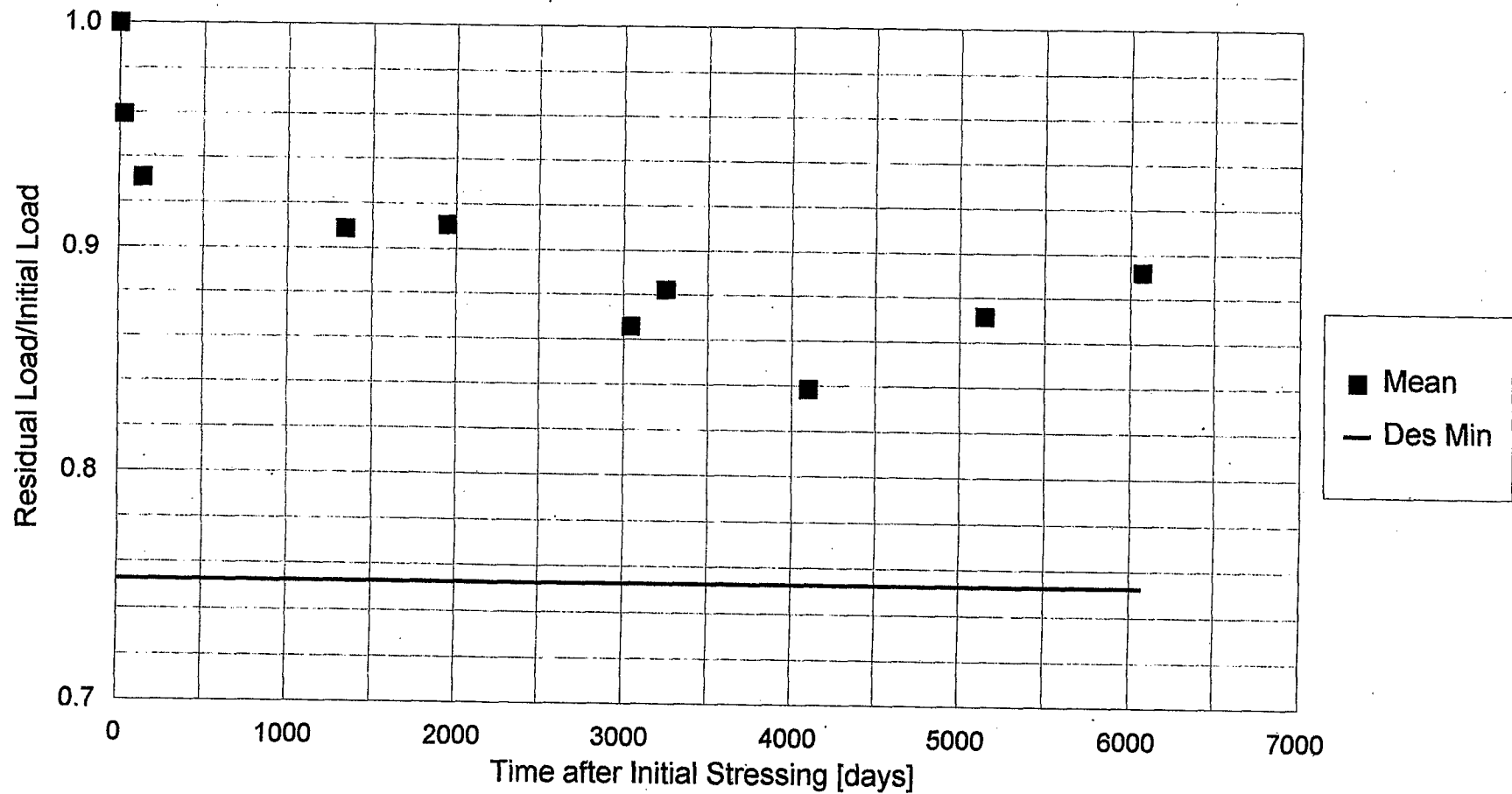


Figure 6 - Dungeness B PCPV R21 - Residual Anchorage Loads

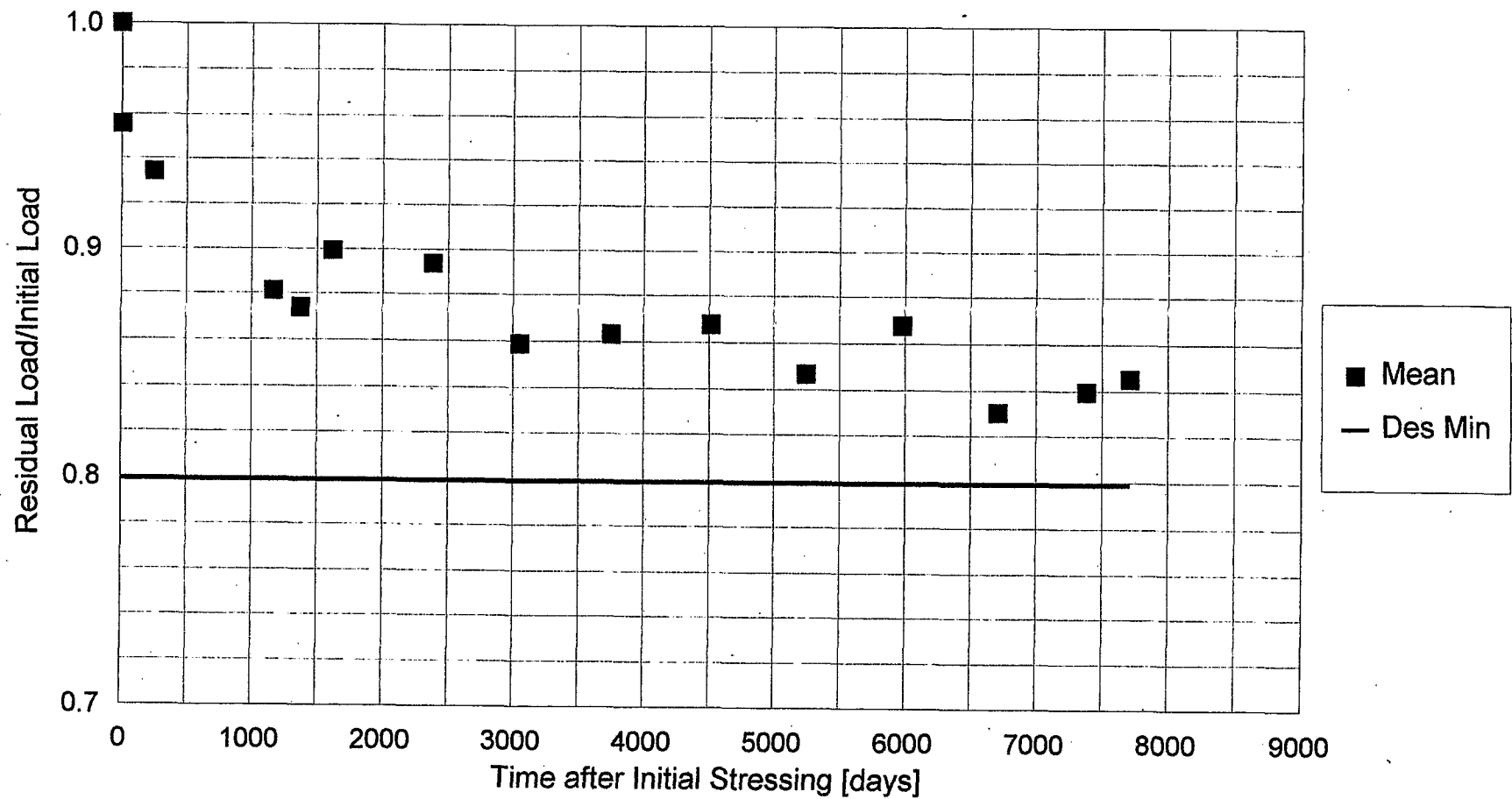


Figure 7 - Hinkley Point B PCPV R3 - Residual Anchorage Loads

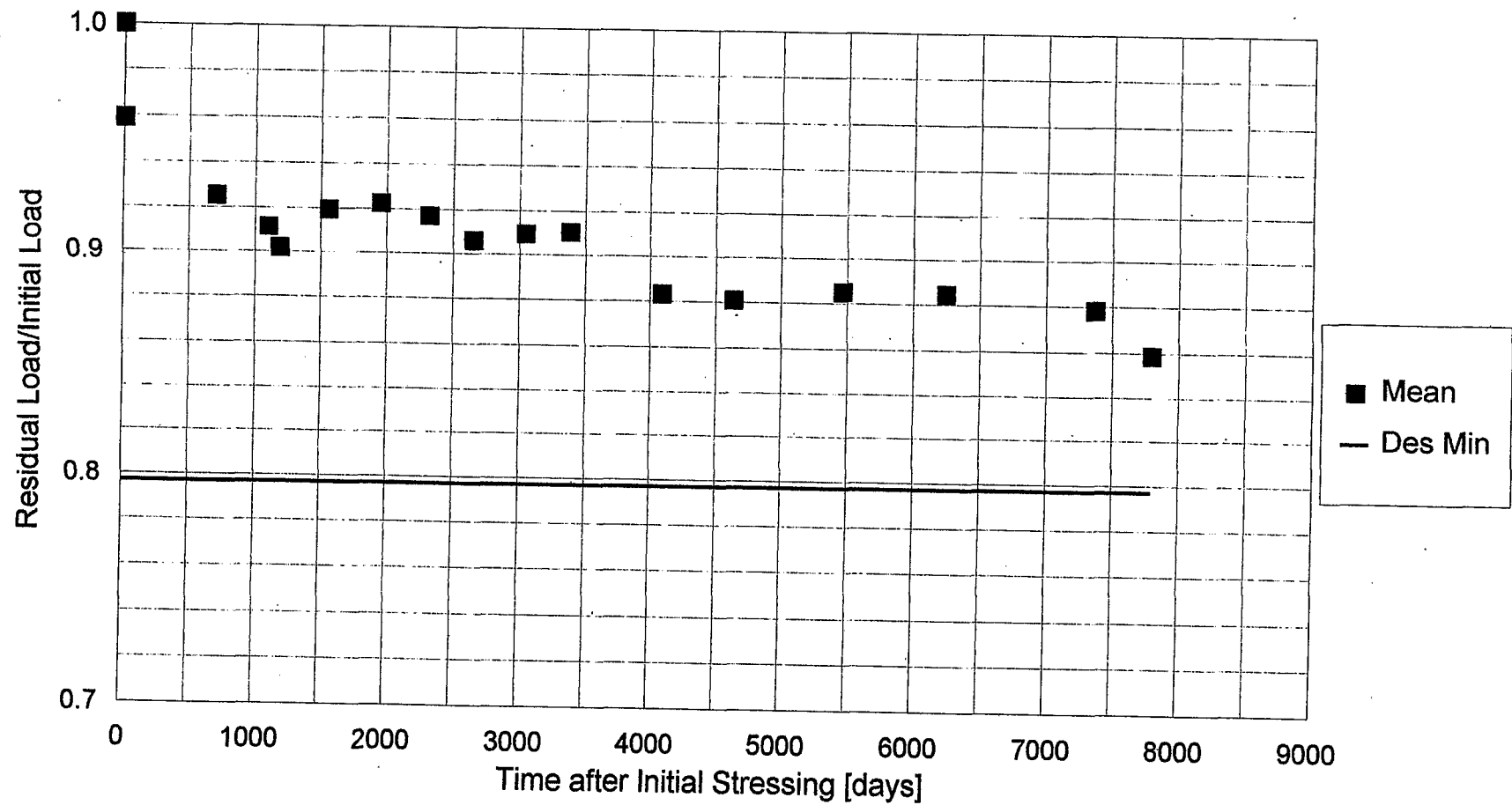


Figure 8 - Hunterston B PCPV R3 - Residual Anchorage Loads

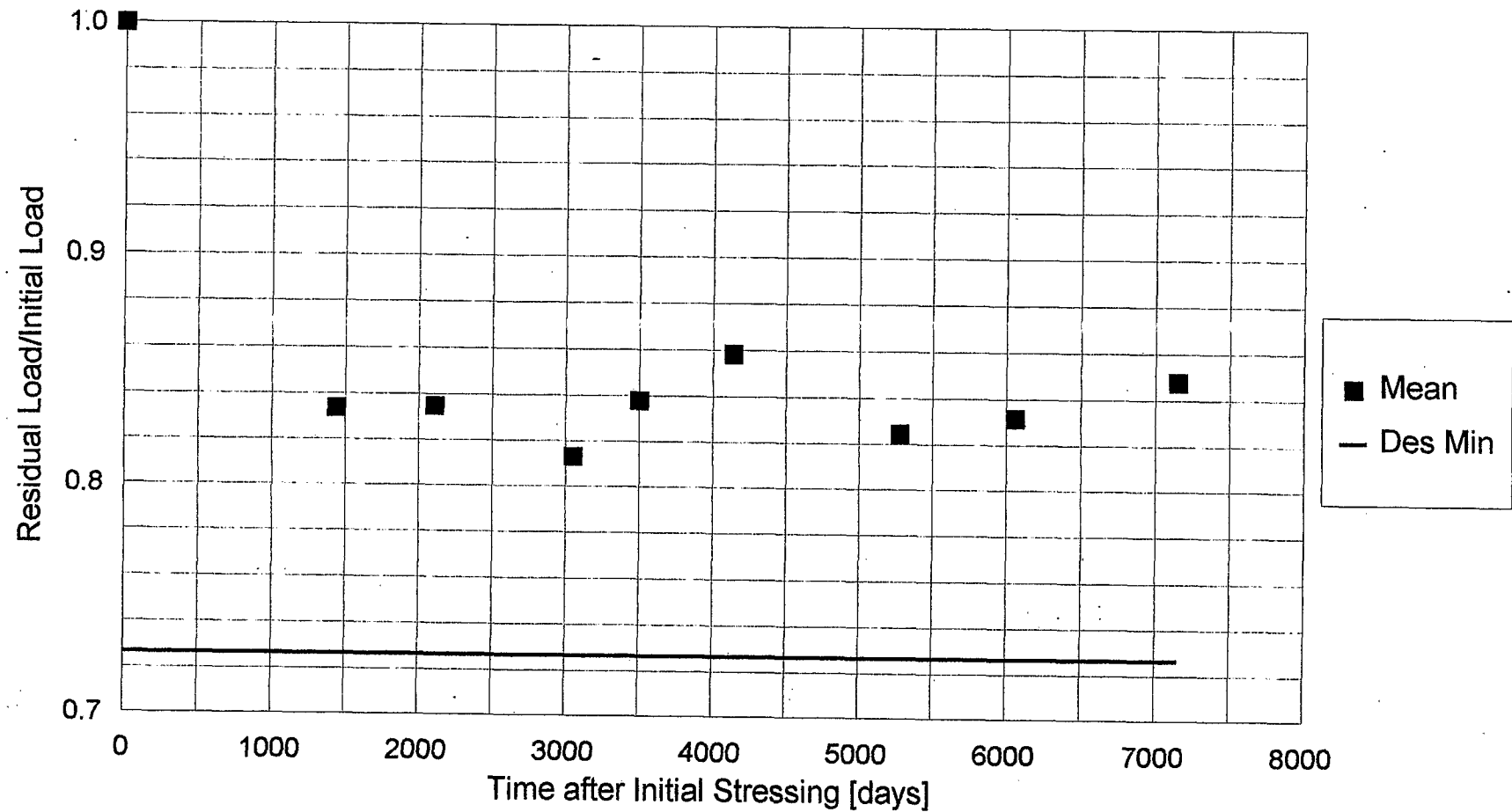


Figure 9 - Hartlepool PCPV R1 - Residual Anchorage Loads

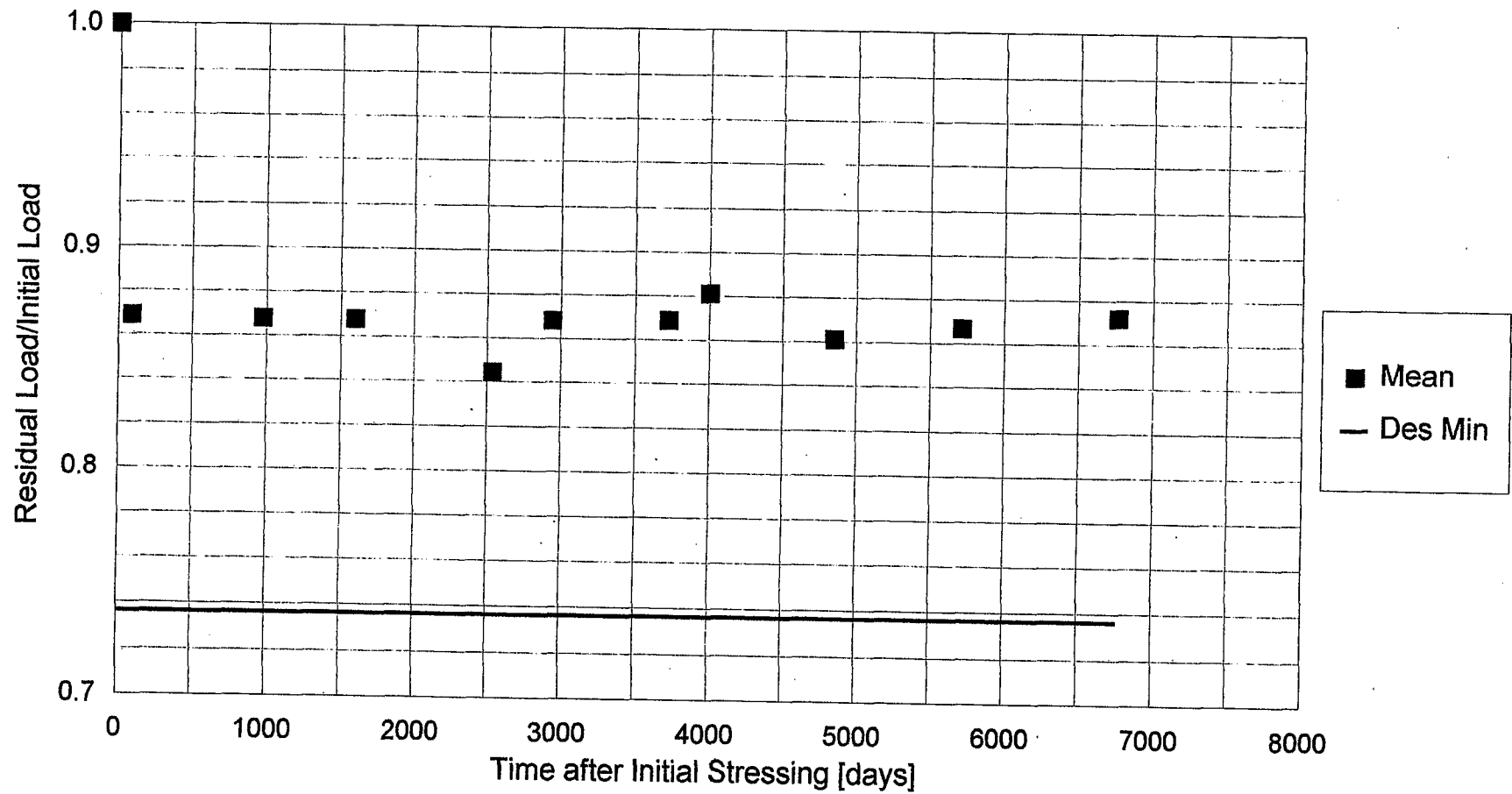
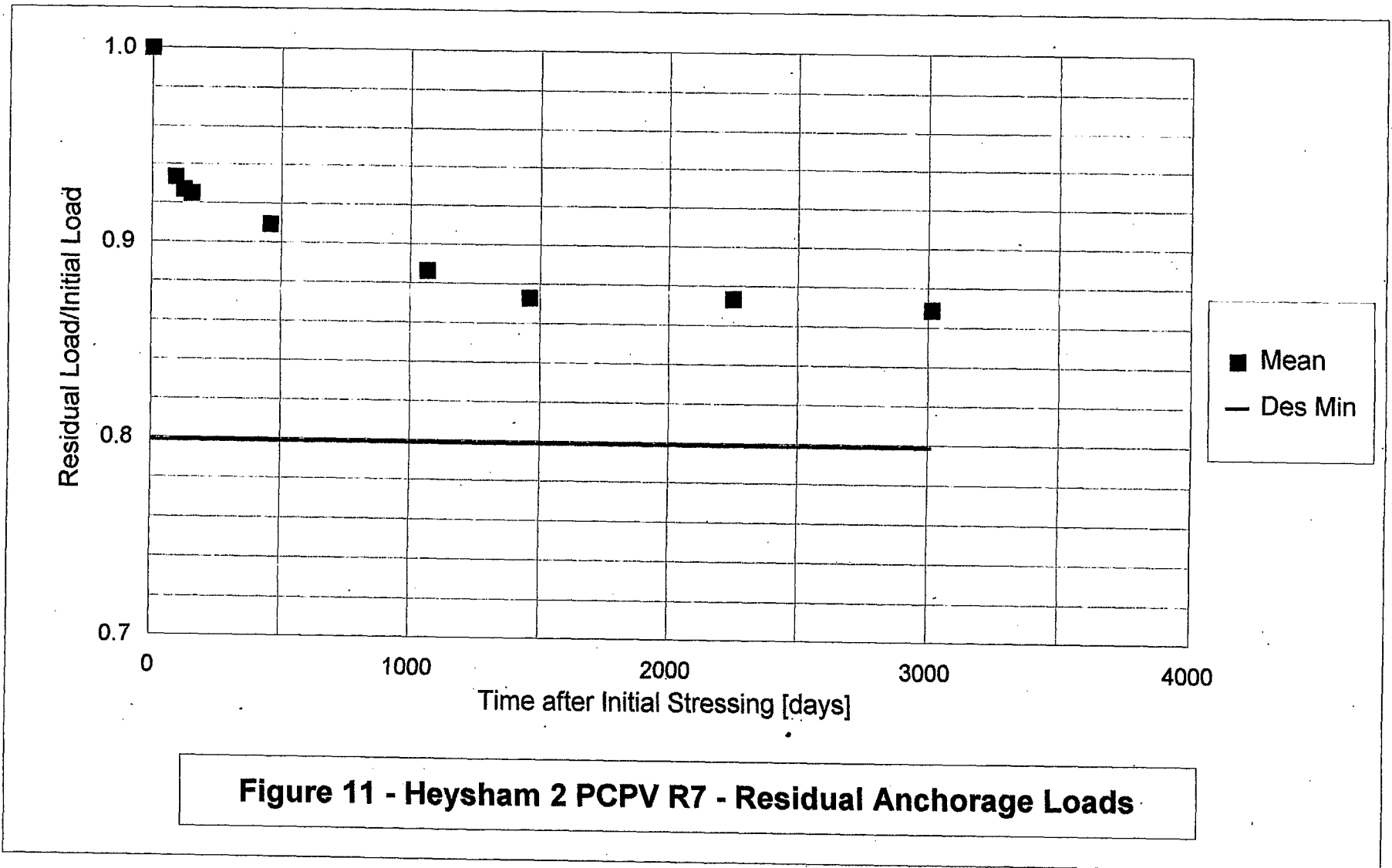
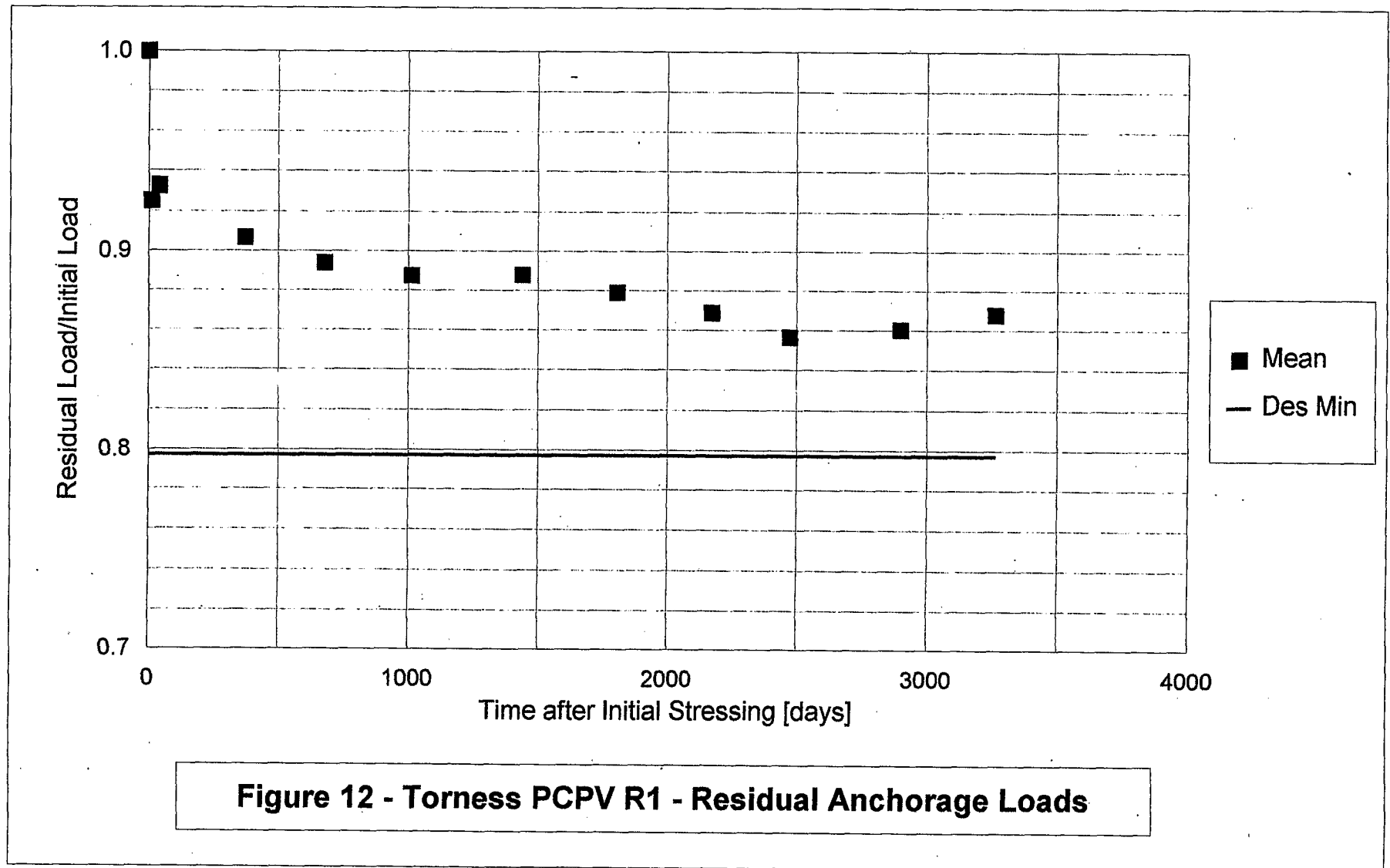


Figure 10 - Heysham 1 PCPV R1 - Residual Anchorage Loads





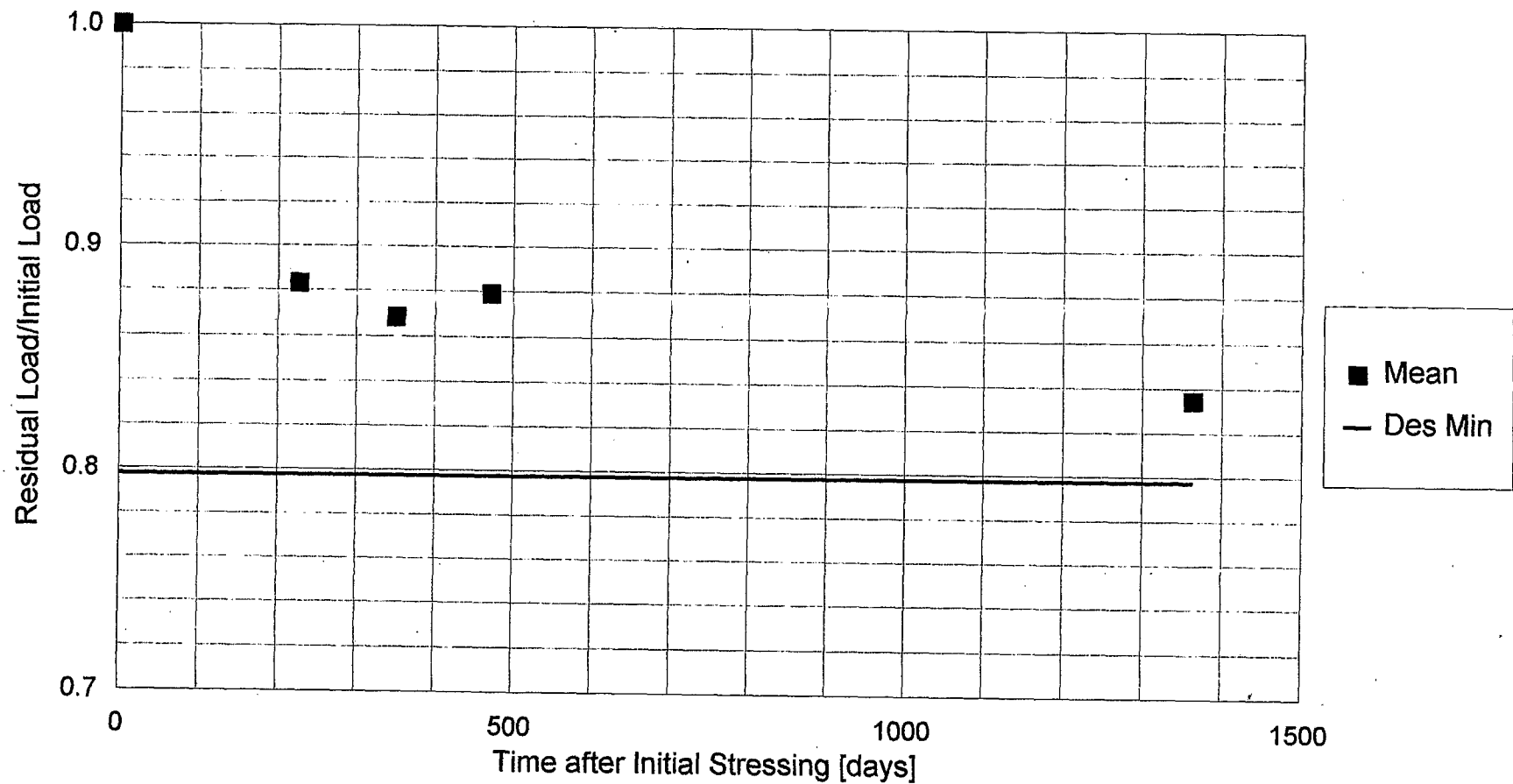


Figure 13 - Sizewell B PCC - Residual Anchorage Loads

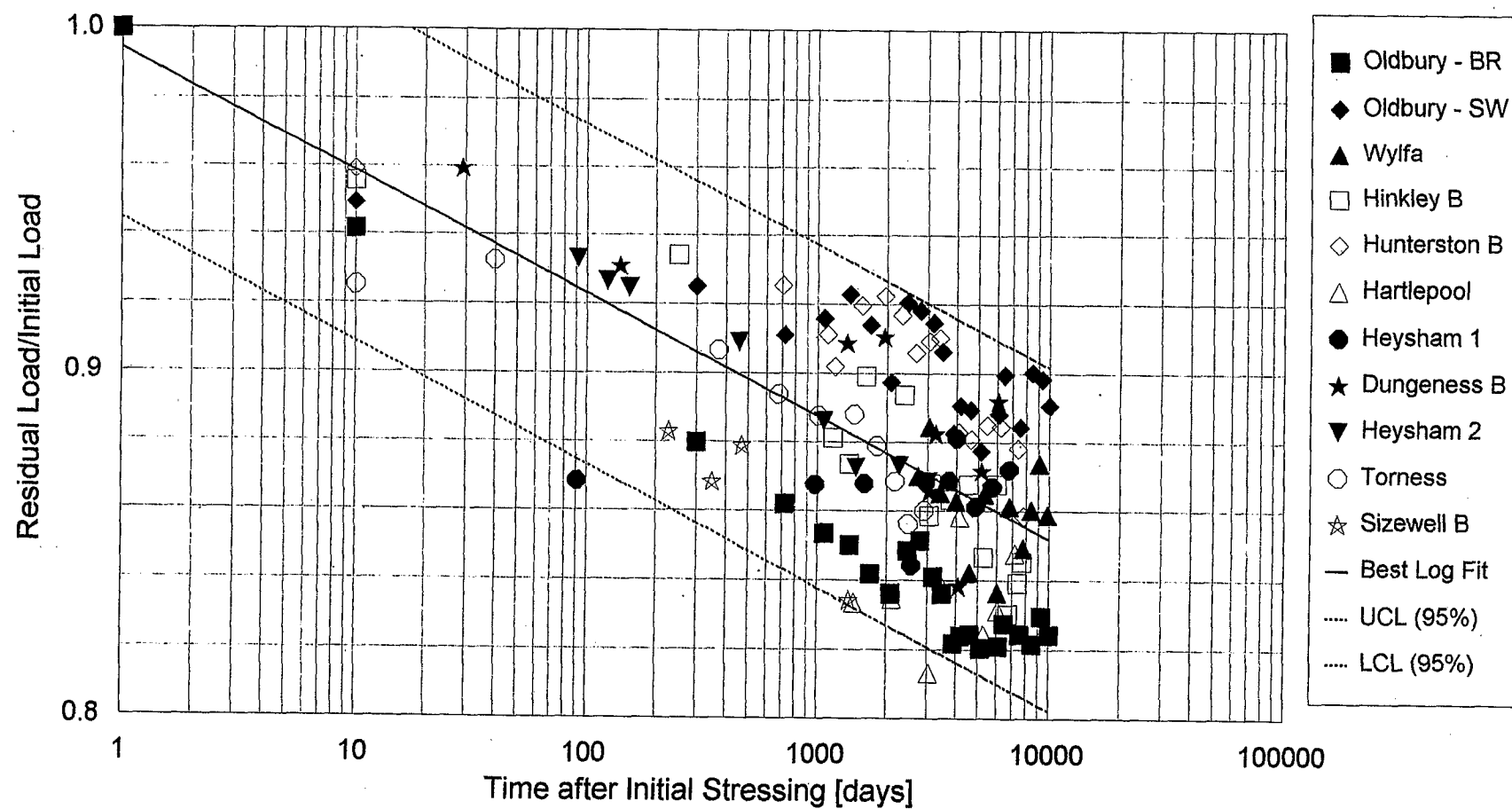


Figure 14 - Summary of all PCPV & PCC data against log(time)
Sample Means of Residual Anchorage Loads for First Vessel Completed

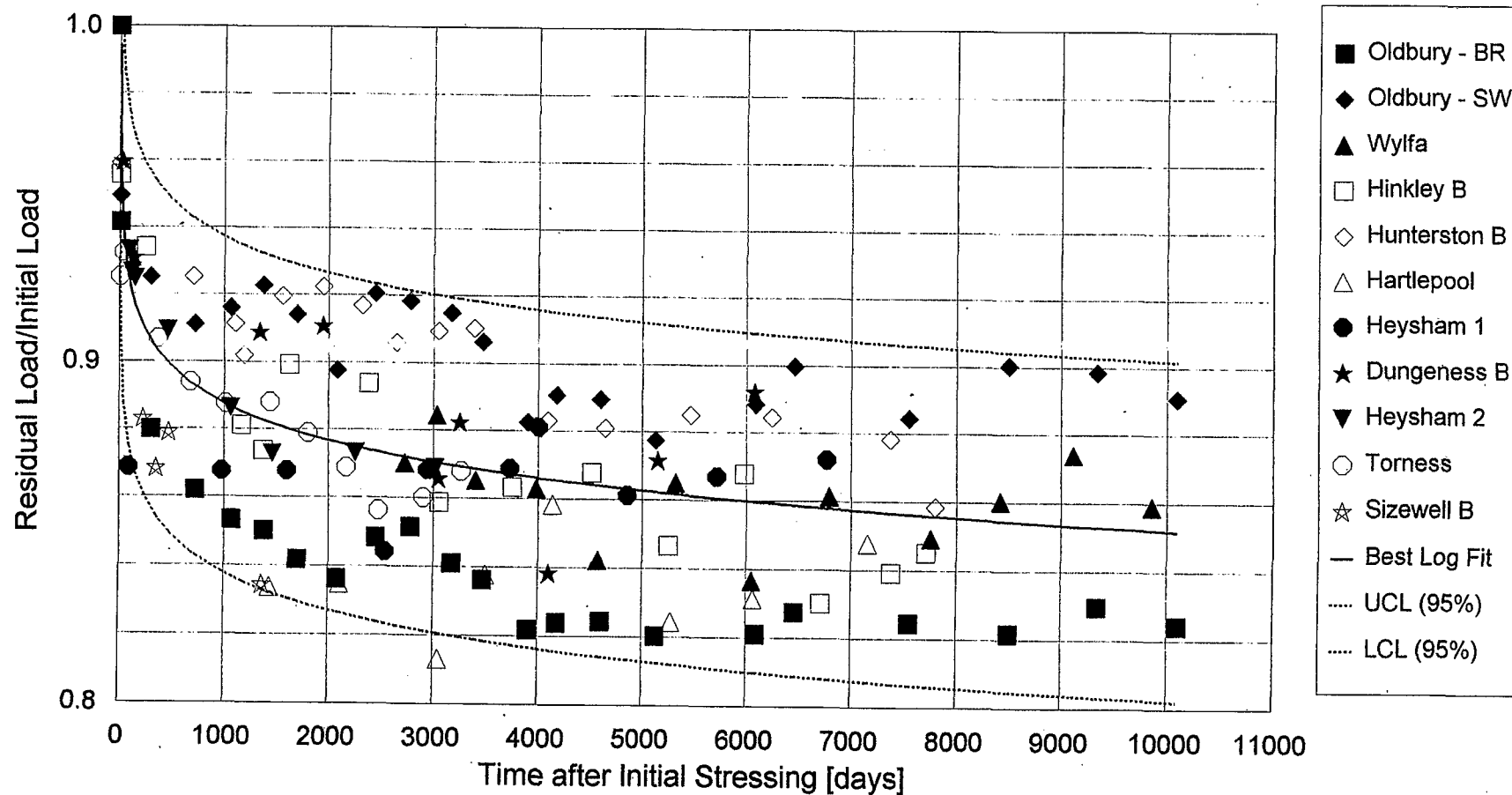


Figure 15 - Summary of all PCPV & PCC data against time
 Sample Means of Residual Anchorage Loads for First Vessel Completed

The Long Term In-service Performance of Corrosion Protection to Prestressing Tendons in AGR Prestressed Concrete Pressure Vessels

Authors: **LM Smith TD, BSc, PhD, CEng, MICE, MStructE, MINucE, FGS**
Scottish Nuclear Limited

MF Taylor BSc, PhD, CEng, FICorr, MIM
NNC Limited

SYNOPSIS

The structural performance of prestressed concrete pressure vessels (PCPVs) and prestressed concrete containment vessels (PCCVs) is dependent on the maintenance of prestress levels within the concrete. In post-tensioned, ungrouted systems the condition and performance of the tendons and the anchorage system at the end of the tendons is of prime importance. The tendons and anchorage components are normally protected from corrosion by a layer of thick viscous grease or wax which is applied at the time of installation.

Little work has been done previously to investigate the performance of the corrosion protection medium for prestressing tendons in AGR (Advanced Gas-cooled Reactor) PCPVs in service. This paper reports the results of investigations carried out on samples of grease collected as tendons were withdrawn for examination under routine maintenance, inspection and test programmes on the PCPVs at the Torness and Hunterston B Nuclear Power Plants.

The paper briefly describes the constituents of the grease and factors affecting its in-service performance as a corrosion protection medium in its long term operational environment. The method of testing is outlined, being based on the requirements of ASME XI but with modifications to allow the processing of relatively small test samples. The effect of ageing is considered and the changes in the material properties and ability to provide corrosion protection are described.

The paper concludes that, although the grease has lost some of its lighter oily constituents with time, it is still capable of providing corrosion protection to the prestressing tendons.

Introduction - number, age, location and type of NPP

Scottish Nuclear Limited and Nuclear Electric Limited are subsidiaries of British Energy PLC and operate seven nuclear power stations with Advanced Gas-cooled Reactors (AGRs) and one Pressurised Water Reactor (PWR) Station.

There are 7 Advanced Gas Cooled Reactor (AGR) nuclear power stations in the UK with a total of 14 Prestressed Concrete Pressure Vessels (PCPVs). Of these vessels, 10 are operated by Nuclear Electric Limited, and 4 by Scottish Nuclear Limited. In addition 2 older Magnox stations with 4 PCPVs are run by Magnox Electric PLC (Table 1). This paper particularly considers PCPVs types operated by Scottish Nuclear Limited although reference will be made to the other stations where appropriate. The results described in this paper are directly relevant to the sister station operated by Nuclear Electric Limited and indirectly relevant

Table 1 Listing of Stations & Operators

Station	Type	Operator *1	Proof Pressure Test *2	Power Raise *2
Oldbury	Magnox	MEL	1966/1966	1967/1968
Wylfa	Magnox	MEL	1968/1969	1971/1971
Hinkley Pt B	AGR	NEL	1973/1975	1976/1976
Hunterston B	AGR	SNL	1973/1975	1976/1977
Dungeness B	AGR	NEL	1979/1981	1983/1986
Heysham I	AGR	NEL	1980/1981	1983/1984
Hartlepool	AGR	NEL	1980/1982	1983/1984
Heysham II	AGR	NEL	1985/1986	1988/1988
Torness	AGR	SNL	1986/1987	1988/1989
Sizewell B	PWR	NEL	1994	1995

*1 Operators
MEL Magnox Electric Limited
NEL Nuclear Electric Limited
SNL Scottish Nuclear Limited

*2 Dates refer to each vessel where a station has two vessels

General Design - Prestressed Concrete Pressure Vessels

In most cases the PCPVs contain the nuclear reactor and the boilers used to produce steam in order to generate electricity. In the case of Heysham I and Hartlepool the boilers are housed in individual cylindrical cavities within the thickness of the vessel wall and the reactor is contained in main vault of the vessel. The principal structural functions of the vessels are to support the reactor and boilers and to provide support to the steel PCPV liner and penetration liners thus creating the pressure enclosure for the carbon dioxide gas circuit which transports heat from the reactor core to the boilers. The PCPVs are therefore the primary structural containment for the reactor. In addition they additionally provide biological shielding from radiation generated by it. The thicknesses of the wall and end cap concrete (see Table 2) are however determined by the primary function of support for the pressure boundary and are far in excess of that required for radiation shielding.

A steel liner on the inside of the concrete pressure vessel, together with the penetration liners, provides a gas-tight membrane, retaining the reactor coolant. The liner, which is anchored to the PCPV concrete, contributes to reactor coolant gas leak prevention but does not contribute to the load resisting capacity of the PCPV. Therefore the PCPV's ultimate strength does not rely on the presence of either an intact or leaking liner. The temperature of this liner, and that of the surrounding concrete, is maintained within design limits by internal insulation and by circulation of cooling water through pipes welded to the liner and embedded in the concrete. More detailed descriptions of the various UK PCPV designs and locations of the nuclear power plants are given in Reference 1 and general details are given in Table 2 for comparison. The designs evolved with time

and, following experience gained on the design of the vessels for the earlier Magnox station at Oldbury on Severn, the Hinkley Point B/Hunterston B vessels design was developed. As for Oldbury, the basic vessel design is based on a vertical concrete cylinder with post tensioned steel prestressing tendons. The more compact nature of the AGR core, however, allowed a significant reduction in internal diameter (18.9 m at Hunterston B/Hinkley Point B compared to 23.45 m at Oldbury), whilst retaining a similar internal height at 19.4 m. Experience gained at Oldbury and increasing confidence in vessel design also allowed a similar wall thickness (5 m), despite an increase in design pressure.

The Torness and Heysham II PCPVs are also in the form of a vertical, right circular cylinder which contains the fuel, core and its support structure, the boilers and gas circulators. These vessels are an evolution of the Hunterston B/Hinkley Point B PCPV design uprated to take account of the higher internal reactor gas pressure. As with all PCPV designs, the inner face of the PCPV is lined with a mild steel liner; this is extended at major penetrations by way of the penetration liners (See Figure 1 for a comparison of the Hunterston B & Torness vessels).

Table 2 UK PCPV/PCCV Types & Dimensions (metres)

Station/ Vessels	PCPV/ PCCV Shape	Internal Diameter	Internal Height	External Diameter	External Height	Minimum Wall Thickness	Minimum Top Cap Thickness	Minimum Bottom Slab Thickness
Oldbury 2 x PCPVs	PCPV Short vertical cylinder, flat ends	23.45	18.30	33.85	32.35	4.58	6.40	6.71
Wylfa 2 x PCPVs	PCPV Flat ended cylinder, spherical cavity	29.25	29.25	35.50	36.30	3.36	3.66	3.36
Hinkley Pt B 2 x PCPVs	PCPV Short vertical cylinder, flat ends	18.90	19.40	28.95	34.2	5.03	5.49	7.51
Hunterston B 2 x PCPVs	PCPV Short vertical cylinder, flat ends	18.90	19.40	28.95	34.2	5.03	5.49	7.51
Dungeness B 2 x PCPVs	PCPV Short vertical cylinder, flat ends	19.95	17.70	27.60	29.95	3.81	6.33	5.95
Heysham 2 x PCPVs	PCPV Short vertical cylinder, flat ends, Poddled boilers in walls	13.10	18.30	25.90	29.25	6.40	5.49	5.49
Hartlepool 2 x PCPVs	PCPV Short vertical cylinder, flat ends, Poddled boilers in walls	13.10	18.30	25.90	29.25	6.40	5.49	5.49
Torness 2 x PCPVs	PCPV Short vertical cylinder, flat ends	20.28	21.9	31.8	40.9	5.76	5.395	7.484
Heysham II 2 x PCPVs	PCPV Short vertical cylinder, flat ends	20.28	21.9	31.8	40.9	5.76	5.395	7.484
Sizewell B 1 x PCCV	PCCV Flat base, circular barrel, hemi- spherical top dome	45.73	64.63	48.48	77.03	1.37	1.00 (Dome)	1.71

Safety Criteria

The structural performance of prestressed concrete pressure vessels is dependent on the maintenance of prestress levels within the concrete. In post-tensioned, ungrouted systems the condition and performance of the tendons and the anchorage system at the end of the tendons is of prime importance. The tendons and anchorage components are normally protected from corrosion by a layer of thick viscous grease or wax which is applied at the time of installation.

Little work has been done previously to investigate the performance of the corrosion protection medium for prestressing tendons in AGR PCPVs in service. This paper reports the results of investigations carried out on samples of grease collected as tendons were withdrawn for examination under routine maintenance, inspection and test programmes on the PCPVs at the Torness and Hunterston B Nuclear Power Plants.

Prestressing Type

The Hinkley Point B/Hunterston B and Torness/Heysham II pressure vessels are prestressed by an ungrouted helical tendon system contained within mild steel tendon duct tubes in the cylinder walls of the vessels (CCL barrel and cone wedge system as shown in Figure 2). In the former design a total of 2816 tendons are arranged in 16 layers, and in the latter a total of 3744 tendons are arranged in 20 layers, with alternate twin layers arranged clockwise and anticlockwise in plan to avoid horizontal torque. In contrast to the Oldbury design, no tendons penetrate the end slabs. The necessary prestress in the top and bottom slabs is provided by the inward radial component of the tendon loads in the helical stressing system which extends beyond the vault walls to terminate in two stressing galleries at the top and bottom of the vessel. This change from the Oldbury arrangement allowed much closer spacing of the standpipes and a more compact core design. Details of the various prestressing systems used in UK PCPVs are given in Table 3 for comparison. Various corrosion protection systems have been used on the different vessel designs and these are listed in Table 4 for comparison.

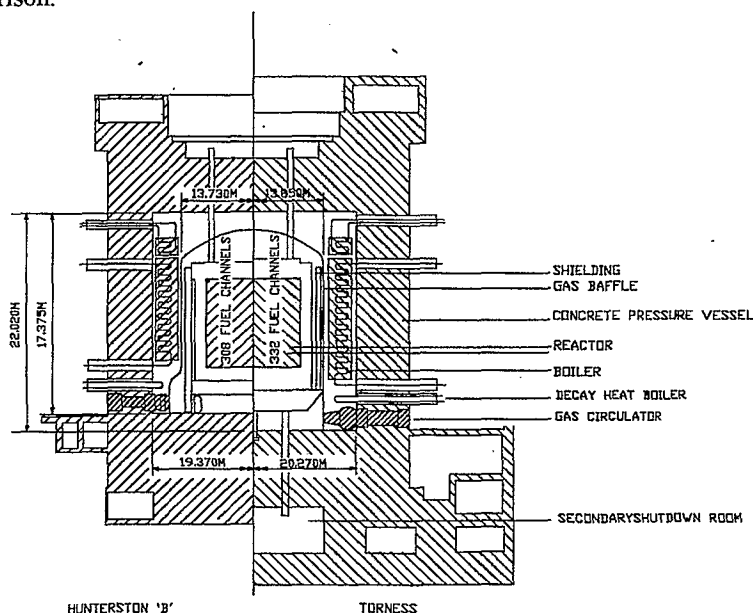
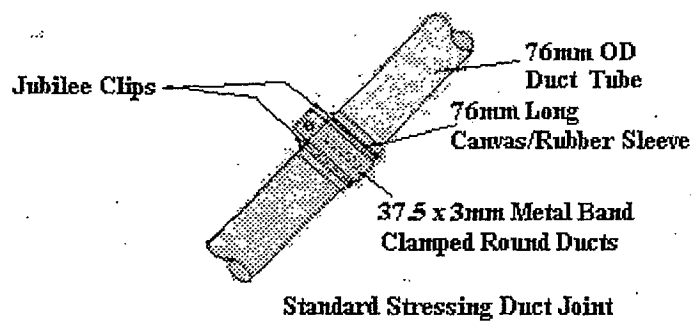


FIGURE 1 COMPARISON OF REACTOR PRESSURE VESSEL CROSS SECTIONS FOR HUNTERSTON 'B' AND TORNESS



TENDON DUCT & JOINT

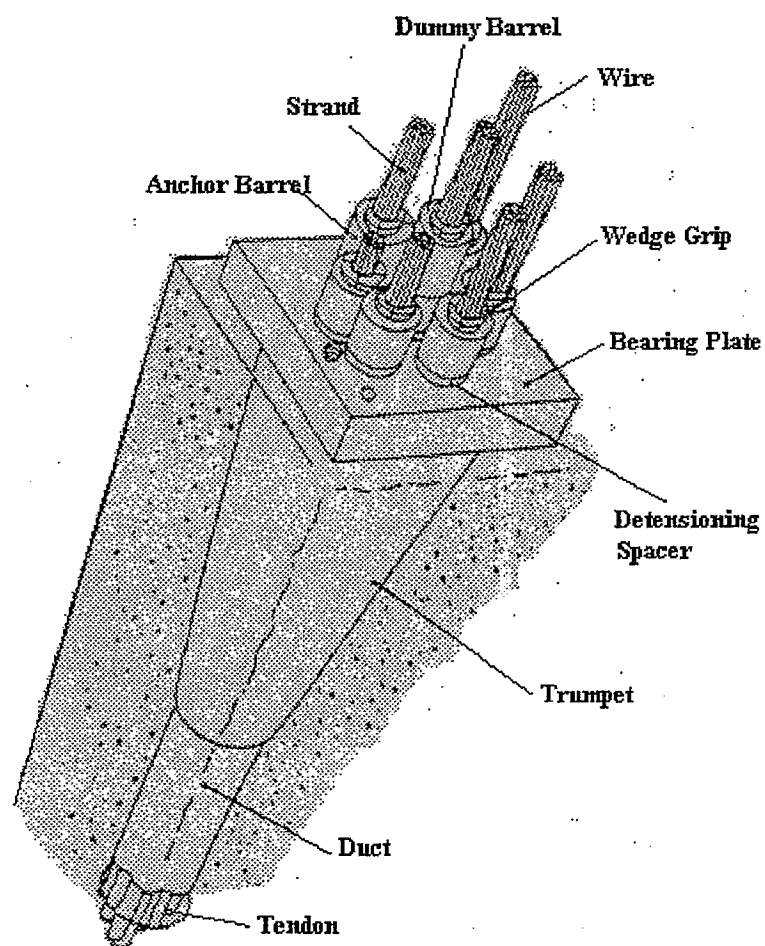


FIGURE 2 - TENDON ANCHORAGE DETAIL

Table 3 PCPV/PCCV Prestressing Systems

Station/ Vessels	Tendon GUTS *1 (tons)	Prestressing System	No. of Tendons per Vessel	Strands per Tendon	PS Strand Diameter/Wire Type
Hinkley Pt B 2 x PCPVs	260	CCL Barrel & Cone Wedge Alternate pairs of rows of helical tendons clockwise / anti-clockwise	R3 - 2814 R4 - 2813	7	18mm Dyform (7 wire) Low relaxation Stabilised
Hunterston B 2 x PCPVs	260	CCL Barrel & Cone Wedge Alternate pairs of rows of helical tendons clockwise / anti-clockwise	R3 - 2814 R4 - 2813	7	18mm Dyform (7 wire) Low relaxation Stabilised
Dungeness B 2 x PCPVs	975	BBRV Buttonhead ie Cold upset nailhead	Wall - 366 Top Slab - 108 Bottom Slab - 108 Wall (vertical) - 384 Total - 966	163 x 7mm parallel wires	7mm wire Low relaxation Stabilised
Heysham I 2 x PCPVs	1040	Longitudinal - CCL Bearing Plate & Cone Wedge	Longitudinal - 272	28	18mm Dyform (7 wire) Low relaxation Stabilised
	Wire 3.46	Circumferential - TWC Wire wound system Barrel & Cone Wedge	700 Layers, 20 Channels with 33/35 layers / channel, 119/120 turns / layer	Each Layer 9.72 km of 5mm wire	5mm wire Low relaxation Stabilised
Hartlepool 2 x PCPVs	1040	Longitudinal - CCL Bearing Plate & Cone Wedge	Longitudinal - 272	28	18mm Dyform (7 wire) Low relaxation Stabilised
	Wire 3.46	Circumferential - TWC Wire wound system Barrel & Cone Wedge	700 Layers, 20 Channels with 33/35 layers / channel, 119/120 turns / layer	Each Layer 9.72 km of 5mm wire	5mm wire Low relaxation Stabilised
Torness 2 x PCPVs	267	CCL Barrel & Cone Wedge Alternate pairs of rows of helical tendons clockwise / anti-clockwise	R1- 3744 R2- 3744	7	18mm Dyform (7 wire) Low relaxation Stabilised
Heysham II 2 x PCPVs	267	CCL Barrel & Cone Wedge Alternate pairs of rows of helical tendons clockwise / anti-clockwise	R7 - 3744 R8 - 3744	7	18mm Dyform (7 wire) Low relaxation Stabilised
Sizewell B 1 x PCCV	1114 (SCUTS)*2	PSC Freyssinet K Series	Meridional - 74 Hoop - 107	37	15.2mm Dyform (7 wire) Low relaxation Stabilised

*1 GUTS - Guaranteed Ultimate Tensile Strength *2 SCUTS - Specified Characteristic Ultimate Tensile Strength

Table 4 Corrosion Protection to Prestressing System

Station	Works Applied	Site Applied
Hinkley Pt B	Phosphate coating + Gulf NoRust 2/9	Shell Alvania EP1
Hunterston B	Phosphate coating + Gulf NoRust 2/9	Shell Alvania EP1
Dungeness B	Phosphate coating + ICI Kephos 253	Rustban 324 (Rustban 381 - hand application)
Hartlepool	Phosphate coating + Castrol Rustillo DW 932* ¹	Castrol S202* ¹
	Phosphate coating* ²	Castrol S203* ²
Heysham I	Phosphate coating + Castrol Rustillo DW 932* ¹	Castrol S202* ¹
	Phosphate coating* ²	Castrol S203* ²
Heysham II	Phosphate coating + Castrol Rustillo DWX41	Shell Alvania EP1
Torness	Phosphate coating + Castrol Rustillo DWX41	Shell Alvania EP1
Sizewell B	Viscosity Oil Visconorust 1601 Amber	Viscosity Oil Visconorust 2090P-4

*¹ Vertical Tendons*² Circumferential Tendons**Monitoring & Data Treatment**

The power stations are complex, combining heavy civil structures with a variety of different types of plant of both conventional and nuclear types. Comprehensive in-service inspection is carried out which is designed to ensure that nuclear safety is maintained and that the Civil structures are in a serviceable condition and support essential plant and systems to allow continued electricity generation and commercial operation (Reference 2). Data is collected on a regular basis and is assessed at, or shortly after, collection. The information collected on the PCPVs is collated and presented to the Regulator after each statutory plant outage. A combination of engineering judgement and fixed acceptance criteria are used to confirm continued fitness for purpose. This is based on consideration of original design criteria, external hazards, and any subsequent changes in loading conditions and design codes.

Historical records and databases and comparison with the performance of similar structures are used to identify the effects of ageing and any identified trending. Inspection and monitoring activities on the Nuclear Power Plants operated by Nuclear Electric and Scottish Nuclear over the last 25 years have allowed a pattern of behaviour to be established and the results of Periodic Safety Reviews have demonstrated that the Civil Engineering Structures are performing in accordance with the design intent.

Ageing Management Programme

Each site is covered by a nuclear site licence which is issued to the operator under the provisions of the Nuclear Installations Act 1965 (and subsequent amendments)(Reference 3) by HM Nuclear Installations Inspectorate (NII) which is part of the Nuclear Safety Division of the UK Health and Safety Executive (HSE). The licence currently contains 35 standard conditions which must be met by the operator by means of established and approved compliance arrangements. However, the rules are not prescriptive and the licensee retains absolute responsibility for nuclear safety under UK law. It is the duty of the NII to; ensure that the appropriate standards are developed, achieved and maintained by the licensee; ensure that the necessary safety precautions are taken; and monitor and regulate the safety of the plant by means of its powers under the licence and relevant regulations (Reference 4).

In addition to the specific requirements of the Nuclear Site Licence, the Stations are covered by other legislation that would affect any other large industrial plant. With regard to structural inspection requirements, however, the provisions of the Pressurised Systems & Transportable Gas Containers Regulations 1989 (Reference 5) as they affect the PCPVs are of particular note.

A safety case containing the relevant information with regard to design and operational parameters and limits is produced by the licensee in accordance with arrangements approved by the NII. Structures must be maintained throughout their operational life in such a way that they are always fit for purpose and capable of meeting their nuclear safety role as required by this safety case which identified in the licence conditions. In order to do this they must be examined, inspected and tested in a manner and at a frequency which is adequate to confirm that the structural integrity, performance and reliability claims made in the safety case continue to be met throughout the operational life of the station.

The PCPVs at each of the AGR stations must be inspected under the terms of Site Licence Condition 28 (LC28), covering the examination, inspection, maintenance and testing of all plant and structures that may affect nuclear safety. The PCPVs are the most critical of the civil structures monitored on the Stations and this is reflected in the range and frequency of the inspections carried out on them under the Maintenance Inspection and Test Schedule (MITS) or Maintenance Schedule (MS), depending on the station. The results obtained from tests carried out under the MITS/MS are combined with other relevant information to produce a report for start-up which must be available prior to NII giving consent to return to power.

The current revision of BS 4975 (Reference 6) contains a specific section (Section 9) on the testing and surveillance of PCPVs. Both the minimum range of inspections to be carried out and a supplementary set which may be used are covered. However, the full range of examinations is routinely carried out and reported by both Scottish Nuclear Ltd and Nuclear Electric PLC (Reference 7).

Minimum program:

- Tendon load checks and strand withdrawal
- Tendon anchorage examinations
- Concrete surface examinations

Supplementary program:

- Vibrating wire strain gauge readings
- Concrete and liner temperature readings
- Main reactor coolant leakage summaries
- PCPV deflection surveys
- Foundation settlement surveys
- Operating history review

In-service monitoring of the condition of the protective grease applied to the pre-stressing strand and to the external surfaces of the anchorage components during installation is not specifically addressed as a requirement under the MITS or Section 9 of BS 4975. However, it is usual for the grease to be visually inspected and reapplied as necessary to maintain surface protection on the tendon and anchorage components. Replacement tendon strands for those which have been removed for inspection are greased during installation. Special emphasis is placed on the detection of Pressure Vessel Cooling Water System (PVCS) leakage and the identification of any other source of water leakage during examination of the surface of the vessels.

The statutory report for start-up following an outage is prepared by the Appointed Examiner (APEX) who is a nominated suitably qualified and experienced chartered civil or structural engineer responsible for the implementation of the monitoring programme and the assessment and reporting of the results.

Investigation of Corrosion Protection to PCPV Prestressing Systems

Background

During routine inspections of the Hunterston B Reactor 3 Upper Stressing Gallery in April 1994, as part of the normal tendon load checking operations, surface corrosion was noted at several anchorage locations. Investigations showed that the water causing this corrosion originated from rainwater ingress that had occurred due to leakage of the main charge hall roof as a result of storm damage. Some of this water had subsequently percolated through construction joints on the Reactor 3 Upper Stressing Gallery roof. The leaking water fell upon local areas of the PCPV prestressing tendons and anchorages located directly beneath the construction joints in the stressing gallery roof.

An initial visual inspection was carried out to gauge the extent of the problem and a precautionary inspection of the Reactor 4 upper stressing gallery was carried out. This indicated that, although there was no damage to Reactor 4 stressing components, the level of protection provided could be improved.

The initial engineer's and metallurgist's reports on the Reactor 3 stressing components concluded that the appearance and extent of the observed rusting was of a superficial nature with no significant penetration of the underlying material. The lower stressing gallery was also inspected visually but, as was expected, there were no signs of water at the lower anchorages of the affected tendons.

The visual surveys were used to identify the two worst affected tendons and these were then withdrawn and examined as an extension to the normal tendon withdrawal and testing programme.

It was important to establish whether the water which had led to external surface corrosion of the anchorage components had affected hidden areas and particularly the interface between the prestressing strand and the anchor wedges. As the tendons were withdrawn the anchorage components were removed and the tendons lifted up into the upper stressing gallery to allow a visual inspection of the anchor zone to be carried out. Each of the tendons was inspected and found to be unaffected and there was sufficient grease present within the anchorage to prevent water from entering and causing corrosion.

Where corrosion did occur it was limited to the external surface areas of anchorage components and exposed tendon tails. The internal load bearing components of the anchorages and the tendon strands were not affected and there was consequently no loss in load carrying ability.

Selected sections of prestressing strand and the anchorage components were taken from the tendons for laboratory testing. This confirmed that the tendon strands and anchorage components exhibited only minor surface corrosion with the deepest corrosion of 90µ being on a spacer.

The remedial works following the removal and inspection of the tendons involved the replacement of the withdrawn material with new strand and anchorage components. A 100% photographic record was taken of all tendon anchorages in the upper stressing galleries of both Reactors 3 and 4. The tendon tails and anchorage components were then cleaned down and totally regreased. The level of grease protection is now far superior to that previously provided and regular inspection and maintenance of the Upper Stressing Galleries will prevent a recurrence of the problem.

During the investigations it became clear that there was very little information available on the long term performance of the grease used to protect the tendons and their anchorage components and this was therefore raised as an item on the Nuclear Research Index. This Nuclear Research Index contains a list of issues that it is considered would benefit from research activity and is prepared, reviewed and updated on an annual basis by the Health and Safety Executive (HSE).

The Health and Safety Commission (HSC) Co-ordinated Programme consists of research to address the safety issues presented in the Nuclear Research Index produced by HSE and takes into account research undertaken by the Licencees for their own purposes, by other government departments and elsewhere. The programme is managed by HSE on behalf of the HSC.

The HSC Co-ordinated Programme is concerned with nuclear safety research activity related to UK thermal reactor sites and comprises two elements:

- The HSE Levy Programme - that part of the HSC Co-ordinated Programme which is identified and placed by HSE and paid for through a levy on the Nuclear Licencees
- The Industry Management Committee (IMC) Programme - that part of the HSC Co-ordinated Programme which is identified, placed and paid for directly by the Nuclear Licencees

The question of the long term performance of corrosion protection to prestressing system tendons and anchorage components was therefore addressed by a project which was run under the IMC Programme.

Research and Development

Previous Research

The first phase of the investigations involved a desk study of existing information relating to the greases used as protection for prestressing tendons and their anchorage components on all the UK nuclear power plants with PCPVs and PCCVs. The purpose of this study, under the IMC research programme, was to consider the long term performance of the corrosion protection applied to pre-stressing tendons.

The resulting NNC report (Reference 8) included a study of the corrosion likely to be suffered by tendons in PCPVs and PCCVs in UK nuclear power plants. It centred on two aspects : the performance of the corrosion protection applied to the tendons during installation and the environment in the tendon ducts during construction and operation. The study also looked forward to continuing operation and considered any corrosion likely to occur during the early stages of decommissioning. The work was based on a survey of archived records and published reports and also reviewed relevant experimental corrosion tests on steels.

It was concluded that most tendons are not at risk even if station operational lifetimes are extended to 40 years. The most damaging form of attack on tendons is pitting (since pits act as stress raisers) but pits will grow only if water enters the tendon ducts. During construction, the tendons were greased and, occasionally, the ducts were filled with wax after the tendons had been installed. It was identified that the risk of pitting depends on the type of grease used as some greases form stable emulsions with water and their presence can actually be deleterious while others were judged to be functioning well. Apart from tendon replacement, the prevention of corrosion is difficult once water has entered a tendon duct. However, relatively few tendons are thought to be susceptible to attack and the best way of minimising corrosion is prompt plant maintenance supported by the careful examination of drawn tendons and water leakage searches during PCPV surface examinations.

The aim of the study was to review the corrosion protection of tendons in PCPVs and to comment on the likely corrosion behaviour of tendons during future service. The first point to emerge was that most tendons are not at risk during continued operation. The normal environment inside a tendon duct is dry enough to prevent any significant rusting. The grease on tendons in dry ducts is therefore not essential for the prevention of corrosion so even if areas on a tendon were to be uncovered (either because the grease has slumped or was scraped off during installation) would not be damaged by corrosion. Tendons in PCPVs awaiting decommissioning would begin to corrode if the humidity in the duct or moisture content of the concrete is allowed to rise, but at a relatively slow rate.

With regard to any tendons which experience a fault condition, the study suggested that pitting could initiate if water enters a tendon duct and rates could increase further if CO₂ is also present since this will acidify the

water. However, CO₂ leaks have been rare and some protection would be derived from an iron carbonate surface film which will form on the tendons in this environment. The main source of water during reactor operation would be the Pressure Vessel Cooling Water (PVCW) system but any attack caused by this would be slow since this water is buffered to suppress corrosion. Short term leaks would also derive some alkalinity from the concrete and this too would make the water less corrosive. However, it was noted that, during the start of decommissioning when tendon integrity may still be important, there may be other sources of water which will be more aggressive towards carbon steel.

In all of the cases considered, attempts were made to judge the condition of the grease on the tendons, to predict the environment inside tendon ducts and to estimate likely corrosion rates. The only materials which are still likely to be giving any corrosion protection are the greases or duct fillers which were applied either during or after tendon insertion. The dip-type oils which were intended to provide temporary protection while the strands were in storage will have gone long ago - either by evaporation or by amalgamation into the grease.

The protective greases used on tendons on the different stations were of varied types. Details of the properties for each of the coatings used in the corrosion protection of tendons is given in Table 5.

	Alvania EP1	Astrolan 39	Castrol S200	Castrol S202	RustBan 324	IL 1978	2090P-4
Base	Li grease	wax	wax/grease	wax/grease	wax	wax	wax
Slump Temp °C	>72	62		72**		65	48
Emulsion	stable	unstable	stable	stable*	stable		nd
Water pick-up	fast	slow	fast	slow	fast		v.slow
Base neutrality	3	low	low	6	low	low	45
Leachable impurities	low	low	high SO ₄	low	high S		high SO ₄
Inhibitor	sulphonates	VPI	sulphonates	succinates	sulphonates	naphthanates	sulphonates
Healing	poor	n/a***	good	good	good	good	v.good

* reversible ** oil separates before slumping *** contains VPI nd : not detected

Table 5 Properties of Grease Type Coatings for Tendons in UK PCPVs & PCCVs

Most of the coatings form emulsions with water; some of these emulsions can be reversed by drying out but others seem to be too stable and could continue to trap water against the tendons. The central problem is that greases are not usually formulated with the prime aim of inhibiting the rusting of steel; they are lubricants with protection as a secondary function. In a worst case scenario, greases could prevent drying out and cause more corrosion than would occur on ungreased tendons.

The conclusions from the study were as follows :

- All tendons in UK PCPVs were coated with a grease or wax during installation.
- The great majority of tendons has remained dry because no water has entered the tendon ducts. Under these conditions, tendons will have suffered no significant corrosion during service and will suffer none unless the duct becomes wet.
- If water were to enter a tendon duct, the amount of corrosion would depend not only on the water chemistry but on the type of grease present. Some greases rapidly form stable emulsions and this helps determine the time of wetness of the tendons.
- Tendons remaining wet for long periods could suffer the additional risk of microbiological attack because some ingredients in greases can act as biological substrates.

- If structural integrity is to be maintained during the early stages of decommissioning, care must be taken to prevent water leaks into the PCPV tendon ducts. Corrosion pitting damage would increase when the vessel is cold and the humidity in the concrete and ducts rises. Under these conditions, any water would remain longer in a duct and the water chemistry may also be more aggressive.
- The elimination of water leaks into PCPV tendon ducts is therefore of prime importance and any leak searching should be tied in with a survey of signs of leakage from tendon anchorages.
- Little quantitative work had been done on the protection of tendons with grease over the longer term and it was suggested that the best source of this information would come from the examination of tendons routinely pulled from PCPVs.

SNL Stations - Hunterston B and Torness

Despite the fact that no problems had been encountered with the in-service performance of protective grease, it was decided prudent, following the publication of the NNC study, to take samples of grease from prestressing tendon strands withdrawn under the normal MITS requirements on the Torness Reactor 2 PCPV in February 1996 and on the Hunterston B Reactor 4 PCPV during May 1996.

As stated above, the in-service monitoring of the condition of the protective grease applied to the pre-stressing strand and to the external surfaces of the anchorage components in PCPVs is not specifically addressed as a requirement under the MITS or Section 9 of BS 4975. However, under Section XI "Rules for In-service Inspection of Nuclear Power Plant Components" of the American Society of Mechanical Engineers (ASME) Boiler and Pressure Vessel Code (Reference 9) there are specified tests and acceptance criteria which may be applied during inspection of the corrosion protection to prestressing tendons and their anchorage components in PCCVs. This was therefore used as the starting point for the investigation of the performance of the grease used at Torness and Hunterston B. One major difference between the concept of testing given in ASME XI for testing corrosion protection in PCCVs and testing on AGR stations is that the size of available sample for testing is smaller in the latter case. This is because the tendons in a PCPV are surface coated with grease during installation whereas the ducts on PCCVs are generally filled with protective grease or wax.

Alvania grease has been used in the protection of tendons in UK PCPVs for at least 20 years. It is a lithium soap grease whose main purpose is to provide lubrication under severe pressure. Its major constituents are oil (at least 50%) and the lithium soap which together make the stable gel. To this are added organic leaded and sulphurised compounds (either lead oleate and sulphurised lard oil or lead carbamate) which act as high pressure lubricants and an anti-rust inhibitor which is probably a sulphonate. Some lanolin may also be present but, as with all greases, the exact make-up is not disclosed by the manufacturer. Lanolin acts as a film healer: it possesses the peculiar ability to creep over a surface. Corrosion protection is derived from the oily constituents in the grease which probably comprise 70 to 80% of the total. These act to displace moisture from the surface of the tendon and thereby provide general protection in contrast to the sulphonate inhibitor which acts by coating only the anodic sites on the tendon such as active centres of rust pits.

During construction of the Hunterston B PCPVs a small amount of Castrol S200 grease was also used. Castrol S200 grease had a similar basic make-up (oil, soap and lanolin) but lacked the extreme pressure additives (which have no influence on corrosion protection). It is likely that the inhibitor was again sulphonate. Compared to Alvania, relatively little S200 grease was used at Hunterston and all the samples tested were of Alvania grease.

Determination of moisture in grease

The technique specified in ASME XI is ASTM D95 (equivalent to IP74/82, API 2560 and BS 4385) which is a Dean and Stark method. This needs a large glass rig and cannot handle small samples and is therefore unsuitable for this work. However, for measuring water in crude oils, ASTM D4006/IP 358 specifies a Karl Fischer technique and this was used here.

A known weight of grease was dispersed in a mixture of 60% toluene, 40% methanol in a closed cell. The moisture content was then titrated by a Karl Fischer technique using a Metrohm 701 KF Titrino automatic titrator. It was the high accuracy of this equipment (it can feed reagent at rates as low as 0.1 µl/minute) which enabled NNC to analyse grease samples as small as 0.25 gm.

Determination of water soluble ions

The general method is as given in Note (1) to Table IWL-2525-1 in ASME XI, Division 1 but, for this work, it was modified to permit the analysis of small samples of grease. In the ASME method, 100 gm. grease is used to coat the internal surfaces of a 1 litre beaker which is then filled with water and allowed to stand so that impurities are leached out of the grease. The water is then analysed. This method was used in the present work but the grease (approximately 0.1 to 0.4 gm.) was smeared onto the surface of a test-tube and extraction was done into approximately 5 ml. water. The water was analysed using a Dionex Ion Chromatograph using techniques which are standard throughout the UK Nuclear Industry and the results related back to the weight of grease used. With such small samples, it is likely that a larger proportion of the solubles is extracted so results will be pessimistic.

Determination of oil in grease

Samples of grease were immersed in petroleum ether which was then decanted leaving the soaps behind. The extract was allowed to evaporate for 48 hours at ambient temperature before weighing. The dried residue was also weighed. In a few cases, the dynamic viscosity of the oil remaining from the extract was measured, in samples from Torness, using an ICI Cone and Plate viscometer.

Grease Sampling at Torness

Grease samples were taken from three tendons, numbers 119F, 146C and 190H as they were pulled through the top anchorages and before they had been handled. Approximately 6 samples per tendon were collected and each was identified by its position on the strand measuring from the top. In addition, some grease was taken from two anchorages, 362K and 354K (selected at random) and from a stock of new Alvania EP1 grease. All were bagged and taken to NNC laboratories, Risley for examination.

Examination

All of the grease which was collected from the tendon strands came from the crevices between the wires; there were no significant amounts on the free surfaces of the strands due to withdrawal through the anchorage and stressing equipment. The grease samples were small : typically weighing less than 1 gram each and this shaped the analytical techniques which were developed. The following determinations were made :

- Oil content
- Water soluble chlorides
- Water soluble nitrates
- Water soluble sulphates and
- Moisture content

Some of the above tests form part of the ASME Codes for construction and inspection of containment prestressing. In particular, Tables CC-2442-1 of Section III (Reference 10) and IWL-2525-1 of Section XI (Reference 9) define maximum acceptance limits for chloride, nitrate and sulphate, along with test methods for their determination. In addition, the Section XI table gives a maximum value for water content.

Torness Results

Oil content in the grease

The analysis technique used here consisted of separating the oily constituents of the grease by extracting in petroleum ether and then evaporating to constant weight as described above. Results are given in Table 6 which give the proportions of both "oil" and non-soluble residue. The latter would contain the soap and may be regarded as including those materials which provide no protection for the steel. Protection will be derived from the "oily" fraction.

New grease was found to contain about 80% oily constituents and these levels were also found in samples taken from grease recently applied to anchorages. Results for samples taken from tendons found lower amounts of oils and correspondingly higher amounts of the non-protective constituents in the grease. The greatest difference came from grease on tendon 190H. This was the nearest of the three to the core and therefore had probably been the warmest. Grease taken from the centre part of this tendon contained about 56% oily components and 42% solids. The samples from this tendon were noticeably thicker than others but with the small sample sizes available, this could not be quantified with any accuracy. However, attempts were made to measure the viscosities of these extracted oils using an ICI Cone and Plate viscometer. The viscosity of the oil extracted from grease 50 metres from the top on tendon 190H was about twice as high as that for new Alvania (10 poise compared with 4.8 poise). This showed that it was the lighter constituents of these oils which had been lost during service.

Location	Distance from top of Tendon (metres)	% oil in grease	% residue
New Alvania EP1		74	21
New Alvania EP1		80	20
New Alvania EP1		82	16
Anchorage 354H		80	15
Anchorage 362K		80	14
Tendon 119F	12	67	27
	40	65	28
	60	64	34
Tendon 146C	20	69	28
	40	67	30
	60	60	36
Tendon 190H	30	70	29
	50	56	42
	66	70	27

Table 6 Oil Content in Samples of Grease from Torness PCPV (Age ~ 9 years)

Water soluble anions

The concentrations of water soluble ions in grease were measured using a method similar to that described in ASME XI, Table IWL-2525-1, Note (1). The results (see Table 7) were good; there was generally a low level of leachable ions in the samples collected. Only one sample gave results significantly higher than the ASME guideline levels; that was taken from tendon 119F, 12 metres from the top. The chloride values are the most important here since these can promote pitting and local attack of the tendon. The more generally high levels of sulphate in the samples could have been caused by concrete dust embedded in the grease and are of less importance. The only other sample to show a raised soluble anion concentration came from tendon 146C, 60 metres from the top but this did not greatly exceed the guideline concentration. It should be noted that, as stated above, the use of small samples will result in a larger proportion of solubles being extracted and lead to more pessimistic results.

Identification	Distance from top of Tendon (metres)	Concentration in grease (ppm)		
		Chloride	Nitrate	Sulphate
New Alvania EP1		9.5	1.7	6.5
Tendon 119F	12	55	20	90
	60	5.4	nil	3.8
Tendon 146C	20	7.6	nil	29
	60	15.5	0.6	30
Tendon 190H	66	3.1	nil	4.4
ASME maxima		10	10	10

Table 7 Water Soluble Anions in Samples of Grease from Torness PCPV (Age ~ 9 years)

Moisture content in the grease

Analyses were obtained using an automatic titrator and a Karl Fischer technique. Results are given in Table 8. The moisture content in new Alvania grease was indistinguishable from background. All the grease samples taken from tendons and anchorages had absorbed some moisture with one higher result for tendon 119F. However, the average moisture level was about 0.3% which is a highly satisfactory result. The maximum permitted level in ASME XI is 10%.

Identification	Distance from top of Tendon (metres)	% moisture in grease
New Alvania EP1	-	0.0
Anchorage 362K	-	0.13
Tendon 119F	26	0.44
	40	1.05
	50	0.36
	60	0.21
Tendon 146C	5	0.36
	30	0.17
	50	0.27
	70	0.38
Tendon 190H	20	0.25
	30	0.23
	50	0.25
	66	0.29
ASME XI maximum		10.0

Table 8 Moisture Content in Samples of Grease from Torness PCPV (Age ~ 9 years)

Discussion of Torness results

The samples of grease examined here were collected from three tendon strands in a reactor which had been in service for about 9 years with no history of water leaks into the PCPV. The results obtained in this study provide the first long term exposure data for grease operating under fault-free reactor conditions. This information will be of great value when comparisons are made with greases taken from stations where conditions have not been so benign, for instance, where there have been leaks of CO₂ or PVCW water into the tendon ducts or anchorages.

The grease taken from the three tendons was still in excellent condition; the principal change which has occurred has been the loss of some of the oily components which provide corrosion protection to the steel. About 20% of the oil has been lost from the grease since the tendons were coated. Greases are intended to "bleed" oil and the loss may have occurred in this way although greases near the bottoms of tendons did not contain noticeably more oil than those at the top. The other way in which oil may have been lost is by evaporation and this seems more likely. The attempts at measuring viscosity suggest a significant loss of the lighter components in the "oily fraction". The grease is therefore slowly drying out leaving the heavier oils and the soap constituents behind. These will continue to provide corrosion protection to the tendon but with some reduction in effectiveness. However, this will only be of concern if water enters the tendon duct at some future date. At present, it is judged that the grease is still offering substantial protection.

The greases have picked up some moisture even though conditions in the ducts are dry and warm. The amounts found, in the range 0.1 to 1.0%, are small and will cause no corrosion. Grease can tolerate much higher levels of water before the underlying steel starts to rust. The maximum moisture permitted by the ASME code is 10% but this is considered high especially for long term exposure. Despite the high pH of water which has passed through concrete, research at NNC (Reference 11) has shown that rust may spread beneath grease containing 10% moisture. Attack will be focused at any sites where there is a local concentration of chloride. A safer limit, especially for a grease which emulsifies as rapidly as Alvania, would be lower, say 5%, and the present results should be judged against this.

The concentrations of chloride, nitrate and sulphate in the samples of grease are low and meet the ASME guidelines except where noted above. It should be noted that the samples examined here were scraped from the tendons using a spatula and this would remove some of any surface deposits present on the tendon when they were installed in the ducts. The levels of salts in the stock Alvania grease are low. There will have been a batch-to-batch variation in the grease as originally used so most of the results in Table 7 suggest that there was no chloride contamination present on the tendons when installed and none has occurred since. The higher result for tendon 119F relates to an isolated patch of marginally higher salt contamination and is typical for a steel surface in a nuclear station.

If contaminants were deposited in the grease (as opposed to being present on the surface of the tendon), then some concentration in apparent anion concentration will have occurred as oil evaporates from the grease. A typical concentration value of 20% may be assumed from the results given in Table 6.

The study, commissioned under the Plant Life Management Programme (Reference 8), estimated the likely condition of tendon greases under different environmental conditions. For ducts that have remained water-free, it was predicted that the grease would dry out and eventually crack but that no corrosion of the underlying steel would occur. The work reported here is the first to yield information on grease ageing and it supports the view expressed in that report.

Hunterston B

A total of 15 samples of grease (each between 0.5 and 1 g) were collected from 5 tendon strands : 263F, 59H, 121B, 100A and 169D as they were withdrawn from Hunterston R4. Three samples were taken from each strand, from near the top, at the centre and at the bottom. In addition, a sample of a newer Shell grease, Calithia (similar to Alvania but based on calcium/lithium soap), was supplied. Each sample was chemically tested and the following determinations were made :

- oil content
- soap content
- water content
- water soluble anions (chloride, fluoride, nitrate and sulphate)

With regard to standards relating to the presence of contaminants in grease used on prestressing systems, ASME XI gives maximum limits for water content and water soluble ions (and also reserve alkalinity) (Reference 9). The ASTM test methods associated with these determinations are also given but could not be used as stated because of the large amounts of grease (typically 10 to 100 g) needed for each measurement.

Hunterston B Results

Appearance

Most of the samples of grease looked to be in good condition; they were visibly oily. However, 6 samples showed signs of deterioration and these are listed in Table 9. In three cases, the grease had retained the normal dark brown colour of Alvania but appeared to be drier than usual. The other three samples were pale coloured and had dried out. Each of these three had come from the mid-point of a tendon.

Location	Condition	% oil (see Table 2)
59H mid	dark, drying out	67
100A top	dark, drying out	70
121B top	dark, drying out	68
169D mid	light brown, dry	42
121B mid	light brown, dry	37
100A mid	light brown/white, dry	36

Table 9 Appearance of Samples of Grease from Hunterston B PCPV (Age ~ 24 years)

Oil content

The analysis technique used here consisted of extracting the "oily" constituents from samples of grease using petroleum ether and then evaporating this to a constant weight at room temperature. The vapour pressure of the oil is low compared to the ether and over a 24 hour period after drying, no further weight loss could be measured. The residue (which was insoluble in ether) contained the soaps and other constituents and was also weighed. Unless water is also present, the weights of extract plus residue should equal the weight of the sample. Results are given in Table 10.

Location	% oil	% residue	% total
263F top	68	30	98
263F mid	77	23	100
263F bot	81	14	95
59H top	60	37	97
59H mid	67	27	94
59H bot	83	12	95
169D top	72	26	98
169D mid	42	40	82
169D bot	68	28	96
121B top	68	30	98
121B mid	37	49	86
121B bot	70	32	102
100A top	70	27	97
100A mid	36	51	87
100A bot	68	29	97
Calithia	69	30	99
Alvania	79	19	98

Table 10 Oil Contents and Residues in Samples of Grease from Hunterston B PCPV (Age ~ 24 years)

Water soluble ions

The concentrations of water soluble ions in the samples of grease were determined using a method similar to that specified in ASME XI Table IWL-2525-1, Note (1). Results are given in Table 11 and have been corrected for the different ratio of water to grease so that they may be compared with the limiting values given in ASME XI. All samples contained low levels of soluble impurities.

Location	Soluble anions in grease (ppm)			
	Fluoride	Chloride	Nitrate	Sulphate
100A top	0.5	2	nd	2
100A bot	1.5	2	0.5	1
121B top	1	5	0.5	5
121B bot	1.5	2	2	6
169D top	nd	7	nd	4
169D bot	0.2	nd	nd	0.5
59H top	nd	2	nd	3
59H bot	nd	2	3	14
263F top	nd	8	nd	3
263F bot	nd	1	nd	7
Calithia	2	0.5	0.5	0.5
ASME XI	ns	10	10	ns

ns - no limit specified nd - below detection limit

Table 11 Water Soluble Anions in Samples of Grease from Hunterston B PCPV (Age ~ 24 years)

Water content

The amount of water in each sample is given in Table 12. With four of the tendon strands, the greases taken from the mid-points had high water contents - up to 18%. Two of these values exceeded the limit set in the ASME Code (see table IWL-2525-1) and in all, six of the fifteen samples contained more than 2% water.

Location	Water content (%)
100A top	2.71
100A mid	17.30
100A bot	0.81
121B top	1.21
121B mid	18.15
121B bot	1.49
169D top	1.45
169D mid	8.94
169D bot	0.94
59H top	0.60
59H mid	7.56
59H bot	1.31
263F top	2.48
263F mid	0.61
263F bot	1.14
New Calithia	0.15
ASME XI maximum	10.00

Table 12 Water Content in Samples of Grease from Hunterston B PCPV (Age ~ 24 years)

Discussion

The samples of Alvania grease taken from tendons at Torness NPS were examined and found to be in good condition after 9 years service as reported above. The samples removed from Hunterston B and discussed here have seen much longer service (~ 24 years). It is therefore possible to make general comments on any deterioration which has occurred during this time and the principal one is loss of oil.

On visual inspection, some of the Hunterston B grease samples were drying out. These came from the mid points of four out of the five tendons removed and from the tops of two of the same four tendons (Table 10). In the worst case, the grease felt dry although, on analysis, even this had retained 50% of its original oil (see 100A in Table 10). The grease therefore changes its visual appearance and "feel" while still containing a considerable quantity of oil. In time, oil separates from the soaps in grease and can either run down the tendon or evaporate. Oil has been lost from the hottest parts of the tendons while grease on the cooler parts has remained less affected. Evaporation therefore seems the likely cause of oil loss. The average oil contents for the top, middle and bottom samples are 68%, 52% and 74% respectively. New Alvania contains about 79% oily constituents (as measured by our technique) so grease at all positions sampled has lost some oil during service even though run-down might have been expected to boost the amounts of oil in grease on the bottoms of tendons.

Because of the different locations where samples were taken, it is difficult to compare these results with their direct equivalents at Torness but the lowest oil content found in any Torness sample was 56% (this was 50 metres down a 70 metre long strand) compared with 37% at Hunterston (half-way down tendon strand 121B). None of the samples from Torness had the dry, pale appearance of some of the Hunterston samples and this supports the belief that the grease is drying out with time.

If the oil and grease residues are added together, it can be seen that several sets of results showed an apparent shortfall (see Table 10). This is attributed to the presence of water in the grease which evaporated from extracts during the 24 hour drying time and whose weight was therefore lost. This was confirmed by analysis using an automated Karl Fischer apparatus which found quantities of water in these samples. The highest values, in the range 7 to 18%, came from the mid points of four tendon strands, 100A, 121B, 169D and 59H.

Water contents were greatest at the centres of the four tendons listed above. There was much less water at the tops and bottoms of the tendons. The most likely source of water entering the middle of tendon ducts is from leaks in the PVCW system but Hunterston R4 has an excellent history here. NNC leak sealing records list only one pipe on R4 which has ever needed sealing. Even this had a very small leak rate and it is unlikely that a PVCW leak had gone unnoticed taking into account the emphasis on water leakage detection during vessel monitoring.

Unlike some greases, Alvania forms stable emulsions with water so wetting of the ducts might have occurred some time ago. At temperatures of, say 50°C, the greases will eventually dry out unless water is still entering the ducts.

The extraction of soluble impurities done on these greases was more rigorous than that stipulated in ASME XI Table IWL-2525-1 because of the small sample size. The ASTM method uses 100 g of grease which is wetted for only 4 hours before the water is analysed. This extracts only those impurities in the surface layers of the grease. With total sample weights of ½ to 1 g taken from the Hunterston tendons, all soluble impurities would have been extracted so the results given in Table 11 are highly pessimistic. Despite this, all 20 chloride and nitrate results still fall well below the ASME guidelines; there are no fluoride and sulphate limits in ASME XI but those found in the Hunterston samples are excellent and will greatly reduce the risk of pitting corrosion of the tendons. Any chance of corrosion will arise from the moist environments around the centres of some tendons. At an early stage of this investigation, it was suggested that during the standard metallurgical examination which these tendon strands were to receive, special attention should be given to the condition of the central parts of strands 169D, 100A and 121B. During the metallurgical examination (Reference 12), only superficial staining was found on these five tendons; no deep pitting was found. This staining was most extensive on 100A and covered about half of 169D and 121B. There was less staining on 59H and much less

on 263F. Thus there was a general agreement between the condition of the tendon and of the overlying grease but no corrosion of any significance had occurred.

Future Research and Development

The assessment which was carried out by NNC under the IMC programme was based on available information and provided much useful information but, as little work had been done to investigate the performance of prestressing tendon grease protection in service, its conclusions were restricted. It was suggested in the recommendations from that study that the best source of information would be the investigation of samples of grease collected as tendons are withdrawn for examination under routine maintenance, inspection and test programmes. Currently, an extension of the previous study to carry out an investigation into the long term properties and performance of the protective grease on prestressing tendons and anchorage components by sampling of grease as tendons are withdrawn is in progress under the IMC programme. This will include the results of the testing that has been carried out at Torness and Hunterston B by Scottish Nuclear which has been reported here and further sampling from the majority of the UK nuclear power plants with a view to consolidation of the information in order for conclusions to be drawn. The current study will include a greater range of grease of different types and ages and from varied operating conditions to be considered.

Conclusions

- The samples of tendon grease taken at Torness are drying with time but after 9 years reactor operation, they still retain the ability to protect the steel.
- The impurity contents of the grease samples comply with the acceptance limits given in ASME XI.
- The Torness results describe the condition of Alvania grease after 9 years exposure in dry tendon ducts and therefore provide an excellent baseline with which to judge greases taken from other PCPVs.
- The grease tested from tendon strands removed from Hunterston B R4 has lost up to 50% of the oil components during approximately 24 years service. This is consistent with results for Torness where grease has started to dry out after 9 years service having lost up to 29% of the oil components. Its ability to provide corrosion protection to the tendons will therefore have been reduced but significant protection will still be provided.
- Some of the older samples of grease contained relatively high levels of water. There seems to be a general association of surface condition of the tendons with moisture level in the grease but no pitting was found on these tendons.
- It is concluded that, although the grease has lost some of its lighter oily constituents with time, it is still capable of providing corrosion protection to the prestressing tendons.

References

- 1.) Irving, J, Hinley, MS and McCluskey, DJ, "The Measurement of Unbonded Tendon Loads in PCPV and Primary Containment Buildings", Joint WANO-PC/OECD-NEA Workshop on Prestress Loss in NPP Containments, Civaux, France, August 23- 25 1997
- 2.) Smith, LM, "In-service Monitoring of Nuclear Safety Related Structures", The Structural Engineer, Volume 74, No.12, Pages 210-211, The Institution of Structural Engineers, UK, 18 June 1996.
- 3.) "The Nuclear Installations Act 1965", HMSO, UK, 1965 (*et seq*)

- 4.) Bradford PM, and McNair, IJ, "A Regulatory View of Nuclear Containment on UK Licenced Sites", Institution of Nuclear Engineers, International Conference on Nuclear Containment, Cambridge, UK, September 23-25 1996
- 5.) "The Pressure Systems and Transportable Gas Containers Regulations 1989", Statutory Instruments, 1989 No. 2169 Health and Safety, HMSO, UK, 1989
- 6.) BS 4975, "British Standard Specification for Prestressed Concrete Pressure Vessels for Nuclear Engineering", British Standards Institution, London, UK, 1990
- 7.) MacFarlane, JP, Smith, LM, Davies, DR, and McCluskey, DT, "In-service Monitoring of AGR and PWR Nuclear Safety Related Structures in the UK", Institution of Nuclear Engineers, International Conference on Nuclear Containment, Cambridge, UK, September 23-25 1996
- 8.) Taylor, MF, "An Assessment of the Corrosion Protection Applied to Tendons Used in Pre-stressed Concrete Pressure Vessels in the Nuclear Power Stations ", NNC Report C9837/TR/001, NNC Ltd., Knutsford, UK, September 1995.
- 9.) ASME Boiler and Pressure Vessel Code, Section XI, "Rules for In-service Inspection of Nuclear Power Plant Components", American Society of Mechanical Engineers, New York, USA, July 1995
- 10.) ASME Boiler and Pressure Vessel Code, Section III, Division 2, "Code for Concrete Reactor Vessels and Containments", American Society of Mechanical Engineers, New York, USA, July 1995
- 11.) Williams L & Taylor M F., NNC Report PWR/TM1016, Issue B, October 1990.
- 12.) McNair K and Pollock J A, " Hunterston B Power Station - Reactor 4. Metallurgical examination of five PCPV pre-stressing strands", Scottish Power Report 5223/203/R/96/6036, July 1996.

PRESTRESS FORCE LOSSES IN CONTAINMENTS OF U.S. NUCLEAR POWER PLANTS

Hans Ashar, James Costello, and Herman Graves^{1,2}

Abstract: In the design of prestressed concrete containment structures in the United States, allowances are made for losses due to elastic shortening of the structure, creep and shrinkage of the concrete, and relaxation of the prestressing steel. Prestressing losses higher than the initially projected losses have been reported by the licensees of a number of nuclear power plants with prestressed concrete containment structures. The higher losses have been attributed, generally, to higher than estimated losses due to relaxation of the prestressing steel. As the tendons of the affected containment structures have been protected from corrosion by means of grease (i.e., the tendons are not bonded), it is not difficult to retension the tendons to the required level of prestressing force. This paper describes general design bases, the inservice inspection criteria, and give details related to the plants where higher prestress losses have been reported. The paper concludes with a note that the actual factors contributing to the higher losses need further investigation.

Keywords: Prestress, containment, nuclear power plant, cement grout, bond, corrosion inhibiting grease, unbonded, elastic shortening, creep, shrinkage, relaxation.

INTRODUCTION

Prestressed concrete has been used in U.S. nuclear power plants for a number of structures, that is, containments, a reactor pressure vessel, missile shield members, reactor cavity walls, spent fuel pool girders, and structural supports for ice condenser floors. Prestressed concrete, however, is used principally in the construction of containment structures (or containments). Hence, this paper is based mostly on experience with prestressed concrete containments (PCCs).

In the United States, 109 nuclear reactors are in operation, and each reactor has its own containment. Of the 109 containments, 41 are PCCs, 31 are reinforced concrete containments, and 37 are steel containments.

¹ Senior Structural Engineers, U.S. Nuclear Regulatory Commission, Washington DC, 20555, U.S.A.

² The opinions expressed in this paper are those of the authors and not necessarily those of the U.S. Nuclear Regulatory Commission.

EVOLUTION OF PCCs IN THE U.S.

The functional and performance requirements for containments can be satisfied by various types of composite and hybrid steel-concrete constructions. Originally, the containment was envisioned as a static pressure envelope fabricated of steel in various configurations (e.g., spherical, cylindrical with an elliptical bottom and hemispherical dome, and cylindrical with a hemispherical dome and flat slab). A separate reinforced concrete structure surrounding the containment served as a biological and missile shield. As the capacity of the nuclear power plants increased, the fabrication of high-pressure steel containment structures with post-weld heat treatment became too costly and in some cases technologically difficult. Thereafter it seemed prudent to combine the containment and shielding functions into a composite steel-lined reinforced (conventional or prestressed) concrete structure. In this concept, the welded steel liner, typically less than 13 mm (0.5 in.) thick and anchored to the concrete by studs or rolled sections, provides leak-tightness for the concrete containment. The concrete envelope is designed to withstand the postulated loadings with an adequate margin of safety.

With the introduction of concrete containment construction, the vertical cylinder with a shallow or hemispherical dome and a flat foundation mat became a preferred shape for containments. In the 1960s, the first PCCs were prestressed only in the vertical direction with non-prestressed reinforcing in the circumferential (hoop) direction of the cylinder and in the dome (e.g., containments at the R. E. Ginna and the H. B. Robinson Unit 2 nuclear stations).

Fully prestressed PCCs were first built in the late 1960s and typically consisted of a cylindrical wall, a shallow dome, a large ring girder at the intersection of the dome and wall, six buttresses, and a flat reinforced concrete base slab. The wall was prestressed by hoop tendons anchored at two alternate buttresses and spanning 120° (six buttresses total) and by vertical tendons anchored at the top of the ring girder and at the bottom of the foundation mat in a specially constructed tendon gallery. The dome was prestressed by three sets of tendons oriented at 120° to each other. The dome tendons were anchored to the ring girder. Because of the number of tendons (>900), which required a very labor-intensive activity to fabricate, install, tension, and corrosion-proof, and because the plants were increasing in size, a second generation of fully prestressed concrete containment designs with three or four buttresses evolved. Although the use of three buttresses, instead of six, increased the length of hoop tendons and the friction force, the reduced number of buttresses and anchorages produced considerable cost savings. Another change was that the capacity of the post-tensioning tendons was approximately doubled, significantly reducing the total number of tendons. In the third generation of PCCs, the shallow dome was replaced with a hemispherical dome, the ring girder was eliminated, and the dome and vertical tendons were replaced by inverted U-shaped tendons. The inverted U-shaped tendons were divided into two sets of tendons oriented at 90° to each other. Hoop tendons were still anchored to the three buttresses. Figure 1 shows some of the common configurations.

Prestressing Systems

There are three major categories of post-tensioning systems: wire, strand, or bar. The tendons are installed within preplaced ducts in the containment structure and are post-tensioned from one or both ends after the concrete has achieved sufficient strength. The primary evolution in prestressing systems over the years has been in system capacity. Before the advent of PCCs, prestressing systems were relatively small, that is, with an ultimate capacity of less than 4.45 meganewtons (MN) (500 tons). The requirements to withstand high forces resulting from a combination of increased volumes and pressures of the dry containments of the pressurized water reactors necessitated the development of tendon systems with capacities ranging from 8.0 MN (900 tons) to 10.7 MN (1200 tons). This development permitted increased spacing of tendons and reduced congestion; the number of tendons, tendon ducts, and anchorages was almost halved. The large tendons were developed using groupings of multiwire or multistrand systems. The satisfactory performance of the large tendons was verified by a number of static and cyclic tests on prototype full-size tendons and detailed stress analyses of anchorage hardware. Current material and performance test requirements for the post-tensioning systems are provided in Reference 11. In the United States, the 8.9-MN (1000-ton) systems approved for use are: (1) the Birkenmaier Brandestioni RVS and Vogt (BBRV) wire system, (2) Vorspann System Losinger (VSL) strand system, and (3) Stresssteel S/H strand system. The BBRV and VSL are the most commonly used systems for PCCs.

The large-capacity BBRV tendon systems consist of 163, 169, 170 or 186 wires. The wire diameter is 6.35 mm (0.25 in.) except for the 163-wire tendon, where 7-mm (0.28 in.) wires are used. Each wire is anchored by a buttonhead that is cold-formed and bears on anchor heads at each end of the tendon.

The large-capacity VSL tendon system consists of 55 seven wire strands; the wire diameter being 12.7 mm (0.5 in.). Anchorage is provided by a two-piece split cone wedge held tightly against the inner surface of the anchor head.

Corrosion Inhibitors for Prestressing Tendons

Prestressing plays a vital role in ensuring the structural integrity of the PCC throughout its design life (normally 40 years). However, because the tendons and their anchorage hardware are fabricated from high-strength, high-hardness materials and are subjected to sustained high stresses, they are susceptible to stress-corrosion cracking and hydrogen embrittlement. The tendons and their load-bearing hardware are protected against the corroding influences by filling the tendon ducts with Portland cement grout (bonded tendons) or petrolatum-based microcrystalline waxes compounded using organic corrosion inhibitors (unbonded tendons).

Portland Cement Grout

The effectiveness of Portland cement as a deterrent to the corrosion of steel is evidenced by its performance history in prestressed concrete for 50

years and in reinforced concrete construction for over 100 years. A review of the durability performance of post-tensioned tendons in conventional civil engineering structures showed that incidence of corrosion was small (less than 1 in 100,000) and related to either ill-conceived detailing, poor construction practices, or the presence of contaminants¹. This performance history was supplemented by extensive tests conducted to ensure adequate penetration of grout through vertical bars and curved hoop and long vertical strand tendons.²⁻⁵ The regulators, however, were concerned about not being able to positively check the integrity of the post-tensioning system throughout the service life of the structure. As a result of discussions and public meetings, the NRC developed two regulatory guides (RGs).^{6,7} RG 1.107 (Ref. 6) provides recommendations for qualifying Portland cement grout, and RG 1.90 (Ref. 7) provides two distinct approaches for inservice inspection of PCCs with grouted tendons. Though the intent of these guides was to ensure that grout material and grout installation were thoroughly scrutinized, and that the status of PCCs with grouted tendons was periodically checked, these actions did not encourage the use of grouted tendons in PCCs. At present, there are two PCCs with grouted tendons in the United States. One of them is the PCC at Three Mile Island Unit 2; it has strand tendons and has not operated since the accident in 1979. The second is the PCC at H. B. Robinson Unit 2 (bar tendons).

Petrolatum-Based Grease

Although the use of organic petrolatum-based corrosion protection compounds (greases) is a more recent development it has gained prominence in PCCs in the United States because of the relative ease with which the tendons can be inspected and tested. Additional advantages include the following: (1) encapsulation provides about 50% reduction in the friction factor thus permitting the use of longer tendons and fewer buttresses and anchorages; (2) tendons may be relaxed, retensioned, and replaced as required; and (3) a corrosion-protection coating applied in the shop (before shipment) permits the installation and tensioning of tendons, and the installation of grease to be scheduled efficiently during the construction sequence.

The petrolatum-based filler greases have evolved over the years to make the products more suitable to the application of unbonded (greased) tendons in PCCs. Initially, the product was a sheathing filler containing polar wetting agents, rust-prevention additives, microcrystalline waxes, and proprietary constituents formulated to be water displacing, self-healing, and resistant to electrical conductivity. The next generation of materials was formed by adding a plugging agent to raise the low-flow point of the products [$\approx 39^{\circ}\text{C}$ (100°F)] to keep them from seeking loose sheathing joints and flowing into hairline cracks in concrete. A subsequent refinement involved incorporation of a light base number to provide alkalinity (3 mg KOH/gm of product) for improved corrosion protection. The current generation of products has been formulated to (1) increase the viscosity without sacrificing pumpability, (2) raise the congealing point to $57\text{--}63^{\circ}\text{C}$ ($135\text{--}145^{\circ}\text{F}$), (3) increase the resistance to flow from sheathing joints, (4) increase water-displacing characteristics, and (5) raise the base number (35 mg KOH/gm of product) to provide higher reserve alkalinity.^{8,9}

DESIGN CONSIDERATIONS

The containment is a vital engineering safety feature of a nuclear power plant. It encloses the entire reactor and the reactor coolant system and serves as a final barrier against the release of radioactive fission products to the environment under various accident conditions. Containment design is based on pressure and temperature loadings associated with a loss-of-coolant accident (LOCA) resulting from a double-ended rupture of the largest pipe in the reactor coolant system. The containment is also designed to retain its integrity under low-probability ($< 10^{-4}$) environmental loadings such as those generated by an earthquake, tornado, hurricane, seiche, or tsunami. Additionally, it is required to provide biological shielding under normal and accident conditions and to protect the internal equipment from external missiles, such as tornado or turbine generated missiles and aircraft impact (where postulated).

Safety-related concrete structures (e.g., containments) of early light-water reactor plants were designed and constructed using the provisions of American Concrete Institute (ACI) 318¹⁰, supplemented by the specific loads and load combinations pertinent to their design, as stipulated by the Nuclear Regulatory Commission (NRC). Current requirements for the design and construction of concrete reactor vessels and containments are delineated in ASME Code Section III, Division 2¹¹. Supplemental criteria (or endorsement of Reference 11) are delineated in RG 1.136¹² and Standard Review plan (SRP) Section 3.8.1.¹³

The design for the required prestressing forces (F) in a PCC is principally governed by the conservatively calculated internal pressure load (P) imposed on the containment during a LOCA event. Prestressing forces required in each of the major directions (i.e., hoop and vertical in cylinders, and two-way or three-way in the dome) are estimated so as to neutralize the tensile forces generated by P, 1.25P, or 1.5P (depending upon the design requirements). For a preliminary design, the effective prestressing force in a tendon is the initial force (F_i) [approximately 70 percent of the guaranteed ultimate tensile strength (GUTS) of the tendon], minus 15 to 25 percent of F_i , to account for the initial and time-dependent losses. The final design incorporates the detailed calculations of the losses and predicted forces for the tendons.

RG 1.35.1¹⁴ provides guidelines for calculating the losses and the predicted forces that could be used to compare with the measured prestressing forces during the periodic inspection of the containment post-tensioning tendons. The initial losses to be considered in computing the predicted forces are the losses due to (1) the slip of prestressing elements at the anchorages, and (2) the elastic shortening of the structure. The time-dependent losses are those induced by (1) concrete shrinkage, (2) concrete creep, and (3) the relaxation of prestressing steel. The RG also recommends that appropriate consideration be given to the effects of potential degradation of prestressing elements and variation in sustained temperature. For discussion of the initial prestressing losses, see Reference 14. Major contributors to the time-dependent losses are discussed in detail in the following paragraphs.

Concrete Shrinkage

The construction schedule of a typical prestressed concrete containment is such that a substantial portion of the expected long-term shrinkage takes place before the structure is prestressed. Reference 15 presents formulas for predicting the long-term shrinkage based on the assumption that the shrinkage approximately follows the laws of diffusion and supports the formulas by experimental investigation. An appropriate extrapolation of these formulas (for the volume-to-surface ratio of the structure in excess of 60 cm (24 in.) and the contributing shrinkage as that could occur 100 days after the average time of construction of the structure) would yield a value of 100×10^{-6} , which is considered to be a reasonable value at a temperature of 21° C (70° F) and a relative humidity of 50%. The safety analysis reports of several plants indicate that a 40-year shrinkage value of 100×10^{-6} has been used in the design.

This value, however, needs to be modified to account for the significantly higher shrinkage in a low-humidity environment and the significantly lower shrinkage in a high-humidity environment. Table 1 provides typical shrinkage values that could be used for computation of prestressing losses caused by shrinkage.

Concrete Creep

One of the most significant and variable factors in the computation of time-dependent losses in prestressed concrete containment structures is the influence of concrete creep. Creep is thought to consist of two components: basic creep and drying creep. Drying creep, also sometimes termed stress-induced shrinkage, is due to the exchange of moisture between the structure and its environment. Its characteristics are similar to those of shrinkage, except that they represent an additional moisture movement resulting from the stressed condition of a structure. The amount of drying creep depends mainly on the volume-to-surface ratio of the structure and the mean relative humidity of the environment. For prestressed concrete containment structures having a volume-to-surface ratio in excess of 60 cm (24 in.), the relative influence of drying creep (compared to basic creep) is negligible.¹⁶

Four parameters significantly influence the magnitude of basic creep:

1. concrete mix (Cement and aggregate type; proportion of cement, water, and aggregates; and the influence of admixtures)
2. age at loading (the basic creep value being a function of the degree of hydration that has taken place at the time of loading)
3. the magnitude of the average sustained stress
4. temperature

Almost all investigators support the assumption that basic creep varies linearly with the intensity of sustained stress, as long as the average stress

in the concrete is not greater than 40% of the ultimate strength of the concrete. The specific creep is thus defined as the ratio of total creep to the average stress intensity.

A literature review of the effect of temperature on basic creep (sealed or water-stored concrete specimens) is compiled in Reference 16. The average temperature of a prestressed concrete containment structure could vary between 5°C (40°F) and 38°C (100°F). Basic creep is shown to vary linearly with temperature in this range of temperatures.

An acceptable method of determining basic creep at various times for a given concrete mix as a function of age at loading is provided in Appendix A of RG 1.35.1.¹⁴ The method is based on concepts and equations derived by Hansen¹⁷ from a rheological model representing concrete creep. Reference 18 uses the method of Reference 17 in determining long-term creep for a given concrete mix. Most investigators agree that no one formula can be generally applicable in determining the long-term creep for various concrete mixes. Hence Reference 14 recommends a method of predicting the long-term basic creep from the results of short-term creep tests.

Relaxation of Prestressing Steel

The stress relaxation properties of prestressing steel vary with its chemical composition and thermal/mechanical treatment. Manufacturers should be able to provide data on the long-term loss in prestressing steel stress from pure relaxation. Section CC-2424 of Reference 11 requires a minimum of three 1000-hour relaxation tests for the prestressing steel proposed for use. There should be a sufficient number of data points in each of the three tests to extrapolate the 1000-hour pure relaxation data to the planned useful life of the structure.

Losses Caused by Tendon Degradation

Utilities make allowance for breakage of wires on an overall basis as well as on a localized basis. Such an allowance in the design of the containment would allow a breakage of a few wires during construction without a need for replacing these wires. For a tendon with a few broken wires, care should be taken not to overstress intact wires to bring the tendon force to a prescribed value. Instead, the tendon should be extended to the same strain level as other similar tendons (without broken wires). The procedure will leave the tendon at a prestress level lower than the prescribed (generally 70% of the guaranteed ultimate tensile strength (GUTS)) level. This is acceptable provided the design includes an allowance for the breakage of wires.

Variations in Temperature

Of particular importance for the purpose of comparing the prestress forces is the effect of differences between the average temperature of the structure during installation and that during inspections. Localized hot spots and temperature variations along the length of a tendon can cause variations in the force along the length of the tendon. The differences between the coefficients of expansion or contraction of concrete and steel can

also cause modifications of tendon forces. These effects, as appropriate, should be considered in comparing the measured prestressing forces with the predicted forces.

INSERVICE INSPECTION OF POST-TENSIONING SYSTEM

Grouted Tendon Containments

Because grouted tendons cannot be inspected directly, a number of alternative methods of assessing the integrity of the PCCs with grouted tendons were investigated in the early 1970s, when some utilities were exploring the use of grouted tendons for their PCCs. After a number of public meetings and discussions among knowledgeable professionals, the regulatory staff promulgated the final provisions for inspecting the PCCs with grouted tendons in Revision 1 of Regulatory Guide (RG) 1.90.⁷ Two distinct alternatives are provided in the guide. The first alternative requires the monitoring of prestress level in the PCC with strategically located instrumentation (strain gages, stress meters, load indicators, etc.). The second alternative requires the monitoring of deformations of the PCC at critical locations under prescribed pressures. The monitoring of prestressing forces in strategically located ungrouted tendons and visual examination of tendon-anchorage areas and structurally critical areas are the common inspection provisions for both the alternatives.

Greased Tendon Containments

Inservice inspection (ISI) programs for the earlier PCCs (i.e., those licensed before 1973) with greased tendons were developed on a case-by-case basis. In general, the inspection consisted of (1) monitoring nine selected tendons for prestressing force, grease, and condition of anchor hardware, and (2) visually examining the exterior of the containment. The inspections were to be performed more frequently in the early years (typically the first five) and less often during the later years. The practice of repeatedly inspecting the same tendons was a subject of considerable discussion in the early 1970s. A number of industry professionals and members of the regulatory staff felt that monitoring the same nine tendons out of approximately 1000 tendons would not provide adequate information about the condition of the entire tendon population. It was also recognized that repeatedly tensioning and detensioning the same tendons during all inspections would increase the possibility of damaging these tendons. The consensus was that it was necessary to inspect the tendons on a random but representative basis to ensure the effectiveness of the inspection program.

After a number of discussions with industry groups and after taking into consideration the performance of prestressing systems in other civil engineering structures, the NRC staff decided that 21 tendons should be inspected during each of the first three inspections. If no significant problems with the post-tensioning system were found during these inspections, the subsequent inspections were to be performed using a reduced sample size. The first effective version (i.e., Revision 1) of RG 1.35¹⁹ prescribed a scheme in which 21 tendons (10 hoop, 5 vertical, and 6 dome tendons) were to

be inspected during the first three inspections and 9 tendons (3 from each group) during subsequent inspections. Additionally, the RG provided for (1) inspecting tendon-anchorage areas, (2) checking for grease coverage in the selected tendons, (3) testing the material properties of the prestressing elements removed from the tendons, and (4) visually examining of the exterior surfaces of the PCC. Revision 2 of RG 1.35 incorporated provisions for Type III (Figure 1) PCCs.

The regulatory staff issued Revision 3 to the RG in July 1990 to update and clarify the guide on the basis of experience obtained during prior inspections. Various interpretations by the utilities of the acceptability of measured prestressing forces in tendons concerned the regulatory staff enough to issue a companion guide (RG 1.35.1¹⁴) together with Revision 3 of RG 1.35. Additional information on the development of ISI provisions and an assessment of their effectiveness are given in References 20 and 21.

In August 1996, the NRC staff issued an amendment to its regulation for the use of Codes and Standards. The amended regulation endorsed Subsection IWL²² of Section XI of the ASME Boiler and Pressure Vessel Code. Subsection IWL on inservice inspection of reinforced and prestressed concrete containments incorporated the provisions of Revision 3 of RG 1.35 for ISI of post-tensioning tendons.

PERFORMANCE DATABASE

A discussion of problems encountered during the construction of prestressed concrete containment are described by Ashar et. al.²³ Unusual incidents, related to post-tensioning tendons reported during the operation, are described in Reference 24. The incidents related to the losses in prestressing forces are summarized in the following paragraphs.

Plant 1

The containment structure at the plant is a reinforced concrete structure, post-tensioned in the vertical direction of the containment cylinder by 160 vertical tendons. The structure is reinforced in the hoop direction of the cylinder and in the dome by non-prestressed reinforcing bars. The vertical tendons are coupled to prestressed rock anchors at the bottom of the tendons (Figure 2). A tendon consists of ninety, 6.4 mm (1/4 in.) diameter, stress-relieved, American Society of Testing and Materials (ASTM) A416 wires. The GUTS of the wire is 52.31 kN (11.76 Kips). During the original stressing operation, the tendons were overstressed to 0.8 of the GUTS and locked-off at 0.7 of the GUTS. The stressing operations were performed in March-April of 1969. Twenty-three tendons were retensioned and locked-off at 0.7 of the GUTS, approximately 1000 hours after the original lift-off.

Between the dates of the original lock-off and October 1979, the utility performed five lift-off tests of the selected tendons (i.e., approximately at 6 months, 1 year, 3 years, 8 years, and 10 years after the original lock-off dates). During each lift-off test, the utility observed that the individual as well as the average tendon forces were lower than those predicted for the

time of the tests. At the 10th year lift-off tests, the average of the measured tendon lift-off forces was marginally higher than would be expected at 40 years. A consultant to the utility investigated the potential causes and solution for the problem.²⁵

The consultant identified 10 potential causes as part of its investigation: (1) coupling at rock anchors, (2) rock creep, (3) rock failure, (4) tendon wire stresses, (5) tendon thermal expansion, (6) stressing equipment calibration and lift-off procedure, (7) 6 per cent overstressing of wires, (8) elastomeric pad creep, (9) stress relaxation, and (10) tendon type. After studying each of these effects in detail, the consultant determined that cause 9, high stress relaxation of wires, is the dominant contributor to the higher than predicted losses in prestressing forces.

The wires used in the tendons at this plant were determined (by the wire fabricator) to have a 40-year design relaxation loss of 12 percent of the prestressing force in the wires. To confirm the finding about high relaxation losses in wires, the utility awarded a contract to Fritz Engineering Laboratory of Lehigh University to test production wires obtained from the prestressing tendons at the plant. A total of 14 specimens was tested at temperatures of 20°C (68°F), 25°C (78°F), and 40°C (104°F); and at initial prestressing forces of 0.70 and 0.75 of GUTS.

Typical results of the relaxation tests are shown in Figure 3. The results clearly show appreciably higher relaxation of wires at 25°C and 40°C than at 20°C. Based on the information regarding the outdoor temperatures and the operating temperatures in the containment structure at the plant, the consultant estimated the average temperature around the tendons to be between 30°C and 35°C. The interpolation of the tested relaxation loss values at these temperatures gave a relaxation loss of 17.5 percent compared to the 12 percent loss value used in the design. The utility retensioned 137 tendons to the average lock-off force of 0.72 of the GUTS of the tendons in June 1980, and based its estimate of the predicted forces in the tendons on the relaxation test data.

In July 1981, the prestressing forces in 18 selected tendons were measured to assess the behavior of the retensioned tendons. The results showed that the average of the measured forces was 0.99 of the average of the predicted forces for the same tendons. In June 1983, another set of 18 tendons was selected for lift-off measurement. The average of the measured forces in this surveillance was found to be 1.014 of the average of the predicted forces. In a SMIRT conference paper, Fulton et al.²⁶ describe the results of these measurements. The utility performed such surveillances in 1988 and 1993, and has not reported any unusual behavior of the retensioned tendons.

Plant 2 (two Units)

The containment structures of this plant are PCCs with Type I configuration (Figure 1). The inside diameter of the cylindrical wall of each PCC is 35.35 m (116 ft), the thickness of the wall is 1.143 m (3.75 ft), and the thickness of the shallow dome is 0.99 m (3.25 ft). Each PCC has 165 dome

tendons, 180 vertical tendons, and 489 hoop tendons. Each tendon consists of ninety-6.4 mm (0.25 in) wires anchored at their ends by BBRV button-head anchorages. During the performance of 20th year tendon surveillance in November-December 1992, it was found that the measured prestressing forces of a number of randomly selected tendons in both Units were appreciably lower than the predicted forces. The lower tendon forces were found in all groups of tendons. The utility, with the assistance of its consultant, investigated the root cause and implemented necessary corrective actions.

The root cause investigation indicated that the most probable cause for lower prestressing forces (higher prestressing losses) was an increased tendon wire steel relaxation resulting from the sustained high temperatures around the tendons. The analysis of the meteorological data indicated that the average sustained temperatures around the tendons could be estimated as 32°C (90°F). The supplier of the prestressing wire had provided 8 percent as the wire relaxation losses at 20°C, and had indicated higher relaxation losses at higher temperatures. In estimating prestressing forces, the utility had used 8 percent of the prestressing force in the tendons as the loss due to relaxation. Also, the investigations performed at other nuclear power plants indicated the relaxation losses at such temperature (i.e., 32° C) could be 14 percent.

In this case, instead of retensioning the tendons, the utility demonstrated to the regulatory authority (the NRC) that the design basis containment internal pressure was at least 10 percent higher than the calculated peak internal pressure. Thus, using the original load combinations and reduced pressure load (reduced prestressing forces), the utility demonstrated that the containment design basis was satisfied without exceeding the original acceptance criteria for stresses in concrete, reinforcing steel, and prestressing steel.

Plant 3

The containment at this plant is a Type II PCC (Figure 1). During the fourth surveillance of tendon forces in February 1990, the utility discovered that the forces in the 115 vertical tendons were lower than expected. As the wires used in the prestressing tendons were of the same size, type, and relaxation property as those used in Plant 1 tendons, the utility concluded that the reason for low prestressing forces was the higher (than considered) relaxation of prestressing wires. As in the case of Plant 1 and Plant 2 containments, the average temperature around the tendons was determined to be 32° C. The utility retensioned the vertical tendons at an average lock-off force of 0.685 of the GUTS of the wires.

DISCUSSION

In all the cases discussed above, the utilities concluded that the dominant contributor to the higher losses was the high relaxation of the prestressing steel. In the U.S., the stress relaxation tests for materials and structures are conducted in accordance with the standard method developed by the ASTM in ASTM E-328.²⁷ The general stress relaxation test is performed

by isothermally loading a specimen to a fixed value of constraint. During the entire test period, the ASTM method requires the specimen to have specified temperature with a tolerance of $\pm 3^{\circ}\text{C}$. A normal duration of the test, as required by Reference 11, is 1000 hours. A minimum of three tests are required. Unless explicitly specified otherwise by the purchaser, the tests are conducted at $23^{\circ}\text{C} \pm 3^{\circ}\text{C}$. The prestressing steel fabricator conducts the relaxation tests, performs the regression analysis of the data, and provides the total relaxation values to be considered in the design.

As noted in the discussion above, the average temperatures around the prestressing tendons could vary between 28°C and 33°C . The tests conducted at Lehigh University clearly indicated that the relaxation losses increase appreciably at high temperatures (Figure 3).

Other potential factors contributing to higher than estimated prestressing losses are high shrinkage and creep of concrete at high temperatures. As discussed in RG 1.35.1 (Ref. 14), the shrinkage and drying creep do not contribute appreciably to the total losses in prestressing forces. The contribution of basic creep in the estimated prestress force losses could be as much as that of the stress relaxation of prestressing steel. It is also recognized that the basic creep increases with temperature, but not as much as the relaxation of prestressing steel. Moreover, the U.S. utilities found that a good part of the higher prestressing losses can be explained by the high relaxation losses of prestressing steel. Thus, no additional plant-specific research is being performed to understand the potential contribution of high creep at high temperatures.

Revision 3 of RG 1.35 (Ref. 19) and Subsection IWL (Ref. 22) require the utilities to monitor the prestressing forces in tendons at the end anchorages. The design of the containment is based on the minimum prestressing forces in tendons, estimated considering the initial losses, time-dependent losses, and friction losses. In monitoring the tendon prestressing forces at end anchorages, it is assumed that the estimated losses are conservatively calculated for the operating life of the plant and that these forces accurately represent the minimum forces in the tendons. Based on a limited study of the tendon lift-off data, Hill²⁸ indicated in a letter report to NRC that there does not seem to be any consistent relation between end anchorage force and the remaining forces along the length of the tendon. In fact, he emphasized that the actual minimum force in a tendon could be lower than that obtained from the measured end anchorage force, implying that the time-dependent losses along the length of the tendons could be higher than those at the end anchorages. In arriving at this conclusion, Hill considered the average tendon force calculated from the corrected elongation of the tendons as the actual average force, and the force calculated by subtracting the friction force from the measured lift-off force as the measured force.

Without making any judgement on the validity of the conclusions reached in Dr. Hill's study, the authors believe that if the tendon end anchorage forces are accurately measured and if they are well above the conservatively calculated lower limits (see Ref. 14), the prestressing tendon behavior can be considered as acceptable.

CONCLUDING REMARKS

The periodic surveillance of post-tensioning tendons in prestressed concrete containments in the United States has shown that the deterioration of the tendon hardware, such as bearing plates, anchor heads, wedges, button-heads, has been insignificant. A small amount of water is occasionally found in end caps, but is not found to cause deterioration of anchor hardware. Leakage of sheathing filler (corrosion inhibiting grease) from the end caps stains the concrete and creates messy clean-up work. However, the filler is protecting the tendon hardware effectively. Losses in prestressing forces higher than those considered in the design have been reported at a number of plants. The primary reason for the higher losses appears to be higher than anticipated temperature. Based on the extensive investigative work sponsored by the owner of Plant 1, the utilities have concluded that the main factor in higher (than estimated) prestressing force losses is the high relaxation of prestressing wires at relatively high temperature.

REFERENCES

1. M. Schupack, "A Survey of Durability Performance of Post-Tensioning Tendons," *Journal of American Concrete Institute*, 75(10):501-10, October 1978.
2. A. Wern, M. Schupack, and W. Larsen, "Prestressing System for H. B. Robinson Nuclear Power Plant," *Journal of the Power Division*, American Society of Civil Engineers (ASCE), Vol. 97, March 1971.
3. G. Harstead and E. Kummerle, "Grouted Tendons for Nuclear Containments," *Journal of the Power Division*, ASCE, Vol. 95, October 1969.
4. G. Harstead, E. Kummerle, J. Archer, and M. Porat, "Testing of Large Curved Prestressing Tendons," *Journal of the Power Division*, ASCE, Vol. 97, March 1971.
5. M. Schupack, "Grouting Aid for Controlling the Separation of Water for Cement Grout for grouting Vertical Tendons in Nuclear Concrete Pressure Vessels," Conference Paper 151/75, *Experience in Design, Construction and Operation of Prestressed Concrete Pressure Vessels and Containments for Nuclear Reactors*, Institution of Mechanical Engineers, London, September 1975.
6. U.S. Nuclear Regulatory Commission (NRC), "Qualification of Cement Grouting for Prestressing Tendons in Containment Structures," Regulatory Guide 1.107.
7. NRC, "Inservice Inspection of Prestressed Concrete Containment With Grouted Tendon," Regulatory Guide 1.90, Rev. 1.
8. C. W. Novak, Viscosity Oil Company, Chicago, Illinois, personal communication to H. Ashar, NRC, November 11, 1982.

9. D. Naus, "An Evaluation of the Effectiveness of Selected Corrosion Inhibitors for Protecting Prestressing Steels in PCPVs," ORNL/TM-6479, Oak Ridge National Laboratory (ORNL), Oak Ridge, Tennessee, March 1979.
10. American Concrete Institute (ACI), "Building Code Requirements for Reinforced Concrete," ACI Standard 318, ~~Detroit~~, 1963.
11. ASME Code Section III, Division 2 (or ACI Standard 359), "Code for Concrete Reactor Vessels and Containments," 1995.
12. NRC, "Materials, Construction and Testing of Concrete Containment," Regulatory Guide 1.136, Rev. 2 (endorsement of ASME Section III, Division 2, with exceptions).
13. NRC, "Standard Review Plan for the Review of Safety Analysis Reports," NUREG-0800, Section 3.8.1, "Concrete Containments," July 1981.
14. NRC, "Determining Prestressing Forces for Inspection of Prestressed Concrete Containments," Regulatory Guide 1.35.1.
15. T. C. Hansen and A. H. Mattock, "Influence of Size and Shape of Member on the Shrinkage and Creep of Concrete," *Journal of the American Concrete Institute*, Vol. 63, February 1966 (also published as PCA Development Bulletin D103).
16. H. G. Geymayer, "Effect of Temperature on Creep of Concrete: A Literature Review," Paper 31 of ACI SP-34, "Concrete for Nuclear Reactors," Vol. 1, ACI, ~~Farmington Hills, MI~~, 1972.
17. T. C. Hansen, "Creep and Stress Relaxation of Concrete," Swedish Cement and Concrete Research Institute, Stockholm, 1960.
18. Schupack and Associates, "Report on Recommended Concrete Creep and Shrinkage Values for Computing Prestressing Losses." This nonproprietary report is filed in the NRC Public Document Room as Appendix 5J in Amendment 2 of the "Preliminary Safety Analysis Report for the Three Mile Island Nuclear Power Station, Unit 2," Docket No. 50-32, June 1968.
19. NRC, "Inservice Inspection of Ungrouted Tendons in Prestressed Concrete Containments," Regulatory Guide 1.35, Rev. 3.
20. J. Dougan, "Evaluation of In-Service Inspections of Greased Prestressing Tendons," NUREG/CR-2719 (ORNL/TM-8278), September 1982.
21. H. Ashar and D. Jeng, "Effectiveness of In-Service Inspection Requirements of Prestressed Concrete Containments - U.S. Experience," *Proceedings of the Second International Conference on Containment Design and Operation*, Toronto, October 1990.
22. American Society of Mechanical Engineers (ASME), *Boiler and Pressure Vessel Code*, 1992 and 1995 editions, Subsection IWL of ASME Section XI,

"Requirements for Class CC Concrete Components of Light-Water Cooled Plants," New York.

23. H. Ashar, D. Naus, and C. P. Tan, "Prestressed Concrete in U.S. Nuclear Power Plants," Part 1, *Concrete International*, ACI, Farmington Hills, MI, May 1994.
24. H. Ashar, C. P. Tan, D. Naus, "Prestressed Concrete in U. S. Nuclear Power Plants," Part 2, *Concrete International*, ACI, Farmington Hills, MI, June 1994.
25. Gilbert Associates, Inc. (GAI), "Containment Building Tendon Investigation for R. E. Ginna Nuclear Power Station," GAI Report 2347, prepared for Rochester Gas and Electric Corporation, January 1982.
26. J. F. Fulton and C.A. Forbes, "Inservice Inspection Forces Measured in Retensioned Tendons," Paper D8/5, *Structural Mechanics in Reactor Technology: 8th Conference*, Brussels, August 1985.
27. American Society for Testing and Materials (ASTM), "Standard Method for Stress Relaxation Tests for Materials and Structures," ASTM Standard E 328, Philadelphia, 1996.
28. H. Hill, "Concrete Containment Post-Tensioning System Aging Study," Letter Report 95/13 to NRC, ORNL, Oak Ridge, Tennessee, July 1995.

Table 1
Variation of Shrinkage Strain With Relative Humidity

Mean Daily Relative Humidity ¹	40-Year Shrinkage Strain ²
Under 40%	130×10^{-6}
40 to 80%	100×10^{-6}
Above 80%	50×10^{-6}

Note 1. Mean daily relative humidities for various areas in the U.S. can be found in: "Climates of the United States," published by the U. S. Department of Commerce.

Note 2. These values are applicable to containments in which inside operating temperatures do not exceed 49°C (120°F)) and that are subject to the ambient outside environment. The maximum value of 130×10^{-6} may be substantially increased if the containment is exposed to a controlled dry high-temperature environment after completion of prestressing.

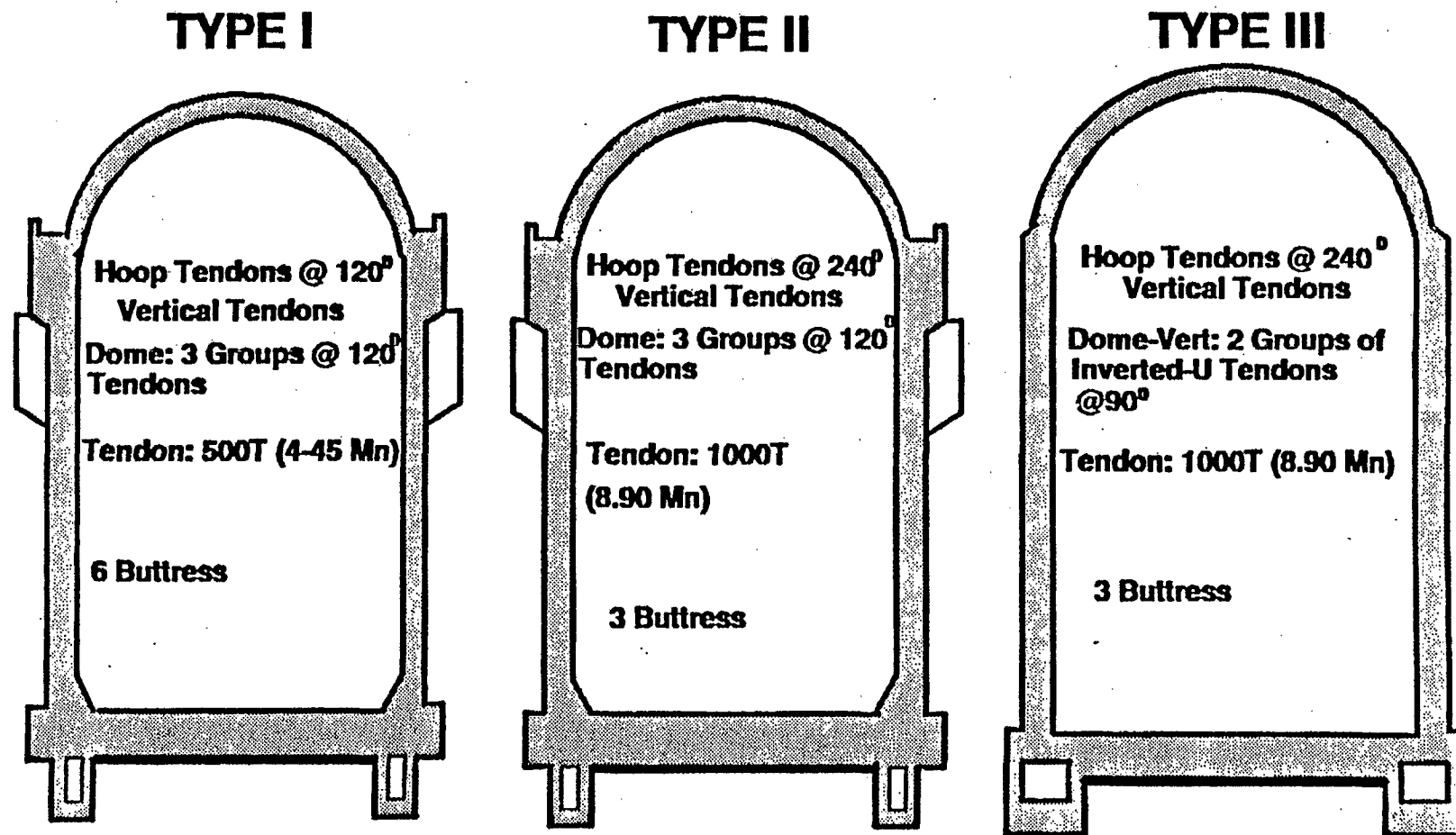


Figure 1. Generic types of prestressed concrete containments

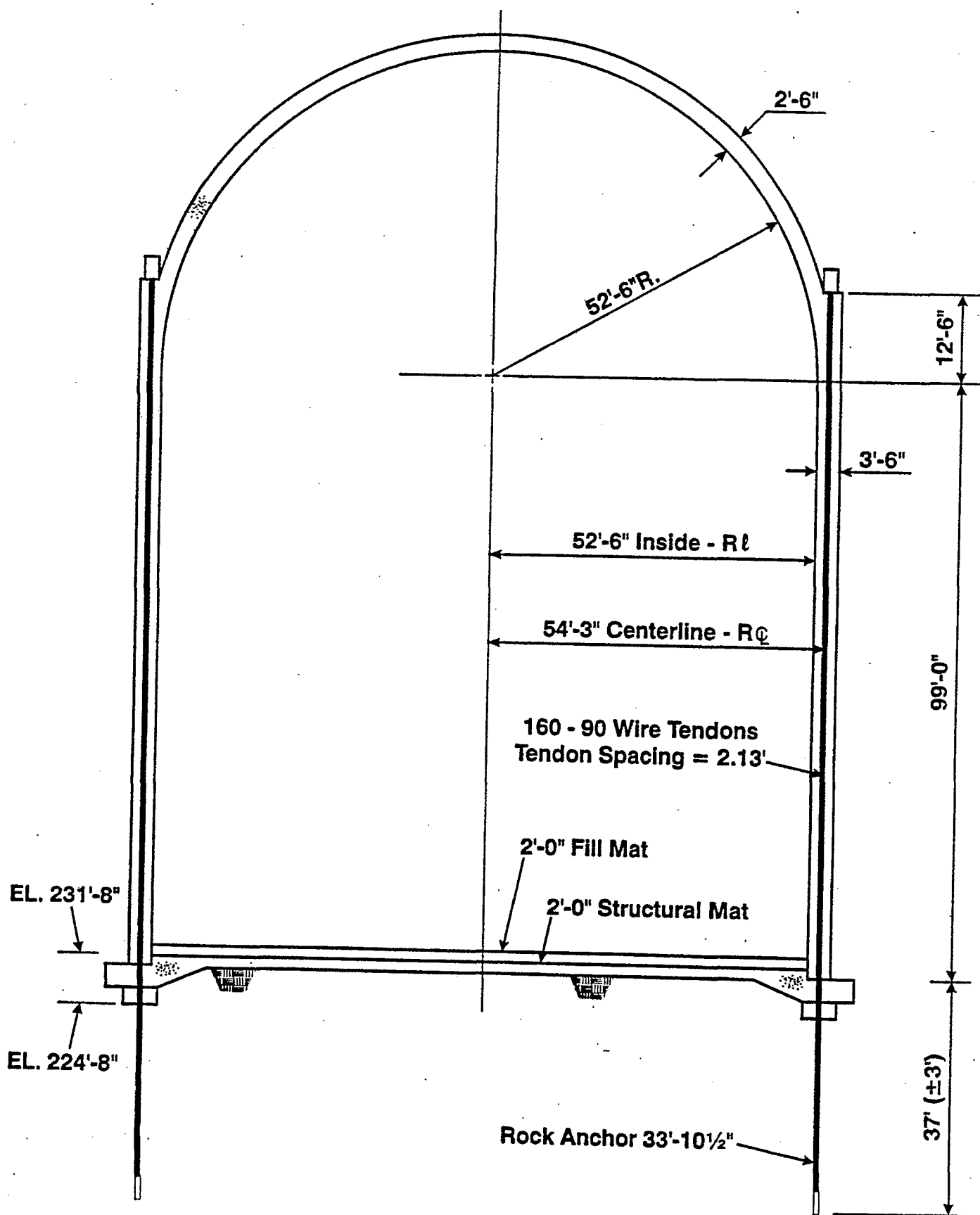
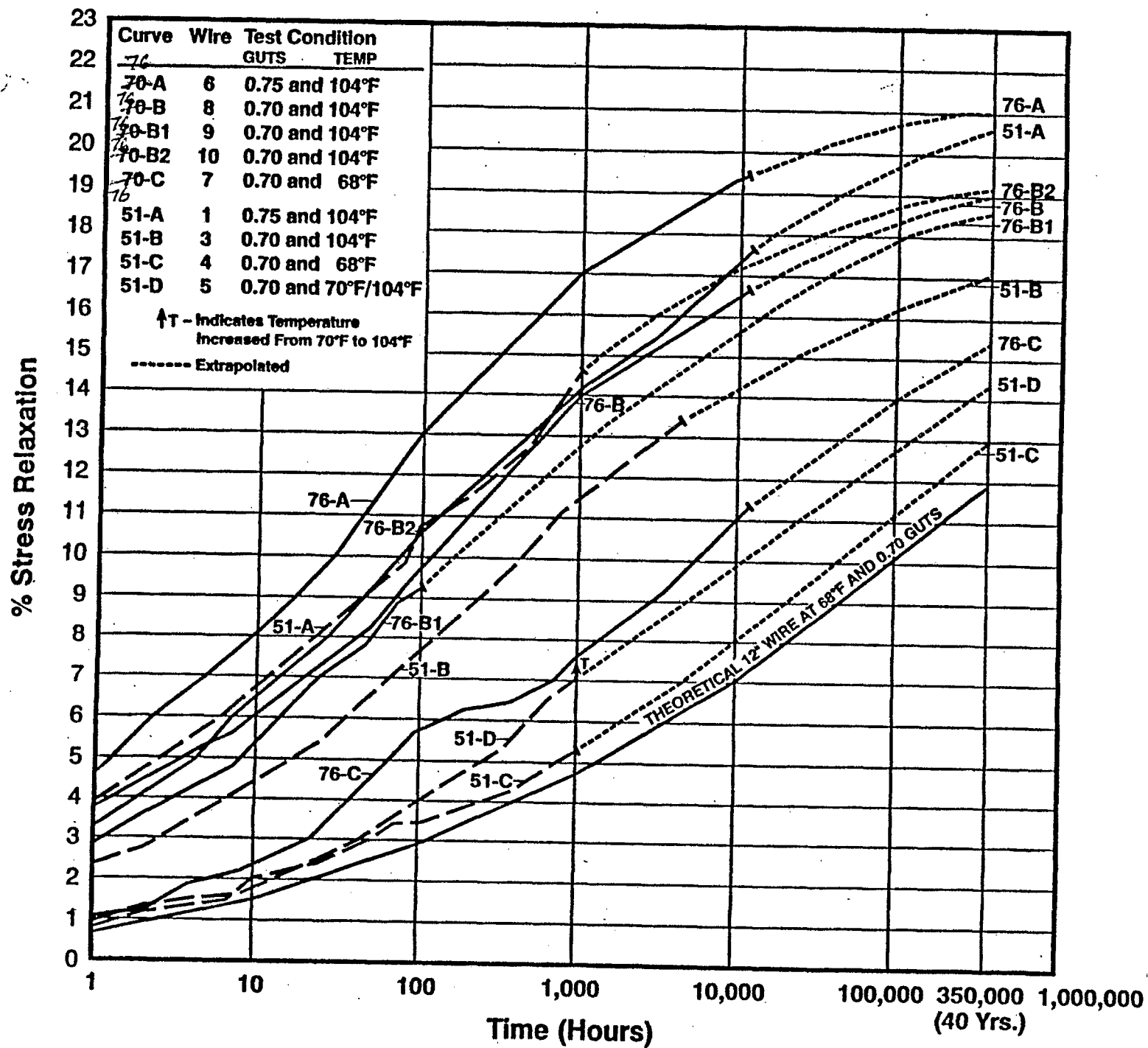


Figure 2.
Containment Building

Figure 3.
Stress Relaxation of Wires from Tendons 76 and 51



Discussion following each paper

Paper by Ulm

Dr. Ulm said that the effect of volume to surface ratio was only significant at very long times when creep became important.

The extension to a 3D model was not difficult. Another test rig was needed, such as a torsional arrangement as Prof Bazant had used for creep in the 1970s. The biaxial effect was not yet studied.

Concrete shrinkage will depend on time of loading and will be higher if the concrete was loaded at an early age.

Paper by Bazant

There was no geometry factor in the model because volume to surface ratio was not important until the final stage of drying, which was not reached until after 30-50 years for very thick structures.

Reinforcement also affected shrinkage, but it was modelled by a coupled separate restraining effect. In some simpler cases (but not the containment), it was modelled by empirical reduction factor. The bifurcation problem which made extrapolation to long times difficult applied to both creep and shrinkage, but the creep part was easy to treat.

Hydration was included in the model.

A large database on concrete ageing exist at the University of Karlsruhe

RILEM paper by Granger

The comparison for Flamanville was not as good as for Paluel. Both represented 10 years. For the other 4 stations compared, there was not yet enough time, but the initial results were well predicted.

In real life the contractor decided the concrete mix at a late stage, and it was site dependent. This could be controlled by requiring concrete tests in the contract. The results would be available in time to increase the prestressing if necessary. Concrete was considered representative if the diameter of the cylinder was greater than 6 times the aggregate size.

Belgian paper

The operator preferred instrumentation to pressure testing for economic reasons. Mr. Ashar commented that at least one country (Belgium) is utilising the provisions of RG 1.90. The RG has not been used in the US, as grouted tendon containments have been constructed in the US since the issue of the RG.

French paper

The steel tension could not directly be measured, as the tendons were grouted. Nevertheless there was confidence that the prestress measurements were real. Most work had been done on the concrete behaviour. The tendons could not be retensioned, but a liner could maybe be inserted to limit the leak rate in an ultimate case not foreseen for the time being.

The differences in behaviour were hard to correlate with causes, such as coastal or inland location. Two neighbouring stations, Flamanville and Paluel, had similar concrete, with only the gravel (limestone vs granite) being

different. However the prestress loss results were different. There was no obvious geographical effect.

The rules for conventional structures are not valid/applicable for containment. It was not possible to separate the steel relaxation from the total loss of prestress.

German paper

There were no rules or codes for measurements of the prestress. There was confidence in the predictions, and the only scatter taken into account was for the measurements. They had benefited from UK and French experience.

The measurements were on the 10 ungrouted tendons. The rest were grouted. The overestimation of the concrete compressive deformations by up to 40% could be explained by delays during erection. The later concrete age and the later time of prestress application, consequently, led to less concrete deformability - less than predicted, in the beginning, on the basis of a younger concrete. The ungrouted cables were representative. Most of the load was the prestress.

Indian paper

They had very few test results to date. They hypothesised 5% tension loss per year. The tendons were grouted. No monitoring or comparison of prestress loss and prediction were performed.

Pakistan paper

Pakistan has two stations only, one built in 1972 and one in construction.

Russian paper

The prestress loss was higher than anticipated.

Spanish paper

The UK experience was that load cells which were removed from the jacks for calibration purposes could be unreliable. The experience with these load cells in high capacity jacks had been that the errors could be as high as 15-20% depending on the geometry of the load cell and jack. Short squat load cells were particularly prone to error.

UK Magnox paper

There were 2 different manufacturers of strands, but only one was low relaxation. ISI was performed at Wylfa every 2 years, and at Oldbury the interval had just been increased to every 3 years. There was a 5 yearly review, when the vibrating wire and strain gauge results were compared with the analyses. Six wires were taken out at the inspection to inspect for corrosion. The cable temperature was 60-70C for the hottest, and maybe 100C at penetrations. This was modelled in the predictions, and the inner row was discounted for strength purposes in the analyses. A 60°C operating temperature was accounted for at the cables from the beginning.

UK Scottish paper

The standard was BS 4975 1973. There was now a testing programme. New greases according to the new standard BS 4975 (1990) were not degrading. In the early days storage had not been good, with just a short term protection for indoor storage. Defective or contaminated strands had been rejected. The Li based

grease had now been replaced by a LiCa grease. The oil migrated, with the salt (a corrosion inhibitor) staying on the surface. It was a powder which could easily be removed, so now there were visual inspections for drying out. The grease content was a commercial secret, but there was a high organic content, which led to bacteriological attack. They were not in high flux regions, so there had been no study of irradiation effects. For Sizewell B grease had been pumped at high pressure, leading to leaks as in the US.

US paper

In response to the question whether the results of the temperature were just an acceleration, or whether the amplitude was changed also, the response was that the results were an extrapolation from 1000hrs to 40 years, so the question could not be answered. Dr. Ulm said that the LCPC tests showed that there was no asymptote to the creep relaxation. The temperature effect were an acceleration leading to a greater prestress loss.

Similar grease leaking effect as in the UK had been observed. There had been no early regulation to keep grease inside, but it was easy to solve.

Round table on Prestressing for long serving structures: trends for the future

Members: Dr. Fuzier, Prof. Labbé, Prof. Lacroix, Dr. Tilly

Prof. Lacroix said that codes were more important in civil engineering than elsewhere. In mechanical engineering testing was easier. In civil engineering all structures were prototypes. Codes were a mixture of recommendations and regulations. There were two different trends, firstly for a short performance based code, and secondly for a detailed code. Codes quickly became obsolete, so he preferred a short code with recommendations. The Eurocode had been in the process of being developed for 15-20 years, but there were differences between countries as to whether they should be regarded as law or as recommendations. The first 3 codes were completed or nearly completed, on general aspects and buildings, bridges and tanks/silos. There would be future codes on offshore structures and buildings, and an execution code (firstly buildings). A nuclear code was envisaged later.

Dr. Tilly described bridge construction and gave failure examples, which were mainly due to corrosion. There were also problems with creep in bridges; creep had been observed in cantilever bridges, forming a collapse mechanism. The present creep codes were inadequate.

Dr. Fuzier said that costing of construction should include the cost of maintenance. Owners often require a 100-120 year lifespan for structures. The first prestressed structure (by Freyssinet in 1908), had shown excellent behaviour. External prestressing with grouting was now commonly used, as this facilitated survey and replacement. Another new development was the use of petroleum wax for corrosion protection. Bridge conditions were now periodically measured and recorded. He stressed the differences between bridges and NPPs.

There was discussion about corrosion. Dr. Fuzier commented that only the Scottish Nuclear paper had addressed this topic. He said that the petroleum wax being investigated by Freyssinet was being used on its own, but it contained an admixture of additives. The wax became liquid at 110C. It wetted the steel, which had positive effects. In NPPs the average temperature was 50C, but in an accident the temperature could reach 160C, although this was not relevant to the corrosion issue as the time was short. The environment in NPPs was protected, leading to reduced corrosion in comparison with bridges. Brennilis (Monts d'Arrée), an early heavy water reactor, would be dismantled, and it would be interesting to get results from this. Cathodic protection was sometimes used in specific cases. Corrosion had been discussed 2 years ago in a RILEM symposium. It should be possible to design cable materials that did not rust. The question was raised whether marine site NPPs could suffer from chlorides as a result of exposure in the construction phase.

In Sweden they also had plant where the tendons were kept in a dehumidified circulating air environment, which was monitored. Some corrosion had been found in Marcoule PV, an early gas cooled reactor designed in 1956. The corrosion was very localised, at 1m from the anchor point. Similarly after this discovery a desiccated flow of dried air had been put into operation, and after this the problem was solved. Corrosion had been found in Early NPP at the anchor heads and at the Fort St. Vrain PCPV, now decommissioned. This had been microbiological corrosion.

There was discussion on the difference between bridges and NPPs. The consequence of accidents was not the same, and public perception was not the same, partly because there were alternative energy sources, whereas there was no real alternative to bridges. The construction time and cost pressure were similar. The main NPP concerns were creep and shrinkage, whereas the main

concern for bridges was corrosion. Bridges saw their full design load occasionally, whereas NPP containment were passive for most of their life.

Professor Labbé pointed out differences between bridges and NPPs from the point of view of safety: for a bridge loss of prestressing is a safety concern because mechanical capacity is the safety function of a bridge; for a NPP containment, the safety function is leaktightness, thus loss of prestressing is not a priori a safety concern. This point is confirmed by the fact that we have no evidence of correlation between creep and leakage of operating containments. In the case of a containment we have to deal with radiological consequences; this safety goal is first converted into admissible leaks and after that into mechanical criteria; loss of prestressing is only related to the last step (mechanical criteria) while each conversion process introduces margins. For instance, there are assumptions made about the relationship between air leak rates and steam leak rates which need to be tested; the Maeva mock-up, here in Civaux, is devoted to analysis of these margins. In case of excessive loss of prestressing in a containment, the situation has to be examined from the point of view of a possible leak before drawing conclusions.

There was discussion about failure probabilities. The view was expressed that these figures were very often purely empirical and tradition. There had not been enough accidents loading the containment to establish a figure. The methods were defended as giving guidance. The main problem was incorrect scenarios. However knowledge was improving, and it was a main way to progress. Used as relative probabilities the figures were more useful than used as absolute probabilities.

There was discussion on the relative merits of grouted and ungrouted tendons. The view was expressed that structures having grouted tendons were more ductile than those with ungrouted tendons, and this led to a more favourable cracking pattern in the concrete, which would reduce tearing in the liner (if any) and hence reduce the leak rate. The alternative view was expressed that structures with ungrouted tendons have multiple diverse safety arguments, such as monitoring and replacement possibilities. Another possibility was to remove the prestressing and have only reinforced concrete. A related distinction could be made between bonded and unbonded tendons. It was possible to have grouted but unbonded tendons.

Prof. Lacroix and Dr. Fuzier summarised by saying that topics for future research and development were the development of new materials with less corrosion in the steel (the main concern for bridges) and less creep and shrinkage in the concrete (the main concern for NPPs), but innovation and new materials had always a part of uncertainties. There was a trend to unbonded tendons. There was a need to monitor grouted tendons. It was necessary to develop methods for new construction and methods for managing the existing structures.

Synthesis

Mr. Seni presented a synthesis of the papers, followed by discussion and contributions from the workshop participants. He presented the attached table and preliminary conclusions:

1. The reports from 12 countries have provided a large variety of cases including:
 - grouted system (72 containments) and un-grouted system (88 containments)
 - Freyssinet, BBRV, VSL and SH type cables.
2. The accumulated ageing experience was ranging from 4 to 39 years
3. Prestress loss > Predicted on some containments in 3 countries
4. Prestress loss < Predicted on some containments in 5 countries
5. No report on loss vs. prediction from 4 countries.
6. It appears that the prestressing loss is not a generic problem and it can not be associated with a type of prestressing cables or prestressing system. It is not dependent on the geographical location either.
7. More information is required in each case to define the reason for a higher loss than anticipated and its evolution in time. It is not clear yet if the loss is only quicker than anticipated or will also end up to be higher than anticipated at the end of the service life.
8. Among the main reasons for higher than anticipated loss were: early application of prestressing, high temperature in the vicinity of the cables, inadequate code provisions.

Three main topics were analysed:

- Corrosion protective media,
- Lift-off test instrumentation,
- Prestress loss

In the following 'O' indicates applicability to operational and 'N' to new plants.

Corrosion protective media

a/ Synthesis

The main features retained from papers were:

Pakistan (M. Ahmad)

The current generation of greases has (N)

- increased viscosity without sacrificing pumpability
- raised congealing point
- increased resistance to flow at sheathing joints
- increased water displacing characteristics
- raised base number thus higher reserve alkalinity
- increased electrical conductivity resistance

Scotland (L. M. Smith)

- Grease lost 29% of oil components after 9 years but retains protection ability (ON)

- Grease lost 50% of oil components after 24 years but still can provide protection. (ON)

Japan (Y. Watanabe)

- Grease performance was good. (ON)

b/Discussion

L. M. Smith (UK)

- The indoor storage time is important
- There is a need of visual inspection every 3 months since there is a danger of grease wash-out
- The grease content (components) is kept confidential and the organic content is not known. When it was high this has led to bacteriological attack.

H. Ashar (USA)

- The effect of irradiation is not known/quantified.

J-P. Fuzier (France)

- To note that there are also other corrosion inhibitors besides grease and the generic name used by ASME is "Corrosion protective media"

J. Irving UK)

- There is a danger of chloride ingress at the anchorages where problems were encountered.

H.Ashar (USA)

- The cable ducts (and joints) have improved, and chloride ingress is less probable.

c/Summary.

1. Presently available products are reliable
2. Risk factor: no risk identified
3. Action suggested:
 - gather from Users the brand names used with feed-back of performance
 - create a database and distribute to interested parties
 - develop guidelines

Lift-off test

a/ Synthesis

The main features retained from papers were:

Belgium (L. de Marneffe)

- Vibrating wires are robust (ON)
- Pressure cells are not so good (ON)
- Lift-off force translates additional strain to the first meters of the tendon only (ON)
- Lift-off with insertion of gauges is lacking accuracy (ON)
- A new generation of measuring devices is required to replace the mechanical procedure. (ON)

Germany (F. Stangenberg)

- Prestressing force transducers performed well (ON)

Spain (L. Ubalde)

- The lift-off used in the 80's with callipers was not accurate (O)
- Lift-off presently used, with computerised reading is accurate. (ON)

UK (J. Irving, D. W. Twidale)

- Load cells which are removed from the jacks for calibration purposes can be unreliable (ON)

b/ Discussion

J-P. Fuzier (France)

There is a problem with the stressing of the strands since they are not parallel in the area close to the anchorage. Freyssinet had developed a method in which each strand was stressed first separately and at a lower level.

L. de Marneffe (Belgium).

R&D work is required to develop means to prevent the formation of a knot by the strands close to the bearing plate

C. Seni (Canada)

More details could have been provided by the Spain delegate (L. Ubalde) who described in his paper a method which gave satisfaction but unfortunately he was not present and it would be useful to request more detailed information from him.

The initiative created with this Workshop should continue and collect, organise and distribute data available

V. D. Souza (WANO)

WANO could be used for further collection and distribution of data

c/Summary

1. Mechanical procedures (callipers, gauges insertion) are not reliable
2. Computerised reading instrumentation is reliable and available
3. Pressure cells should be abandoned
4. Risk factor
 - no risk identified with proper instrumentation
5. Action suggested
 - gather from Users specific data on instrumentation used and performance feed-back
 - create a database and distribute to participants

Loss of prestressing force

a/Synthesis.

The main features retained from papers were:

France (L. Granger)

- Concrete mix affects prestress loss (N)
- Regulation provisions are not well tested (N)
- Undertake study of delayed concrete behaviour at start (N)

Germany (F. Stangenberg)

- The discrepancy design/actual prestress loss depends on concrete age at first loading. (not considered by design) (ON)

India (A. S. Warudkar)

- Prestress loss code values have large variation (ON)
- Code values are for 20° C and corrections are required to the actual temperatures to which cables are exposed. (ON)

Pakistan (M. Ahmad)

-Prestress losses due to various factors (creep, shrinkage, relaxation, corrosion) can be monitored but can not be isolated quantitatively. (O)

Ukraine (J. Klimov)

-The highest prestress loss takes place during the first years, e.g. after 4-5 years. (O)

-Prestress loss also depends on concept of transfer of forces and could reach 20-25% with additional 1-3.45% per year from creep, shrinkage, etc. (O)

UK (J. Irving, D. W. Twidale)

-Tendon prestress loss is affected by temperature (ON)

USA (H. Ashar)

-Primary reason for prestress loss higher than anticipated was higher temperature in the vicinity of the cables. (ON)

-Losses alone the tendons could be higher than at the end anchorage (O)

b/Discussion

F. J. Ulm (France)

Where higher than anticipated prestress loss was detected this trend will continue till the end of the service life due to the continuous concrete creep.

P. Labbé (France)

The prestress loss did not affect the plant life. It affected the leak tightness only.

c/Summary

1. The loss of prestressing in containment is different from other concrete structures

2. The phenomenon is local, not generic and can not be associated with a type of prestressing or cable system or geographical location.

3. Additional and more specific data is required to understand each case and be able to draw general conclusions.

4. Risk factor:

-it appears not to be a plant life limiting factor since it affects the leak tightness only, which can be controlled,

-there are so far no available repair methods for grouted cables

5. Action suggested

(i) gather and harmonise data available to make it interchangeable

(ii) identify and fill gaps

(iii) distribute data to the participants

	Country	Years ageing	system	grouted	ungouted	loss >predict	loss <predict	loss n/a
1	Belgium	10 -- 20	Freyssinet	x(5)			x	
2	China	4	n/a	x(2)			x	
3	France		Freyssinet?	x(54)		x		
4	Germany	19	BBRV	x(1)				
5	India	27	n/a	x(8)				x
6	Japan	3/5/10	BBRV-3, VSL-2		x(5)		x	
7	Pakistan	n/a	n/a	n/a	n/a			?
8	Spain	15	Freyssinet		x(8)			x
9	Ukraine	10 -- 15	n/a		x(10)			x
10	UK1/2/Scotld	30	BBRV/Freyssinet		x(19)		x	
11	US	39	BBRV/VSL/SH	x(2)	x(39)	x		
12	Russia	20			x(7)	x		
	Total			6(72)	6(88)	3	5	4
	Grouted			6		2	3	1
	Ungouted				5	1	2	2
	Freyssinet	4		2	2	1	2	
	VSL	3		1	2	2	1	
	BBRV	5		2	3	2	3	

Summary of tendon prestress information

5th and 6th columns are no. of countries (no. of power stations)

Workshop on Prestress Losses in NPP Containment

Monday 25th August 1997	
8h00	Departure from the hotels to Civaux NPP
9h00	Introduction : OECD by A. Miller and EDF by P. Labbé
9h30	P. Acker : "Creep and Shrinkage of concrete : physical origins, practical measurements"
10h00	Z. P. Bazant : "Prediction of concrete creep and shrinkage : past, present and future"
10h30	BREAK
11h00	French presentation by E. Martinet et al.
11h20	Belgian presentation by L. De Marneffe
11h40	Indian presentation by A. S. Warudkar
12h00	U. K. Presentation by D. W. Twidale
12h20	LUNCH
13h30	Visit to the Merovingian cemetery in Civaux
14h30	Ukrainian presentation by J. Klimov
14h50	Russian presentation by V. Maliavine and J. Chataignier
15h10	German presentation by F. Stangenberg et al.
15h30	BREAK
16h00	U. K. Presentation by L. M. Smith et al.
16h20	Japanese presentation by Watanabe Yukio et al.
16h40	Pakistani presentation by Munir Ahmad
17h00	BREAK
17h15	Panel session : "Prestressing for long serving structures : trends for future design".
19h00	Soirée : Departure by bus to hotel
20h30	Restaurant in Poitiers

Workshop on Prestress Losses in NPP Containment

	Tuesday 26th of August
8h15	Departure from the hotels to Civaux NPP
9h00	RILEM Task Committee on Methodology for life prediction in NPP L. Granger : "What kind of prediction for prestress losses in NPP Containment ? "
9h30	Chinese presentation by Xu Yao Zhang
9h50	U.K. presentation by J. Irving and M. S. Hinley
10h10	BREAK
10h40	Spanish presentation by S. Luis Ubalde
11h00	USA presentation by H. Ashar
11h20	Discussions and conclusions (C. Seni)
12h00	J. -L. Costaz "Civaux 2 nuclear containment and the MAEVA mock-up"
12h30	LUNCH
14h00	Visit of the mock-up (2 Groups)
15h00	Visit of the Civaux 2 reactor building (2 Groups)
16h30	Departure by bus to Poitiers railway station and airport

List of Participants

BELGIUM

DE MARNEFFE, Luc
Principal Engineer
TRACTEBEL
7, Avenue Ariane
B-1200 BRUSSELS

Tel: +32 2 773 81 48
Fax: +32 2 773 89 70
Eml: luc.demarneffe@tractebel.be

CANADA

SENI, Claude
Specialist Civil Engineering
AECL CANDU
2251 Speakman Drive
MISSISSAUGA, Ont L5K 1B2

Tel: +1 (905) 823 9060 X3103
Fax: +1 (905) 823 9754
Eml: senic@aecl.ca

FRANCE

ACKER, Paul
Lab Centrale Ponts&Chaussees
58 bd Lefebvre
75015 PARIS

Tel: +33 1 40 43 62 86
Fax: +33 1 40 43 54 98
Eml:

BARBE, Bernard
DES/SAMS
CE FAR
CEA IPSN
B P 6
92265 FONTENAY-AUX-ROSES

Tel: +33 1 4654 7644
Fax: +33 1 4746 1014
Eml:

CHATAIGNER, Jacques
Coyne & Bellier
Agence de Lyon
Tour Credit Lyonnais
129 rue Servient
69431 LYON Cedex 3

Tel: +33 + 33 4 78 63 69 25
Fax: +33 + 33 4 78 63 69 29
Eml: coyne@worldnet.net

COSTAZ, Jean-Louis
Manager
Civil Engineering Branch
EDF
12-14, ave Dutriévoz
69628 VILLEURBANNE CEDEX

Tel: +33 4 78 94 44 44
Fax: +33 4 78 94 47 98
Eml:

FUZIER, Jean-Philippe
Directeur Scientifique
FREYSSINET
10 rue Paul Dautier
78140 VELIZY

Tel: +33 + 33 1 34 63 16 81
Fax: +33 + 33 1 34 63 16 77
Eml:

GRANGER, Laurent
EDF SEPTEN Div. Génie Civil
12-14 Avenue Dutriévoz
69628 Villeurbanne Cedex

Tel: +33 + 33 4 72 82 76 12
Fax: +33 + 33 4 72 82 77 07
Eml: laurent.granger@de.edfgdf.fr

GUINET, Patrice
EDF SEPTEN Div. Génie Civil
12-14 Avenue Dutriévoz
69628 Villeurbanne Cedex

Tel: +33 + 33 4 72 82 71 60
Fax: +33 + 33 4 72 82 77 07
Eml: @de.edfgdf.fr

LABBE, *Pierre
EDF SEPTEN
12-14 av Dutriévoz
69628 VILLEURBANNE Cedex

Tel: +33 4 72 82 72 22
Fax: +33 4 72 82 77 13
Eml:

LACROIX, Roger
65 rue de Javelot
75013 PARIS

Tel: +33 1 34 63 16 82
Fax: +33 1 45 83 91 40
Eml:

LE CORFF, Bertrand
Attache - Relations Internat.
EDF Production Transport
Exploitation Centre Nucleaire
Centre Affaires Michelet
92060 PARIS LA DEFENSE

Tel: +33 + 33 1 49 02 02 11
Fax: +33 + 33 1 49 02 06 95
Eml:

MARTINET, Eric
EDF-DTG
12 rue St Sidoine
69000 LYON

Tel:
Fax: +33 (33) 4 72 33 55 49
Eml:

NAHAS, Georges
DES/SAMS
CE FAR
CEA IPSN
B P 6
92265 FONTENAY-AUX-ROSES CEDEX

Tel: +33 1 4654 88 95
Fax: +33 1 4746 1014
Eml: nahas@sodium.far.cea.fr

PICAUT, Jack
Directeur
Dept. Geothech. et Structures
COYNE ET BELLIER
9, allée des Barbanniers
92632 Gennevilliers Cedex

Tel: +33 + 33 1 41 85 03 69
Fax: +33 + 33 1 41 85 03 74
Eml: coyne@worldnet.net

ROBERT, Lucien
EDF-DTG
12 rue St Sidoine
69000 LYON

Tel:
Fax: +33 (33) 4 72 33 55 49
Eml:

ROUSSELLE, Henri
EDF EPN-DM
Quartier Michelet
13-27 Esplanade Ch. de Gaulle
92060 PARIS-LA DEFENSE Cdx 57

Tel: +33 1 49 02 7777
Fax: +33 1 49 02 07 69
Eml:

TERRAILLON, Eric
EDF-UNIFE

Tel:
Fax:
Eml:

TOURET, *Jean-Pierre
Group Dynamique et Seisme
Div. Mécanique des Structures
EDF/SEPTEN
12-13 ave Dutrievoz
69628 VILLEURBANNE Cedex

Tel: +33 4 72 82 75 54
Fax: +33 4 72 82 77 13
Eml: jean-pierre.touret@de.edfgdf.f

ULM, Franz-Josef
Laboratoire Central des Ponts et Chaussée
59 boulevard Lefebvre
F-75732 Paris Cedex 15

Tel: +33 1 40 43 53 25
Fax: +33 1 40 43 54 98
Eml: ulm@lcp.fr

GERMANY

ALEX, Herbert
Gesellschaft für Anlagen-und
Reaktorsicherheit (GRS) mbH
Schwertnergasse 1
50667 KOLN

Tel: +49 221 2068 742
Fax: +49 221 2068 888
Eml: ale@grs.de

BUSCH, Dieter
Junior Assistant Manager
RWE Energie AG Bereich Bau
Kruppstrasse 5
45128 ESSEN

Tel: +49 + 49 201 12 24 476
Fax: +49 + 49 201 12 22 486
Eml:

KOBLER, Gerhard
Universität Karlsruhe
Institut für Massivbau
Am Fasanengarten
D-76128 KARLSRUHE

Tel: +49 721 608.22.77/38.86
Fax: +49 721 69 30 75
Eml:

LIERSCH, Ing. Gunter
Director
Dep. of Civil Engineering
BAYERNWERK

Tel: +49 + 49 89 12 54 34 47
Fax: +49 + 49 89 12 54 30 00
Eml:

STANGENBERG, Friedhelm
Stangenberg und Partner
Ingenieur-GmbH
Viktoriastrasse 47
D-44787 BOCHUM

Tel: +49 + 49 234 9613012
Fax: +49 + 49 234 9613048
Eml:

INDIA

RAJESHIRKE, Umesh K.
STUP Consultants Limited
301 Nirman Vyapar Kendra
Plot No. 10, Sector 17, Vashi
Navi Mumbai - 400 703

Tel: ++ 7670 995, 7672 521
Fax: ++ 7630 173
Eml: stup@bom2.vsi.net.in

WARUDKAR, Aniruddha S.
Nuclear Power Corporation
8-14 floor
Vikram Sarabhai Bhavan
Central Ave. Anushaktinagar
MUMBAI 400-094

Tel: ++91 (22) 556 4210 / 0140
Fax: ++91 (22) 556 3350
Eml:

JAPAN

AKITA, Shodo
The Kansai Electric Co. Inc.
3-3-22, Nakanoshima
Kita-ku
Osaka, 530-70

Tel: +81 + 81 6 446 9656
Fax: +81 + 81 6 441 3879
Eml: k439455@kepco.co.jp

CHANG, Chao-Bin
WANO Tokyo Centre
2-11-1 Iwatokita
Komae
TOKYO 201

Tel: +81 3 3480 4809
Fax: +81 3 3480 5379
Eml:

KAWAI, Ikurou
Manager of Civil Engineering
Japan Atomic Power Co.
Ohtemachi Bldg.6-1-1 Chome,
Ohtemachi,Chiyoda-ku
TOKYO 100

Tel: +81 + 81 3 3201 66 31
Fax: +81 + 81 3 3212 84 63
Eml: ikurou-kawai@japc.co.jp

KOYANAGI, Mitsuo
Chief Research Engineer
Technical Research Institute
Obayashi Corporation
4-640 Shimo-Kiyoto
Kiyose-shi, Tokyo

Tel: +81 + 81 424 95 0970
Fax: +81 + 81 424 95 0908
Eml:

SONO, Youichi
Manager
Civil Engineering Department
Kyushu Electric Power Co.Inc.
1-82 Watanabe-dori
2-chome, Chuo-ku, Fukuoka

Tel: +81 + 81 92 761 3031
Fax: +81 + 81 92 761 4237
Eml:

YAMAMOTO, Mikio
Deputy General Manager
Engineering Department
Obayashi Corporation
Shinjuku Park Tower 3-7-1
Nishi-Shinjuku, Tokyo

Tel: +81 + 81 (3) 5323 35 59
Fax: +81 + 81 (3) 5323 35 50
Eml: m.yama@o-net.obayashi.co.jp

P.R. OF CHINA

ZHANG, Xuyao
Guangdong Nuclear Power Joint Venture Co.
BX Building
Daya Bay Nuclear Power Station
SHENZHEN Guangdong

Tel: ++86 (755) 3349349 X 3257
Fax: ++86 (755) 3385513
Eml:

PAKISTAN

AHMAD, Munir
CHASNUPP
P O Box 1133
Islamabad

Tel: ++92 51 9205600
Fax: ++92 51 9217864
Eml:

RUSSIAN FEDERATION

MALIAVINE, Vladimir
Atomenergoproekt
Bakuninskaya 7 str 1
107815 GSP-6
MOSCOW B-5

Tel: +7 095 267 4975
Fax: +7 095 265 0974
Eml:

SPAIN

UBALDE SERRA, Luis
Civil Eng Dept Head
Asco NPP
Tres Torres 7
BARCELONA 08017

Tel: +34 (3) 2532900
Fax: +34 (3) 2040421
Eml:

SWEDEN

SUNDQUIST, Håkan
Prof. Structural Design
Royal Institute of Technology
Dept Structural Engineering
SE-100 44 STOCKHOLM

Tel: +46 (8) 790 80 30
Fax: +46 (8) 21 69 49
Eml: hsund@struct.kth.se

UKRAINE

KLIMOV, Julij
State Research Institute
Building Construction
5/2 Kimenko str
KIEV 252680

Tel: +380 44 276 0366
Fax: +380 44 276 6269
Eml:

UNITED KINGDOM

HINLEY, Malcom
Multi-Design Consultants
175 Moathouse Drive
Crewe
Cheshire
GB-CW2 8LG

Tel: +44 1270 651824 / 0370 954164
Fax: +44 161 477 6768/1242 582260
Eml:

IRVING, Jim
Multi-Design Consultants
9 Pinetrees
Charlton Kings
Cheltenham
Glos GB-GL53 0NB

Tel: +44 1242 582260
Fax: +44 1242 582260
Eml:

MCNULTY, Tony
NII, HSE
St Peter's House
Balliol Road
Bootle, Merseyside L20 3LZ

Tel: +44 151 951 3624
Fax: +44 151 951 3942
Eml: tony.mcnulty@hse.gov.uk

SMITH, Leslie M.
Civil Design, Scottish Nuclear
3 Redwood Cresc., Peel Park
East Kilbride
GLASGOW
GB-G74 5PR

Tel: +44 13552 62385
Fax: +44 13552 62459
Eml: les.smith@snl.co.uk

TILLY, Graham
Gifford & Partners
Carlton House, Ringwood Road
Woodlands
SOUTHAMPTON
GB-SO40 7HT

Tel: +44 (1703) 813461
Fax: +44 (1703) 813462
Eml: mail@giffeng.co.uk

TWIDALE, David
Magnox Electric plc
Berkeley Centre
BERKELEY
Gloucestershire GL13 9PB

Tel: +44 (1453) 812165
Fax: +44 (1453) 812944
Eml:

UNITED STATES OF AMERICA

ASHAR, Hansraj
Senior Civil Engineer
U.S. Nuclear Regulatory
Commission
11555 Rockville Pike
Rockville, Md. 20852-2738

Tel: +1 + 1 (301) 415 2851
Fax: +1 + 1 (301) 415 2444
Eml: hga@nrc.gov

BAZANT, Zdenek P.
Depart. of Civil Engineering
The Technological Institute
Northwestern University
EVANSTON, IL 60208-3109

Tel: +1 (847) 491 4025
Fax: +1 (847) 467 1078
Eml:

COSTELLO, James F.
Structural & Seismic Eng Branch
NRC
Off. of Nucl. Regulatory Res.
WASHINGTON DC 20555

Tel: +1 301 415 6009
Fax: +1 301 415 5074
Eml: jfc2@nrc.gov

GRAVES, Herman L
US NRC
Mail Stop T-10L1
Regulatory Research
WASHINGTON DC 20555

Tel: +1 301 415 5880
Fax: +1 301 415 5074
Eml: hlg1@nrc.gov

International Organisations

DE SOUZA, Vaner Diniz
World Association of Nuclear Operators
Paris Centre
39 avenue de Friedland
FR- 75008 PARIS

Tel: +33 1 4042 7056
Fax: +33 1 4561 9277
Eml:

ICHER, Jean
WANO Paris centre
39 avenue de Friedland
75008 PARIS

Tel: +33 1 4042 4596
Fax: +33 1 4561 9277
Eml:

MILLER, Alex G.
OECD-NEA
Nuclear Safety Division
Le Seine St-Germain
12 bd des Iles
F-92130 ISSY-LES-MOULINEAUX

Tel: +33 1 4524 1057
Fax: +33 1 4524 1110
Eml: alex.miller@oecd.org